UNIVERSITEIT VAN PRETORIA
UNIVERSITY OF PRETORIA
YUNIBESITHI YA PRETORIA

AN INVESTIGATION INTO THE RELATIONSHIP BETWEEN VERTICAL AND LATERAL FORCES, SPEED AND SUPERELEVATION IN RAILWAY CURVES

ALEXANDER FRANK POWELL

A dissertation submitted in fulfilment of the requirements for the degree of

MASTER OF ENGINEERING (TRANSPORTATION ENGINEERING)

In the

FACULTY OF ENGINEERING

UNIVERSITY OF PRETORIA

November 2016

© University of Pretoria

UNIVERSITEIT VAN PRETORIA
UNIVERSITY OF PRETORIA
YUNIBESITHI YA PRETORIA

DISSERTATION SUMMARY

AN INVESTIGATION INTO THE RELATIONSHIP BETWEEN VERTICAL AND LATERAL FORCES, SPEED AND SUPERELEVATION IN RAILWAY CURVES

AF POWELL

Supervisor: Professor PJ Gräbe

Department: Civil Engineering

University: University of Pretoria

Degree: Master of Engineering (Transportation Engineering)

The Gautrain Rapid Rail Link (GRRL) is a rail transit system in South Africa that links Johannesburg and Pretoria, as well as Johannesburg and the O.R. Tambo International Airport. Travelling at speeds of up to 160 km/h, the Gautrain system is the first of its kind on the African continent. This dissertation covers an investigation into the relationship between the vertical and lateral forces, speed and superelevation in a GRRL curve.

The process followed in the investigation was to select an experimental curve, to determine all the curve parameters and to instrument the curve in order to be able to collect vertical and lateral rail force data. An experiment was then undertaken which involved running a test train at various speeds, changing the cant of the curve, through tamping the ballast, and repeating the test train runs at the same varying speeds.

The selected curve was found to be experiencing high leg contact to the gauge side of the rail, while the low leg contact was to the field side of the rail. In order to move the high leg contact band away from the gauge side of the rail the cant needs to be reduced (as was done in this dissertation) or alternatively the operational speed of the train needs to be increased.

The theoretical effect of changing the cant in a curve is well known. The primary purpose of this dissertation was to experimentally assess what the actual effect of changing the cant is and compare these results to the theoretically expected results.

© University of Pretoria

Assessing the before and after tamping test data independently did validate the existence of the expected relationships between the vertical and lateral rail forces, speed and superelevation. When comparing the before and after tamping results using trend analysis these relationships were again identified, but were less rigorous than those established for the independent sets of data.

The most significant finding when comparing the before and after tamping results to one another was that while the theory indicates that the reduction of the cant in this specific test curve, given all of the other curve characteristics, should have resulted in an increase in the lateral forces, there was in fact a roughly 50% reduction in the maximum lateral forces after the cant was reduced. The wear of the rail and wheels is strongly linked to the magnitude of forces that they experience. Although other factors also need to be taken into account, it is not unreasonable to presume that a 50% reduction in the maximum lateral forces could lead to a halving of the wear rate of the rail and wheels in this curve.

The reduction of the cant had a minimal effect on the magnitude of the vertical forces, but did result in a transfer of loading between the high and the low legs.

© University of Pretoria

DECLARATION

I, the undersigned hereby declare that:

I understand what plagiarism is and I am aware of the University's policy in this regard;

The work contained in this thesis is my own original work;

I did not refer to work of current or previous students, lecture notes, handbooks or any other study material without proper referencing;

Where other people's work has been used, this has been properly acknowledged and referenced;

I have not allowed anyone to copy any part of my thesis;

I have not previously in its entirety or in part submitted this thesis at any university for a degree.

Signature of student

AF Powell

21185710

November 2016

© University of Pretoria

ACKNOWLEDGEMENTS

Soli Deo Gloria, with sincere thanks and appreciation to the following persons and organisations:

a) Professor PJ Gräbe, my supervisor for his ongoing and patient mentorship, guidance and support. His dedication to his students is unwavering.

b) The Chair in Railway Engineering at the University of Pretoria for financial support, as well as the use of various equipment and facilities during the course of the study.

c) This dissertation is based on a research project of Bombela Maintenance Company. Permission to use the material is gratefully acknowledged. The opinions expressed are those of the author and do not necessarily represent the policy of Bombela Maintenance Company.

d) Bombela Maintenance Company and Bombardier Transportation for the provision of data.

e) The following persons are gratefully acknowledged for their invaluable assistance:

   i) The 2015 team of Chair in Railway Engineering research assistants at the University of Pretoria, specifically Mr P Vorster, Mr R Vandoorne, Mr R du Plooy and Mr A Ronda, as well as the 2015 final year undergraduate research students Mr T Mabotha and Mr T Heenop. Also a special thanks to Mrs C Bezuidenhout (Information Specialist) for critical help in the sourcing of literature.

   ii) The Gautrain Wayside Team at Bombela Maintenance Company, specifically Mr H Mkiti, Mr D de Lange, Mr E Khechane, Mr M Uys, Mr C Greeff, Mr M Ximba and the whole Track Department crew, as well as Mr S Dayanand, Mr N Karatela, Mr S Madanda and Mr K Seethal.

   iii) The Gautrain Services Team at Bombardier Transportation, specifically Mr J van Biljon, Mr C Engelbrecht, Mr G Gretten, Mr W van Rooyen and Mr W Snyders.

   iv) Mr P Louw and Mr JC Kleynhans at Bombela Operating Company.

   v) Ms N Gilfillan from Bombardier Bogies Division, Mr B Cousins from TLC Engineering Solutions, Mr F Shaw from Tubular Track and Mr J Vorster from Aurecon.

f) My family and friends for their encouragement and support during the study, specifically:

   i) My wife, Karen, for her love, support and never-ending belief that I could complete this dissertation. And close family and friends for checking in on my progress.

   ii) Little James, for walks every afternoon to clear my head and keep me future-focused.

   iii) James's little brother (DHP), who we expect to be joining our family in January 2017.

© University of Pretoria

TABLE OF CONTENTS

PAGE

© University of Pretoria

© University of Pretoria

LIST OF TABLES

© University of Pretoria

© University of Pretoria

© University of Pretoria

© University of Pretoria

© University of Pretoria

LIST OF FIGURES

© University of Pretoria

© University of Pretoria

© University of Pretoria

© University of Pretoria

© University of Pretoria

© University of Pretoria

© University of Pretoria

LIST OF SYMBOLS

a_y	Acceleration parallel to the track plane
a_z	Acceleration perpendicular to the track plane
CL	Cord length
F	Lateral reaction force on outside of raised wheel
g	Gravitational acceleration
h	Cant
h_{eq}	Equilibrium cant
h_e	Cant excess
h_d	Cant deficiency
H	Resultant height of vehicle's centre of gravity above the rail
M	Total mass of vehicle
p_d	Dynamic wheel load
p_s	Static wheel load
R	Radius of curve
R_{LL}	Vertical reaction force of low leg rail
R_{HL}	Vertical reaction force of high leg rail
R^2	Coefficient of determination
r_0	Wheel radius
Δr	Rolling radius difference
R_W	Wheel profile radius
R_R	Rail profile radius
U	Resultant centrifugal force on vehicle
v	Speed of vehicle
v_{eq}	Equilibrium speed
X	Dynamic wheel load factor
y	Lateral displacement of the wheelset from the centre position of the track
2a	Effective gauge (For a rail gauge of 1435 mm, 2a ≈ 1500 mm)
2b	Lateral distance of axle box suspension
δ	Angle between the plane of contact and track level
γ	Conicity of the wheel tread
γ_e	Equivalent conicity of the wheel tread
θ	Cant angle

© University of Pretoria

LIST OF ABBREVIATIONS

A	Axle
AT	After Tamping
BCC	Bombela Concession Company
BMC	Bombela Maintenance Company
BOC	Bombela Operating Company
BT	Before Tamping
D	Down
DMOA	Driving Motor Open Airport
DMOS	Driving Motor Open Standard
DR	Derailment Ratio
EMU	Electric Multiple Unit
FIFA	The Fédération Internationale de Football Association
GMA	Gautrain Management Agency
GRRL	Gautrain Rapid Rail Link
HL	High Leg
LB	Leading Bogie
LL	Low Leg
MOS	Motor Open Standard
OHTE	Overhead Traction Equipment
ORE	Office of Research and Experiments
PPP	Public Private Partnership
PRASA	Passenger Rail Agency of South Africa
PTOA	Pantograph Trailer Open Airport
PTOS	Pantograph Trailer Open Standard
RCF	Rolling Contact Fatigue
STD	Standard Deviation
S1	Site 1
S2	Site 2
TB	Trailing Bogie
TGMS	Track Geometry Measuring System
U	Up
UIC	International Union of Railways
W	Wheel

© University of Pretoria

CHAPTER 1 INTRODUCTION

1.1 BACKGROUND

Railways worldwide form an integral component of any transportation system. The movement of freight on rail can be done much more efficiently from an energy, time and cost point of view when compared to roads, while simultaneously protecting the road infrastructure by decreasing the loads travelling on the roads. Through decreasing the loads on the roads the maintenance attention that needs to be given to overused roads is drastically decreased which gives rise to another long list of benefits. The movement of passengers on rail versus roads has the same benefits, although the reduction in road loads is insignificant when compared to freight. However, the benefits that passenger railways provide to society in the form of good reliable public transport, which allows for a better quality of life and the stimulation of the economy, are extensive. Even in the case of unreliable passenger railway services, such as those that can be found in many third world countries, the fact that the users don’t have any alternative options for getting to and from work means that they would rather have an unreliable passenger train service than no train service at all. As such the economy is still stimulated, although inefficiently. The goal of any railway service whether freight or passenger is to be the customers’ preferred choice of transportation through continuously striving for increased safety, reliability and cost-effectiveness.

Railway engineering is one of the most multi-disciplinary engineering industries, with civil, mechanical, electrical, electronic and industrial engineers all often working together within the same railway focused organizations.

As a very crude outline of responsibilities it is often said that the civil (or track) engineer is responsible for the rails down, the mechanical engineer is responsible for the vehicles running on the rails, the electrical engineer is responsible for the electrification system that powers the trains (in the case of electrically powered trains versus diesel powered trains), the electronic engineer is responsible for the signalling system that controls the movement of the trains and the industrial engineer is responsible for the efficient day to day operation of the railway network.

As can be concluded from the above description, there are several areas where the different engineering disciplines overlap and therefore need to work together to ensure an optimal interaction. The two most important areas of interaction include the interaction of the wheels with the rails, and of the pantograph with the catenary wire, which forms part of the overhead traction equipment (OHTE).

© University of Pretoria

The Gautrain Rapid Rail Link (GRRL) is a rail transit system that links the two cities of Johannesburg and Pretoria in the province of Gauteng, South Africa. The system also provides an airport service between Johannesburg and the O.R. Tambo International Airport. Travelling at speeds of up to 160 km/h, the Gautrain system is the first of its kind in South Africa and in fact in Africa.

The first part of the system, between Sandton and the O.R. Tambo International Airport, opened to the public on 8 June 2010, in time for the 2010 FIFA World Cup. The route from Rosebank to Pretoria and Hatfield commenced operations on 2 August 2011, while the remaining section from Rosebank to Johannesburg Park Station opened on 7 June 2012, due to higher than anticipated underground water ingress into the railway tunnel (Wikipedia, 2015). Therefore at the time of writing the GRRL airport service has been operational for 6 years and the commuter service has been operational for 5 years. The relative newness and uniqueness of this state-of-the-art railway engineering project in the South African context therefore provides an excellent opportunity for a variety of research studies to be undertaken.

1.2 OBJECTIVES OF THE STUDY

The main objective of the study was to investigate whether or not certain characteristics of a GRRL curve could be optimized from a track point of view.

This main objective was achieved by means of identifying an experimental curve in which the high leg (HL) rail contact was predominantly to the gauge side of the rail, with the corresponding low leg (LL) rail contact being predominantly to the field side of the rail. This situation allowed for one of two approaches to be taken in order to move the high leg contact band away from the gauge side of the rail. Either the cant could be reduced (as was done in this dissertation) or alternatively the operational speed of the train could be increased.

Once an appropriate experimental curve had been found within the GRRL network the selected curve was assessed in terms of the curve’s design characteristics, as well as the curve’s current operational performance versus the curve’s operational performance at the modified level of cant.

© University of Pretoria

1.3 SCOPE OF THE STUDY

The main focus of the study was to investigate the interaction between the wheels of trains operating on the GRRL network and the rails of the GRRL system. The study was limited to the vehicle and track components having a direct influence on the wheel/rail interaction, and was further limited by means of focusing the research on a particular curve on the GRRL network. It is believed that the results obtained from the experimental test curve can readily be extrapolated to the other curves on the GRRL system.

Although the GRRL system is comprised of both ballasted track and tunnel slab track, only 14% of the total system is on tunnel slab track, with the remaining 86% all being on ballasted track. This study therefore focused solely on ballasted track with the findings being deemed as being applicable to tunnel slab track as well.

1.4 METHODOLOGY

The dissertation was undertaken by pursuing the methodology as outlined by the following points:

- A literature review was undertaken during which the topic of railway line infrastructure and its associated terminology, as well as track geometry and its associated terminology were introduced. This was followed by discussions focussing on cant and the wheel/rail interface. Finally information pertaining to the current wheel/rail interface of the GRRL system was introduced.
- Following on from the literature review a test curve site was selected for the collection of data relating to the dissertation objectives. For redundancy purposes two similar sites were selected within the experimental test curve.
- The design of the experiment pivoted around collecting data at the curve's design/operational cant and then changing the cant and repeating the data collection process. Data was therefore collected before and after tamping. Data collected included track geometry information, rail forces and wheel/rail interaction videos.
- Analyses of the before tamping data measurements' results and the comparison of these results to the theoretically expected results.
- Analyses of the after tamping data measurements' results and the comparison of these results to the theoretically expected results.
- Finally the comparison of the before and after tamping results to one another.

© University of Pretoria

1.5 ORGANISATION OF THE DISSERTATION

The dissertation consists of the following chapters and appendices:

- **Chapter 1** serves as an introduction to the dissertation.
- **Chapter 2** contains the technical introduction based on a literature review.
- **Chapter 3** describes the experimental work done.
- **Chapter 4** presents the experimental results and describes the analyses undertaken.
- **Chapter 5** contains the conclusions and recommendations of the dissertation.
- **Chapter 6** provides a list of the references used in the dissertation.
- **Appendix A** contains all of the test train speed information.
- **Appendix B** contains all of the test curve rail forces data for the wheels.
- **Appendix C** contains all of the test curve rail forces trends for the wheels.
- **Appendix D** contains all of the trend line information for the wheels.
- **Appendix E** contains all of the test curve rail forces data for the bogies, cars and trains.
- **Appendix F** contains details with regard to the train positions of the maximum and minimum train to rail forces.
- **Appendix G** contains all of the test curve rail forces trends for the bogies.
- **Appendix H** contains all of the test curve rail forces trends for the cars.
- **Appendix I** contains all of the test curve rail forces trends for the trains.
- **Appendix J** contains all of the trend line information for the bogies, cars and trains.
- **Appendix K** contains all of the force balancing data for the bogies and cars.
- **Appendix L** contains all of the test curve rail forces data for the bogies and cars at 85 km/h.

© University of Pretoria

CHAPTER 2 LITERATURE REVIEW

2.1 INTRODUCTION

The literature study starts with an overview of the Gautrain Rapid Rail Link (GRRL) system, followed by a brief description of some track infrastructure components and track geometry parameters. An in depth literature study with regard to cant and the wheel/rail interface is then presented, followed by a discussion of the current wheel/rail interface of the GRRL system.

2.2 GAUTRAIN RAPID RAIL LINK SYSTEM OVERVIEW

The GRRL system comprises a total of 143 km of railway track (excluding the Depot tracks), of which 20 km is tunnel slab track and 123 km is ballasted track. The tunnel section runs from the Portal (close to Marlboro Station) to Johannesburg Park Station, with the first 5 km between the Portal and Sandton being a double-line and the remaining tunnel section linking Sandton to Johannesburg Park Station via Rosebank being a single-line, 10 km in length. The ballasted section includes 46.5 km of double-line track stretching from Marlboro to Hatfield via Midrand, Centurion and Pretoria. Another double-line ballasted section of 15 km links Marlboro to the O.R. Tambo International Airport via Rhodesfield.

Ten stations and dedicated bus feeder and distribution services line the route. The route alignment is shown in Figure 2.1. Of the ten stations, four of them are at-grade (Hatfield, Pretoria, Midrand and Marlboro), three of them are elevated (Centurion, Rhodesfield and O.R. Tambo International Airport) and 3 of them are underground (Sandton, Rosebank and Park).

The GRRL system is the first rapid rail train in South Africa, achieving operational speeds of up to 160 km/h and using a standard gauge track width (1435 mm). Most other South African railways operate narrow gauge track (1067 mm).

© University of Pretoria

Figure 2.1: Gautrain Route Alignment

The project consisting of the design, construction and financing of the system, as well as the ongoing operation and maintenance, has brought together government, the private sector, and a host of local and international specialists in an unprecedented manner. The Public-Private Partnership (PPP) Project has the Government of the Province of Gauteng as the client and the concessionaire (Bombela Concession Company, BCC) will transfer the system back to the client at the end of the 15-year Operating Period. The Gautrain project not only addresses a critical transport need in the province but also meets the Government's objectives of promoting and stimulating economic growth, development and employment creation.

The Gauteng Province has appointed the Gautrain Management Agency (GMA) to oversee the Gautrain Project. The concessionaire (BCC) has subcontracted the operation of the Gautrain system to Bombela Operating Company (BOC) and BOC has subcontracted the perway and rolling stock maintenance to Bombela Maintenance Company (BMC). Bombardier Transportation supplied the Electric Multiple Units (EMUs) or trains that run on the network.

© University of Pretoria

2.3 TRACK INFRASTRUCTURE AND TERMINOLOGY

Descriptions and figures of the track components are taken from the book "The Railway Track and Its Long Term Behaviour" (Tzanakakis, 2013), unless stated otherwise.

Track components are grouped into two main categories (Figure 2.2),

- The superstructure which consists of the
  - Rails,
  - Sleepers and
  - A fastening system to hold the components together
  - Ballast, and
- The substructure which consists of the
  - Subballast and the
  - Subgrade or formation

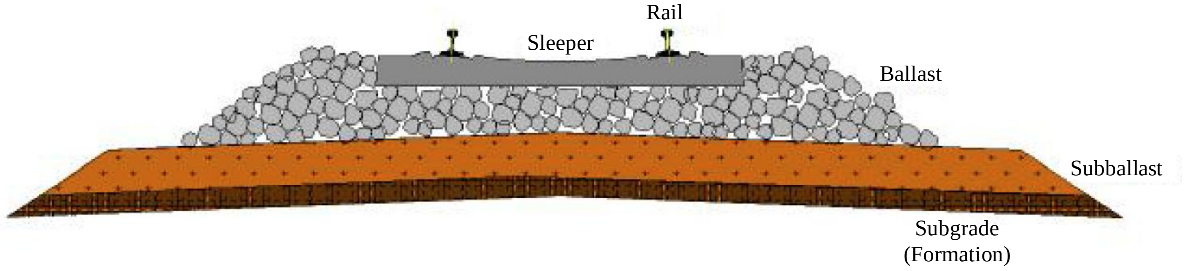

Figure 2.2: Typical Ballasted Track System, from Tzanakakis (2013)

2.3.1 Rails

Rails are the longitudinal steel members that directly guide the train wheels evenly and continuously. They must have sufficient stiffness to serve as beams that transfer the concentrated wheel loads to the spaced sleeper supports without excessive deflection between supports.

2.3.2 Fasteners

Fasteners are typically required to retain the rails on the sleepers, to maintain the track gauge and to resist vertical, lateral, longitudinal and overturning movements of the rails. Causing these movements are forces from the wheels and from temperature change in the rails.

A fastener must meet the following criteria:

- The longitudinal resistance of the fastener must be greater than that of the longitudinal resistance between the sleeper and the ballast.
- There must exist a safety factor for the longitudinal resistance, able to cover the longitudinally unequal distribution of clamping forces, dynamic phenomena, etc.
- In case of rail rupture, the resulting gap should remain small.

2.3.3 Rail Pads

Rail pads are required between the rail seat and the sleeper surface to fulfil various functions. From a track dynamics point of view the rail pads play an important role. They influence the overall track stiffness:

- When the track is loaded by the train, a soft rail pad permits a larger deflection of the rails and the axle load from the train is distributed over more sleepers.
- Soft rail pads isolate high-frequency vibrations. They suppress the transmission of high frequency vibrations down to the sleepers and further down into the ballast.

Modern rail pads, taking into account today's environment where the axle loads and speeds are being increased, shall:

1. Reduce vibration and impact transmission from the rail to the sleeper by providing resilience and impact attenuation.
2. Give adequate resistance to longitudinal and rotational movement of the rail.
3. Ensure long life (minimum 10 years).
4. Ensure that the rail pad properties are stable over a wide range of operating temperatures during life.
5. Not deform, abrade or move out of the fastening system under dynamic loads.
6. Not be adversely affected by ozone, ultraviolet light, oils and related chemicals.
7. Reduce the possibility of rail foot corrosion and concrete sleeper erosion.
8. Provide more resistance to longitudinal rail movement due to creep or thermal expansion.
9. Provide electrical resistance between the rail and the sleeper.
10. Provide a conforming layer between the rail and the sleeper to avoid contact areas of high pressure.

© University of Pretoria

2.3.4 Sleepers

Sleepers are essentially beams that span across and tie together the two rails.

The sleepers (among others):

- Receive the load from the rail and distribute it over the supporting ballast at an acceptable ballast pressure level.
- Hold the fastening system to maintain proper track gauge.
- Restrain lateral, longitudinal and vertical rail movements by the anchorage of the superstructure in the ballast.
- Provide a cant to the rails to help develop proper wheel/rail contact by matching the inclination of the conical wheel shape.

2.3.5 Ballast

Ballast is the layer of crushed stone on which the sleepers rest.

The ballast (among others):

- Distributes load from the sleepers uniformly over the subgrade assisting in track stability.
- Assists in absorbing shock from dynamic loads by having only a limited spring like action (due to the rough interlocking particles).
- Anchors the track in place against lateral, vertical and longitudinal movement by way of irregular shaped ballast particles that interlock with each other.
- Easily drains any moisture introduced into the system through the ballast away from the rails and sleepers.
- Assists in track maintenance operations due to its easy manipulation.

© University of Pretoria

2.3.6 Subballast

Subballast is material chosen as a transition layer between the upper layer of large particle, good quality ballast and the lower layer of fine-graded subgrade.

Subballast (among others):

- Assists in reducing the stress at the bottom of the ballast layer to a tolerable level for the top of the subgrade.
- Can prevent the inter-penetration of the subgrade and ballast, thereby reducing migration of fine material into the ballast which affects drainage.
- Acts as a surface to shed water away from the subgrade into drainage along the side of the track.

The usual thickness of the gravel subballast layer is 15 cm. However, some railways do not use a subballast layer and they simply use a greater thickness of the subgrade (formation) layer.

2.3.7 Subgrade (or Formation)

Sometimes an extra layer (a formation layer), is put on the earth so as to give the correct profile to receive the foundation of the track bed. The subgrade, or formation, is usually a surface of earth or rock levelled off to receive the track bed (subballast and ballast layers).

Subgrade (among others):

- Offers the final support to the track structure.
- Bears and distributes the resultant load from the train vehicle through the track structure.
- Facilitates drainage and provides a smooth platform, at an established grade, for the track structure to rest upon.

© University of Pretoria

2.4 TRACK GEOMETRY AND TERMINOLOGY

Descriptions and figures of track geometry are taken from the book "Track Geotechnology and Substructure Management" (Selig & Waters, 1994), unless stated otherwise.

Track geometry is the projection that each rail occupies in space. Track geometry is important as it controls the behaviour of the vehicles on the track. The primary track geometry parameters that can be measured in the horizontal, longitudinal vertical, transverse vertical and track planes are as follows:

- Gauge (Track plane - a plane located 15 mm below the top of both rails along the centre line)
- Superelevation (also known as Cant, Transverse vertical plane)
- Twist (A parameter calculated from the cant measurements in the transverse vertical plane)
- Alignment (Horizontal plane)
- Profile (Longitudinal vertical plane)

2.4.1 Track Gauge

Gauge is the distance measured normal to the track axis between the inside of the rail heads 15 mm below the top of the rail surface (Figure 2.3).

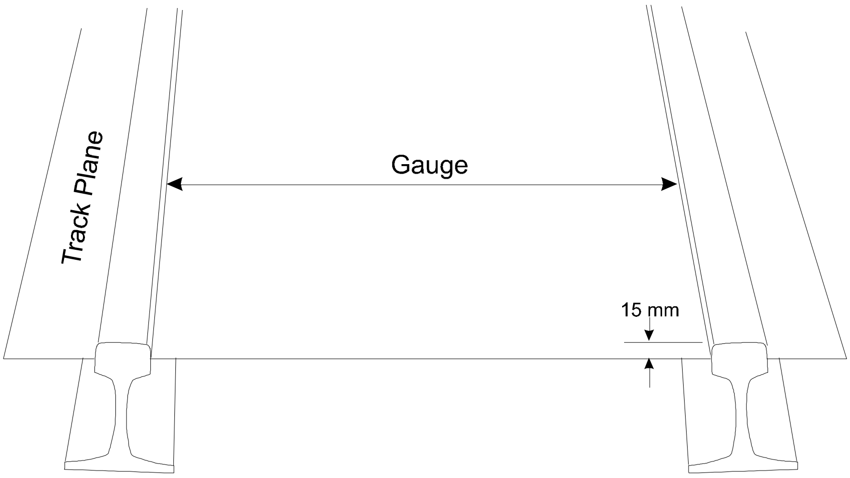

Figure 2.3: Track Plane, from University of Pretoria (2010)

2.4.2 Superelevation (or Cant)

Superelevation is the difference in elevation between a point on one rail and elevation of a point on the other rail measured along a line perpendicular to the track centre line as indicated in Figure 2.4.

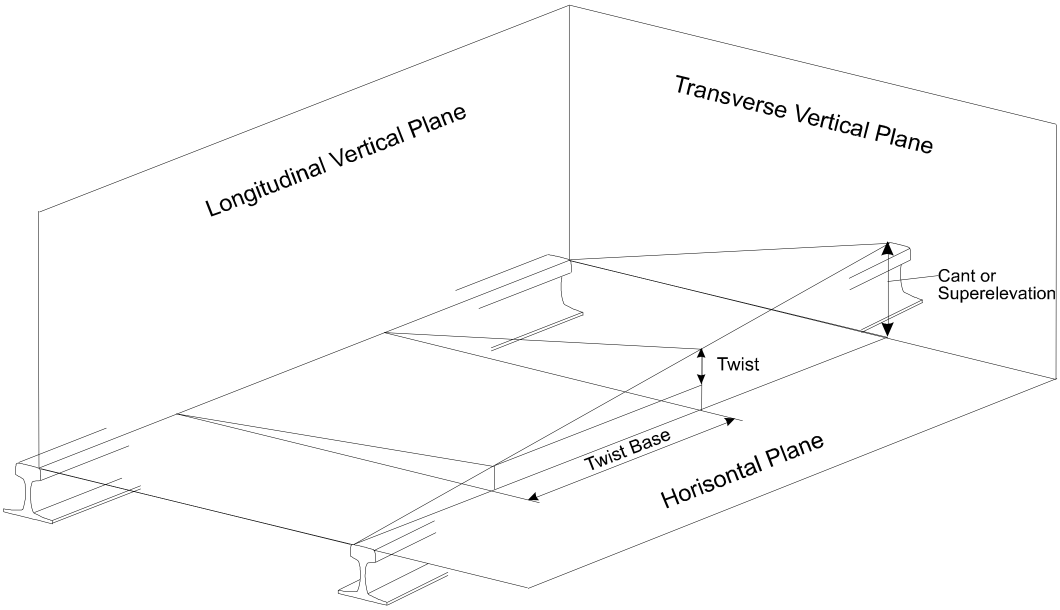

Figure 2.4: Superelevation and Twist in the Transverse Vertical Plane, from University of Pretoria (2010)

In Figure 2.5 cant is denoted by h, while the cant angle is denoted by θ. 2a is known as the effective gauge and is 1500 mm for standard gauge track.

© University of Pretoria

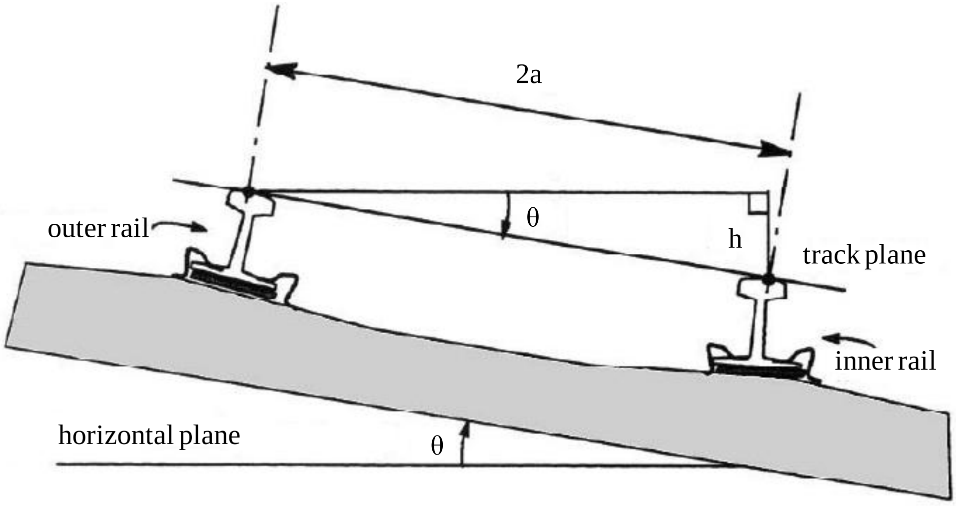

Figure 2.5: Illustration of Cant, from Lindahl (2001)

A detailed cant discussion is given in Section 2.6, but it is worth noting here that the maximum value of cant that is used, is determined by considering the possibility of trains having to come to a standstill in a curve and/or slowly running trains. A maximum value is therefore set for cant because of the following problems which arise if a train is forced to stop or run slowly in a curve (Lindahl, 2001):

- Passenger discomfort.
- Possible derailment due to cant excess. Cant excess leads to high lateral forces and low vertical forces on the outer wheel at low speeds, the combined effect of which can lead to derailment.
- Possible displacement of wagon load.

2.4.3 Twist

Twist is the variation in cant over a given distance along the length of the track as indicated in Figure 2.4. The distance between the two points is referred to as the twist base.

2.4.4 Curve Radius

The horizontal radius of a curve can be calculated using the mid-cord ordinate method. The offsets from the middle of a cord are measured throughout the curve. Using the Pythagorean

© University of Pretoria

formula the average offset is then used to calculate the curve radius, as shown in Figure 2.6 and Equation 2-1 below.

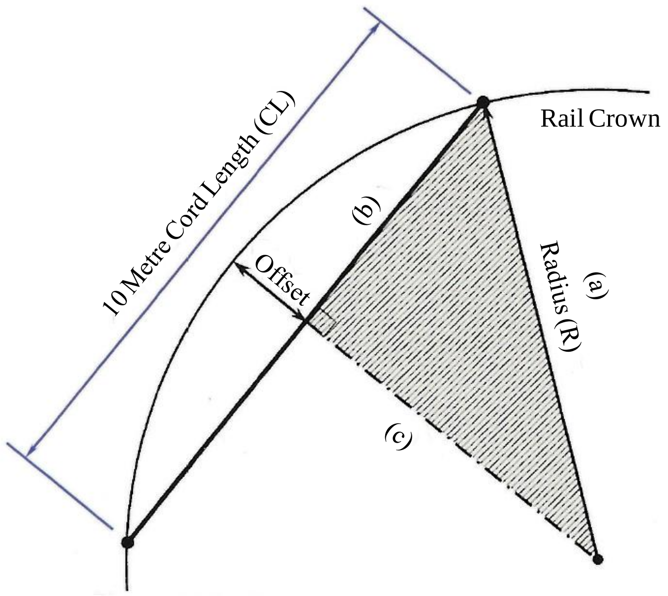

Figure 2.6: Calculating the Curve Radius, from Zaayman (2013)

$$\boldsymbol{Curve\ Radius\ (R) = \frac{CL \times CL \times 125}{Offset}}$$ **Equation 2-1**

Where: CL = Cord length in metres (10 metres)

R = Radius of curve (m)

2.5 TRACK FORCES

Descriptions of track forces are taken from the book "Track Geotechnology and Substructure Management" (Selig & Waters, 1994), unless stated otherwise.

Understanding the type and magnitude of forces that the track structure must support is basic to track design. Forces imposed on the track can be either mechanical (static and dynamic) or thermal in nature. The track structure must restrain repeated vertical, lateral and longitudinal forces resulting from traffic and changing temperature.

The dynamic interactions between rail vehicle wheels and the rails are a function of track, vehicle, and train characteristics, operating conditions, and environmental conditions. Forces

© University of Pretoria

applied to the track by moving rail vehicles are a combination of a static load and a dynamic component superimposed on the static load.

High frequency vibrations also result from dynamic loading. Vibrations can affect track superstructure and substructure component performance significantly, particularly at high speeds.

Temperature changes induce thermal stresses in the rail which cause expansion or contraction of the steel. Any restraint to the change in length, as in continuous welded rail, will set up internal stresses generally represented by a force acting in a longitudinal direction in the rail. Without sufficient resistance, track buckling can occur in a vertical or lateral direction due to the longitudinal compression forces in the rails, or rail breaks can occur from tension forces.

The vertical, lateral and longitudinal force components discussed above are shown in Figure 2.7 below.

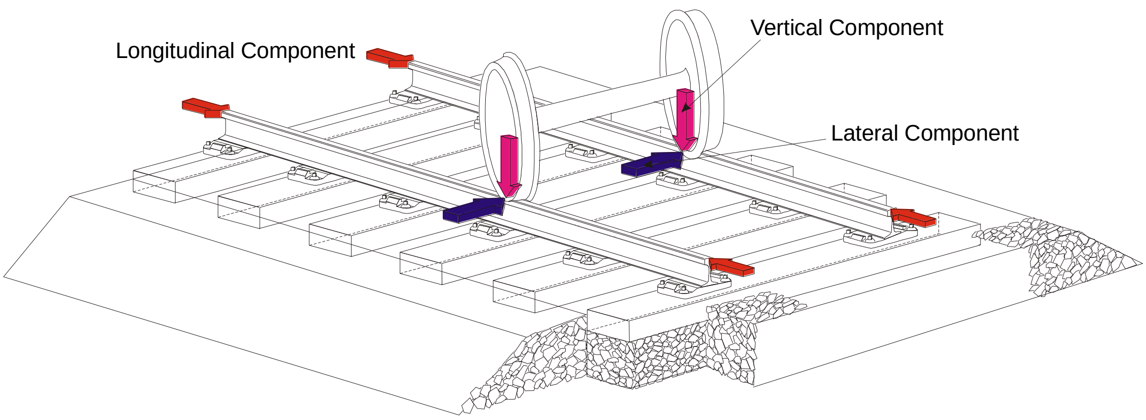

Figure 2.7: Track Forces, from University of Pretoria (2010)

2.5.1 Vertical Forces

Vertical forces are considered those that are perpendicular to the plane of the rails. As such, the actual direction is a function of the track cant. In the vertical plane the track superstructure acts as a beam supported on an elastic substructure (see Section 2.3 for a description of what makes up the superstructure and substructure). This "beam" distributes the high vertical load into the track structure. Figure 2.8 indicates the load distribution characteristics of the track structure (University of Pretoria, 2010).

© University of Pretoria

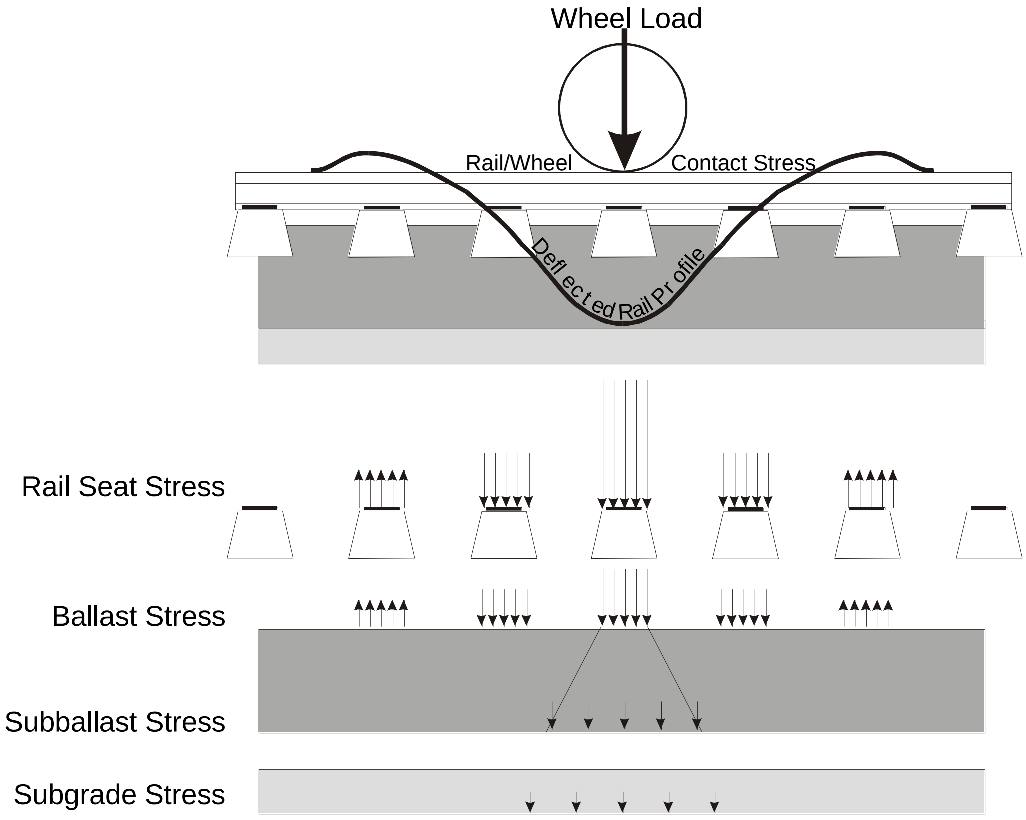

Figure 2.8: Vertical Load Distribution, from University of Pretoria (2010)

2.5.2 Lateral Forces

Lateral forces considered those that are parallel to the long axis of the sleepers. Lateral forces originate from two principle sources:

1) Lateral wheel forces, and
2) Buckling reaction forces.

The lateral wheel forces come from the lateral component of the friction force between the wheel and the rail, and from the lateral forces applied by the wheel flange against the rail. Sources of lateral wheel forces are train reactions to geometry deviations, self-excited hunting motions which result from bogie instability at high speeds, and centrifugal forces in curves. Lateral wheel forces are very complex and much harder to predict than vertical forces.

Lateral forces acting on the rail tend to shift the track horizontally, as shown in Figure 2.9 below. This tendency is resisted by the lateral stiffness of the sleepers and rail, as well as the ballast in the shoulder (edge of the sleeper on either side of the track) and the resistance on the side and bottom of the sleepers in the ballast bed.

© University of Pretoria

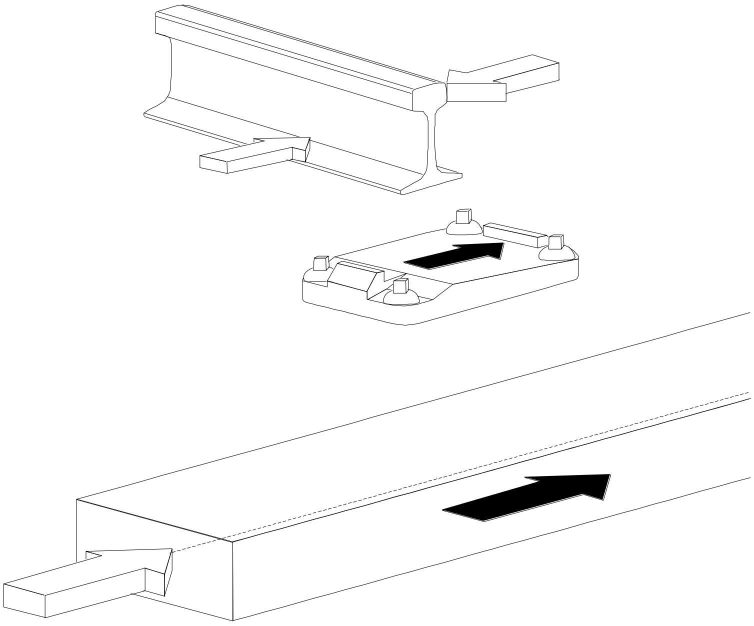

Figure 2.9: Lateral Load Absorption, from University of Pretoria (2010)

2.5.3 The Effect of Speed on Track Forces

The two main factors influencing track forces are the weight and the speed of the train. The higher the weight and speed of the train the higher the track forces. Assuming that the weights of trains are fixed according to rolling stock type, passenger/freight capacity etc., speed becomes the primary variable factor that has the greatest effect on track forces.

As train speeds increase the dynamic loading effect of the train wheels increases according to a dynamic wheel load factor applicable to the operating conditions in question. For this reason design wheel loads are therefore higher than static wheel loads to account for this increase due to speed, and are determined by means of an applicable equation such as Equation 2-2 shown below:

$$p_d = \chi . p_s$$ **Equation 2-2**

Where:

p_d = dynamic wheel load

X = dynamic wheel load factor

p_s = static wheel load

© University of Pretoria

The dynamic wheel load factor is typically developed empirically using field data and is expressed in terms of train speed. Historically, there have been many efforts undertaken to quantify the increase of load expected at the wheel/rail interface due to speed, with the most comprehensive dynamic factors having been developed by the Office of Research and Experiments (ORE) of the International Union of Railways (UIC), which incorporates factors such as track geometry, vehicle suspension, vehicle speed, vehicle centre of gravity, age of track, curve radius, superelevation, and cant deficiency (Van Dyk, et al., 2013).

2.6 CANT DISCUSSION

The definition of cant (also known as superelevation) is given in Section 2.4.2. Descriptions, figures and the derivations of the various formulae used in this discussion of cant are taken from Lindahl (2001) and Esveld (2001).

Cant is the term used to denote the raising of the outer rail on curved track to allow higher speeds than if the two rails were level. Cant compensates for the centrifugal force arising from a train traversing a curve. If a track was canted to the level required for the maximum speed of the fastest train, the level of tilt would be too high for a slower train. A compromise degree of cant is therefore used, known as ‘cant deficiency’. However, inappropriate matching of cant to vehicle speed can adversely influence the curving performance of the vehicle and, in turn, the wear and stresses in the rail and the wheel (Harris, et al., 2001).

From a curving point of view, a stationary train in a curve with cant, will be experiencing overbalance in the form of an excess of cant, at which point the train will be experiencing negative lateral accelerations, and given a situation with sufficient cant excess the stationary train may rollover to the inside of the curve.

As the train’s speed increases from stationary, this overbalance situation (cant excess) will reduce up until the speed where a balance is achieved, at which point the train will be experiencing zero lateral accelerations.

Train speeds beyond the balance speed will result in the train experiencing underbalance in the form of a deficiency of cant, at which point the train will be experiencing positive lateral accelerations, and given a situation with sufficient cant deficiency the train may derail due to rail roll over, the car rolling over or simply derailing to the outside of the curve.

© University of Pretoria

2.6.1 Track Plane Acceleration

Quasi-static curving can be defined as curving during which a train travels at a constant speed (v) through a curve with perfect track geometry, including a constant radius (R) and constant cant (h). In the case of quasi-static curving the vehicle is exposed to two accelerations: horizontal centrifugal acceleration ($\frac{v^2}{R}$) and gravitational acceleration (g) (see Figure 2.10 (a)). The resultant of the acceleration vector can be split into two components, namely a_y which is parallel to the track plane and a_z which is perpendicular to the track plane (see Figure 2.10 (b)) (Lindahl, 2001).

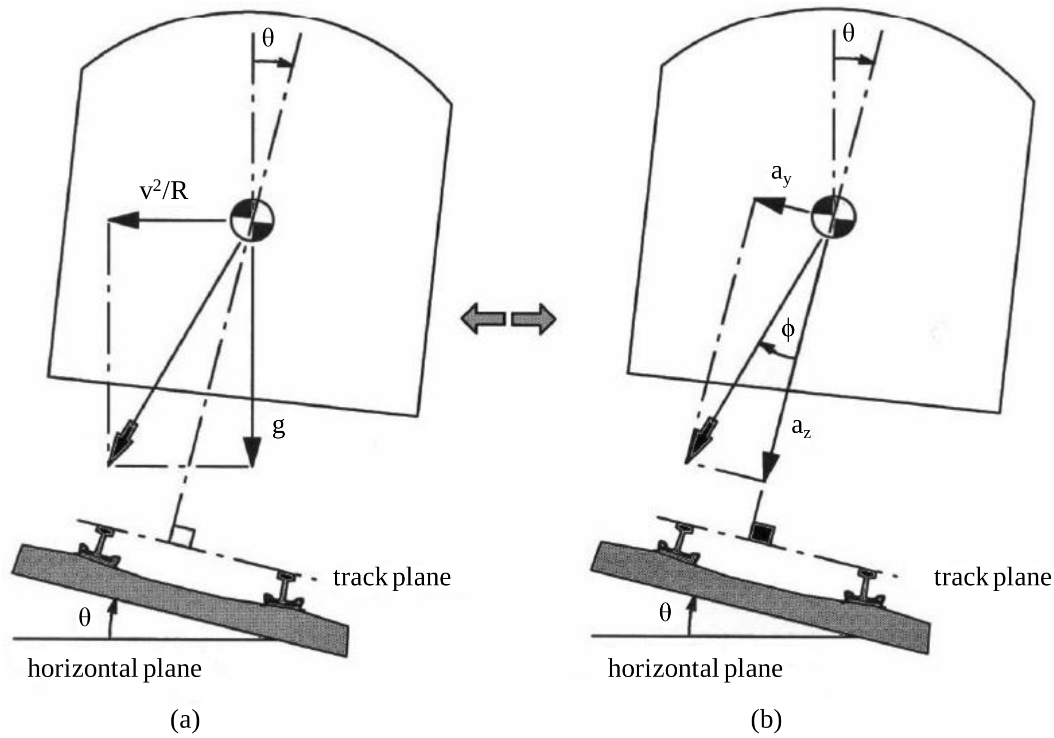

Figure 2.10: Definition of Track Plane Acceleration & Lateral Force Angle, from Lindahl (2001)

For the derivations of Equation 2-3 to Equation 2-6 it is assumed that θ is a small angle ($\theta \leq 0.15$ rad). (Lindahl, 2001) For standard gauge track, θ will be less than 0.15 rad for all cant values of 224 mm or less.

From Figure 2.10 (b) the acceleration a_y is known as the lateral acceleration on the vehicle, while the acceleration a_z is known as the vertical acceleration on the vehicle.

For non compensated acceleration, as is the case for rigid vehicles, the equations for a_y and a_z are as follows (Lauriks, et al., 2003):

$$a_y \approx \frac{v^2}{R} - g.\frac{h}{2a}$$ **Equation 2-3**

$$a_z \approx \frac{v^2}{R}.\frac{h}{2a} + g$$ **Equation 2-4**

For compensated acceleration, through for example the ability of a train to tilt during curving, the equations for a_y and a_z are as follows (Lauriks, et al., 2003):

$$a_y \approx \frac{v^2}{R}$$ **Equation 2-5**

$$a_z \approx g$$ **Equation 2-6**

The above equations can be used in determining the forces experienced during curving by means of the rudimentary physics equation of force being equal to mass times acceleration.

2.6.2 Equilibrium Cant, Balance Speed and Curving Forces

The balance speed is the speed at which the compensation due to cant (or superelevation) balances the acceleration due to curving. Relative to the track plane, the perceived lateral acceleration is then zero.

The cant which gives $a_y = 0$ at a given radius (R) and given vehicle speed (v) is called the equilibrium cant (h_{eq}) and is calculated by the following equation:

$$h_{eq} = \frac{2a.v^2}{g.R}$$ **Equation 2-7**

The equilibrium speed or balance speed (v_{eq}) is the vehicle speed at which $a_y = 0$ at a given radius (R) and a given cant (h) and is calculated by the following equation:

$$v_{eq} = \sqrt{\frac{R.g.h}{2a}}$$ **Equation 2-8**

© University of Pretoria

Further equations that can be derived from first principles include the following:

$$R_{LL} = \frac{\left(M * g * \frac{h}{2a} * H\right) + \left(M * g * \frac{\sqrt{(2a^2 - h^2)}}{2a} * a\right) + \left(U * \frac{h}{2a} * a\right) - \left(U * \frac{\sqrt{(2a^2 - h^2)}}{2a} * H\right)}{2a}$$

Equation 2-9

$$R_{HL} = \frac{\left(-M * g * \frac{h}{2a} * H\right) + \left(M * g * \frac{\sqrt{(2a^2 - h^2)}}{2a} * a\right) + \left(U * \frac{h}{2a} * a\right) + \left(U * \frac{\sqrt{(2a^2 - h^2)}}{2a} * H\right)}{2a}$$

Equation 2-10

$$U = M * \frac{v^2}{R}$$ **Equation 2-11**

$$F = \left(U * \frac{\sqrt{(2a^2 - h^2)}}{2a}\right) - \left(M * g * \frac{h}{2a}\right)$$ **Equation 2-12**

Where:

R_{LL} = Vertical reaction force of low leg rail

R_{HL} = Vertical reaction force of high leg rail

M = Total mass of vehicle

H = Resultant height of vehicle’s centre of gravity above the rail

U = Resultant centrifugal force on vehicle

F = Lateral reaction force on outside of raised wheel

© University of Pretoria

2.6.3 Cant Deficiency and Cant Excess

For several reasons, fully compensated track plane acceleration cannot be achieved in all cases and some of these reasons have been discussed earlier in Section 2.4.2. The primary reason is due to the possibility that a train may come to a standstill in a curve and/or run slowly.

Operating systems that run various different traffic types over their network would also mention that not all trains travel at the same speed. For the GRRL system however only one type of rolling stock is used (the Bombardier Electrostar) and all trains are scheduled to run at the same speed through each section as every other train. Nonetheless, the possibility that a train may come to a standstill in a curve and/or run slowly due to mechanical problems, signalling problems, human error etc. will always be present in all train networks.

The maximum cant has to therefore be limited. It is thus desirable to allow a cant deficiency, i.e. a certain amount of uncompensated lateral acceleration (a_y) remains in the track plane.

At speeds under the balance speed, the lateral acceleration term is less than the superelevation term. This is termed cant excess, meaning the track has excessive cant for the present speed. With cant excess, perceived accelerations are to the inside of the curve.

At speeds over the balance speed, the lateral acceleration term is greater than the superelevation term. This is termed cant deficiency, meaning the track has insufficient cant for the present speed. With cant deficiency, perceived accelerations are to the outside of the curve.

Cant excess and cant deficiency can therefore be mathematically represented by means of the following expressions:

Cant Excess (h_e): $\frac{v^2}{R} < g.\frac{h}{2a}$

Cant Deficiency (h_d): $\frac{v^2}{R} > g.\frac{h}{2a}$

The left hand term in each expression is the lateral acceleration. This is given by the square of the speed (v), divided by the curve radius (R). The compensating effect of superelevation is the right hand term. This is the acceleration of gravity (g) (roughly 9.81 m/s^2) times the superelevation (h), divided by the distance between rail centres (2a) (roughly 1500 mm for standard gauge track).

© University of Pretoria

Cant Excess (h_e) is the difference between the actual cant (h) and equilibrium cant (h_{eq}) and is thus determined by the following equation:

$$h_e = h - h_{eq}$$ **Equation 2-13**

Cant Deficiency (h_d) is the difference between equilibrium cant (h_{eq}) and actual cant (h) and is thus determined by the following equation:

$$h_d = h_{eq} - h$$ **Equation 2-14**

2.7 THE WHEEL/RAIL INTERFACE

Tribology, the science and technology of friction, wear, and lubrication, is an interdisciplinary subject. It can therefore be addressed from several different viewpoints. This literature review focuses on the friction, wear, and lubrication of the tiny contact zone (roughly 1 cm^2), where the steel wheel meets the steel rail. The wheel/rail contact is an open system, which is exposed to dirt and particles and natural lubrication, such as high humidity, rain and leaves, all of which can seriously affect the contact conditions and the forces transmitted through the contact (Olofsson & Lewis, 2006).

The contact patch is small, with correspondingly high-contact stresses. Typically, contact is made over a quasi-elliptical contact patch the size of a small coin of half an inch (13 mm) diameter (see Figure 2.11). Approximating the quasi-elliptical contact patch to be equivalent to a small circular coin with a diameter of 13 mm, means that the contact area is approximately 1.33 cm^2 in size ($A = \pi r^2 = \pi * (0.65\text{ cm})^2 = 1.33\text{ cm}^2$) (Harris, et al., 2001).

© University of Pretoria

Figure 2.11: Contact Between Wheel and Rail: Wheel Centrally Placed on the Track, from Harris, et al. (2001)

2.7.1 Wheel/Rail Interface Research and Development

It is no longer adequate to change one part of the railway system without examining its impact on the other parts of the system. Increasing car weight can have a profound effect on the track and bridges. Changing rail properties can lead to unexpected wheel behaviour. It is therefore of critical importance to deal with the wheel/rail interface as a system. A systems approach to the design and maintenance of the wheel and rail interface can be expected to result in the minimisation of rail gauge face and wheel flange wear, the avoidance of detrimental wheel and rail defects, stable vehicle performance, including safety issues, and the minimisation of noise generation (Harris, et al., 2001).

“An important aspect of a part’s performance is how it interacts with other parts to affect the performance of the whole.” Russel Ackof.

A scheme for the systematic approach to wheel/rail interface research and development is shown in Figure 2.12 which emphasises the consideration of all aspects including wheel/rail materials, wheelset dynamics, contact mechanics and friction management. Nothing can really be treated in isolation (Iwnicki, 2006).

© University of Pretoria

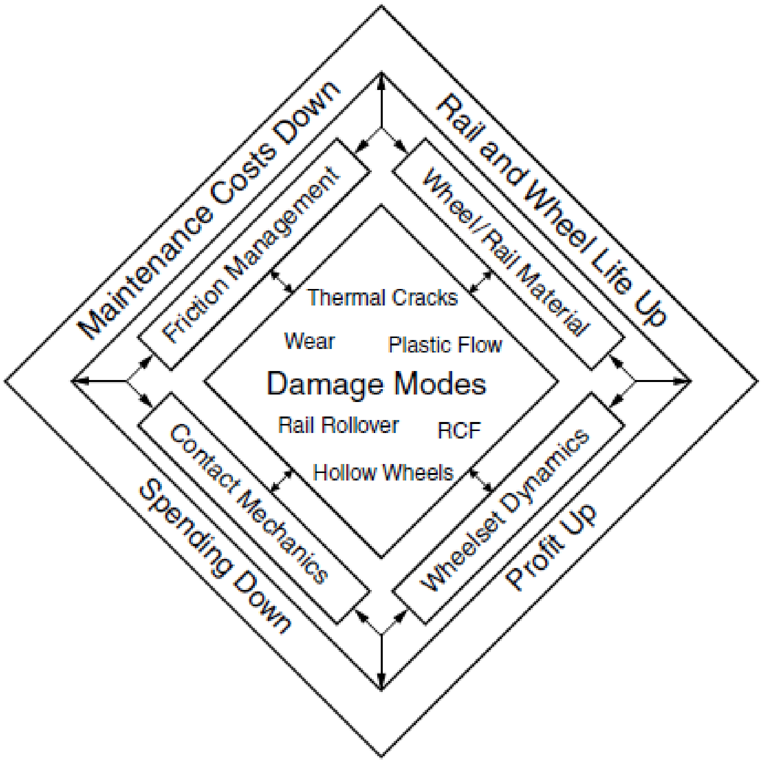

Figure 2.12: Systems Approach to Wheel/Rail Interface Research and Development, from Kalousek & Magel (1997)

While many railway engineers are exploring the benefits of the latest lubrication technologies, bogie types and metallurgies, the wheel/rail contact mechanics are often overlooked or poorly controlled. The geometry of the wheel/rail contact permeates every facet of the wheel/rail interaction, having profound effects on wear, fatigue, corrugation, stability and derailment potential (Magel & Kalousek, 2002). In approaching the wheel/rail interface from a systems point of view it must be realised that everything plays a role, including lubrication technologies, bogie types and metallurgies, but in tandem with wheel/rail contact mechanics and the whole array of the wheel/rail system parameters.

2.7.2 Railway Wheelset and Track

Track infrastructure and geometry are discussed in detail in Section 2.3 and Section 2.4. Some basic concepts from these sections will however be retouched upon in this section.

© University of Pretoria

Figure 2.13 shows a typical railway wheelset comprised of two wheels that are fixed rigidly to a common axle, with the rolling surfaces of the wheels (wheel treads), having been cut to a cone angle, γ (Roney, et al., 2015).

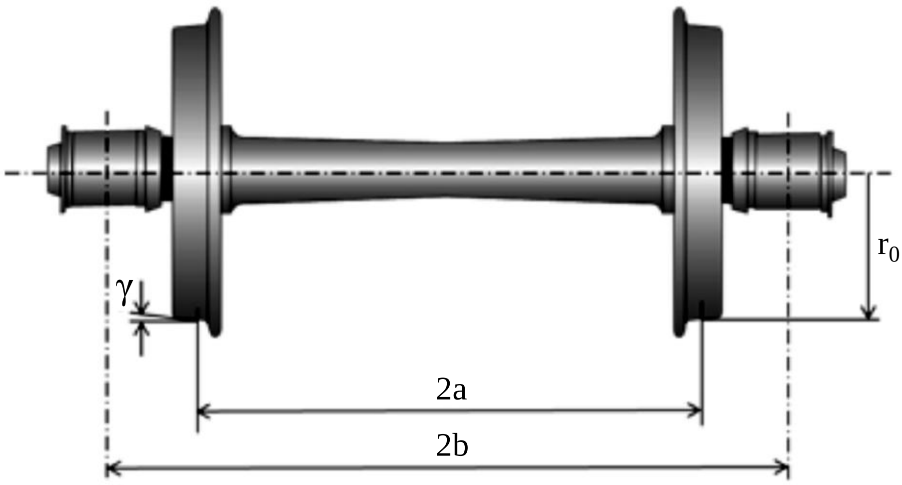

Figure 2.13: The Railway Wheelset, from Roney, et al. (2015)

Figure 2.14 shows a track comprising of two rails laid on sleepers at an angle, β, to the sleeper to generally match the angle, γ, of the wheelset profile. This centralizes contact on the centre of the head of the rail on tangent track and assists in stabilizing the rail against rollover as the normal reaction to the contact of the wheel generally passes through the base of the rail (Roney, et al., 2015).

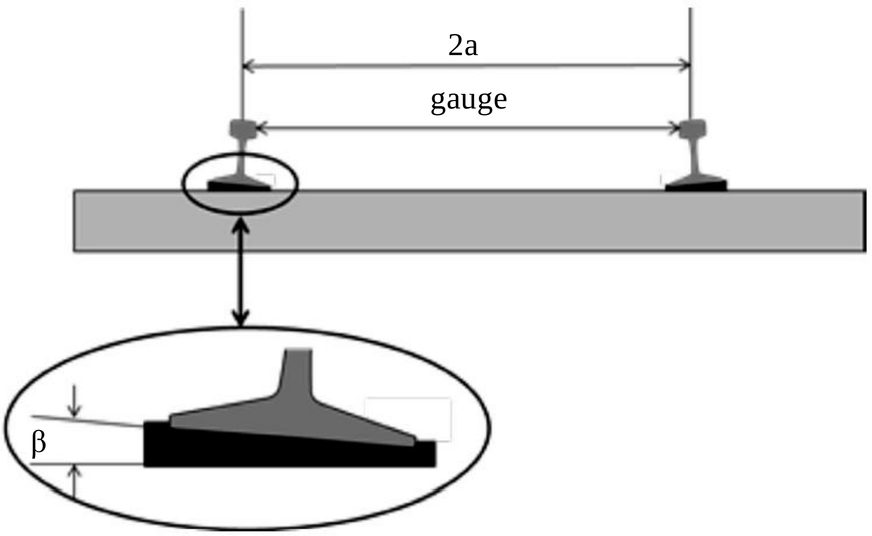

Figure 2.14: Cross Section of the Railway Track, from Roney, et al. (2015)

© University of Pretoria

Self-guidance of a wheelset is facilitated by the geometry of the wheelset, which is mathematically described as being a di-cone (two cones placed back to back having a cone angle, 2γ). Figure 2.15 shows the self-centering self-guidance ability of a wheelset on tangent track, while Figure 2.16 shows the ability of a self-guiding wheelset to negotiate a curve (Roney, et al., 2015).

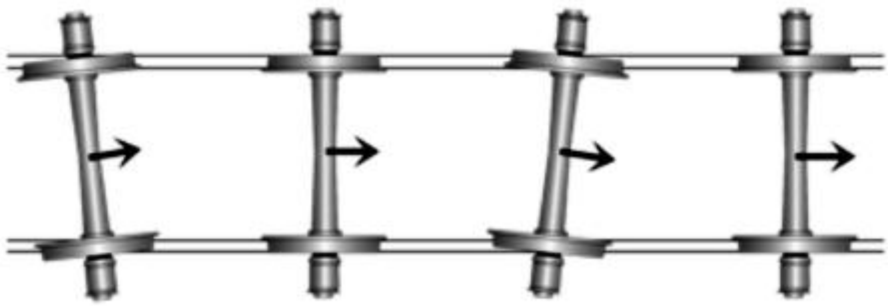

Figure 2.15: Self-Centering Motion on Tangent Track, from Roney, et al. (2015)

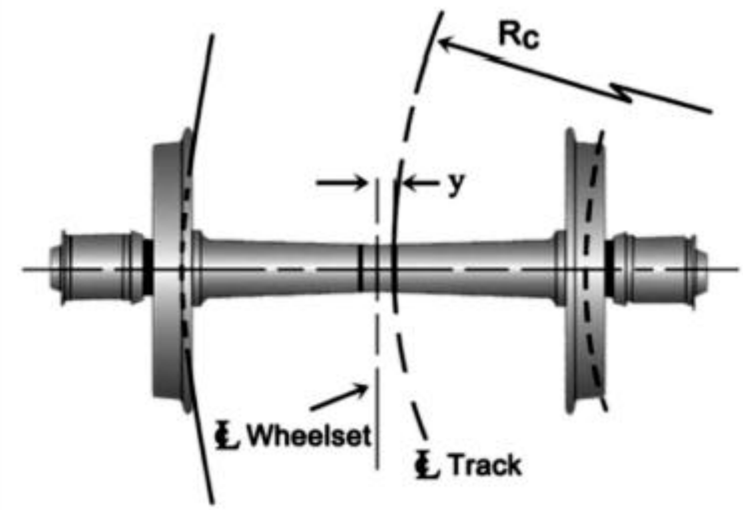

Figure 2.16: The Generation of a Radius Differential in a Curve, from Roney, et al. (2015)

© University of Pretoria

2.7.3 Rolling Radius Difference

The difference between the rolling radii on a wheelset is known as the “rolling radius difference” and is an important parameter in analyzing the behaviour of the railway wheelset. The rolling radius difference is the difference between the radii of the wheel/rail contact points on the wheel running on the low versus the high rail (Roney, et al., 2015).

As shown in Figure 2.17 the rolling radius difference (Δr) is defined as follows:

$$\Delta r = \gamma y$$ **Equation 2-15**

Where:

y = Lateral displacement of the wheelset from the centre position of the track

γ = Conicity of the wheel tread

A wheelset with coned wheels in a curve can maintain a pure rolling motion if it moves outward and adopts a radial position. Redtenbacher provided the first theoretical analysis of this concept in 1855. Figure 2.17 and Equation 2-16 illustrates Redtenbacher’s analysis. From the geometry in Figure 2.17 it can be seen that there is a simple geometric relationship between the lateral movement (y) of the wheelset in a curve, the radius (R) of the curve, the wheel radius (r_0), the lateral distance between the points of contact of the wheels with the rails (2a) and the conicity (γ) of the wheels in order to sustain pure rolling. In practice a wheelset can only roll round moderate curves without flange contact, and a more realistic consideration of curving requires the analysis of the forces acting between the vehicle and the track (Wickens, 2003).

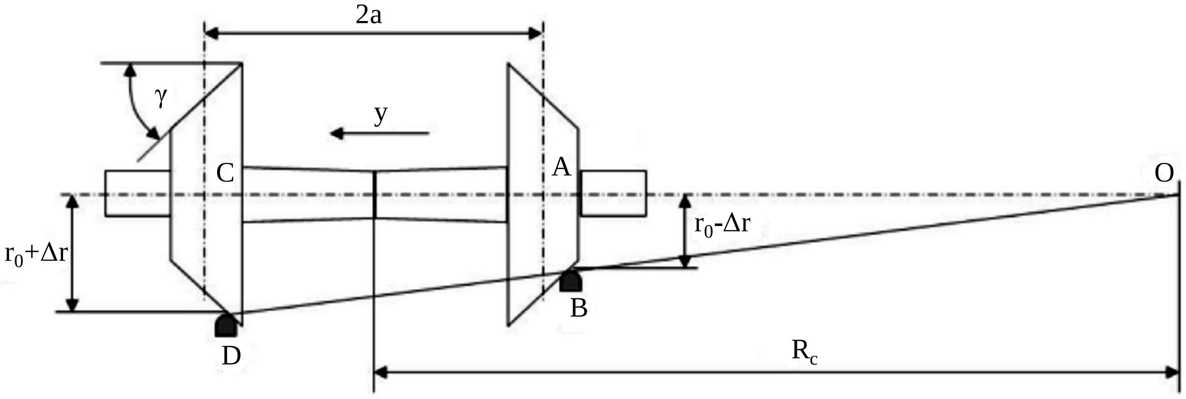

Figure 2.17: Rolling of a Coned Wheelset on a Curve, from Roney, et al. (2015)

© University of Pretoria

$$OAB = OCD$$

$$\frac{(r_0 - \gamma y)}{(R_c - a)} = \frac{(r_0 + \gamma y)}{(R_c + a)}$$

$$y = \frac{r_0 a}{R\gamma}$$ **Equation 2-16**

2.7.4 Conicity

For wheelsets with conical wheels, the conicity is derived from the mean slope of the rolling radius versus lateral wheelset displacement and from Equation 2-15 is defined as:

$$\gamma = \frac{\Delta r}{y}$$ **Equation 2-17**

Figure 2.18 shows an example of circular wheel/rail contact geometry which results in a so-called “equivalent conicity”. Equivalent conicity (γ_e) in terms of profile radii is defined as follows:

$$\gamma_e = \frac{R_W \delta}{R_W - R_R}$$ **Equation 2-18**

Where:

δ = Angle between the plane of contact and track level

R_W = Wheel profile radius

R_R = Rail profile radius

When R_W is set to infinity and R_R is small (a typical rail profile), Equation 2-18 becomes:

$$\gamma_e = \delta = Angle\ of\ the\ wheel\ profile$$ **Equation 2-19**

© University of Pretoria

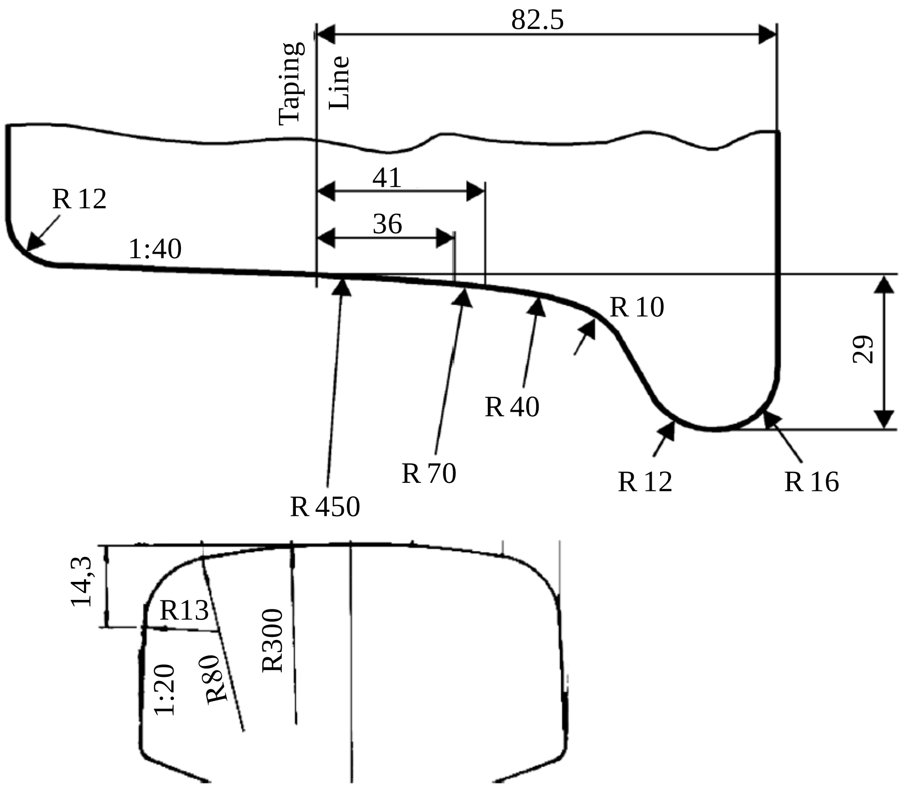

Figure 2.18: Profiled Wheel and Rail, from Roney, et al. (2015)

2.7.5 Creepage

Creepage is the partial sliding motion that takes place in the wheel/rail contact patch resulting in relative slip. Creepages occur in the lateral and longitudinal directions, as well as rotational creep around the normal axis that is known as spin creep.

2.7.6 Wheel and Rail Profiles

The selection of the cross sectional profile for the wheel of railway vehicles is a typical engineering compromise and has challenged railway engineers since the early 1800s (Iwnicki, 2009). Figure 2.19 and Figure 2.20 show examples of typical wheel and rail profiles, including the typical terminology used for the different sections of the wheel and the rail.

© University of Pretoria

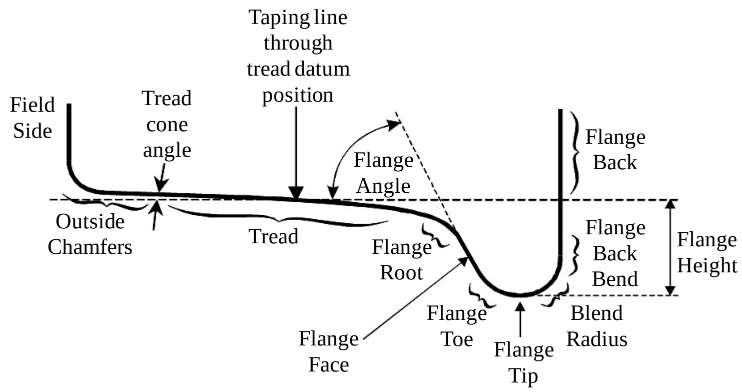

Figure 2.19: Typical Wheel Profile, from Roney, et al. (2015)

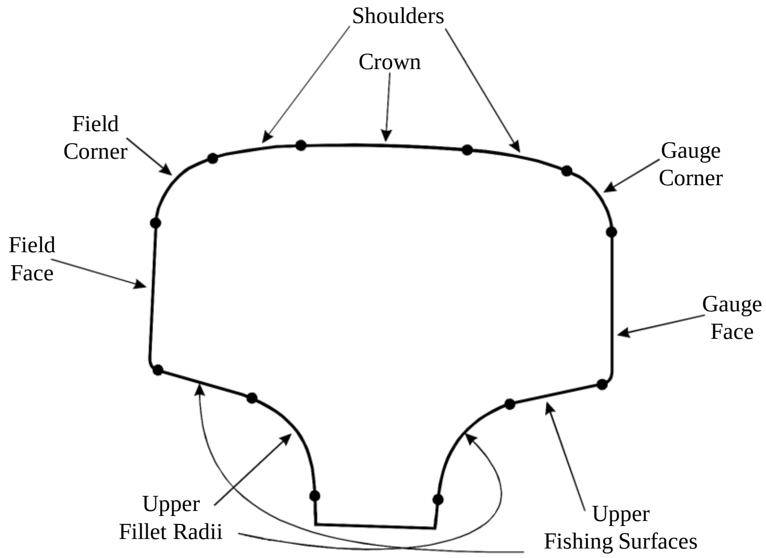

Figure 2.20: Typical Rail Profile, from Roney, et al. (2015)

As very well stated by Iwnicki (2009), the early railway pioneers understood that a conical wheel profile would give better vehicle performance but could also lead to unstable behaviour when running at speed. A high level of conicity will allow good curving behaviour even in the tightest curve without flange contact. This could, however, lead to a relatively low critical speed and possibly dangerous hunting instability. A low level of conicity on the other hand will allow very high speed stable operation but the flangeway clearance will quickly be used up in curves, resulting in flange contact and possible flange climb derailment. Flange angle and root radius are also variables that can have a significant effect on the possibility of derailment. In practice most modern wheel profiles are a more complex shape and often based on an observed worn profile in an attempt to increase the intervals between re-profiling. This

© University of Pretoria

increased complexity makes the problem of profile selection to ensure smooth and safe running even more difficult.

In addition to the vehicle behaviour, engineers must consider the stresses on the wheel and on the rail. These have a major influence on the development of rolling contact fatigue which can have expensive and sometimes dangerous consequences. Rail profiles for main line operation have also historically been developed according to fairly simple ‘rules of thumb’ with a large radius at the rail head where contact with the tread of the wheel normally occurs and a smaller radius at the corner of the rail head where contact with the flange occurs. In practice this pattern has been fairly stable as changes to the wheel profile have been easier to make. But changes to either radii can have a big effect on stress levels in the contact patch and also on the likelihood of two point contact occurring.

As discussed in Section 2.7.1 wheel and rail profiles are two integral parts of the wheel/rail system and can therefore not be dealt with in isolation. In applying a systems approach to the optimisation of wheel/rail performance regular re-profiling of the rails to shapes that conform to the worn wheel to reduce high stress contact and the avoidance of wheel tread hollowing through re-profiling is of utmost importance. As part of profile management it is assumed that an average stable profile exists which is formed on all wheels and rails if the wheels and rails are not changed during operation. The goal of profile management is to achieve a tendency for the average profiles of the rails and wheels to be tending towards the optimal profiles for the system (Zakharov, et al., 2008).

On wheels, the most common problem is flange wear. To restore the thickness of the flange requires substantial metal removal from the wheel tread (Kalousek, 2002).

2.7.7 Contact Conditions

Control of the wheel/rail contact interface commences with control of the size and position of the contact patch on both the wheel and the rail together with the forces transmitted across this interface (Tournay, 2008). Figure 2.21 provides an indication of the various forces acting on a wheelset, where (Zeng & Wu, 2008):

P_L, P_R, F_S = Vertical and lateral suspension forces on wheelset;

P_1, P_2 = Left and right wheel/rail vertical forces;

Q_1, Q_2 = Left and right wheel/rail lateral forces;

© University of Pretoria

mg	=	Gravitational force of wheelset;
F_n, F_{cy}	=	Normal force and lateral creep force on the wheel/rail contact point;
δ_L, δ_R	=	Contact angles of left and right wheel contact point;
r_0, r_L, r_R	=	Wheel nominal rolling radius, left and right wheel contact radii;
2a, 2b	=	Lateral distances of wheel/rail nominal contact points and axle box suspension;
Δ_L, Δ_R	=	Distances of left and right wheel/rail contact points to their nominal points.

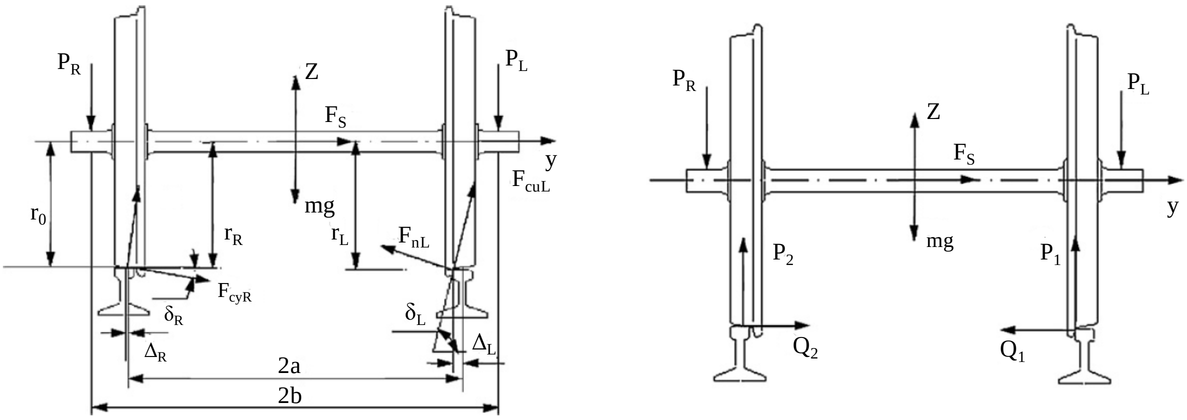

Figure 2.21: Wheel/Rail Interaction and Forces on Wheelset, from Zeng and Wu (2008)

From the multitude of forces and geometrical properties presented in Figure 2.21 it can be seen that contact mechanics can become quite involved which is why there is often a gulf that exists between practical engineers and the academic community. In some instances, the practical engineer may consider the researcher too remote from the commercial and regulatory pressures to which they are exposed, and equally distant from the need to make daily decisions using whatever incomplete information is available. Likewise, the researcher may consider statements and observations made by the practical engineer superfluous or even un-publishable because they lack the rigour of proper documentation and scientific proof (Kalousek, 2005).

Another situation that arises frequently in wheel/rail contact and makes solving the problem much more complex is the double point contact. At certain positions of the wheel on the rail two contact patches are produced simultaneously. Creepages and normal forces appear separately in each contact area. A typical double point contact scenario, when the rail vehicle is negotiating a tight curve is shown in Figure 2.22 when the wheelset is rotated at a large yaw angle and laterally displaced, one contact patch is created on the wheel thread and another on the wheel flange, and the flange contact is displaced from the vertical diametral section (Santamaria, et al., 2009).

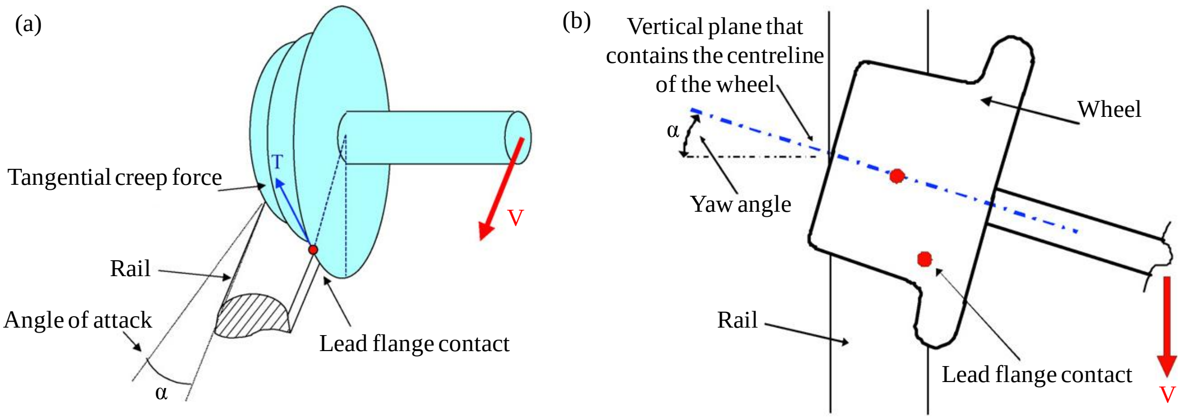

Figure 2.22: (a) Wheel/Rail Contact Point When the Wheelset Rotates at Yaw Angle α (b) Top View of the Double Contact Point Scenario with a Large Yaw Angle. The Contact Patch on the Wheel Thread is Located on the Wheel's Vertical Diametral Section, Whereas the Flange Contact Patch is Displaced Longitudinally, from Santamaria, et al. (2009)

In most cases, the rails are connected to the sleeper with fasteners (see Figure 2.23). The elastic fastener and rubber pad in a fastening system are the main components that allow the rail to move, and it is this elasticity that provides the possibility for rail deformation under the action of wheel/rail interaction forces. On tangent track, the wheel load produced by gravity is the main component of the wheel/rail vertical force. Therefore, vertically downward movements of the rails are the common phenomena. But in curves, vertical deformations of the outer and inner rails are unequal due to their different wheel loads. Wheel load reduction will decrease rail deformation while an increase of wheel load enlarges it. In curves, severe wheel/rail lateral interaction commonly occurs on the outer rail. Track gauge is widened owing to rail deformation, as shown in Figure 2.24. A large track gauge enlargement could cause the wheels on the inner rail to drop thereby damaging the track components.

© University of Pretoria

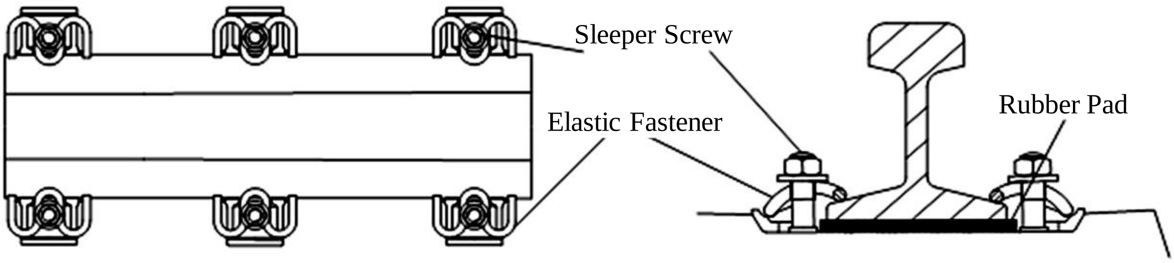

Figure 2.23: Typical Rail Fastening System, from Roney, et al. (2015)

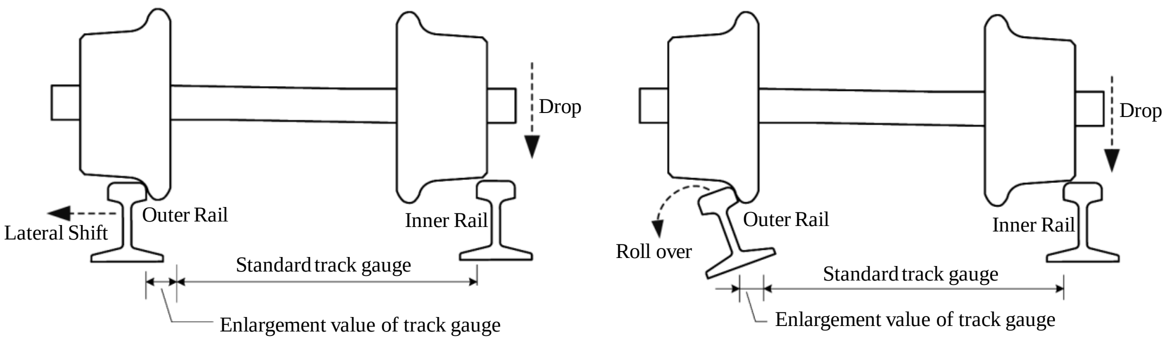

Figure 2.24: Track Gauge Widening, from Roney, et al. (2015)

Referring to Figure 2.25 the rail rotational motion is determined by the resultant moment (M), which is calculated as follows:

$$M = Uh_r + F_L a - Re + (F_{V1} - F_{V2})b$$ **Equation 2-20**

There are three different possible cases for the resultant moment (M):

- Case 1: M = 0, no rail rotation occurs.
- Case 2: M > 0, the rail rotates clockwise.
- Case 3: M < 0, the rail rotates counter-clockwise.

© University of Pretoria

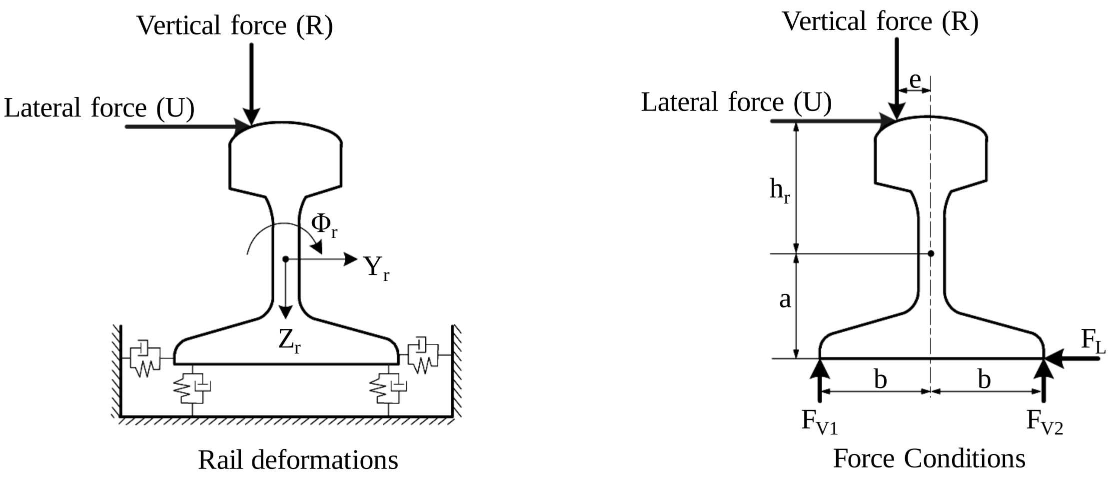

Figure 2.25: Rail Motion and Forces, from Roney, et al. (2015)

An effective method for reducing lateral forces is to control the friction on the top of the low rail. A second (complementary) technique is to avoid saturating friction by minimising creepage, i.e. engineer wheel and rail profile combinations that develop (strong) positive steering moments to take advantage of the limited wheelset alignment permitted by the bogie (Magel & Kalousek, 2002).

2.7.8 Flange Forces

The flange makes contact, laterally, with the rail under the following conditions (Roney, et al., 2015):

- When the wheelset runs with a significant angle of attack for a significant distance, thereby forcing one flange into contact with the rail.
- When a vehicle runs through a curve at a speed that is higher than the equilibrium speed the wheelset can be forced into contact with the high leg rail, whereas if a vehicle runs through a curve at a speed that is lower than the equilibrium speed the wheelset can be forced into contact with the low leg rail.
- When a vehicle/wheelset momentarily loses its steering ability or negotiates a track discontinuity where it is unable to steer (typically turnouts).

2.7.9 Shakedown Theory

The lifetime of railway wheels and rails is limited by wear and rolling contact fatigue (RCF), both of which are deterioration phenomena. A competition exists between wear and surface-initiated RCF. Wear can worsen the contact geometry between wheel and rail, which may accelerate crack growth, but at higher wear rates, RCF does not have the opportunity to develop further. Cracks can initiate, but will be worn off due to the high wear rate and will not be able to propagate beneath the surface. Care must therefore be taken, when optimizing to reduce the wear, since RCF can in that case become the dominant problem (Dirks & Enblom, 2011).

The shakedown diagram is often used to compare the contact conditions with the shakedown limit (see Figure 2.26). The "shakedown limit" for surface plasticity is denoted by the curve BC. The surface fatigue index is indicated by the horizontal dashed line. The location of the limit in the shakedown diagram is a function of the maximum contact pressure (p_0 in [N/m^2]) divided by the material yield stress in shear (k in [N/m^2]), and the utilized friction coefficient (μ) (Dirks & Enblom, 2011).

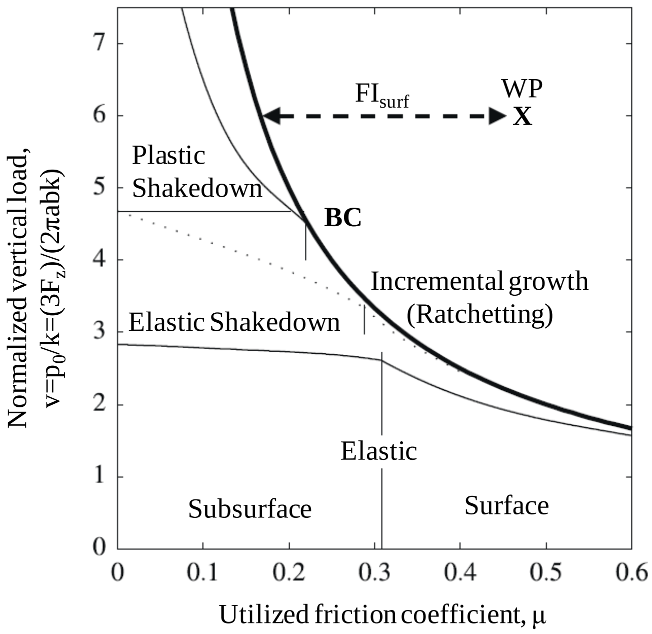

Figure 2.26: Shakedown Diagram with Working Point (WP) Indicated by "X", from Dirks and Enblom (2011)

© University of Pretoria

RCF is often observed in different locations for wheels and rails. For wheels severe RCF commonly shows up on the outside of the wheel tread, whereas for the rail it is more severe on the gauge corner. These observations indicate that RCF mainly develops on the inner wheel and on the outer rail in curves. This seems confusing, since the same forces work on both the wheels and the rail. The explanation for this can be found in the propagation mechanism of cracks. The presence of fluid plays an important role in the propagation rate of cracks, since fluid can get entrapped in a crack, causing high pressure inside the crack under a wheel load. Due to the longitudinal creep forces on the inner wheel and on the outer rail in a curve, the cracks on the wheel and the rail get orientated in such a way that fluid can get entrapped inside the cracks, as shown in Figure 2.27. This is because the crack opening enters the contact first, causing the crack to close. If the orientation of the cracks is in the opposite direction (due to creep forces on the outer wheel and inner rail) fluid will get squeezed out of the cracks instead (Dirks & Enblom, 2011).

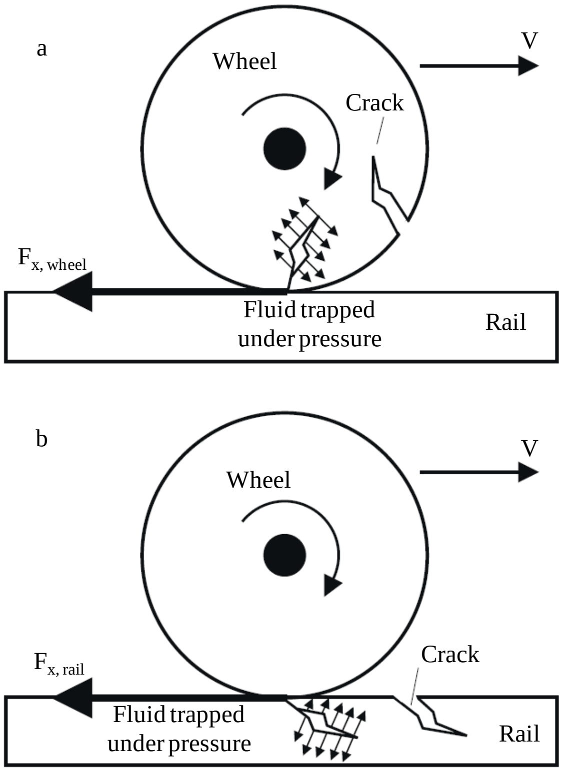

Figure 2.27: Influence of Fluid on the Crack Propagation (a) Longitudinal Force on the Inner Wheel ($F_{x,wheel}$) Causes Fluid Entrapment Inside a Crack on the Wheel (b) Longitudinal Force on the Outer Rail ($F_{x,rail}$) Causes Fluid Entrapment Inside a Crack on the Rail, from Dirks and Enblom (2011)

© University of Pretoria

2.7.10 Wear

When simulating wheel/rail wear, it is necessary to consider the inter-relation of the wear process with the dynamics of the vehicle/track interaction, the contact mechanics parameters and the tribological properties of the interacting materials. The theoretical study of two mutually wearing bodies has shown that their steady-state worn profiles do depend on their initial profiles. This conclusion enables one to suggest two schemes of control over the wheel/rail stable-state worn profile, which is direct and non-direct control. Direct control includes selection of the initial wheel/rail profiles and the use of rail grinding and wheel turning. A non-direct control is, for example, the developing of surfaces possessing variable wear resistance properties over profile length by means of surface treatment techniques, such as plasma, weld-on, induction-metallurgical methods, etc. But, before developing any method of control it is necessary to know what profiles provides for the best results in terms of the minimum wear rate or the minimum pressure distribution (Zakharov & Zharov, 2002).

The improved tracking characteristics of modern rail vehicles together with straighter track, rail grinding procedures “concentrating” contact on the rail crown, and tighter gauge control have led us from the “wear regime” to the “stress regime”.

Wheel and rail profiles are designed to meet certain desired properties of conicity, gravitational suspension stiffness and resultant contact stresses. The wheel and rail then enter service and change shape over time. The nature of this shape change is a function of the wear and material flow caused by various contact conditions between the two bodies. These contact conditions depend inter alia on track curvature, vehicle alignment, axle load, vehicle speed, vehicle type, traction and braking. The wear regime is characterised by high flange wear rates. Improvements in the tracking performance of the vehicle generally reduce, or can eliminate wheel flange wear, concentrating what wear does occur over the tread of the wheel profile. This reduction in wear between rail and wheel can result in the formation of higher contact stresses under worn conditions.

The transition from a wear to a stress regime due to tighter gauge tolerances, rail crown grinding producing tighter contact bands and improved vehicle tracking properties, have concentrated contact on the wheel profile enhancing hollow wear, which gives rise to the generation of high contact stresses and conicities (Tournay & Mulder, 1996).

Increased stress and reduced wear across the wheel/rail interface may be altering the wear modes of both components. Wheel flange and rail gauge corner wear continues to be reduced in proportion to tread and rail crown wear. This change must impact worn wheel and rail shapes (Tournay, 2008).

© University of Pretoria

The wear that shapes wheel and rail profiles has a profound effect on the curving performance and the dynamic stability of bogies. Reducing the spread between worn and unworn profiles, and in particular reducing the concavity of worn wheels, can significantly improve the curving and the ride quality of bogies, decrease wheel/rail damage and increase wheel and rail lifespan (Kalousek, 2005).

2.7.11 Bogie Parameters

It has been established that the bogie does not necessarily rotate about the common geometric centre of the centre plate and bowl but about a centre of rotation that is not necessarily coincident with the geometric centre of the bowl. Depending on bogie/body interface conditions and vehicle and curve geometry, this off-centre rotation can result in sidewall contact. Sidewall contact can appreciably increase the bogie rotational resistance to the carbody, as Figure 2.28 shows (Tournay, 2008).

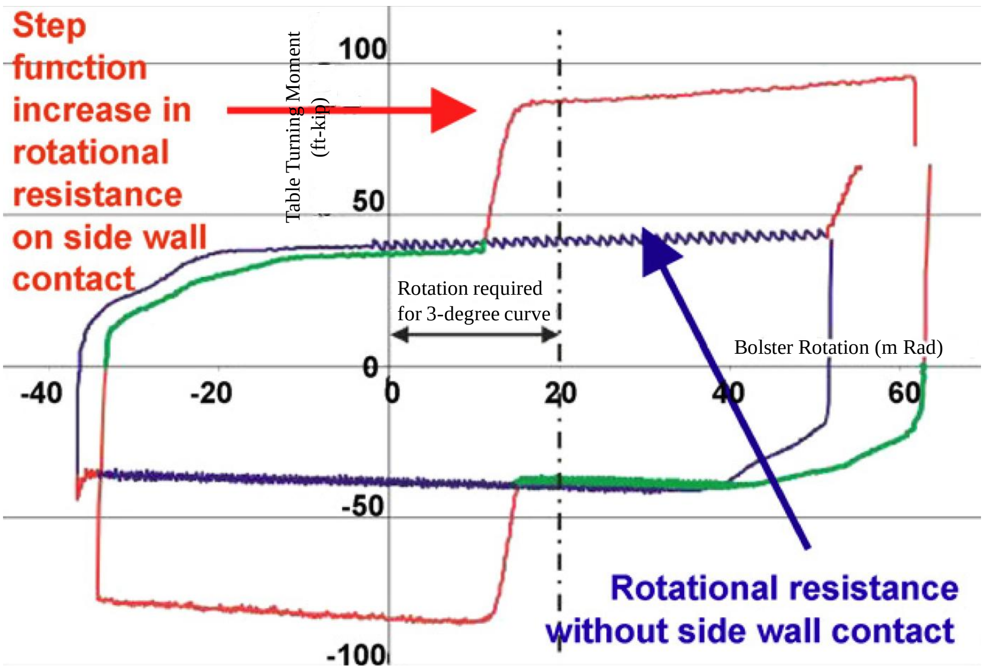

Figure 2.28: Step Function Increase in Bogie Rotational Resistance on Sidewall Contact, from Tournay (2008)

2.7.12 Derailment Ratio

To estimate vehicle safety one can analyze the possibility of derailment. Various formulae exist as a guide for the derailment process, which gives the ratio between lateral and vertical forces for a particular wheel/rail combination. This ratio, usually called the “derailment ratio”, is calculated by dividing the lateral forces by the vertical forces at the flange contact. The derailment ratio is used as a measure of the running safety of railway vehicles (Esveld, 2004).

According to UIC leaflet 518 a maximum derailment ratio value of 0.8 over 2 m is considered to be safe (UIC Code 518, 2005).

2.8 GAUTRAIN SYSTEM WHEEL/RAIL INTERFACE

The GRRL system is a dedicated railway line with dedicated vehicles and dedicated track. The system was opened in phases between June 2010 and June 2012 and the system can therefore, at the time of writing, still be considered as being relatively new.

When designing, constructing, operating and maintaining a new railway system the choice of rail section and metallurgy has a significant and long term impact on the ride comfort and maintenance of the system. The rail section is the initial structural element in the support of the trains. Not only must it be strong enough to support the load for decades, but the shape of the head must also work with the wheels and bogies on the vehicles to ensure proper tracking on both tangents and curves. The metallurgy also has long term effects. Rolling contact fatigue problems have revealed a relationship between rail wear and fatigue cracks in the rail head. A rail that is too strong can have significant rail problems that require extra inspection and maintenance, compared to a rail with lower metallurgical strength (Cornwell, 2005).

2.8.1 Gautrain Rail Grades

When designing the GRRL there was much debate with regard to whether to use a CEN Grade 260 rail (Brinell Hardness 260, Non Heat Treated), a CEN Grade 350 HT (Brinell Hardness 350, Heat Treated) or a CEN Grade 350 LHT rail (Brinell Hardness 350, Heat Treated). The only difference between the CEN Grade 350 HT and CEN Grade 350 LHT rails is the maximum chromium content, 0.1% and 0.3% respectively. The wheels were being manufactured to meet BS 5892, P+3 grade R8T (Brinell Hardness between 255 and 285). Therefore a rail with a Brinell hardness of 350 is significantly harder than the wheel, whereas a rail with a Brinell hardness of 260 is within the

© University of Pretoria

same range as the wheels (Cornwell, 2005). Table 2-1 provides an overview of some of the more common rail grades.

It is a common perception that reducing the wear rate of the material on one side of the wheel/rail interface will result in an increase in wear on the other side of the interface. However in 1993 an internal British Rail Research report, “Effect of differential hardness on wheel/rail wear literature survey” (Benson, 1993), reviewed available sets of test data and published papers on wheel and rail wear. One of the main conclusions was that “the belief that an increase in the hardness of the rail, while giving a decrease in the rail wear rate, will give an increase in wheel wear is not generally felt to be justified”. This conclusion was based on a review of a large number of studies from different organisations and researchers in the UK and abroad (Burstow, 2012).

In the end CEN Grade 350 LHT rail was used to construct all the Mainline track, while CEN Grade 260 rail was used to construct all the Depot track.

Table 2-1: Rail Grades

Steel grade		Hardness range (HBW)	Description	Branding lines
Steel name	Steel number			
R200	1.0521	200 to 240	Non-alloy (C-Mn) Non heat treated	No branding lines
R220	1.0524	220 to 260	Non-alloy (C-Mn) Non heat treated	— — — —
R260	1.0623	260 to 300	Non-alloy (C-Mn) Non heat treated	— — — — — —
R260Mn	1.0624	260 to 300	Non-alloy (C-Mn) Non heat treated	— — — — — — — —
R320Cr	1.0915	320 to 360	Alloy (1% Cr) Non heat treated	— — — — — — — — — — — —
R350HT	1.0631	350 to 390	Non-alloy (C-Mn) Heat treated	— — — — — — — — — —
R350LHT	1.0632	350 to 390	Non-alloy (C-Mn) Heat treated	— — — — — — — — — — — —
R370CrHT	t.b.a	370 to 410	Alloy (C-Mn) Heat treated	— — — — — — — — — — — — — —
R400HT	t.b.a	400 to 440	Non-alloy (C-Mn) Heat treated	— — — — — — — — — — — —

© University of Pretoria

2.8.2 Gautrain Electrostar Bogie Information

The rolling stock used on the GRRL system is the Bombardier Electrostar. The Gautrain Electrostar bogie system utilises a conventional "H" frame design with air secondary suspension. Two air springs per bogie are used to support the vehicle body and to provide the required ride comfort. The primary suspension comprises radial arm axle location and a pair of interleaved rubber springs mounted above of the axle-box. This arrangement allows the bogie to negotiate track irregularities safely whilst ensuring vehicle stability and reducing wheel wear in curves (Mutsvene, 2007).

2.8.3 Gautrain Cant Design Limitations

Geometric design limitations on the GRRL dictate that the maximum cant allowable is 125 mm, while the desirable maximum cant deficiency is 75 mm and the absolute maximum cant deficiency is 100 mm.

The Gautrain track is maintained according to Network Rail Standards and as per Network Rail's Track Design Handbook NR/L2/TRK/2049 (Network Rail, 2010) the maximum cant value for the Gautrain's operating conditions is given as 110 mm. The standard also specifies an exceptional maximum cant value of 150 mm that is applicable to passenger type bogie rolling stock, where no track features are likely to contribute to lateral misalignment on the curve where 110 mm cant deficiency is exceeded.

Due to the abovementioned geometric design limitations, no design cants exist in the GRRL system that will result in cant excess problems for stationary trains. Focus can therefore be entirely given to the correct design of cant with cant deficiency as the dominant concern.

This implies that primary attention can be given to the determination of the forces generated in curves by moving trains.

2.8.4 Gautrain Track Information

Table 2-2 provides some general Gautrain system information, while Table 2-3 provides some general Gautrain track information and Table 2-4 provides a list of all curves on the Gautrain system with a radius of 1000 m or less, of which there are 28 such curves.

© University of Pretoria

Table 2-2: General Gautrain System Information

Number of Passenger Stations	10
Main Line Slab Track (track - m)	20000
Main Line Ballasted Track (track - m)	123000
Total Length of Mainline Permanent way (track - m)	143000
Length of Track in DEPOT including workshop (track - m)	8300
Total Length of Single-lane Permanent way (track - m)	151300
Tunnel (Southern end – continuous) (single track - m) Viaduct (single track - m) Cut and Cover Tunnel (Northern end) (single track - m) At-grade (single track - m)	20000 16500 1300 105200 143000
Maximum Grade - Main Line (absolute) (%) - Main Line (normal) (%) - DEPOT Access Track (%)	 4.0 2.5 2.5
Minimum Radius of Vertical Curve Main Line (m) DEPOT Access Track (m)	 2000 2000
Minimum Radius of Horizontal Curve Main Line (m) DEPOT Access Track (m) DEPOT Track (m)	 250 1000 190

Table 2-3: General Gautrain Track Information

Track	Track Gauge	1435 mm
	Rail Inclination	1:20 (based on Electrostar)
	Mainline Rail Fasteners	Pandrol fast clips (FC1501)
	Depot Rail Fasteners	Pandrol fast clips (FC1501) and Pandrol e-clips
	Mainline Ballast Depth (minimum)	300 mm
	Depot Ballast Depth (minimum)	250 mm
	Slab Track (in tunnel)	Low Vibration Track - Sonneville blocks system
	Typical Track Centre to Centre Spacing	4000 mm
Rail	Mainline and Depot Running Rail Profile	Network Rail 60E2 (CEN 60E1 Alternate E2)
	Mainline Rail Grade	CEN Grade 350 LHT
	Depot Rail Grade	CEN Grade 260
Sleepers	Mainline Sleepers (Concrete)	Infraset B70 (1:20 inclination on the rail seat)
	Depot Sleepers (Concrete)	Infraset B70 Flat (no inclination on the rail seat)
	Sleeper spacing	700 mm centre to centre

© University of Pretoria

Table 2-4: Gautrain Track Curves

CURVES			
Number	**Radius (m)**	**Turning**	**Length (m)**
JA713	250	Left Hand	186
JB712	250	Right Hand	166
JA712	254	Right Hand	169
JB713	254	Left Hand	189
HA604	260	Right Hand	46
HB602	260	Left Hand	345
PA503	260	Left Hand	105
HA601	264	Left Hand	342
HB605	264	Right Hand	47
PB503	264	Left Hand	108
HA602	300	Right Hand	160
HB604	300	Left Hand	56
HA603	304	Left Hand	58
HB603	304	Right Hand	163
JA701	400	Right Hand	102
HB606	405	Left Hand	318
HA605	409	Left Hand	322
HA606	495	Right Hand	192
HB607	500	Right Hand	194
PB504	500	Right Hand	41
PC301	500	Right Hand	41
PC302	500	Right Hand	41
PA212	700	Left Hand	837
PB210	704	Left Hand	843
PA101	870	Left Hand	119
HB608	905	Left Hand	27
JA702	1000	Left Hand	124
JB701	1000	Right Hand	195

© University of Pretoria

2.9 DISCUSSION

Considerable benefits can be gained through appropriate wheel/rail interface management, including reduced defect rates, improved safety, extended wheel and rail life, improved vehicle/track interaction, reduced wheel/rail noise and the development of suitable standards and maintenance procedures (Monash University, no date).

As per the closing statement made by Joseph Kalousek (2002) during his keynote address at the 5th International Conference on Contact Mechanics and Wear of Rail/Wheel Systems in Tokyo, Japan in 2000, “I encourage you all to continue your efforts to improve our understanding of the wheel/rail interface and follow the wise advice of a Sufi master D. Rumi, who lived over 700 years ago.

When you eventually see through the veils,
To know how things really are,
You will keep saying again and again,
This is certainly not like we thought it was!”

© University of Pretoria

CHAPTER 3 FIELD AND LABORATORY TESTS

3.1 INTRODUCTION

The basis of the field and laboratory tests was to determine how to minimise wheel and rail wear, by optimising the interaction between the wheel and rail, with the focus of the investigation being the relationship between cant and speed.

In order to do this, two sites were selected on the Gautrain line between Pretoria and Hatfield Stations. The two sites, 40 m apart in the same curve, were instrumented with strain gauges to measure the vertical and lateral forces being exerted on the rail by the wheels of a train at different track cants as the train ran through the curve at different speeds.

3.2 PURPOSE OF THE INVESTIGATION

In designing an experiment to assess the interaction between the wheel and rail, parameters that could be changed as part of a wheel/rail interaction experiment included amongst others:

1. The rail profile
2. The wheel profile
3. Train characteristics
4. Track characteristics

Due to design, operational and maintenance constraints making rail profile, wheel profile or train characteristic modifications was not possible. The experiment therefore had to be set up in such a way as to collect data by means of varying track characteristics, while still remaining complaint with all the applicable system design requirements.

3.2.1 Methodology

The process followed to set up a wheel/rail interaction experiment was as follows:

Firstly, sites where the collection of data concerning the vertical and lateral forces being exerted on the rail by the wheels of a train had to be identified. As the studying of lateral forces, as well the loading and unloading of vertical forces, played a critical role in the proposed research, it was known that the selected sites had to be situated in a curve.

© University of Pretoria

Thereafter, strain gauges capable of measuring vertical and lateral forces were attached to the rail at two different sites within the identified curve. The measurements were then conducted by means of using an empty 4-car test train at night during engineering hours when the GRRL system was closed to all traffic. The test train was run at varying speeds through the curve in both directions, with data being collected during each run. This whole process was done twice, firstly at the original site conditions in terms of cant, and then again with a modified cant.

To evaluate the site conditions, both hand measured track geometry data, as well as laser-based track geometry measuring system track geometry data were recorded and analysed and this is discussed further in Section 3.3.

During the test train runs, some video footage was also obtained of the wheel/rail interface by means of using cameras that were attached in such a way so as to capture the running of the train wheel on the rail. The wheel/rail interaction videos are discussed further in Section 3.4.4.

Upon completion of the site experimentation, the site was left at its modified track cant, until the completion of the study, so as to ascertain whether its original cant or modified cant was more favourable to the daily operational wheel/rail interaction.

3.3 SITE DESCRIPTION AND SELECTION

A curve on the Gautrain line between Pretoria Station (Operational Chainage: km 0.000) and Hatfield Station (Operational Chainage: km 5.425) was identified. This section of the Gautrain line runs parallel with a section of the Metrorail line that runs between Loftus Versveldpark Station and Walker Street Station on the Passenger Rail Agency of South Africa (PRASA) line that connects Panpoort to Pretoria. Figure 3.1 indicates the geographical location of the selected experimental curve, while Figure 3.2 provides an aerial view of the selected experimental curve.

© University of Pretoria

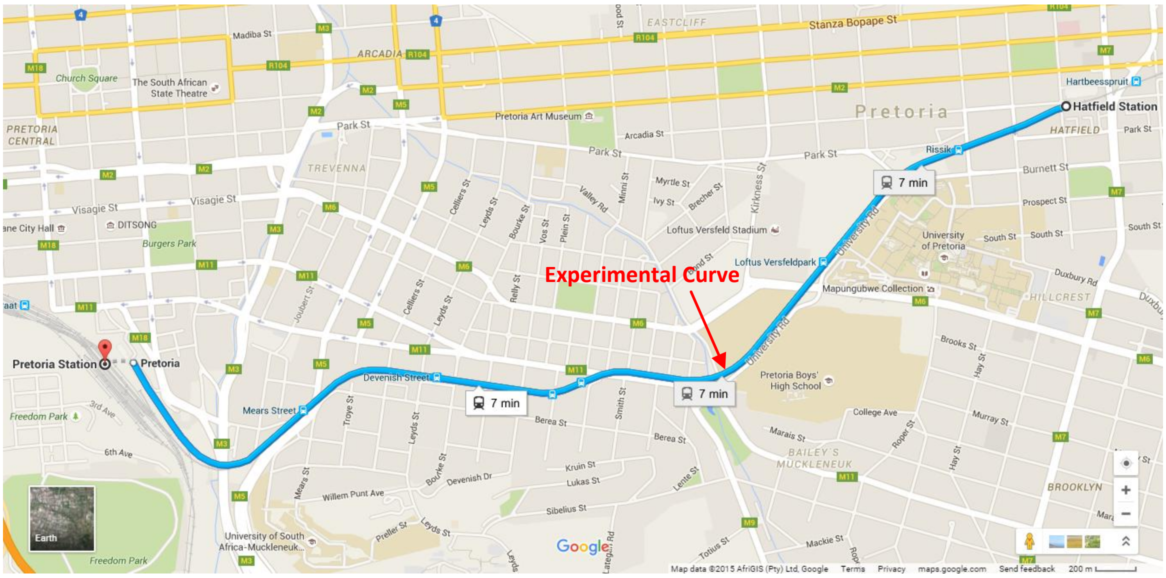

Figure 3.1: Geographical Location of Experimental Curve, from Google Earth (2015)

Figure 3.2: Aerial View of Location of Experimental Curve, from Google Earth (2015)

The experimental curve was selected based on the fact that the curve in question was found to be experiencing high leg contact to the gauge side of the rail (see Figure 3.3), while the low leg contact was to the field side of the rail (see Figure 3.4). In order to move the high leg contact band away from the gauge side of the rail the cant needed to be reduced (as was done in this dissertation) or alternatively the operational speed of the train needed to be increased.

© University of Pretoria

Figure 3.3: High Leg Contact to the Gauge Side of the Rail in the Experimental Curve

Figure 3.4: Low Leg Contact to the Field Side of the Rail in the Experimental Curve

© University of Pretoria

Figure 3.5 shows the construction chainages and design radius of the selected curve. Curve HB 606 was chosen, with the normal traffic direction on the HB Line being from Hatfield to Pretoria in the decreasing kilometre chainage direction, while on the HA Line the normal traffic flow direction is from Pretoria to Hatfield in the increasing kilometre chainage direction. Curve HB 606 has a design radius of 405 m and design cant of 120 mm. Table 3-1 and Table 3-2 provide a summary of the information shown in Figure 3.5.

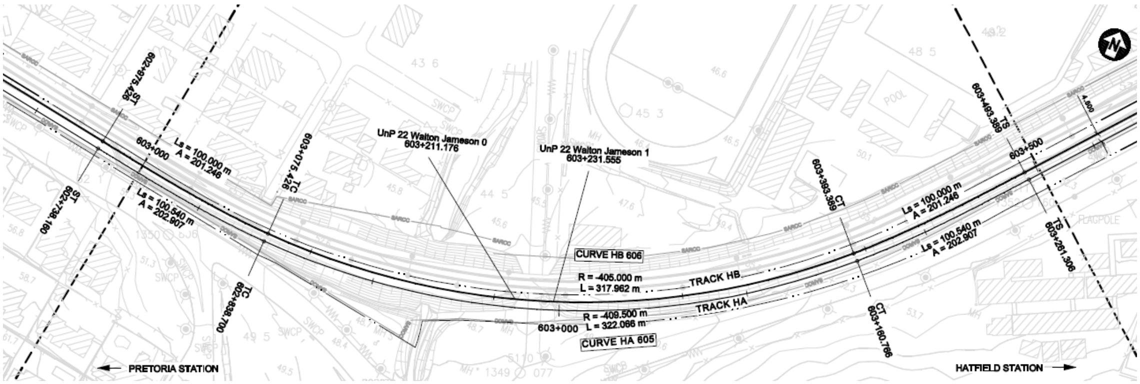

Figure 3.5: Track Alignment Design (Hatfield – Pretoria, km 2.985 – 3.535)

Table 3-1: Curve HB606 Design Parameters

Direction	Radius (m)	Transition 1 (m)	Curve Length (m)	Transition 2 (m)	Cant (m)	Speed (km/h)
Left Hand	405.0	100.0	318.0	100.0	0.120	85.0

Table 3-2: Curve HB606 Construction Chainages [Operational Chainages]

Beginning Transition Curve BTC (km)	Beginning Circular Curve BCC (km)	End Circular Curve ECC (km)	End Transition Curve ETC (km)
602.975 [3.000]	603.075 [3.100]	603.393 [3.418]	603.493 [3.518]

Figure 3.6 and Figure 3.7 below represent GPS data (coordinates, speed and elevation) that were captured from a train running between Pretoria and Hatfield on the HA Line and between Hatfield and Pretoria on the HB Line. The GPS data was manipulated in such a way as to be able to graphically present the horizontal curves between Hatfield and Pretoria and it can be seen that the horizontal curves shown in Figure 3.6 (as determined from the GPS data) correspond nicely with the Hatfield to Pretoria route given by Google Earth in Figure 3.1.

© University of Pretoria

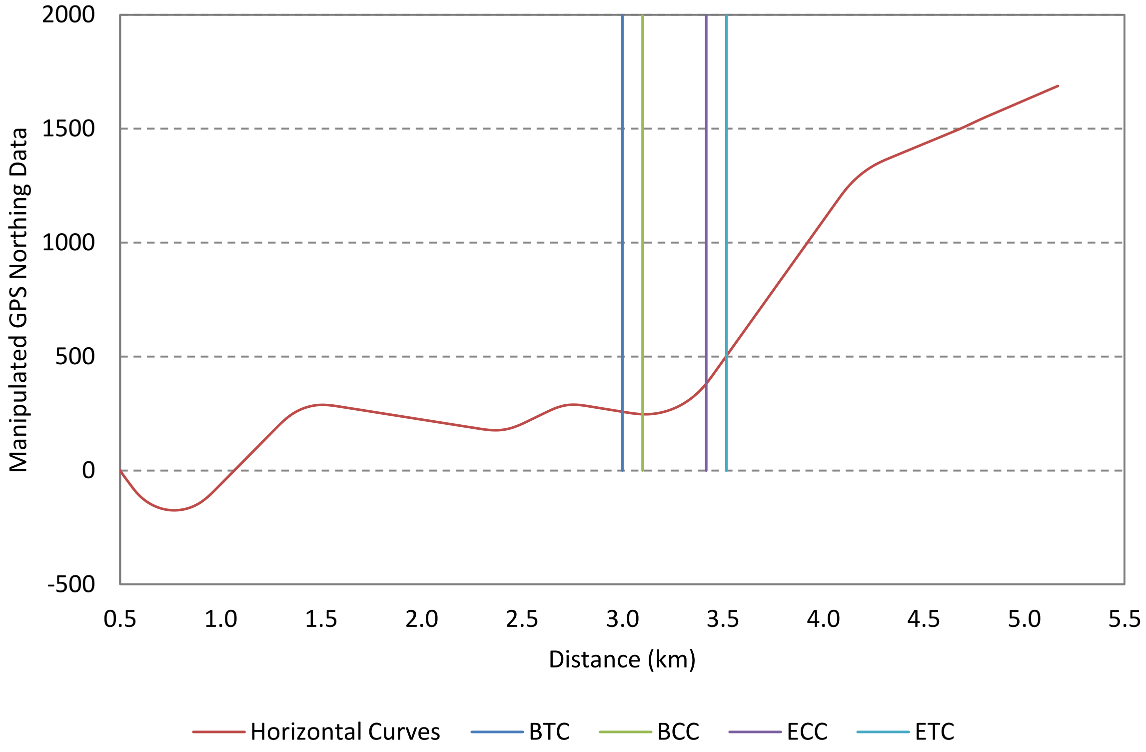

Figure 3.6: Horizontal Curvature Layout between Pretoria and Hatfield

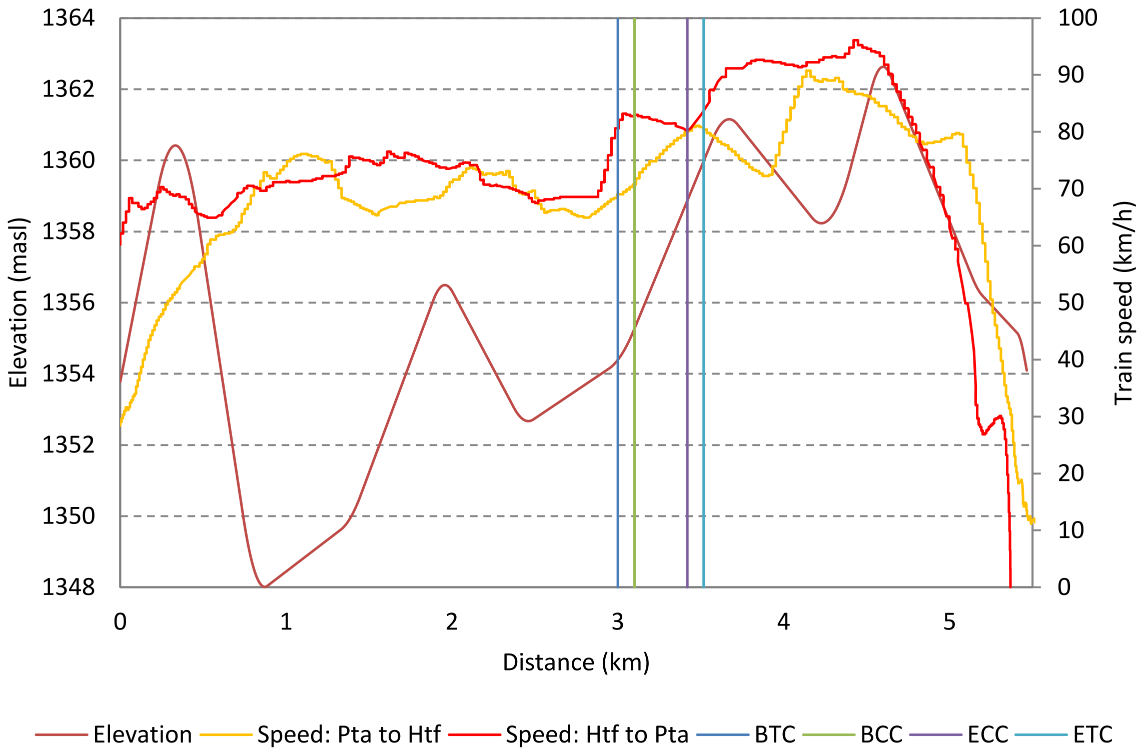

Figure 3.7: Elevation vs. Train Speed between Pretoria and Hatfield

© University of Pretoria

The curve direction convention used by the Gautrain system is to determine the direction of the curve by looking at the curve towards the increasing chainage direction. Therefore although the normal traffic direction through Curve HB606 sees the curve as a right hand curve it is nonetheless designated as a left hand curve as per the Gautrain convention. Similarly the left and right rails are also determined in this fashion, with the left rail being the rail on the left hand side and the right rail being the rail on the right hand side when looking in the increasing chainage direction. In the case of Curve HB606 the left hand rail is the low leg and the right hand rail is the high leg, but throughout this dissertation the legs will simply be referred to as either the low or high leg with no reference to left or right leg.

Two test sites, 40 m apart, were instrumented as part of the experiment in the selected curve. Site 1 (S1) was located at km 3.215 and Site 2 (S2) was located at km 3.175. Figure 3.8 and Figure 3.9 show the locations of Site 1 and Site 2 within the selected experimental curve. Figure 3.10 shows a view from the leading cab while travelling through the experimental curve from Hatfield towards Pretoria.

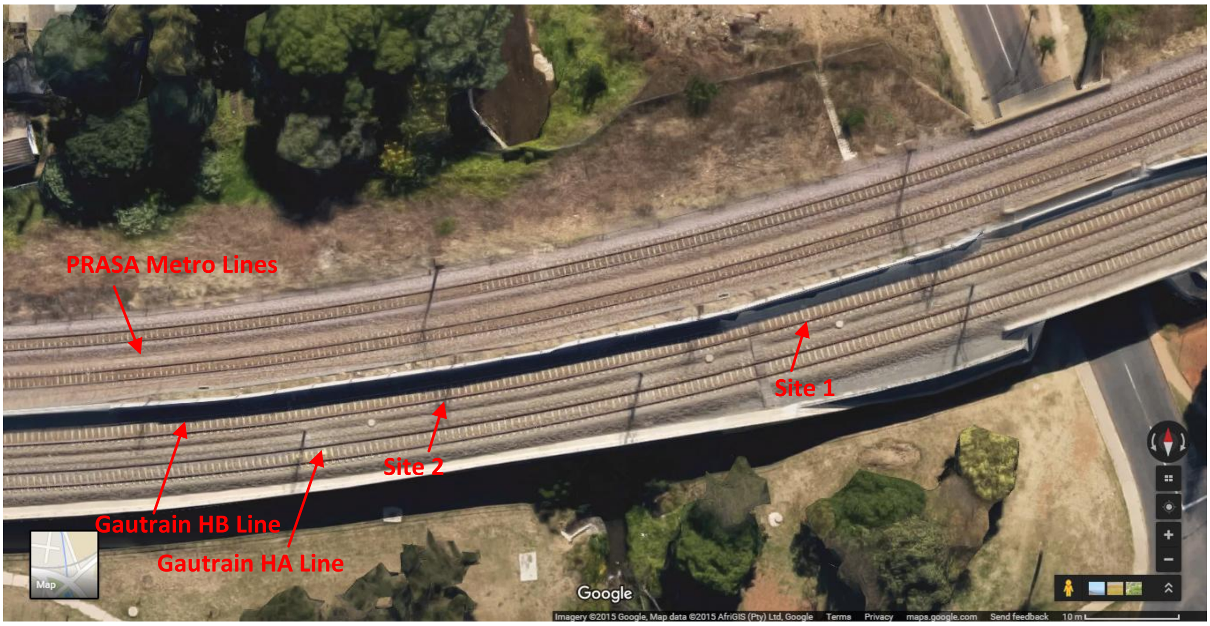

Figure 3.8: Overview of Site 1 and Site 2 Locations

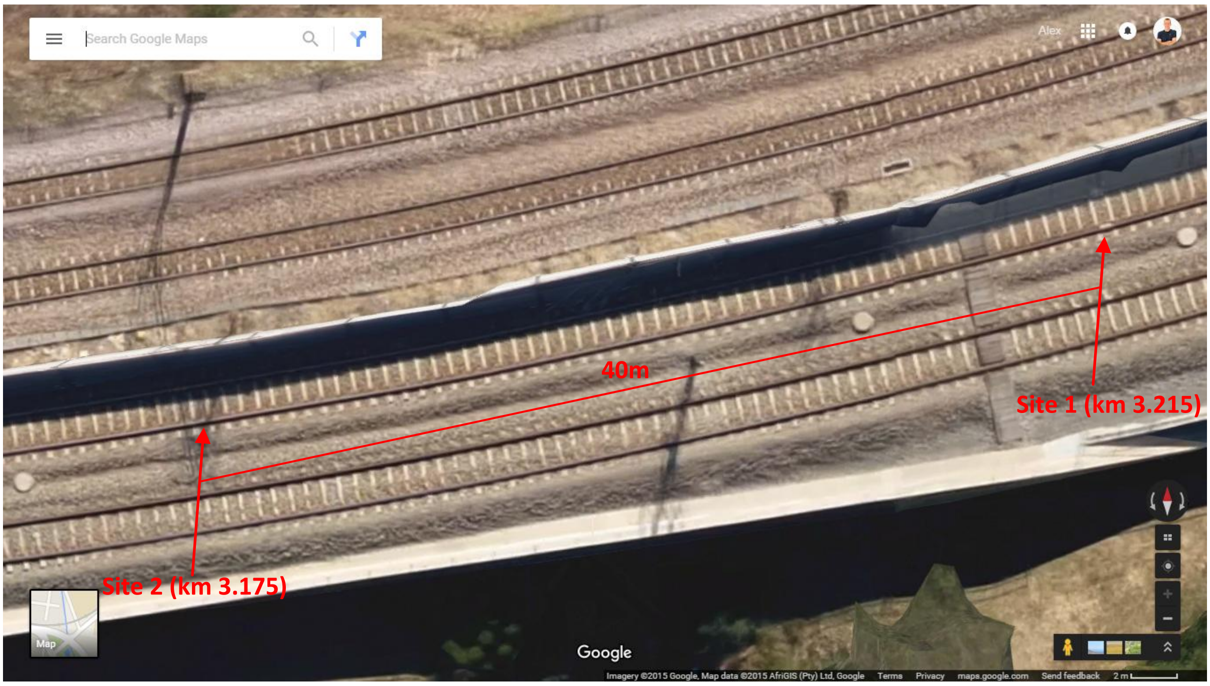

Figure 3.9: Site 1 and Site 2 Location Details

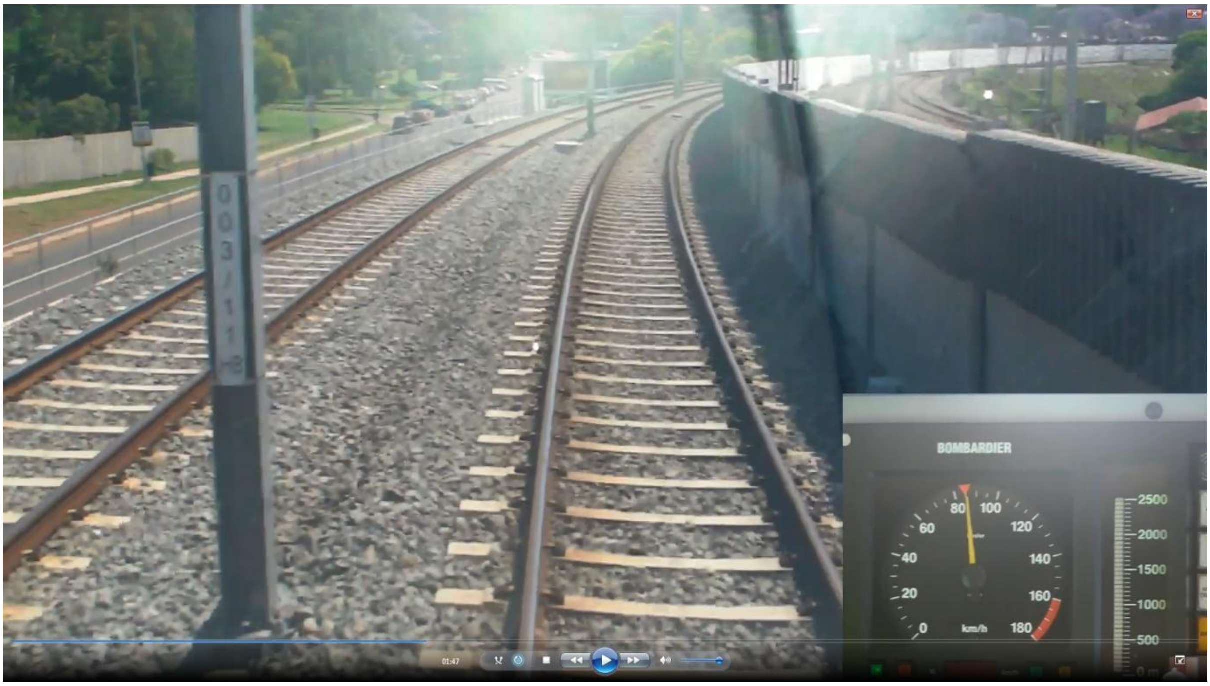

Figure 3.10: A View From the Leading Cab While Travelling Through the Experimental Curve from Hatfield Towards Pretoria (Also Showing the Train Speedometer)

© University of Pretoria

3.3.1 Curve Tamping

In addition to instrumenting the selected test sites in the experimental curve with strain gauges the other key activity that needed to take place in order to complete this dissertation was the tamping of the curve in order to change the cant between data collection campaigns. Rail force data were collected from the site as described in Section 3.4 on the 12th of February 2015 and 21st of July 2015, with tamping taking place in the week of 15 – 19 June 2015. Figure 3.11 below shows the tamper on-site in the experimental curve.

Figure 3.11: Tamping of Experimental Curve

3.3.2 Cant

Train speed and cant were the primary variables in this research project. Experimental curve cant measurements before and after tamping were collected by means of a laser-based Track Geometry Measuring System (TGMS). Spot cant measurements for comparison purposes were also taken using a track gauge (see Figure 3.12).

© University of Pretoria

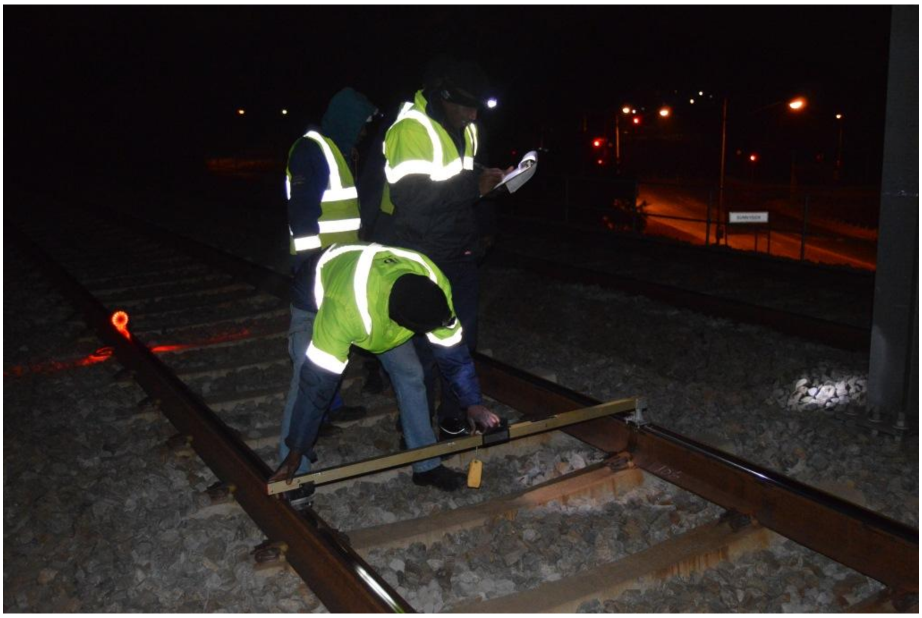

Figure 3.12: Hand Cant Measurements

Figure 3.13 shows the cant measurements before and after tamping in the experimental curve. The cant at Site 1 before and after tamping was 109.9 mm and 91.5 mm respectively and the cant at Site 2 before and after tamping was 105.9 mm and 92.8 mm respectively. The tamping of the experimental curve therefore reduced the cant at Site 1 and Site 2 by 18.4 mm and 13.1 mm respectively. The average cant for the circular curve before and after tamping was 107.1 mm and 92.0 mm respectively. This indicates that the cant of the curve before tamping was not set to its design value of 120 mm.

The decision to reduce the cant, thereby further increasing the cant deficiency in the curve was made based on field observations that at the normal operational speed of the test curve, the wheels were generating some flanging noise emanating from the low leg. The selected curve was also found to be experiencing high leg contact to the gauge side of the rail, while the low leg contact was to the field side of the rail. In order to move the high leg contact band away from the gauge side of the rail the cant needed to be reduced (as was done in this dissertation) or alternatively the operational speed of the train needed to be increased.

Railway curve first principles theory indicates that decreasing the cant while keeping the operational speed the same, in a curve that already has a cant deficiency, thereby increasing the cant deficiency, should result in the lateral forces in the curve increasing. The intention of reducing the cant was not to increase the lateral forces experienced in the curve. The experiment of reducing the cant was nonetheless carried out based on the perceived

© University of Pretoria

operational train dynamics through the curve at the original cant. The aim of the experiment was therefore to determine if the measured before and after tamping results confirmed or contradicted the first principles theory in this case.

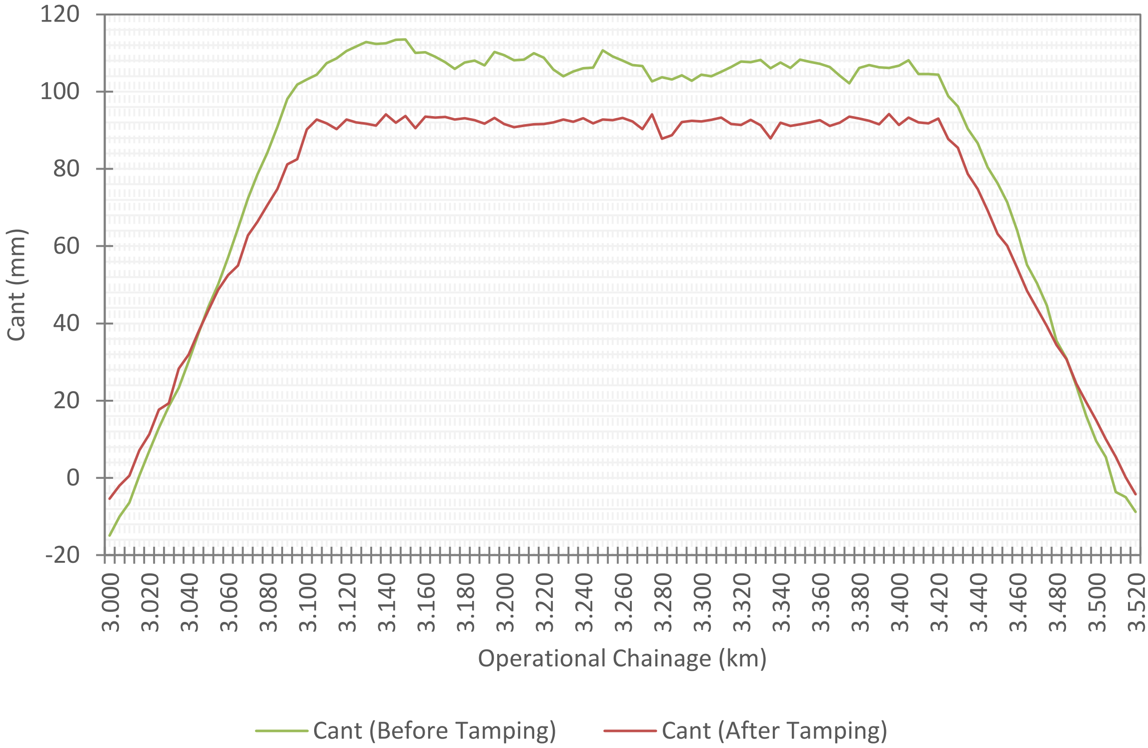

Figure 3.13: Cant Measurements Before and After Tamping in the Experimental Curve

3.3.3 Horizontal Alignment

In order to compare the given design radius value of 405 m with the actual site radius the mid-cord ordinate method was used to verify the on-site radius. The offset from the middle of a 10 m cord at 5 metre intervals was measured throughout the curve, including the transition curves (see Figure 3.14).

© University of Pretoria

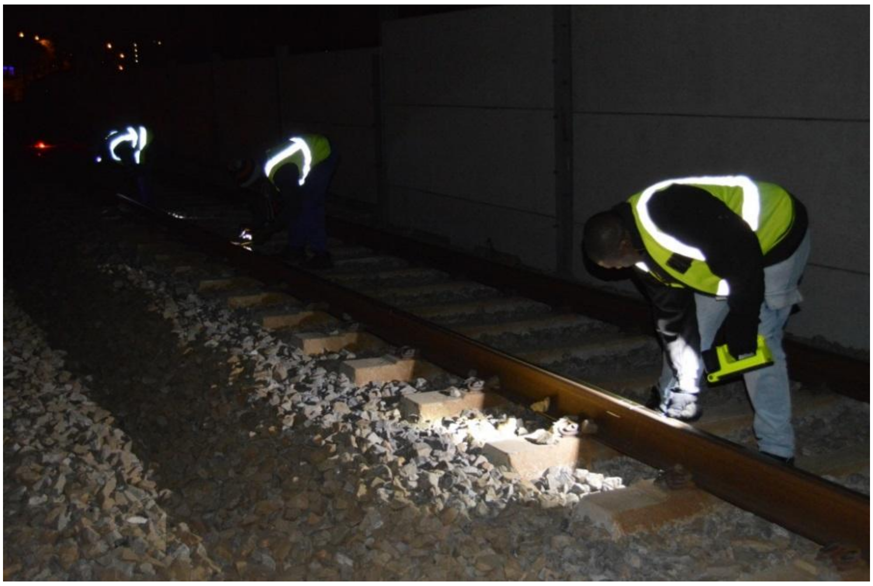

Figure 3.14: Hand Horizontal Alignment Measurements

Figure 3.15 shows the offset measurements before and after tamping in the experimental curve. The average offset for the circular curve before and after tamping was 29.631 mm and 30.323 mm respectively.

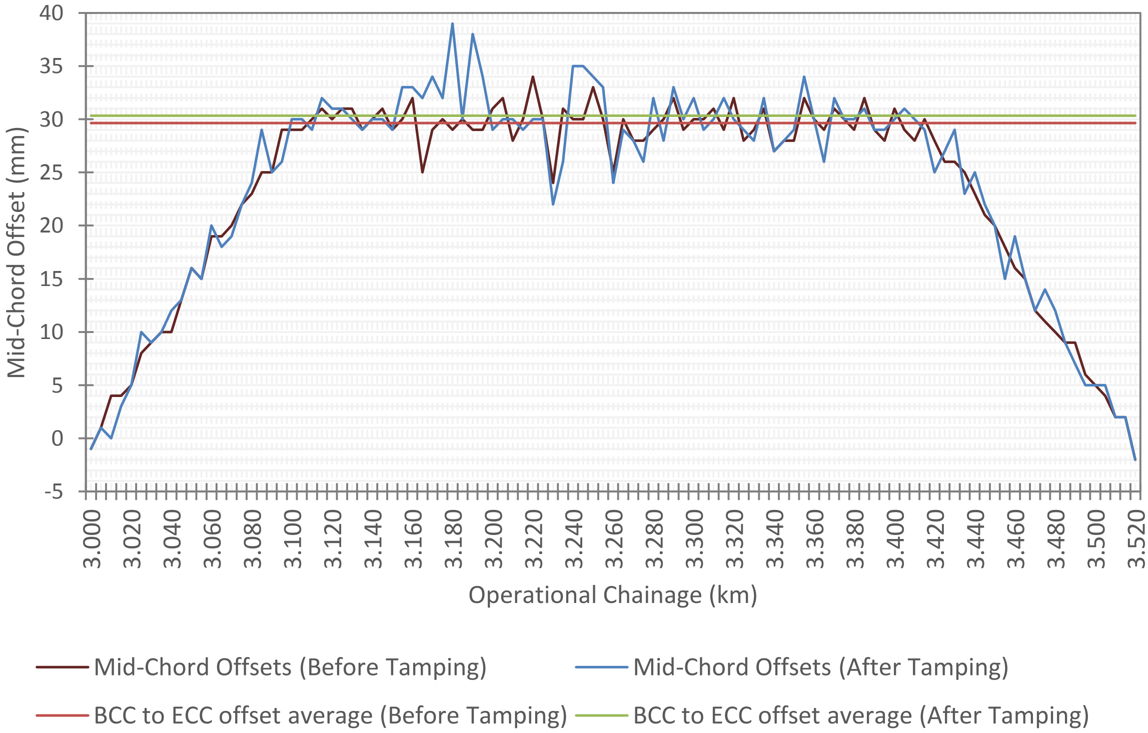

Figure 3.15: Curve Mid-Cord Offset Measurements Before and After Tamping

Using Equation 2-1, the radius of the curve before tamping was 421.9 m and due to the tamping activity the radius after tamping had been reduced slightly to 412.2 m.

$$Before\ Tamping: Curve\ Radius\ (R) = \frac{10\ m \times 10\ m \times 125}{29.631\ mm} = 421.9\ m$$

$$After\ Tamping: Curve\ Radius\ (R) = \frac{10\ m \times 10\ m \times 125}{30.323\ mm} = 412.2\ m$$

3.3.4 Rail and Wheel Wear

The rail grade of the experimental curve is CEN Grade 350 LHT 60 kg/m rail with a 60E2 rail profile (see Figure 3.17). This is therefore a relatively large, heavy and hard rail considering the light axle loads and single traffic type of the network (10.4 t/axle empty, 13.4 t/axle full as shown in Table 3-14). The wheel profile in use on the Gautrain system is a P8 (see Figure 3.18).

Rail wear within the experimental curve was checked using the rail MiniProf full contact measurement system (see Figure 3.16) as well as a handheld rail wear gauge (see Figure 3.19). The rail wear of the experimental curve was found to be negligible with most of the hand measurements indicating no wear. The rail MiniProf profiles were not analysed in detail, as the initial on-site verification of the measured profiles indicated very close matching to the design 60E2 rail profile.

© University of Pretoria

UNIVERSITEIT VAN PRETORIA
UNIVERSITY OF PRETORIA
YUNIBESITHI YA PRETORIA

Figure 3.16: Rail Miniprof Device

With regard to wheel wear the wheels profiles are managed by the engineering teams to stay within maintenance limits and are replaced when the worn profiles have reached their allowable wear limits and can no longer be re-profiled back to the required P8 profile. Wheel re-profiling is done according to mileage and the measured wheel profile based on a preventative maintenance schedule.

A rail wheel typically has a wear life of about 240,000 km, which for a standard freight wheel is about 8×10^7 (or 80 million) revolutions (Magel & Kalousek, 2002). A new Gautrain Electrostar wheel has a diameter of 840 mm, while a worn Gautrain Electrostar wheel has a diameter of 776 mm. The average between a new and a worn wheel's diameter is 808 mm. For a wheel with a diameter of 808 mm to cover a distance of 240,000 km will require approximately 94.5 million revolutions.

The total amount of loadings seen by the rail in the experimental curve at the time of the "before" and "after" tamping testing campaigns can be seen in Table 3-3 below. As at the 21st of July 2015, the trains in the GRRL system fleet had covered on average 800,000 – 900,000 km each.

Table 3-3: Experimental Curve Total Mega Gross Tons

Experimental Curve (HB606)	Total Mega Gross Tons
As at 12 February 2015 (Before Tamping)	16.77
As at 21 July 2015 (After Tamping)	18.93

© University of Pretoria

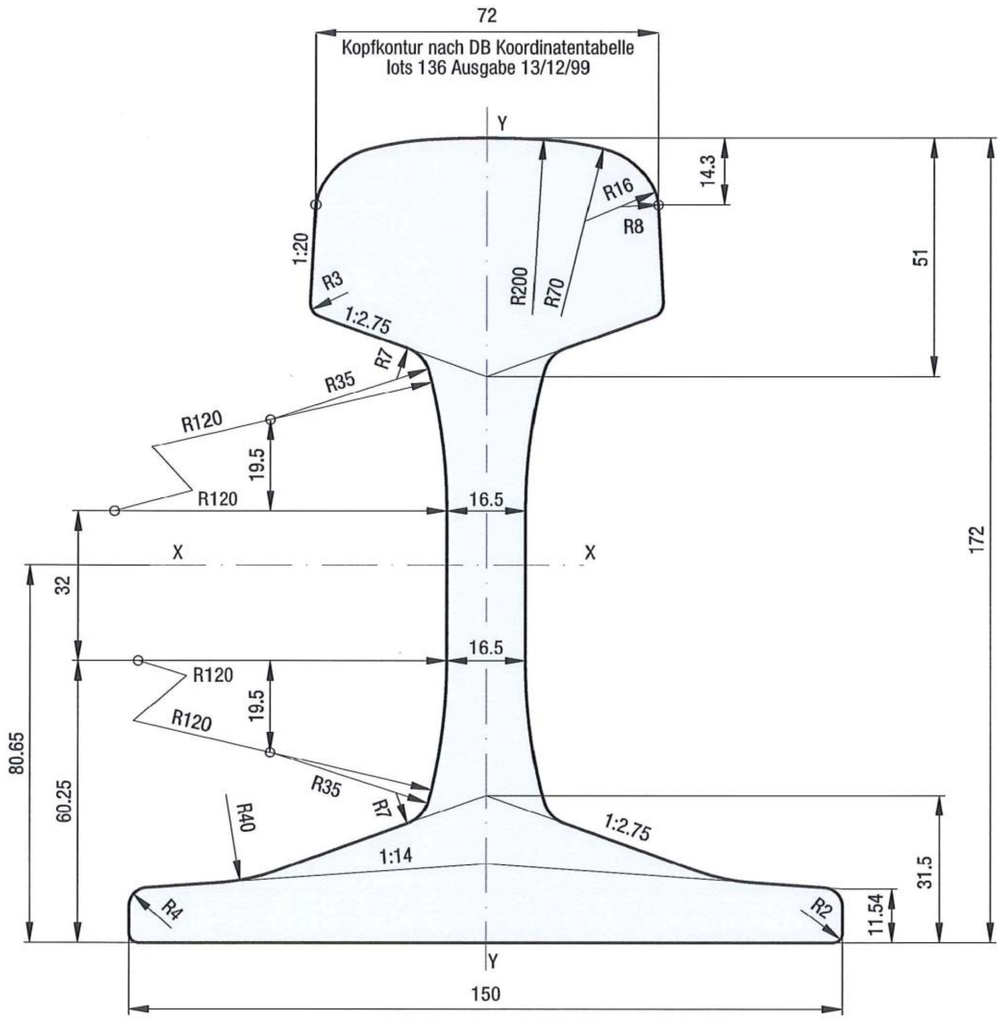

Figure 3.17: An Example of a New 60E2 Rail Profile

© University of Pretoria

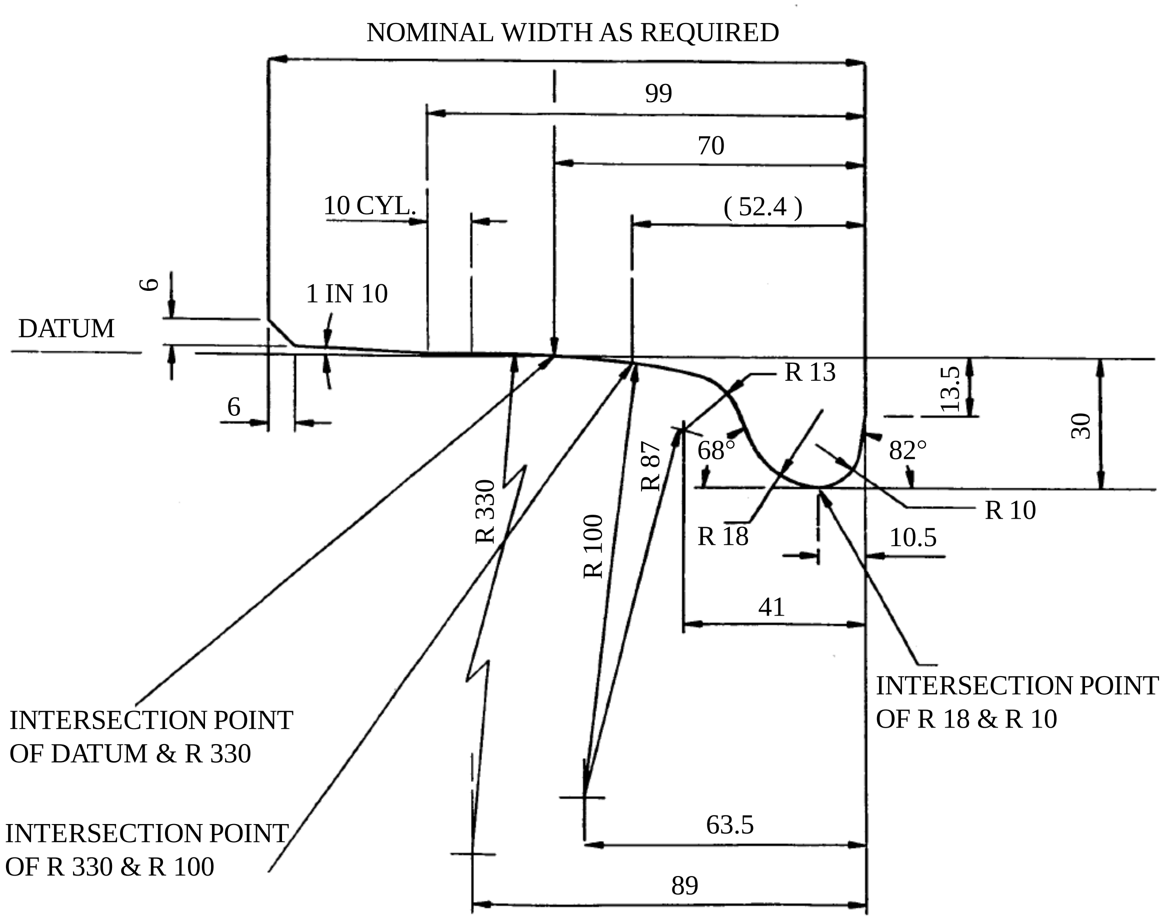

Figure 3.18: An Example of a New P8 Wheel Profile

Figure 3.19: Handheld Rail Wear Gauge Measurements

© University of Pretoria

3.4 EXPERIMENTAL SETUP

In order to measure the vertical and lateral forces experienced by each of the rail legs in the experimental curve during the passing of trains, strain gauges were installed on the rail as shown in Figure 3.20 and Figure 3.21 below. The strain gauges that can be seen attached to the web of the rail allow for the measuring of vertical rail forces, while the strain gauges that can be seen attached to the foot of the rail allow for the measuring of lateral rail forces.

Figure 3.20: Longitudinal View of Installed Encapsulated Strain Gauges

Figure 3.21: Side View of Installed Encapsulated Strain Gauges

© University of Pretoria

3.4.1 Strain Gauge Configuration

The base chevron strain gauge configuration method (as can be seen in Figure 3.22) was used for the measuring of vertical and lateral forces. The base chevron method is an alternative to the more widely used web bending strain gauge configuration method (as can be seen in Figure 3.23).

The base chevron method and the web bending method both measure the vertical forces in the same way by means of attaching the vertical strain gauges to the web of the rail. With regard to the measurement of lateral forces however, the two methods differ in that when using the base chevron method, the lateral strain gauges are attached to the foot of the rail, while the web bending method measures lateral forces by means of attaching the lateral strain gauges in a vertical orientation on the web of the rail.

It is believed that the web-bending technique of strain gauging the rail to measure the lateral rail forces is subject to cross talk from the vertical rail forces. The initial results of tests conducted by Transnet Freight Rail (Reitmann, 2013) indicate that the base chevron method measures lateral forces more accurately.

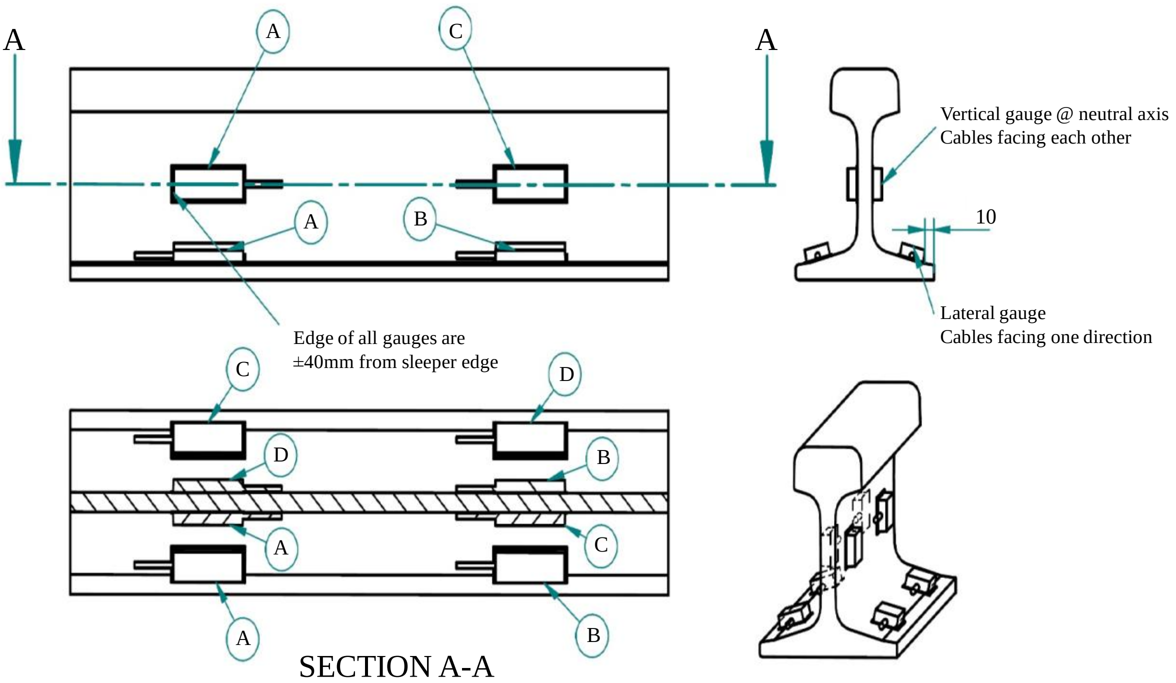

Figure 3.22: Vertical and Lateral Strain Gauges Configuration for Base Chevron Method

© University of Pretoria

UNIVERSITEIT VAN PRETORIA
UNIVERSITY OF PRETORIA
YUNIBESITHI YA PRETORIA

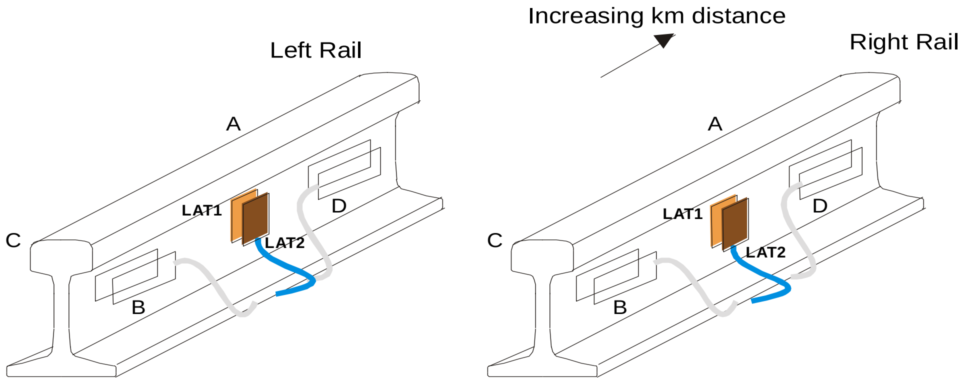

Figure 3.23: Vertical and Lateral Strain Gauges Configuration for Web Bending Method

As strain gauges measure strain at singular point(s), considerable skill is required to ensure that the critical elements of the rails behaviour are captured. Strain gauges are particularly delicate items, and considerable care is required when mounting them on the rail if accurate and reliable measurements are to be achieved. The gauges that can be seen in Figure 3.20 and Figure 3.21 were encapsulated in a laboratory environment so as to prevent the ingress of water and other contaminants and to ensure the long term usability of the installed strain gauges. The areas on the rail where the strain gauges were mounted were polished to a good surface finish and then cleaned with specialist solvents and cleaning agents to remove any oil contamination and oxides and to ensure that the surface was at the optimum pH for bonding (Iwnicki, 2006).

Following the installation of the encapsulated strain gauges at Site 1 (km 3.215) and Site 2 (km 3.175) further strain gauge protection measures were put in place in the form of permanently plastic putty with aluminium foil (see Figure 3.24) at one of the sites and stainless steel cover plates (see Figure 3.25) at the other site. The reason for two different methods of protection at each site was due to insufficient quantities of either protection material to do both sites using the same method.

© University of Pretoria

Figure 3.24: Encapsulated Strain Gauges Covered in Permanently Plastic Putty with Aluminium Foil (ABM75)

Figure 3.25: Encapsulated Strain Gauges Covered by Stainless Steel Cover Plates

© University of Pretoria

3.4.2 Strain Gauge Calibration

The strain gauges then had to be calibrated, which needed to be done separately for the vertical and lateral gauges. A Loadtech 10 t load cell, model LT200, and a 10 t hydraulic jack were used for the calibration. The initial set up of the lateral calibration rig proved to have some alignment challenges, with rods on either side of the load cell. The alignment problems were compensated for by means of placing an I-beam underneath the set up (see Figure 3.26). The set up was however improved at a later stage, with only one rod being needed on one side of the load cell as can be seen in Figure 3.27. The vertical calibration rig can be seen in Figure 3.28.

The lateral force calibration was performed by means of taking lateral force measurements at 0 t and then again at 3 t, while the vertical force calibration was performed by means of taking vertical force measurements at 0 t and then again at 10 t.

Figure 3.26: Original Set Up of the Calibration Rig for the Lateral Strain Gauges

© University of Pretoria

Figure 3.27: Improved Set Up of the Calibration Rig for the Lateral Strain Gauges

Figure 3.28: Calibration Rig for the Vertical Strain Gauges

The amplification instrument used with the strain gauges was a Quantum X, MX840A 8-channel universal amplifier and the collection of data throughout the experimental process was done at a sampling rate of 1200 Hz.

© University of Pretoria

As discussed in detail in Chapter 4, a 4-car test train was expected to exert a total vertical load of approximately 166 t on the track (see Table 3-16 in which axle, vehicle and 4-car loads are presented for load state AW0 (service ready train, including full working fluids and one driver. No passengers. No other consumables – as per Table 3-12)). The information used in determining the estimated vertical load of 166 t was obtained from design documents during the bidding phase of the Gautrain project and therefore does not represent final as-built loads.

After the completion of the analysis of the measured raw data the average measured vertical track force and standard deviation for each site was calculated and can be seen in Table 3-4 below. For Site 1 (175.1 t and 177.4 t) and Site 2 (173.0 t and 171.4 t) before tamping and for Site 2 (171.2 t and 173.0 t) after tamping the measured vertical track forces can therefore be considered as being true reflections of actual vertical track forces. The vertical track forces measured at Site 1 (154.7 t and 150.7 t) after tamping however did not provide results that were as accurate as the other 3 measurement set ups. Although great care was taken with regard to the calibration of each measurement site before each measurement campaign the most likely source of the measured versus expected loadings differences would be related to calibration issues, more specifically a scaling issue.

Table 3-4: Average Raw Data Vertical Track Forces and Standard Deviations (STD)

SITE	Before Tamping		After Tamping	
	Avg. VERT force (t)	Std Dev (t)	Avg. VERT force (t)	Std Dev (t)
Site 1 Down	175.1	3.7	154.7	2.2
Site 1 Up	177.4	4.9	150.7	3.8
Site 2 Down	173.0	2.8	171.2	3.7
Site 2 Up	171.4	2.3	173.0	4.3

In order to correct this scaling issue the measured data from Site 1 and Site 2 before tamping and from Site 2 after tamping were used as reference points and a correction factor of 1.154 was calculated to be used on all the Site 1 after tamping vertical force data. The results presented in Chapter 4 related to the vertical force data of Site 1 after tamping have therefore all undergone the applicable scaling correction.

The corrected vertical track force and standard deviation after applying the correction factor of 1.154 for Site 1 after tamping can be seen in Table 3-5 below.

© University of Pretoria

Table 3-5: Average Calibrated Vertical Track Forces and Standard Deviations (STD)

SITE	Before Tamping		After Tamping	
	Avg. VERT force (t)	Std Dev (t)	Avg. VERT force (t)	Std Dev (t)
Site 1 Down	175.1	3.7	178.6	2.5
Site 1 Up	177.4	4.9	173.9	4.4
Site 2 Down	173.0	2.8	171.2	3.7
Site 2 Up	171.4	2.3	173.0	4.3

3.4.3 Sign Convention and Test Train Direction

During the calibration process, signs needed to be assigned to the various force directions. For the lateral forces, any forces pulling the outer or inner rail of the curve towards the middle of the track were considered to be a negative force, while any lateral forces to the outside of the track were considered to be positive. Figure 3.29 illustrates a simple plan view of the described sign convention for the lateral forces.

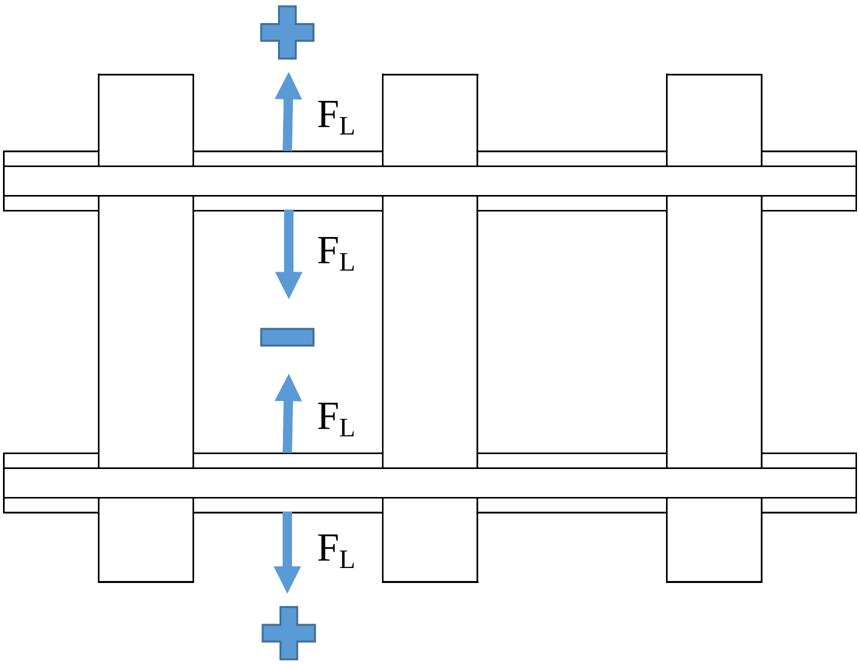

Figure 3.29: Sign Convention for Lateral Rail Forces

For the vertical forces, any forces pushing down onto the rail were considered to be positive. From a practical point of view, rails should never experience a negative vertical force, with the smallest force that they should be able to be exposed to being 0 in the case of a wheel totally lifting (unloading) from the track, for example during a derailment. Figure 3.30 illustrates a simple longitudinal view of the described sign convention for the vertical forces (with the previously described lateral forces sign convention also being shown).

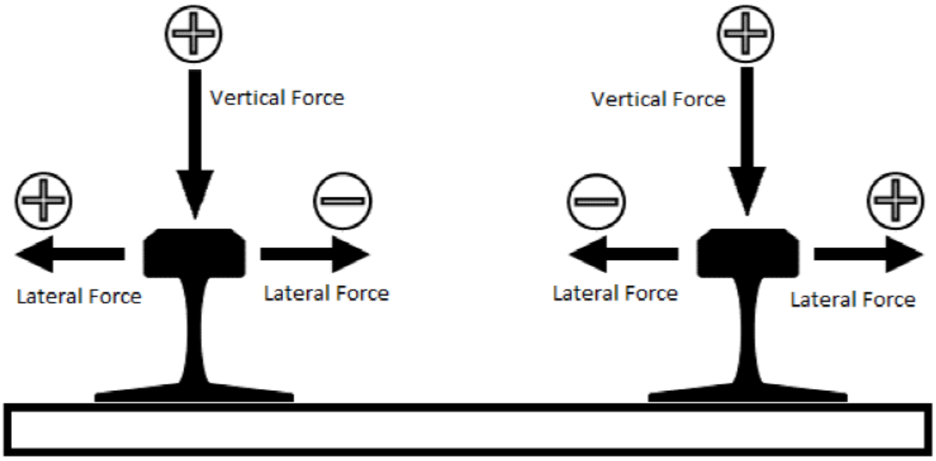

Figure 3.30: Sign Convention for Lateral and Vertical Rail Forces

For testing purposes, directions were also assigned to the various test train runs. The direction of trains running through the experimental curve from Pretoria towards Hatfield was considered as being in the "Up" direction, while trains running through the experimental curve from Hatfield towards Pretoria was considered as being in the "Down" direction.

3.4.4 Wheel/Rail Interaction Videos

In an attempt to supplement the rail forces data gathered through the strain gauges, Garmin GoPro video cameras were also set up in front of Wheel 1 and Wheel 8 on Axle 1 of DMOS B (see Section 3.5 for train configuration details) with LED spotlights so as to be able to record video footage of the wheel/rail interaction during the test runs. This exercise proved to be difficult due to challenges with controlling the video cameras remotely and insufficient battery life. There is however much room for this type of wheel/rail interaction investigation method to be further developed and improved upon. A sampling of photos of the set up are shown in Figure 3.31 to Figure 3.34 below. Images from some of the videos captured are presented and discussed in Chapter 4.

© University of Pretoria

Figure 3.31: View from under the Train of Cameras and Spotlights Installed in front of Wheel 1 and Wheel 8 on Axle 1 of DMOS B on the Workshop Maintenance Line

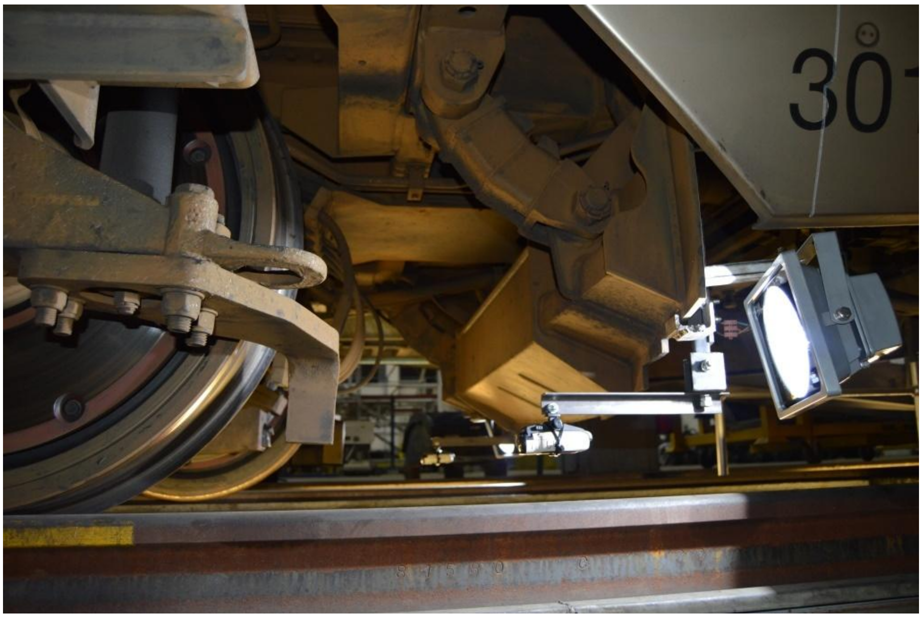

Figure 3.32: Side View of Cameras and Spotlights Installed in front of Wheel 1 and Wheel 8 on Axle 1 of DMOS B on the Workshop Maintenance Line

© University of Pretoria

Figure 3.33: Side View of Cameras and Spotlights Installed in front of Wheel 1 and Wheel 8 on Axle 1 of DMOS B on Ballasted Track

Figure 3.34: Front View of Cameras and Spotlights Installed in front of Wheel 1 and Wheel 8 on Axle 1 of DMOS B on Ballasted Track

© University of Pretoria

3.5 TEST TRAIN

The standard GRRL train configuration is that of either a 4-car or 8-car train on the Commuter Line and exclusively 4-car trains on the Airport Line. There are nineteen 4-car trains servicing the Commuter Lines (i.e. 76 Commuter vehicles in total) and five 4-car trains servicing the Airport Lines (i.e. 20 Airport vehicles in total). The 4-car Commuter train sets are numbered sequentially from 301001 to 301019, while the 4-car Airport train sets are numbered sequentially from 301101 to 301105. 8-car trains for the Commuter service are created by means of coupling two of the 4-car Commuter train sets together.

A typical Gautrain Bombardier Electrostar 4-car Commuter train set was used for the test runs through the instrumented experimental curve. The before tamping test train test runs on the 12th of February were done using Train 301012 (Commuter 12), while the after tamping test train test runs on the 21st of July were done using Train 301011 (Commuter 11). The standard Gautrain 4-car Commuter train configuration is as follows:

DMOS A + MOS + PTOS + DMOS B

The standard Gautrain 4-car Airport train configuration is as follows:

DMOS A + MOS + PTOA + DMOA

Both of the above configuration are shown in Figure 3.35, while a 4-car Commuter train configuration is shown Figure 3.36. Descriptions of the car names are given in Table 3-6. Figure 3.37 shows the wheels (W) and axles configuration for a 4-car Commuter train.

With reference to the above configurations it can be seen that the configuration of a standard Gautrain 4-car Airport train is slightly different from that of the 4-car Commuter train. From a technical point of view there are no differences between the PTOS and PTOA, as well the DMOS B and DMOA. The reason for differentiating between these vehicles is due to the fact that they have different seat layouts from one another, which has a slight effect on the train loadings. The loadings of a Commuter and an Airport train can be seen in Table 3-14.

© University of Pretoria

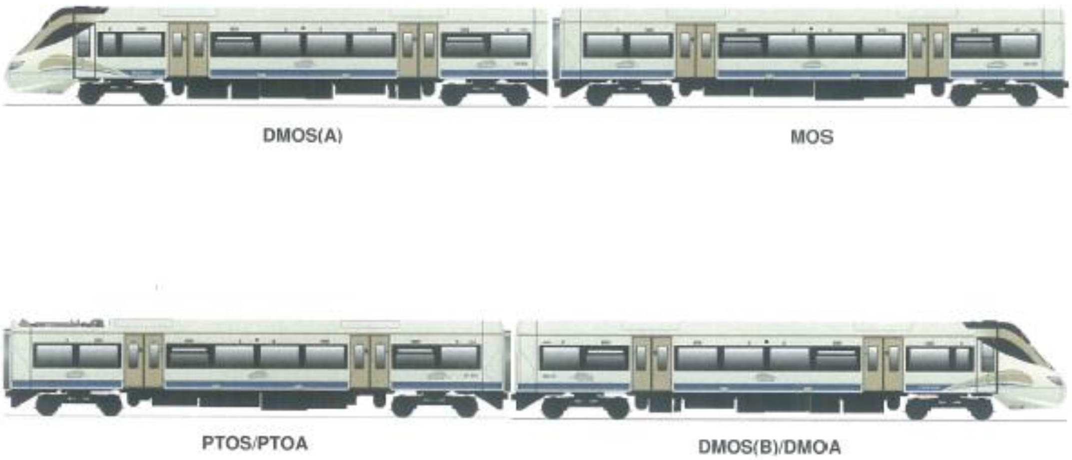

Figure 3.35: Gautrain 4-Car Train Set Configuration

Figure 3.36: Typical Gautrain 4-Car Commuter Train Set

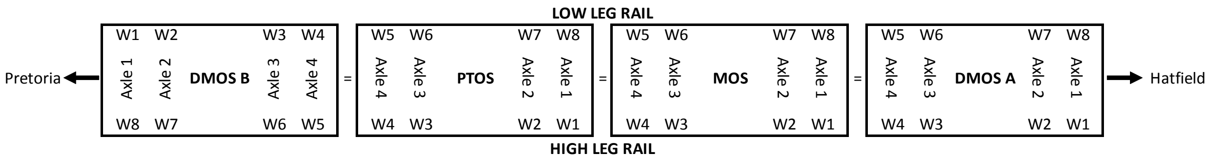

Figure 3.37: Gautrain 4-Car Commuter Train Wheels and Axles Configuration

© University of Pretoria

Table 3-6: Gautrain Car Descriptions

CAR TYPE	DESCRIPTION
DMOS A/B	Driving Motor Open Standard
DMOA	Driving Motor Open Airport
MOS	Motor Open Standard
PTOS	Pantograph Trailer Open Standard
PTOA	Pantograph Trailer Open Airport

DMOS A/B are identical, with one on either end of the train from which a driver drives the train. Between Pretoria and Hatfield, when trains are running in the up direction (Pretoria to Hatfield) DMOS A is in the front of the train, and when trains are running in the down direction (Hatfield to Pretoria) DMOS B is in the front of the train.

During the data collection process testing had to be done at night while the line was closed to revenue-earning traffic. The Gautrain system operates daily from 04h50 to 21h18, with daily maintenance taking place during a full closure of the system between 22h00 and 04h00. Testing of the experimental curve could only efficiently be done at night due to the fact that trains needed to be run through the curve at a variety of speeds. The testing equipment in the form of amplifiers, laptops and a generator, as well as the testing team manning the track side equipment would also have resulted in operational clearance issues with trains passing on both lines during normal operations. The special test train used for the collection of rail force data in the experimental curve was therefore an unloaded train with only a driver and test team assistant in the cab of each DMOS.

Figure 3.38 below shows the 4-car test train parked on the HA Line adjacent to the experimental curve on the HB Line prior to testing during engineering hours. The test train changed tracks from the HA Line to the HB Line at the Hatfield Station turnouts, after which test runs were conducted through the test curve in the up and down directions at speeds varying from 10 km/h to 110 km/h in 10 km/h increments and then repeated again after the cant of the experimental curve had been modified.

© University of Pretoria

Figure 3.38: Gautrain 4-Car Test Train Adjacent to the Experimental Curve

3.5.1 Test Train Runs

During the running of the test train through the experimental curve at speeds varying from 10 km/h to 110 km/h in 10 km/h increments the drivers attempted to achieve the target speed for each test run, but given the nature of train handling achieving the exact target speed was not practically possible.

In order to have some data redundancy two test runs were done in each direction as close to each target speed as possible. For the before tamping tests the speeds varied from 10 km/h to 110 km/h in 10 km/h increments, with three tests being done in the down direction at 100 km/h and three tests being done in the up direction at 110 km/h. For the after tamping tests the speeds varied from 10 km/h to 105 km/h in 10 km/h increments, with the final sets of test runs being done at 100 km/h and 105 km/h. 105 km/h was set as the limit for the after tamping test runs, due to the decreased cant (as described in Section 3.3.2) and the extraordinarily high risks associated with taking a train at too high a speed through a curve. The on-site conditions needed to be taken into account, with the possibility of track irregularities such as proud or dipped welded rail joints and track geometry defects. Travelling in the down direction from Hatfield towards Pretoria, the right hand curve that immediately follows the left hand experimental curve (see Figure 3.1) has a design radius of 264.5 m and therefore the test train running in the down direction needed to have slowed down sufficiently to be able to safely negotiate this adjacent curve. In the up direction the test train also needed a sufficient length of track once exiting this adjacent curve in order to get up

© University of Pretoria

to the target speed before reaching the experimental curve. These various on-site conditions therefore governed the maximum test speeds of 110 km/h and 105 km/h before and after tamping respectively.

With reference to Table 3-7 and Table 3-8 a total of 46 test runs were completed before tamping (23 in the up direction and 23 in the down direction), while a total of 44 test runs were completed after tamping (22 in the up direction and 22 in the down direction). There were therefore a total of 90 test runs completed before and after tamping and as there were two test sites within the experimental curve this resulted in 180 data files being recorded.

Table 3-7: Before Tamping Test Train Runs

12-Feb-15	Down	Up
Target Speed (km/h)	No. of Runs	No. of Runs
10.00	2	2
20.00	2	2
30.00	2	2
40.00	2	2
50.00	2	2
60.00	2	2
70.00	2	2
80.00	2	2
90.00	2	2
100.00	3	2
110.00	2	3

Table 3-8: After Tamping Test Train Runs

21-Jul-15	Down	Up
Target Speed (km/h)	No. of Runs	No. of Runs
10.00	2	2
20.00	2	2
30.00	2	2
40.00	2	2
50.00	2	2
60.00	2	2
70.00	2	2
80.00	2	2
90.00	2	2
100.00	2	2
105.00	2	2

© University of Pretoria

3.5.2 Test Train Speeds

With reference to the 46 test runs (see Table 3-7) done before tamping and the 44 test runs (see Table 3-8) done after tamping, before any data analysis could take place, it firstly had to be decided which of the test run files would be analysed in detail. As described in Section 3.5.1 in order to create data redundancy at least 2 test runs were completed in each direction as close to each target speed as possible. All the required data was successfully collected for all 90 test runs, therefore for the purposes of detailed data analysis 1 run in each direction at each speed for test runs before and after tamping was selected based on which of the 2 test runs was closest to the target speed (3 test runs for 100 km/h in the down direction before tamping and 3 test runs for 110 km/h in the up direction before tamping). As mentioned in Section 3.5.1, due to the fact that there were 2 test sites within the experimental curve a total of 180 data files were successfully recorded from the 90 test runs. Once a single data file for each test run speed in each direction had been selected the 180 data files were reduced to 88 data files that needed to be analysed in detail. These 88 data files were the result of there being 2 sites, 2 directions, 11 different speeds, i.e. 2 x 2 x 11 = 44 data files before tamping and 2 sites, 2 directions, 11 different speeds, i.e. 2 x 2 x 11 = 44 after tamping, giving a total of 88 data files before and after tamping.

In order to accurately determine the speed of each test run, the distance between Axle 1 of DMOS A and Axle 1 of DMOS B, as well as the time taken from the recording of the greatest vertical and lateral forces on the high and low legs at each of these two axles, was taken. The Gautrain axle spacing's can be seen in Figure 3.39 and Table 3-9 below. The letters used as spacing symbols in Figure 3.39 are defined in Table 3-9.

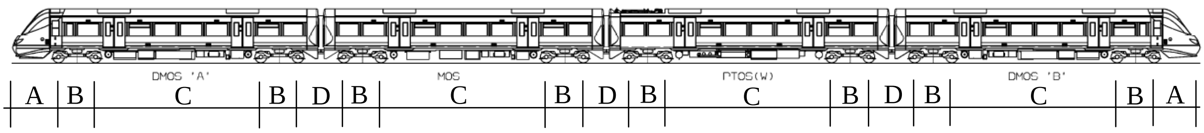

Figure 3.39: Gautrain Axle Spacing's Diagram

© University of Pretoria

Table 3-9: Gautrain Axle Spacing's Table

Axle to Axle Descriptions	Distance (mm)	Spacing Symbol (Fig 4.1)
Front of DMOS A to DMOS A Axle 1	3212	A
DMOS A Axle 1 to DMOS A Axle 2	2600	B
DMOS A Axle 2 to DMOS A Axle 3	11573	C
DMOS A Axle 3 to DMOS A Axle 4	2600	B
DMOS A Axle 4 to MOS A Axle 1	2917	D
MOS Axle 1 to MOS Axle 2	2600	B
MOS Axle 2 to MOS Axle 3	11573	C
MOS Axle 3 to MOS Axle 4	2600	B
MOS Axle 4 to PTOS Axle 1	2917	D
PTOS Axle 1 to PTOS Axle 2	2600	B
PTOS Axle 2 to PTOS Axle 3	11573	C
PTOS Axle 3 to PTOS Axle 4	2600	B
PTOS Axle 4 to DMOS B Axle 4	2917	D
DMOS B Axle 4 to DMOS B Axle 3	2600	B
DMOS B Axle 3 to DMOS B Axle 2	11573	C
DMOS B Axle 2 to DMOS B Axle 1	2600	B
DMOS B Axle 1 to Front of DMOS B	3212	A
TOTAL LENGTH OF TRAIN	82267	

The distance between Axle 1 of DMOS A and Axle 1 of DMOS B is 75843 mm. At a speed of 10 km/h it takes approximately 27.3 s between Axle 1 of DMOS A and Axle 1 of DMOS B to pass over a particular point on the track, while at 110 km/h this time is reduced to 2.5 s.

The average of the speeds calculated at the relevant axles for the greatest vertical forces on the high and low leg and the greatest lateral forces on the high and low leg were used and the test run speeds that were closest to the target speed can be seen in Table 3-10 for the before tamping test runs and in Table 3-11 for the after tamping test runs. The speeds for each of the forces on each of the legs can be seen in their entirety in Appendix A (Table A-1 to Table A-8).

© University of Pretoria

Table 3-10: Actual Speeds of Selected Before Tamping Test Train Runs

12-Feb-15	Site 01 - Down		Site 02 - Down		Site 01 - Up		Site 02 - Up	
Target Speed (km/h)	Run #	Speed (km/h)	Run #	Speed (km/h)	Run #	Speed (km/h)	Run #	Speed (km/h)
10.00	1	11.04	1	11.13	2	11.30	1	11.31
20.00	1	20.75	2	21.60	1	20.79	1	20.79
30.00	1	30.65	2	30.12	2	30.28	2	30.50
40.00	1	40.11	1	39.90	2	39.49	1	39.82
50.00	1	49.64	1	49.26	2	49.84	1	49.92
60.00	2	59.56	1	59.48	2	59.20	2	59.11
70.00	1	68.83	1	68.74	2	69.59	1	68.98
80.00	1	79.17	1	79.08	1	79.30	2	78.94
90.00	1	89.02	1	88.32	1	90.32	1	89.23
100.00	1	101.78	1	102.21	1	97.59	1	97.48
110.00	2	109.18	2	108.75	2	106.32	2	104.81

Table 3-11: Actual Speeds of Selected After Tamping Test Train Runs

21-Jul-15	Site 01 - Down		Site 02 - Down		Site 01 - Up		Site 02 - Up	
Target Speed (km/h)	Run #	Speed (km/h)	Run #	Speed (km/h)	Run #	Speed (km/h)	Run #	Speed (km/h)
10.00	2	11.10	2	11.09	2	10.97	2	11.01
20.00	2	21.02	2	20.87	2	20.55	1	20.39
30.00	2	30.50	2	30.69	1	30.32	1	29.80
40.00	2	40.07	2	40.32	2	40.09	2	39.92
50.00	2	50.15	1	50.09	1	50.10	2	49.68
60.00	2	60.01	2	60.03	2	59.61	2	59.45
70.00	1	69.38	1	69.41	2	69.90	2	69.57
80.00	2	79.42	2	79.57	2	79.84	2	79.66
90.00	2	89.55	2	89.30	2	89.37	2	90.09
100.00	2	98.74	2	99.05	2	99.02	2	99.10
105.00	2	104.02	2	104.12	2	104.70	2	104.24

Typical examples of the data collected during the running of the test trains can be seen in Figure 3.40 and Figure 3.41 below. Figure 3.40 shows typical vertical and lateral rail forces data for a train running at a low speed (approximately 10 km/h), while Figure 3.41 shows typical vertical and lateral rail forces data for a train running at a high speed (approximately 105 km/h). As already mentioned the time taken to cover the distances between the different wheels is entirely speed dependent and this can be seen in the differences between Figure 3.40 (measurements recorded at a low test train run speed) and Figure 3.41 (measurements recorded at a high test train run speed).

© University of Pretoria

As can be seen in Figure 3.40 and Figure 3.41 at low speeds (speeds below the equilibrium speed) the low leg experiences the greatest vertical forces, while at high speeds (speeds above the equilibrium speed) the high leg experiences the greatest vertical forces. Given ideal track and train conditions the low and high leg should experience equal vertical forces at the equilibrium speed. With regard to the lateral forces it is interesting to note how the signs switch from positive to negative and vice versa for specific train wheels in the low versus high speed measurements.

The loading/unloading of the high and low legs dependent on the speed of the train will be analysed in further detail in Chapter 4.

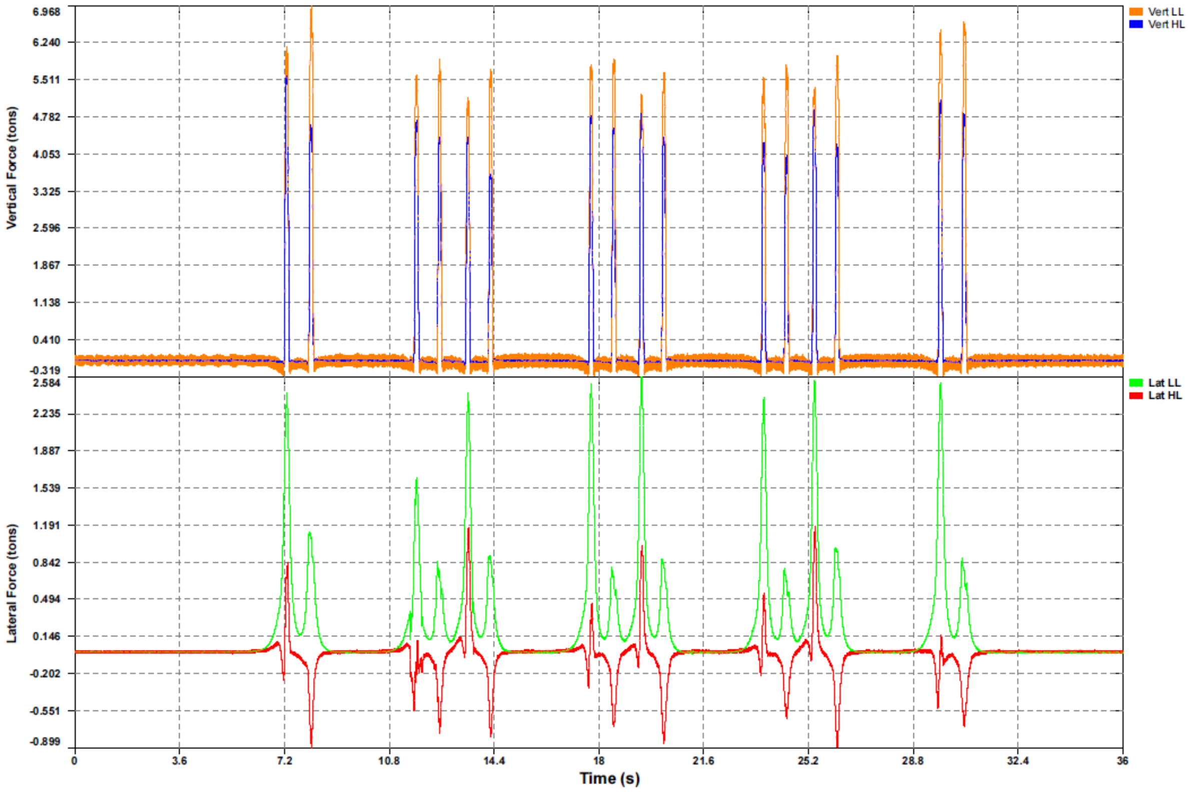

Figure 3.40: Vertical and Lateral Rail Forces After Tamping (10km/h, S2 Up)

© University of Pretoria

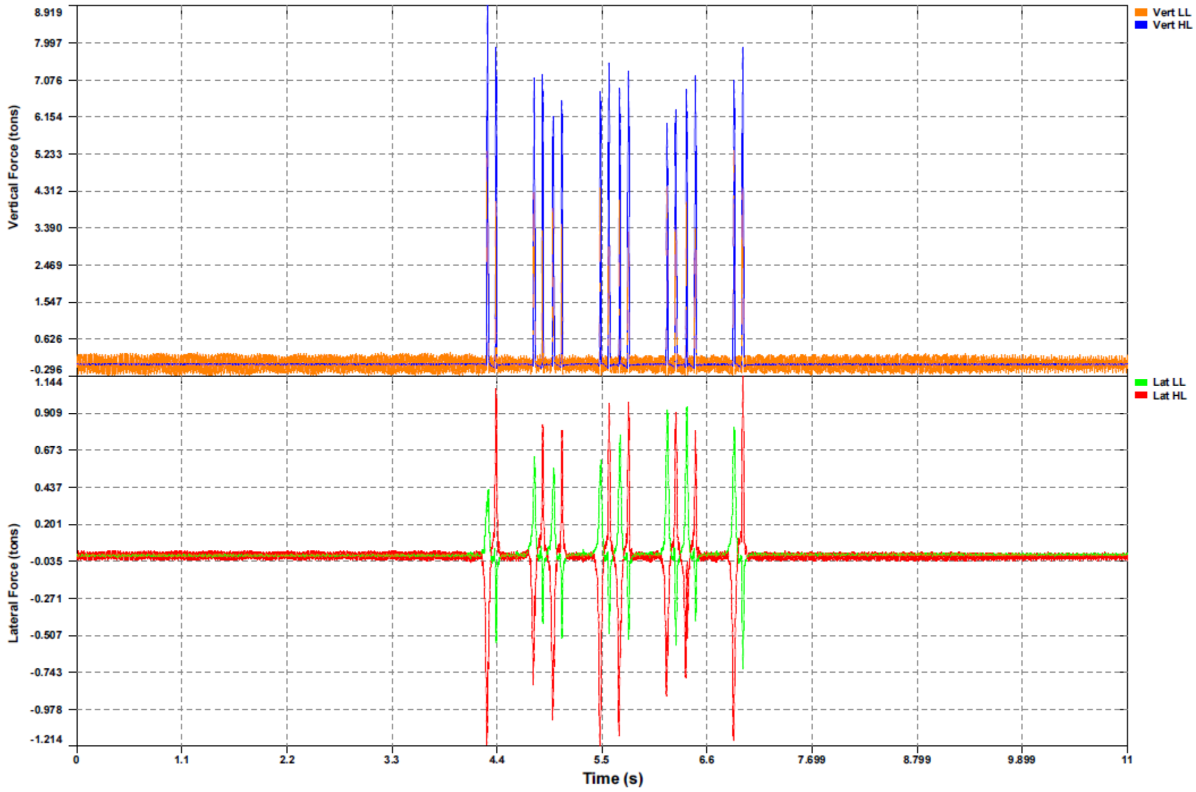

Figure 3.41: Vertical and Lateral Rail Forces After Tamping (105km/h, S2 Up)

Figure 3.40 and Figure 3.41 show a typical 4-car Gautrain consist. The initial four measurements make up either DMOS A or DMOS B of the train depending on the direction of travel. Figure 3.40 and Figure 3.41 show the measurements of rail forces for a train travelling in the up direction (from Pretoria to Hatfield), and therefore the initial four measurements shown are for DMOS A. See Figure 3.39 and Table 3-9 for the distances that the train travelled between the various rail force measurements at the different speeds.

© University of Pretoria

3.5.3 Test Train Loads

In order to be able to interpret the rail force data accurately a detailed understanding of the test train loads was required.

Typical definitions, specifications, mass properties and load balance diagrams are given for the Gautrain cars in Table 3-12 to Table 3-15 and Figure 3.42 below. It must be noted that the information shown is design information which dates back to before the actual building and commissioning of the Gautrain Bombardier Electrostars took place. This information therefore provides guidance in terms of what rail forces to expect in the experimental curve, but the actual forces experienced will provide an indication of what the final actual as-built weights are.

In Table 3-12 passenger weights are 75 kg each throughout.

Table 3-12: Definition of Load States

Tare (AW0)	Service ready, including full working fluids and one driver. No passengers. No other consumables.
Laden (AW1)	As tare plus all seats (fixed and tip-up) occupied.
Fully Laden (AW2)	Laden plus 25% additional passengers standing.
Fully Laden (AW3)	Laden plus 43% additional passengers standing.
Crush (AW4)	All fixed seats occupied (not tip-ups) plus all standing areas occupied at 5.4 passengers/m^2, except aisles <= 0.55 m wide occupied at 1.885 passengers/m. Maximum load for performance calculations.
Crush (AW5)	All fixed seats occupied (not tip-ups) plus all standing areas occupied at 5.4 passengers/m^2. Maximum load for structural calculations and route availability.

© University of Pretoria

Table 3-13: Gautrain Design Specifications for Commuter Units

Weight	DMOS A/B 43457 kg MOS 43457 kg PTOS 39976 kg	
Length	82267 mm	
Width	2800 mm	
Height	3774 mm	
Bogie	Series 3 (Bombardier Bogie Division) 14173 mm between centers 2600 mm Wheel Base	
Wheel Diameter	New Worn	840 mm 776 mm
Axle Load	Mass Tare (AW0) Fully Seated + 43% standing (AW3)	10.4 t 12.4 t
Traction System	12 x 200 kW (268 hp) 3 phase AC squirrel cage asynchronous traction motors	
Battery	2 sets (one per DMOS) nominal voltage 90 V with capacity 80 Ah Nickel Cadmium Cells	
Acceleration Rate	Notch 1 0.23 m/s Notch 2 0.45 m/s Notch 3 0.68 m/s Notch 4 0.90 m/s	
Braking Rate	Step 1 0.29 m/s Step 2 0.59 m/s Step 3 0.88 m/s Emergency 1.17 m/s	

© University of Pretoria

Table 3-14: 4-Car Train Mass Properties

Car Type	Load Condition	Vehicle Mass (kg)	Average Axle Load (kg)	Average Axle Load (t)
4-car Commuter Train (DMOS(B) + PTOS + MOS + DMOS(A))	TARE (AW0)	165935	10371	10.37
	LADEN (AW1)	189195	11825	11.82
	FULLY LADEN (AW2)	195045	12190	12.19
	FULLY LADEN (AW3)	199170	12448	12.45
	CRUSH (AW4)	213795	13362	13.36
	CRUSH (AW5)	214095	13381	13.38
4-car Airport Train (DMOA + PTOA + MOS + DMOS(A))	TARE (AW0)	165191	10324	10.32
	LADEN (AW1)	184701	11544	11.54
	FULLY LADEN (AW2)	AW2 and AW3 loads are not applicable to airport cars, since in normal operation these vehicles are reserved seating only.		
	FULLY LADEN (AW3)			
	CRUSH (AW4)	209526	13095	13.10
	CRUSH (AW5)	210651	13166	13.17

© University of Pretoria

Table 3-15: Commuter Vehicle Mass Properties

Car Type	Load Condition	Passenger Capacity	Vehicle Mass (kg)	Axle Loads (kg)			
				Axle 1	Axle 2	Axle 3	Axle 4
DMOS A/B	TARE (AW0)	0	43250	11434	11369	10249	10198
	LADEN (AW1)	74	48955	12746	12680	11790	11739
	FULLY LADEN (AW2)	93	50380	13088	13023	12160	12109
	FULLY LADEN (AW3)	106	51355	13323	13257	12413	12362
	CRUSH (AW4)	152	54805	14154	14088	13307	13256
	CRUSH (AW5)	153	54880	14168	14102	13331	13280
PTOS	TARE (AW0)	0	40001	10594	10590	9409	9408
	LADEN (AW1)	78	45851	12058	12053	10871	10869
	FULLY LADEN (AW2)	98	47351	12375	12370	11304	11303
	FULLY LADEN (AW3)	113	48476	12485	12480	11756	11755
	CRUSH (AW4)	167	52526	13558	13553	12708	12707
	CRUSH (AW5)	168	52601	13581	13577	12722	12721
MOS	TARE (AW0)	0	39434	9690	9706	10027	10011
	LADEN (AW1)	80	45434	11233	11248	11485	11468
	FULLY LADEN (AW2)	100	46934	11619	11635	11848	11832
	FULLY LADEN (AW3)	114	47984	11890	11905	12102	12086
	CRUSH (AW4)	163	51659	12841	12856	12989	12973
	CRUSH (AW5)	164	51734	12859	12875	13008	12992

© University of Pretoria

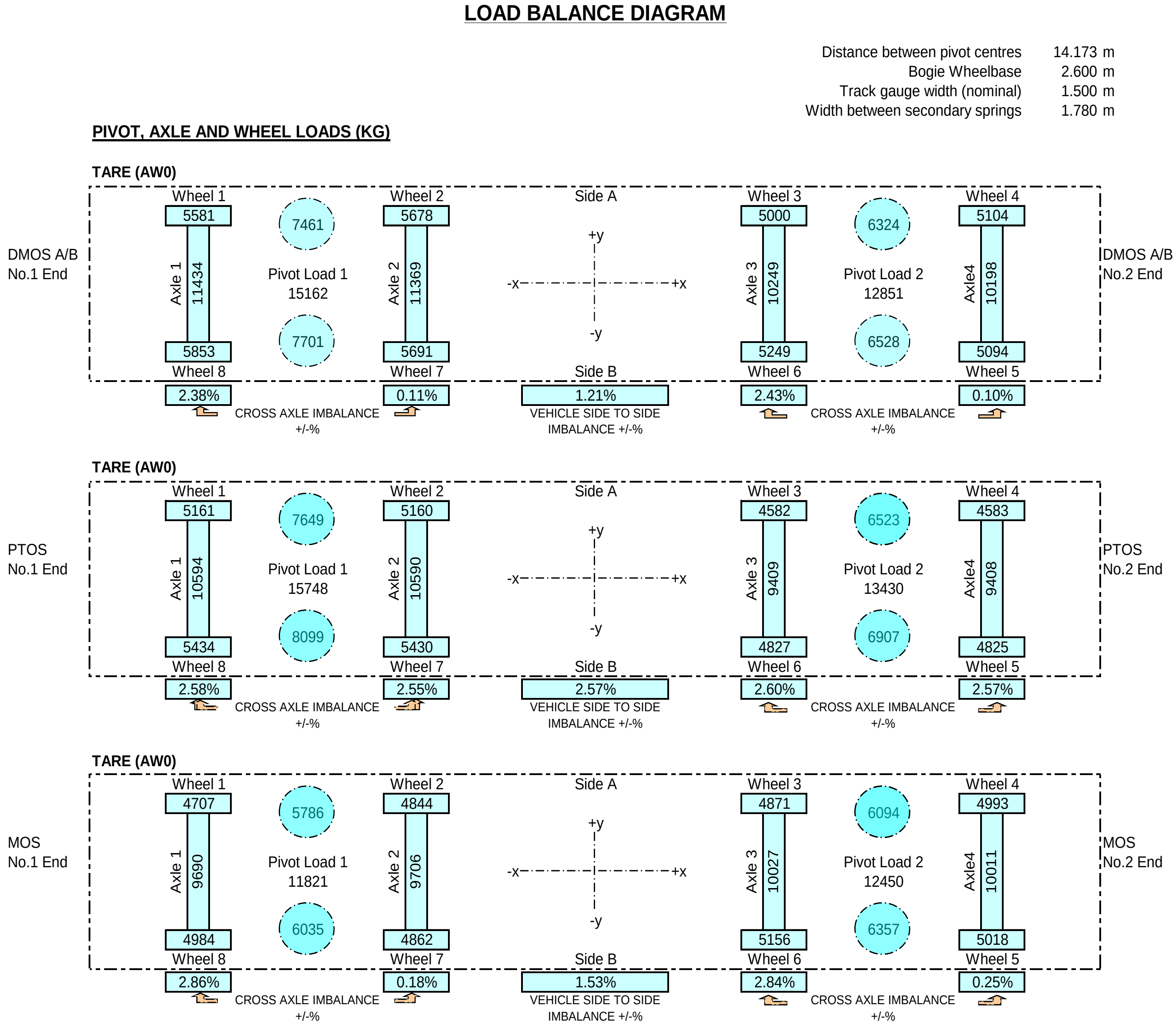

Figure 3.42: Typical Load Balance Diagrams for DMOS A/B, PTOS and MOS

From Table 3-14 it can therefore be concluded that for the purpose of the test train runs load case AW0 was applicable, which refers to a service ready train (including full working fluids and one driver), with no passengers and no other consumables. There were other testing personnel present on the train, but in total there were 4 – 5 people on the train during testing. To classify as load case AW1 all seats need to be occupied, which for a 4-car train means 306 passengers (74 passengers in DMOS(B) + 78 passengers in PTOS + 80 passengers in MOS +74 passengers in DMOS(A)).

From Table 3-14 it can be seen that the applicable average axle loading for the test train could therefore be accepted as being 10.37 t. Summarising Table 3-14 and Table 3-15 to only show the AW0 load case axle loads of the 4-car commuter test train, as well as each commuter test train vehicle results in Table 3-16.

Table 3-16: Axle Loads for Commuter Test Train Load Condition AW0

Car Type	Load Condition	Passenger Capacity	Vehicle Mass (t)	Axle Loads (t)			
				Axle 1	Axle 2	Axle 3	Axle 4
4-car train (DMOS(B) + PTOS + MOS + DMOS(A))	TARE (AW0)	0	165.93	Avg Axle Load = 10.37 t			
DMOS A/B	TARE (AW0)	0	43.25	11.43	11.37	10.25	10.20
PTOS	TARE (AW0)	0	40.00	10.59	10.59	9.41	9.41
MOS	TARE (AW0)	0	39.43	9.69	9.71	10.03	10.01

The information shown in Table 3-16 can be used to determine the vertical wheel load of each of the two wheels on each axle. This is done by simply dividing the axle load in half. The resulting vertical wheel loads for load condition AW0 are shown in Table 3-17.

© University of Pretoria

Table 3-17: Vertical Wheel Loads for Commuter Test Train Load Condition AW0

Car Type	Load Condition	Vertical Wheel Loads (t)							
		Axle 1		Axle 2		Axle 3		Axle 4	
		W1	W8	W2	W7	W3	W6	W4	W5
DMOS A/B	TARE (AW0)	5.72	5.72	5.68	5.68	5.12	5.12	5.10	5.10
PTOS	TARE (AW0)	5.30	5.30	5.29	5.29	4.70	4.70	4.70	4.70
MOS	TARE (AW0)	4.85	4.85	4.85	4.85	5.01	5.01	5.01	5.01

The information shown in Table 3-17 can be used to determine the lateral wheel load of each wheel as a result of the 1:20 rail inclination. This is done by dividing the wheel load by 20. The resulting 1:20 rail inclination lateral wheel loads for load condition AW0 are shown in Table 3-18.

Table 3-18: 1:20 Rail Inclination Lateral Wheel Loads for Load Condition AW0

Car Type	Load Condition	Lateral Wheel Loads (t) due to 1: 20 Rail Inclination							
		Axle 1		Axle 2		Axle 3		Axle 4	
		W1	W8	W2	W7	W3	W6	W4	W5
DMOS A/B	TARE (AW0)	0.29	0.29	0.28	0.28	0.26	0.26	0.25	0.25
PTOS	TARE (AW0)	0.26	0.26	0.26	0.26	0.24	0.24	0.24	0.24
MOS	TARE (AW0)	0.24	0.24	0.24	0.24	0.25	0.25	0.25	0.25

© University of Pretoria

UNIVERSITEIT VAN PRETORIA
UNIVERSITY OF PRETORIA
YUNIBESITHI YA PRETORIA

3.6 DISCUSSION

This chapter commenced by presenting the purpose of the investigation, followed by a detailed description of the experimental sites, and ended off with a comprehensive discussion of the experimental setup.

From a quantitative point of view the vertical and lateral rail forces changed significantly after changing the cant and this will be discussed in detail in Chapter 4. The wheel/rail interaction videos were assessed qualitatively and using this approach made it much harder to determine any clear conclusions from the footage gathered, but the videos are discussed in Chapter 4 nonetheless.

© University of Pretoria

CHAPTER 4 ANALYSIS OF FIELD AND LABORATORY DATA

4.1 INTRODUCTION

This chapter deals with the results from the experimental curve field tests discussed in the previous chapter. The experimental curve field tests are evaluated and the results for the two different curve cant settings are given (February 2015, Average Cant = 107.1 mm and July 2015, Average Cant = 92.0 mm). The experimental curve field test results are then compared against the theoretically expected results.

4.2 ANALYSIS OF CURVE PARAMETERS

With reference to the curve information presented in Section 3.3 and the cant related formulas presented in Section 2.6 the before and after tamping information shown in Table 4-1 could be determined.

Table 4-1: Curve Characteristics Before and After Tamping

	Curve Parameter	Curve Design	Curve Actual	Site 1	Site 2
Before Tamping	Radius Before Tamping (m)	405.0	421.9	Curve Actual	Curve Actual
	Cant Before Tamping (mm)	120.0	107.1	109.9	105.9
	Speed Before Tamping (km/h)	85.0	85.0	85.0	85.0
	h_{eq} Before Tamping (mm)	210.5	202.1	202.1	202.1
	v_{eq} Before Tamping (km/h)	64.2	61.9	62.7	61.5
	h_d Before Tamping (mm)	90.5	95.0	92.2	96.2
After Tamping	Radius After Tamping (m)	405.0	412.2	Curve Actual	Curve Actual
	Cant After Tamping (mm)	120.0	92.0	91.5	92.8
	Speed After Tamping (km/h)	85.0	85.0	85.0	85.0
	h_{eq} After Tamping (mm)	210.5	206.8	206.8	206.8
	v_{eq} After Tamping (km/h)	64.2	56.7	56.5	56.9
	h_d After Tamping (mm)	90.5	114.8	115.3	114.0

From Table 4-1 it can be seen that the designed curve has a cant of 120 mm, an operational speed of 85 km/h and a cant deficiency of 90.5 mm. For the purpose of the design characteristics it is assumed that the design parameters stay constant for the before and after

© University of Pretoria

tamping comparisons that are done with regard to the actual curve data, as well as the site specific data at Site 1 and Site 2 respectively.

For the actual curve, the before tamping properties were a cant of 107.1 mm, with an operational speed of 85 km/h and a cant deficiency of 95.0 mm. After tamping, the cant became 92.0 mm, the operational speed remained 85 km/h and this resulted in a cant deficiency of 114.8 mm.

For Site 1, the before tamping properties were a cant of 109.9 mm, with an operational speed of 85 km/h and a cant deficiency of 92.2 mm. After tamping the Site 1 cant became 91.5 mm, the operational speed remained 85 km/h and this resulted in a cant deficiency of 115.3 mm.

For Site 2, the before tamping properties were a cant of 105.9 mm, with an operational speed of 85km/h and a cant deficiency of 96.2 mm. After tamping, the Site 2 cant became 92.8 mm, the operational speed remained 85 km/h and this resulted in a cant deficiency of 114.0 mm.

In addition to the information shown in Table 4-1, certain speed determined properties as shown in Table 4-2 for before tamping and in Table 4-3 for after tamping could be determined.

Table 4-2: Speed Determined Cant & Acceleration Properties of Curve Before Tamping

Before Tamping						
Speed (km/h)	h_{eq} (mm) (Site 1 & 2)	h_d (mm) (Site 1)	h_d (mm) (Site 2)	Compensated Accelerations (m/s^2) (Site 1 & 2)	Quasi-Static Accelerations (m/s^2) (Site 1)	Quasi-Static Accelerations (m/s^2) (Site 2)
0	0.000	-109.900	-105.900	0.000	-0.719	-0.693
10	2.797	-107.103	-103.103	0.018	-0.700	-0.674
20	11.187	-98.713	-94.713	0.073	-0.646	-0.619
30	25.172	-84.728	-80.728	0.165	-0.554	-0.528
40	44.750	-65.150	-61.150	0.293	-0.426	-0.400
50	69.922	-39.978	-35.978	0.457	-0.262	-0.235
60	100.687	-9.213	-5.213	0.658	-0.060	-0.034
70	137.047	27.147	31.147	0.896	0.177	0.204
80	179.000	69.100	73.100	1.170	0.452	0.478
90	226.547	116.647	120.647	1.481	0.763	0.789
100	279.687	169.787	173.787	1.829	1.110	1.136
110	338.421	228.521	232.521	2.213	1.494	1.520
120	402.749	292.849	296.849	2.634	1.915	1.941

© University of Pretoria

Table 4-3: Speed Determined Cant & Acceleration Properties of Curve After Tamping

After Tamping						
Speed (km/h)	h_{eq} (mm) (Site 1 & 2)	h_d (mm) (Site 1)	h_d (mm) (Site 2)	Compensated Accelerations (m/s^2) (Site 1 & 2)	Quasi-Static Accelerations (m/s^2) (Site 1)	Quasi-Static Accelerations (m/s^2) (Site 2)
0	0.000	-91.500	-92.800	0.000	-0.598	-0.607
10	2.863	-88.637	-89.937	0.019	-0.580	-0.588
20	11.451	-80.049	-81.349	0.075	-0.524	-0.532
30	25.764	-65.736	-67.036	0.168	-0.430	-0.438
40	45.803	-45.697	-46.997	0.300	-0.299	-0.307
50	71.567	-19.933	-21.233	0.468	-0.130	-0.139
60	103.057	11.557	10.257	0.674	0.075	0.067
70	140.272	48.772	47.472	0.917	0.319	0.310
80	183.212	91.712	90.412	1.198	0.600	0.591
90	231.878	140.378	139.078	1.516	0.918	0.909
100	286.269	194.769	193.469	1.872	1.274	1.265
110	346.385	254.885	253.585	2.265	1.667	1.658
120	412.227	320.727	319.427	2.696	2.097	2.089

The information shown in Table 4-1, Table 4-2 and Table 4-3 was used to graphically represent the cant excess and cant deficiency of Site 1 before and after tamping as shown in Figure 4.1 and of Site 2 before and after tamping as shown in Figure 4.2. All cant values to the left of the equilibrium speed are cant excess (i.e. cant < 0 mm), while all cant values to the right of the equilibrium speed are cant deficiency (i.e. cant > 0 mm).

As can be seen numerically in Table 4-1 and graphically in Figure 4.1 and Figure 4.2, the theoretically calculated equilibrium speed for Site 1 before and after tamping is 62.7 km/h and 56.5 km/h respectively and the theoretically calculated equilibrium speed for Site 2 before and after tamping is 61.5 km/h and 56.9 km/h respectively. Reducing the cant from 109.9 mm to 91.5 mm for Site 1 and from 105.9 mm to 92.8 mm for Site 2 therefore resulted in a decrease in the theoretically calculated equilibrium speed for Site 1 and Site 2 of 6.1 km/h and 4.6 km/h respectively. Operating the trains through the curve at the indicated speeds for either site within the curve would result in a 0 mm cant deficiency, as opposed to the cant deficiencies that exist for the current operational speed of 85 km/h as indicated in Table 4-1. The results from the measured data are discussed in Section 4.4.

Table 4-4 shows the relationship between a decrease in cant with the corresponding decrease in equilibrium speed. It is interesting to note that if the percentage cant change is known the corresponding percentage equilibrium speed change can be calculated by multiplying the

© University of Pretoria

percentage cant change by 0.6 or alternatively if the percentage equilibrium speed change is known the corresponding percentage cant change can be calculated by multiplying the percentage equilibrium speed change by 1.7. It must be noted that these factors only hold true if the larger cant and equilibrium speed values are used as references for the percentage changes.

Table 4-4: Speed Determined Properties of Curve Before and After Tamping

Curve Parameter	Curve Design	Curve Actual	Site 1	Site 2
Cant Before Tamping (mm)	120.0	107.1	109.9	105.9
Cant After Tamping (mm)	120.0	92.0	91.5	92.8
Δ Cant (mm) (Cant Decrease)	0.0	15.1	18.4	13.1
% Cant Change	0.0	14.1	16.7	12.4
V_{eq} Before Tamping (km/h)	64.2	61.9	62.7	61.5
V_{eq} After Tamping (km/h)	64.2	56.7	56.5	56.9
Δ V_{eq} (km/h) (V_{eq} Decrease)	0.0	5.2	6.1	4.6
% V_{eq} Change	0.0	8.4	9.8	7.5
% V_{eq} Change : % Cant Change	N/A	0.6	0.6	0.6
% Cant Change : % V_{eq} Change	N/A	1.7	1.7	1.7

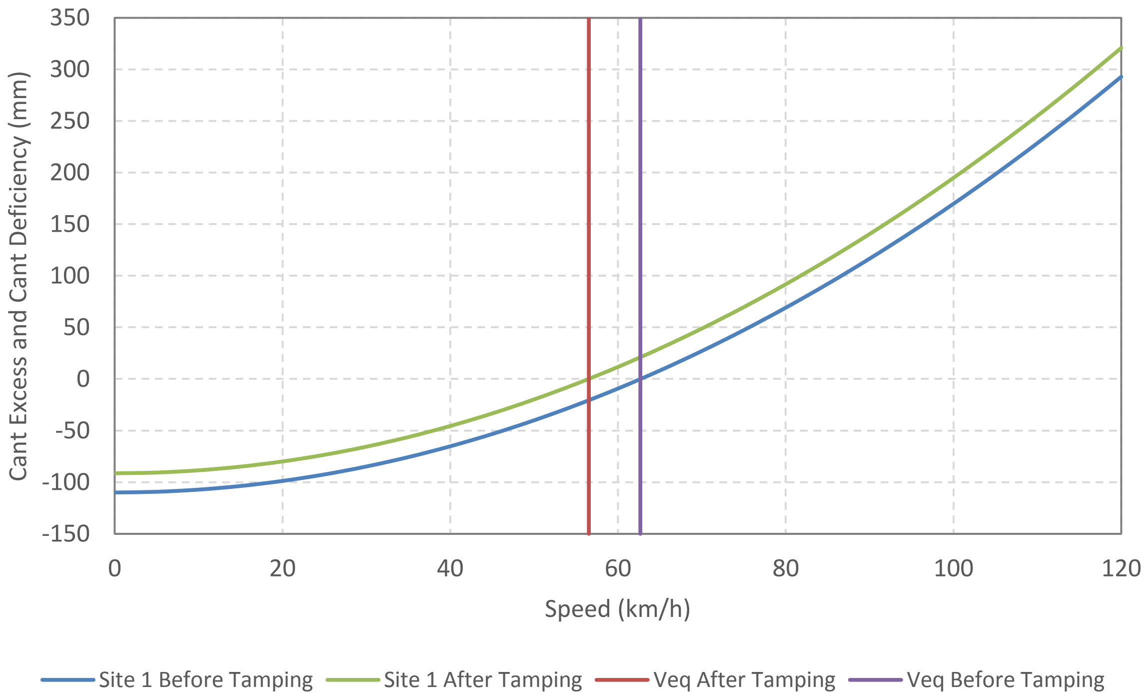

Figure 4.1: Cant Excess and Cant Deficiency Before and After Tamping – S1

© University of Pretoria

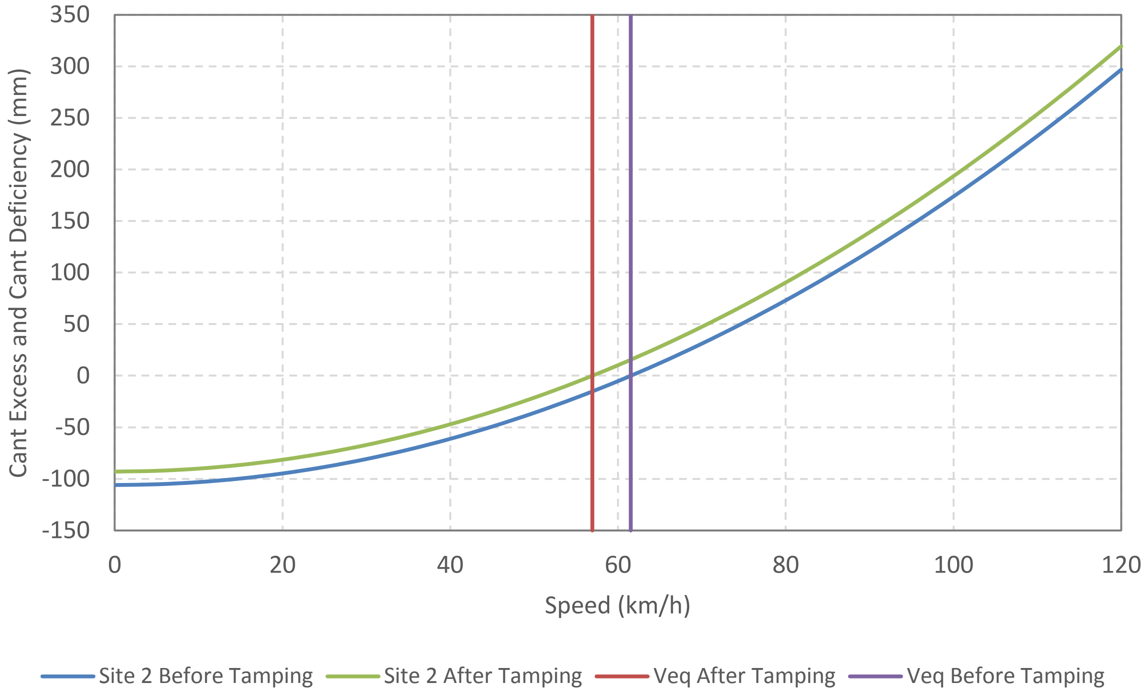

Figure 4.2: Cant Excess and Cant Deficiency Before and After Tamping – S2

4.3 WHEEL UNLOADING CALCULATIONS

With reference to the formulas derived in Section 2.6.2 with regard to wheel unloading, the forces resulting from a train negotiating the experimental sites could be calculated.

The "Vehicle Mass" and "Vehicle Centre of Gravity" parameters used were those for a DMOS A/B vehicle as these are the vehicles where the maximum vertical and lateral forces were measured during the test runs. Figure 4.3 provides an overview of how the centre of gravity coordinates system is defined, while Figure 3.42 provides further clarity with regard to the definition of the x and y coordinates (in terms of No. 1 and No. 2 end, Side A and Side B, as well as the signage of the x and y coordinates).

Table 4-5 provides the centre of gravity coordinates for the DMOS A/B, PTOS and MOS vehicles for the various possible load conditions.

The calculated forces resulting from a train negotiating the experimental sites at equilibrium speed are shown in Table 4-6 and Table 4-7. The variables used in Table 4-6 and Table 4-7 were the actual measured radii's of the curve before and after tamping, as well as the actual measured cants of Site 1 and Site 2 before and after tamping.

© University of Pretoria

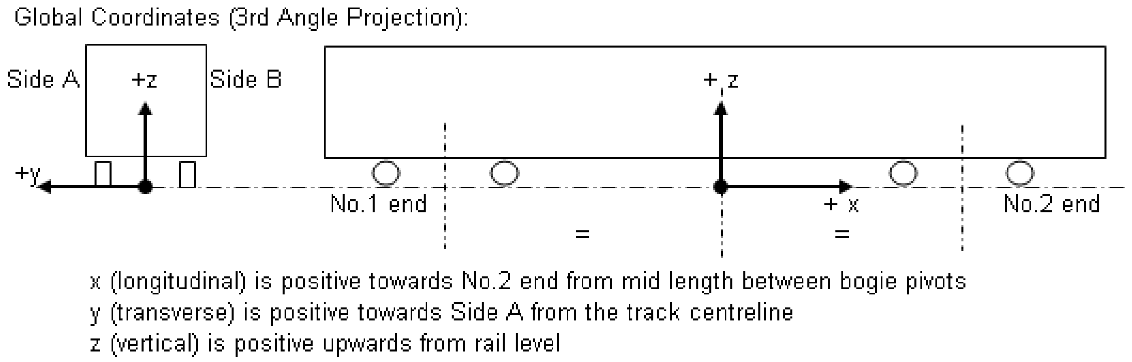

Figure 4.3: Centre of Gravity Coordinate System on the Gautrain

Table 4-5: Gautrain Centre of Gravity Information

Car Type	Load Condition	Mass (kg)	Centre of Gravity (m)		
			x	y	z
DMOS A/B	TARE (AW0)	43250	-0.390	-0.009	1.277
	LADEN (AW1)	48955	-0.278	-0.010	1.332
	FULLY LADEN (AW2)	50380	-0.263	-0.010	1.353
	FULLY LADEN (AW3)	51355	-0.253	-0.010	1.367
	CRUSH (AW4)	54805	-0.220	-0.011	1.414
	CRUSH (AW5)	54880	-0.217	-0.011	1.415
PTOS	TARE (AW0)	40001	-0.420	-0.019	1.345
	LADEN (AW1)	45851	-0.367	-0.018	1.398
	FULLY LADEN (AW2)	47351	-0.320	-0.018	1.420
	FULLY LADEN (AW3)	48476	-0.213	-0.018	1.435
	CRUSH (AW4)	52526	-0.229	-0.020	1.491
	CRUSH (AW5)	52601	-0.231	-0.020	1.492
MOS	TARE (AW0)	39434	0.115	-0.012	1.289
	LADEN (AW1)	45434	0.074	-0.017	1.351
	FULLY LADEN (AW2)	46934	0.064	-0.016	1.375
	FULLY LADEN (AW3)	47984	0.058	-0.016	1.390
	CRUSH (AW4)	51659	0.036	-0.015	1.442
	CRUSH (AW5)	51734	0.036	-0.015	1.443

© University of Pretoria

In order to determine the equilibrium speeds as highlighted in green in Table 4-6 and Table 4-7 an iteration process was followed in which the "Vehicle Speed" variable was continually adjusted until R_{LL} equalled R_{RL}.

Table 4-6: Wheel Unloading Calculations Before and After Tamping – S1

Curving Wheel Unloading Calculations				
SITE 1				
Variables Needed:	Before Tamping		After Tamping	
Curve radius (R)	421.9	m	412.2	m
Vehicle mass (M)	43250	kg	43250	kg
Track gauge (2a)	1.500	m	1.500	m
Vehicle Centre of Gravity (H)	1.277	m	1.277	m
Gravitational acceleration (g)	9.81	m/s^2	9.81	m/s^2
Track cant (to calculate alpha)	0.1099	m	0.0915	m
Vehicle Speed (v)	62.8	km/h	56.6	km/h
Calculated Variables:				
Alpha (θ)	0.073	rad	0.061	rad
Axle load	10.813	t	10.813	t
h_{eq} (Equation 2-7)	0.110	m	0.092	m
Calculated Forces:				
R_{LL} (Equation 2-9)	21.69	t	21.67	t
R_{HL} (Equation 2-10)	21.69	t	21.67	t
U (Equation 2-11)	3.18	t	2.64	t
F (Equation 2-12)	0.00	t	0.00	t

© University of Pretoria

Table 4-7: Wheel Unloading Calculations Before and After Tamping – S2

Curving Wheel Unloading Calculations				
SITE 2				
Variables Needed:	Before Tamping		After Tamping	
Curve radius (R)	421.9	m	412.2	m
Vehicle mass (M)	43250	kg	43250	kg
Track gauge (2a)	1.500	m	1.500	m
Vehicle Centre of Gravity (H)	1.277	m	1.277	m
Gravitational acceleration (g)	9.81	m/s^2	9.81	m/s^2
Track cant (to calculate alpha)	0.1059	m	0.0928	m
Vehicle Speed (v)	61.6	km/h	57.0	km/h
Calculated Variables:				
Alpha (θ)	0.071	rad	0.062	rad
Axle load	10.813	t	10.813	t
h_{eq} (Equation 2-7)	0.106	m	0.093	m
Calculated Forces:				
R_{LL} (Equation 2-9)	21.69	t	21.67	t
R_{HL} (Equation 2-10)	21.69	t	21.67	t
U (Equation 2-11)	3.06	t	2.68	t
F (Equation 2-12)	0.00	t	0.00	t

Referring to the "Vehicle Speed" results from Table 4-6 and Table 4-7 that were determined by balancing the R_{LL} and R_{RL} results and comparing them to the "Equilibrium Speed" results from Equation 2-9 (as shown in Table 4-1), it can be seen that the first principle calculations as defined in Section 2.6.2 correspond almost exactly with the results from "Equilibrium Speed" equation. Table 4-8 provides a summary between the Equation 2-9 "Equilibrium Speed" results and the first principle "Vehicle Speed" results.

Table 4-8: Equilibrium Speed Calculation Comparisons

Equilibrium Speed (km/h)	Site 1		Site 2	
	Before Tamping	After Tamping	Before Tamping	After Tamping
V_{eq} (Equation 2-9)	62.7	56.5	61.5	56.9
V_{eq} (1st Principles)	62.8	56.6	61.6	57.0

© University of Pretoria

Further calculations were performed to assess what the theoretically expected forces at the operational speed of 85 km/h before and after tamping were.

The calculated forces resulting from a train negotiating the experimental sites at the operational speed of 85 km/h are shown in Table 4-9 and Table 4-10. As with the calculations shown in Table 4-6 and Table 4-7, the variables used in Table 4-9 and Table 4-10 were the actual measured radii's of the curve before and after tamping, as well as the actual measured cants of Site 1 and Site 2 before and after tamping.

It can be seen from the calculations shown in Table 4-9 and Table 4-10 that reducing the cant at Site 1 resulted in the calculated lateral force on the outside of the raised wheel increasing from 2.64 t to 3.31 t (25.4% increase), while reducing the cant at Site 2 resulted in the calculated lateral force on the outside of the raised wheel increasing from 2.76 t to 3.28 t (18.8% increase). The intention of reducing the cant was not to increase the lateral forces experienced in the curve. The experiment of reducing the cant was nonetheless carried out based on the perceived operational train dynamics through the curve at the original cant. The measured before and after tamping field test results are discussed in detail in Section 4.4 and Section 4.5.

© University of Pretoria

Table 4-9: Operational Speed Force Calculations Before and After Tamping – S1

Curving Wheel Unloading Calculations				
SITE 1				
Variables Needed:	Before Tamping		After Tamping	
Curve radius (R)	421.9	m	412.2	m
Vehicle mass (M)	43250	kg	43250	kg
Track gauge (2a)	1.500	m	1.500	m
Vehicle Centre of Gravity (H)	1.277	m	1.277	m
Gravitational acceleration (g)	9.81	m/s^2	9.81	m/s^2
Track cant (to calculate alpha)	0.1099	m	0.0915	m
Vehicle Speed (v)	85.00	km/h	85.00	km/h
Calculated Variables:				
Alpha (θ)	0.073	rad	0.061	rad
Axle load	10.813	t	10.813	t
h_{eq} (Equation 2-7)	0.202	m	0.207	m
Calculated Forces:				
R_{LL} (Equation 2-9)	19.54	t	18.95	t
R_{HL} (Equation 2-10)	24.04	t	24.60	t
U (Equation 2-11)	5.83	t	5.96	t
F (Equation 2-12)	2.64	t	3.31	t

© University of Pretoria

Table 4-10: Operational Speed Force Calculations Before and After Tamping – S2

Curving Wheel Unloading Calculations				
SITE 2				
Variables Needed:	Before Tamping		After Tamping	
Curve radius (R)	421.9	m	412.2	m
Vehicle mass (M)	43250	kg	43250	kg
Track gauge (2a)	1.500	m	1.500	m
Vehicle Centre of Gravity (H)	1.277	m	1.277	m
Gravitational acceleration (g)	9.81	m/s^2	9.81	m/s^2
Track cant (to calculate alpha)	0.1059	m	0.0928	m
Vehicle Speed (v)	85.00	km/h	85.00	km/h
Calculated Variables:				
Alpha (θ)	0.071	rad	0.062	rad
Axle load	10.813	t	10.813	t
h_{eq} (Equation 2-7)	0.202	m	0.207	m
Calculated Forces:				
R_{LL} (Equation 2-9)	19.44	t	18.99	t
R_{HL} (Equation 2-10)	24.13	t	24.56	t
U (Equation 2-11)	5.83	t	5.96	t
F (Equation 2-12)	2.76	t	3.28	t

4.4 ANALYSIS OF TEST TRAIN RAIL AND TRACK FORCES DATA

When no train is present on a particular point of rail the vertical and lateral rail forces are both zero. This can be seen in Figure 3.40 and Figure 3.41 by the fact that even when a train is passing over the test site the measured forces become zero in between wheels (albeit with some measurement signal noise about zero on the Y-axis and/or the effect of strain build up in the rails).

For vertical forces only positive rail forces are measured, as the presence of the train results in positive forces being measured (as per the sign convention shown in Figure 3.30), while the absence of a train implies the presence of no vertical forces.

For lateral forces both positive and negative rail forces are measured (as per the sign convention shown in Figure 3.30), while the absence of a train implies the presence of no lateral forces.

© University of Pretoria

Tables were drawn up that show all the forces measured for each wheel on each leg for each analysed test run. Table 4-11 provides an example of one these tables, while the rest of these wheel force data summary tables are shown in Appendix B (Table B-1 to Table B-15).

A 3-colour scale is used to visually present the results for each test run, so as to provide an indication of the trend as to where the maximum and minimum (both positive and negative) forces occur. The lowest value of the 32 measured wheel forces for each test train is highlighted in red, while the highest value is highlighted in green. The midpoint value is highlighted in white, with the scale progressing through lighter shades of red and green towards the midpoint value. For ease of reference, the maximum and minimum values for each run are also shown in bold italics and are double underlined.

© University of Pretoria

Table 4-11: Vertical Forces Before Tamping (Wheels) – S1 Down

Hatfield to Pretoria (Down) km 3.215 (Site 1) Before Tamping		km/h										
		11.04	20.75	30.65	40.11	49.64	59.56	68.83	79.17	89.02	101.78	109.18
Car Type and Axle	Wheel and Rail Leg	Vertical Force (t)										
DMOS B Axle 1	Wheel 8 - High Leg	6.15	5.52	5.50	5.84	***6.14***	***6.36***	6.50	6.86	6.98	7.57	8.12
	Wheel 1 - Low Leg	6.90	6.42	6.38	6.27	6.01	5.62	5.41	5.13	5.10	4.74	4.80
DMOS B Axle 2	Wheel 7 - High Leg	4.94	4.97	5.12	5.13	5.95	6.20	***6.51***	***6.96***	***7.27***	***8.05***	***8.44***
	Wheel 2 - Low Leg	7.02	6.76	***6.77***	6.51	5.91	5.87	5.32	5.23	4.72	4.45	4.66
DMOS B Axle 3	Wheel 6 - High Leg	5.43	4.82	4.87	4.97	5.19	5.33	5.61	5.86	6.31	7.19	7.68
	Wheel 3 - Low Leg	6.08	5.80	5.78	5.63	5.31	5.40	5.04	4.97	4.62	4.08	3.79
DMOS B Axle 4	Wheel 5 - High Leg	4.50	4.53	4.77	4.71	5.09	5.33	5.68	6.22	6.78	7.39	7.79
	Wheel 4 - Low Leg	6.20	5.98	5.87	5.81	5.29	5.18	4.85	4.50	4.23	3.67	***3.24***
PTOS Axle 4	Wheel 4 - High Leg	5.31	4.35	4.41	4.48	5.08	5.14	5.38	5.56	5.75	6.30	6.57
	Wheel 5 - Low Leg	5.67	5.45	5.37	5.33	5.01	4.91	***4.61***	***4.04***	***4.02***	3.98	3.49
PTOS Axle 3	Wheel 3 - High Leg	***3.64***	***3.58***	***3.75***	***3.80***	***4.33***	***4.58***	4.99	5.39	5.78	6.29	6.68
	Wheel 6 - Low Leg	6.38	6.08	6.00	5.86	5.48	5.26	4.78	4.40	4.07	3.78	3.56
PTOS Axle 2	Wheel 2 - High Leg	5.70	4.91	4.93	5.00	5.49	5.54	5.67	6.03	6.54	7.18	7.56
	Wheel 7 - Low Leg	6.32	5.97	6.03	5.82	5.38	5.56	5.30	5.16	4.67	4.34	4.04
PTOS Axle 1	Wheel 1 - High Leg	4.77	4.92	5.07	5.13	5.67	5.79	6.13	6.42	6.92	7.70	8.06
	Wheel 8 - Low Leg	6.38	5.98	5.81	5.72	5.16	5.04	4.73	4.50	4.12	3.63	3.37
MOS Axle 4	Wheel 4 - High Leg	5.48	4.92	4.92	5.07	5.45	5.70	5.84	6.09	6.54	7.13	7.44
	Wheel 5 - Low Leg	5.91	5.54	5.46	5.41	4.83	4.81	4.72	4.38	4.18	***3.55***	3.52
MOS Axle 3	Wheel 3 - High Leg	4.20	4.23	4.31	4.34	4.87	5.22	5.61	6.09	6.55	7.17	7.33
	Wheel 6 - Low Leg	6.29	6.09	6.07	6.04	5.46	5.22	5.07	4.51	4.21	3.57	3.43
MOS Axle 2	Wheel 2 - High Leg	5.13	4.74	4.92	5.06	5.35	5.45	5.58	5.96	6.23	6.77	7.12
	Wheel 7 - Low Leg	5.60	5.35	5.27	5.22	4.82	4.79	4.86	4.27	4.32	3.95	4.07
MOS Axle 1	Wheel 1 - High Leg	4.06	4.09	4.34	4.35	4.72	4.84	5.06	5.37	5.63	6.45	6.75
	Wheel 8 - Low Leg	6.06	5.84	5.72	5.63	5.26	5.21	4.95	4.81	4.44	3.95	3.69
DMOS A Axle 4	Wheel 4 - High Leg	5.39	4.96	4.95	5.15	5.62	5.75	6.06	6.29	6.83	7.23	7.76
	Wheel 5 - Low Leg	5.86	5.63	5.56	5.41	5.13	4.76	4.62	4.37	4.23	3.89	3.49
DMOS A Axle 3	Wheel 3 - High Leg	4.04	4.03	4.18	4.20	4.70	5.09	5.37	5.91	6.43	6.92	7.37
	Wheel 6 - Low Leg	6.56	6.43	6.33	6.47	5.86	5.52	5.27	5.09	4.56	3.85	3.84
DMOS A Axle 2	Wheel 2 - High Leg	5.86	5.49	5.64	5.94	6.13	6.33	6.35	6.60	6.70	7.31	7.91
	Wheel 7 - Low Leg	6.67	6.31	6.22	5.99	5.72	5.60	5.56	5.37	5.34	4.67	4.62
DMOS A Axle 1	Wheel 1 - High Leg	4.70	4.95	5.07	5.07	5.66	5.88	6.22	6.56	6.81	7.63	8.04
	Wheel 8 - Low Leg	***7.15***	***6.87***	6.69	***6.70***	6.06	5.93	5.82	5.47	4.94	4.41	3.95

© University of Pretoria

In order to interpret the measured data, a selection process had to be undertaken in order to assess which wheels, on which axle, on which bogie and on which car were contributing to the greatest loadings (both positive and negative) on each rail leg.

As a starting point the before tamping data was analysed in order to determine which wheels to focus the analysis on, and from the before tamping wheel selections, the same wheels were assessed after tamping and compared to the before tamping results.

Figure 4.4 shows which wheels were chosen for analysis for the test runs in the down (Hatfield – Pretoria) and up (Pretoria – Hatfield) directions.

© University of Pretoria

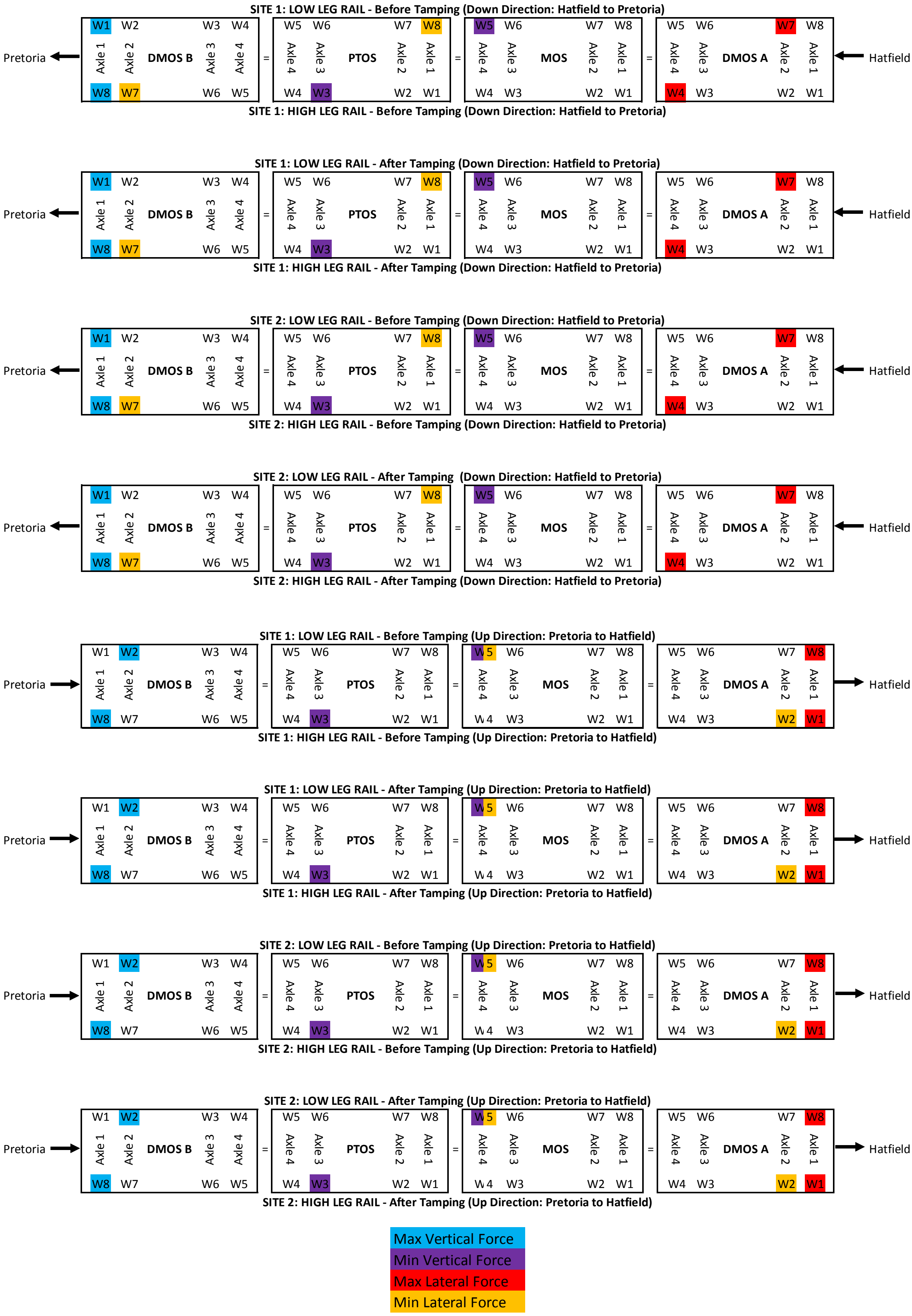

Figure 4.4: Before and After Tamping Analysed Wheels

© University of Pretoria

In Section 4.4.1 and Section 4.4.2 the locations of the various analysed wheel positions, specifically with reference to the direction in which the test train was travelling are discussed.

4.4.1 Maximum and Minimum Vertical Force Wheel Positions

The maximum vertical force on the high leg remained in the same absolute bogie, axle and wheel position (DMOS B 8) on the train for both directions of travel. In the down direction DMOS B 8 is on leading axle of the leading bogie of the leading vehicle of the 4-car train (DMOS B), whereas in the up direction DMOS B 8 is on trailing axle of the trailing bogie of the rear vehicle of the 4-car train (DMOS B).

The maximum vertical force on the low leg remained in the same absolute bogie position, and remained in the same relative axle position in reference to this bogie, namely DMOS B 1 in the down direction and DMOS B 2 in the up direction. In the down direction DMOS B 1 is on leading axle of the leading bogie of the leading vehicle of the 4-car train (DMOS B), whereas in the up direction DMOS B 2 is on leading axle of the trailing bogie of the rear vehicle of the 4-car train (DMOS B).

The minimum vertical force on the high leg remained in the same absolute bogie, axle and wheel position (PTOS 3) on the train for both directions of travel. In the down direction PTOS 3 is on trailing axle of the leading bogie of the second vehicle of the 4-car train (PTOS), whereas in the up direction PTOS 3 is on leading axle of the trailing bogie of the third vehicle of the 4-car train (PTOS).

The minimum vertical force on the low leg remained in the same absolute bogie, axle and wheel position (MOS 5) on the train for both directions of travel. In the down direction MOS 5 is on leading axle of the leading bogie of the third vehicle of the 4-car train (MOS), whereas in the up direction MOS 5 is on trailing axle of the trailing bogie of the second vehicle of the 4-car train (MOS).

In summary it is therefore interesting to note that of the four vertical forces under consideration (vertical maximum and minimum for both the high leg and the low leg), three of them (DMOS B 8, PTOS 3 and MOS 5) stayed in the exact same absolute position on the train for both the down and the up direction, while the other one (DMOS B 1 vs. DMOS B 2) stayed in the same absolute bogie position and the same relative axle position in reference to this bogie for the down versus the up direction.

© University of Pretoria

4.4.2 Maximum and Minimum Lateral Force Wheel Positions

The maximum lateral force on the high leg remained in the same relative position (DMOS A 4 vs. DMOS A 1) on a specific vehicle for the down versus the up direction. In the down direction DMOS A 4 is on leading axle of the leading bogie of the trailing vehicle of the 4-car train (DMOS A), whereas in the up direction DMOS A 1 is on leading axle of the leading bogie of the leading vehicle of the 4-car train (DMOS A).

The maximum lateral force on the low leg remained in the same relative axle position on the same bogie on the same vehicle (DMOS A 7 vs. DMOS A 8) for the down versus the up direction. In the down direction DMOS A 7 is on leading axle of the trailing bogie of the rear vehicle of the 4-car train (DMOS A), whereas in the up direction DMOS A 8 is on leading axle of the leading bogie of the leading vehicle of the 4-car train (DMOS A).

The minimum lateral force on the high leg remained in the same relative position (DMOS B 7 vs. DMOS A 2) on the train for both directions of travel. In the down direction DMOS B 7 is on trailing axle of the leading bogie of the leading vehicle of the 4-car train (DMOS B), whereas in the up direction DMOS A 2 is on trailing axle of the leading bogie of the leading vehicle of the 4-car train (DMOS A).

The minimum lateral force on the low leg remained in the same relative position (PTOS 8 vs. MOS 5) on the train for both directions of travel. In the down direction PTOS 8 is on trailing axle of the trailing bogie of the second vehicle of the 4-car train (PTOS), whereas in the up direction MOS 5 is on trailing axle of the trailing bogie of the second vehicle of the 4-car train (MOS).

In summary it is interesting to note that of the four lateral forces under consideration (lateral maximum and minimum for both the high leg and the low leg), none of them stayed in the exact same absolute position on the train for both the up and the down directions. Instead two of them (DMOS B 7 vs. DMOS A 2 and PTOS 8 vs. MOS 5) stayed in the same relative position on the train for the down versus the up direction. One of them (DMOS A 4 vs. DMOS A 1) stayed in the same relative position on a specific vehicle for the down versus the up direction. The last one (DMOS A 7 vs. DMOS A 8) stayed in the same relative axle position on the same bogie on the same vehicle for the down versus the up direction.

© University of Pretoria

4.4.3 Maximum and Minimum Force Values for Wheels

Using the forces summary data shown in Table 4-11 and Appendix B in conjunction with the wheels referred to in Figure 4.4, balancing force graphs for the vertical and lateral forces at the various speeds could be plotted as shown in Appendix C.

Adding trend lines and determining the equations of these trend lines (as shown on the graphs in Appendix C) allowed for the intersection points between the high and low legs, vertical and lateral forces before and after tamping to be determined. Appendix D summarises the trend line information for each of the balancing force graphs. For the wheel forces data linear trend lines provided acceptable levels of reliability and were therefore used.

Although the wheel positions and magnitudes of the minimum forces were assessed for Site 1 and Site 2 in the up and down directions, these results relative to the results that were assessed for the maximum forces turned out to be insignificant in terms of the overall wheel/rail interaction forces. Beyond being shown in Table 4-12 to Table 4-15 there were therefore no further discussions around the results of the minimum forces.

Solving for the equations shown on the balancing force graphs and summarised in Appendix D yields the balance forces and speeds shown in Table 4-12 to Table 4-15. The Δ x (%) and Δ y (%) refers to the percentage change relative to the before tamping results. Table 4-12 shows the balance forces and speeds for Site 1 in the down direction.

Table 4-12: Force Balancing (Wheels) – S1 Down

	SITE 1: DOWN	Before Tamping		After Tamping		Δ x	Δ x	Δ y	Δ y
		x (km/h)	y (t)	x (km/h)	y (t)	(km/h)	(%)	(t)	(%)
Verticals	HL Max DMOS B 8 LL Max DMOS B 1	42.3	6.1	76.8	6.8	34.6	81.8	0.7	11.8
Verticals	HL Min PTOS 3 LL Min MOS 5	59.2	4.8	82.9	5.2	23.6	39.9	0.4	8.7
Laterals	HL Max DMOS A 4 LL Max DMOS A 7	139.3	2.0	163.4	-0.2	24.1	17.3	-2.2	-109.5
Laterals	HL Min DMOS B 7 LL Min PTOS 8	57.0	-0.2	63.6	-0.1	6.6	11.6	0.1	54.3

© University of Pretoria

For Site 1 in the down direction the balanced maximum vertical forces for the high and low legs were analysed for the following wheels: DMOS B 8 and DMOS B 1. Referring to Table 3-17, both these wheels have the same expected vertical loading of 5.72 t each (for load condition AW0). The before tamping balancing forces for these wheels were 6.1 t each at a speed of 42.3 km/h, while the after tamping balancing forces for these wheels were 6.8 t each at a speed of 76.8 km/h.

For the lateral forces the balanced maximum lateral forces for the high and low legs were analysed for the following wheels: DMOS A 4 and DMOS A 7. The before tamping balancing forces for these wheels were 2.0 t each at a speed of 139.3 km/h, while the after tamping balancing forces for these wheels were -0.2 t each at a speed of 163.4 km/h.

Figure 4.5 graphically shows what is presented in Table 4-12 in terms of maximum forces, as described above.

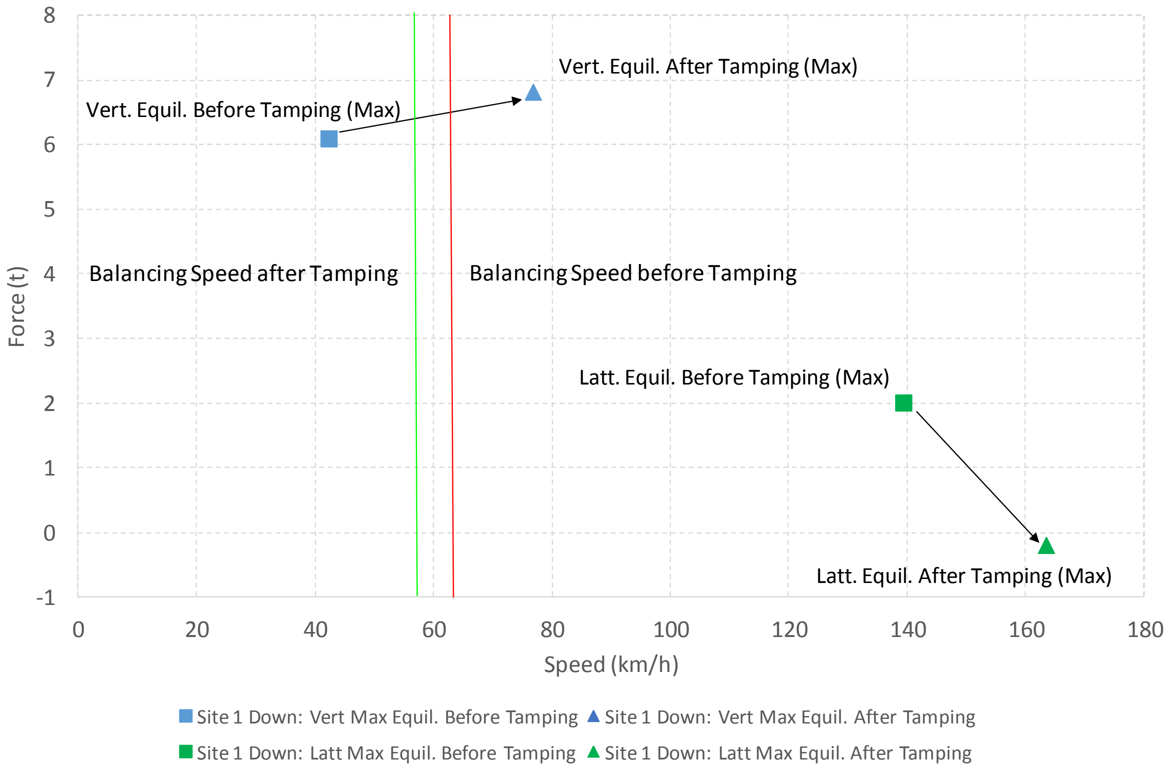

Figure 4.5: Before & After Tamping Balance Speeds & Max Forces (Wheels) – S1 Down

From Figure 4.5 it can be seen that the theoretically calculated balancing speed for Site 1 before tamping was 62.7 km/h and was reduced to 56.5 km/h after tamping, with a reduction in cant of 18.4 mm (from 109.9 mm to 91.5 mm). From Figure 4.5 (and Table 4-12) it can be seen that at Site 1 in the down direction the maximum forces balancing speeds for both the

© University of Pretoria

vertical and lateral forces increased after tamping. The balancing force of the maximum vertical force increased after tamping, while the balancing force of the maximum lateral force decreased after tamping.

Table 4-13 shows the balance forces and speeds for Site 1 in the up direction.

Table 4-13: Force Balancing (Wheels) – S1 Up

	SITE 1: UP	Before Tamping		After Tamping		Δ x	Δ x	Δ y	Δ y
		x (km/h)	y (t)	x (km/h)	y (t)	(km/h)	(%)	(t)	(%)
Verticals	HL Max DMOS B W8 LL Max DMOS B W2	50.2	6.2	70.2	6.4	19.9	39.7	0.1	2.2
Verticals	HL Min PTOS W3 LL Min MOS W5	55.8	4.8	71.3	4.7	15.5	27.8	-0.2	-3.5
Laterals	HL Max DMOS A W1 LL Max DMOS A W8	149.1	2.2	71.8	2.5	-77.4	-51.9	0.3	12.4
Laterals	HL Min DMOS A W2 LL Min MOS W5	62.5	-0.4	63.1	-0.2	0.6	0.9	0.2	56.7

For Site 1 in the up direction the balanced maximum vertical forces for the high and low legs were analysed for the following wheels: DMOS B 8 and DMOS B 2. Referring to Table 3-17, DMOS B 8 has an expected vertical loading of 5.72 t, while DMOS B 2 has an expected vertical loading of 5.68 t (for load condition AW0). The before tamping balancing forces for these wheels were 6.2 t each at a speed of 50.2 km/h, while the after tamping balancing forces for these wheels were 6.4 t each at a speed of 70.2 km/h.

For the lateral forces the balanced maximum lateral forces for the high and low legs were analysed for the following wheels: DMOS A 1 and DMOS A 8. The before tamping balancing forces for these wheels were 2.2 t each at a speed of 149.1 km/h, while the after tamping balancing forces for these wheels were 2.5 t each at a speed of 71.8 km/h.

Figure 4.6 graphically shows what is presented in Table 4-13 in terms of maximum forces, as described above.

© University of Pretoria

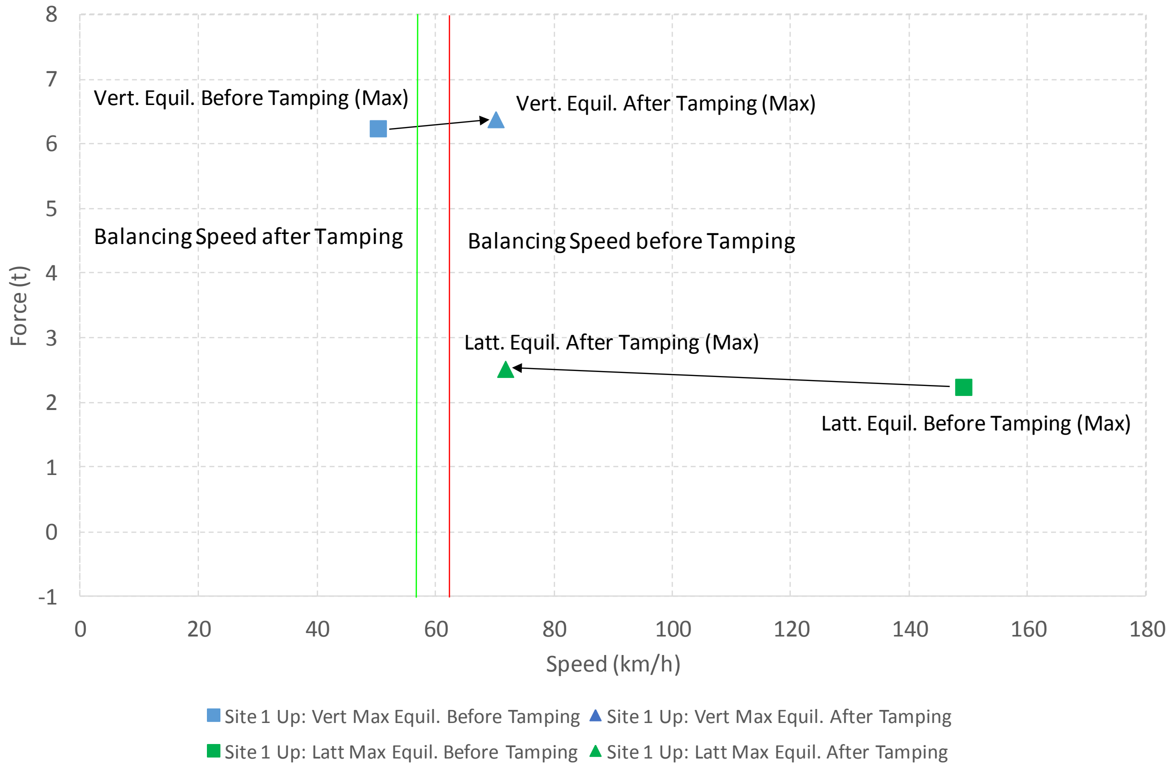

Figure 4.6: Before & After Tamping Balance Speeds & Max Forces (Wheels) – S1 Up

From Figure 4.6 it can be seen that the theoretically calculated balancing speed for Site 1 before tamping was 62.7 km/h and was reduced to 56.5 km/h after tamping, with a reduction in cant of 18.4 mm (from 109.9 mm to 91.5 mm). From Figure 4.6 (and Table 4-13) it can be seen that at Site 1 in the up direction the balancing speed of the maximum vertical forces increased, while the balancing speed of maximum lateral forces decreased. The balancing forces of both the maximum vertical and maximum lateral forces increased slightly after tamping.

Table 4-14 shows the balance forces and speeds for Site 2 in the down direction.

© University of Pretoria

Table 4-14: Force Balancing (Wheels) – S2 Down

	SITE 2: DOWN	Before Tamping		After Tamping		Δ x	Δ x	Δ y	Δ y
		x (km/h)	y (t)	x (km/h)	y (t)	(km/h)	(%)	(t)	(%)
Verticals	HL Max DMOS B W8 LL Max DMOS B W1	42.8	6.1	39.9	6.1	-2.9	-6.7	0.0	0.1
	HL Min PTOS W3 LL Min MOS W5	63.1	4.7	56.7	4.8	-6.5	-10.2	0.1	2.2
Laterals	HL Max DMOS A W4 LL Max DMOS A W7	82.0	2.7	-295.5	9.8	-377.5	-460.6	7.1	266.5
	HL Min DMOS B W7 LL Min PTOS W8	53.3	-0.3	65.3	0.1	12.0	22.5	0.3	128.4

For Site 2 in the down direction the balanced maximum vertical forces for the high and low legs were analysed for the following wheels: DMOS B 8 and DMOS B 1. Referring to Table 3-17 both these wheels have the same expected vertical loadings of 5.72 t each (for load condition AW0). The before tamping balancing forces for these wheels were 6.1 t each at a speed of 42.8 km/h, while the after tamping balancing forces for these wheels were 6.1 t each at a speed of 39.9 km/h.

For the lateral forces the balanced maximum lateral forces for the high and low legs were analysed for the following wheels: DMOS A 4 and DMOS A 7. The before tamping balancing forces for these wheels were 2.7 t each at a speed of 82.0 km/h, while the after tamping balancing forces for these wheels were 9.8 t each at a speed of -295.5 km/h.

Figure 4.7 graphically shows what is presented in Table 4-14 in terms of maximum forces, as described above.

© University of Pretoria

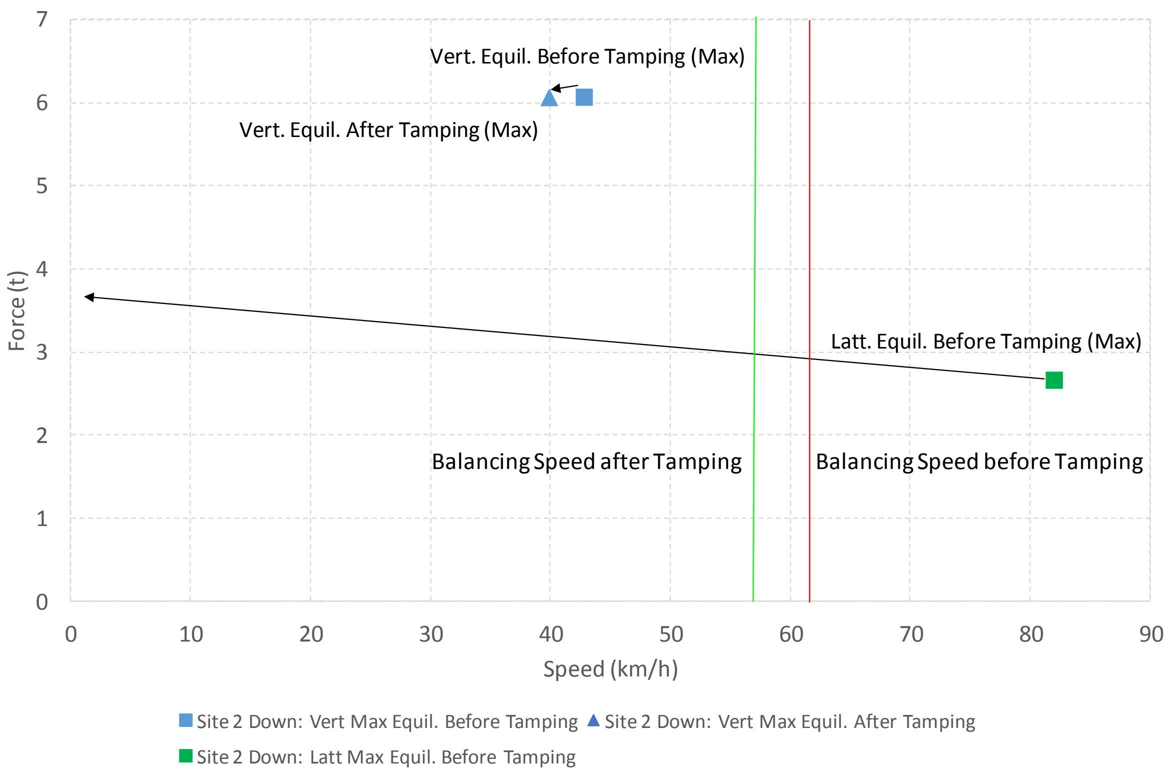

Figure 4.7: Before & After Tamping Balance Speeds & Max Forces (Wheels) – S2 Down

From Figure 4.7 it can be seen that the theoretically calculated balancing speed for Site 2 before tamping was 61.5 km/h and was reduced to 56.9 km/h after tamping, with a reduction in cant of 13.1 mm (from 105.9 mm to 92.8 mm). From Figure 4.7 (and Table 4-14) it can be seen that at Site 2 in the down direction the balancing speed of the maximum vertical forces decreased, while the balancing speed of the maximum lateral forces decreased significantly after tamping. The balancing force of the maximum vertical forces decreased slightly (6.07 t to 6.06 t), while the balancing force of the maximum lateral forces increased significantly after tamping.

Table 4-15 shows the balance forces and speeds for Site 2 in the up direction.

© University of Pretoria

Table 4-15: Force Balancing (Wheels) – S2 Up

	SITE 2: UP	Before Tamping		After Tamping		Δ x	Δ x	Δ y	Δ y
		x (km/h)	y (t)	x (km/h)	y (t)	(km/h)	(%)	(t)	(%)
Verticals	HL Max DMOS B W8 LL Max DMOS B W2	52.7	6.0	47.3	6.2	-5.5	-10.4	0.3	4.4
	HL Min PTOS W3 LL Min MOS W5	54.1	4.8	54.4	4.7	0.4	0.7	-0.1	-1.5
Laterals	HL Max DMOS A W1 LL Max DMOS A W8	77.0	2.9	2444.1	-67.6	2367.1	3074.4	-70.5	-2416.9
	HL Min DMOS A W2 LL Min MOS W5	65.8	-0.4	60.8	0.0	-5.0	-7.6	0.4	108.8

For Site 2 in the up direction the balanced maximum vertical forces for the high and low legs were analysed for the following wheels: DMOS B 8 and DMOS B 2. Referring to Table 3-17 DMOS B 8 has an expected vertical loading of 5.72 t, while DMOS B 2 has an expected vertical loading of 5.68 t (for load condition AW0). The before tamping balancing forces for these wheels were 6.0 t each at a speed of 52.7 km/h, while the after tamping balancing forces for these wheels were 6.2 t each at a speed of 47.3 km/h.

For the lateral forces the balanced maximum lateral forces for the high and low legs were analysed for the following wheels: DMOS A 1 and DMOS A 8. The before tamping balancing forces for these wheels were 2.9 t each at a speed of 77.0 km/h, while the after tamping balancing forces for these wheels were -67.6 t each at a speed of 2444.1 km/h.

Figure 4.8 graphically shows what is presented in Table 4-15 in terms of maximum forces, as described above.

© University of Pretoria

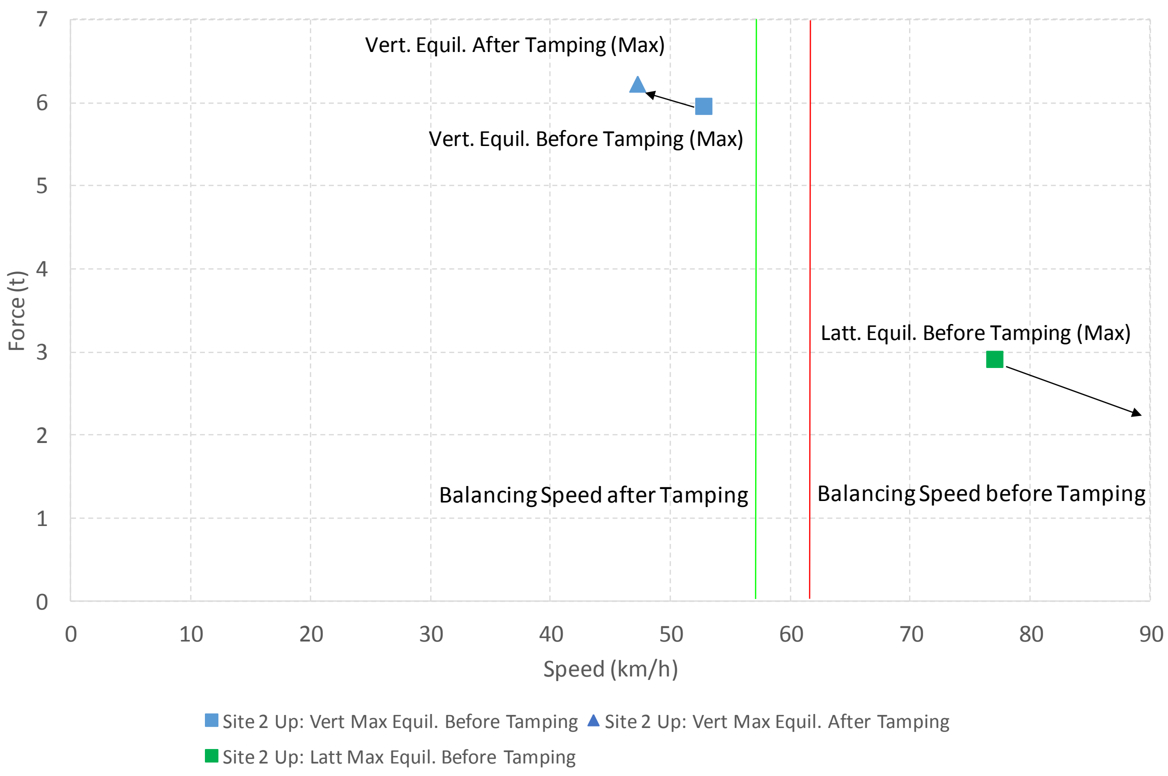

Figure 4.8: Before & After Tamping Balance Speeds & Forces (Wheels) – S2 Up

From Figure 4.8 it can be seen that the theoretically calculated balancing speed for Site 2 before tamping was 61.5 km/h and was reduced to 56.9 km/h after tamping, with a reduction in cant of 13.1 mm (from 105.9 mm to 92.8 mm). From Figure 4.8 (and Table 4-15) it can be seen that at Site 2 in the up direction the balancing speed of the maximum vertical forces decreased after tamping, while the balancing speed of the maximum lateral forces increased significantly after tamping. The balancing force of the maximum vertical forces decreased after tamping, while the balancing force of the maximum lateral forces decreased significantly after tamping.

4.4.4 Maximum and Minimum Force Changes for Wheels

With reference to the percentage changes of the speeds and balancing forces before and after tamping shown in Table 4-12 to Table 4-15 it can be seen that the vertical forces trend line balancing calculations showed good consistency. The lateral forces trend line balancing calculations were significantly less consistent.

© University of Pretoria

For Site 1 Down, Site 1 Up, Site 2 Down and Site 2 Up the largest percentage change in the vertical force balancing was 11.8%, and if Site 1 Down (the biggest vertical force balancing difference) is excluded the maximum percentage change in the vertical force balancing drops to 4.4%.

For Site 1 Down, Site 1 Up, Site 2 Down and Site 2 Up the largest percentage change in the lateral force balancing was -2416.9%, and if Site 2 Up (the biggest lateral force balancing difference) is excluded the maximum percentage change in the vertical force balancing drops to 266.5%.

4.4.5 Vertical Loads on the High and Low Legs as a Function of Speed

In order to discuss the vertical loads on the high and low legs as a function of speed, the forces summary tables presented in Appendix E were used to plot balancing force diagrams for the vertical forces induced by the 4-car test train at the various test run speeds.

Figure 4-9 below provides an example of one these plots for Site 2 in the up direction, showing both the before and after tamping vertical force data, while Appendix I shows the rest of the balancing force diagrams for the 4-car trains for both the vertical and the lateral forces (while Appendices G and H show the balancing force diagrams for the vertical and lateral forces induced by the bogies and the cars respectively).

Using the data for the 4-car trains allowed for an overview, as opposed to the detail involved with assessing the data on a wheel, bogie or car level. However all of the aforementioned balancing force diagrams are available in Appendices C, G and H respectively, with the accompanying balancing speed discussions presented in Section 4.4.3 and Section 4.4.6.

© University of Pretoria

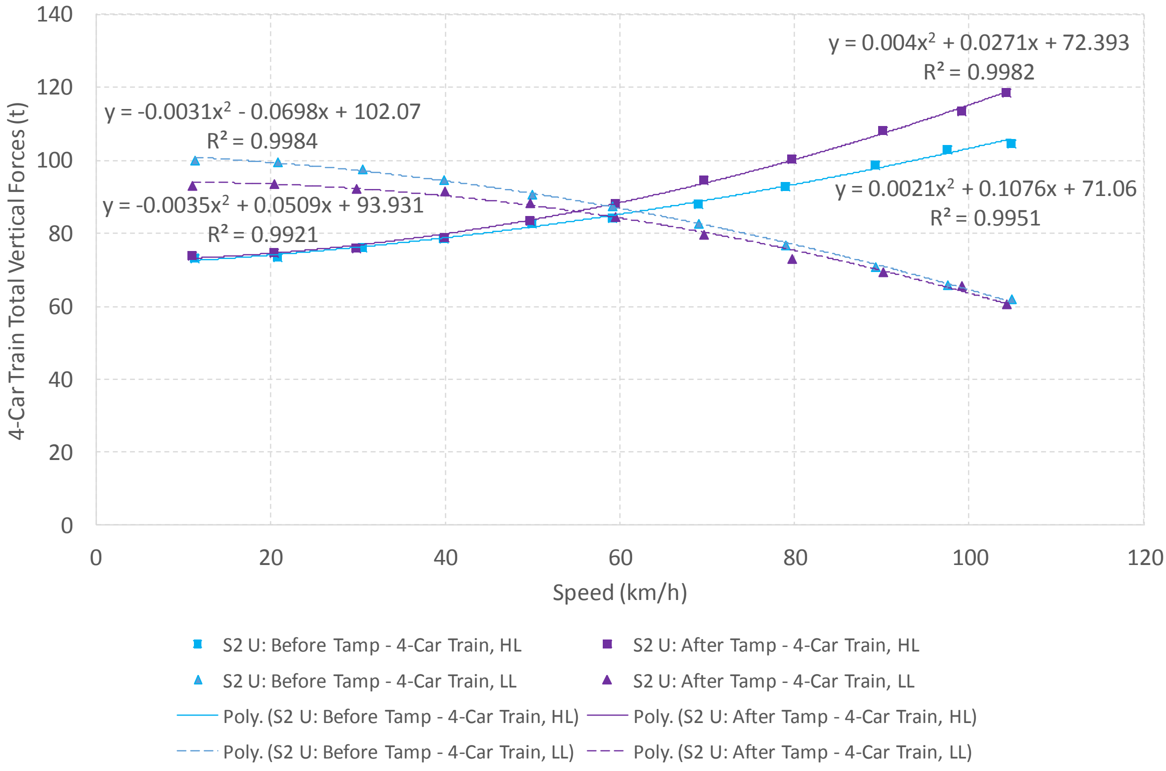

Figure 4.9: Vertical Forces (4-Car Train) – S2 Up

As would be expected, at low speeds the vertical loads are higher on the low leg than the high leg, with a transfer of loading from the low leg to high leg taking place as the train speed increases. The balancing speeds applicable to the data presented in Figure 4-9 are discussed in Section 4.4.6 and presented in Table 4-19.

For Site 2 in both the up and the down direction the reduction in cant resulted in a lowering of the low leg vertical forces at the lower speeds, but it should be noted that this was not the case for the Site 1 data, as can be seen in Appendix I. The reasons for the differences in behaviour between Site 1 and Site 2 are not clear, but discussions relating to the balancing speeds of each of the sites for both the vertical and lateral forces are presented in further detail Section 4.4.6.

4.4.6 Maximum and Minimum Force Values for Bogies, Cars and 4-Car Trains

Using the forces summary tables in Appendix E balancing force diagrams for the vertical and lateral forces induced by the bogies, cars and 4-car trains respectively at the various speeds could be plotted as shown in Appendices G, H and I, as well as Figure 4-9.

© University of Pretoria

Adding trend lines and determining the equations of these trend lines (as shown on the graphs in Appendices G, H and I, as well as Figure 4.9.) allowed for the intersection points between the high and low legs, vertical and lateral forces before and after tamping to be determined. Appendix J summarises the trend line information for each of the force graphs. For the bogies, cars and 4-car train forces data 2nd order polynomial trend lines provided acceptable levels of reliability and were therefore used.

Solving for the equations shown on the balancing force graphs and summarised in Appendix J yields the balance forces and speeds shown in Appendix K for the bogies and cars and shown in Table 4-16 to Table 4-19 for the 4-car trains. The Δ x (%) and Δ y (%) refers to the percentage change relative to the before tamping results.

Table 4-16: Force Balancing (4-Car Trains) – S1 Down

	SITE 1: DOWN		Before Tamping		After Tamping		Δ x (km/h)	Δ x (%)	Δ y (t)	Δ y (%)
	Forces	Rail	x (km/h)	y (t)	x (km/h)	y (t)				
4-Car Train	Verticals	High Leg Low Leg	56.45	85.96	78.07	89.27	21.62	38.29	3.31	3.85
	Laterals	High Leg Low Leg	85.82	16.77	84.63	7.43	-1.20	-1.39	-9.34	-55.71

Table 4-17: Force Balancing (4-Car Trains) – S1 Up

	SITE 1: UP		Before Tamping		After Tamping		Δ x (km/h)	Δ x (%)	Δ y (t)	Δ y (%)
	Forces	Rail	x (km/h)	y (t)	x (km/h)	y (t)				
4-Car Train	Verticals	High Leg Low Leg	60.31	88.10	74.43	86.31	14.12	23.41	-1.78	-2.03
	Laterals	High Leg Low Leg	89.13	13.08	71.02	16.72	-18.11	-20.32	3.64	27.84

Table 4-18: Force Balancing (4-Car Trains) – S2 Down

	SITE 2: DOWN		Before Tamping		After Tamping		Δ x (km/h)	Δ x (%)	Δ y (t)	Δ y (%)
	Forces	Rail	x (km/h)	y (t)	x (km/h)	y (t)				
4-Car Train	Verticals	High Leg Low Leg	61.28	85.35	56.27	84.94	-5.01	-8.18	-0.40	-0.47
	Laterals	High Leg Low Leg	76.48	18.94	103.22	-0.40	26.73	34.95	-19.34	-102.12

© University of Pretoria

Table 4-19: Force Balancing (4-Car Trains) – S2 Up

	SITE 2: UP		Before Tamping		After Tamping		Δ x (km/h)	Δ x (%)	Δ y (t)	Δ y (%)
	Forces	Rail	x (km/h)	y (t)	x (km/h)	y (t)				
4-Car Train	Verticals	High Leg	62.03	85.81	55.20	86.08	-6.83	-11.01	0.26	0.31
		Low Leg								
	Laterals	High Leg	77.83	18.34	96.04	1.79	18.20	23.39	-16.55	-90.23
		Low Leg								

The data presented in Appendix K with regard to the rail forces generated by the bogies and individual cars is not discussed beyond the presentation of the data in these tables. The data presented in Table 4-16 to Table 4-19 with regard to the rail forces generated by the 4-car trains as a whole is however discussed in further detail below.

With reference to Table 4-16, for Site 1 in the down direction the balanced vertical forces generated by the 4-car train as a whole for the high and low legs were 85.96 t at a speed of 56.45 km/h before tamping and 89.27 t at a speed of 78.07 km/h after tamping. For the lateral forces the balanced lateral forces generated by the 4-car train as a whole for the high and low legs were 16.77 t at a speed of 85.82 km/h before tamping and 7.43 t at a speed of 84.63 km/h after tamping. Figure 4.10 graphically shows what is presented in Table 4-16 as described above.

With reference to Table 4-17, for Site 1 in the up direction the balanced vertical forces generated by the 4-car train as a whole for the high and low legs were 88.10 t at a speed of 60.31 km/h before tamping and 86.31 t at a speed of 74.43 km/h after tamping. For the lateral forces the balanced lateral forces generated by the 4-car train as a whole for the high and low legs were 13.08 t at a speed of 89.13 km/h before tamping and 16.72 t at a speed of 71.02 km/h after tamping. Figure 4.11 graphically shows what is presented in Table 4-17 as described above.

With reference to Table 4-18, for Site 2 in the down direction the balanced vertical forces generated by the 4-car train as a whole for the high and low legs were 85.35 t at a speed of 61.28 km/h before tamping and 84.94 t at a speed of 56.27 km/h after tamping. For the lateral forces the balanced lateral forces generated by the 4-car train as a whole for the high and low legs were 18.94 t at a speed of 76.48 km/h before tamping and -0.40 t at a speed of 103.22 km/h after tamping. Figure 4.12 graphically shows what is presented in Table 4-18 as described above.

© University of Pretoria

With reference to Table 4-19, for Site 2 in the up direction the balanced vertical forces generated by the 4-car train as a whole for the high and low legs were 85.81 t at a speed of 62.03 km/h before tamping and 86.08 t at a speed of 55.20 km/h after tamping. For the lateral forces the balanced lateral forces generated by the 4-car train as a whole for the high and low legs were 18.34 t at a speed of 77.83 km/h before tamping and 1.79 t at a speed of 96.04 km/h after tamping. Figure 4.13 graphically shows what is presented in Table 4-19 as described above.

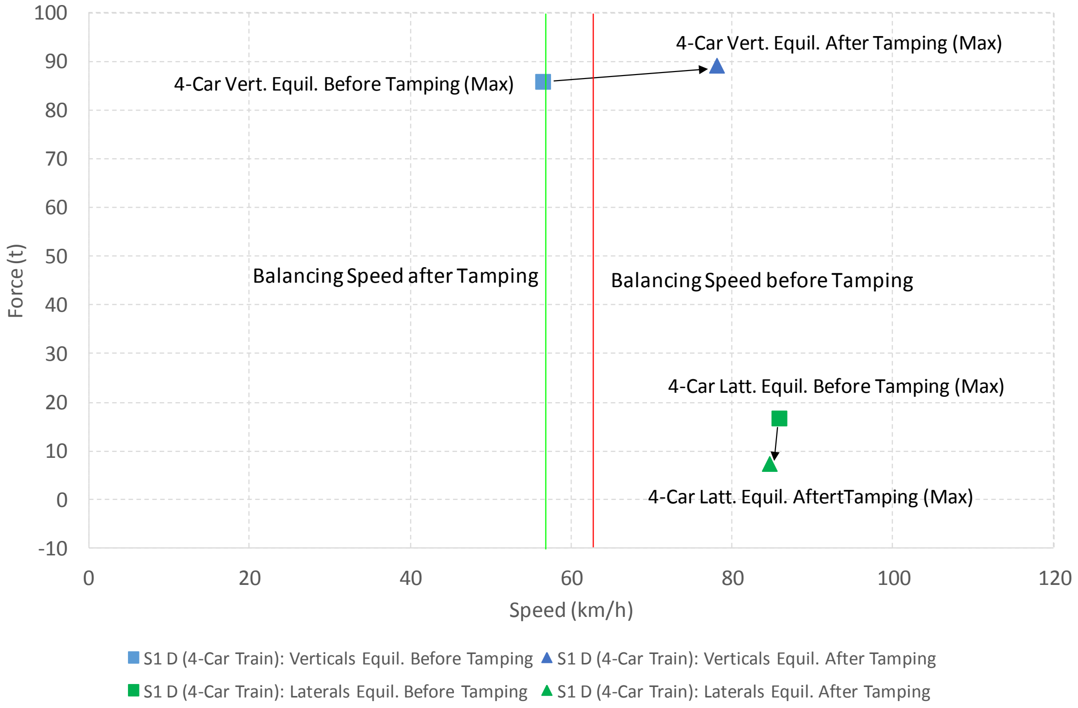

Figure 4.10: Before & After Tamping Balance Speeds & Forces (4-Car Train) – S1 Down

© University of Pretoria

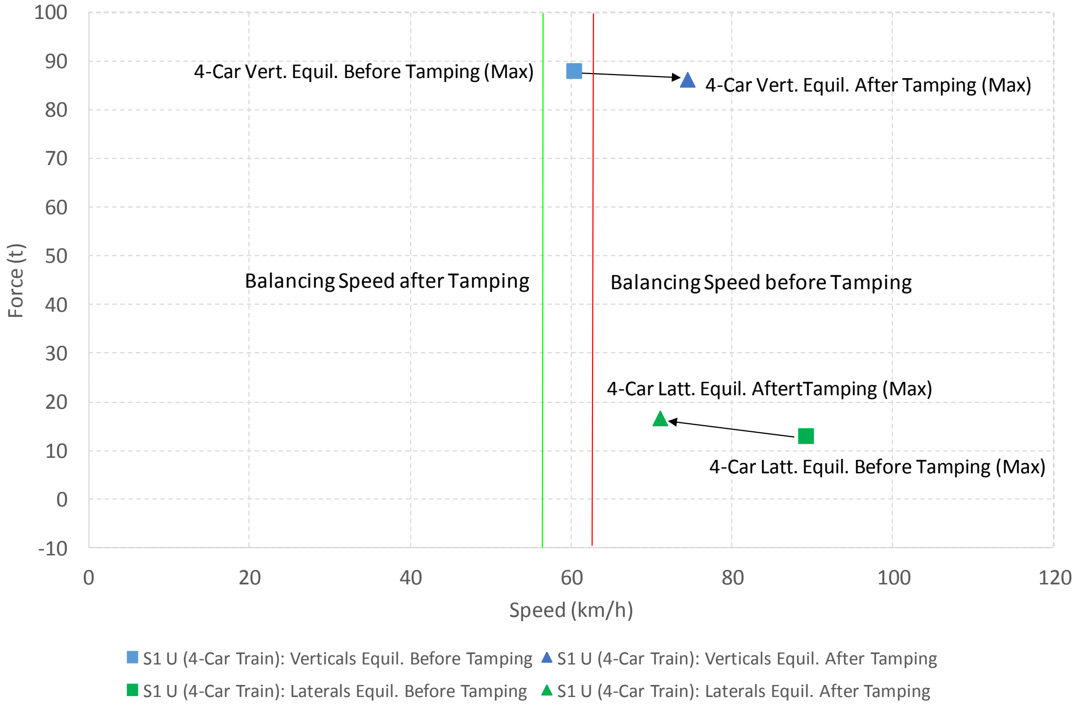

Figure 4.11: Before & After Tamping Balance Speeds & Forces (4-Car Train) – S1 Up

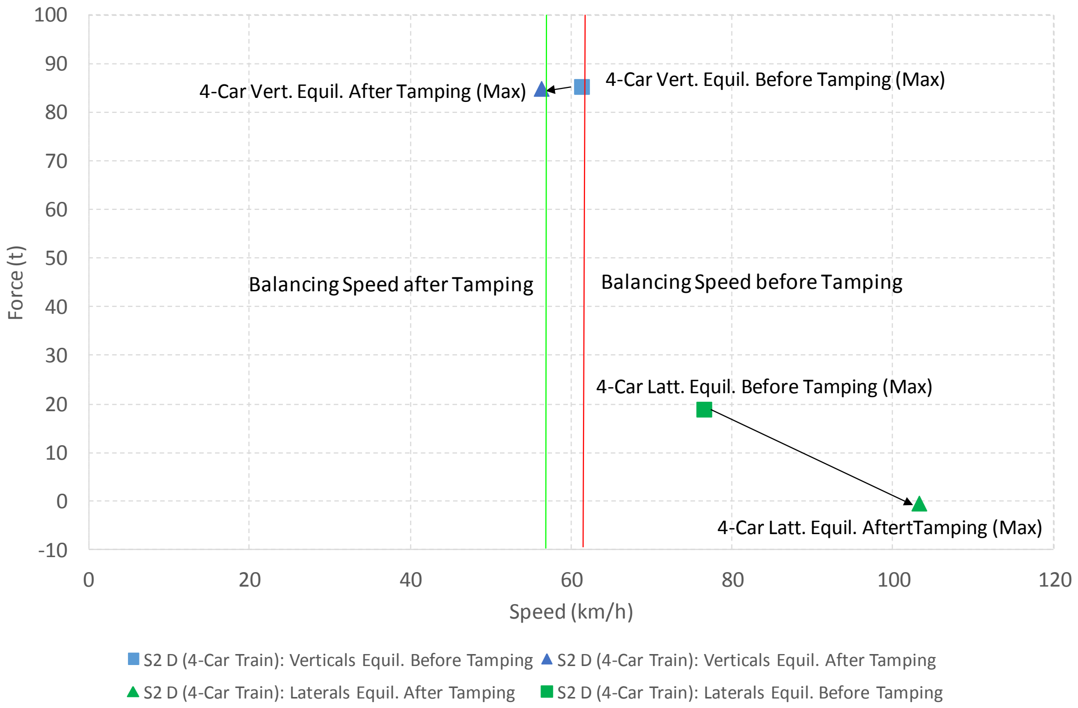

Figure 4.12: Before & After Tamping Balance Speeds & Forces (4-Car Train) – S2 Down

© University of Pretoria

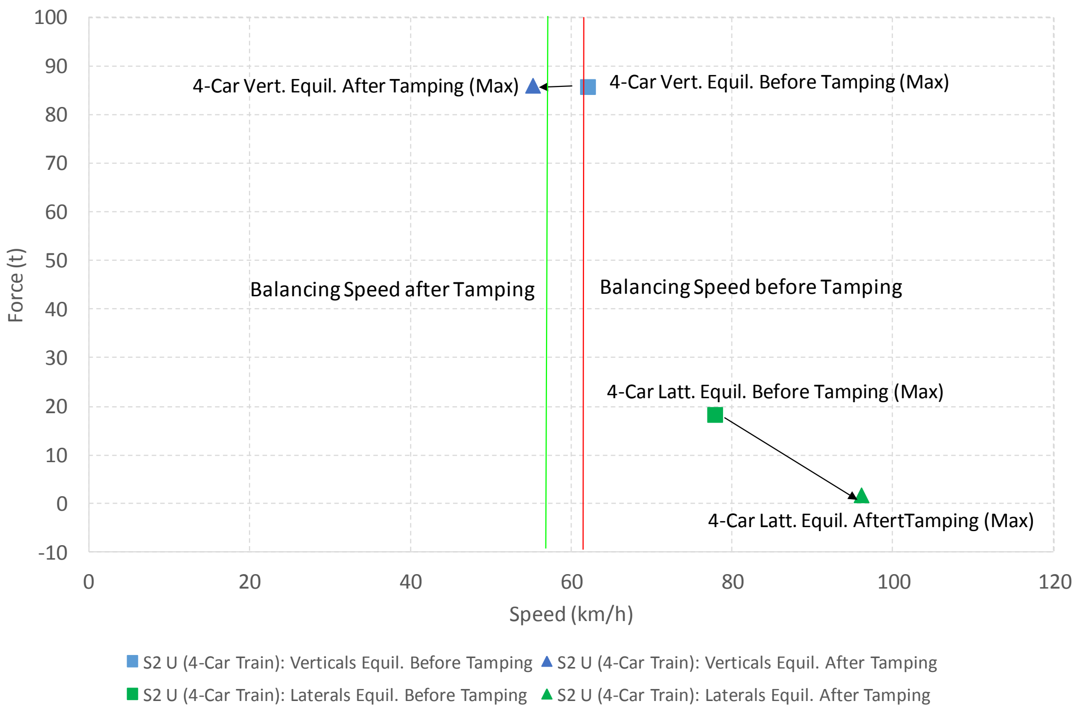

Figure 4.13: Before & After Tamping Balance Speeds & Forces (4-Car Train) – S2 Up

4.4.7 Rail Forces at Operational Speed for Wheels

The operational speed of the experimental curve is one of the variables that remained constant both before and after tamping, and there is no intention of changing the operational speed, due to the effect that this will have on the timetable, signalling system etc. Therefore the specific effect that changing the cant had on the rail forces at a train speed of 85 km/h is discussed in this section.

Solving for the equations shown on the balancing force graphs and summarised in Appendix D, the minimum and maximum vertical and lateral rail forces, on the high and low legs, before and after tamping, for a train speed of 85 km/h could be calculated and are presented in Table 4-20 to Table 4-23.

It can be seen in Table 4-20 to Table 4-23 that no consistent trends applicable to Site 1 and Site 2 in the up and the down directions could be established. For discussion purposes focus will be given to the trend of the maximum vertical forces on the high legs, with the same reasoning holding true for the other rail forces.

For Site 1 in the down direction the high leg maximum force stayed the same after tamping, while the low leg maximum force increased after tamping. For Site 1 in the up direction the

© University of Pretoria

high leg maximum force decreased after tamping, while the low leg maximum force increased after tamping. For Site 2 in the down direction the high leg maximum force decreased after tamping, while the low leg maximum increased after tamping. For Site 2 in the up direction the maximum force on both the high and low legs increased after tamping.

Table 4-20: Rail Forces Before and After Tamping at 85 km/h (Wheels) – S1 Down

	SITE 1: DOWN	Operational Speed (km/h)	Before Tamping y (t)	After Tamping y (t)	Δ y (%)
Verticals	HL Max (DMOS B W8)	85.0	7.08	7.08	0 (0%)
	LL Max (DMOS B W1)	85.0	5.16	6.65	+1.49 (+28.89%)
	HL Min (PTOS W3)	85.0	5.63	5.25	-0.37 (-6.57%)
	LL Min (MOS W5)	85.0	4.16	5.15	+0.99 (+23.8%)
Laterals	HL Max (DMOS A W4)	85.0	2.13	1.11	-1.01 (-47.5%)
	LL Max (DMOS A W7)	85.0	2.70	1.72	-0.98 (-36.34%)
	HL Min (DMOS B W7)	85.0	0.17	0.38	+0.21 (+124.85%)
	LL Min (PTOS W8)	85.0	-0.69	-0.71	-0.01 (-1.44%)

Table 4-21: Rail Forces Before and After Tamping at 85 km/h (Wheels) – S1 Up

	SITE 1: UP	Operational Speed (km/h)	Before Tamping y (t)	After Tamping y (t)	Δ y (%)
Verticals	HL Max (DMOS B W8)	85.0	7.59	6.91	-0.67 (-8.82%)
	LL Max (DMOS B W2)	85.0	5.54	6.05	+0.5 (+9.01%)
	HL Min (PTOS W3)	85.0	5.68	4.88	-0.79 (-13.9%)
	LL Min (MOS W5)	85.0	4.05	4.16	+0.1 (+2.46%)
Laterals	HL Max (DMOS A W1)	85.0	2.01	2.53	+0.51 (+25.35%)
	LL Max (DMOS A W8)	85.0	2.83	2.30	-0.53 (-18.71%)
	HL Min (DMOS A W2)	85.0	-0.07	0.36	+0.42 (+612.24%)
	LL Min (MOS W5)	85.0	-0.76	-0.75	0 (0%)

© University of Pretoria

Table 4-22: Rail Forces Before and After Tamping at 85 km/h (Wheels) – S2 Down

	SITE 2: DOWN	Operational Speed (km/h)	Before Tamping y (t)	After Tamping y (t)	Δ y (%)
Verticals	HL Max (DMOS B W8)	85.0	7.38	7.21	-0.17 (-2.3%)
	LL Max (DMOS B W1)	85.0	4.98	5.46	+0.47 (+9.43%)
	HL Min (PTOS W3)	85.0	5.23	5.72	+0.48 (+9.17%)
	LL Min (MOS W5)	85.0	4.13	4.39	+0.25 (+6.04%)
Laterals	HL Max (DMOS A W4)	85.0	2.68	-0.34	-3.02 (-112.64%)
	LL Max (DMOS A W7)	85.0	2.62	1.10	-1.51 (-57.63%)
	HL Min (DMOS B W7)	85.0	0.37	0.56	+0.18 (+48.56%)
	LL Min (PTOS W8)	85.0	-0.75	-0.27	+0.48 (+63.66%)

Table 4-23: Rail Forces Before and After Tamping at 85 km/h (Wheels) – S2 Up

	SITE 2: UP	Operational Speed (km/h)	Before Tamping y (t)	After Tamping y (t)	Δ y (%)
Verticals	HL Max (DMOS B W8)	85.0	6.89	7.68	+0.78 (+11.32%)
	LL Max (DMOS B W2)	85.0	5.23	5.55	+0.32 (+6.12%)
	HL Min (PTOS W3)	85.0	5.20	5.47	+0.27 (+5.19%)
	LL Min (MOS W5)	85.0	3.84	3.81	-0.02 (-0.52%)
Laterals	HL Max (DMOS A W1)	85.0	3.00	-0.38	-3.37 (-112.5%)
	LL Max (DMOS A W8)	85.0	2.83	1.50	-1.32 (-46.59%)
	HL Min (DMOS A W2)	85.0	-0.12	0.61	+0.72 (+581.11%)
	LL Min (MOS W5)	85.0	-0.69	-0.40	+0.28 (+40.86%)

4.4.8 Rail Forces at Operational Speed for Bogies, Cars and 4-Car Trains

As discussed in Section 4.4.7 the operational speed of the experimental curve is one of the variables that remained constant both before and after tamping. The specific effect that changing the cant had on the rail forces due to the bogies, cars and 4-car trains at a train speed of 85 km/h is discussed in this section.

Solving for the equations shown on the balancing force graphs and summarised in Appendix J, the vertical and lateral rail forces due to the bogies, cars and 4-car trains, on the high and low legs, before and after tamping, for a train speed of 85 km/h could be calculated and are shown in Appendix L for the bogies and cars and shown in Table 4-24 to Table 4-27 for the 4-car trains. The Δ y (%) refers to the percentage change relative to the before tamping results.

Table 4-24: Rail Forces Before and After Tamping at 85 km/h (4-Car Trains) – S1 Down

4 Car Train	SITE 1: DOWN		Operational Speed (km/h)	Before Tamping	After Tamping	Δ y (%)
	Forces	Rail		y (t)	y (t)	
	Verticals	High Leg	85.0	101.53	94.08	-7.44 (-7.32%)
		Low Leg	85.0	73.81	84.97	+11.16 (+15.12%)
	Laterals	High Leg	85.0	16.63	7.43	-9.19 (-55.27%)
		Low Leg	85.0	17.03	7.20	-9.83 (-57.72%)

Table 4-25: Rail Forces Before and After Tamping at 85 km/h (4-Car Trains) – S1 Up

4 Car Train	SITE 1: UP		Operational Speed (km/h)	Before Tamping	After Tamping	Δ y (%)
	Forces	Rail		y (t)	y (t)	
	Verticals	High Leg	85.0	103.51	91.21	-12.29 (-11.87%)
		Low Leg	85.0	77.07	79.46	+2.38 (+3.08%)
	Laterals	High Leg	85.0	12.21	19.12	+6.9 (+56.51%)
		Low Leg	85.0	14.56	9.58	-4.97 (-34.14%)

Table 4-26: Rail Forces Before and After Tamping at 85 km/h (4-Car Trains) – S2 Down

4-Car Train	SITE 2: DOWN		Operational Speed (km/h)	Before Tamping	After Tamping	Δ y (%)
	Forces	Rail		y (t)	y (t)	
	Verticals	High Leg	85.0	99.48	100.60	+1.11 (+1.11%)
		Low Leg	85.0	73.26	73.66	+0.4 (+0.54%)
	Laterals	High Leg	85.0	20.81	-2.94	-23.74 (-114.09%)
		Low Leg	85.0	15.87	7.97	-7.89 (-49.72%)

© University of Pretoria

Table 4-27: Rail Forces Before and After Tamping at 85 km/h (4-Car Trains) – S2 Up

	SITE 2: UP		Operational Speed (km/h)	Before Tamping	After Tamping	Δ y (%)
	Forces	Rail		y (t)	y (t)	
4-Car Train	Verticals	High Leg	85.0	95.38	103.60	+8.21 (+8.6%)
		Low Leg	85.0	73.74	72.97	-0.76 (-1.03%)
	Laterals	High Leg	85.0	20.05	1.62	-18.43 (-91.9%)
		Low Leg	85.0	16.08	8.24	-7.83 (-48.7%)

4.4.9 Rail Forces Discussion for Wheels

The maximum forces being exerted on the rail by individual wheels in the experimental curve were measured in order to physically assess what the effect of reducing the cant was. Figure 4.5 to Figure 4.8 graphically presents what the effects of reducing the cant on the balancing forces and the corresponding balancing speeds were.

The effect that reducing the cant had on the maximum vertical forces is described in the following bullets:

- At Site 1 in the down direction reducing the cant resulted in a higher maximum vertical balancing force at a higher balancing speed (see Table 4-12).
- At Site 1 in the up direction reducing the cant resulted in a slightly higher maximum vertical balancing force at a higher balancing speed (see Table 4-13).
- At Site 2 in the down direction reducing the cant resulted in a negligible increase to the maximum vertical balancing force, but after tamping this similar vertical balancing force was achieved at a slightly lower balancing speed (see Table 4-14).
- At Site 2 in the up direction reducing the cant resulted in a slightly higher maximum vertical balancing force at a lower balancing speed (see Table 4-15).

From the above bullets it can be seen that at Site 1 in the down and up directions the maximum vertical forces increased after tamping with a corresponding increase in the balancing speed. At Site 2 however in the down direction the maximum vertical force increased negligibly after tamping with a corresponding decrease in the balancing speed, while at Site 2 in the down direction the maximum vertical force increased after tamping with a corresponding decrease in the balancing speed. There were therefore no consistent trends with regard to the maximum vertical forces results before and after tamping.

© University of Pretoria

The minimum vertical forces are of less interest, as only positive vertical forces are measured (see Figure 3.30) therefore the various minimum vertical forces that were assessed in detail throughout Chapter 4 are covered by default when interpreting the maximum vertical forces experienced by the rail.

For the lateral forces data, the maxima and minima were of much more interest than was the case for the vertical forces data, as negative lateral forces made up a significant proportion of the data collected, due to the fact the sign of the force indicates in which direction the lateral force was acting on the rail (see Figure 3.29 and Figure 3.30). Assessing the minimums therefore covered all of the forces to the inside of the rail.

On a test by test basis some interesting lateral force information was collected, and this has been presented in detail in this chapter. In terms of this discussion however the lack of clear consistency provided by the lateral force data when assessing the experimental curve in its entirety led to an assessment of the average percentage changes in the lateral force data, as opposed to a direct quantitative trend assessment.

The percentage changes presented in Table 4-20 to Table 4-23 which show the change in forces before and after tamping at the operational speed of 85 km/h are summarised in Table 4-28 below.

Table 4-28: Percentage Change in Forces After Tamping (Wheels)

Site	Leg	% Change in Forces at 85 km/h after tamping (Wheels)			
		Max Verticals	Min Verticals	Max Laterals	Min Laterals
Site 1 Down	High Leg	0.0	-6.6	-47.5	124.9
	Low Leg	28.9	23.8	-36.3	-1.4
Site 1 Up	High Leg	-8.8	-13.9	25.4	612.2
	Low Leg	9.0	2.5	-18.7	0.0
Site 2 Down	High Leg	-2.3	9.2	-112.6	48.6
	Low Leg	9.4	6.0	-57.6	63.7
Site 2 Up	High Leg	11.3	5.2	-112.5	581.1
	Low Leg	6.1	-0.5	-46.6	40.9
High Leg Average		0.0	-1.5	-61.8	341.7
Low Leg Average		13.4	7.9	-39.8	25.8
Overall Average		6.7	3.2	-50.8	183.7

© University of Pretoria

The cant of the curve before tamping was 107.1 mm and this was reduced to 92.0 mm after tamping, which equates to a 14% reduction in cant. Assessing the percentage change in forces presented in Table 4-28, at the operational speed of 85 km/h, revealed the following results for this 14% reduction in cant:

- For the Site 1 and Site 2 in the down and up directions the maximum and minimum vertical and lateral forces at 85 km/h after tamping decreased in 13 out of the 32 cases, increased in 17 out of the 32 cases and was neither increased nor decreased in 2 out of the 32 cases.
- There was a zero net effect on the average maximum vertical high leg forces, with a corresponding 13.4% increase in the maximum vertical low leg forces. The average maximum vertical forces therefore increased by 6.7%.
- As discussed previously the minimum vertical forces are of less interest, as only positive vertical forces are measured (see Figure 3.30).
- An average reduction of 50.8% in maximum lateral forces, with a 61.8% reduction in the maximum lateral high leg forces and an average 39.8% reduction in the maximum lateral low leg forces.
- There are some large percentage changes in the minimum lateral forces (a 612.2% increase at Site 1 in the up direction on the high leg and a 581.1% increase at Site 2 in the up direction on the high leg). Assessing the absolute values (Table 4-20 to Table 4-23) of these changes reveals that all of the minimum lateral forces are between -1 t and 1 t, therefore the forces themselves are small, but the percentage changes relative to the small forces are large.

4.4.10 Rail Forces Discussion for Bogies, Cars and 4-Car Trains

As a follow on from the discussion in Section 4.4.9 which dealt with the rail forces generated by individual wheels, this section discusses the rail forces generated by the bogies, cars and 4-car trains.

The percentage changes presented in Appendix L and in Table 4-24 to Table 4-27 are summarised in Table 4-29 to Table 4-35 below. The data presented in Table 4-29 to Table 4-34 with regard to the percentage changes in the rail forces generated by the bogies and individual cars are not discussed beyond the presentation of the data in the tables. The data presented in Table 4-35 with regard to the percentage changes in the rail forces generated by the 4-car trains as a whole is however discussed in further detail below.

© University of Pretoria

Table 4-29: Percentage Change in Vertical Forces After Tamping (Leading Bogies)

Site	Leg	% Change in Vertical Forces at 85 km/h after tamping – Leading Bogies			
		DMOS B	PTOS	MOS	DMOS A
Site 1 Down	High Leg	-2.0	-8.7	-9.1	-10.0
	Low Leg	20.8	6.2	14.4	15.3
Site 1 Up	High Leg	-22.7	-24.9	-22.8	-26.8
	Low Leg	-11.2	-13.4	-5.5	-9.5
Site 2 Down	High Leg	0.2	5.0	2.3	-0.5
	Low Leg	2.3	-4.4	-2.8	-7.6
Site 2 Up	High Leg	9.6	9.7	2.0	8.0
	Low Leg	-5.8	-9.3	-5.1	-6.0
High Leg Average		-3.7	-4.7	-6.9	-7.3
Low Leg Average		1.5	-5.2	0.3	-1.9
Overall Average		-1.1	-5.0	-3.3	-4.6

Table 4-30: Percentage Change in Lateral Forces After Tamping (Leading Bogies)

Site	Leg	% Change in Lateral Forces at 85 km/h after tamping – Leading Bogies			
		DMOS B	PTOS	MOS	DMOS A
Site 1 Down	High Leg	-79.7	-56.0	-63.6	-32.9
	Low Leg	-65.1	-28.0	-60.3	-47.1
Site 1 Up	High Leg	89.3	58.7	35.8	40.3
	Low Leg	-46.0	-17.6	-31.3	-42.3
Site 2 Down	High Leg	-112.8	-102.1	-97.2	-102.8
	Low Leg	-53.0	-44.3	-52.7	-16.9
Site 2 Up	High Leg	-86.8	-94.9	-95.7	-92.1
	Low Leg	-74.4	-21.2	-54.0	-52.6
High Leg Average		-47.5	-48.6	-55.2	-46.9
Low Leg Average		-59.6	-27.8	-49.6	-39.7
Overall Average		-53.5	-38.2	-52.4	-43.3

© University of Pretoria

Table 4-31: Percentage Change in Vertical Forces After Tamping (Trailing Bogies)

Site	Leg	% Change in Vertical Forces at 85 km/h after tamping – Trailing Bogies			
		DMOS B	PTOS	MOS	DMOS A
Site 1 Down	High Leg	-6.7	-11.8	-8.0	-8.3
	Low Leg	10.9	16.0	17.3	13.1
Site 1 Up	High Leg	-20.6	-25.2	-21.4	-23.6
	Low Leg	-8.3	-9.7	-13.6	-12.3
Site 2 Down	High Leg	-0.7	0.3	-0.4	3.2
	Low Leg	1.1	-2.5	3.8	-1.5
Site 2 Up	High Leg	11.0	8.5	7.1	5.8
	Low Leg	6.0	4.4	-1.4	-5.5
High Leg Average		-4.3	-7.0	-5.7	-5.7
Low Leg Average		2.4	2.1	1.5	-1.5
Overall Average		-0.9	-2.5	-2.1	-3.6

Table 4-32: Percentage Change in Lateral Forces After Tamping (Trailing Bogies)

Site	Leg	% Change in Lateral Forces at 85 km/h after tamping - Trailing Bogies			
		DMOS B	PTOS	MOS	DMOS A
Site 1 Down	High Leg	-19.6	-68.9	-88.6	-34.4
	Low Leg	-40.5	-38.8	-73.4	-74.2
Site 1 Up	High Leg	171.2	66.6	31.2	92.7
	Low Leg	-48.8	-38.1	-33.1	-36.3
Site 2 Down	High Leg	-122.1	-147.2	-115.2	-133.4
	Low Leg	-57.2	-59.9	-65.4	-77.7
Site 2 Up	High Leg	-96.4	-80.4	-81.9	-82.0
	Low Leg	-63.2	-20.2	-61.5	-21.9
High Leg Average		-16.7	-57.5	-63.6	-39.3
Low Leg Average		-52.4	-39.3	-58.3	-52.5
Overall Average		-34.6	-48.4	-61.0	-45.9

© University of Pretoria

Table 4-33: Percentage Change in Vertical Forces After Tamping (Cars)

Site	Leg	% Change in Vertical Forces at 85 km/h after tamping (Cars)			
		DMOS B	PTOS	MOS	DMOS A
Site 1 Down	High Leg	-4.3	-10.4	-8.6	-6.4
	Low Leg	19.7	11.2	15.9	14.1
Site 1 Up	High Leg	-14.9	-11.9	-12.7	-10.3
	Low Leg	5.3	4.9	2.9	2.8
Site 2 Down	High Leg	2.5	5.6	1.0	-1.3
	Low Leg	1.8	-3.4	0.5	-0.7
Site 2 Up	High Leg	10.3	6.0	7.7	10.1
	Low Leg	0.3	-2.9	-3.4	-2.1
High Leg Average		-1.6	-2.7	-3.1	-2.0
Low Leg Average		6.8	2.4	4.0	3.5
Overall Average		2.6	-0.1	0.4	0.8

Table 4-34: Percentage Change in Lateral Forces After Tamping (Cars)

Site	Leg	% Change in Lateral Forces at 85 km/h after tamping (Cars)			
		DMOS B	PTOS	MOS	DMOS A
Site 1 Down	High Leg	-44.3	-57.5	-76.4	-36.4
	Low Leg	-43.7	-55.2	-66.9	-61.4
Site 1 Up	High Leg	69.1	64.3	65.5	66.0
	Low Leg	-47.2	-28.5	-32.2	-24.7
Site 2 Down	High Leg	-63.7	-107.4	-106.1	-112.4
	Low Leg	-121.6	-50.4	-41.7	-51.2
Site 2 Up	High Leg	-90.2	-95.1	-99.2	-83.4
	Low Leg	-62.7	-42.8	-57.7	-48.9
High Leg Average		-32.3	-48.9	-54.0	-41.5
Low Leg Average		-68.8	-44.2	-49.6	-46.5
Overall Average		-50.5	-46.6	-51.8	-44.0

© University of Pretoria

Table 4-35: Percentage Change in Forces After Tamping (4-Car Trains)

Site	Leg	% Change in Forces at 85 km/h after tamping (4-Car Trains)	
		Vertical	Lateral
Site 1 Down	High Leg	-7.3	-55.3
	Low Leg	15.1	-57.7
Site 1 Up	High Leg	-11.9	56.5
	Low Leg	3.1	-34.1
Site 2 Down	High Leg	1.1	-114.1
	Low Leg	0.5	-49.7
Site 2 Up	High Leg	8.6	-91.9
	Low Leg	-1.0	-48.7
High Leg Average		-2.4	-51.2
Low Leg Average		4.4	-47.6
Overall Average		1.0	-49.4

By referring to Table 4-35 an assessment can be done as to what the effect of changing the cant was on the rail forces as a result of the 4-car trains as a whole. The cant of the curve before tamping was 107.1 mm and this was reduced to 92.0 mm after tamping, which equates to a 14% reduction in cant. Assessing the percentage change in forces presented in Table 4-35, at the operational speed of 85 km/h, revealed the following results for this 14% reduction in cant:

- For the Site 1 and Site 2 in the down and up directions the vertical and lateral forces at 85 km/h after tamping decreased in 10 out of the 16 cases and increased in the other 6 cases. The cases where increased forces were observed were at Site 1 in the down direction for the low leg vertical forces, Site 1 in the up direction for the low leg vertical forces, Site 2 in the down direction for both the high and low leg vertical forces, at Site 2 in the up direction for the high leg vertical forces, and Site 1 in the up direction for the high leg lateral forces.
- There was an average reduction of 2.4% in the vertical high leg forces and an average increase of 4.4% in the vertical low leg forces.
- There was an average reduction of 51.2% in the lateral high leg forces and an average reduction of 47.6% in the lateral low leg forces.

© University of Pretoria

The information shown in Table 4-28 to Table 4-35 is summarised in Table 4-36 for the percentage change in vertical forces after tamping and in Table 4-37 for the percentage change in lateral forces after tamping at wheel, bogie, car and 4-car train level. The highlighted values indicate the largest changes at each level of assessment.

The summarised information presented in Table 4-36 and Table 4-37 shows good consistency between the changes in vertical and lateral forces at the various levels of assessment (wheel, bogie, car and 4-car train). Although the changes in vertical and lateral forces after tamping were not empirically predictable, the relatively small range of the after tamping vertical force changes (-5.0% to 6.7%) and the relatively small range of the after tamping lateral force changes (-61.0% to -50.8%) indicates that the data at the various levels of assessment is reliable.

Table 4-36: Percentage Change in Vertical Forces After Tamping Summary

% Change in Vertical Forces at 85 km/h after tamping (Overall Average)			
WHEELS			
Max Verticals		Min Verticals	
6.7		3.2	
LEADING BOGIES			
DMOS B	PTOS	MOS	DMOS A
-1.1	-5.0	-3.3	-4.6
TRAILING BOGIES			
DMOS B	PTOS	MOS	DMOS A
-0.9	-2.5	-2.1	-3.6
CARS			
DMOS B	PTOS	MOS	DMOS A
2.6	-0.1	0.4	0.8
4-CAR TRAIN			
Vertical			
1.0			

© University of Pretoria

Table 4-37: Percentage Change in Lateral Forces After Tamping Summary

% Change in Lateral Forces at 85 km/h after tamping (Overall Average)			
WHEELS			
Max Laterals		Min Laterals	
-50.8		183.7	
LEADING BOGIES			
DMOS B	PTOS	MOS	DMOS A
-53.5	-38.2	-52.4	-43.3
TRAILING BOGIES			
DMOS B	PTOS	MOS	DMOS A
-34.6	-48.4	-61.0	-45.9
CARS			
DMOS B	PTOS	MOS	DMOS A
-50.5	-46.6	-51.8	-44.0
4-CAR TRAIN			
Lateral			
-49.4			

4.4.11 Track Forces Discussion for the Curve

Following on from the data analysis that was done for the rail forces experienced due to the wheels, the bogies, the cars and the 4-car train, as discussed in Sections 4.4.1 to 4.4.10, the final step that was taken was to analyse the forces experienced by the railway track in the curve as whole. The sign convention that was used for analysing the track forces can be seen in Figure 4.14. The vertical track forces convention is the same as for the vertical rail forces, with positive forces being in the downward direction. The lateral track forces convention is slightly different to the lateral rail forces in that positive lateral track forces are taken to be acting to the outside of the curve, while negative lateral track forces are taken to be acting to the inside of the curve.

© University of Pretoria

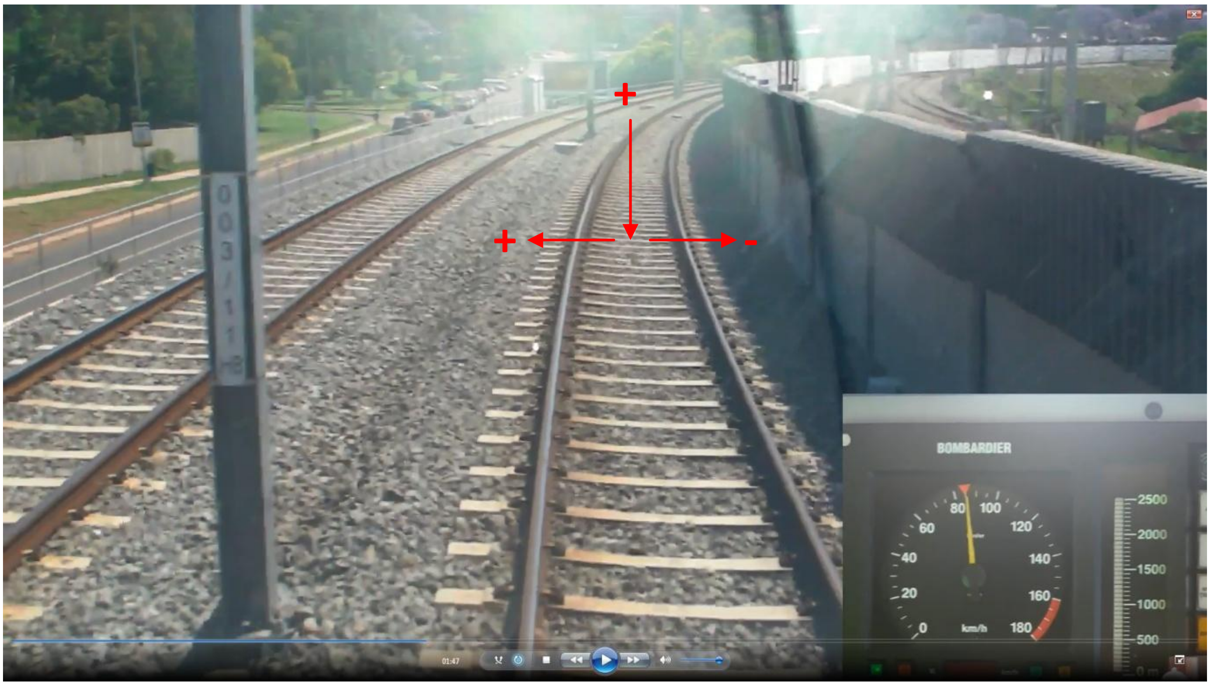

Figure 4.14: Sign Convention for Lateral and Vertical Track Forces

In order to assess the vertical forces experienced by the railway track in the curve as a whole, all the vertical forces experienced by both the high and low leg rails were summed and presented as a single force value for each of the test run speeds, as shown in Table 4-38 to Table 4-45 below for Site 1 Down, Site 1 Up, Site 2 Down and Site 2 Up before and after tamping respectively.

In order to assess the lateral forces experienced by the railway track in the curve as a whole, all the lateral forces experienced by both the high and low leg rails were summed and presented as a single force value for each of the test run speeds, as shown in Table 4-38 to Table 4-45 below for Site 1 Down, Site 1 Up, Site 2 Down and Site 2 Up before and after tamping respectively. Special care had to be taken when summing the lateral forces to ensure that positive high leg lateral rail forces and negative low leg lateral rail forces were seen as creating lateral track forces to the outside of the curve and vice-versa for positive low leg lateral rail forces and negative high leg lateral rail forces.

© University of Pretoria

Table 4-38: Track Forces Before Tamping – S1 Down

Site 1 Down	km/h										
	11.0	20.8	30.6	40.1	49.6	59.6	68.8	79.2	89.0	101.8	109.2
4 Car Train	Before Tamping - Track Force (t)										
Lateral	-27.0	-21.1	-20.3	-19.0	-13.7	-11.8	-8.6	-5.0	1.6	7.8	12.8
Vertical	180.4	171.5	172.1	172.1	172.1	173.2	173.5	174.4	175.8	178.8	182.2

Table 4-39: Track Forces After Tamping – S1 Down

Site 1 Down	km/h										
	11.1	21.0	30.5	40.1	50.2	60.0	69.4	79.4	89.5	98.7	104.0
4 Car Train	After Tamping - Track Force (t)										
Lateral	-23.8	-23.6	-22.0	-20.4	-18.0	-14.6	-6.3	-1.7	4.1	8.2	14.5
Vertical	177.1	178.2	178.3	181.2	179.0	177.3	177.1	174.7	176.6	183.1	181.8

Table 4-40: Track Forces Before Tamping – S1 Up

Site 1 Up	km/h										
	11.3	20.8	30.3	39.5	49.8	59.2	69.6	79.3	90.3	97.6	106.3
4 Car Train	Before Tamping - Track Force (t)										
Lateral	-23.6	-22.5	-22.3	-20.0	-18.4	-14.3	-9.9	-5.8	0.5	4.8	9.9
Vertical	173.0	172.5	172.5	172.4	174.3	177.1	178.2	180.1	182.3	184.0	185.0

Table 4-41: Track Forces After Tamping – S1 Up

Site 1 Up	km/h										
	11.0	20.5	30.3	40.1	50.1	59.6	69.9	79.8	89.4	99.0	104.7
4 Car Train	After Tamping - Track Force (t)										
Lateral	-22.6	-21.8	-19.6	-16.5	-12.6	-7.1	-1.7	7.4	16.0	19.9	23.0
Vertical	177.6	179.7	177.7	177.1	177.2	175.9	172.3	170.6	169.5	168.1	167.4

Table 4-42: Track Forces Before Tamping – S2 Down

Site 2 Down	km/h										
	11.1	21.6	30.1	39.9	49.3	59.5	68.7	79.1	88.3	102.2	108.8
4 Car Train	Before Tamping - Track Force (t)										
Lateral	-20.3	-18.9	-17.8	-16.1	-12.4	-8.6	-4.7	2.1	9.0	17.2	20.3
Vertical	175.0	173.3	173.4	174.5	171.5	170.3	169.4	170.1	171.1	176.2	178.4

© University of Pretoria

Table 4-43: Track Forces After Tamping – S2 Down

Site 2 Down	km/h										
	11.1	20.9	30.7	40.3	50.1	60.0	69.4	79.6	89.3	99.1	104.1
4 Car Train	After Tamping - Track Force (t)										
Lateral	-28.4	-27.6	-27.2	-27.1	-24.2	-21.5	-19.3	-13.7	-7.3	-3.2	0.1
Vertical	167.3	167.5	168.2	168.7	169.8	169.5	171.9	170.8	174.7	176.9	177.8

Table 4-44: Track Forces Before Tamping – S2 Up

Site 2 Up	km/h										
	11.3	20.8	30.5	39.8	49.9	59.1	69.0	78.9	89.2	97.5	104.8
4 Car Train	Before Tamping - Track Force (t)										
Lateral	-21.1	-20.8	-19.1	-15.5	-12.7	-8.5	-4.8	0.0	5.6	11.7	15.6
Vertical	173.3	173.2	173.9	173.4	173.5	171.8	170.8	169.8	169.7	169.0	166.8

Table 4-45: Track Forces After Tamping – S2 Up

Site 2 Up	km/h										
	11.0	20.4	29.8	39.9	49.7	59.5	69.6	79.7	90.1	99.1	104.2
4 Car Train	After Tamping - Track Force (t)										
Lateral	-25.9	-25.7	-24.5	-23.3	-21.0	-18.9	-15.8	-7.5	-1.2	2.8	4.9
Vertical	167.1	168.4	168.3	170.6	171.9	172.8	174.4	173.6	177.7	179.3	179.3

The data presented in Table 4-38 to Table 4-45 is presented graphically in Figure 4.15 to Figure 4.18 below for the vertical track forces and in Figure 4.19 to Figure 4.22 below for the lateral track forces.

© University of Pretoria

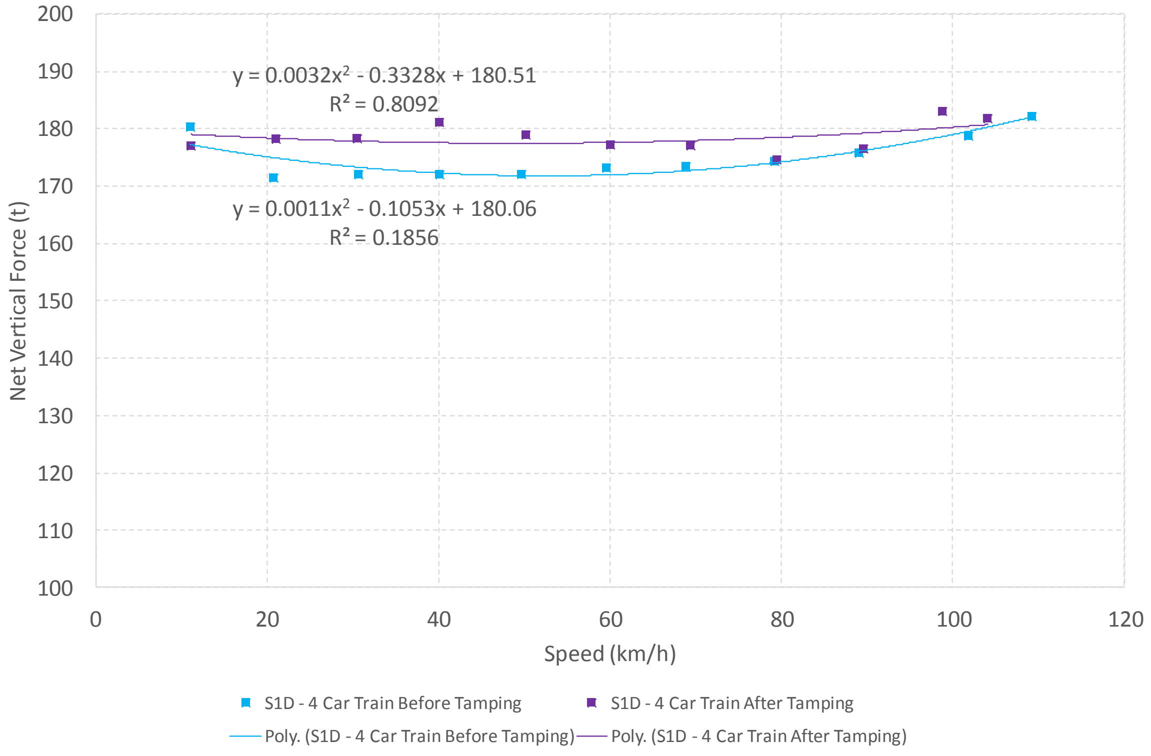

Figure 4.15: Vertical Track Forces Before and After Tamping – S1 Down

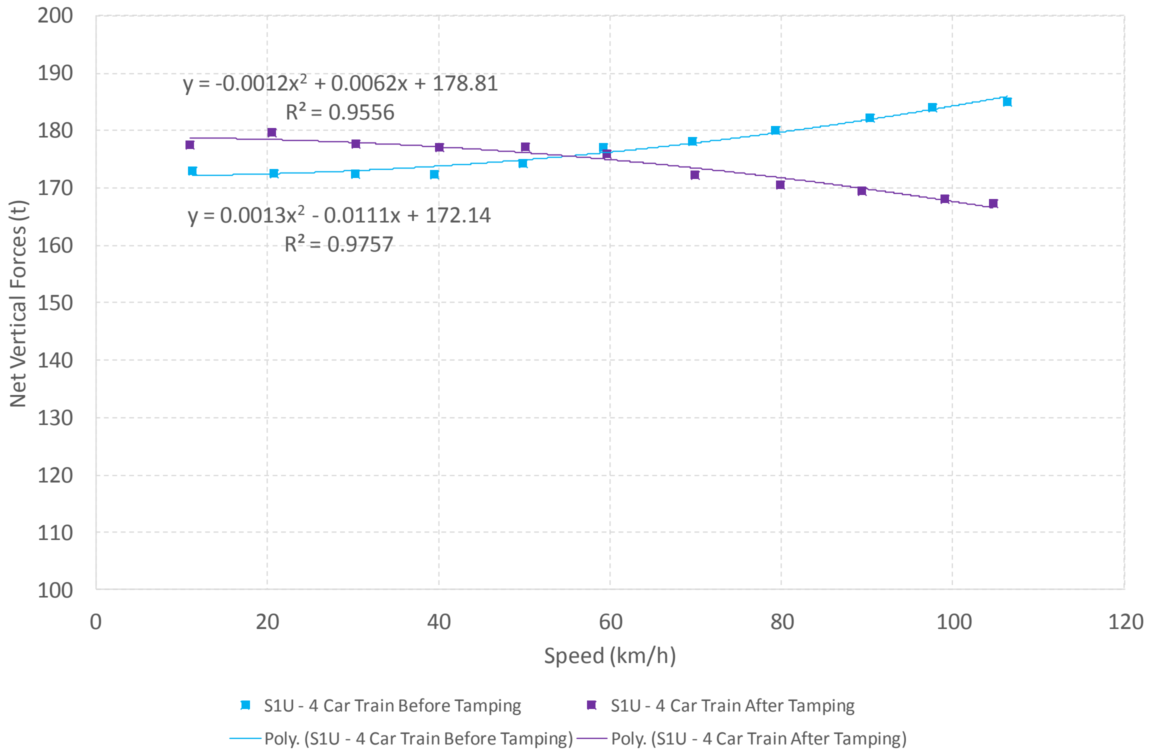

Figure 4.16: Vertical Track Forces Before and After Tamping – S1 Up

© University of Pretoria

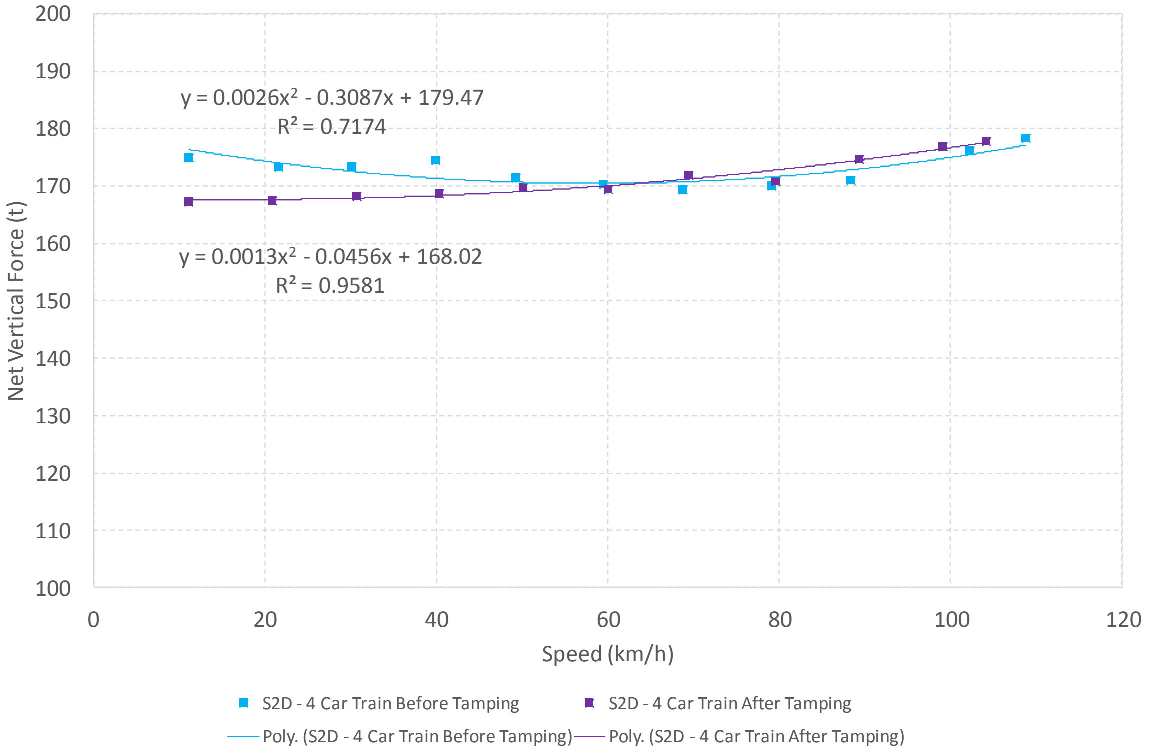

Figure 4.17: Vertical Track Forces Before and After Tamping – S2 Down

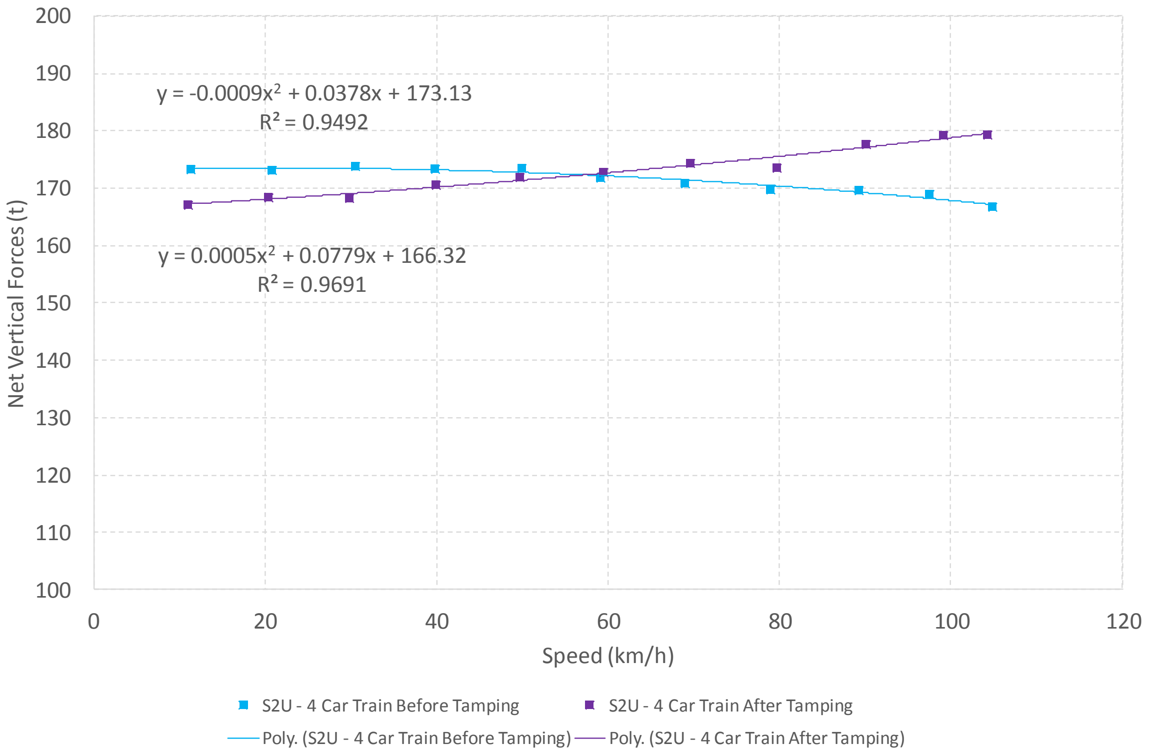

Figure 4.18: Vertical Track Forces Before and After Tamping – S2 Up

© University of Pretoria

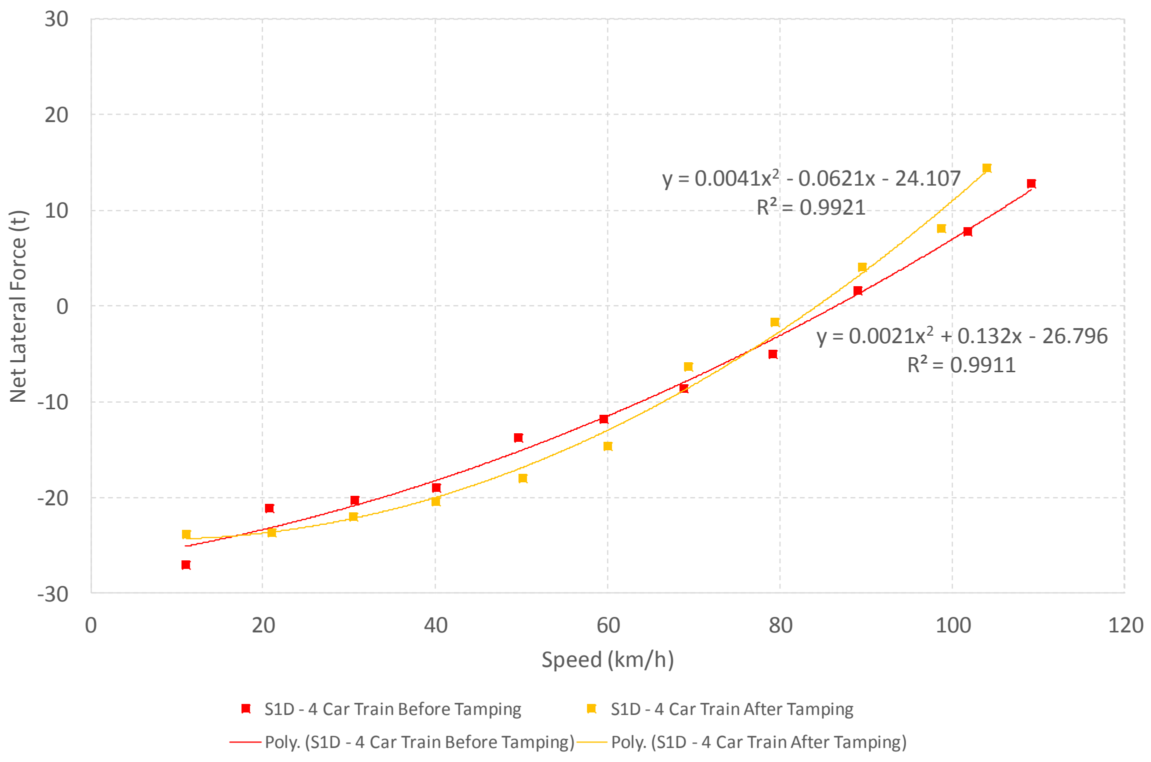

Figure 4.19: Lateral Track Forces Before and After Tamping – S1 Down

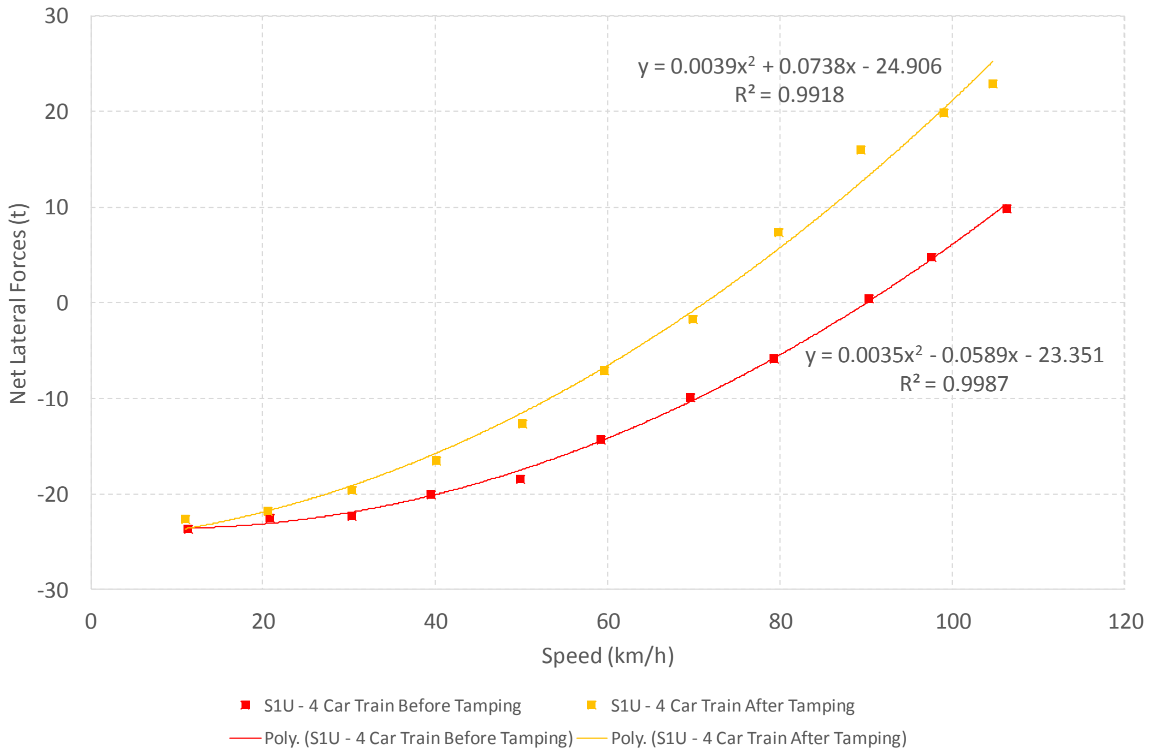

Figure 4.20: Lateral Track Forces Before and After Tamping – S1 Up

© University of Pretoria

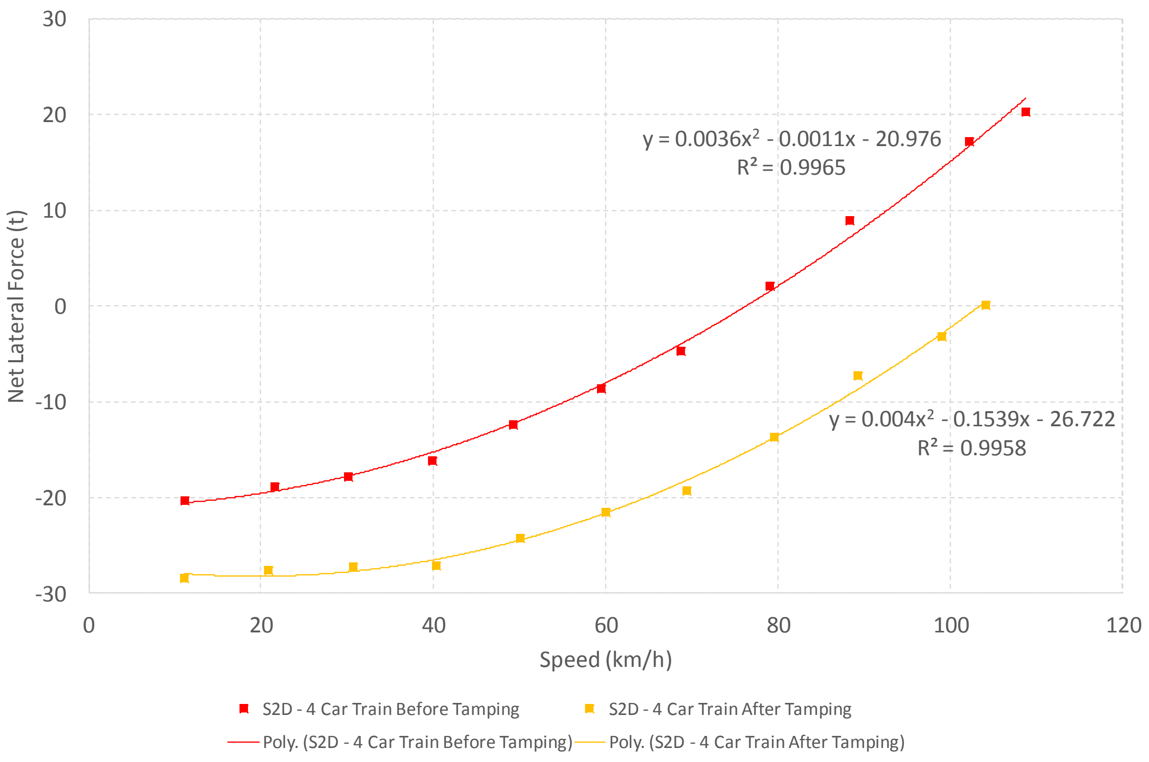

Figure 4.21: Lateral Track Forces Before and After Tamping – S2 Down

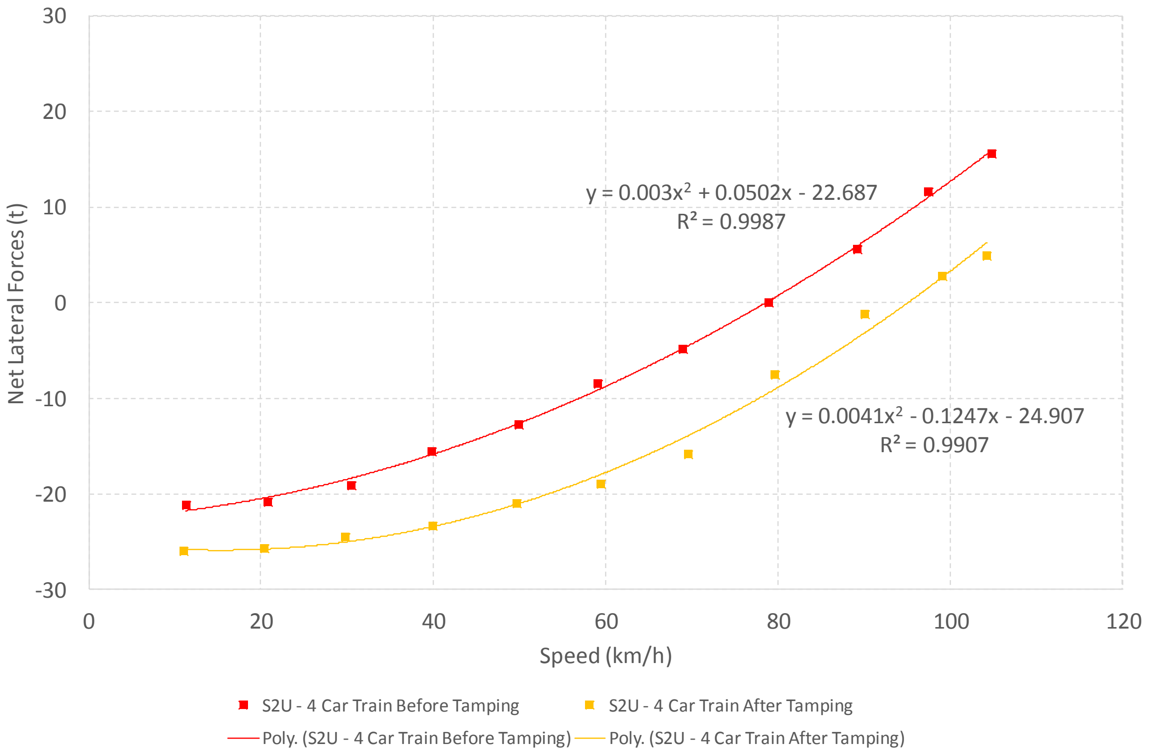

Figure 4.22: Lateral Track Forces Before and After Tamping – S2 Up

© University of Pretoria

With reference to Figure 4.15 to Figure 4.18 the average measured vertical track force and standard deviation for each site can be seen in Table 4-46 below (which is a repeat of Table 3-5). As discussed in Section 3.4.2 the Site 1 after tamping results were scaled prior to the presentation of the Chapter 4 information.

With reference to Table 3-16 in which axle, vehicle and 4-car loads were presented for load state AW0 (service ready train, including full working fluids and one driver; no passengers; no other consumables – as per Table 3-12) it can be seen that a 4-car train is expected to exert a vertical load of 166 t. The information used in determining the estimated vertical load of 166 t was obtained from design documents during the bidding phase of the Gautrain project and therefore does not represent final as-built loads.

The measured vertical track forces can therefore be considered as being true reflections of actual vertical track forces (which include the effect of a dynamic load factor as discussed in Section 2.5.3).

Table 4-46: Average Calibrated Vertical Track Forces and Standard Deviations (STD)

SITE	Before Tamping		After Tamping	
	Avg. Vertical forces (t)	STD (t)	Avg. Vertical forces (t)	STD (t)
Site 1 Down	175.1	3.7	178.6	2.5
Site 1 Up	177.4	4.9	173.9	4.4
Site 2 Down	173.0	2.8	171.2	3.7
Site 2 Up	171.4	2.3	173.0	4.3

With reference to Figure 4.19 to Figure 4.22 and using the trend line equations shown on the graphs the lateral track forces at the operational speed of 85 km/h and the speed at which the lateral forces are equal to zero were calculated and are shown in Table 4-47 and Table 4-48 below.

From Table 4-47 it can be seen that for Site 1 the lateral track forces changed from being to the inside of the curve (negative) before tamping to being to the outside of the curve (positive) after tamping, while for Site 2 the lateral track forces changed from being to the outside of the curve (positive) before tamping to being to the inside of the curve (negative) after tamping.

© University of Pretoria

Table 4-47: Lateral Track Forces at 85 km/h

SITE	Lateral Forces (t) at 85 km/h		
	Before Tamping	After Tamping	% Change after tamping
Site 1 Down	-0.40	0.24	158.7
Site 1 Up	-3.07	9.54	410.9
Site 2 Down	4.94	-10.90	-320.7
Site 2 Up	3.26	-5.88	-280.8

Table 4-48: Speeds at Which Lateral Track Forces are 0 t

SITE	Speed (km/h) for Lateral Forces to = 0 t	
	Before Tamping	After Tamping
Site 1 Down	85.82	84.63
Site 1 Up	90.53	71.01
Site 2 Down	76.49	103.21
Site 2 Up	79.00	94.62

4.4.12 Coefficient of Determination Discussion

Some of the information presented in this section was interpreted from notes found on the NYU Stern's website (www.stern.nyu.edu) and the University of Reading's website (www.reading.ac.uk), but these have not been formally referenced in the list of references presented in Chapter 6, due to the generic non-descriptive nature of the notes found and the fact that the applicable points were adjusted in terms of their context to apply to the research being presented in this dissertation.

At this point it is appropriate to discuss the implications of the wide ranging coefficients of determination (R^2) that are presented as part of the analysis of the data in this chapter, as well as in Appendices C, D, G, H, I and J.

R^2 is known to always be between 0 and 1 and is a measure of the strength of a relationship between variables, ranging from no relationship if $R^2 = 0$ to a perfect correlation if $R^2 = 1$.

In the case of this research the relationship in question was train speed versus force (both vertical forces and lateral forces), with the only variable that was changed being that of the cant of the experimental curve. Due to the nature of an operational railway environment and the understandably rigorous procedures that need to be followed in order to change any design condition on an operational railway line, the cant could only be changed once, and

© University of Pretoria

therefore only two sets of data were obtainable from the field tests undertaken (before and after tamping).

From the collected data, linear regression analysis was used for the analysis at “wheel” level, while 2nd order polynomial regression analysis was used for the analysis at “bogie”, “car” and “4-car train” level.

In this chapter sixteen coefficients of determination are presented (all from 2nd order polynomial regression analyses). Eight in total in Figure 4.15 to Figure 4.18, that deal with the vertical forces for a 4-car train, and eight in total in Figure 4.19 to Figure 4.22, that deal with the lateral forces for a 4-car train.

All eight of the coefficients of determination in Figure 4.19 to Figure 4.22 are greater than 0.99, which indicates very good correlation between the speed of the train and the net lateral forces.

The eight coefficients of determination in Figure 4.15 to Figure 4.18 however indicate a much weaker overall correlation between the speed of the train and the net vertical forces, ranging from 0.1856 for “Site 1 Down Before Tamping” to 0.9757 for “Site 1 Up Before Tamping”, although other than the R^2 of 0.1856, all of the other seven R^2 values are greater than 0.71.

In Appendices C and D the linear regression analysis of the data at “wheel” level is presented. Several very low R^2 values are presented, ranging from 0.0045 for the maximum high leg lateral forces at “Site 1 Up Before Tamping” to 0.9818 for the minimum low leg lateral forces at “Site 2 Down Before Tamping”. Both low and high R^2 values were also found for the various vertical forces analyses that were done, and there is no clear pattern defining what determines a low versus a high R^2 value in terms of the data. An R^2 value of 0.0045 indicates that there is almost no relationship in these particular sets of data, but it should be noted that while the aim of the use of regression analysis in this study was to assess the relationship between the train speed and forces, in such a way as to use the train speed to explain the forces at the differing cant values, this explanation may not always be one of cause and effect.

With specific reference to the analysis dealing with lateral forces, possible explanations for the large variance in R^2 values, could be due to the low forces involved when dealing with lateral forces. One train could measure a maximum lateral force of -0.5 t, while the next train measures a maximum later force of +0.5 t, which is only a absolute difference of 1 t, but equates to a 200% increase in force. Several train runs could then fluctuate between negative and positive values, which would have a noticeably detrimental effect on the R^2 value.

© University of Pretoria

Under certain operating conditions train wheels may struggle to find their desired or preferred running path and then enter into a state of hunting in order to try and achieve their preferred running path, with hunting oscillation being defined as a periodic motion in lateral displacement. Hunting could therefore also have a significant effect on the lateral loads and to a certain degree the vertical loads as well, dependant on the wheel positions on the rail heads of the both the high and low legs at the location of the strain gauges.

Lastly driver behaviour, such as braking or accelerating in the vicinity of the strain gauges could also influence the measured values, thus also undermining a good R^2 value for the data, while nonetheless still providing insights into the general trend line shapes, albeit with a less than ideal R^2 value. In this experiment the drivers were cautious not to compromise the integrity of the data, and took care to drive as consistently as possibly, but nonetheless varying a train's speed from 10 – 110 km/h through a 318 m long curve will invariably incorporate some inconsistencies between test runs.

4.4.13 Derailment Ratio Analysis

Using the measured vertical and lateral wheel forces data as presented in Table 4-11 and Appendix B, a derailment ratio (DR) analysis was undertaken to assess the running safety of the test trains through the experimental curve before and after tamping.

The derailment ratio was calculated by dividing the maximum measured lateral forces by the maximum measured vertical forces for each wheel at each test train run speed. Using the maximum lateral and vertical forces for each wheel may not strictly give the worst case scenario in terms of a derailment ratio, but does provide a good indication of what effect tamping had on the derailment ratio.

Table 4-49 below indicates the maximum derailment ratio values for each site in both directions. As discussed in Section 2.7.12 a derailment ratio of less than or equal to 0.8 over 2 m is considered to be safe, therefore all the calculated derailment ratios in this case are considered to be safe.

© University of Pretoria

It can be seen that tamping reduced the maximum derailment ratio at both sites and in both directions of travel, indicating that from a running safety point of view reducing the cant of the experimental curve made the running of trains through this curve safer. The speed at which the maximum derailment ratios were measured also all reduced after tamping, meaning that for this curves' normal operational speed of 85 km/h, the risk of derailment has also been reduced.

Table 4-49: Maximum Derailment Ratio Values for Each Site in Both Directions

SITE	Before Tamping		After Tamping		% Change after tamping	
	DR	Speed (km/h)	DR	Speed (km/h)	DR	Speed
S1 Down	0.66	79.17	0.52	30.50	-21.4	-61.5
S1 Up	0.59	106.32	0.55	69.90	-7.5	-34.3
S2 Down	0.62	79.08	0.51	20.87	-16.9	-73.6
S2 Up	0.56	89.23	0.53	20.39	-5.9	-77.2

4.5 RAIL AND TRACK FORCES RESULTS DISCUSSION

The research involved reducing the cant of an experimental curve, while leaving the operational speed of 85 km/h unchanged. The actual original cant of the experimental curve (107.1 mm) translated into a theoretical equilibrium speed of 61.9 km/h and a cant deficiency of 95.0 mm for the given curve characteristics as presented in Table 4-1. After the cant was reduced from 107.1 mm to 92.0 mm, the theoretical equilibrium speed dropped to 56.7 km/h and the cant deficiency increased to 114.8 mm. With specific reference to the exact locations of Site 1 and Site 2, the cant was reduced from 109.9 mm to 91.5 mm for Site 1 and from 105.9 mm to 92.8 mm for Site 2.

The theory indicates that the reduction of the cant in this specific test curve, given all of the other curve characteristics, should have resulted in an increase in the lateral forces, but this was not found to be consistently the case, with the majority of the scenarios that were investigated (i.e. wheel, bogie, car, 4-car train and track lateral forces) indicating a reduction in lateral forces when comparing the before and after tamping results.

The specific results and some suggested reasons for the variations between the theoretically expected results and the results derived from the experimental results measured on-site in the experimental curve are discussed in further detail in Chapter 5.

© University of Pretoria

4.6 WHEEL/RAIL INTERACTION VIDEOS DATA

As discussed in Section 3.4.4 some video footage of the wheel/rail interaction during the test runs was recorded. Images from the captured videos are shown in Figure 4.23 to Figure 4.26 below.

Figure 4.23: HL Before Tamping – DMOS B W1 A1 110 km/h in the Up Direction

Figure 4.24: HL Before Tamping – DMOS B W1 A1 110 km/h in the Down Direction

© University of Pretoria

Figure 4.25: LL After Tamping – DMOS B W8 A1 70 km/h in the Down Direction

Figure 4.26: LL After Tamping – DMOS B W8 A1 60 km/h in the Up Direction

No vertical force information could be assessed from the wheel/rail interaction video footage. If the method were to be used on a section of track where track discontinuities, such as proud or dipped welded rail joints were present, the observation of the displacement of the train wheel in the vertical direction would be evidence of the presence of vertical impact forces in the vicinity of the track discontinuity.

As described in Section 2.7.7 and Section 2.7.8 lateral forces at the wheel/rail interface are generated when a wheelset negotiates a sharp curve, due to the leading wheelset needing to assume an angle of attack to the curve and thereby developing lateral forces. When the wheelset runs with a significant angle of attack for a significant distance, one of the flanges will be forced into contact with the rail, in accordance with one of the following two cases:

- Case 1: If a train negotiates a curve at a speed higher than the equilibrium speed (see Figure 4.1 and Figure 4.2) then a situation in which cant deficiency exists is created. Cant deficiency produces flanging on the high leg and thus lateral wear of the high leg rail head.
- Case 2: If a train negotiates a curve at a speed lower than the equilibrium speed (see Figure 4.1 and Figure 4.2) then a situation in which cant excess exists is created. Cant excess produces flanging on the low leg and thus lateral wear of the low leg rail head.

Table 4-50 below provides details with regard to the scenario applicable to each wheel/rail interaction image shown in Figure 4.23 to Figure 4.26.

Table 4-50: Summary of Wheel/Rail Interaction Images

Figure	Leg	Tamping	Speed (km/h)	Cant	Wheel
4.26	High	Before	110	Deficiency	Wheel 1 on Axle 1 of DMOS B
4.27	High	Before	110	Deficiency	Wheel 1 on Axle 1 of DMOS B
4.28	Low	After	70	Deficiency	Wheel 8 on Axle 1 of DMOS B
4.29	Low	After	60	Deficiency	Wheel 8 on Axle 1 of DMOS B

For all the images shown cant deficiency is applicable, as the equilibrium speed of the curve is 56.7 km/h, and all the images shown are for speeds greater than the equilibrium speed. It can however be seen that for the low leg the wheel flange is closer to the low rail head at 60 km/h than at 70 km/h. The further the wheel flange is from the low rail head the closer the wheel flange will be to the high rail head. Therefore as expected the situation of cant

© University of Pretoria

deficiency produces flanging on the high leg. The greater the cant deficiency the greater the high leg flanging. The camera set up on the high leg wheel did not provide the best angle in terms of assessing flange contact, but Figure 4.23 and Figure 4.24 do confirm that at the high speed of 110 km/h high leg flange contact was present.

Figure 4.23 to Figure 4.26 also clearly show the position of the wheel/rail contact band for both the high leg and the low leg. For the high leg, the contact band can be seen on the gauge side of the rail, while the low leg contact was to the field side of the rail. In order to move the high leg contact band away from the gauge corner the cant needs to be reduced (as was done in this dissertation) or alternatively the operational speed of the train through this curve needs to be increased.

In curves, severe wheel/rail lateral interaction commonly occurs on the outer rail, with RCF mainly developing on the outer rail in curves. For the experimental curve in question no RCF on either rail has been observed.

© University of Pretoria

CHAPTER 5 CONCLUSIONS AND RECOMMENDATIONS

The conclusions and recommendations from the investigation are discussed in this chapter. The use of trend analysis allowed various conclusions to be drawn, and highlighted the differences between the theoretical and experimental results.

The main objective of this study, namely attempting to optimize the experimental GRRL curve from a track point of view, can be considered to have been achieved, as the reduction of cant did result in a significant reduction in the lateral forces experienced by the curve, while having a negligible effect on the vertical forces. This outcome was counterintuitive to what was theoretically expected. The next step in the optimization process would have been to look beyond the track and to investigate whether any realistically practical changes to the trains can be made to optimize the train's curving performance.

5.1 CONCLUSIONS

The following section will provide some concluding remarks with regard to the findings from the research.

The body of theoretical first principles knowledge with regard to the negotiation of a curve by a train is extensive, comprehensive and technically sound from a physics point of view. Accurately reproducing and/or measuring the expected data from a train negotiating a curve is difficult to achieve. Furthermore it is difficult to simultaneously assess vertical and lateral forces. As presented in Chapter 4, vertical and lateral forces need to be analysed separately from one another, with separate balancing forces and balancing speeds being calculated for each one. This implies that an overarching equilibrium speed would be very difficult to achieve in practise, as a multitude of factors lead to variations in the vertical and lateral forces experienced by the rail.

In this investigation the scope was purposefully limited in an attempt to use strain gauge technology to capture rail force data that could then be compared to the expected first principle calculations.

Assessing each set of test data independently did validate the existence of the expected relationships between the vertical and lateral rail forces, the speed and the superelevation. This was done by means of comparing the mathematical solution used in the design process to the measured forces on the track.

© University of Pretoria

When comparing the before and after tamping results using trend analysis, various relationships between the vertical and lateral rail forces, the speed and the superelevation were again identified, but these relationships were less rigorous than those established for the independent sets of data.

5.1.1 Lateral Forces

The most significant finding when comparing the before and after tamping results to one another was that while the theory indicates that the reduction of the cant in this specific test curve, given all of the other curve characteristics, should have resulted in an increase in the lateral forces, there was in fact a roughly 50% reduction in the lateral forces. With reference to Table 4-37 there was a 50.8% reduction in the maximum lateral wheel forces after the cant was reduced, a 53.5% reduction in the maximum lateral leading bogie forces, a 61.0% reduction in the maximum lateral trailing bogie forces, a 51.8% reduction in the maximum lateral car forces and a 49.4% reduction in the maximum lateral 4-car train forces.

The reason for the counter-intuitive experimental setup was due to the fact that the selected curve was found to be experiencing high leg contact to the gauge side of the rail, while the low leg contact was to the field side of the rail. In order to move the high leg contact band away from the gauge side of the rail the cant needs to be reduced (as was done in this dissertation) or alternatively the operational speed of the train needs to be increased.

The most likely explanation for the lateral forces decreasing instead of increasing is believed to be related to the wheels and bogies of the Gautrain Bombardier Electrostars performing better in the curve than theoretically expected. The mechanical set up and response of the wheels and bogies of the trains in terms of steering, primary suspension, secondary suspension, anti-roll bars, vertical dampers, lateral dampers, yaw dampers, bump stops etc. was beyond the scope of this study, but should form part of future studies investigating the results of this dissertation.

Furthermore even the slightest amount of hunting oscillation of the wheels in the lateral direction causes significant variations in the measurements of the lateral forces. As the strain gauges were pasted at discreet points on the rail, variations in the position of the wheel on the rail due to hunting at these discreet points will have a noteworthy influence on the measured forces.

© University of Pretoria

In terms of the applied cant it was shown by Elkins and Eickhoff (1982) that an increase in cant deficiency makes both the wheelsets run further out in a curve, to reduce the angle of attack of the leading wheelset and bring about a small negative angle of attack of the trailing wheelset. Expressed from a different perspective, Fröhling (2012) explains that cant excess reduces the curving performance of rolling stock, due to the inner wheel running on a larger radius than the outer wheel in a curve with cant excess.

Grassie and Elkins (2005) also mention how cant deficiency has a favourable effect on curving performance due to the fact that cant deficiency brings about a change in distribution of tangential force between wheels, so that there is a more even distribution of creep forces and for all but the highest levels of tractive effort, traction on the high rail wheels is lower than that on the low rail wheels. As a result of the more even distribution of tangential force, the traction ratios overall are lower than for curving at balance speed. Grassie (2012) went on further to state that rail maintenance would be reduced if mixed traffic lines were canted for lower speed freight traffic than for higher speed passenger traffic. The converse is common, if not universal, practice.

5.1.2 Vertical Forces

In the vertical direction the results proved useful and relationships were discovered that did agree with the theoretically expected results as discussed in Chapter 4. The reduction of cant had a minimal effect on the magnitude of the vertical forces, but did result in a transfer of loading between the high and low legs.

5.1.3 Maximum and Minimum Vertical and Lateral Force Positions

The positions of the maximum and minimum vertical and lateral forces on the train in each travel direction were interesting to note (see Figure 4.4):

- All the maximum vertical and lateral forces before and after tamping occurred at wheels on the DMOS A/B vehicles.
- The minimum vertical and lateral forces before and after tamping occurred at wheels on the PTOS and MOS vehicles, except for the minimum high leg lateral forces which occurred at a wheel on the trailing axle of the lead bogie of the DMOS A/B vehicles.

© University of Pretoria

The travel direction had a minimal effect on where the maximum and minimum vertical and lateral forces occurred, as the positions of these forces were dependent on the mass properties (see Table 3-15) and load balancing (see Figure 3.42) of the train.

5.1.4 Balancing Speeds

The theoretical equilibrium speed before and after tamping for Site 1 was 62.7 km/h and 56.5 km/h respectively, while for Site 2 it was 61.5 km/h and 56.9 km/h respectively (see Table 4-4).

The balancing speeds for the maximum vertical forces varied between 42.3 km/h and 76.8 km/h for Site 1 before and after tamping in the up and down directions (see Table 4-12 and Table 4-13) and between 39.9 km/h and 52.7 km/h for Site 2 before and after tamping in the up and down directions (see Table 4-14 and Table 4-15).

The balancing speeds for the maximum lateral forces varied between 71.8 km/h and 163.4 km/h for Site 1 before and after tamping in the up and down directions (see Table 4-12 and Table 4-13) and between 77.0 km/h and 82.0 km/h for Site 2 before and after tamping in the up and down directions (see Table 4-14 and Table 4-15). The speeds given for Site 2 disregard the impractical calculated balancing speeds of -295.5 km/h and 2444.1 km/h.

As stated previously, to assess vertical and lateral forces simultaneously and to determine an overarching equilibrium speed would be very difficult to achieve in practise. Furthermore the results of this research, specifically with regard to the measured lateral forces generally being lower after tamping (contradictory to the expected first principles theory) could indicate that the first principles balancing speed calculation may in fact not be resulting in the curve experiencing the optimal vertical and lateral forces combination. This observation would however need to be studied in further detail in follow-up research.

© University of Pretoria

5.1.5 Rail Forces

The cant of the curve before tamping was 107.1 mm and this was reduced to 92.0 mm after tamping, which equates to a 14% reduction in cant. Assessing the percentage change in forces at wheel level at the operational speed of 85 km/h (see Table 4-28) revealed the following results for this 14% reduction in cant:

- There was a zero net effect on the average maximum vertical high leg forces, with a corresponding 13.4% increase in the maximum vertical low leg forces. The average maximum vertical forces therefore increased by 6.7%.
- As discussed previously the minimum vertical forces are of less interest, as only positive vertical forces are measured (see Figure 3.30).
- An average reduction of 50.8% in maximum lateral forces, with a 61.8% reduction in the maximum lateral high leg forces and an average 39.8% reduction in the maximum lateral low leg forces.
- There are some large percentage changes in the minimum lateral forces (a 612.2% increase at Site 1 in the up direction on the high leg and a 581.1% increase at Site 2 in the up direction on the high leg). Assessing the absolute values (Table 4-20 to Table 4-23) of these changes however reveals that all of the minimum lateral forces are between -1 t and 1 t, therefore the forces themselves are small, but the percentage changes relative to the small force are large.

From the above results it is significant to take note of the 50.8% reduction in maximum lateral wheel forces that occurred as a result of the 14% reduction in cant, as well as the 53.5% reduction in the maximum lateral leading bogie forces, the 61.0% reduction in the maximum lateral trailing bogie forces, the 51.8% reduction in the maximum lateral car forces and the 49.4% reduction in the maximum lateral 4-car train force (see Table 4-37).

The wear of the rail and wheels is strongly linked to the magnitude of forces that they experience. Although other factors also need to be taken into account it is not unreasonable to presume that a 50% reduction in maximum lateral forces could lead to a halving of the wear rate of the rail and wheels in this curve.

© University of Pretoria

5.1.6 Track Forces

With specific reference to the lateral track forces (see Table 4-47 and Table 4-48) the reasons for the lack of conformity with regard to the before and after tamping lateral track forces and the speeds at which the lateral forces would be equal to 0 t have not been identified, but may include the following possibilities:

- As the strain gauges are pasted at discreet points on the rail, variations in the position of the wheels on the rail at different speeds due to train vehicle hunting will have a noteworthy influence on the measured forces at these discreet points.
- The mechanical set up and response of the wheels and bogies of the Gautrain Bombardier Electrostars at differing speeds (primary suspension, secondary suspension, anti-roll bars, vertical dampers, lateral dampers, yaw dampers, bump stops etc.).
- In a 4-car Gautrain Electrostar consist, 12 of the axles are powered. The 4 non-powered axles are all on the PTOS car, therefore all 4 axles on each of the DMOS A, MOS and DMOS B cars are powered. This powered versus non-powered axle set up may have an effect on the rail/track forces, specifically during acceleration or deceleration (braking) conditions. The acceleration/braking conditions specific to the track geometry of the test curve in question are discussed in Section 5.1.7 below.

5.1.7 Track Geometry Aspects Affecting the Measured Forces

From a track geometry point of view it is worth noting that on the Pretoria side of the test curve in close proximity to the left hand test curve there is a right hand curve, while on the Hatfield side there is a long section of straight track (see Figure 3.6).

In the down direction (Hatfield towards Pretoria) the long section of straight track approaching the test curve allowed the test train driver to reach the desired test speed before entering the test curve, but at the higher test speeds (95 km/h and above) upon exiting the curve, the train driver needed to immediately apply brakes to ensure that the train entered the adjacent opposite direction curve at a safe speed. The desired down direction test speeds were all achieved, but the forces measured at Site 2 for the higher test run speeds, might have been measured with the test train in its initial stages of deceleration.

© University of Pretoria

During the return runs in the up direction (Pretoria towards Hatfield) the test train driver needed to negotiate the adjacent opposite direction curve at a safe speed before accelerating to reach the desired test speeds before entering the test curve. The desired up direction test speeds were all achieved, but the forces measured at Site 2 for the higher test run speeds, might have been measured with the test train in its final stages of acceleration.

5.2 RECOMMENDATIONS

The first follow-up research step that could be taken with specific reference to this dissertation would be to repeat the same experiment in another similar curve or curves.

There are many further interesting aspects of railway curves that can be studied in great detail, but as was shown in this relatively narrow study, many limitations exist in terms of matching theoretically expected results with experimental results. Any further research would therefore need to pay very close attention to the accurate capturing of real world experimental data that proves or disproves the first principle knowledge. This is true of all scientific research, but in the case of wheel/rail interaction the control of variables is significantly challenging.

While this research focused on the relationship between vertical and lateral forces, speed and superelevation in railway curves, further research into these same relationships for transition curves, specifically looking into the transition curves cant gradient as a function of time and distance, as well the rate of cant deficiency as a function of time and distance could prove useful.

The supplementation of all wheel/rail interaction research to simultaneously include track and vehicle data collection would also go a long way in eliminating some of the unknowns. The use of accelerometers on the train, but preferably on the track side of the suspension system would provide insights into the movements of the train. Further supplementing this with a comprehensive wheel/rail interaction video capturing system would eliminate many of the parameters that in the context of this study were unknown. Furthermore, detailed research can be done from a mechanical railway engineering perspective in terms of wheels, bogies, vehicle and train steering and suspension.

Lastly further strides can be made in terms of refining the consolidation of the theoretical results with the experimental results if additional curves are tested using rigorously repeatable experimental designs, as well as by adding more track side measuring stations in the curve(s).

© University of Pretoria

CHAPTER 6 REFERENCES

Benson, M. (1993). *Effect of differential hardness on wheel/rail wear literature survey.* Derby: British Rail Research.

Burstow, M. (2012). *Wheel/rail hardness and total 'system' wear.* London: Railway Safety and Standards Board.

Cornwell, N. (2005). *Rail Supply.* Johannesburg: Bombardier.

Dirks, B. & Enblom, R. (2011). Prediction model for wheel profile wear and rolling contact fatigue. *Wear*, 210-217.

Elkins, J. A. & Eickhoff, B. M. (1982). Advances in non-linear wheel/rail force prediction methods and their validation. *Journal of Dynamic Systems, Measurement, and Control*, 133-142.

Esveld, C. (2004). *Investigation of the train accident on 22 July 2004 near Pamukova, Turkey.* Zaltbommel: ECS.

Esveld, C. (2001). *Modern Railway Track.* Delft: MRT-Productions.

Fröhling, R. (2012). *Cant and Maximum Permissible Speed in Curves Between Piet Retief and RBCT.* Pretoria: Transnet Freight Rail.

Grassie, S. L. (2012). Traction, Curving and Surface Damage of Rails, Part 2: Rail Damage. *9th Internatinal Conference on Contact Mechanics and Wear of Rail/Wheel Systems*, (pp. 1-8). Chengdu.

Grassie, S. L. & Elkins, J. A. (2005). Tractive effort, curving and surface damage of rail Part 1. Forces exerted on the rails. *Wear*, 1235-1244.

Harris, J. W., Ebersohn, W., Lundgren, J., Tournay, H. & Zakharov, S. (2001). *Guidelines to Best Practices for Heavy Haul Railway Operations: Wheel and Rail Interface Issues.* Virginia Beach: International Heavy Haul Association.

Iwnicki, S. D. (2006). *Handbook of Railway Vehicle Dynamics.* Boca Raton: CRC Press.

© University of Pretoria

Iwnicki, S. D. (2009). The Effect of Profiles on Wheel and Rail Damage. *International Journal of Vehicles Structures & Systems*, 99-104.

Kalousek, J. (2002). Keynote Address: light to heavy, snail to rocket. *Wear*, 1-8.

Kalousek, J. (2005). Wheel/rail damage and its relationship to track curvature. *Wear*, 1330-1335.

Kalousek, J. & Magel, E. (1997, January). OWRI: Optimizing the wheel/rail interface. *Railway Track and Structures*, 28-X3.

Lauriks, G., Evans, J., Forstberg, J., Balli, M. & Barron de Angoiti, I. (2003). *UIC comfort tests (VTI notat 56A-2003).* UIC.

Lindahl, M. (2001). *Track geometry for high-speed railways.* Stockholm: Royal Institute of Technology.

Magel, E. & Kalousek, J. (2002). The application of contact mechanics to rail profile design and rail grinding. *Wear*, 308-316.

Monash University. (n.d.). Advancing the Railway Industry through Technology. Victoria, Australia: Institute of Railway Technology.

Mutsvene, P. (2007). *System Design Description.* Johannesburg: Bombardier.

Network Rail. (2010). *Track Desing Handbook NR/L2/TRK/2049.* London: Network Rail.

Olofsson, U. & Lewis, R. (2006). *Handbook of Railway Vehicle Dynamics.* Boca Raton: CRC Press.

Redtenbacher, F. J. (1855). *Die Gesetze des Locomotiv-Baues.* Mannheim.

Reitmann, E. (2013). *Vertical Load Cross-Talk Investigation on Web-Bending vs Base-Chevron Lateral Force Measurement Techniques.* Pretoria: Transnet Freight Rail.

Roney, M., Tournay, H., Lonsdale, C., Allen, R., Reinschmidt, A., Kalay, S., et al. (2015). *Guidelines to Best Practices for Heavy Haul Railway Operations: Wheel and Rail Interface Issues*. Virginia Beach: International Heavy Haul Association.

Santamaria, J., Vadillo, E. G. & Oyarzabal, O. (2009). Wheel-rail wear index prediction considering multiple contact patches. *Wear*, 1100-1104.

© University of Pretoria

Selig, E. T. & Waters, J. M. (1994). *Track Geotechnology and Substructure Management.* Townbridge, England: Thomas Telford.

Tournay, H. M. (2008). A future challenge to wheel/rail interaction analysis and design: Predicting worn shapes and resulting damage modes. *Wear*, 1259-1265.

Tournay, H. M. & Mulder, J. M. (1996). The transition from the wear to the stress regime. *Wear*, 107-112.

Tzanakakis, K. (2013). *The Railway Track and Its Long Term Behaviour.* Berlin: Springer.

UIC Code 518. (2005). *Testing and Approval of Railway Vehicles from the Point of View of their Dynamic Behaviour – Safety – Track Fatigue – Ride Quality.* Paris: International Union of Railways.

University of Pretoria. (2010, September 13). Course Notes. *Introductory Course on Multi-Disciplinary Concepts in Railway Engineering* . Pretoria, Gauteng, South Africa: Continuing Education at the University of Pretoria.

Van Dyk, B. J., Dersch, M. S., Edwards, J. R., Rupert Jr., C. J. & Barkan, C. P. (2013, November 15). Evaluation of Dynamic and Impact Wheel Load Factors and their Application for Design. *Transportation Research Board 93rd Annual Meeting* . Washington, D.C.

Wickens, A. H. (2003). *Fundamentals of Rail Vehicle Dyanmics.* Lisse: Swets & Zeitlinger.

Wikipedia. (2015, November 20). Retrieved from Wikepedia: https://en.wikipedia.org/wiki/Gautrain

Zaayman, L. (2013). *Mechanisation of track work in developing countries.* Plasser.

Zakharov, S. & Zharov, I. (2002). Simulation of mutual wheel/rail wear. *Wear*, 100-106.

Zakharov, S., Goryacheva, I., Bogdanov, V., Pogorelov, D., Zharov, I., Yazykov, V., et al. (2008). Problems with wheel and rail profiles selection and optimization. *Wear*, 1266-1272.

Zeng, J. & Wu, P. (2008). Study on the wheel/rail interaction and derailment safety. *Wear*, 1452-1459.

© University of Pretoria

APPENDIX A. TEST TRAIN RUN SPEEDS

Table A-1: Test Run Speeds Before Tamping – S1 Down

Target Speed (km/h)	Run #	Site 1 Down Before Tamping: Actual Speed (km/h) at greatest Force				AVG. SPEED (km/h)
		Vert HL	Lat HL	Vert LL	Lat LL	
10	1	11.05	11.03	11.05	11.03	11.04
	2	11.40	11.40	11.41	11.41	11.41
20	1	20.77	20.75	20.70	20.80	20.75
	2	21.78	21.77	21.75	21.77	21.77
30	1	30.61	30.64	30.62	30.71	30.65
	2	30.67	30.69	30.63	30.72	30.68
40	1	40.06	40.13	40.07	40.18	40.11
	2	40.23	40.26	40.20	40.31	40.25
50	1	49.65	49.62	49.54	49.77	49.64
	2	48.72	48.74	48.66	48.87	48.75
60	1	59.45	59.66	59.43	59.68	59.56
	2	59.47	59.58	59.54	59.63	59.56
70	1	68.63	69.01	68.70	68.98	68.83
	2	68.47	68.73	68.54	68.70	68.61
80	1	79.06	79.35	78.97	79.31	79.17
	2	78.80	79.14	78.82	79.06	78.95
90	1	89.06	88.99	89.01	89.04	89.02
	2	87.56	87.54	87.63	87.51	87.56
100	1	101.84	101.75	101.72	101.82	101.78
	2	98.27	98.36	98.24	98.25	98.28
	3	97.69	97.60	97.66	97.57	97.63
110	1	105.08	105.08	105.05	105.01	105.05
	2	109.21	109.18	109.14	109.18	109.18

© University of Pretoria

Table A-2: Test Run Speeds Before Tamping – S2 Down

Target Speed (km/h)	Run #	Site 2 Down Before Tamping: Actual Speed (km/h) at greatest Force				AVG. SPEED (km/h)
		Vertical HL	Lateral HL	Vertical LL	Lateral LL	
10	1	11.13	11.12	11.13	11.13	11.13
	2	11.19	11.21	11.20	11.21	11.20
20	1	18.38	18.39	18.38	18.42	18.39
	2	21.57	21.61	21.60	21.60	21.60
30	1	30.58	30.61	30.58	30.68	30.61
	2	30.11	30.13	30.12	30.12	30.12
40	1	39.90	39.88	39.83	39.98	39.90
	2	40.33	40.31	40.36	40.50	40.37
50	1	49.30	49.21	49.14	49.39	49.26
	2	48.78	48.80	48.80	48.96	48.83
60	1	59.54	59.40	59.38	59.59	59.48
	2	59.35	59.29	59.45	59.68	59.44
70	1	68.70	68.56	68.72	68.96	68.74
	2	67.95	68.53	68.25	68.56	68.32
80	1	78.91	79.47	78.91	79.03	79.08
	2	78.74	79.26	78.72	78.68	78.85
90	1	88.27	88.41	88.24	88.36	88.32
	2	87.42	87.49	87.60	87.51	87.50
100	1	102.23	102.16	102.20	102.26	102.21
	2	96.20	96.28	96.25	96.11	96.21
	3	97.34	97.48	97.63	97.54	97.50
110	1	104.81	104.98	104.88	104.88	104.89
	2	108.78	108.81	108.67	108.74	108.75

Table A-3: Test Run Speeds Before Tamping – S1 Up

Target Speed (km/h)	Run #	Site 1 Up Before Tamping: Actual Speed (km/h) at greatest Force				AVG. SPEED (km/h)
		Vertical HL	Lateral HL	Vertical LL	Lateral LL	
10	1	11.38	11.37	11.38	11.35	11.37
	2	11.30	11.29	11.30	11.29	11.30
20	1	20.81	20.79	20.76	20.80	20.79
	2	20.88	20.87	20.84	20.88	20.87
30	1	30.77	30.73	30.70	30.69	30.72
	2	30.29	30.27	30.30	30.25	30.28
40	1	39.51	39.55	39.51	39.33	39.48
	2	39.60	39.51	39.46	39.37	39.49
50	1	49.58	49.60	49.56	49.40	49.53
	2	49.91	49.91	49.82	49.74	49.84
60	1	58.59	58.40	58.57	58.56	58.53
	2	59.26	59.04	59.20	59.30	59.20
70	1	69.46	69.64	69.52	69.52	69.53
	2	69.61	69.74	69.40	69.62	69.59
80	1	79.33	79.39	79.18	79.31	79.30
	2	78.99	78.87	78.74	78.97	78.89
90	1	90.28	90.36	90.33	90.31	90.32
	2	88.65	88.67	88.60	88.62	88.64
100	1	97.51	97.63	97.60	97.63	97.59
	2	97.51	97.60	97.63	97.57	97.58
110	1	101.75	101.78	101.75	101.81	101.78
	2	106.24	106.34	106.38	106.31	106.32
	3	106.24	106.21	106.34	106.24	106.26

© University of Pretoria

Table A-4: Test Run Speeds Before Tamping – S2 Up

Target Speed (km/h)	Run #	Site 2 Up Before Tamping: Actual Speed (km/h) at greatest Force				AVG. SPEED (km/h)
		Vertical HL	Lateral HL	Vertical LL	Lateral LL	
10	1	11.31	11.31	11.31	11.32	11.31
	2	11.45	11.44	11.44	11.44	11.44
20	1	20.80	20.78	20.80	20.79	20.79
	2	20.81	20.83	20.82	20.82	20.82
30	1	30.65	30.67	30.63	30.67	30.65
	2	30.51	30.47	30.51	30.52	30.50
40	1	39.81	39.74	39.79	39.94	39.82
	2	39.57	39.61	39.57	39.68	39.60
50	1	49.93	49.83	49.79	50.12	49.92
	2	49.80	49.89	49.97	49.82	49.87
60	1	58.85	58.92	58.94	58.83	58.89
	2	59.13	58.99	59.14	59.16	59.11
70	1	69.27	68.62	68.96	69.07	68.98
	2	69.74	69.28	69.65	69.79	69.62
80	1	78.89	79.03	78.89	78.84	78.91
	2	78.85	78.97	79.03	78.89	78.94
90	1	89.25	89.23	89.23	89.20	89.23
	2	87.58	87.70	87.67	87.65	87.65
100	1	97.57	97.54	97.37	97.45	97.48
	2	96.96	97.05	97.17	97.08	97.06
110	1	100.14	100.14	99.89	100.14	100.08
	2	104.88	104.85	104.68	104.84	104.81
	3	104.81	104.71	104.78	104.74	104.76

Table A-5: Test Run Speeds After Tamping – S1 Down

Target Speed (km/h)	Run #	Site 1 Down After Tamping: Actual Speed (km/h) at greatest Force				AVG. SPEED (km/h)
		Vertical HL	Lateral HL	Vertical LL	Lateral LL	
10	1	11.37	11.38	11.37	11.40	11.38
	2	11.09	11.10	11.09	11.12	11.10
20	1	21.42	21.39	21.38	21.45	21.41
	2	20.99	21.02	20.99	21.07	21.02
30	1	30.64	30.61	30.70	30.78	30.68
	2	30.47	30.46	30.48	30.58	30.50
40	1	40.42	40.24	40.37	40.45	40.37
	2	40.13	39.92	40.04	40.19	40.07
50	1	49.68	49.57	49.70	49.82	49.69
	2	50.17	50.00	50.12	50.32	50.15
60	1	59.58	59.80	59.52	59.47	59.59
	2	60.04	60.17	59.97	59.87	60.01
70	1	69.39	69.56	69.33	69.25	69.38
	2	69.23	69.62	69.14	69.04	69.26
80	1	79.46	79.44	79.34	79.04	79.32
	2	79.58	79.33	79.49	79.29	79.42
90	1	93.91	93.75	93.99	93.67	93.83
	2	89.69	89.37	89.62	89.50	89.55
100	1	98.09	97.86	98.01	97.71	97.92
	2	99.02	98.51	98.90	98.54	98.74
105	1	101.44	101.03	101.47	100.84	101.19
	2	104.24	104.11	104.04	103.68	104.02

© University of Pretoria

Table A-6: Test Run Speeds After Tamping – S2 Down

Target Speed (km/h)	Run #	Site 2 Down After Tamping: Actual Speed (km/h) at greatest Force				AVG. SPEED (km/h)
		Vertical HL	Lateral HL	Vertical LL	Lateral LL	
10	1	11.74	11.74	11.74	11.77	11.75
	2	11.08	11.09	11.07	11.11	11.09
20	1	21.33	21.34	21.32	21.38	21.34
	2	20.85	20.87	20.83	20.92	20.87
30	1	30.78	30.76	30.78	30.86	30.80
	2	30.68	30.70	30.64	30.75	30.69
40	1	40.56	40.60	40.54	40.67	40.59
	2	40.25	40.29	40.33	40.41	40.32
50	1	50.02	49.97	50.11	50.27	50.09
	2	50.54	50.69	50.54	50.70	50.62
60	1	59.71	59.87	59.47	59.81	59.72
	2	59.95	59.99	60.01	60.17	60.03
70	1	69.39	69.07	69.44	69.74	69.41
	2	69.34	68.95	69.43	69.27	69.25
80	1	79.39	79.01	79.37	79.27	79.26
	2	79.74	79.41	79.70	79.43	79.57
90	1	94.04	93.72	93.85	93.99	93.90
	2	89.30	88.99	89.42	89.50	89.30
100	1	98.33	98.01	98.36	98.57	98.32
	2	99.17	98.72	99.04	99.29	99.05
105	1	102.13	101.78	102.04	102.36	102.08
	2	104.14	103.78	104.11	104.45	104.12

Table A-7: Test Run Speeds After Tamping – S1 Up

Target Speed (km/h)	Run #	Site 1 Up After Tamping: Actual Speed (km/h) at greatest Force				AVG. SPEED (km/h)
		Vertical HL	Lateral HL	Vertical LL	Lateral LL	
10	1	11.72	11.70	11.71	11.66	11.70
	2	10.97	10.98	10.98	10.94	10.97
20	1	20.64	20.65	20.62	20.57	20.62
	2	20.57	20.57	20.55	20.50	20.55
30	1	30.37	30.34	30.33	30.25	30.32
	2	30.48	30.43	30.40	30.36	30.41
40	1	40.60	40.68	40.50	40.44	40.55
	2	40.09	40.23	40.06	39.98	40.09
50	1	50.17	50.28	50.07	49.88	50.10
	2	50.31	50.46	50.23	50.10	50.28
60	1	61.14	61.41	61.09	61.26	61.22
	2	59.57	59.73	59.52	59.61	59.61
70	1	69.92	69.55	70.04	70.05	69.89
	2	70.05	69.59	69.93	70.01	69.90
80	1	78.95	79.06	78.85	79.14	79.00
	2	79.74	79.82	79.89	79.93	79.84
90	1	88.86	89.01	88.98	89.20	89.01
	2	89.18	89.45	89.35	89.50	89.37
100	1	98.42	98.39	98.30	98.36	98.37
	2	98.84	99.04	98.99	99.20	99.02
105	1	103.32	103.36	103.29	103.52	103.37
	2	104.68	104.68	104.57	104.88	104.70

© University of Pretoria

Table A-8: Test Run Speeds After Tamping – S2 Up

Target Speed (km/h)	Run #	Site 2 Up After Tamping: Actual Speed (km/h) at greatest Force				AVG. SPEED (km/h)
		Vertical HL	Lateral HL	Vertical LL	Lateral LL	
10	1	11.46	11.47	11.42	11.86	11.55
	2	11.03	11.01	11.00	10.98	11.01
20	1	20.38	20.41	20.41	20.35	20.39
	2	20.55	20.53	20.55	20.46	20.52
30	1	29.83	29.81	29.84	29.72	29.80
	2	30.31	30.24	30.30	30.21	30.26
40	1	39.83	39.61	39.83	39.64	39.73
	2	39.98	39.94	39.92	39.83	39.92
50	1	49.43	49.31	49.53	49.30	49.39
	2	49.75	49.63	49.72	49.63	49.68
60	1	60.73	60.60	60.83	60.50	60.66
	2	59.58	59.33	59.58	59.30	59.45
70	1	69.49	69.31	69.50	69.30	69.40
	2	69.67	69.64	69.68	69.31	69.57
80	1	79.06	79.16	79.12	79.10	79.11
	2	79.70	79.52	79.72	79.72	79.66
90	1	91.09	90.81	91.14	91.19	91.06
	2	90.06	90.11	90.09	90.11	90.09
100	1	98.33	98.16	98.18	98.66	98.33
	2	99.11	98.93	99.04	99.31	99.10
105	1	103.62	103.36	103.58	103.88	103.61
	2	104.24	103.91	104.21	104.57	104.24

© University of Pretoria

APPENDIX B. CURVE RAIL FORCES DATA FOR WHEELS

Table B-1: Lateral Forces Before Tamping (Wheels) – S1 Down

Hatfield to Pretoria (Down) km 3.215 (Site 1) Before Tamping		km/h										
		11.04	20.75	30.65	40.11	49.64	59.56	68.83	79.17	89.02	101.78	109.18
Car Type and Axle	Wheel and Rail Leg	Lateral Force (t)										
DMOS B Axle 1	Wheel 8 - High Leg	1.40	1.51	1.63	1.37	1.62	1.66	1.59	1.77	1.83	2.04	2.24
	Wheel 1 - Low Leg	3.04	3.21	3.31	3.09	2.99	2.93	2.81	2.66	2.49	2.17	2.14
DMOS B Axle 2	Wheel 7 - High Leg	-0.75	-0.68	-0.64	-0.51	-0.44	-0.38	-0.25	-0.22	0.33	0.61	0.72
	Wheel 2 - Low Leg	0.93	0.68	0.64	0.49	0.35	0.26	-0.18	-0.38	-0.59	-0.83	-0.99
DMOS B Axle 3	Wheel 6 - High Leg	1.19	1.34	1.46	1.39	1.70	1.52	1.55	1.33	1.49	1.46	1.64
	Wheel 3 - Low Leg	2.81	2.93	3.08	2.93	2.94	2.85	2.69	2.54	2.10	1.73	1.60
DMOS B Axle 4	Wheel 5 - High Leg	-0.78	-0.51	-0.44	-0.45	-0.28	-0.24	-0.15	0.16	0.38	0.78	0.99
	Wheel 4 - Low Leg	0.82	0.38	0.25	0.25	-0.06	-0.13	-0.31	-0.43	-0.63	-0.92	-0.92
PTOS Axle 4	Wheel 4 - High Leg	1.93	2.02	2.20	2.12	2.04	2.15	2.03	2.14	2.10	2.09	2.27
	Wheel 5 - Low Leg	3.04	3.09	3.26	3.25	2.91	2.92	2.70	2.54	2.32	2.07	1.95
PTOS Axle 3	Wheel 3 - High Leg	-0.85	-0.58	-0.54	-0.53	-0.35	-0.30	-0.24	-0.15	0.29	0.49	0.63
	Wheel 6 - Low Leg	1.35	0.58	0.48	0.38	0.13	-0.04	-0.18	-0.34	-0.50	-0.65	-0.72
PTOS Axle 2	Wheel 2 - High Leg	1.28	1.29	1.34	1.31	1.38	1.47	1.41	1.59	1.65	1.54	1.85
	Wheel 7 - Low Leg	3.18	3.22	3.32	3.31	3.05	3.10	2.98	2.73	2.51	2.14	1.89
PTOS Axle 1	Wheel 1 - High Leg	-0.81	-0.44	-0.37	-0.36	-0.23	-0.23	0.20	0.42	0.48	0.73	0.83
	Wheel 8 - Low Leg	0.80	0.21	0.19	-0.05	-0.27	-0.39	-0.52	-0.68	-0.72	-0.86	-0.96
MOS Axle 4	Wheel 4 - High Leg	1.57	1.78	1.77	1.74	1.80	1.96	1.88	1.85	1.72	1.73	1.84
	Wheel 5 - Low Leg	2.86	3.04	3.06	2.95	2.81	2.66	2.55	2.34	2.18	1.88	1.78
MOS Axle 3	Wheel 3 - High Leg	-0.92	-0.64	-0.61	-0.60	-0.41	-0.32	-0.27	-0.14	0.25	0.52	0.70
	Wheel 6 - Low Leg	1.10	0.55	0.47	0.39	0.20	-0.07	-0.19	-0.38	-0.51	-0.68	-0.76
MOS Axle 2	Wheel 2 - High Leg	1.72	1.84	2.03	1.98	2.13	2.21	2.28	2.16	2.26	2.09	2.02
	Wheel 7 - Low Leg	2.91	2.99	3.10	3.03	2.85	2.91	2.81	2.81	2.39	2.21	1.94
MOS Axle 1	Wheel 1 - High Leg	-0.70	-0.57	-0.57	-0.55	-0.50	-0.43	-0.30	-0.26	0.17	0.32	0.46
	Wheel 8 - Low Leg	1.18	0.89	0.78	0.73	0.61	0.58	0.47	0.32	0.21	-0.32	-0.39
DMOS A Axle 4	Wheel 4 - High Leg	2.02	2.19	2.22	2.28	2.44	2.37	2.28	2.17	2.07	1.97	1.91
	Wheel 5 - Low Leg	3.25	3.39	3.42	3.33	3.13	3.11	3.01	2.83	2.42	2.26	2.11
DMOS A Axle 3	Wheel 3 - High Leg	-0.88	-0.62	-0.65	-0.63	-0.45	-0.37	-0.29	-0.16	0.27	0.45	0.80
	Wheel 6 - Low Leg	1.19	0.64	0.56	0.48	0.21	0.09	-0.12	-0.28	-0.46	-0.61	-0.77
DMOS A Axle 2	Wheel 2 - High Leg	1.66	1.80	1.83	1.84	1.95	2.01	2.07	2.00	1.81	1.97	2.03
	Wheel 7 - Low Leg	3.33	3.43	3.45	3.33	3.23	3.20	3.10	2.89	2.70	2.44	2.06
DMOS A Axle 1	Wheel 1 - High Leg	-0.96	-0.71	-0.73	-0.67	-0.47	-0.38	-0.34	-0.25	0.26	0.52	1.07
	Wheel 8 - Low Leg	1.33	0.90	0.85	0.83	0.59	0.49	0.41	0.26	-0.22	-0.52	-0.78

© University of Pretoria

Table B-2: Vertical Forces Before Tamping (Wheels) – S2 Down

Hatfield to Pretoria (Down) km 3.175 (Site 2) Before Tamping		km/h										
		11.13	21.60	30.12	39.90	49.26	59.48	68.74	79.08	88.32	102.21	108.75
Car Type and Axle	Wheel and Rail Leg	Vertical Force (t)										
DMOS B Axle 1	Wheel 8 - High Leg	5.97	5.59	5.66	5.69	6.00	6.06	***6.48***	6.66	7.09	***8.48***	***8.94***
	Wheel 1 - Low Leg	6.80	6.41	6.47	6.32	5.89	5.67	5.38	5.39	5.03	4.38	4.19
DMOS B Axle 2	Wheel 7 - High Leg	4.80	4.93	5.20	5.15	5.54	6.01	6.04	6.29	6.84	7.49	7.92
	Wheel 2 - Low Leg	7.00	6.74	6.49	6.60	6.18	5.69	5.22	5.12	4.63	4.48	3.83
DMOS B Axle 3	Wheel 6 - High Leg	4.89	4.76	4.80	4.95	5.18	5.22	5.46	6.17	6.45	7.09	7.90
	Wheel 3 - Low Leg	6.03	6.11	6.02	5.89	5.47	5.36	5.07	4.84	4.56	4.03	3.52
DMOS B Axle 4	Wheel 5 - High Leg	4.19	4.23	4.45	4.49	4.73	5.07	5.49	5.92	6.04	6.31	7.24
	Wheel 4 - Low Leg	6.31	6.16	6.02	6.13	5.53	5.38	4.98	4.48	3.90	3.90	3.44
PTOS Axle 4	Wheel 4 - High Leg	4.53	4.48	4.51	4.52	4.64	5.12	5.13	5.34	5.48	6.59	6.75
	Wheel 5 - Low Leg	5.77	5.54	5.51	5.55	5.24	4.65	***4.63***	***4.22***	4.10	3.55	3.51
PTOS Axle 3	Wheel 3 - High Leg	***3.59***	***3.69***	***3.85***	4.13	***3.87***	***4.42***	4.72	5.03	5.19	5.61	6.31
	Wheel 6 - Low Leg	6.22	5.99	5.81	5.76	5.66	5.08	4.79	4.32	3.93	***3.44***	3.15
PTOS Axle 2	Wheel 2 - High Leg	4.85	4.93	4.98	5.09	5.42	5.28	5.60	5.92	6.19	7.20	7.71
	Wheel 7 - Low Leg	6.46	6.17	6.28	6.29	5.64	5.57	5.27	4.99	4.62	4.11	3.63
PTOS Axle 1	Wheel 1 - High Leg	4.45	4.53	4.73	5.04	5.01	5.23	5.52	5.68	6.24	7.16	7.48
	Wheel 8 - Low Leg	6.38	6.29	6.12	5.93	5.76	5.37	5.02	4.80	4.24	3.58	3.52
MOS Axle 4	Wheel 4 - High Leg	5.04	5.08	5.12	5.11	5.36	5.52	5.39	6.04	6.63	7.28	7.58
	Wheel 5 - Low Leg	5.62	5.48	5.58	5.62	5.11	4.76	4.65	4.23	4.17	3.59	3.39
MOS Axle 3	Wheel 3 - High Leg	4.10	4.17	4.31	4.36	4.53	4.96	5.04	5.52	5.91	6.89	6.86
	Wheel 6 - Low Leg	6.22	6.11	5.93	5.96	5.79	5.21	4.93	4.44	4.14	3.60	***3.14***
MOS Axle 2	Wheel 2 - High Leg	4.74	4.88	4.93	5.16	5.27	5.23	5.61	5.94	6.38	7.05	7.64
	Wheel 7 - Low Leg	5.71	5.56	5.52	5.42	5.00	4.94	4.63	4.40	4.02	3.73	3.76
MOS Axle 1	Wheel 1 - High Leg	3.88	3.83	4.02	***4.04***	4.41	4.67	4.88	5.04	5.64	5.90	5.88
	Wheel 8 - Low Leg	6.24	6.19	6.00	6.09	5.64	5.36	5.20	4.80	4.31	4.33	3.56
DMOS A Axle 4	Wheel 4 - High Leg	5.11	5.20	5.18	5.18	5.24	5.75	5.59	6.55	***7.09***	7.86	8.18
	Wheel 5 - Low Leg	5.82	5.75	5.60	5.57	5.33	4.78	4.82	4.40	***3.87***	3.54	3.66
DMOS A Axle 3	Wheel 3 - High Leg	4.10	4.14	4.17	4.24	4.30	4.88	5.14	5.55	6.06	6.78	7.46
	Wheel 6 - Low Leg	6.52	6.47	6.30	6.25	6.28	5.63	4.97	4.62	4.49	3.72	3.60
DMOS A Axle 2	Wheel 2 - High Leg	5.38	5.52	5.46	5.75	5.98	5.94	6.40	***6.71***	7.07	7.99	8.01
	Wheel 7 - Low Leg	6.53	6.53	6.48	6.41	5.77	5.82	5.43	5.27	5.08	4.52	4.44
DMOS A Axle 1	Wheel 1 - High Leg	4.51	4.73	4.83	4.98	5.32	5.49	6.12	5.90	6.53	7.32	7.84
	Wheel 8 - Low Leg	***7.24***	***7.19***	***7.09***	***6.84***	***6.40***	***6.19***	5.81	5.48	5.13	4.68	4.34

© University of Pretoria

Table B-3: Lateral Forces Before Tamping (Wheels) – S2 Down

Hatfield to Pretoria (Down) km 3.175 (Site 2) Before Tamping		km/h										
		11.13	21.60	30.12	39.90	49.26	59.48	68.74	79.08	88.32	102.21	108.75
Car Type and Axle	Wheel and Rail Leg	Lateral Force (t)										
DMOS B Axle 1	Wheel 8 - High Leg	1.70	2.05	2.15	2.14	2.19	2.29	2.40	2.49	2.45	2.60	***2.93***
	Wheel 1 - Low Leg	2.89	3.27	3.45	3.28	3.02	3.00	2.84	2.72	2.22	2.03	2.08
DMOS B Axle 2	Wheel 7 - High Leg	***-0.81***	-0.74	-0.67	-0.65	-0.48	-0.34	-0.30	0.26	0.54	0.75	1.11
	Wheel 2 - Low Leg	0.89	0.70	0.63	0.56	0.36	0.23	-0.25	-0.51	-0.74	-0.95	***-1.09***
DMOS B Axle 3	Wheel 6 - High Leg	1.50	1.76	1.92	2.03	1.94	1.87	1.95	1.95	1.86	1.72	1.97
	Wheel 3 - Low Leg	2.71	3.07	3.25	3.22	2.92	2.91	2.69	2.48	1.98	1.61	1.60
DMOS B Axle 4	Wheel 5 - High Leg	-0.61	-0.52	-0.45	-0.41	-0.30	-0.26	-0.20	0.26	0.60	0.69	0.86
	Wheel 4 - Low Leg	0.54	0.41	0.30	0.30	0.20	-0.15	-0.35	-0.54	-0.83	-0.91	-0.94
PTOS Axle 4	Wheel 4 - High Leg	2.06	2.26	2.46	2.48	2.46	2.46	2.36	2.50	2.40	2.49	2.65
	Wheel 5 - Low Leg	2.84	3.06	3.23	3.19	3.06	2.72	2.63	2.47	2.16	1.83	1.90
PTOS Axle 3	Wheel 3 - High Leg	-0.76	-0.65	-0.60	-0.58	-0.50	-0.34	-0.21	0.18	0.45	0.81	0.89
	Wheel 6 - Low Leg	0.74	0.47	0.44	0.36	0.31	-0.11	-0.32	-0.46	-0.71	-0.97	-1.02
PTOS Axle 2	Wheel 2 - High Leg	1.57	1.73	1.87	1.88	1.84	1.84	1.86	1.85	1.77	1.47	1.88
	Wheel 7 - Low Leg	3.25	3.32	3.45	3.51	3.12	3.06	2.89	2.60	2.33	1.80	1.75
PTOS Axle 1	Wheel 1 - High Leg	-0.51	-0.50	-0.43	-0.35	-0.34	-0.29	-0.19	0.33	0.56	1.08	1.08
	Wheel 8 - Low Leg	0.31	0.27	0.22	-0.01	-0.15	-0.36	***-0.48***	***-0.66***	***-0.89***	***-1.11***	-1.02
MOS Axle 4	Wheel 4 - High Leg	1.95	2.05	2.05	2.09	2.09	2.13	2.21	2.30	2.05	2.23	2.42
	Wheel 5 - Low Leg	2.96	2.99	3.06	3.08	2.73	2.56	2.63	2.36	2.02	1.69	1.65
MOS Axle 3	Wheel 3 - High Leg	-0.77	-0.73	-0.59	-0.59	-0.56	-0.41	-0.22	0.17	0.41	0.78	1.03
	Wheel 6 - Low Leg	0.67	0.53	0.47	0.42	0.30	-0.09	-0.19	-0.43	-0.66	-0.96	-1.00
MOS Axle 2	Wheel 2 - High Leg	1.87	2.08	2.22	2.45	2.38	2.45	2.52	2.50	2.55	2.55	2.38
	Wheel 7 - Low Leg	2.92	3.04	3.16	3.07	2.86	2.83	2.65	2.63	2.28	1.90	1.85
MOS Axle 1	Wheel 1 - High Leg	-0.53	-0.60	-0.55	-0.60	-0.50	***-0.54***	-0.35	-0.19	-0.20	0.60	0.85
	Wheel 8 - Low Leg	0.83	0.86	0.72	0.74	0.53	0.54	0.34	0.24	-0.34	-0.61	-0.62
DMOS A Axle 4	Wheel 4 - High Leg	2.21	2.44	2.44	2.58	2.49	2.62	2.60	2.71	***2.80***	***2.75***	2.63
	Wheel 5 - Low Leg	3.22	3.31	3.38	3.33	3.16	2.86	2.88	2.72	2.32	1.89	1.78
DMOS A Axle 3	Wheel 3 - High Leg	-0.72	-0.68	-0.67	-0.60	***-0.58***	-0.46	-0.23	0.19	0.32	0.86	1.13
	Wheel 6 - Low Leg	0.65	0.60	0.49	0.44	0.32	-0.04	-0.23	-0.53	-0.65	-0.88	-0.99
DMOS A Axle 2	Wheel 2 - High Leg	2.13	2.18	2.32	2.39	2.40	2.41	2.55	2.55	2.59	2.26	2.23
	Wheel 7 - Low Leg	***3.45***	***3.44***	***3.59***	***3.53***	***3.19***	***3.21***	***3.08***	***2.95***	2.70	2.01	2.02
DMOS A Axle 1	Wheel 1 - High Leg	-0.75	***-0.77***	***-0.68***	***-0.67***	-0.48	-0.39	-0.28	-0.22	0.45	1.04	1.24
	Wheel 8 - Low Leg	0.92	0.88	0.75	0.71	0.50	0.46	0.33	-0.32	-0.58	-0.90	-1.00

© University of Pretoria

Table B-4: Vertical Forces Before Tamping (Wheels) – S1 Up

Pretoria to Hatfield (Up) km 3.215 (Site 1) Before Tamping		km/h										
		11.30	20.79	30.28	39.49	49.84	59.20	69.59	79.30	90.32	97.59	106.32
Car Type and Axle	Wheel and Rail Leg	Vertical Force (t)										
DMOS A Axle 1	Wheel 1 - High Leg	5.60	5.41	5.33	5.51	5.59	6.18	6.46	6.75	6.75	7.03	7.44
	Wheel 8 - Low Leg	6.79	6.57	6.50	6.40	6.45	***6.35***	5.82	5.70	5.29	5.32	4.73
DMOS A Axle 2	Wheel 2 - High Leg	4.83	4.92	5.10	5.42	5.61	5.85	6.39	6.66	7.30	7.50	8.28
	Wheel 7 - Low Leg	***7.02***	***6.87***	***6.75***	6.41	6.46	6.21	5.89	5.51	5.37	4.78	4.89
DMOS A Axle 3	Wheel 3 - High Leg	4.56	4.56	4.59	4.67	5.02	5.46	5.88	6.29	6.43	6.71	7.21
	Wheel 6 - Low Leg	6.14	6.14	6.09	5.94	5.93	5.41	5.28	4.91	4.81	4.69	4.06
DMOS A Axle 4	Wheel 4 - High Leg	4.36	4.45	4.48	4.66	4.93	5.37	5.87	6.41	6.92	7.48	8.06
	Wheel 5 - Low Leg	6.14	6.16	6.05	5.86	5.72	5.42	4.93	4.58	4.09	3.81	3.61
MOS Axle 1	Wheel 1 - High Leg	4.80	4.62	4.62	4.84	4.82	5.23	5.67	5.88	6.04	6.28	6.48
	Wheel 8 - Low Leg	5.45	5.45	5.41	5.38	5.30	5.13	4.95	4.62	4.53	4.38	3.76
MOS Axle 2	Wheel 2 - High Leg	4.11	4.20	4.29	4.51	4.73	4.96	5.33	5.82	6.34	6.53	6.85
	Wheel 7 - Low Leg	6.03	5.90	5.72	5.52	5.54	5.44	5.01	4.73	4.47	4.46	4.15
MOS Axle 3	Wheel 3 - High Leg	4.31	4.41	4.40	4.41	4.61	5.08	5.49	5.94	6.19	6.48	6.99
	Wheel 6 - Low Leg	6.12	6.04	6.18	5.85	5.83	5.57	5.18	5.14	4.89	4.49	4.12
MOS Axle 4	Wheel 4 - High Leg	4.62	4.75	4.75	5.04	4.92	5.65	6.15	6.69	7.34	7.78	8.28
	Wheel 5 - Low Leg	5.77	5.60	5.57	5.52	5.38	4.98	***4.47***	***4.00***	***3.89***	3.68	***3.33***
PTOS Axle 1	Wheel 1 - High Leg	4.92	5.06	5.00	5.20	5.13	5.59	6.02	6.41	6.98	7.07	7.44
	Wheel 8 - Low Leg	6.06	6.03	5.99	5.75	5.93	5.70	5.38	5.08	4.66	4.84	4.26
PTOS Axle 2	Wheel 2 - High Leg	4.60	4.71	4.80	5.14	5.11	5.51	6.09	6.39	7.07	7.51	7.78
	Wheel 7 - Low Leg	6.26	6.20	6.15	5.76	5.77	5.61	5.08	4.80	4.15	4.09	3.60
PTOS Axle 3	Wheel 3 - High Leg	***3.90***	***4.04***	***4.01***	***4.11***	4.32	4.88	5.28	5.59	5.81	6.01	6.51
	Wheel 6 - Low Leg	5.90	5.79	5.88	5.78	5.60	5.39	5.08	4.98	4.42	4.57	4.11
PTOS Axle 4	Wheel 4 - High Leg	3.95	4.05	4.04	4.18	***4.29***	***4.80***	5.29	5.88	6.43	6.78	7.12
	Wheel 5 - Low Leg	5.86	5.78	5.67	5.47	5.42	5.15	4.67	4.45	4.03	***3.43***	3.35
DMOS B Axle 4	Wheel 5 - High Leg	4.67	4.75	4.80	4.87	5.00	5.44	5.90	6.19	6.63	6.86	7.37
	Wheel 4 - Low Leg	5.96	5.76	5.80	5.79	5.72	5.52	5.19	4.65	4.74	4.61	4.03
DMOS B Axle 3	Wheel 6 - High Leg	4.50	4.57	4.68	4.93	5.20	5.43	6.00	6.55	6.79	7.25	7.83
	Wheel 3 - Low Leg	6.11	6.01	5.87	5.58	5.74	5.37	4.92	4.56	4.33	4.01	3.62
DMOS B Axle 2	Wheel 7 - High Leg	5.10	5.14	5.16	5.32	5.66	5.99	6.42	6.93	7.47	7.55	7.93
	Wheel 2 - Low Leg	6.76	6.75	6.63	***6.58***	***6.49***	6.26	5.94	5.57	5.49	5.27	4.87
DMOS B Axle 1	Wheel 8 - High Leg	5.13	5.31	5.42	5.70	5.80	6.33	***6.67***	***7.38***	***7.83***	***8.32***	***8.67***
	Wheel 1 - Low Leg	6.72	6.55	6.73	6.26	6.29	5.84	5.49	5.09	4.75	4.49	4.32

© University of Pretoria

Table B-5: Lateral Forces Before Tamping (Wheels) – S1 Up

Pretoria to Hatfield (Up) km 3.215 (Site 1) Before Tamping		km/h										
		11.30	20.79	30.28	39.49	49.84	59.20	69.59	79.30	90.32	97.59	106.32
Car Type and Axle	Wheel and Rail Leg	Lateral Force (t)										
DMOS A Axle 1	Wheel 1 - High Leg	1.87	1.66	1.84	1.85	1.90	1.85	1.93	1.91	2.24	2.03	2.06
	Wheel 8 - Low Leg	***3.28***	***3.25***	***3.39***	***3.37***	***3.40***	***3.24***	***3.04***	***2.93***	***2.85***	***2.53***	***2.46***
DMOS A Axle 2	Wheel 2 - High Leg	***-0.96***	***-0.81***	***-0.89***	***-0.73***	***-0.65***	***-0.52***	-0.39	-0.28	-0.25	0.31	0.50
	Wheel 7 - Low Leg	1.28	0.93	0.91	0.73	0.67	0.45	0.33	0.24	-0.29	-0.53	-0.66
DMOS A Axle 3	Wheel 3 - High Leg	1.38	1.46	1.46	1.47	1.38	1.50	1.24	1.14	1.15	0.88	1.30
	Wheel 6 - Low Leg	3.02	3.10	3.20	3.13	2.95	2.85	2.57	2.38	2.19	1.79	1.95
DMOS A Axle 4	Wheel 4 - High Leg	-0.64	-0.62	-0.58	-0.47	-0.41	-0.28	-0.19	0.23	0.44	0.71	0.86
	Wheel 5 - Low Leg	0.56	0.48	0.40	0.28	0.21	-0.13	-0.29	-0.43	-0.63	-0.78	-0.87
MOS Axle 1	Wheel 1 - High Leg	1.51	1.53	1.61	1.65	1.75	1.81	1.66	1.73	1.67	1.53	1.82
	Wheel 8 - Low Leg	2.81	2.86	2.99	2.97	3.03	2.99	2.69	2.66	2.43	2.27	2.22
MOS Axle 2	Wheel 2 - High Leg	-0.78	-0.72	-0.64	-0.59	-0.51	-0.48	-0.30	-0.23	0.17	0.37	0.46
	Wheel 7 - Low Leg	1.14	0.95	0.85	0.71	0.60	0.51	0.35	0.28	-0.21	-0.37	-0.48
MOS Axle 3	Wheel 3 - High Leg	1.00	1.03	0.96	1.03	0.83	0.85	0.58	0.58	0.60	0.44	0.93
	Wheel 6 - Low Leg	2.99	3.00	3.08	3.10	2.82	2.67	2.38	2.21	1.89	1.72	1.78
MOS Axle 4	Wheel 4 - High Leg	-0.50	-0.44	-0.36	-0.37	-0.25	-0.19	0.36	0.51	0.90	1.08	1.21
	Wheel 5 - Low Leg	0.31	0.25	0.21	0.13	0.11	-0.31	***-0.54***	-0.72	***-0.97***	-1.00	-1.06
PTOS Axle 1	Wheel 1 - High Leg	1.51	1.54	1.52	1.43	1.44	1.36	1.24	1.08	0.93	0.90	1.19
	Wheel 8 - Low Leg	2.95	2.99	3.02	2.89	3.02	2.68	2.38	2.17	1.87	1.62	1.58
PTOS Axle 2	Wheel 2 - High Leg	-0.69	-0.66	-0.60	-0.49	-0.46	-0.31	-0.19	0.14	0.40	0.69	0.94
	Wheel 7 - Low Leg	0.59	0.51	0.44	0.24	0.21	0.06	-0.20	-0.42	-0.64	-0.83	-0.92
PTOS Axle 3	Wheel 3 - High Leg	1.34	1.29	1.33	1.22	1.22	1.06	0.90	0.77	0.80	0.76	1.01
	Wheel 6 - Low Leg	3.03	3.05	3.11	3.03	2.88	2.67	2.47	2.24	2.02	1.78	1.73
PTOS Axle 4	Wheel 4 - High Leg	-0.45	-0.43	-0.42	-0.32	-0.25	-0.14	0.28	0.51	0.79	0.97	1.13
	Wheel 5 - Low Leg	0.35	0.28	0.26	0.13	-0.04	-0.27	-0.46	***-0.74***	-0.96	-1.04	-1.16
DMOS B Axle 4	Wheel 5 - High Leg	1.47	1.62	1.41	1.40	1.59	1.27	1.10	0.94	0.82	0.75	1.39
	Wheel 4 - Low Leg	3.07	3.11	3.08	3.07	3.10	2.78	2.48	2.25	1.99	1.71	1.84
DMOS B Axle 3	Wheel 6 - High Leg	-0.65	-0.65	-0.54	-0.41	-0.39	-0.23	-0.16	0.25	0.48	0.77	0.97
	Wheel 3 - Low Leg	0.57	0.50	0.36	0.21	0.18	-0.11	-0.29	-0.48	-0.67	-0.87	-0.94
DMOS B Axle 2	Wheel 7 - High Leg	0.95	1.01	1.03	0.82	0.70	0.67	0.67	0.63	0.64	0.55	1.34
	Wheel 2 - Low Leg	3.02	3.08	3.18	2.98	2.71	2.54	2.31	2.16	1.98	1.79	2.08
DMOS B Axle 1	Wheel 8 - High Leg	-0.61	-0.58	-0.59	-0.40	-0.34	-0.19	0.17	0.33	0.63	0.81	1.06
	Wheel 1 - Low Leg	0.41	0.36	0.34	0.13	0.11	-0.27	-0.46	-0.66	-0.91	***-1.06***	***-1.23***

© University of Pretoria

Table B-6: Vertical Forces Before Tamping (Wheels) – S2 Up

Pretoria to Hatfield (Up) km 3.175 (Site 2) Before Tamping		km/h										
		11.31	20.79	30.50	39.82	49.92	59.11	68.98	78.94	89.23	97.48	104.81
Car Type and Axle	Wheel and Rail Leg	Vertical Force (t)										
DMOS A Axle 1	Wheel 1 - High Leg	5.22	5.31	5.26	5.62	5.95	5.70	***6.22***	6.22	6.34	6.81	6.64
	Wheel 8 - Low Leg	7.02	6.94	6.62	6.42	6.49	***6.21***	5.88	5.57	5.31	5.29	4.76
DMOS A Axle 2	Wheel 2 - High Leg	4.67	4.73	4.90	5.25	5.13	5.38	5.75	6.06	6.48	6.47	6.95
	Wheel 7 - Low Leg	***7.16***	***7.07***	***7.02***	***6.79***	***6.50***	6.15	5.79	5.52	5.18	4.74	4.35
DMOS A Axle 3	Wheel 3 - High Leg	4.72	4.70	4.79	5.18	5.08	5.07	5.36	5.57	5.97	6.20	6.44
	Wheel 6 - Low Leg	6.08	6.11	5.99	5.69	5.68	5.50	5.27	4.90	4.30	4.24	4.07
DMOS A Axle 4	Wheel 4 - High Leg	4.33	4.40	4.42	4.67	4.99	5.23	5.59	5.85	6.56	6.83	6.64
	Wheel 5 - Low Leg	6.11	6.13	6.03	5.83	5.36	5.10	4.82	4.35	4.09	3.41	3.46
MOS Axle 1	Wheel 1 - High Leg	4.59	4.59	4.78	4.86	4.95	5.06	5.31	5.64	5.66	6.11	5.92
	Wheel 8 - Low Leg	5.79	5.79	5.53	5.53	5.20	5.21	4.92	4.53	4.33	4.15	3.84
MOS Axle 2	Wheel 2 - High Leg	3.94	4.02	4.21	4.26	***4.54***	***4.59***	4.99	5.34	5.32	5.85	5.71
	Wheel 7 - Low Leg	6.11	6.10	5.96	5.76	5.56	5.27	5.02	4.70	4.49	3.83	3.82
MOS Axle 3	Wheel 3 - High Leg	4.49	4.43	4.74	4.77	4.94	4.89	5.33	5.50	5.80	5.90	6.09
	Wheel 6 - Low Leg	6.12	5.93	5.96	5.88	5.63	5.57	5.28	4.95	4.52	4.16	3.92
MOS Axle 4	Wheel 4 - High Leg	4.57	4.57	4.68	4.80	5.32	5.67	5.72	6.36	6.62	6.88	6.90
	Wheel 5 - Low Leg	5.69	5.69	5.62	5.33	5.07	4.79	***4.42***	***3.94***	3.76	***3.17***	***3.24***
PTOS Axle 1	Wheel 1 - High Leg	4.89	4.94	5.13	5.27	5.40	5.41	5.74	5.95	6.24	6.33	6.76
	Wheel 8 - Low Leg	6.26	6.21	6.15	6.04	5.75	5.55	5.29	4.77	4.55	4.21	4.03
PTOS Axle 2	Wheel 2 - High Leg	4.34	4.37	4.66	4.53	4.99	5.25	5.37	5.85	6.13	6.88	6.87
	Wheel 7 - Low Leg	6.48	6.48	6.31	6.16	5.81	5.51	5.25	4.82	4.35	4.01	3.67
PTOS Axle 3	Wheel 3 - High Leg	4.16	4.26	4.38	4.49	4.87	4.89	4.91	5.04	5.35	5.49	5.32
	Wheel 6 - Low Leg	5.77	5.76	5.74	5.55	5.43	5.30	4.85	4.81	4.40	4.11	3.86
PTOS Axle 4	Wheel 4 - High Leg	***3.91***	***3.91***	***4.04***	***4.14***	4.55	4.90	4.86	5.38	6.01	6.26	6.54
	Wheel 5 - Low Leg	5.80	5.73	5.64	5.43	5.01	4.76	4.53	4.16	***3.71***	3.40	3.25
DMOS B Axle 4	Wheel 5 - High Leg	4.69	4.68	4.91	4.91	5.17	5.28	5.31	5.65	6.23	6.46	6.53
	Wheel 4 - Low Leg	6.14	6.15	6.04	5.84	5.69	5.54	5.02	4.78	4.23	4.04	3.64
DMOS B Axle 3	Wheel 6 - High Leg	4.39	4.31	4.45	4.59	4.91	5.05	5.41	5.75	6.45	6.49	6.86
	Wheel 3 - Low Leg	6.27	6.29	6.04	5.97	5.71	5.56	5.16	4.60	4.07	3.99	3.47
DMOS B Axle 2	Wheel 7 - High Leg	5.26	5.20	5.55	5.77	6.00	5.96	6.05	6.06	6.44	6.71	6.95
	Wheel 2 - Low Leg	6.68	6.65	6.57	6.29	6.16	5.87	5.74	5.38	5.09	4.97	4.56
DMOS B Axle 1	Wheel 8 - High Leg	5.00	5.10	5.24	5.50	5.95	5.92	6.17	***6.71***	***7.13***	***7.35***	***7.55***
	Wheel 1 - Low Leg	6.64	6.65	6.51	6.25	5.72	5.70	5.55	5.09	4.54	4.25	4.17

© University of Pretoria

Table B-7: Lateral Forces Before Tamping (Wheels) – S2 Up

Pretoria to Hatfield (Up) km 3.175 (Site 2) Before Tamping		km/h										
		11.31	20.79	30.50	39.82	49.92	59.11	68.98	78.94	89.23	97.48	104.81
Car Type and Axle	Wheel and Rail Leg	Lateral Force (t)										
DMOS A Axle 1	Wheel 1 - High Leg	2.37	2.28	2.59	2.63	2.54	2.69	2.75	2.90	***3.15***	***3.00***	***3.31***
	Wheel 8 - Low Leg	***3.53***	***3.39***	***3.51***	***3.31***	***3.32***	***3.18***	***3.04***	***2.94***	2.85	2.61	2.50
DMOS A Axle 2	Wheel 2 - High Leg	***-0.87***	***-0.93***	***-0.93***	***-0.79***	***-0.69***	***-0.59***	-0.42	-0.32	-0.26	0.25	0.37
	Wheel 7 - Low Leg	1.05	1.06	1.02	0.79	0.72	0.57	0.36	0.29	0.19	-0.48	-0.59
DMOS A Axle 3	Wheel 3 - High Leg	1.81	1.82	1.94	1.90	1.97	1.98	2.04	1.96	2.04	1.99	2.24
	Wheel 6 - Low Leg	3.10	3.14	3.15	2.97	2.86	2.83	2.71	2.57	2.27	2.03	1.98
DMOS A Axle 4	Wheel 4 - High Leg	-0.73	-0.74	-0.69	-0.52	-0.44	-0.27	-0.17	0.17	0.31	0.67	0.73
	Wheel 5 - Low Leg	0.50	0.52	0.43	0.23	0.20	-0.19	-0.32	-0.49	-0.63	-0.81	-0.86
MOS Axle 1	Wheel 1 - High Leg	2.14	2.07	2.37	2.29	2.35	2.47	2.44	2.48	2.67	2.54	2.98
	Wheel 8 - Low Leg	3.06	2.97	3.09	3.03	2.88	2.86	2.73	2.46	2.44	2.18	2.07
MOS Axle 2	Wheel 2 - High Leg	-0.80	-0.80	-0.69	-0.66	-0.62	-0.48	-0.39	-0.25	-0.21	0.43	0.38
	Wheel 7 - Low Leg	0.98	0.96	0.79	0.75	0.64	0.50	0.36	0.27	0.22	-0.41	-0.34
MOS Axle 3	Wheel 3 - High Leg	1.45	1.49	1.50	1.57	1.57	1.56	1.56	1.52	1.80	1.65	1.96
	Wheel 6 - Low Leg	3.15	3.07	3.15	2.98	2.88	2.84	2.63	2.41	2.29	2.01	1.97
MOS Axle 4	Wheel 4 - High Leg	-0.58	-0.61	-0.50	-0.33	-0.30	-0.15	0.17	0.42	0.55	0.87	0.78
	Wheel 5 - Low Leg	0.35	0.36	0.27	0.20	-0.15	-0.33	***-0.45***	***-0.68***	-0.79	-0.92	-0.88
PTOS Axle 1	Wheel 1 - High Leg	2.33	2.21	2.33	2.42	2.47	2.57	2.57	2.51	2.65	2.67	2.84
	Wheel 8 - Low Leg	3.37	3.19	3.29	3.17	2.99	2.99	2.73	2.32	2.19	2.04	1.85
PTOS Axle 2	Wheel 2 - High Leg	-0.82	-0.81	-0.78	-0.69	-0.54	-0.37	-0.27	-0.20	0.19	0.49	0.63
	Wheel 7 - Low Leg	0.66	0.63	0.54	0.45	0.26	-0.04	-0.14	-0.32	-0.45	-0.68	-0.75
PTOS Axle 3	Wheel 3 - High Leg	1.82	1.68	1.73	1.80	1.78	1.87	1.85	1.90	1.87	1.63	2.14
	Wheel 6 - Low Leg	3.17	3.01	3.10	2.95	2.82	2.81	2.57	2.45	2.10	1.89	1.92
PTOS Axle 4	Wheel 4 - High Leg	-0.55	-0.54	-0.51	-0.37	-0.23	-0.07	0.13	0.34	0.62	0.82	0.94
	Wheel 5 - Low Leg	0.37	0.29	0.25	0.17	-0.16	-0.28	-0.36	-0.59	-0.81	***-0.94***	-0.95
DMOS B Axle 4	Wheel 5 - High Leg	2.18	2.06	2.27	2.36	2.18	2.37	2.41	2.28	2.28	2.46	2.72
	Wheel 4 - Low Leg	3.37	3.28	3.36	3.20	3.07	3.06	2.79	2.50	2.14	2.00	1.90
DMOS B Axle 3	Wheel 6 - High Leg	-0.77	-0.76	-0.66	-0.54	-0.53	-0.39	-0.31	-0.17	0.32	0.44	0.53
	Wheel 3 - Low Leg	0.63	0.59	0.48	0.37	0.25	-0.04	-0.12	-0.31	-0.59	-0.65	-0.77
DMOS B Axle 2	Wheel 7 - High Leg	1.69	1.63	1.67	1.71	1.74	2.04	2.04	2.08	1.85	2.21	2.52
	Wheel 2 - Low Leg	3.35	3.23	3.33	3.06	2.93	2.96	2.89	2.56	2.18	2.24	2.25
DMOS B Axle 1	Wheel 8 - High Leg	-0.68	-0.70	-0.60	-0.42	-0.33	-0.18	-0.13	0.23	0.54	0.76	0.83
	Wheel 1 - Low Leg	0.49	0.46	0.37	0.23	0.16	-0.20	-0.35	-0.58	***-0.84***	-0.92	***-1.01***

Table B-8: Vertical Forces After Tamping (Wheels) – S1 Down

Hatfield to Pretoria (Down) km 3.215 (Site 1) After Tamping		km/h										
		11.10	21.02	30.50	40.07	50.15	60.01	69.38	79.42	89.55	98.74	104.02
Car Type and Axle	Wheel and Rail Leg	Greatest Vertical Force (t)										
DMOS B Axle 1	Wheel 8 - High Leg	5.09	5.14	5.27	5.66	5.86	5.82	6.20	6.30	**7.23**	**8.46**	7.75
	Wheel 1 - Low Leg	7.41	7.46	7.74	**8.91**	**8.30**	6.55	**7.13**	6.46	5.76	6.98	6.02
DMOS B Axle 2	Wheel 7 - High Leg	4.41	4.45	4.53	4.71	4.97	5.51	5.95	6.07	6.66	7.39	7.51
	Wheel 2 - Low Leg	**7.87**	**7.83**	**7.77**	7.68	7.18	6.78	6.41	5.49	5.01	4.98	5.28
DMOS B Axle 3	Wheel 6 - High Leg	4.35	4.47	4.54	4.57	4.73	4.87	5.24	5.47	6.22	6.96	7.00
	Wheel 3 - Low Leg	6.57	6.61	6.56	6.66	6.40	6.12	5.73	5.45	5.06	4.59	4.28
DMOS B Axle 4	Wheel 5 - High Leg	3.99	4.00	4.28	4.20	4.66	4.80	5.15	5.81	6.36	6.59	6.89
	Wheel 4 - Low Leg	6.79	6.84	6.66	6.67	6.26	6.07	5.45	4.95	4.33	4.05	3.67
PTOS Axle 4	Wheel 4 - High Leg	4.06	4.11	4.03	4.23	4.42	4.61	4.88	4.68	4.95	5.80	6.15
	Wheel 5 - Low Leg	6.08	6.12	6.05	6.04	5.65	5.36	5.21	5.15	5.05	4.53	4.55
PTOS Axle 3	Wheel 3 - High Leg	**3.46**	**3.50**	**3.63**	**3.57**	**4.00**	**4.25**	4.70	5.09	5.35	5.80	6.08
	Wheel 6 - Low Leg	6.52	6.51	6.35	6.59	5.89	5.56	5.31	4.76	4.23	4.09	3.74
PTOS Axle 2	Wheel 2 - High Leg	4.42	4.47	4.59	4.47	4.81	4.88	5.15	5.14	5.54	6.27	6.51
	Wheel 7 - Low Leg	6.86	6.83	6.73	6.93	6.48	6.35	6.14	5.72	5.48	4.88	4.51
PTOS Axle 1	Wheel 1 - High Leg	4.19	4.23	4.42	4.43	4.66	5.13	5.36	5.88	6.34	6.71	7.09
	Wheel 8 - Low Leg	6.86	6.83	6.51	6.61	6.38	6.14	5.74	5.10	4.31	**3.93**	**3.44**
MOS Axle 4	Wheel 4 - High Leg	4.50	4.48	4.48	4.67	4.80	5.08	5.16	5.35	5.79	6.47	6.57
	Wheel 5 - Low Leg	6.21	6.24	6.24	6.09	5.79	5.53	5.40	5.29	5.16	4.82	4.79
MOS Axle 3	Wheel 3 - High Leg	4.13	4.22	4.30	4.26	4.63	4.98	5.25	6.03	6.43	6.83	6.92
	Wheel 6 - Low Leg	6.33	6.35	6.16	6.36	5.91	5.31	5.08	**4.35**	**4.07**	4.02	3.86
MOS Axle 2	Wheel 2 - High Leg	3.96	4.01	4.05	4.05	4.34	4.53	**4.57**	4.59	5.20	5.94	6.37
	Wheel 7 - Low Leg	6.52	6.74	6.51	6.78	6.41	6.15	5.82	5.97	5.73	5.36	5.19
MOS Axle 1	Wheel 1 - High Leg	3.69	3.72	3.98	3.87	4.08	4.39	4.62	5.34	5.95	6.32	5.92
	Wheel 8 - Low Leg	6.62	6.70	6.47	6.42	6.07	5.92	5.64	4.92	4.58	4.74	4.04
DMOS A Axle 4	Wheel 4 - High Leg	4.56	4.56	4.61	4.81	4.90	5.44	5.38	5.33	5.93	6.53	7.15
	Wheel 5 - Low Leg	6.38	6.55	6.55	6.20	6.04	6.01	5.50	5.71	5.04	4.77	4.60
DMOS A Axle 3	Wheel 3 - High Leg	3.95	4.02	4.09	4.24	4.50	4.95	5.27	5.71	6.19	6.80	7.01
	Wheel 6 - Low Leg	6.92	6.76	6.69	6.76	6.47	5.91	5.46	4.90	4.30	4.19	3.98
DMOS A Axle 2	Wheel 2 - High Leg	4.69	4.82	4.84	4.91	5.18	5.15	5.30	5.35	5.86	6.53	6.99
	Wheel 7 - Low Leg	7.66	7.70	7.61	7.69	7.20	**6.99**	6.75	**6.58**	6.41	5.78	5.68
DMOS A Axle 1	Wheel 1 - High Leg	4.45	4.55	4.85	4.76	5.09	5.37	5.70	6.04	6.70	7.05	**7.83**
	Wheel 8 - Low Leg	7.60	7.43	7.24	7.40	6.92	6.75	6.46	5.68	5.37	4.94	4.47

© University of Pretoria

Table B-9: Lateral Forces After Tamping (Wheels) – S1 Down

Hatfield to Pretoria (Down) km 3.215 (Site 1) After Tamping		km/h										
		11.10	21.02	30.50	40.07	50.15	60.01	69.38	79.42	89.55	98.74	104.02
Car Type and Axle	Wheel and Rail Leg	Lateral Force (t)										
DMOS B Axle 1	Wheel 8 - High Leg	1.68	1.63	1.28	1.23	1.33	1.44	1.48	-0.81	-0.73	-0.71	0.93
	Wheel 1 - Low Leg	2.76	2.84	2.26	2.22	2.14	2.07	1.78	1.12	0.95	0.76	0.81
DMOS B Axle 2	Wheel 7 - High Leg	-0.82	***-0.94***	***-0.91***	***-0.82***	***-0.71***	-0.61	-0.49	0.22	0.62	0.98	1.19
	Wheel 2 - Low Leg	1.31	1.25	1.12	0.96	0.88	0.73	0.55	-0.64	-1.08	-1.11	-1.24
DMOS B Axle 3	Wheel 6 - High Leg	1.26	1.59	1.68	1.62	1.57	1.39	1.32	0.82	0.78	0.82	1.10
	Wheel 3 - Low Leg	2.45	2.75	2.80	2.69	2.60	2.44	2.07	1.61	***1.38***	1.23	1.28
DMOS B Axle 4	Wheel 5 - High Leg	-0.66	-0.71	-0.64	-0.57	-0.51	-0.33	-0.24	0.47	0.91	1.26	1.34
	Wheel 4 - Low Leg	1.04	1.03	0.85	0.89	0.77	0.59	-0.61	-0.87	-1.05	-1.11	-1.15
PTOS Axle 4	Wheel 4 - High Leg	1.81	1.93	2.08	1.87	1.91	1.83	1.85	0.80	-0.61	-0.59	0.68
	Wheel 5 - Low Leg	2.56	2.60	2.85	2.66	2.50	2.33	2.22	1.39	0.96	0.90	0.98
PTOS Axle 3	Wheel 3 - High Leg	-0.72	-0.78	-0.74	-0.70	-0.62	-0.52	-0.42	0.21	0.69	0.99	1.12
	Wheel 6 - Low Leg	1.13	1.03	0.97	0.97	0.86	0.68	0.57	-0.61	-0.93	-1.05	-1.16
PTOS Axle 2	Wheel 2 - High Leg	1.48	1.53	1.59	1.53	1.58	1.43	1.12	-0.65	-0.92	-0.89	-0.69
	Wheel 7 - Low Leg	2.96	2.98	3.06	3.09	2.78	2.60	2.34	1.49	0.85	0.92	0.86
PTOS Axle 1	Wheel 1 - High Leg	-0.69	-0.66	-0.62	-0.52	-0.49	-0.36	-0.21	0.53	1.02	1.34	1.49
	Wheel 8 - Low Leg	0.99	0.92	0.81	0.79	0.76	0.63	-0.65	-0.81	-1.10	-1.17	-1.12
MOS Axle 4	Wheel 4 - High Leg	1.72	1.70	1.68	1.66	1.83	1.75	1.77	-0.60	-0.85	-0.85	-0.55
	Wheel 5 - Low Leg	2.80	2.83	2.87	2.67	2.60	2.54	2.34	1.25	0.82	0.85	0.88
MOS Axle 3	Wheel 3 - High Leg	-0.84	-0.77	-0.71	-0.64	-0.58	-0.50	-0.29	0.48	0.79	1.16	1.19
	Wheel 6 - Low Leg	0.93	0.88	0.80	0.71	0.66	0.58	-0.50	-0.81	-0.92	-1.11	-1.05
MOS Axle 2	Wheel 2 - High Leg	1.21	1.19	1.17	1.28	1.45	1.49	1.25	-0.92	-0.99	-1.10	-0.82
	Wheel 7 - Low Leg	2.57	2.59	2.59	2.46	2.53	2.50	2.15	0.96	0.74	0.78	0.72
MOS Axle 1	Wheel 1 - High Leg	-0.61	-0.59	-0.51	-0.43	-0.39	-0.31	0.26	0.73	1.03	1.39	1.40
	Wheel 8 - Low Leg	0.89	0.88	0.74	0.67	0.70	0.54	-0.55	-1.08	-1.08	-1.30	-1.13
DMOS A Axle 4	Wheel 4 - High Leg	1.91	1.91	2.02	2.02	2.06	1.91	2.12	0.93	0.77	0.59	0.64
	Wheel 5 - Low Leg	2.76	2.83	2.92	2.70	2.63	2.54	***2.45***	1.48	1.13	0.86	0.99
DMOS A Axle 3	Wheel 3 - High Leg	***-0.84***	-0.88	-0.83	-0.73	-0.67	-0.61	-0.39	0.26	0.72	1.00	1.27
	Wheel 6 - Low Leg	1.20	1.15	1.02	0.85	0.84	0.65	0.51	-0.63	-0.87	-1.03	-1.10
DMOS A Axle 2	Wheel 2 - High Leg	1.32	1.43	1.61	1.55	1.48	1.17	0.89	-0.54	-0.65	-0.70	0.70
	Wheel 7 - Low Leg	***3.06***	***3.13***	***3.15***	***3.11***	***2.85***	***2.67***	2.29	***1.62***	1.32	1.22	1.29
DMOS A Axle 1	Wheel 1 - High Leg	-0.65	-0.62	-0.53	-0.51	-0.44	-0.37	-0.24	0.77	1.25	***1.59***	***1.76***
	Wheel 8 - Low Leg	0.96	0.90	0.82	0.80	0.66	***-0.68***	***-0.87***	***-1.10***	***-1.40***	***-1.54***	***-1.57***

© University of Pretoria

Table B-10: Vertical Forces After Tamping (Wheels) – S2 Down

Hatfield to Pretoria (Down) km 3.175 (Site 2) After Tamping		km/h										
		11.09	20.87	30.69	40.32	50.09	60.03	69.41	79.57	89.30	99.05	104.12
Car Type and Axle	Wheel and Rail Leg	Vertical Force (t)										
DMOS B Axle 1	Wheel 8 - High Leg	5.59	5.62	5.77	5.98	***6.45***	***6.26***	***7.00***	6.51	7.13	7.91	7.99
	Wheel 1 - Low Leg	6.30	6.50	6.33	5.91	5.78	5.36	6.71	5.07	5.37	5.48	5.01
DMOS B Axle 2	Wheel 7 - High Leg	4.62	4.74	4.74	5.05	5.51	5.80	6.23	6.82	7.19	***8.00***	***8.25***
	Wheel 2 - Low Leg	***6.87***	***6.72***	***6.99***	***6.67***	6.18	5.89	5.65	4.81	4.62	4.35	4.71
DMOS B Axle 3	Wheel 6 - High Leg	4.66	4.64	4.68	4.95	5.25	5.26	5.43	5.90	6.21	6.60	6.86
	Wheel 3 - Low Leg	5.67	5.65	5.65	5.37	5.27	5.38	5.16	4.96	4.35	4.22	4.16
DMOS B Axle 4	Wheel 5 - High Leg	4.31	4.52	4.48	4.50	5.09	5.20	5.78	5.95	6.59	6.74	6.94
	Wheel 4 - Low Leg	6.00	5.80	5.97	5.63	5.20	5.18	4.79	4.15	4.38	3.55	3.44
PTOS Axle 4	Wheel 4 - High Leg	4.35	4.36	4.52	4.75	4.93	5.03	5.40	5.40	5.50	6.06	6.47
	Wheel 5 - Low Leg	5.09	5.08	5.00	4.92	4.69	4.70	***4.33***	4.62	4.20	3.92	3.73
PTOS Axle 3	Wheel 3 - High Leg	***3.66***	***3.74***	***3.79***	***4.00***	***4.27***	4.64	4.96	5.53	5.95	6.41	6.56
	Wheel 6 - Low Leg	5.66	5.62	5.56	5.41	5.12	5.00	4.61	***4.10***	***3.64***	3.52	***3.22***
PTOS Axle 2	Wheel 2 - High Leg	4.84	4.79	4.74	5.24	5.49	5.46	5.60	5.78	6.24	6.66	6.98
	Wheel 7 - Low Leg	5.80	5.81	5.85	5.66	5.24	5.19	5.24	5.05	4.96	4.50	4.31
PTOS Axle 1	Wheel 1 - High Leg	4.58	4.74	4.77	4.75	5.45	5.67	6.08	6.65	6.91	7.27	7.60
	Wheel 8 - Low Leg	5.90	5.82	5.71	5.84	5.07	4.92	4.64	4.33	3.72	3.58	3.29
MOS Axle 4	Wheel 4 - High Leg	4.85	4.93	4.95	5.25	5.47	5.61	5.55	5.84	6.05	6.60	6.99
	Wheel 5 - Low Leg	5.22	5.21	5.15	5.14	4.86	4.70	4.67	4.59	4.34	4.16	4.02
MOS Axle 3	Wheel 3 - High Leg	4.33	4.42	4.53	4.64	4.94	5.33	5.55	6.35	6.91	7.18	7.38
	Wheel 6 - Low Leg	5.66	5.70	5.60	5.30	5.34	***4.60***	4.47	4.18	3.81	***3.06***	3.38
MOS Axle 2	Wheel 2 - High Leg	4.30	4.27	4.33	4.64	5.04	4.84	5.02	4.71	5.59	5.92	5.51
	Wheel 7 - Low Leg	5.54	5.57	5.51	5.42	5.22	5.15	5.01	5.23	4.87	4.81	4.17
MOS Axle 1	Wheel 1 - High Leg	3.95	4.11	4.17	4.16	4.62	4.97	4.96	5.42	6.31	6.51	6.84
	Wheel 8 - Low Leg	5.89	5.64	5.63	5.66	5.15	5.11	4.69	4.37	4.40	3.82	3.83
DMOS A Axle 4	Wheel 4 - High Leg	4.90	4.87	5.04	5.27	5.50	5.59	6.01	5.99	6.28	6.35	7.23
	Wheel 5 - Low Leg	5.42	5.35	5.24	5.20	5.04	5.00	4.71	4.59	4.38	4.11	3.62
DMOS A Axle 3	Wheel 3 - High Leg	4.20	4.27	4.31	4.51	4.79	5.17	5.43	6.03	6.79	7.04	7.27
	Wheel 6 - Low Leg	6.04	6.05	6.05	5.79	5.59	5.32	4.88	4.24	4.08	3.47	3.47
DMOS A Axle 2	Wheel 2 - High Leg	5.11	5.06	5.09	5.31	5.77	5.75	5.83	6.08	6.38	6.95	7.12
	Wheel 7 - Low Leg	6.49	6.39	6.48	6.25	5.95	5.77	5.88	5.69	5.40	5.53	5.53
DMOS A Axle 1	Wheel 1 - High Leg	4.84	5.02	5.02	5.02	5.70	6.13	6.27	***6.83***	***7.31***	7.95	7.93
	Wheel 8 - Low Leg	6.66	6.52	6.61	6.54	5.82	5.47	5.37	5.08	4.85	4.68	4.01

© University of Pretoria

Table B-11: Lateral Forces After Tamping (Wheels) – S2 Down

Hatfield to Pretoria (Down) km 3.175 (Site 2) After Tamping		km/h										
		11.09	20.87	30.69	40.32	50.09	60.03	69.41	79.57	89.30	99.05	104.12
Car Type and Axle	Wheel and Rail Leg	Lateral Force (t)										
DMOS B Axle 1	Wheel 8 - High Leg	0.83	0.78	0.52	0.76	-0.53	-0.52	-0.50	-1.21	-1.32	-1.21	-1.00
	Wheel 1 - Low Leg	2.47	2.45	2.12	2.14	1.87	1.64	1.64	0.75	0.57	0.51	0.71
DMOS B Axle 2	Wheel 7 - High Leg	-0.85	-0.87	-0.76	-0.72	-0.57	-0.42	-0.26	0.31	0.73	***1.16***	***1.43***
	Wheel 2 - Low Leg	1.11	1.05	1.03	0.92	0.67	0.55	0.47	0.28	-0.48	-0.64	-0.77
DMOS B Axle 3	Wheel 6 - High Leg	-0.39	0.54	0.64	-0.43	-0.44	-0.59	-0.75	-0.94	-1.01	-1.04	-0.78
	Wheel 3 - Low Leg	2.06	2.34	2.36	1.95	1.90	1.64	1.32	1.01	0.73	0.55	0.70
DMOS B Axle 4	Wheel 5 - High Leg	-0.69	-0.66	-0.65	-0.55	-0.33	-0.23	-0.06	0.27	0.44	0.75	0.89
	Wheel 4 - Low Leg	0.82	0.76	0.78	0.71	0.49	0.44	0.32	0.23	-0.29	-0.41	-0.46
PTOS Axle 4	Wheel 4 - High Leg	1.28	1.20	1.16	0.98	0.84	0.78	0.62	-1.01	-1.05	-1.10	-0.58
	Wheel 5 - Low Leg	2.52	2.50	2.44	2.24	1.96	1.88	1.70	0.88	0.87	0.62	0.91
PTOS Axle 3	Wheel 3 - High Leg	-0.74	-0.73	-0.69	-0.60	-0.51	-0.35	-0.18	0.31	0.70	0.83	0.90
	Wheel 6 - Low Leg	0.89	0.88	0.78	0.72	0.61	0.48	0.37	-0.22	-0.48	-0.48	-0.50
PTOS Axle 2	Wheel 2 - High Leg	0.61	0.48	-0.42	-0.62	-0.59	-0.76	-0.90	-1.25	***-1.42***	-1.29	-0.96
	Wheel 7 - Low Leg	***2.66***	2.67	2.50	2.15	1.97	1.83	1.53	1.04	0.75	0.61	0.70
PTOS Axle 1	Wheel 1 - High Leg	-0.70	-0.65	-0.54	-0.57	-0.29	-0.15	0.19	0.61	0.81	1.00	1.06
	Wheel 8 - Low Leg	0.81	0.75	0.69	0.70	0.43	0.34	0.21	-0.43	-0.50	-0.52	-0.57
MOS Axle 4	Wheel 4 - High Leg	1.10	1.15	1.08	1.00	0.71	0.58	0.35	-1.18	-1.20	-1.14	-0.58
	Wheel 5 - Low Leg	2.64	***2.67***	***2.63***	***2.54***	2.12	1.92	1.89	1.02	0.77	0.74	1.23
MOS Axle 3	Wheel 3 - High Leg	-0.84	-0.82	-0.77	-0.67	-0.62	-0.47	-0.42	0.21	0.73	1.01	1.11
	Wheel 6 - Low Leg	0.86	0.84	0.79	0.74	0.56	0.48	0.43	-0.16	-0.41	-0.60	-0.71
MOS Axle 2	Wheel 2 - High Leg	0.51	0.49	0.51	-0.37	-0.39	-0.41	-0.50	-1.12	-1.17	-1.11	-0.72
	Wheel 7 - Low Leg	2.36	2.43	2.37	1.98	1.91	1.86	1.81	***1.17***	0.90	0.91	0.99
MOS Axle 1	Wheel 1 - High Leg	-0.61	-0.59	-0.51	-0.52	-0.35	-0.31	-0.15	0.41	0.66	0.88	0.93
	Wheel 8 - Low Leg	0.78	0.73	0.69	0.77	0.47	0.40	0.37	-0.32	-0.49	-0.56	-0.63
DMOS A Axle 4	Wheel 4 - High Leg	1.13	1.14	1.10	1.00	1.06	1.16	0.73	-1.11	-1.02	-1.01	-0.53
	Wheel 5 - Low Leg	2.51	2.53	2.46	2.38	***2.36***	***2.13***	***1.95***	0.89	0.79	0.79	1.11
DMOS A Axle 3	Wheel 3 - High Leg	***-0.87***	***-0.87***	***-0.83***	-0.69	-0.63	-0.48	-0.34	0.16	0.41	0.71	0.90
	Wheel 6 - Low Leg	1.00	0.97	0.87	0.83	0.69	0.53	0.43	0.25	-0.26	-0.39	-0.47
DMOS A Axle 2	Wheel 2 - High Leg	-0.43	-0.55	-0.52	***-0.73***	***-0.80***	***-1.05***	***-1.25***	***-1.48***	-1.39	***-1.35***	***-1.03***
	Wheel 7 - Low Leg	2.65	2.56	2.56	2.17	1.96	1.61	1.38	1.06	***0.95***	0.84	0.77
DMOS A Axle 1	Wheel 1 - High Leg	-0.68	-0.65	-0.63	-0.61	-0.32	-0.22	0.23	0.43	0.72	1.05	1.29
	Wheel 8 - Low Leg	0.91	0.82	0.82	0.79	0.49	0.38	0.27	-0.39	-0.54	-0.68	-0.78

© University of Pretoria

Table B-12: Vertical Forces After Tamping (Wheels) – S1 Up

Pretoria to Hatfield (Up) km 3.215 (Site 1) After Tamping		km/h										
		10.97	20.55	30.32	40.09	50.10	59.61	69.90	79.84	89.37	99.02	104.70
Car Type and Axle	Wheel and Rail Leg	Greatest Vertical Force (t)										
DMOS A Axle 1	Wheel 1 - High Leg	4.81	4.92	5.07	5.33	5.69	5.61	5.52	5.95	6.17	6.41	6.47
	Wheel 8 - Low Leg	7.57	7.43	7.24	6.96	6.85	***6.92***	***6.38***	6.11	6.10	5.41	5.44
DMOS A Axle 2	Wheel 2 - High Leg	4.29	4.37	4.50	4.77	4.98	5.40	5.29	5.71	6.34	6.73	6.35
	Wheel 7 - Low Leg	***7.74***	7.90	***7.81***	***7.25***	7.03	6.47	6.34	6.05	5.28	4.64	4.23
DMOS A Axle 3	Wheel 3 - High Leg	4.51	4.57	4.78	5.01	5.02	4.97	5.22	5.53	5.82	5.85	6.23
	Wheel 6 - Low Leg	6.45	6.49	6.24	5.93	6.19	5.90	5.31	4.91	4.84	4.72	4.09
DMOS A Axle 4	Wheel 4 - High Leg	3.99	3.98	4.16	4.59	4.65	5.05	5.16	5.67	5.93	6.70	6.90
	Wheel 5 - Low Leg	6.75	6.78	6.76	6.29	5.89	5.82	5.52	4.85	3.84	3.65	3.11
MOS Axle 1	Wheel 1 - High Leg	4.04	4.11	4.27	4.46	4.79	4.64	4.76	4.75	4.93	5.23	5.38
	Wheel 8 - Low Leg	6.47	6.47	6.05	6.01	5.93	5.65	5.65	5.32	5.04	4.60	4.63
MOS Axle 2	Wheel 2 - High Leg	***3.63***	***3.62***	3.78	***4.03***	4.47	4.52	4.61	5.04	5.46	5.69	6.18
	Wheel 7 - Low Leg	6.95	7.11	7.00	6.43	6.42	6.21	5.69	5.29	4.20	4.02	3.73
MOS Axle 3	Wheel 3 - High Leg	4.47	4.57	4.66	4.85	5.00	5.07	5.21	5.50	5.55	5.80	6.02
	Wheel 6 - Low Leg	6.37	6.23	6.03	5.80	5.73	5.70	5.32	4.73	4.69	4.23	4.31
MOS Axle 4	Wheel 4 - High Leg	4.09	4.07	4.19	4.59	4.76	4.85	5.11	5.74	6.30	6.61	6.60
	Wheel 5 - Low Leg	6.45	6.53	6.39	5.97	5.50	5.55	5.15	4.47	***3.81***	3.44	3.14
PTOS Axle 1	Wheel 1 - High Leg	4.57	4.68	4.90	5.06	5.41	5.29	5.36	5.63	5.79	5.80	6.28
	Wheel 8 - Low Leg	6.75	6.69	6.43	6.28	5.74	5.77	5.73	5.13	5.10	4.66	4.15
PTOS Axle 2	Wheel 2 - High Leg	4.06	4.12	4.18	4.51	4.89	4.95	5.20	5.62	6.18	6.53	6.75
	Wheel 7 - Low Leg	7.03	7.01	6.83	6.52	5.95	5.79	5.48	4.78	4.19	3.80	3.56
PTOS Axle 3	Wheel 3 - High Leg	3.88	3.95	4.07	4.35	4.45	***4.27***	***4.48***	4.74	4.69	5.11	5.56
	Wheel 6 - Low Leg	6.29	6.32	6.05	5.82	5.77	5.68	5.25	5.13	4.97	4.37	4.00
PTOS Axle 4	Wheel 4 - High Leg	3.69	3.71	***3.78***	4.21	***4.42***	4.58	4.92	5.13	5.45	5.86	6.23
	Wheel 5 - Low Leg	6.16	6.20	6.15	5.71	5.34	5.39	5.01	***4.31***	4.15	***3.41***	***2.99***
DMOS B Axle 4	Wheel 5 - High Leg	4.51	4.52	4.67	4.89	5.10	5.17	5.39	5.73	5.64	6.09	6.44
	Wheel 4 - Low Leg	6.53	6.44	6.25	6.21	5.97	5.66	5.27	4.79	4.50	4.17	4.21
DMOS B Axle 3	Wheel 6 - High Leg	3.98	3.95	4.05	4.29	4.66	4.69	5.09	5.39	5.84	6.31	6.62
	Wheel 3 - Low Leg	6.84	6.95	6.68	6.66	6.03	5.93	5.35	5.01	4.35	3.94	3.65
DMOS B Axle 2	Wheel 7 - High Leg	4.85	4.99	5.21	5.38	5.25	5.66	5.71	5.89	5.94	6.46	6.58
	Wheel 2 - Low Leg	7.39	7.45	7.33	6.77	***7.36***	6.85	6.23	***6.47***	6.19	5.79	4.99
DMOS B Axle 1	Wheel 8 - High Leg	4.76	4.82	4.92	5.18	5.53	5.52	5.76	6.12	***7.57***	***7.46***	***8.33***
	Wheel 1 - Low Leg	7.68	***8.72***	7.28	7.01	6.43	6.42	5.79	5.12	4.62	4.63	4.21

© University of Pretoria

Table B-13: Lateral Rail Forces After Tamping (Wheels) – S1 Up

Pretoria to Hatfield (Up) km 3.215 (Site 1) After Tamping		km/h										
		10.97	20.55	30.32	40.09	50.10	59.61	69.90	79.84	89.37	99.02	104.70
Car Type and Axle	Wheel and Rail Leg	Lateral Force (t)										
DMOS A Axle 1	Wheel 1 - High Leg	2.22	2.29	2.38	2.55	2.78	2.64	***2.85***	***2.97***	***2.69***	***2.33***	1.90
	Wheel 8 - Low Leg	***3.27***	***3.26***	***3.21***	***3.08***	2.99	***3.02***	2.84	2.71	2.37	1.79	1.48
DMOS A Axle 2	Wheel 2 - High Leg	***-0.99***	***-1.03***	-0.89	-0.74	***-0.72***	-0.52	-0.46	-0.41	0.58	1.11	1.32
	Wheel 7 - Low Leg	1.14	1.10	1.03	0.97	0.85	0.71	0.53	-0.60	-1.10	-1.28	-1.28
DMOS A Axle 3	Wheel 3 - High Leg	1.86	1.93	2.06	2.03	2.11	2.16	2.20	2.10	1.50	1.25	1.25
	Wheel 6 - Low Leg	2.86	2.87	2.87	2.68	2.63	2.58	2.42	2.20	1.65	1.43	1.17
DMOS A Axle 4	Wheel 4 - High Leg	-0.84	-0.87	-0.78	-0.62	-0.55	-0.46	-0.23	0.22	0.97	1.48	1.74
	Wheel 5 - Low Leg	0.93	0.94	0.89	0.78	0.67	0.57	-0.43	-0.66	-0.99	-1.17	-1.26
MOS Axle 1	Wheel 1 - High Leg	1.99	2.05	2.28	2.22	2.23	2.47	2.60	2.31	2.10	1.66	1.54
	Wheel 8 - Low Leg	2.74	2.73	2.72	2.57	2.38	2.38	2.28	2.10	1.77	1.33	1.13
MOS Axle 2	Wheel 2 - High Leg	-0.96	-0.88	***-0.92***	-0.76	-0.65	-0.55	-0.43	-0.40	0.72	0.92	1.07
	Wheel 7 - Low Leg	1.00	0.94	0.89	0.85	0.70	0.60	0.49	-0.53	-0.99	-1.05	-1.18
MOS Axle 3	Wheel 3 - High Leg	1.56	1.82	1.72	1.72	1.78	2.07	1.93	1.75	1.26	0.99	0.91
	Wheel 6 - Low Leg	2.78	2.90	2.78	2.61	2.55	2.40	2.34	1.91	1.47	1.10	1.06
MOS Axle 4	Wheel 4 - High Leg	-0.80	-0.79	-0.70	-0.53	-0.45	-0.36	-0.24	0.45	1.12	1.36	1.52
	Wheel 5 - Low Leg	0.89	0.84	0.79	0.69	0.58	0.45	-0.65	-0.90	-1.14	-1.18	-1.14
PTOS Axle 1	Wheel 1 - High Leg	2.14	2.17	2.31	2.39	2.43	2.47	2.62	2.37	1.90	1.38	1.71
	Wheel 8 - Low Leg	3.11	3.13	3.03	2.94	2.74	2.64	2.56	2.16	1.70	1.12	1.14
PTOS Axle 2	Wheel 2 - High Leg	-0.94	-0.88	-0.86	***-0.78***	-0.60	-0.55	-0.51	-0.29	0.56	0.83	1.03
	Wheel 7 - Low Leg	1.01	0.96	0.89	0.89	0.68	0.52	0.42	-0.65	-0.95	-1.12	-1.13
PTOS Axle 3	Wheel 3 - High Leg	1.60	1.70	1.77	1.85	1.88	1.87	1.87	1.71	1.44	0.94	1.35
	Wheel 6 - Low Leg	2.92	2.99	2.88	2.80	2.62	2.58	2.34	1.94	1.53	0.97	1.07
PTOS Axle 4	Wheel 4 - High Leg	-0.58	-0.58	-0.53	-0.42	-0.29	-0.24	-0.16	0.56	0.93	1.21	1.52
	Wheel 5 - Low Leg	0.80	0.77	0.71	0.67	0.48	-0.54	-0.63	-1.00	-1.08	-1.14	-1.27
DMOS B Axle 4	Wheel 5 - High Leg	2.11	2.26	2.24	2.58	2.40	2.57	2.57	2.40	2.20	1.74	1.75
	Wheel 4 - Low Leg	2.93	2.98	2.84	2.80	2.60	2.50	2.30	1.88	1.82	1.14	1.15
DMOS B Axle 3	Wheel 6 - High Leg	-0.85	-0.87	-0.77	-0.76	-0.58	-0.47	-0.40	-0.23	0.44	0.76	0.98
	Wheel 3 - Low Leg	0.48	0.44	0.43	0.44	-0.43	-0.52	-0.66	-0.80	-1.09	-1.12	-1.23
DMOS B Axle 2	Wheel 7 - High Leg	1.83	1.78	1.72	2.04	1.83	2.04	2.08	1.78	1.42	0.70	0.84
	Wheel 2 - Low Leg	3.25	3.20	3.11	3.06	***3.06***	2.73	2.48	2.22	1.89	1.30	1.35
DMOS B Axle 1	Wheel 8 - High Leg	-0.86	-0.90	-0.73	-0.60	-0.49	-0.26	-0.28	0.85	1.50	1.83	***2.12***
	Wheel 1 - Low Leg	0.98	0.93	0.79	0.82	0.62	***-0.66***	***-0.91***	***-1.25***	***-1.56***	***-1.53***	***-1.47***

© University of Pretoria

Table B-14: Vertical Rail Forces After Tamping (Wheels) – S2 Up

Pretoria to Hatfield (Up) km 3.175 (Site 2) After Tamping		km/h										
		11.01	20.39	29.80	39.92	49.68	59.45	69.57	79.66	90.09	99.10	104.24
Car Type and Axle	Wheel and Rail Leg	Vertical Force (t)										
DMOS A Axle 1	Wheel 1 - High Leg	4.98	5.13	5.20	5.45	5.71	5.87	6.29	6.66	6.59	6.99	7.12
	Wheel 8 - Low Leg	6.44	6.40	***6.50***	6.23	6.25	6.00	5.93	5.61	5.60	5.62	4.92
DMOS A Axle 2	Wheel 2 - High Leg	5.00	4.99	5.12	5.54	5.77	***6.12***	6.29	6.68	***7.72***	7.77	8.66
	Wheel 7 - Low Leg	6.48	6.41	6.22	6.13	6.02	5.67	5.51	4.92	4.65	3.92	4.21
DMOS A Axle 3	Wheel 3 - High Leg	4.62	4.66	4.60	4.95	5.28	5.61	6.07	6.48	6.21	6.46	7.05
	Wheel 6 - Low Leg	5.60	5.67	5.70	5.65	5.52	5.05	4.59	4.65	4.26	4.07	3.83
DMOS A Axle 4	Wheel 4 - High Leg	4.62	4.68	4.76	4.70	5.13	5.45	5.88	6.58	7.55	8.14	7.81
	Wheel 5 - Low Leg	5.75	5.58	5.54	5.82	5.33	5.03	4.49	3.88	3.79	3.53	3.06
MOS Axle 1	Wheel 1 - High Leg	4.22	4.28	4.38	4.53	4.80	5.02	5.23	5.33	5.61	5.47	6.37
	Wheel 8 - Low Leg	5.51	5.60	5.72	5.30	5.35	5.46	5.01	4.97	4.88	4.27	4.16
MOS Axle 2	Wheel 2 - High Leg	4.15	4.19	4.39	4.55	4.81	5.03	5.28	5.43	6.53	6.98	6.98
	Wheel 7 - Low Leg	5.73	5.95	5.44	5.97	5.25	4.92	4.54	4.16	3.75	3.95	3.57
MOS Axle 3	Wheel 3 - High Leg	4.57	4.70	4.64	4.81	5.09	5.46	5.79	6.08	6.39	6.77	7.05
	Wheel 6 - Low Leg	5.47	5.42	5.53	5.30	5.30	5.20	4.86	4.65	3.94	4.17	3.81
MOS Axle 4	Wheel 4 - High Leg	4.70	4.72	4.88	4.76	5.12	5.48	5.91	6.50	7.39	7.85	7.79
	Wheel 5 - Low Leg	5.52	5.47	5.34	5.47	5.02	4.98	4.60	3.82	3.70	3.03	3.07
PTOS Axle 1	Wheel 1 - High Leg	4.75	4.85	4.86	5.11	5.20	5.53	5.86	6.17	6.24	6.59	7.32
	Wheel 8 - Low Leg	5.82	5.79	5.84	5.69	5.60	5.55	5.30	5.06	4.90	4.41	4.26
PTOS Axle 2	Wheel 2 - High Leg	4.71	4.72	4.88	5.07	5.35	5.78	6.20	6.81	7.50	7.89	8.18
	Wheel 7 - Low Leg	5.83	5.77	5.69	5.45	5.39	5.10	4.78	4.08	3.66	3.09	3.09
PTOS Axle 3	Wheel 3 - High Leg	***3.82***	***3.93***	***3.90***	***4.15***	***4.38***	4.77	5.14	5.32	5.67	5.78	6.09
	Wheel 6 - Low Leg	5.62	5.55	5.59	5.53	5.23	5.15	5.01	4.81	4.37	4.25	4.08
PTOS Axle 4	Wheel 4 - High Leg	4.22	4.23	4.33	4.22	4.70	5.05	5.55	6.12	6.53	6.79	6.90
	Wheel 5 - Low Leg	5.19	5.20	5.18	5.21	4.93	***4.67***	***4.23***	***3.54***	***3.16***	***2.98***	3.08
DMOS B Axle 4	Wheel 5 - High Leg	4.70	4.76	4.75	5.06	5.13	5.46	5.73	6.03	6.33	6.38	7.04
	Wheel 4 - Low Leg	5.59	5.51	5.65	5.51	5.25	5.32	4.98	4.70	4.45	4.39	3.98
DMOS B Axle 3	Wheel 6 - High Leg	4.55	4.54	4.67	4.99	5.36	5.45	5.84	6.58	7.18	7.22	7.47
	Wheel 3 - Low Leg	5.67	5.61	5.57	5.32	5.34	5.03	4.64	4.29	4.13	3.63	***3.04***
DMOS B Axle 2	Wheel 7 - High Leg	5.01	4.88	5.07	5.35	5.67	6.07	6.26	6.50	7.13	7.92	7.80
	Wheel 2 - Low Leg	***6.72***	6.57	6.48	***6.63***	***6.43***	5.91	5.89	5.35	5.95	5.32	4.85
DMOS B Axle 1	Wheel 8 - High Leg	5.32	5.46	5.53	5.68	5.99	6.03	***7.30***	***7.16***	7.60	***8.53***	***8.98***
	Wheel 1 - Low Leg	6.25	***7.19***	6.37	6.45	6.21	5.59	5.43	4.66	4.34	5.12	3.72

© University of Pretoria

Table B-15: Lateral Rail Forces After Tamping (Wheels) – S2 Up

Pretoria to Hatfield (Up) km 3.175 (Site 2) After Tamping		km/h										
		11.01	20.39	29.80	39.92	49.68	59.45	69.57	79.66	90.09	99.10	104.24
Car Type and Axle	Wheel and Rail Leg	Lateral Force (t)										
DMOS A Axle 1	Wheel 1 - High Leg	1.38	1.08	1.09	1.04	1.00	1.19	0.79	-0.71	-1.08	-1.16	-0.81
	Wheel 8 - Low Leg	***3.26***	3.10	***3.10***	***2.88***	***2.91***	***2.89***	***2.63***	***1.54***	0.93	0.75	0.83
DMOS A Axle 2	Wheel 2 - High Leg	-0.78	-0.74	-0.65	-0.51	-0.48	-0.43	-0.26	0.47	0.82	1.24	1.34
	Wheel 7 - Low Leg	0.85	0.80	0.78	0.64	0.57	0.50	0.35	-0.40	-0.58	-0.79	-0.82
DMOS A Axle 3	Wheel 3 - High Leg	1.20	1.20	1.20	1.06	1.07	1.21	0.90	-0.67	-1.06	-1.07	-0.93
	Wheel 6 - Low Leg	2.83	2.87	2.88	2.74	2.63	2.49	2.13	1.29	0.69	0.57	0.55
DMOS A Axle 4	Wheel 4 - High Leg	***-0.78***	-0.66	-0.59	-0.62	-0.40	-0.32	-0.16	0.64	1.01	1.30	1.41
	Wheel 5 - Low Leg	0.72	0.67	0.64	0.64	0.52	0.37	0.24	-0.42	-0.58	-0.66	-0.71
MOS Axle 1	Wheel 1 - High Leg	1.02	1.03	0.94	1.02	0.96	0.91	0.53	-0.82	-0.90	-0.82	-0.45
	Wheel 8 - Low Leg	2.60	2.64	2.54	2.48	2.39	2.39	1.98	0.95	0.67	0.52	0.88
MOS Axle 2	Wheel 2 - High Leg	-0.75	-0.73	-0.66	***-0.67***	-0.46	-0.37	-0.26	0.47	0.67	0.78	0.93
	Wheel 7 - Low Leg	0.71	0.70	0.63	0.59	0.50	0.37	0.30	-0.40	-0.46	-0.48	-0.52
MOS Axle 3	Wheel 3 - High Leg	0.91	1.08	0.87	0.86	0.73	0.55	0.31	-1.04	-1.05	-1.10	-0.49
	Wheel 6 - Low Leg	2.74	2.86	2.69	2.71	2.45	2.28	1.84	0.91	0.62	0.52	1.01
MOS Axle 4	Wheel 4 - High Leg	-0.74	-0.71	-0.55	-0.56	-0.42	-0.32	-0.20	0.76	1.12	1.40	***1.51***
	Wheel 5 - Low Leg	0.64	0.62	0.57	0.58	0.43	0.33	0.20	-0.51	-0.68	-0.70	-0.81
PTOS Axle 1	Wheel 1 - High Leg	1.01	1.08	1.05	0.92	0.97	0.82	0.46	-1.03	***-1.39***	***-1.21***	-0.71
	Wheel 8 - Low Leg	2.98	3.07	3.00	2.86	2.86	2.70	2.32	1.47	0.86	0.73	0.92
PTOS Axle 2	Wheel 2 - High Leg	-0.74	-0.71	-0.62	-0.52	-0.46	-0.37	-0.27	0.58	1.03	1.33	1.45
	Wheel 7 - Low Leg	0.71	0.69	0.61	0.58	0.47	0.39	0.26	-0.49	-0.72	-0.83	-0.83
PTOS Axle 3	Wheel 3 - High Leg	0.71	0.80	0.78	0.64	0.69	0.49	-0.35	-1.07	-1.12	-1.00	-0.69
	Wheel 6 - Low Leg	2.87	2.94	2.90	2.76	2.67	2.47	2.03	1.13	0.65	0.61	0.74
PTOS Axle 4	Wheel 4 - High Leg	-0.48	-0.47	-0.43	-0.45	-0.35	-0.28	0.32	0.97	***1.28***	***1.54***	1.36
	Wheel 5 - Low Leg	0.55	0.54	0.51	0.54	0.41	0.32	-0.29	-0.66	-0.78	-0.87	-0.74
DMOS B Axle 4	Wheel 5 - High Leg	1.35	1.33	1.32	1.15	1.36	1.09	0.71	-0.71	-1.03	-0.97	-0.43
	Wheel 4 - Low Leg	2.88	2.84	2.79	2.60	2.64	2.42	2.03	1.13	0.59	0.46	0.91
DMOS B Axle 3	Wheel 6 - High Leg	-0.68	-0.65	-0.57	-0.43	-0.42	-0.29	-0.19	0.43	0.84	1.09	1.26
	Wheel 3 - Low Leg	0.29	0.27	0.18	-0.07	-0.12	-0.20	-0.42	-0.72	-0.88	-0.95	***-0.94***
DMOS B Axle 2	Wheel 7 - High Leg	0.64	0.76	0.74	0.38	0.59	0.42	***-0.72***	***-1.27***	-1.25	-1.16	-0.44
	Wheel 2 - Low Leg	3.12	***3.13***	3.09	2.84	2.84	2.60	1.90	1.08	0.82	0.88	1.18
DMOS B Axle 1	Wheel 8 - High Leg	-0.73	***-0.88***	***-0.76***	-0.61	***-0.59***	***-0.46***	0.26	0.83	1.27	1.52	1.47
	Wheel 1 - Low Leg	0.72	0.75	0.71	0.65	0.56	0.42	0.21	-0.55	-0.81	-0.89	-0.77

© University of Pretoria

APPENDIX C. CURVE RAIL FORCES TRENDS FOR WHEELS (MAXIMUMS AND MINIMUMS)

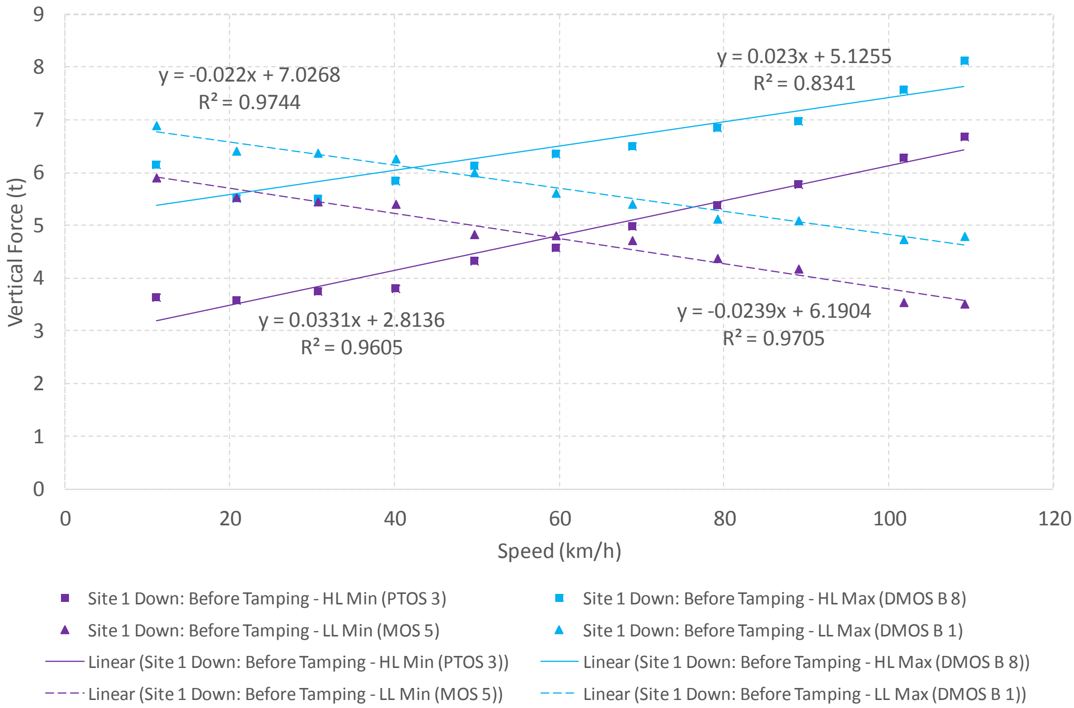

Figure C-1: Vertical Wheel Forces Before Tamping – S1 Down

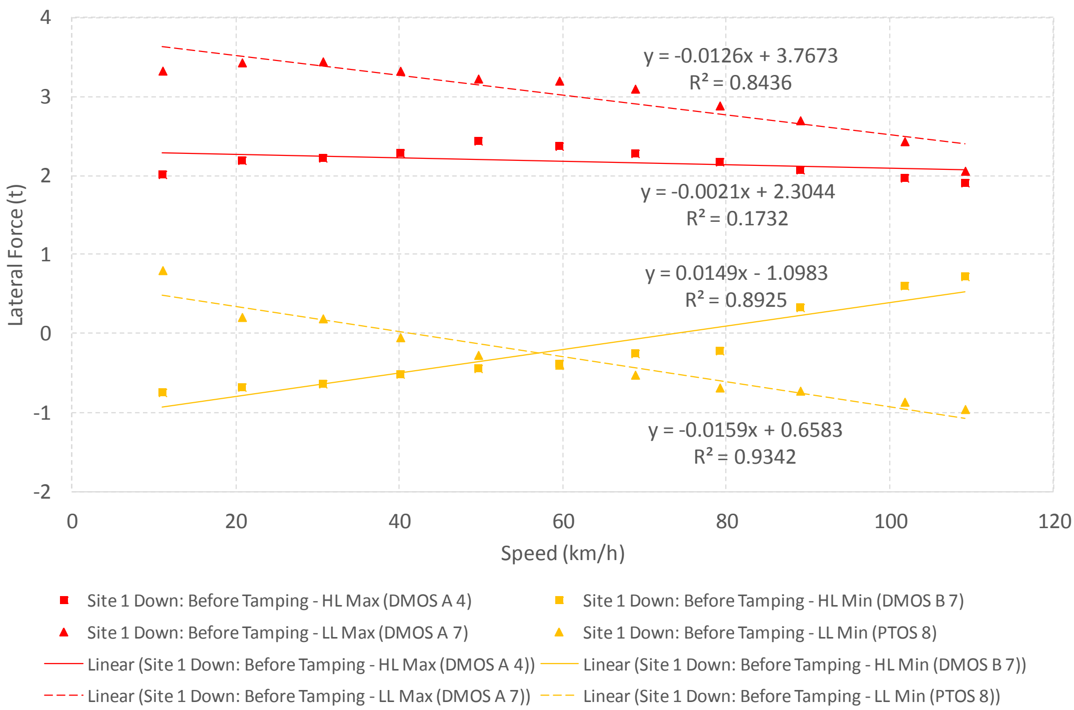

Figure C-2: Lateral Wheel Forces Before Tamping – S1 Down

© University of Pretoria

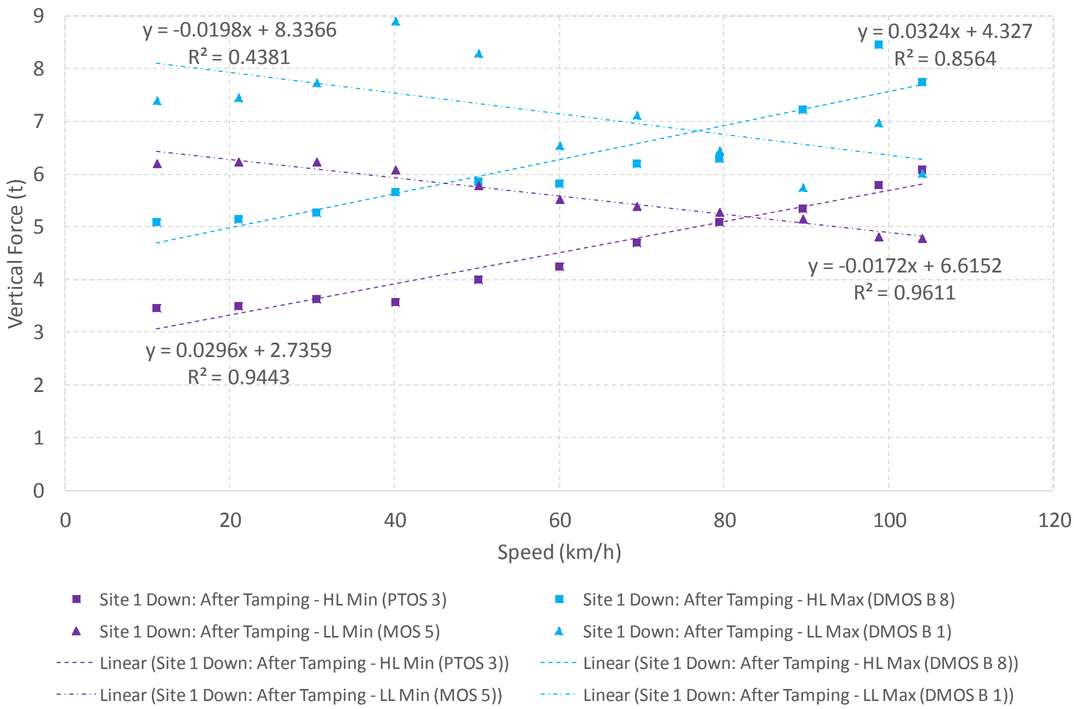

Figure C-3: Vertical Wheel Forces After Tamping – S1 Down

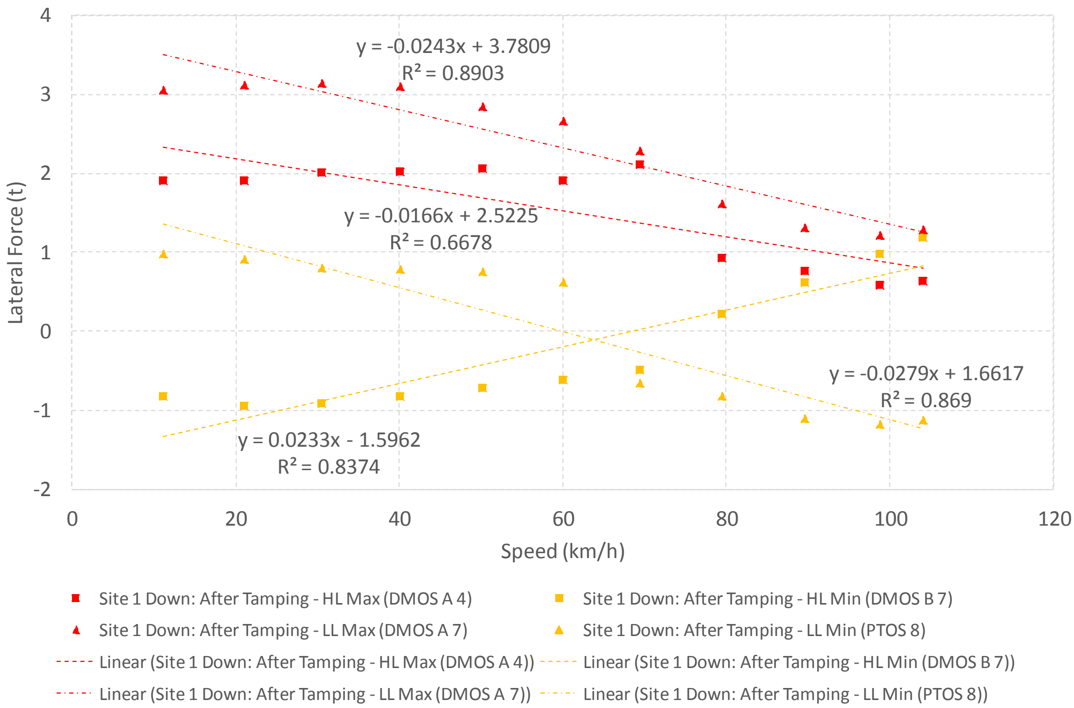

Figure C-4: Lateral Wheel Forces After Tamping – S1 Down

© University of Pretoria

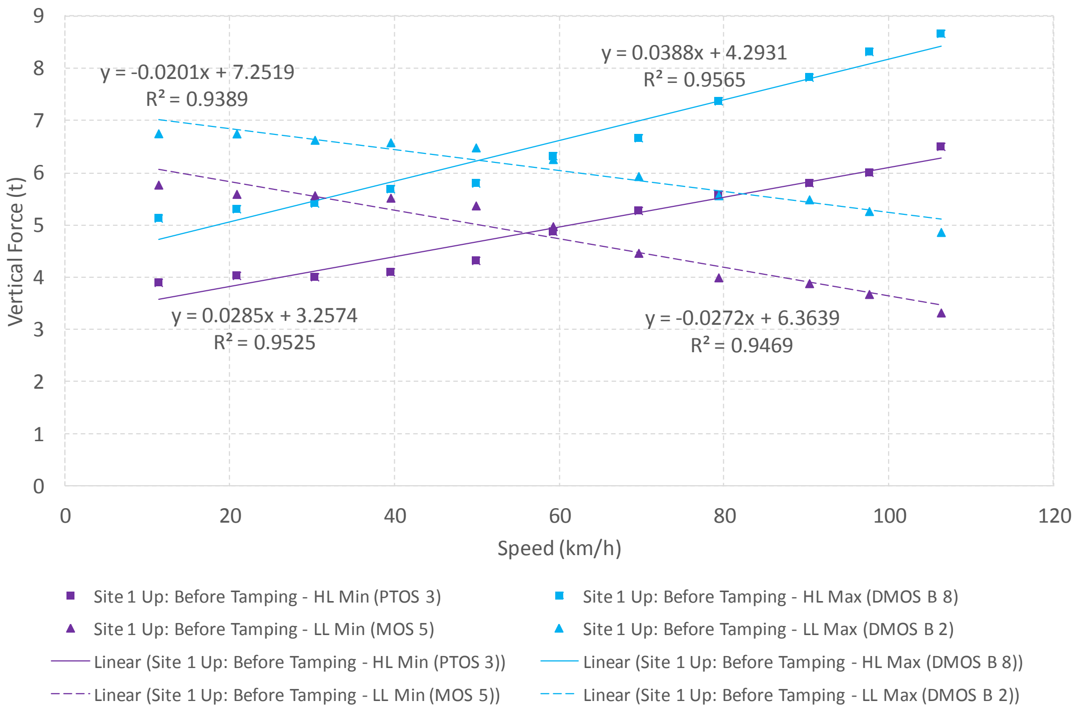

Figure C-5: Vertical Wheel Forces Before Tamping – S1 Up

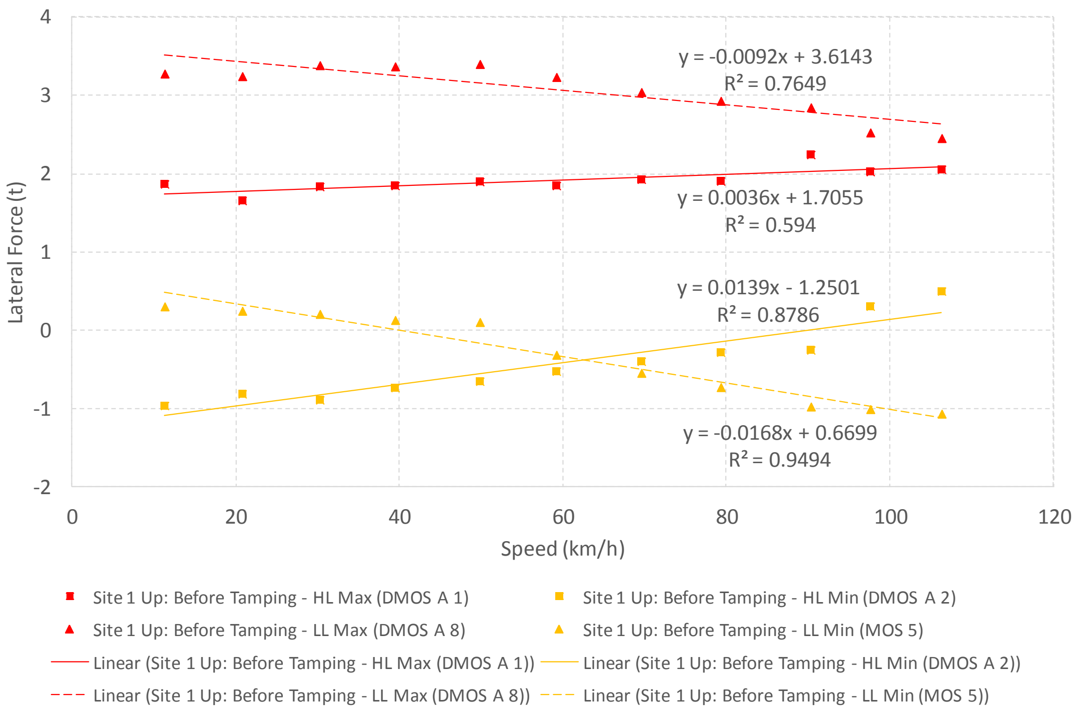

Figure C-6: Lateral Wheel Forces Before Tamping – S1 Up

© University of Pretoria

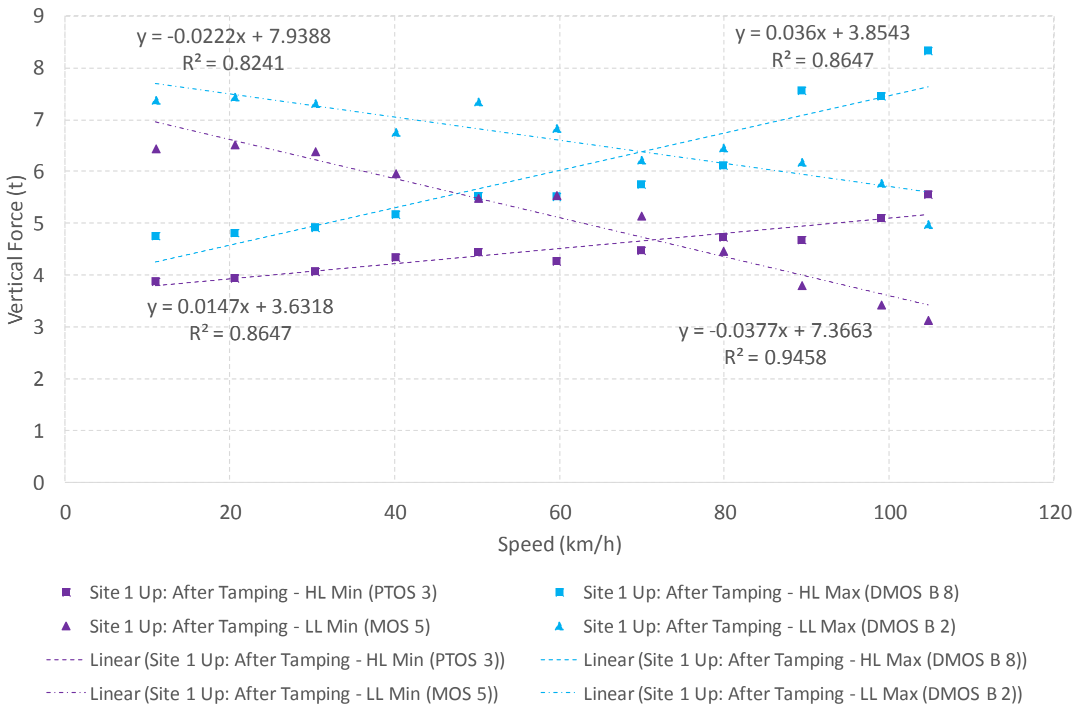

Figure C-7: Vertical Wheel Forces After Tamping – S1 Up

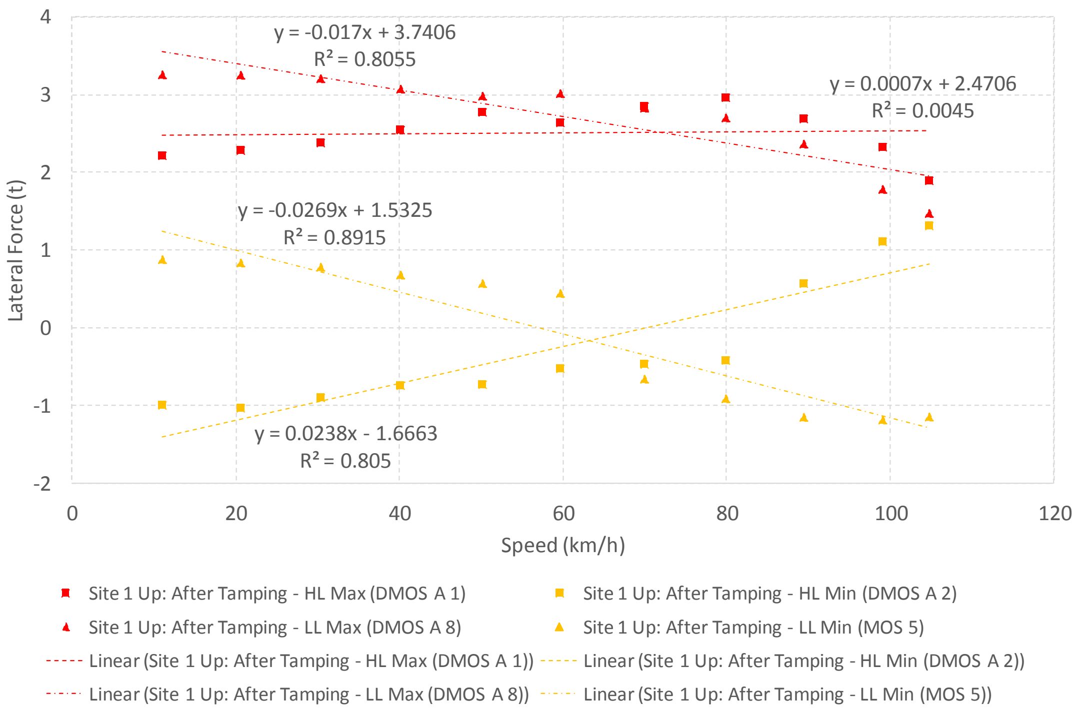

Figure C-8: Lateral Wheel Forces After Tamping – S1 Up

© University of Pretoria

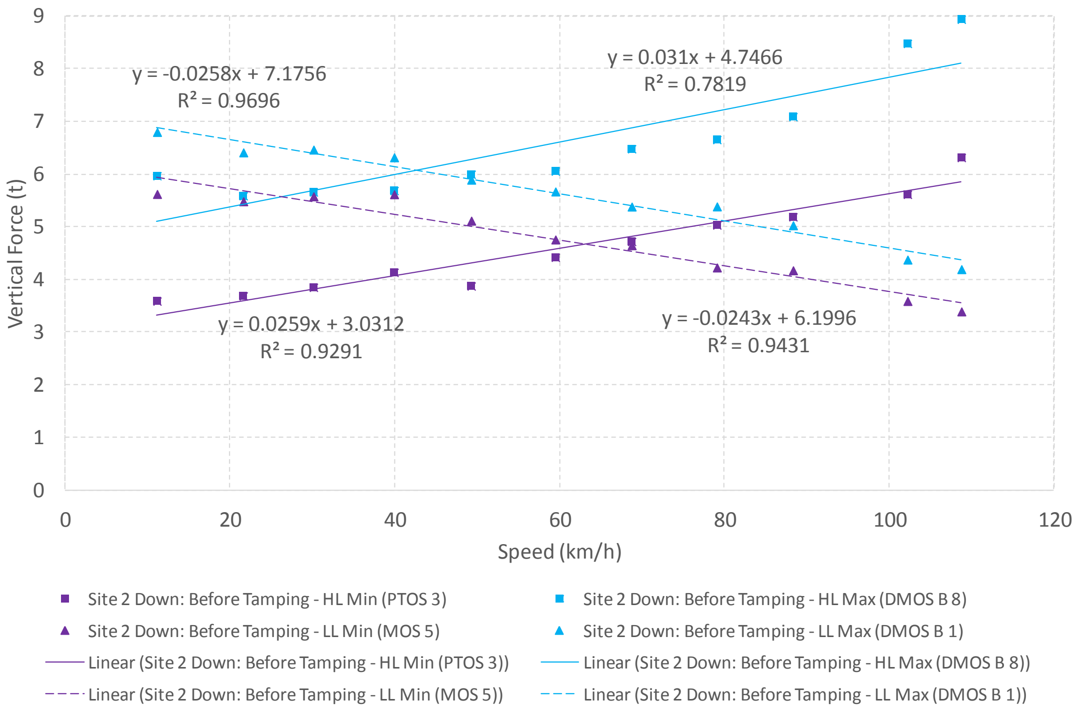

Figure C-9: Vertical Wheel Forces Before Tamping – S2 Down

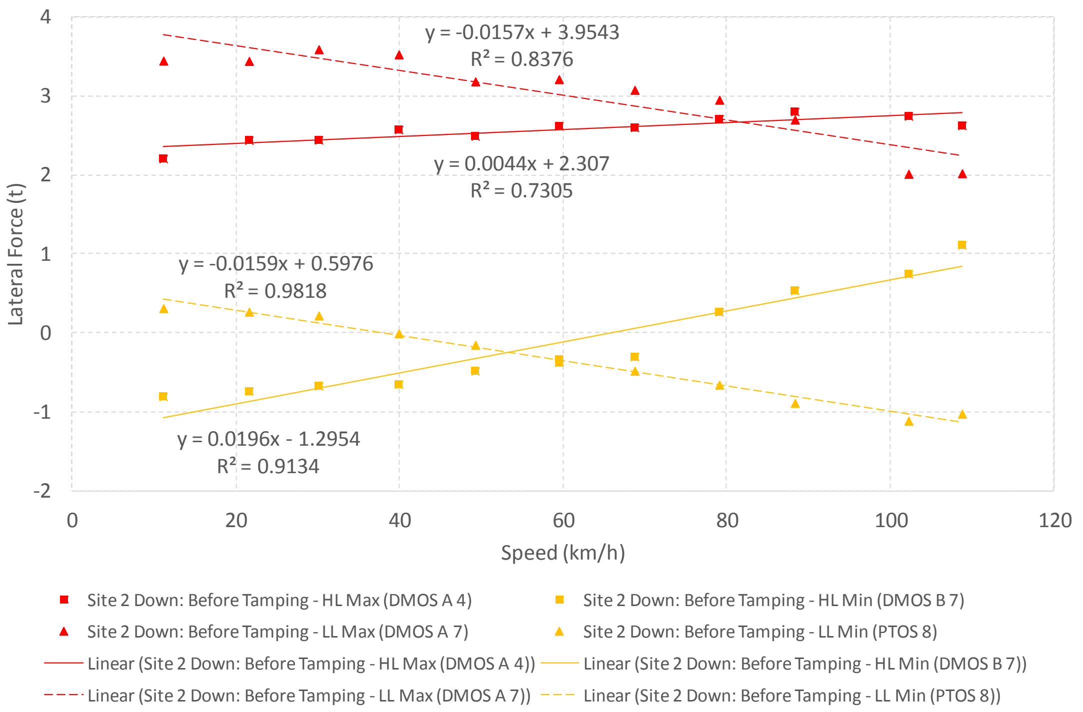

Figure C-10: Lateral Wheel Forces Before Tamping – S2 Down

© University of Pretoria

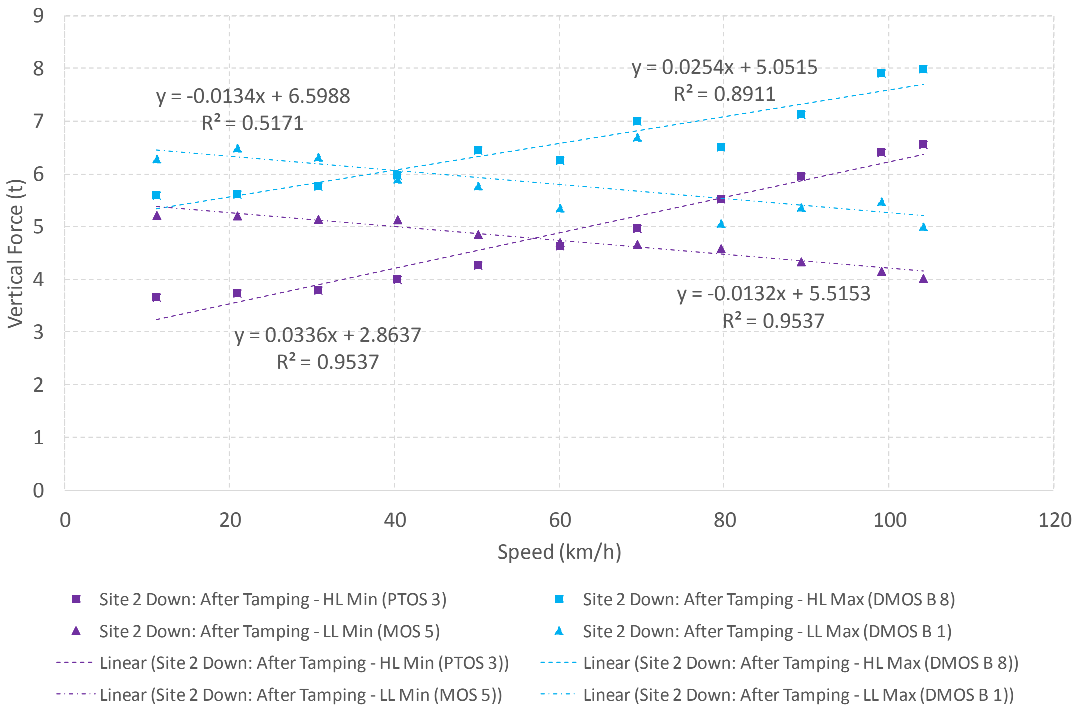

Figure C-11: Vertical Wheel Forces After Tamping – S2 Down

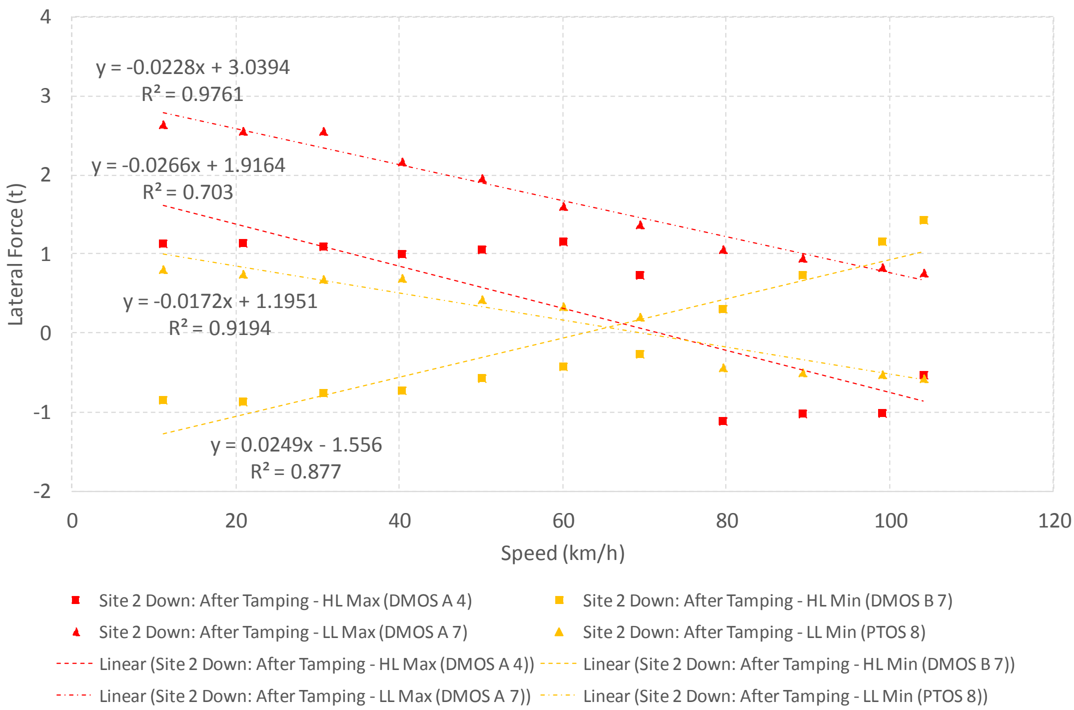

Figure C-12: Lateral Wheel Forces After Tamping – S2 Down

© University of Pretoria

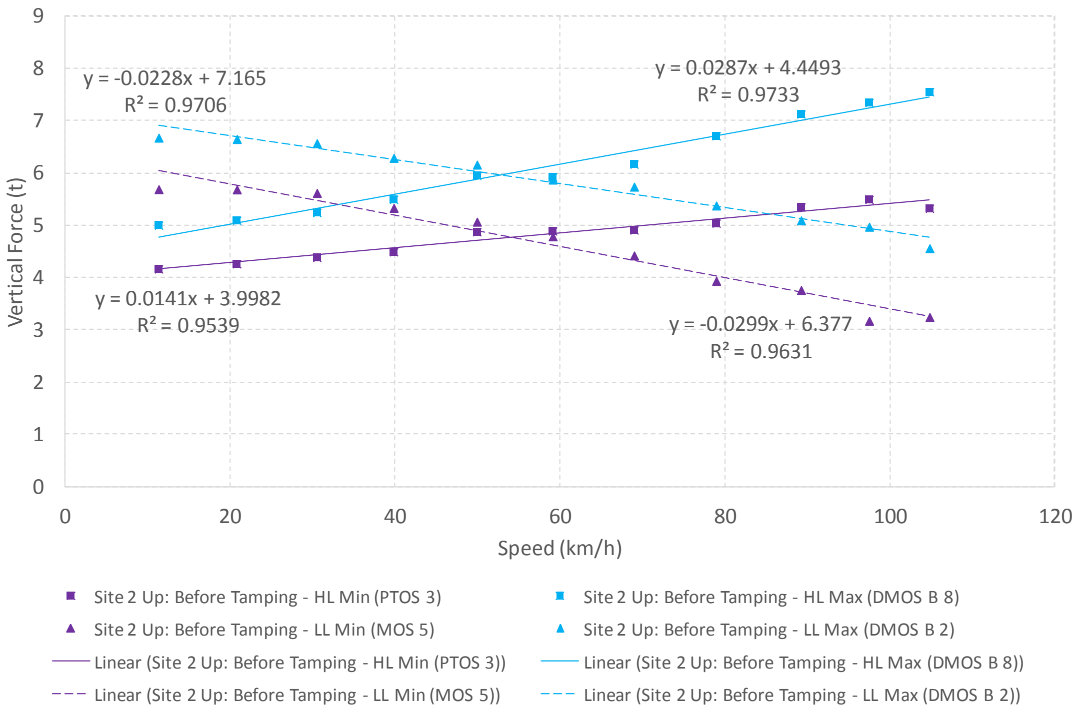

Figure C-13: Vertical Wheel Forces Before Tamping – S2 Up

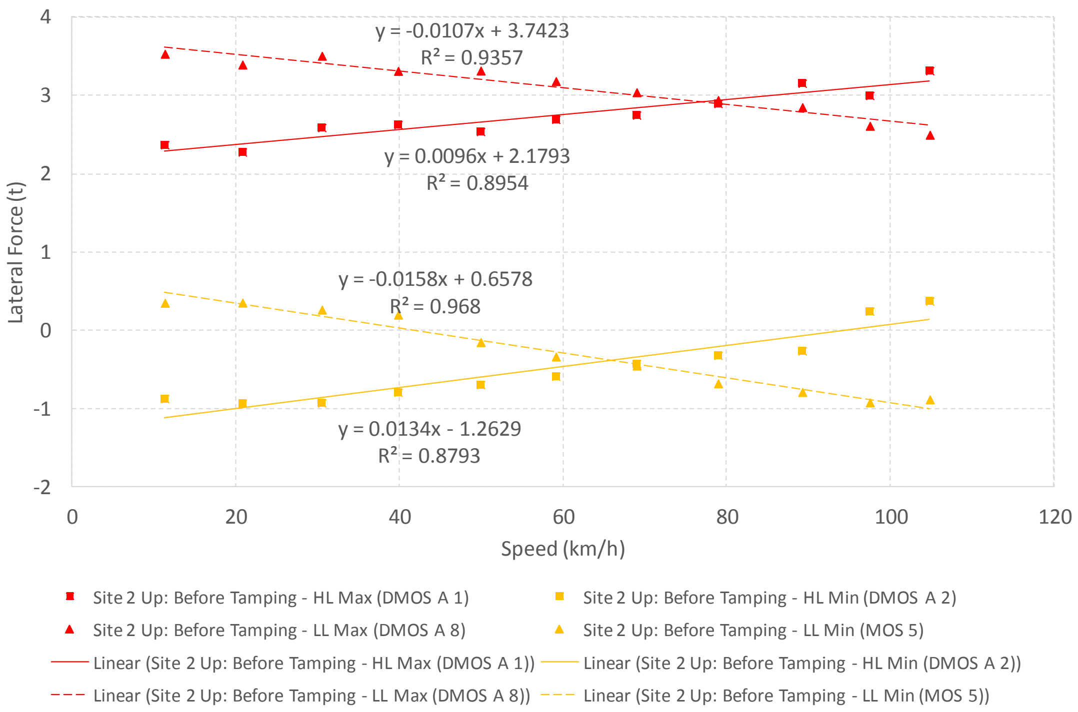

Figure C-14: Lateral Wheel Forces Before Tamping – S2 Up

© University of Pretoria

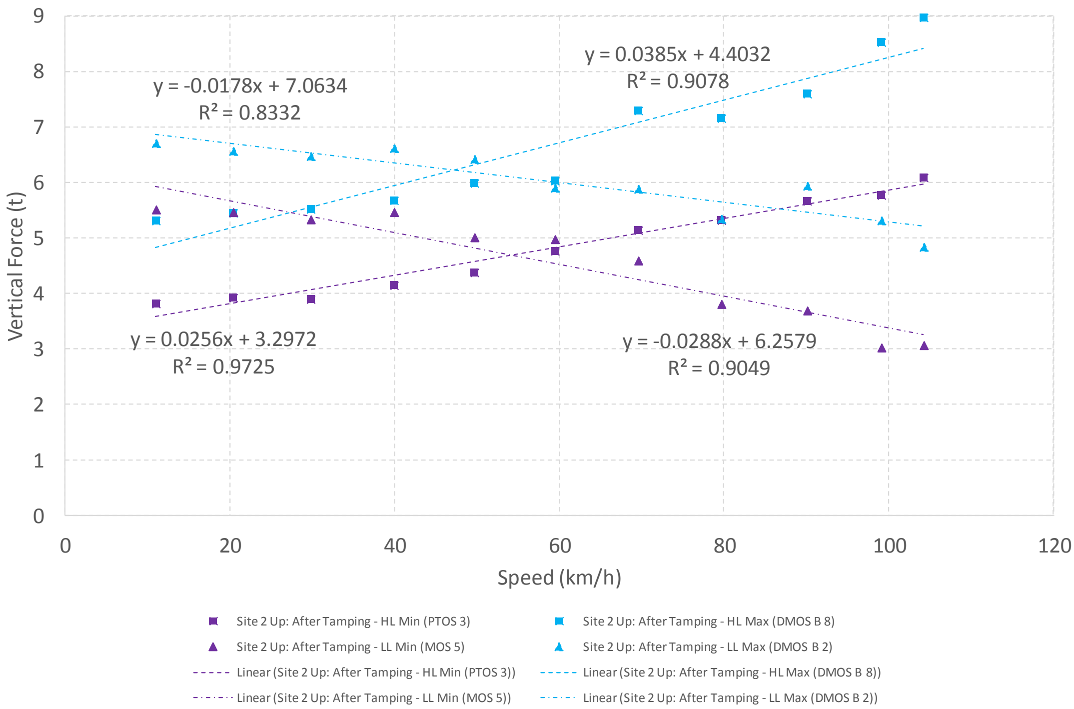

Figure C-15: Vertical Wheel Forces After Tamping – S2 Up

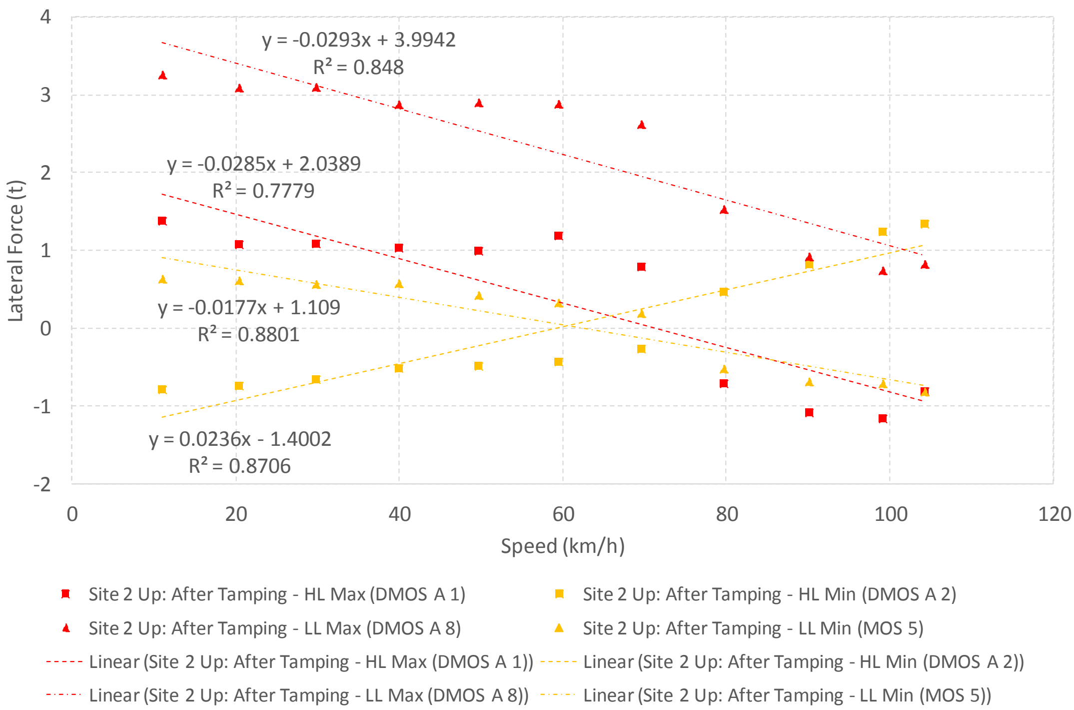

Figure C-16: Lateral Wheel Forces After Tamping – S2 Up

© University of Pretoria

APPENDIX D. TREND LINE INFROMATION FOR WHEELS

Figure D-1: Trend Line Information (Wheels) – S1 Down

	SITE 1: DOWN	Before Tamping		After Tamping	
		Trend Line Equation	R^2	Trend Line Equation	R^2
Verticals	High Leg Max (DMOS B 8)	y = 0.023x + 5.1255	0.8341	y = 0.0324x + 4.3270	0.8564
	Low Leg Max (DMOS B 1)	y = -0.022x + 7.0268	0.9744	y = -0.0198x + 8.3366	0.4381
	High Leg Min (PTOS 3)	y = 0.0331x + 2.8136	0.9605	y = 0.0296x + 2.7359	0.9443
	Low Leg Min (MOS 5)	y = -0.0239x + 6.1904	0.9705	y = -0.0172x + 6.6152	0.9611
Laterals	High Leg Max (DMOS A 4)	y = -0.0021x + 2.3044	0.1732	y = -0.0166x + 2.5225	0.6678
	Low Leg Max (DMOS A 7)	y = -0.0126x + 3.7673	0.8436	y = -0.0243x + 3.7809	0.8903
	High Leg Min (DMOS B 7)	y = 0.0149x - 1.0983	0.8925	y = 0.0233x - 1.5962	0.8374
	Low Leg Min (PTOS 8)	y = -0.0159x + 0.6583	0.9342	y = -0.0279x + 1.6617	0.8690

Figure D-2: Trend Line Information (Wheels) – S1 Up

	SITE 1: UP	Before Tamping		After Tamping	
		Trend Line Equation	R^2	Trend Line Equation	R^2
Verticals	High Leg Max (DMOS B 8)	y = 0.0388x + 4.2931	0.9565	y = 0.036x + 3.8543	0.8647
	Low Leg Max (DMOS B 2)	y = -0.0201x + 7.2519	0.9389	y = -0.0222x + 7.9388	0.8241
	High Leg Min (PTOS 3)	y = 0.0285x + 3.2574	0.9525	y = 0.0147x + 3.6318	0.8647
	Low Leg Min (MOS 5)	y = -0.0272x + 6.3639	0.9469	y = -0.0377x + 7.3663	0.9458
Laterals	High Leg Max (DMOS A 1)	y = 0.0036x + 1.7055	0.5940	y = 0.0007x + 2.4706	0.0045
	Low Leg Max (DMOS A 8)	y = -0.0092x + 3.6143	0.7649	y = -0.017x + 3.7406	0.8055
	High Leg Min (DMOS A 2)	y = 0.0139x - 1.2501	0.8786	y = 0.0238x - 1.6663	0.8050
	Low Leg Min (MOS 5)	y = -0.0168x + 0.6699	0.9494	y = -0.0269x + 1.5325	0.8915

© University of Pretoria

Figure D-3: Trend Line Information (Wheels) – S2 Down

	SITE 2: DOWN	Before Tamping		After Tamping	
		Trend Line Equation	R^2	Trend Line Equation	R^2
Verticals	High Leg Max (DMOS B 8)	y = 0.031x + 4.7466	0.7819	y = 0.0254x + 5.0515	0.8911
	Low Leg Max (DMOS B 1)	y = -0.0258x + 7.1756	0.9696	y = -0.0134x + 6.5988	0.5171
	High Leg Min (PTOS 3)	y = 0.0259x + 3.0312	0.9291	y = 0.0336x + 2.8637	0.9537
	Low Leg Min (MOS 5)	y = -0.0243x + 6.1996	0.9431	y = -0.0132x + 5.5153	0.9537
Laterals	High Leg Max (DMOS A 4)	y = 0.0044x + 2.307	0.7305	y = -0.0266x + 1.9164	0.7030
	Low Leg Max (DMOS A 7)	y = -0.0157x + 3.9543	0.8376	y = -0.0228x + 3.0394	0.9761
	High Leg Min (DMOS B 7)	y = 0.0196x - 1.2954	0.9134	y = 0.0249x - 1.556	0.8770
	Low Leg Min (PTOS 8)	y = -0.0159x + 0.5976	0.9818	y = -0.0172x + 1.1951	0.9194

Figure D-4: Trend Line Information (Wheels) – S2 Up

	SITE 2: UP	Before Tamping		After Tamping	
		Trend Line Equation	R^2	Trend Line Equation	R^2
Verticals	High Leg Max (DMOS B 8)	y = 0.0287x + 4.4493	0.9733	y = 0.0385x + 4.4032	0.9078
	Low Leg Max (DMOS B 2)	y = -0.0228x + 7.165	0.9706	y = -0.0178x + 7.0634	0.8332
	High Leg Min (PTOS 3)	y = 0.0141x + 3.9982	0.9539	y = 0.0256x + 3.2972	0.9725
	Low Leg Min (MOS 5)	y = -0.0299x + 6.377	0.9631	y = -0.0288x + 6.2579	0.9049
Laterals	High Leg Max (DMOS A 1)	y = 0.0096x + 2.1793	0.8954	y = -0.0285x + 2.0389	0.7779
	Low Leg Max (DMOS A 8)	y = -0.0107x + 3.7423	0.9357	y = -0.0293x + 3.9942	0.8480
	High Leg Min (DMOS A 2)	y = 0.0134x - 1.2629	0.8793	y = 0.0236x - 1.4002	0.8706
	Low Leg Min (MOS 5)	y = -0.0158x + 0.6578	0.9680	y = -0.0177x + 1.109	0.8801

© University of Pretoria

APPENDIX E. CURVE RAIL FORCES DATA FOR BOGIES, CARS AND 4-CAR TRAINS

In addition to the wheel force data summary tables presented in Appendix B, tables were also drawn up to show what the total vertical and lateral forces exerted on the track by the test trains were. This was done by assessing the total vertical and lateral forces exerted by the bogies of each car, the total vertical and lateral forces exerted by the cars themselves and finally the total vertical and lateral forces exerted by the full 4- car trains as described in Section 3.4.3. This assessment was done by summing the respective forces and calculating the net effect of the forces on the track, while paying special attention to the sign of the forces during this process.

The tables presented in Appendix E indicate the forces exerted by the bogies, the cars and the 4-car trains respectively.

The values shown in the “bogies” tables are arrived at by summing the relevant data as presented in Appendix B. The values shown in the “cars” tables are arrived at by summing the relevant data as presented in the “bogies” tables. The values shown in the “4-car train” tables are arrived at by summing the relevant data as presented in the “cars” tables. The relevant values were summed using Microsoft Excel and then rounded to 2 decimal places, which resulted in some apparent rounding errors when verifying the data presented in the tables, but which is in fact correct when referring to the raw data before rounding off the values at the various stages in the calculations process.

© University of Pretoria

Table E-1: Vertical Forces Before Tamping (Bogies) – S1 Down

12 Feb 2015: Hatfield to Pretoria (Down) km 3.215 (Site 1)				km/h										
				11.04	20.75	30.65	40.11	49.64	59.56	68.83	79.17	89.02	101.78	109.18
Car Type	Bogie	Axle	Wheel & Rail Leg	Vertical Force (t)										
DMOS B	Leading	Axle 1 & 2	W 8 & 7: HL	11.10	10.48	10.62	10.97	12.09	12.56	13.01	13.81	14.25	15.62	16.56
			W 1 & 2: LL	13.93	13.18	13.15	12.78	11.91	11.48	10.73	10.36	9.81	9.19	9.46
	Trailing	Axle 3 & 4	W 6 & 5: HL	9.93	9.36	9.64	9.68	10.28	10.66	11.29	12.07	13.09	14.58	15.47
			W 3 & 4: LL	12.28	11.78	11.65	11.44	10.59	10.59	9.89	9.47	8.85	7.75	7.03
PTOS	Leading	Axle 4 & 3	W 4 & 3: HL	8.94	7.93	8.16	8.28	9.41	9.72	10.37	10.95	11.53	12.59	13.25
			W 5 & 6: LL	12.06	11.52	11.37	11.19	10.48	10.16	9.39	8.44	8.09	7.76	7.06
	Trailing	Axle 2 & 1	W 2 & 1: HL	10.47	9.83	10.00	10.13	11.16	11.32	11.80	12.45	13.46	14.88	15.62
			W 7 & 8: LL	12.71	11.95	11.84	11.54	10.54	10.60	10.03	9.67	8.80	7.97	7.41
MOS	Leading	Axle 4 & 3	W 4 & 3: HL	9.68	9.14	9.23	9.41	10.32	10.92	11.46	12.18	13.09	14.30	14.77
			W 5 & 6: LL	12.20	11.63	11.53	11.45	10.30	10.03	9.79	8.89	8.39	7.12	6.94
	Trailing	Axle 2 & 1	W 2 & 1: HL	9.18	8.83	9.26	9.40	10.08	10.29	10.64	11.32	11.86	13.21	13.87
			W 7 & 8: LL	11.66	11.19	10.99	10.85	10.08	10.00	9.80	9.09	8.75	7.90	7.75
DMOS A	Leading	Axle 4 & 3	W 4 & 3: HL	9.43	8.99	9.13	9.35	10.32	10.84	11.43	12.20	13.26	14.15	15.13
			W 5 & 6: LL	12.42	12.06	11.89	11.89	10.99	10.29	9.88	9.47	8.79	7.74	7.34
	Trailing	Axle 2 & 1	W 2 & 1: HL	10.56	10.44	10.71	11.01	11.79	12.21	12.57	13.16	13.52	14.95	15.95
			W 7 & 8: LL	13.82	13.18	12.90	12.69	11.78	11.53	11.38	10.84	10.28	9.08	8.58

Table E-2: Vertical Forces Before Tamping (Cars) – S1 Down

12 Feb 2015: Hatfield to Pretoria (Down) km 3.215 (Site 1)			km/h										
			11.04	20.75	30.65	40.11	49.64	59.56	68.83	79.17	89.02	101.78	109.18
Car Type	Rail Leg	Wheel	Vertical Force (t)										
DMOS B	HL	W 8 & 7 & 6 & 5	21.02	19.84	20.26	20.65	22.37	23.22	24.30	25.89	27.34	30.20	32.03
	LL	W 1 & 2 & 3 & 4	26.20	24.95	24.79	24.22	22.51	22.07	20.61	19.83	18.66	16.94	16.49
PTOS	HL	W 4 & 3 & 2 & 1	19.41	17.77	18.16	18.41	20.57	21.04	22.17	23.40	24.99	27.47	28.87
	LL	W 5 & 6 & 7 & 8	24.76	23.47	23.21	22.73	21.02	20.76	19.42	18.10	16.89	15.73	14.47
MOS	HL	W 4 & 3 & 2 & 1	18.86	17.97	18.49	18.81	20.40	21.21	22.10	23.51	24.96	27.51	28.64
	LL	W 5 & 6 & 7 & 8	23.86	22.82	22.52	22.30	20.38	20.03	19.59	17.98	17.14	15.02	14.70
DMOS A	HL	W 4 & 3 & 2 & 1	19.99	19.42	19.83	20.36	22.11	23.05	24.00	25.36	26.78	29.09	31.08
	LL	W 5 & 6 & 7 & 8	26.24	25.25	24.79	24.57	22.77	21.82	21.27	20.31	19.07	16.81	15.91

Table E-3: Vertical Forces Before Tamping (4-Car Train) – S1 Down

12 Feb 2015: Hatfield to Pretoria (Down) km 3.215 (Site 1)		km/h										
		11.04	20.75	30.65	40.11	49.64	59.56	68.83	79.17	89.02	101.78	109.18
Car Type	Rail Leg	Vertical Force (t)										
4 Car Train	HL	79.29	75.00	76.74	78.23	85.44	88.53	92.58	98.16	104.07	114.27	120.62
	LL	101.07	96.49	95.31	93.83	86.68	84.68	80.89	76.23	71.76	64.51	61.57

© University of Pretoria

Table E-4: Lateral Forces Before Tamping (Bogies) – S1 Down

12 Feb 2015: Hatfield to Pretoria (Down) km 3.215 (Site 1)				km/h										
				11.04	20.75	30.65	40.11	49.64	59.56	68.83	79.17	89.02	101.78	109.18
Car Type	Bogie	Axle	Wheel & Rail Leg	Lateral Force (t)										
DMOS B	Leading	Axle 1 & 2	W 8 & 7: HL	0.65	0.83	0.99	0.86	1.18	1.28	1.34	1.55	2.16	2.64	2.97
			W 1 & 2: LL	3.97	3.89	3.95	3.57	3.34	3.19	2.64	2.28	1.90	1.33	1.16
	Trailing	Axle 3 & 4	W 6 & 5: HL	0.41	0.83	1.02	0.94	1.42	1.28	1.40	1.49	1.87	2.24	2.63
			W 3 & 4: LL	3.63	3.31	3.33	3.18	2.88	2.72	2.38	2.10	1.47	0.82	0.68
PTOS	Leading	Axle 4 & 3	W 4 & 3: HL	1.08	1.44	1.66	1.59	1.70	1.84	1.79	1.99	2.39	2.58	2.90
			W 5 & 6: LL	4.39	3.67	3.73	3.63	3.04	2.88	2.52	2.20	1.82	1.42	1.23
	Trailing	Axle 2 & 1	W 2 & 1: HL	0.48	0.85	0.97	0.95	1.15	1.24	1.62	2.01	2.13	2.26	2.68
			W 7 & 8: LL	3.98	3.43	3.51	3.26	2.78	2.71	2.46	2.05	1.79	1.28	0.93
MOS	Leading	Axle 4 & 3	W 4 & 3: HL	0.65	1.13	1.16	1.14	1.39	1.64	1.61	1.71	1.97	2.25	2.54
			W 5 & 6: LL	3.97	3.59	3.53	3.34	3.01	2.59	2.36	1.96	1.67	1.20	1.02
	Trailing	Axle 2 & 1	W 2 & 1: HL	1.02	1.27	1.46	1.43	1.63	1.77	1.97	1.91	2.42	2.41	2.48
			W 7 & 8: LL	4.09	3.88	3.88	3.75	3.46	3.49	3.28	3.14	2.61	1.89	1.55
DMOS A	Leading	Axle 4 & 3	W 4 & 3: HL	1.13	1.58	1.57	1.66	1.99	2.01	1.99	2.01	2.34	2.43	2.71
			W 5 & 6: LL	4.44	4.02	3.98	3.81	3.34	3.20	2.89	2.55	1.96	1.64	1.34
	Trailing	Axle 2 & 1	W 2 & 1: HL	0.70	1.09	1.10	1.17	1.48	1.63	1.73	1.75	2.06	2.50	3.10
			W 7 & 8: LL	4.66	4.34	4.30	4.16	3.82	3.69	3.51	3.15	2.48	1.92	1.28

Table E-5: Lateral Forces Before Tamping (Cars) – S1 Down

12 Feb 2015: Hatfield to Pretoria (Down) km 3.215 (Site 1)			km/h										
			11.04	20.75	30.65	40.11	49.64	59.56	68.83	79.17	89.02	101.78	109.18
Car Type	Rail Leg	Wheel	Lateral Force (t)										
DMOS B	HL	W 8 & 7 & 6 & 5	1.06	1.66	2.01	1.79	2.60	2.56	2.74	3.04	4.03	4.88	5.60
	LL	W 1 & 2 & 3 & 4	7.60	7.20	7.28	6.75	6.22	5.91	5.02	4.39	3.37	2.15	1.83
PTOS	HL	W 4 & 3 & 2 & 1	1.56	2.29	2.63	2.54	2.85	3.08	3.41	4.00	4.52	4.85	5.58
	LL	W 5 & 6 & 7 & 8	8.37	7.10	7.24	6.89	5.82	5.59	4.98	4.24	3.61	2.70	2.16
MOS	HL	W 4 & 3 & 2 & 1	1.67	2.40	2.62	2.57	3.02	3.42	3.58	3.62	4.40	4.66	5.02
	LL	W 5 & 6 & 7 & 8	8.06	7.47	7.40	7.10	6.48	6.08	5.64	5.10	4.28	3.09	2.57
DMOS A	HL	W 4 & 3 & 2 & 1	1.84	2.67	2.68	2.83	3.47	3.63	3.73	3.77	4.40	4.92	5.81
	LL	W 5 & 6 & 7 & 8	9.10	8.36	8.27	7.97	7.16	6.89	6.39	5.70	4.45	3.56	2.63

Table E-6: Lateral Forces Before Tamping (4-Car Train) – S1 Down

12 Feb 2015: Hatfield to Pretoria (Down) km 3.215 (Site 1)		km/h										
		11.04	20.75	30.65	40.11	49.64	59.56	68.83	79.17	89.02	101.78	109.18
Car Type	Rail Leg	Lateral Force (t)										
4 Car Train	HL	6.12	9.02	9.94	9.74	11.93	12.69	13.46	14.44	17.35	19.30	22.01
	LL	33.13	30.12	30.20	28.71	25.67	24.46	22.03	19.43	15.71	11.50	9.19

© University of Pretoria

Table E-7: Vertical Forces Before Tamping (Bogies) – S2 Down

12 Feb 2015: Hatfield to Pretoria (Down) km 3.175 (Site 2)				km/h										
				11.13	21.60	30.12	39.90	49.26	59.48	68.74	79.08	88.32	102.21	108.75
Car Type	Bogie	Axle	Wheel & Rail Leg	Vertical Force (t)										
DMOS B	Leading	Axle 1 & 2	W 8 & 7: HL	10.76	10.51	10.86	10.84	11.54	12.07	12.52	12.95	13.93	15.97	16.86
			W 1 & 2: LL	13.80	13.15	12.96	12.92	12.08	11.36	10.60	10.50	9.66	8.86	8.02
	Trailing	Axle 3 & 4	W 6 & 5: HL	9.08	8.99	9.25	9.44	9.91	10.30	10.95	12.09	12.49	13.40	15.14
			W 3 & 4: LL	12.34	12.26	12.04	12.02	11.00	10.74	10.05	9.31	8.46	7.93	6.96
PTOS	Leading	Axle 4 & 3	W 4 & 3: HL	8.12	8.16	8.36	8.66	8.52	9.54	9.85	10.37	10.67	12.21	13.06
			W 5 & 6: LL	11.99	11.52	11.32	11.30	10.89	9.73	9.42	8.54	8.04	6.98	6.65
	Trailing	Axle 2 & 1	W 2 & 1: HL	9.30	9.46	9.70	10.14	10.43	10.50	11.13	11.60	12.43	14.36	15.19
			W 7 & 8: LL	12.84	12.47	12.40	12.22	11.40	10.94	10.29	9.80	8.86	7.69	7.15
MOS	Leading	Axle 4 & 3	W 4 & 3: HL	9.14	9.25	9.43	9.46	9.89	10.47	10.43	11.56	12.54	14.17	14.44
			W 5 & 6: LL	11.84	11.59	11.51	11.57	10.90	9.97	9.58	8.67	8.31	7.18	6.53
	Trailing	Axle 2 & 1	W 2 & 1: HL	8.61	8.71	8.95	9.19	9.68	9.90	10.48	10.98	12.02	12.95	13.52
			W 7 & 8: LL	11.95	11.74	11.52	11.51	10.63	10.31	9.84	9.20	8.33	8.06	7.31
DMOS A	Leading	Axle 4 & 3	W 4 & 3: HL	9.21	9.34	9.35	9.42	9.54	10.64	10.73	12.10	13.15	14.64	15.64
			W 5 & 6: LL	12.33	12.22	11.90	11.82	11.61	10.40	9.79	9.02	8.36	7.26	7.26
	Trailing	Axle 2 & 1	W 2 & 1: HL	9.89	10.25	10.29	10.73	11.30	11.43	12.52	12.61	13.60	15.32	15.85
			W 7 & 8: LL	13.77	13.72	13.56	13.25	12.16	12.01	11.24	10.76	10.21	9.21	8.78

Table E-8: Vertical Forces Before Tamping (Cars) – S2 Down

12 Feb 2015: Hatfield to Pretoria (Down) km 3.175 (Site 2)			km/h										
			11.13	21.60	30.12	39.90	49.26	59.48	68.74	79.08	88.32	102.21	108.75
Car Type	Rail Leg	Wheel	Vertical Force (t)										
DMOS B	HL	W 8 & 7 & 6 & 5	19.84	19.50	20.11	20.28	21.45	22.37	23.47	25.04	26.42	29.36	32.00
	LL	W 1 & 2 & 3 & 4	26.14	25.41	25.00	24.94	23.07	22.09	20.65	19.82	18.13	16.79	14.98
PTOS	HL	W 4 & 3 & 2 & 1	17.42	17.63	18.06	18.79	18.95	20.05	20.98	21.98	23.10	26.56	28.25
	LL	W 5 & 6 & 7 & 8	24.83	23.99	23.72	23.52	22.29	20.66	19.71	18.33	16.89	14.67	13.81
MOS	HL	W 4 & 3 & 2 & 1	17.75	17.96	18.38	18.65	19.57	20.37	20.91	22.54	24.56	27.12	27.96
	LL	W 5 & 6 & 7 & 8	23.79	23.33	23.03	23.09	21.54	20.28	19.42	17.87	16.65	15.25	13.85
DMOS A	HL	W 4 & 3 & 2 & 1	19.11	19.58	19.64	20.15	20.84	22.07	23.25	24.71	26.75	29.96	31.49
	LL	W 5 & 6 & 7 & 8	26.10	25.94	25.46	25.07	23.77	22.41	21.03	19.78	18.56	16.47	16.04

Table E-9: Vertical Forces Before Tamping (4-Car Train) – S2 Down

12 Feb 2015: Hatfield to Pretoria (Down) km 3.175 (Site 2)		km/h										
		11.13	21.60	30.12	39.90	49.26	59.48	68.74	79.08	88.32	102.21	108.75
Car Type	Rail Leg	Vertical Force (t)										
4 Car Train	HL	74.12	74.67	76.19	77.87	80.80	84.85	88.61	94.26	100.83	113.01	119.70
	LL	100.86	98.68	97.21	96.63	90.67	85.45	80.81	75.80	70.23	63.17	58.68

© University of Pretoria

Table E-10: Lateral Forces Before Tamping (Bogies) – S2 Down

12 Feb 2015: Hatfield to Pretoria (Down) km 3.175 (Site 2)				km/h										
				11.13	21.60	30.12	39.90	49.26	59.48	68.74	79.08	88.32	102.21	108.75
Car Type	Bogie	Axle	Wheel & Rail Leg	Lateral Force (t)										
DMOS B	Leading	Axle 1 & 2	W 8 & 7: HL	0.89	1.31	1.48	1.48	1.71	1.95	2.09	2.76	2.98	3.35	4.04
			W 1 & 2: LL	3.78	3.97	4.08	3.84	3.38	3.23	2.59	2.21	1.48	1.08	0.99
	Trailing	Axle 3 & 4	W 6 & 5: HL	0.89	1.24	1.47	1.61	1.64	1.61	1.75	2.21	2.46	2.40	2.83
			W 3 & 4: LL	3.25	3.48	3.55	3.52	3.13	2.76	2.34	1.94	1.15	0.70	0.66
PTOS	Leading	Axle 4 & 3	W 4 & 3: HL	1.30	1.62	1.85	1.90	1.96	2.13	2.15	2.68	2.85	3.30	3.54
			W 5 & 6: LL	3.58	3.53	3.66	3.55	3.37	2.61	2.30	2.01	1.45	0.86	0.88
	Trailing	Axle 2 & 1	W 2 & 1: HL	1.06	1.23	1.44	1.53	1.50	1.55	1.66	2.18	2.33	2.55	2.96
			W 7 & 8: LL	3.57	3.59	3.67	3.50	2.96	2.69	2.41	1.94	1.45	0.69	0.72
MOS	Leading	Axle 4 & 3	W 4 & 3: HL	1.18	1.32	1.45	1.50	1.53	1.72	1.99	2.47	2.46	3.01	3.45
			W 5 & 6: LL	3.63	3.53	3.52	3.49	3.04	2.47	2.43	1.93	1.36	0.73	0.65
	Trailing	Axle 2 & 1	W 2 & 1: HL	1.33	1.47	1.68	1.85	1.88	1.91	2.17	2.31	2.35	3.15	3.24
			W 7 & 8: LL	3.75	3.90	3.88	3.81	3.38	3.38	2.99	2.87	1.93	1.28	1.23
DMOS A	Leading	Axle 4 & 3	W 4 & 3: HL	1.49	1.76	1.77	1.98	1.91	2.16	2.37	2.90	3.12	3.60	3.76
			W 5 & 6: LL	3.87	3.91	3.87	3.77	3.48	2.82	2.65	2.19	1.67	1.01	0.80
	Trailing	Axle 2 & 1	W 2 & 1: HL	1.37	1.41	1.64	1.72	1.92	2.01	2.27	2.33	3.04	3.30	3.46
			W 7 & 8: LL	4.37	4.32	4.35	4.23	3.69	3.67	3.41	2.63	2.12	1.12	1.03

Table E-11: Lateral Forces Before Tamping (Cars) – S2 Down

12 Feb 2015: Hatfield to Pretoria (Down) km 3.175 (Site 2)			km/h										
			11.13	21.60	30.12	39.90	49.26	59.48	68.74	79.08	88.32	102.21	108.75
Car Type	Rail Leg	Wheel	Lateral Force (t)										
DMOS B	HL	W 8 & 7 & 6 & 5	1.78	2.55	2.95	3.10	3.35	3.56	3.85	4.97	5.44	5.75	6.87
	LL	W 1 & 2 & 3 & 4	7.03	7.44	7.63	7.36	6.50	5.99	4.94	4.14	2.64	1.77	1.65
PTOS	HL	W 4 & 3 & 2 & 1	2.36	2.85	3.29	3.43	3.46	3.67	3.81	4.87	5.18	5.85	6.51
	LL	W 5 & 6 & 7 & 8	7.15	7.12	7.34	7.05	6.34	5.31	4.71	3.95	2.90	1.55	1.61
MOS	HL	W 4 & 3 & 2 & 1	2.51	2.79	3.13	3.35	3.41	3.63	4.16	4.78	4.81	6.16	6.68
	LL	W 5 & 6 & 7 & 8	7.38	7.43	7.40	7.30	6.42	5.85	5.42	4.80	3.29	2.01	1.88
DMOS A	HL	W 4 & 3 & 2 & 1	2.86	3.17	3.42	3.70	3.83	4.18	4.64	5.23	6.16	6.91	7.22
	LL	W 5 & 6 & 7 & 8	8.23	8.23	8.22	8.01	7.17	6.49	6.06	4.82	3.79	2.12	1.82

Table E-12: Lateral Forces Before Tamping (4-Car Train) – S2 Down

12 Feb 2015: Hatfield to Pretoria (Down) km 3.175 (Site 2)		km/h										
		11.13	21.60	30.12	39.90	49.26	59.48	68.74	79.08	88.32	102.21	108.75
Car Type	Rail Leg	Lateral Force (t)										
4 Car Train	HL	9.51	11.36	12.78	13.57	14.05	15.04	16.46	19.85	21.59	24.68	27.28
	LL	29.79	30.22	30.59	29.72	26.43	23.63	21.13	17.72	12.62	7.45	6.96

© University of Pretoria

Table E-13: Vertical Forces Before Tamping (Bogies) – S1 Up

12 Feb 2015: Pretoria to Hatfield (Up) km 3.215 (Site 1)				km/h										
				11.30	20.79	30.28	39.49	49.84	59.20	69.59	79.30	90.32	97.59	106.32
Car Type	Bogie	Axle	Wheel & Rail Leg	Vertical Force (t)										
DMOS A	Leading	Axle 1 & 2	W 1 & 2: HL	10.42	10.33	10.43	10.94	11.20	12.02	12.85	13.41	14.05	14.53	15.72
			W 8 & 7: LL	13.81	13.44	13.24	12.81	12.91	12.57	11.70	11.21	10.67	10.10	9.62
	Trailing	Axle 3 & 4	W 3 & 4: HL	8.92	9.01	9.07	9.32	9.95	10.83	11.75	12.70	13.35	14.19	15.28
			W 6 & 5: LL	12.27	12.29	12.14	11.80	11.66	10.83	10.20	9.49	8.91	8.50	7.67
MOS	Leading	Axle 1 & 2	W 1 & 2: HL	8.91	8.82	8.92	9.35	9.55	10.19	11.00	11.69	12.39	12.81	13.33
			W 8 & 7: LL	11.48	11.34	11.13	10.90	10.84	10.57	9.96	9.35	8.99	8.84	7.91
	Trailing	Axle 3 & 4	W 3 & 4: HL	8.93	9.17	9.15	9.46	9.53	10.73	11.64	12.62	13.53	14.26	15.27
			W 6 & 5: LL	11.90	11.64	11.75	11.38	11.21	10.55	9.65	9.14	8.78	8.17	7.45
PTOS	Leading	Axle 1 & 2	W 1 & 2: HL	9.52	9.77	9.81	10.34	10.24	11.11	12.11	12.81	14.04	14.58	15.22
			W 8 & 7: LL	12.31	12.23	12.13	11.51	11.70	11.31	10.46	9.88	8.81	8.93	7.85
	Trailing	Axle 3 & 4	W 3 & 4: HL	7.85	8.09	8.05	8.29	8.61	9.68	10.57	11.47	12.24	12.79	13.63
			W 6 & 5: LL	11.76	11.57	11.55	11.25	11.02	10.54	9.75	9.42	8.45	8.00	7.46
DMOS B	Leading	Axle 4 & 3	W 5 & 6: HL	9.17	9.32	9.48	9.79	10.19	10.87	11.90	12.73	13.43	14.11	15.20
			W 4 & 3: LL	12.07	11.77	11.67	11.38	11.46	10.90	10.11	9.21	9.07	8.62	7.65
	Trailing	Axle 2 & 1	W 7 & 8: HL	10.23	10.45	10.58	11.01	11.46	12.32	13.09	14.31	15.30	15.87	16.60
			W 2 & 1: LL	13.48	13.31	13.36	12.85	12.78	12.10	11.43	10.66	10.25	9.76	9.18

Table E-14: Vertical Forces Before Tamping (Cars) – S1 Up

12 Feb 2015: Pretoria to Hatfield (Up) km 3.215 (Site 1)			km/h										
			11.30	20.79	30.28	39.49	49.84	59.20	69.59	79.30	90.32	97.59	106.32
Car Type	Rail Leg	Wheel	Vertical Force (t)										
DMOS A	HL	W 1 & 2 & 3 & 4	19.35	19.34	19.50	20.26	21.15	22.85	24.60	26.11	27.41	28.72	30.99
	LL	W 8 & 7 & 6 & 5	26.08	25.73	25.38	24.62	24.56	23.40	21.91	20.70	19.57	18.60	17.29
MOS	HL	W 1 & 2 & 3 & 4	17.84	17.99	18.07	18.81	19.08	20.92	22.64	24.32	25.92	27.06	28.60
	LL	W 8 & 7 & 6 & 5	23.37	22.99	22.88	22.27	22.05	21.12	19.61	18.49	17.77	17.01	15.36
PTOS	HL	W 1 & 2 & 3 & 4	17.37	17.86	17.86	18.62	18.85	20.79	22.68	24.27	26.29	27.36	28.85
	LL	W 8 & 7 & 6 & 5	24.07	23.80	23.68	22.76	22.72	21.84	20.21	19.30	17.27	16.93	15.32
DMOS B	HL	W 5 & 6 & 7 & 8	19.41	19.77	20.06	20.81	21.66	23.19	24.99	27.04	28.73	29.98	31.80
	LL	W 4 & 3 & 2 & 1	25.55	25.07	25.03	24.22	24.24	23.00	21.54	19.87	19.31	18.38	16.83

Table E-15: Vertical Forces Before Tamping (4-Car Train) – S1 Up

12 Feb 2015: Pretoria to Hatfield (Up) km 3.215 (Site 1)		km/h										
		11.30	20.79	30.28	39.49	49.84	59.20	69.59	79.30	90.32	97.59	106.32
Car Type	Rail Leg	Vertical Force (t)										
4 Car Train	HL	73.96	74.96	75.49	78.50	80.75	87.75	94.92	101.74	108.33	113.12	120.24
	LL	99.08	97.59	96.97	93.87	93.58	89.36	83.26	78.37	73.92	70.91	64.80

Table E-16: Lateral Forces Before Tamping (Bogies) – S1 Up

12 Feb 2015: Pretoria to Hatfield (Up) km 3.215 (Site 1)				km/h										
				11.30	20.79	30.28	39.49	49.84	59.20	69.59	79.30	90.32	97.59	106.32
Car Type	Bogie	Axle	Wheel & Rail Leg	Lateral Force (t)										
DMOS A	Leading	Axle 1 & 2	W 1 & 2: HL	0.91	0.85	0.95	1.12	1.25	1.33	1.54	1.63	1.99	2.33	2.56
			W 8 & 7: LL	4.56	4.18	4.30	4.10	4.07	3.68	3.37	3.17	2.56	2.00	1.79
	Trailing	Axle 3 & 4	W 3 & 4: HL	0.74	0.84	0.88	1.00	0.96	1.22	1.05	1.37	1.59	1.59	2.16
			W 6 & 5: LL	3.58	3.59	3.60	3.41	3.16	2.72	2.27	1.95	1.56	1.01	1.08
MOS	Leading	Axle 1 & 2	W 1 & 2: HL	0.72	0.81	0.97	1.05	1.24	1.33	1.36	1.50	1.84	1.90	2.28
			W 8 & 7: LL	3.94	3.82	3.84	3.68	3.63	3.50	3.04	2.93	2.22	1.89	1.74
	Trailing	Axle 3 & 4	W 3 & 4: HL	0.50	0.59	0.59	0.66	0.58	0.66	0.94	1.08	1.50	1.52	2.14
			W 6 & 5: LL	3.30	3.25	3.29	3.24	2.93	2.36	1.84	1.49	0.92	0.72	0.72
PTOS	Leading	Axle 1 & 2	W 1 & 2: HL	0.82	0.88	0.91	0.94	0.98	1.05	1.05	1.22	1.32	1.59	2.13
			W 8 & 7: LL	3.55	3.50	3.45	3.13	3.24	2.74	2.18	1.75	1.23	0.79	0.67
	Trailing	Axle 3 & 4	W 3 & 4: HL	0.89	0.86	0.92	0.91	0.97	0.92	1.18	1.28	1.59	1.73	2.15
			W 6 & 5: LL	3.38	3.33	3.37	3.16	2.84	2.39	2.01	1.51	1.06	0.75	0.56
DMOS B	Leading	Axle 4 & 3	W 5 & 6: HL	0.81	0.97	0.87	1.00	1.21	1.04	0.94	1.20	1.31	1.52	2.37
			W 4 & 3: LL	3.64	3.61	3.44	3.29	3.28	2.67	2.19	1.77	1.32	0.84	0.89
	Trailing	Axle 2 & 1	W 7 & 8: HL	0.34	0.43	0.44	0.41	0.36	0.48	0.84	0.96	1.27	1.35	2.40
			W 2 & 1: LL	3.44	3.44	3.52	3.12	2.82	2.27	1.85	1.50	1.07	0.73	0.85

Table E-17: Lateral Forces Before Tamping (Cars) – S1 Up

12 Feb 2015: Pretoria to Hatfield (Up) km 3.215 (Site 1)			km/h										
			11.30	20.79	30.28	39.49	49.84	59.20	69.59	79.30	90.32	97.59	106.32
Car Type	Rail Leg	Wheel	Lateral Force (t)										
DMOS A	HL	W 1 & 2 & 3 & 4	1.65	1.69	1.83	2.11	2.21	2.55	2.58	3.00	3.58	3.92	4.72
	LL	W 8 & 7 & 6 & 5	8.14	7.76	7.90	7.51	7.23	6.40	5.65	5.12	4.12	3.01	2.87
MOS	HL	W 1 & 2 & 3 & 4	1.22	1.40	1.56	1.71	1.82	2.00	2.29	2.58	3.33	3.42	4.42
	LL	W 8 & 7 & 6 & 5	7.24	7.07	7.14	6.92	6.56	5.86	4.89	4.42	3.14	2.61	2.46
PTOS	HL	W 1 & 2 & 3 & 4	1.72	1.74	1.83	1.85	1.95	1.97	2.23	2.50	2.92	3.32	4.28
	LL	W 8 & 7 & 6 & 5	6.92	6.83	6.82	6.29	6.07	5.13	4.18	3.26	2.29	1.53	1.23
DMOS B	HL	W 5 & 6 & 7 & 8	1.16	1.40	1.31	1.41	1.57	1.52	1.78	2.16	2.57	2.87	4.77
	LL	W 4 & 3 & 2 & 1	7.07	7.05	6.95	6.40	6.10	4.94	4.04	3.28	2.40	1.57	1.75

Table E-18: Lateral Forces Before Tamping (4-Car Train) – S1 Up

12 Feb 2015: Pretoria to Hatfield (Up) km 3.215 (Site 1)		km/h										
		11.30	20.79	30.28	39.49	49.84	59.20	69.59	79.30	90.32	97.59	106.32
Car Type	Rail Leg	Lateral Force (t)										
4 Car Train	HL	5.75	6.22	6.53	7.08	7.55	8.03	8.88	10.24	12.41	13.54	18.19
	LL	29.38	28.70	28.81	27.12	25.96	22.33	18.75	16.07	11.94	8.73	8.31

© University of Pretoria

Table E-19: Vertical Forces Before Tamping (Bogies) – S2 Up

12 Feb 2015: Pretoria to Hatfield (Up) km 3.175 (Site 2)				km/h										
				11.31	20.79	30.50	39.82	49.92	59.11	68.98	78.94	89.23	97.48	104.81
Car Type	Bogie	Axle	Wheel & Rail Leg	Vertical Force (t)										
DMOS A	Leading	Axle 1 & 2	W 1 & 2: HL	9.89	10.04	10.16	10.86	11.08	11.08	11.97	12.28	12.83	13.28	13.58
			W 8 & 7: LL	14.18	14.01	13.64	13.21	12.99	12.35	11.67	11.10	10.49	10.02	9.11
	Trailing	Axle 3 & 4	W 3 & 4: HL	9.05	9.11	9.21	9.85	10.07	10.30	10.94	11.41	12.53	13.03	13.09
			W 6 & 5: LL	12.19	12.24	12.02	11.52	11.04	10.60	10.09	9.25	8.39	7.65	7.53
MOS	Leading	Axle 1 & 2	W 1 & 2: HL	8.53	8.61	8.99	9.12	9.49	9.65	10.30	10.99	10.98	11.96	11.62
			W 8 & 7: LL	11.91	11.88	11.49	11.30	10.77	10.48	9.93	9.22	8.81	7.98	7.66
	Trailing	Axle 3 & 4	W 3 & 4: HL	9.07	9.01	9.42	9.57	10.26	10.56	11.05	11.86	12.42	12.78	12.98
			W 6 & 5: LL	11.81	11.62	11.58	11.21	10.69	10.36	9.70	8.89	8.28	7.33	7.16
PTOS	Leading	Axle 1 & 2	W 1 & 2: HL	9.24	9.30	9.80	9.80	10.40	10.66	11.11	11.79	12.37	13.21	13.62
			W 8 & 7: LL	12.74	12.69	12.46	12.21	11.56	11.06	10.54	9.59	8.90	8.22	7.69
	Trailing	Axle 3 & 4	W 3 & 4: HL	8.07	8.17	8.43	8.63	9.43	9.79	9.77	10.42	11.36	11.75	11.87
			W 6 & 5: LL	11.57	11.49	11.38	10.98	10.45	10.06	9.38	8.96	8.10	7.52	7.11
DMOS B	Leading	Axle 4 & 3	W 5 & 6: HL	9.08	8.99	9.36	9.50	10.08	10.34	10.71	11.40	12.68	12.95	13.39
			W 4 & 3: LL	12.41	12.43	12.07	11.81	11.41	11.10	10.17	9.38	8.31	8.03	7.11
	Trailing	Axle 2 & 1	W 7 & 8: HL	10.26	10.29	10.79	11.27	11.95	11.88	12.21	12.77	13.57	14.06	14.50
			W 2 & 1: LL	13.31	13.30	13.08	12.54	11.88	11.57	11.29	10.47	9.64	9.22	8.73

Table E-20: Vertical Forces Before Tamping (Cars) – S2 Up

12 Feb 2015: Pretoria to Hatfield (Up) km 3.175 (Site 2)			km/h										
			11.31	20.79	30.50	39.82	49.92	59.11	68.98	78.94	89.23	97.48	104.81
Car Type	Rail Leg	Wheel	Vertical Force (t)										
DMOS A	HL	W 1 & 2 & 3 & 4	18.94	19.15	19.37	20.72	21.15	21.38	22.91	23.69	25.35	26.31	26.67
	LL	W 8 & 7 & 6 & 5	26.37	26.24	25.65	24.73	24.02	22.96	21.76	20.35	18.89	17.68	16.64
MOS	HL	W 1 & 2 & 3 & 4	17.60	17.62	18.41	18.69	19.75	20.21	21.35	22.85	23.39	24.74	24.61
	LL	W 8 & 7 & 6 & 5	23.72	23.50	23.07	22.51	21.46	20.84	19.64	18.11	17.09	15.31	14.82
PTOS	HL	W 1 & 2 & 3 & 4	17.31	17.47	18.22	18.43	19.82	20.45	20.88	22.22	23.73	24.96	25.49
	LL	W 8 & 7 & 6 & 5	24.31	24.18	23.84	23.19	22.00	21.12	19.92	18.56	17.01	15.73	14.80
DMOS B	HL	W 5 & 6 & 7 & 8	19.35	19.28	20.15	20.77	22.03	22.22	22.93	24.16	26.25	27.01	27.89
	LL	W 4 & 3 & 2 & 1	25.73	25.74	25.15	24.34	23.29	22.68	21.46	19.85	17.94	17.25	15.84

Table E-21: Vertical Forces Before Tamping (4-Car Train) – S2 Up

12 Feb 2015: Pretoria to Hatfield (Up) km 3.175 (Site 2)		km/h										
		11.31	20.79	30.50	39.82	49.92	59.11	68.98	78.94	89.23	97.48	104.81
Car Type	Rail Leg	Vertical Force (t)										
4 Car Train	HL	73.19	73.52	76.16	78.61	82.76	84.26	88.07	92.92	98.73	103.03	104.66
	LL	100.12	99.66	97.71	94.77	90.78	87.59	82.78	76.87	70.93	65.98	62.11

© University of Pretoria

Table E-22: Lateral Forces Before Tamping (Bogies) – S2 Up

12 Feb 2015: Pretoria to Hatfield (Up) km 3.175 (Site 2)				km/h										
				11.31	20.79	30.50	39.82	49.92	59.11	68.98	78.94	89.23	97.48	104.81
Car Type	Bogie	Axle	Wheel & Rail Leg	Lateral Force (t)										
DMOS A	Leading	Axle 1 & 2	W 1 & 2: HL	1.50	1.35	1.66	1.84	1.85	2.11	2.32	2.58	2.89	3.24	3.69
			W 8 & 7: LL	4.58	4.45	4.53	4.10	4.03	3.76	3.40	3.23	3.04	2.14	1.91
	Trailing	Axle 3 & 4	W 3 & 4: HL	1.08	1.08	1.26	1.38	1.54	1.71	1.87	2.13	2.36	2.65	2.97
			W 6 & 5: LL	3.60	3.65	3.58	3.20	3.06	2.64	2.39	2.08	1.64	1.23	1.12
MOS	Leading	Axle 1 & 2	W 1 & 2: HL	1.34	1.27	1.68	1.63	1.74	1.98	2.05	2.24	2.46	2.96	3.36
			W 8 & 7: LL	4.04	3.93	3.89	3.78	3.52	3.36	3.09	2.72	2.66	1.77	1.73
	Trailing	Axle 3 & 4	W 3 & 4: HL	0.86	0.88	1.00	1.24	1.27	1.42	1.73	1.93	2.35	2.52	2.74
			W 6 & 5: LL	3.50	3.42	3.41	3.18	2.73	2.50	2.18	1.73	1.50	1.09	1.09
PTOS	Leading	Axle 1 & 2	W 1 & 2: HL	1.51	1.39	1.55	1.72	1.93	2.20	2.30	2.31	2.84	3.16	3.46
			W 8 & 7: LL	4.02	3.82	3.83	3.62	3.25	2.94	2.60	2.00	1.74	1.36	1.11
	Trailing	Axle 3 & 4	W 3 & 4: HL	1.27	1.13	1.22	1.43	1.55	1.80	1.97	2.24	2.49	2.44	3.08
			W 6 & 5: LL	3.54	3.30	3.34	3.12	2.66	2.53	2.21	1.85	1.30	0.94	0.98
DMOS B	Leading	Axle 4 & 3	W 5 & 6: HL	1.41	1.30	1.61	1.82	1.65	1.98	2.10	2.11	2.59	2.90	3.25
			W 4 & 3: LL	4.00	3.87	3.84	3.57	3.31	3.01	2.67	2.19	1.55	1.35	1.13
	Trailing	Axle 2 & 1	W 7 & 8: HL	1.01	0.93	1.07	1.29	1.41	1.86	1.92	2.31	2.38	2.97	3.35
			W 2 & 1: LL	3.84	3.69	3.70	3.29	3.09	2.76	2.55	1.99	1.33	1.31	1.24

Table E-23: Lateral Forces Before Tamping (Cars) – S2 Up

12 Feb 2015: Pretoria to Hatfield (Up) km 3.175 (Site 2)			km/h										
			11.31	20.79	30.50	39.82	49.92	59.11	68.98	78.94	89.23	97.48	104.81
Car Type	Rail Leg	Wheel	Lateral Force (t)										
DMOS A	HL	W 1 & 2 & 3 & 4	2.58	2.43	2.92	3.22	3.38	3.81	4.20	4.71	5.25	5.90	6.66
	LL	W 8 & 7 & 6 & 5	8.18	8.11	8.11	7.31	7.09	6.39	5.79	5.31	4.68	3.36	3.02
MOS	HL	W 1 & 2 & 3 & 4	2.20	2.15	2.68	2.87	3.01	3.40	3.78	4.17	4.81	5.48	6.10
	LL	W 8 & 7 & 6 & 5	7.54	7.35	7.30	6.96	6.25	5.86	5.27	4.45	4.16	2.87	2.82
PTOS	HL	W 1 & 2 & 3 & 4	2.78	2.53	2.77	3.15	3.48	4.00	4.28	4.55	5.33	5.60	6.54
	LL	W 8 & 7 & 6 & 5	7.56	7.12	7.17	6.75	5.91	5.47	4.80	3.86	3.03	2.31	2.08
DMOS B	HL	W 5 & 6 & 7 & 8	2.42	2.23	2.68	3.10	3.05	3.84	4.02	4.42	4.98	5.87	6.61
	LL	W 4 & 3 & 2 & 1	7.83	7.56	7.54	6.86	6.41	5.77	5.22	4.17	2.88	2.66	2.36

Table E-24: Lateral Forces Before Tamping (4-Car Train) – S1 Up

12 Feb 2015: Pretoria to Hatfield (Up) km 3.175 (Site 2)		km/h										
		11.31	20.79	30.50	39.82	49.92	59.11	68.98	78.94	89.23	97.48	104.81
Car Type	Rail Leg	Lateral Force (t)										
4 Car Train	HL	9.98	9.33	11.04	12.34	12.92	15.05	16.28	17.85	20.37	22.85	25.91
	LL	31.11	30.13	30.12	27.87	25.65	23.50	21.09	17.80	14.76	11.20	10.29

© University of Pretoria

Table E-25: Vertical Forces After Tamping (Bogies) – S1 Down

21 Jul 2015: Hatfield to Pretoria (Down) km 3.215 (Site 1)				km/h										
				11.10	21.02	30.50	40.07	50.15	60.01	69.38	79.42	89.55	98.74	104.02
Car Type	Bogie	Axle	Wheel & Rail Leg	Vertical Force (t)										
DMOS B	Leading	Axle 1 & 2	W 8 & 7: HL	9.50	9.60	9.81	10.37	10.83	11.34	12.15	12.37	13.88	15.85	15.26
			W 1 & 2: LL	15.27	15.29	15.51	16.59	15.48	13.33	13.54	11.95	10.76	11.97	11.30
	Trailing	Axle 3 & 4	W 6 & 5: HL	8.34	8.47	8.82	8.76	9.40	9.67	10.39	11.28	12.58	13.55	13.89
			W 3 & 4: LL	13.35	13.46	13.23	13.33	12.66	12.19	11.17	10.40	9.40	8.64	7.95
PTOS	Leading	Axle 4 & 3	W 4 & 3: HL	7.52	7.61	7.66	7.81	8.42	8.86	9.58	9.77	10.30	11.59	12.23
			W 5 & 6: LL	12.59	12.63	12.39	12.62	11.54	10.92	10.52	9.91	9.28	8.62	8.29
	Trailing	Axle 2 & 1	W 2 & 1: HL	8.61	8.69	9.01	8.90	9.47	10.02	10.52	11.01	11.88	12.98	13.61
			W 7 & 8: LL	13.71	13.65	13.24	13.55	12.86	12.49	11.88	10.82	9.79	8.81	7.95
MOS	Leading	Axle 4 & 3	W 4 & 3: HL	8.63	8.70	8.78	8.93	9.44	10.06	10.41	11.38	12.22	13.30	13.49
			W 5 & 6: LL	12.54	12.59	12.40	12.45	11.70	10.84	10.47	9.64	9.23	8.84	8.65
	Trailing	Axle 2 & 1	W 2 & 1: HL	7.65	7.73	8.03	7.91	8.42	8.92	9.19	9.93	11.14	12.25	12.28
			W 7 & 8: LL	13.14	13.44	12.99	13.21	12.48	12.07	11.46	10.89	10.31	10.10	9.23
DMOS A	Leading	Axle 4 & 3	W 4 & 3: HL	8.51	8.58	8.70	9.05	9.40	10.39	10.65	11.04	12.11	13.32	14.16
			W 5 & 6: LL	13.31	13.31	13.24	12.96	12.51	11.92	10.96	10.61	9.34	8.96	8.58
	Trailing	Axle 2 & 1	W 2 & 1: HL	9.14	9.38	9.69	9.66	10.27	10.52	10.99	11.39	12.56	13.59	14.82
			W 7 & 8: LL	15.26	15.13	14.85	15.09	14.12	13.73	13.21	12.26	11.78	10.72	10.15

Table E-26: Vertical Forces After Tamping (Cars) – S1 Down

21 Jul 2015: Hatfield to Pretoria (Down) km 3.215 (Site 1)			km/h										
			11.10	21.02	30.50	40.07	50.15	60.01	69.38	79.42	89.55	98.74	104.02
Car Type	Rail Leg	Wheel	Vertical Force (t)										
DMOS B	HL	W 8 & 7 & 6 & 5	17.84	18.07	18.63	19.13	20.23	21.00	22.54	23.65	26.46	29.40	29.15
	LL	W 1 & 2 & 3 & 4	28.63	28.74	28.74	29.92	28.14	25.52	24.71	22.34	20.16	20.61	19.25
PTOS	HL	W 4 & 3 & 2 & 1	16.13	16.30	16.67	16.70	17.89	18.88	20.10	20.78	22.18	24.57	25.84
	LL	W 5 & 6 & 7 & 8	26.30	26.28	25.63	26.17	24.40	23.41	22.41	20.73	19.07	17.43	16.24
MOS	HL	W 4 & 3 & 2 & 1	16.28	16.43	16.80	16.84	17.86	18.98	19.60	21.31	23.37	25.56	25.78
	LL	W 5 & 6 & 7 & 8	25.68	26.02	25.38	25.66	24.17	22.91	21.93	20.53	19.53	18.94	17.87
DMOS A	HL	W 4 & 3 & 2 & 1	17.65	17.95	18.39	18.72	19.67	20.91	21.64	22.44	24.67	26.91	28.98
	LL	W 5 & 6 & 7 & 8	28.56	28.44	28.08	28.05	26.62	25.66	24.18	22.87	21.12	19.68	18.73

Table E-27: Vertical Forces After Tamping (4-Car Train) – S1 Down

21 Jul 2015: Hatfield to Pretoria (Down) km 3.215 (Site 1)		km/h										
		11.10	21.02	30.50	40.07	50.15	60.01	69.38	79.42	89.55	98.74	104.02
Car Type	Rail Leg	Vertical Force (t)										
4 Car Train	HL	67.90	68.76	70.49	71.39	75.64	79.76	83.88	88.18	96.68	106.44	109.75
	LL	109.18	109.49	107.84	109.80	103.34	97.49	93.23	86.47	79.89	76.66	72.09

© University of Pretoria

Table E-28: Lateral Forces After Tamping (Bogies) – S1 Down

21 Jul 2015: Hatfield to Pretoria (Down) km 3.215 (Site 1)				km/h										
				11.10	21.02	30.50	40.07	50.15	60.01	69.38	79.42	89.55	98.74	104.02
Car Type	Bogie	Axle	Wheel & Rail Leg	Lateral Force (t)										
DMOS B	Leading	Axle 1 & 2	W 8 & 7: HL	0.86	0.69	0.37	0.40	0.62	0.83	0.99	-0.59	-0.12	0.27	2.12
			W 1 & 2: LL	4.07	4.09	3.37	3.18	3.02	2.80	2.33	0.48	-0.13	-0.35	-0.43
	Trailing	Axle 3 & 4	W 6 & 5: HL	0.60	0.88	1.04	1.06	1.06	1.06	1.08	1.29	1.69	2.07	2.45
			W 3 & 4: LL	3.49	3.78	3.65	3.57	3.37	3.03	1.46	0.74	0.33	0.12	0.12
PTOS	Leading	Axle 4 & 3	W 4 & 3: HL	1.09	1.15	1.34	1.17	1.29	1.31	1.43	1.00	0.07	0.39	1.80
			W 5 & 6: LL	3.69	3.63	3.81	3.63	3.36	3.02	2.79	0.79	0.04	-0.15	-0.19
	Trailing	Axle 2 & 1	W 2 & 1: HL	0.78	0.86	0.97	1.00	1.09	1.08	0.92	-0.11	0.10	0.45	0.80
			W 7 & 8: LL	3.94	3.90	3.87	3.88	3.54	3.23	1.69	0.67	-0.25	-0.25	-0.26
MOS	Leading	Axle 4 & 3	W 4 & 3: HL	0.88	0.93	0.97	1.03	1.24	1.25	1.47	-0.12	-0.06	0.30	0.64
			W 5 & 6: LL	3.72	3.71	3.67	3.38	3.26	3.12	1.85	0.44	-0.10	-0.26	-0.18
	Trailing	Axle 2 & 1	W 2 & 1: HL	0.60	0.60	0.67	0.84	1.05	1.18	1.51	-0.19	0.04	0.29	0.58
			W 7 & 8: LL	3.46	3.46	3.33	3.14	3.22	3.05	1.60	-0.12	-0.35	-0.52	-0.40
DMOS A	Leading	Axle 4 & 3	W 4 & 3: HL	1.06	1.03	1.18	1.30	1.40	1.30	1.73	1.19	1.49	1.58	1.90
			W 5 & 6: LL	3.96	3.98	3.94	3.55	3.48	3.19	2.96	0.85	0.26	-0.17	-0.11
	Trailing	Axle 2 & 1	W 2 & 1: HL	0.67	0.81	1.09	1.04	1.04	0.80	0.65	0.23	0.60	0.89	2.45
			W 7 & 8: LL	4.02	4.03	3.97	3.91	3.52	1.99	1.43	0.52	-0.08	-0.32	-0.28

Table E-29: Lateral Forces After Tamping (Cars) – S1 Down

21 Jul 2015: Hatfield to Pretoria (Down) km 3.215 (Site 1)			km/h										
			11.10	21.02	30.50	40.07	50.15	60.01	69.38	79.42	89.55	98.74	104.02
Car Type	Rail Leg	Wheel	Lateral Force (t)										
DMOS B	HL	W 8 & 7 & 6 & 5	1.46	1.57	1.40	1.46	1.68	1.89	2.08	0.70	1.57	2.34	4.57
	LL	W 1 & 2 & 3 & 4	7.56	7.87	7.02	6.75	6.39	5.83	3.80	1.22	0.21	-0.23	-0.30
PTOS	HL	W 4 & 3 & 2 & 1	1.87	2.01	2.31	2.18	2.38	2.39	2.35	0.89	0.17	0.85	2.59
	LL	W 5 & 6 & 7 & 8	7.63	7.53	7.68	7.51	6.91	6.25	4.48	1.46	-0.21	-0.40	-0.45
MOS	HL	W 4 & 3 & 2 & 1	1.48	1.53	1.64	1.87	2.30	2.44	2.98	-0.31	-0.02	0.59	1.21
	LL	W 5 & 6 & 7 & 8	7.18	7.17	6.99	6.51	6.48	6.16	3.44	0.32	-0.45	-0.78	-0.58
DMOS A	HL	W 4 & 3 & 2 & 1	1.73	1.84	2.27	2.33	2.44	2.10	2.37	1.42	2.09	2.47	4.36
	LL	W 5 & 6 & 7 & 8	7.98	8.01	7.91	7.46	6.99	5.18	4.39	1.37	0.18	-0.49	-0.39

Table E-30: Lateral Forces After Tamping (4-Car Train) – S1 Down

21 Jul 2015: Hatfield to Pretoria (Down) km 3.215 (Site 1)		km/h										
		11.10	21.02	30.50	40.07	50.15	60.01	69.38	79.42	89.55	98.74	104.02
Car Type	Rail Leg	Lateral Force (t)										
4 Car Train	HL	6.54	6.95	7.62	7.84	8.80	8.81	9.78	2.70	3.81	6.25	12.73
	LL	30.35	30.58	29.60	28.23	26.77	23.42	16.10	4.37	-0.27	-1.90	-1.73

Table E-31: Vertical Forces After Tamping (Bogies) – S2 Down

21 Jul 2015: Hatfield to Pretoria (Down) km 3.175 (Site 2)				km/h										
				11.09	20.87	30.69	40.32	50.09	60.03	69.41	79.57	89.30	99.05	104.12
Car Type	Bogie	Axle	Wheel & Rail Leg	Vertical Force (t)										
DMOS B	Leading	Axle 1 & 2	W 8 & 7: HL	10.22	10.35	10.51	11.02	11.96	12.06	13.23	13.34	14.32	15.91	16.25
			W 1 & 2: LL	13.16	13.22	13.32	12.59	11.96	11.25	12.36	9.87	10.00	9.83	9.72
	Trailing	Axle 3 & 4	W 6 & 5: HL	8.97	9.16	9.17	9.45	10.34	10.46	11.21	11.84	12.80	13.34	13.80
			W 3 & 4: LL	11.67	11.45	11.62	11.01	10.47	10.56	9.96	9.11	8.73	7.77	7.60
PTOS	Leading	Axle 4 & 3	W 4 & 3: HL	8.01	8.10	8.31	8.74	9.19	9.66	10.36	10.93	11.46	12.47	13.03
			W 5 & 6: LL	10.74	10.70	10.56	10.33	9.81	9.70	8.94	8.73	7.84	7.45	6.95
	Trailing	Axle 2 & 1	W 2 & 1: HL	9.42	9.53	9.51	9.98	10.94	11.13	11.68	12.43	13.15	13.93	14.58
			W 7 & 8: LL	11.70	11.63	11.56	11.51	10.32	10.11	9.87	9.38	8.68	8.08	7.60
MOS	Leading	Axle 4 & 3	W 4 & 3: HL	9.18	9.35	9.48	9.89	10.41	10.94	11.11	12.19	12.96	13.78	14.37
			W 5 & 6: LL	10.88	10.91	10.74	10.44	10.19	9.30	9.14	8.77	8.15	7.22	7.40
	Trailing	Axle 2 & 1	W 2 & 1: HL	8.25	8.38	8.51	8.80	9.66	9.81	9.99	10.12	11.90	12.43	12.35
			W 7 & 8: LL	11.43	11.20	11.13	11.08	10.37	10.26	9.70	9.60	9.26	8.64	8.00
DMOS A	Leading	Axle 4 & 3	W 4 & 3: HL	9.10	9.14	9.35	9.78	10.28	10.77	11.44	12.02	13.07	13.39	14.50
			W 5 & 6: LL	11.46	11.40	11.28	10.99	10.64	10.33	9.59	8.83	8.46	7.58	7.10
	Trailing	Axle 2 & 1	W 2 & 1: HL	9.95	10.08	10.10	10.33	11.47	11.88	12.10	12.91	13.69	14.90	15.05
			W 7 & 8: LL	13.15	12.91	13.09	12.79	11.77	11.24	11.24	10.77	10.25	10.21	9.54

Table E-32: Vertical Forces After Tamping (Cars) – S2 Down

21 Jul 2015: Hatfield to Pretoria (Down) km 3.175 (Site 2)			km/h										
			11.09	20.87	30.69	40.32	50.09	60.03	69.41	79.57	89.30	99.05	104.12
Car Type	Rail Leg	Wheel	Vertical Force (t)										
DMOS B	HL	W 8 & 7 & 6 & 5	19.19	19.51	19.68	20.48	22.30	22.52	24.44	25.18	27.12	29.25	30.05
	LL	W 1 & 2 & 3 & 4	24.83	24.67	24.93	23.59	22.43	21.81	22.32	18.99	18.72	17.60	17.31
PTOS	HL	W 4 & 3 & 2 & 1	17.43	17.63	17.82	18.73	20.14	20.79	22.04	23.36	24.61	26.40	27.61
	LL	W 5 & 6 & 7 & 8	22.44	22.33	22.12	21.83	20.13	19.81	18.81	18.11	16.52	15.53	14.54
MOS	HL	W 4 & 3 & 2 & 1	17.43	17.73	17.99	18.69	20.07	20.75	21.10	22.31	24.86	26.21	26.72
	LL	W 5 & 6 & 7 & 8	22.31	22.11	21.88	21.51	20.56	19.56	18.85	18.36	17.42	15.86	15.41
DMOS A	HL	W 4 & 3 & 2 & 1	19.05	19.22	19.45	20.11	21.75	22.65	23.54	24.93	26.76	28.28	29.55
	LL	W 5 & 6 & 7 & 8	24.60	24.31	24.37	23.79	22.40	21.57	20.83	19.60	18.70	17.78	16.63

Table E-33: Vertical Forces After Tamping (4-Car Train) – S2 Down

21 Jul 2015: Hatfield to Pretoria (Down) km 3.175 (Site 2)		km/h										
		11.09	20.87	30.69	40.32	50.09	60.03	69.41	79.57	89.30	99.05	104.12
Car Type	Rail Leg	Vertical Force (t)										
4 Car Train	HL	73.10	74.09	74.94	78.00	84.26	86.71	91.11	95.78	103.35	110.15	113.93
	LL	94.19	93.43	93.30	90.73	85.53	82.75	80.81	75.06	71.36	66.77	63.90

© University of Pretoria

Table E-34: Lateral Forces After Tamping (Bogies) – S2 Down

21 Jul 2015: Hatfield to Pretoria (Down) km 3.175 (Site 2)				km/h										
				11.09	20.87	30.69	40.32	50.09	60.03	69.41	79.57	89.30	99.05	104.12
Car Type	Bogie	Axle	Wheel & Rail Leg	Lateral Force (t)										
DMOS B	Leading	Axle 1 & 2	W 8 & 7: HL	-0.02	-0.09	-0.23	0.03	-1.10	-0.94	-0.76	-0.91	-0.59	-0.05	0.43
			W 1 & 2: LL	3.59	3.50	3.15	3.07	2.55	2.18	2.11	1.03	0.09	-0.13	-0.06
	Trailing	Axle 3 & 4	W 6 & 5: HL	-1.07	-0.12	0.00	-0.98	-0.78	-0.82	-0.81	-0.67	-0.57	-0.29	0.11
			W 3 & 4: LL	2.89	3.11	3.14	2.65	2.38	2.08	1.63	1.24	0.44	0.14	0.24
PTOS	Leading	Axle 4 & 3	W 4 & 3: HL	0.54	0.47	0.47	0.38	0.33	0.43	0.44	-0.70	-0.35	-0.27	0.32
			W 5 & 6: LL	3.41	3.38	3.22	2.96	2.57	2.36	2.07	0.66	0.39	0.14	0.41
	Trailing	Axle 2 & 1	W 2 & 1: HL	-0.09	-0.18	-0.97	-1.19	-0.87	-0.91	-0.71	-0.64	-0.61	-0.30	0.10
			W 7 & 8: LL	3.47	3.42	3.19	2.85	2.40	2.17	1.74	0.61	0.26	0.09	0.13
MOS	Leading	Axle 4 & 3	W 4 & 3: HL	0.26	0.33	0.31	0.33	0.09	0.11	-0.07	-0.97	-0.47	-0.13	0.54
			W 5 & 6: LL	3.50	3.51	3.42	3.28	2.68	2.39	2.32	0.86	0.36	0.14	0.52
	Trailing	Axle 2 & 1	W 2 & 1: HL	-0.10	-0.10	0.00	-0.89	-0.74	-0.72	-0.65	-0.71	-0.51	-0.23	0.22
			W 7 & 8: LL	3.14	3.16	3.07	2.75	2.37	2.26	2.17	0.85	0.42	0.35	0.36
DMOS A	Leading	Axle 4 & 3	W 4 & 3: HL	0.26	0.27	0.27	0.31	0.43	0.68	0.40	-0.95	-0.61	-0.30	0.37
			W 5 & 6: LL	3.51	3.50	3.33	3.21	3.05	2.66	2.39	1.15	0.53	0.40	0.64
	Trailing	Axle 2 & 1	W 2 & 1: HL	-1.11	-1.20	-1.15	-1.34	-1.12	-1.27	-1.02	-1.04	-0.67	-0.30	0.26
			W 7 & 8: LL	3.55	3.38	3.38	2.97	2.46	1.99	1.65	0.68	0.42	0.16	-0.01

Table E-35: Lateral Forces After Tamping (Cars) – S2 Down

21 Jul 2015: Hatfield to Pretoria (Down) km 3.175 (Site 2)			km/h										
			11.09	20.87	30.69	40.32	50.09	60.03	69.41	79.57	89.30	99.05	104.12
Car Type	Rail Leg	Wheel	Lateral Force (t)										
DMOS B	HL	W 8 & 7 & 6 & 5	-1.09	-0.21	-0.24	-0.95	-1.87	-1.76	-1.57	-1.58	-1.16	-0.34	0.55
	LL	W 1 & 2 & 3 & 4	6.47	6.61	6.29	5.72	4.93	4.26	3.74	2.27	0.52	0.01	0.17
PTOS	HL	W 4 & 3 & 2 & 1	0.45	0.29	-0.50	-0.81	-0.54	-0.48	-0.28	-1.34	-0.95	-0.57	0.42
	LL	W 5 & 6 & 7 & 8	6.88	6.80	6.41	5.81	4.97	4.52	3.81	1.27	0.65	0.23	0.54
MOS	HL	W 4 & 3 & 2 & 1	0.16	0.23	0.31	-0.56	-0.65	-0.60	-0.72	-1.68	-0.98	-0.36	0.75
	LL	W 5 & 6 & 7 & 8	6.64	6.68	6.49	6.03	5.06	4.65	4.49	1.71	0.77	0.49	0.88
DMOS A	HL	W 4 & 3 & 2 & 1	-0.85	-0.92	-0.89	-1.03	-0.69	-0.59	-0.63	-2.00	-1.28	-0.60	0.63
	LL	W 5 & 6 & 7 & 8	7.07	6.89	6.71	6.18	5.50	4.65	4.04	1.82	0.95	0.56	0.63

Table E-36: Lateral Forces After Tamping (4-Car Train) – S2 Down

21 Jul 2015: Hatfield to Pretoria (Down) km 3.175 (Site 2)		km/h										
		11.09	20.87	30.69	40.32	50.09	60.03	69.41	79.57	89.30	99.05	104.12
Car Type	Rail Leg	Lateral Force (t)										
4 Car Train	HL	-1.34	-0.61	-1.31	-3.35	-3.76	-3.44	-3.19	-6.58	-4.37	-1.87	2.35
	LL	27.07	26.97	25.91	23.74	20.47	18.09	16.08	7.08	2.89	1.29	2.22

© University of Pretoria

Table E-37: Vertical Forces After Tamping (Bogies) – S1 Up

21 Jul 2015: Pretoria to Hatfield (Up) km 3.215 (Site 1)				km/h										
				10.97	20.55	30.32	40.09	50.10	59.61	69.90	79.84	89.37	99.02	104.70
Car Type	Bogie	Axle	Wheel & Rail Leg	Vertical Force (t)										
DMOS A	Leading	Axle 1 & 2	W 1 & 2: HL	9.09	9.29	9.57	10.10	10.67	11.00	10.81	11.66	12.51	13.14	12.82
			W 8 & 7: LL	15.31	15.33	15.05	14.21	13.88	13.39	12.72	12.16	11.38	10.05	9.66
	Trailing	Axle 3 & 4	W 3 & 4: HL	8.50	8.55	8.94	9.60	9.66	10.02	10.39	11.20	11.75	12.55	13.13
			W 6 & 5: LL	13.20	13.27	13.00	12.22	12.08	11.72	10.83	9.76	8.68	8.36	7.20
MOS	Leading	Axle 1 & 2	W 1 & 2: HL	7.67	7.73	8.06	8.48	9.25	9.16	9.37	9.79	10.38	10.92	11.56
			W 8 & 7: LL	13.43	13.58	13.05	12.45	12.35	11.86	11.35	10.61	9.24	8.61	8.36
	Trailing	Axle 3 & 4	W 3 & 4: HL	8.56	8.63	8.85	9.44	9.76	9.92	10.32	11.24	11.85	12.40	12.61
			W 6 & 5: LL	12.82	12.76	12.42	11.77	11.23	11.25	10.47	9.20	8.50	7.67	7.45
PTOS	Leading	Axle 1 & 2	W 1 & 2: HL	8.64	8.80	9.09	9.57	10.31	10.23	10.56	11.25	11.97	12.33	13.03
			W 8 & 7: LL	13.78	13.70	13.26	12.80	11.69	11.55	11.21	9.91	9.29	8.46	7.71
	Trailing	Axle 3 & 4	W 3 & 4: HL	7.57	7.66	7.85	8.56	8.88	8.86	9.40	9.86	10.14	10.97	11.80
			W 6 & 5: LL	12.45	12.52	12.20	11.53	11.11	11.07	10.26	9.44	9.13	7.78	6.99
DMOS B	Leading	Axle 4 & 3	W 5 & 6: HL	8.49	8.47	8.72	9.18	9.76	9.86	10.47	11.12	11.49	12.40	13.06
			W 4 & 3: LL	13.38	13.40	12.92	12.87	12.00	11.59	10.62	9.80	8.85	8.11	7.86
	Trailing	Axle 2 & 1	W 7 & 8: HL	9.61	9.81	10.13	10.56	10.78	11.18	11.47	12.02	13.51	13.92	14.91
			W 2 & 1: LL	15.07	16.17	14.60	13.78	13.79	13.26	12.03	11.58	10.81	10.42	9.20

Table E-38: Vertical Forces After Tamping (Cars) – S1 Up

21 Jul 2015: Pretoria to Hatfield (Up) km 3.215 (Site 1)			km/h										
			10.97	20.55	30.32	40.09	50.10	59.61	69.90	79.84	89.37	99.02	104.70
Car Type	Rail Leg	Wheel	Vertical Force (t)										
DMOS A	HL	W 1 & 2 & 3 & 4	17.59	17.84	18.51	19.70	20.33	21.02	21.19	22.86	24.25	25.69	25.95
	LL	W 8 & 7 & 6 & 5	28.52	28.60	28.05	26.43	25.96	25.12	23.55	21.92	20.06	18.41	16.87
MOS	HL	W 1 & 2 & 3 & 4	16.23	16.36	16.91	17.92	19.01	19.09	19.70	21.03	22.24	23.32	24.17
	LL	W 8 & 7 & 6 & 5	26.24	26.34	25.47	24.22	23.57	23.11	21.82	19.81	17.74	16.28	15.81
PTOS	HL	W 1 & 2 & 3 & 4	16.21	16.46	16.94	18.13	19.18	19.09	19.96	21.11	22.11	23.30	24.83
	LL	W 8 & 7 & 6 & 5	26.23	26.22	25.47	24.32	22.81	22.63	21.47	19.35	18.42	16.24	14.70
DMOS B	HL	W 5 & 6 & 7 & 8	18.09	18.28	18.85	19.74	20.55	21.04	21.95	23.13	24.99	26.32	27.97
	LL	W 4 & 3 & 2 & 1	28.44	29.57	27.53	26.65	25.78	24.85	22.65	21.38	19.67	18.53	17.06

Table E-39: Vertical Forces After Tamping (4-Car Train) – S1 Up

21 Jul 2015: Pretoria to Hatfield (Up) km 3.215 (Site 1)		km/h										
		10.97	20.55	30.32	40.09	50.10	59.61	69.90	79.84	89.37	99.02	104.70
Car Type	Rail Leg	Vertical Force (t)										
4 Car Train	High Leg	68.13	68.94	71.20	75.49	79.08	80.24	82.80	88.13	93.59	98.63	102.92
	Low Leg	109.43	110.74	106.52	101.62	98.12	95.71	89.49	82.47	75.89	69.46	64.43

© University of Pretoria

Table E-40: Lateral Forces After Tamping (Bogies) – S1 Up

21 Jul 2015: Pretoria to Hatfield (Up) km 3.215 (Site 1)				km/h										
				10.97	20.55	30.32	40.09	50.10	59.61	69.90	79.84	89.37	99.02	104.70
Car Type	Bogie	Axle	Wheel & Rail Leg	Lateral Force (t)										
DMOS A	Leading	Axle 1 & 2	W 1 & 2: HL	1.23	1.26	1.49	1.81	2.06	2.12	2.39	2.55	3.27	3.44	3.22
			W 8 & 7: LL	4.41	4.36	4.25	4.05	3.84	3.73	3.37	2.11	1.27	0.51	0.20
	Trailing	Axle 3 & 4	W 3 & 4: HL	1.02	1.06	1.27	1.41	1.57	1.70	1.97	2.32	2.47	2.73	2.99
			W 6 & 5: LL	3.79	3.81	3.76	3.47	3.31	3.15	1.99	1.53	0.66	0.25	-0.09
MOS	Leading	Axle 1 & 2	W 1 & 2: HL	1.03	1.17	1.36	1.46	1.58	1.93	2.17	1.91	2.81	2.57	2.62
			W 8 & 7: LL	3.73	3.67	3.62	3.42	3.08	2.98	2.77	1.57	0.78	0.27	-0.05
	Trailing	Axle 3 & 4	W 3 & 4: HL	0.76	1.03	1.02	1.19	1.33	1.71	1.69	2.20	2.38	2.35	2.43
			W 6 & 5: LL	3.67	3.74	3.57	3.30	3.13	2.85	1.69	1.01	0.32	-0.08	-0.08
PTOS	Leading	Axle 1 & 2	W 1 & 2: HL	1.20	1.29	1.45	1.61	1.83	1.91	2.11	2.08	2.46	2.21	2.74
			W 8 & 7: LL	4.12	4.10	3.92	3.83	3.41	3.16	2.98	1.51	0.75	0.00	0.01
	Trailing	Axle 3 & 4	W 3 & 4: HL	1.02	1.12	1.24	1.43	1.58	1.63	1.71	2.27	2.37	2.14	2.87
			W 6 & 5: LL	3.73	3.76	3.59	3.47	3.10	2.04	1.71	0.94	0.45	-0.18	-0.21
DMOS B	Leading	Axle 4 & 3	W 5 & 6: HL	1.26	1.39	1.47	1.81	1.82	2.11	2.18	2.16	2.64	2.50	2.72
			W 4 & 3: LL	3.41	3.42	3.26	3.24	2.17	1.97	1.64	1.08	0.73	0.02	-0.08
	Trailing	Axle 2 & 1	W 7 & 8: HL	0.97	0.88	0.99	1.44	1.34	1.78	1.80	2.63	2.93	2.53	2.97
			W 2 & 1: LL	4.23	4.13	3.90	3.88	3.68	2.06	1.57	0.97	0.32	-0.23	-0.12

Table E-41: Lateral Forces After Tamping (Cars) – S1 Up

21 Jul 2015: Pretoria to Hatfield (Up) km 3.215 (Site 1)			km/h										
			10.97	20.55	30.32	40.09	50.10	59.61	69.90	79.84	89.37	99.02	104.70
Car Type	Rail Leg	Wheel	Lateral Force (t)										
DMOS A	HL	W 1 & 2 & 3 & 4	2.25	2.32	2.76	3.23	3.62	3.82	4.36	4.87	5.74	6.17	6.20
	LL	W 8 & 7 & 6 & 5	8.20	8.16	8.01	7.51	7.15	6.88	5.36	3.65	1.93	0.77	0.11
MOS	HL	W 1 & 2 & 3 & 4	1.79	2.20	2.38	2.65	2.91	3.63	3.87	4.11	5.19	4.92	5.04
	LL	W 8 & 7 & 6 & 5	7.41	7.41	7.19	6.72	6.21	5.84	4.47	2.58	1.11	0.20	-0.13
PTOS	HL	W 1 & 2 & 3 & 4	2.21	2.41	2.68	3.03	3.41	3.54	3.82	4.35	4.83	4.35	5.60
	LL	W 8 & 7 & 6 & 5	7.85	7.86	7.51	7.30	6.51	5.20	4.69	2.45	1.20	-0.18	-0.19
DMOS B	HL	W 5 & 6 & 7 & 8	2.23	2.27	2.46	3.25	3.16	3.89	3.98	4.80	5.56	5.03	5.69
	LL	W 4 & 3 & 2 & 1	7.64	7.55	7.16	7.12	5.85	4.03	3.21	2.05	1.06	-0.21	-0.20

Table E-42: Lateral Forces After Tamping (4-Car Train) – S1 Up

21 Jul 2015: Pretoria to Hatfield (Up) km 3.215 (Site 1)		km/h										
		10.97	20.55	30.32	40.09	50.10	59.61	69.90	79.84	89.37	99.02	104.70
Car Type	Rail Leg	Lateral Force (t)										
4 Car Train	HL	8.49	9.21	10.29	12.16	13.10	14.88	16.03	18.13	21.32	20.47	22.54
	LL	31.09	30.98	29.87	28.66	25.73	21.95	17.72	10.73	5.29	0.57	-0.41

© University of Pretoria

Table E-43: Vertical Forces After Tamping (Bogies) – S2 Up

21 Jul 2015: Pretoria to Hatfield (Up) km 3.175 (Site 2)				km/h										
				11.01	20.39	29.80	39.92	49.68	59.45	69.57	79.66	90.09	99.10	104.24
Car Type	Bogie	Axle	Wheel & Rail Leg	Vertical Force (t)										
DMOS A	Leading	Axle 1 & 2	W 1 & 2: HL	9.98	10.12	10.31	10.99	11.48	11.99	12.58	13.34	14.31	14.76	15.78
			W 8 & 7: LL	12.92	12.81	12.72	12.36	12.27	11.67	11.43	10.53	10.24	9.54	9.14
	Trailing	Axle 3 & 4	W 3 & 4: HL	9.24	9.34	9.35	9.65	10.41	11.06	11.95	13.06	13.76	14.61	14.86
			W 6 & 5: LL	11.35	11.24	11.24	11.47	10.86	10.08	9.08	8.53	8.04	7.59	6.89
MOS	Leading	Axle 1 & 2	W 1 & 2: HL	8.38	8.47	8.77	9.09	9.62	10.05	10.51	10.76	12.14	12.45	13.35
			W 8 & 7: LL	11.25	11.55	11.16	11.27	10.59	10.39	9.55	9.13	8.64	8.23	7.73
	Trailing	Axle 3 & 4	W 3 & 4: HL	9.27	9.42	9.52	9.57	10.22	10.93	11.71	12.58	13.78	14.61	14.84
			W 6 & 5: LL	10.99	10.89	10.87	10.77	10.32	10.18	9.46	8.47	7.63	7.20	6.88
PTOS	Leading	Axle 1 & 2	W 1 & 2: HL	9.46	9.57	9.74	10.18	10.55	11.31	12.06	12.97	13.74	14.47	15.49
			W 8 & 7: LL	11.64	11.55	11.52	11.14	11.00	10.66	10.08	9.14	8.56	7.50	7.34
	Trailing	Axle 3 & 4	W 3 & 4: HL	8.04	8.16	8.23	8.37	9.09	9.82	10.69	11.44	12.20	12.57	12.99
			W 6 & 5: LL	10.81	10.75	10.77	10.74	10.16	9.82	9.24	8.35	7.53	7.22	7.17
DMOS B	Leading	Axle 4 & 3	W 5 & 6: HL	9.24	9.30	9.42	10.05	10.49	10.91	11.57	12.61	13.51	13.60	14.51
			W 4 & 3: LL	11.26	11.13	11.22	10.83	10.59	10.35	9.62	8.99	8.58	8.02	7.02
	Trailing	Axle 2 & 1	W 7 & 8: HL	10.33	10.34	10.60	11.04	11.66	12.10	13.56	13.66	14.73	16.45	16.78
			W 2 & 1: LL	12.97	13.76	12.86	13.08	12.64	11.50	11.32	10.01	10.29	10.44	8.57

Table E-44: Vertical Forces After Tamping (Cars) – S2 Up

21 Jul 2015: Pretoria to Hatfield (Up) km 3.175 (Site 2)			km/h										
			11.01	20.39	29.80	39.92	49.68	59.45	69.57	79.66	90.09	99.10	104.24
Car Type	Rail Leg	Wheel	Vertical Force (t)										
DMOS A	HL	W 1 & 2 & 3 & 4	19.22	19.46	19.67	20.64	21.89	23.05	24.52	26.40	28.06	29.36	30.64
	LL	W 8 & 7 & 6 & 5	24.27	24.05	23.96	23.83	23.13	21.75	20.51	19.06	18.28	17.13	16.03
MOS	HL	W 1 & 2 & 3 & 4	17.64	17.89	18.29	18.66	19.83	20.99	22.22	23.34	25.92	27.06	28.19
	LL	W 8 & 7 & 6 & 5	22.23	22.44	22.03	22.04	20.91	20.57	19.00	17.59	16.27	15.43	14.61
PTOS	HL	W 1 & 2 & 3 & 4	17.49	17.72	17.97	18.55	19.64	21.13	22.75	24.41	25.94	27.04	28.49
	LL	W 8 & 7 & 6 & 5	22.45	22.31	22.29	21.89	21.16	20.48	19.32	17.50	16.08	14.72	14.51
DMOS B	HL	W 5 & 6 & 7 & 8	19.57	19.63	20.02	21.09	22.15	23.01	25.13	26.27	28.24	30.04	31.30
	LL	W 4 & 3 & 2 & 1	24.22	24.89	24.08	23.91	23.23	21.85	20.94	18.99	18.88	18.46	15.58

Table E-45: Vertical Forces After Tamping (4-Car Train) – S2 Up

21 Jul 2015: Pretoria to Hatfield (Up) km 3.175 (Site 2)		km/h										
		11.01	20.39	29.80	39.92	49.68	59.45	69.57	79.66	90.09	99.10	104.24
Car Type	Rail Leg	Vertical Force (t)										
4 Car Train	HL	73.93	74.72	75.94	78.93	83.51	88.18	94.62	100.42	108.17	113.51	118.61
	LL	93.18	93.69	92.36	91.66	88.43	84.64	79.78	73.15	69.52	65.74	60.73

© University of Pretoria

Table E-46: Lateral Forces After Tamping (Bogies) – S2 Up

21 Jul 2015: Pretoria to Hatfield (Up) km 3.175 (Site 2)				km/h										
				11.01	20.39	29.80	39.92	49.68	59.45	69.57	79.66	90.09	99.10	104.24
Car Type	Bogie	Axle	Wheel & Rail Leg	Lateral Force (t)										
DMOS A	Leading	Axle 1 & 2	W 1 & 2: HL	0.60	0.34	0.44	0.52	0.51	0.77	0.53	-0.24	-0.26	0.09	0.54
			W 8 & 7: LL	4.11	3.90	3.88	3.53	3.48	3.39	2.98	1.14	0.35	-0.04	0.01
	Trailing	Axle 3 & 4	W 3 & 4: HL	0.42	0.54	0.61	0.44	0.68	0.90	0.73	-0.03	-0.04	0.23	0.48
			W 6 & 5: LL	3.55	3.54	3.52	3.38	3.15	2.86	2.37	0.87	0.11	-0.08	-0.16
MOS	Leading	Axle 1 & 2	W 1 & 2: HL	0.27	0.31	0.28	0.35	0.50	0.54	0.27	-0.35	-0.23	-0.04	0.48
			W 8 & 7: LL	3.31	3.34	3.17	3.07	2.89	2.76	2.28	0.55	0.21	0.05	0.36
	Trailing	Axle 3 & 4	W 3 & 4: HL	0.18	0.37	0.32	0.30	0.31	0.22	0.12	-0.27	0.07	0.29	1.03
			W 6 & 5: LL	3.38	3.48	3.26	3.29	2.88	2.61	2.04	0.40	-0.06	-0.18	0.20
PTOS	Leading	Axle 1 & 2	W 1 & 2: HL	0.27	0.37	0.44	0.41	0.50	0.45	0.19	-0.45	-0.36	0.12	0.74
			W 8 & 7: LL	3.69	3.76	3.61	3.44	3.33	3.09	2.58	0.98	0.14	-0.09	0.09
	Trailing	Axle 3 & 4	W 3 & 4: HL	0.23	0.33	0.35	0.19	0.33	0.21	-0.03	-0.10	0.16	0.54	0.67
			W 6 & 5: LL	3.42	3.48	3.41	3.30	3.08	2.79	1.73	0.47	-0.13	-0.25	0.00
DMOS B	Leading	Axle 4 & 3	W 5 & 6: HL	0.67	0.68	0.74	0.72	0.94	0.80	0.53	-0.28	-0.19	0.12	0.83
			W 4 & 3: LL	3.17	3.11	2.97	2.52	2.51	2.23	1.61	0.40	-0.30	-0.48	-0.03
	Trailing	Axle 2 & 1	W 7 & 8: HL	-0.10	-0.12	-0.02	-0.23	-0.01	-0.05	-0.46	-0.44	0.02	0.36	1.03
			W 2 & 1: LL	3.84	3.88	3.80	3.49	3.40	3.02	2.11	0.53	0.01	-0.01	0.41

Table E-47: Lateral Forces After Tamping (Cars) – S2 Up

21 Jul 2015: Pretoria to Hatfield (Up) km 3.175 (Site 2)			km/h										
			11.01	20.39	29.80	39.92	49.68	59.45	69.57	79.66	90.09	99.10	104.24
Car Type	Rail Leg	Wheel	Lateral Force (t)										
DMOS A	HL	W 1 & 2 & 3 & 4	1.02	0.88	1.04	0.96	1.19	1.66	1.26	-0.27	-0.30	0.31	1.02
	LL	W 8 & 7 & 6 & 5	7.66	7.44	7.40	6.90	6.63	6.25	5.35	2.00	0.46	-0.12	-0.15
MOS	HL	W 1 & 2 & 3 & 4	0.45	0.68	0.59	0.66	0.81	0.76	0.39	-0.62	-0.16	0.25	1.51
	LL	W 8 & 7 & 6 & 5	6.69	6.82	6.43	6.36	5.77	5.37	4.31	0.95	0.15	-0.14	0.55
PTOS	HL	W 1 & 2 & 3 & 4	0.50	0.70	0.78	0.60	0.84	0.65	0.16	-0.55	-0.20	0.66	1.41
	LL	W 8 & 7 & 6 & 5	7.12	7.24	7.02	6.74	6.41	5.88	4.32	1.45	0.01	-0.35	0.09
DMOS B	HL	W 5 & 6 & 7 & 8	0.57	0.56	0.72	0.49	0.94	0.76	0.06	-0.72	-0.17	0.48	1.86
	LL	W 4 & 3 & 2 & 1	7.01	6.99	6.78	6.01	5.92	5.24	3.72	0.93	-0.29	-0.49	0.38

Table E-48: Lateral Forces After Tamping (4-Car Train) – S2 Up

21 Jul 2015: Pretoria to Hatfield (Up) km 3.175 (Site 2)		km/h										
		11.01	20.39	29.80	39.92	49.68	59.45	69.57	79.66	90.09	99.10	104.24
Car Type	Rail Leg	Lateral Force (t)										
4 Car Train	HL	2.53	2.82	3.15	2.71	3.77	3.83	1.87	-2.16	-0.83	1.71	5.81
	LL	28.48	28.48	27.63	26.01	24.73	22.75	17.70	5.34	0.34	-1.10	0.88

© University of Pretoria

APPENDIX F. MAXIMUM AND MINIMUM TRAIN TO RAIL FORCE POSITIONS

From Figure 4.4**,** Table F-1 and Table F-2 could be drawn up to provide details as to where on the 4-car train the maximum and minimum rail forces occur. Table F-3 and Table F-4 could also be drawn up to provide details as to which wheels (W) on which axles (A) make up which bogies (leading or trailing) on each car. Whether the bogie on any particular car is leading or trailing depends on the direction of the travel of the train.

Table F-1: Summary of Down Direction Analysed Wheels (Figure 4.4)

	SITE 1 & 2: DOWN	Before & After Tamping				
		Wheel	Car Position	Axle	Axle Position	Bogie Position
Verticals	High Leg Max	DMOS B 8	1st Car	1	Leading Axle	Leading Bogie
	Low Leg Max	DMOS B 1	1st Car	1	Leading Axle	Leading Bogie
	High Leg Min	PTOS 3	2nd Car	3	Trailing Axle	Leading Bogie
	Low Leg Min	MOS 5	3rd Car	4	Leading Axle	Leading Bogie
Laterals	High Leg Max	DMOS A 4	4th Car	4	Leading Axle	Leading Bogie
	Low Leg Max	DMOS A 7	4th Car	2	Leading Axle	Trailing Bogie
	High Leg Min	DMOS B 7	1st Car	2	Trailing Axle	Leading Bogie
	Low Leg Min	PTOS 8	2nd Car	1	Trailing Axle	Trailing Bogie

Table F-2: Summary of Up Direction Analysed Wheels (Figure 4.4)

	SITE 1 & 2: UP	Before & After Tamping				
		Wheel	Car Position	Axle	Axle Position	Bogie Position
Verticals	High Leg Max	DMOS B 8	4th Car	1	Trailing Axle	Trailing Bogie
	Low Leg Max	DMOS B 2	4th Car	2	Leading Axle	Trailing Bogie
	High Leg Min	PTOS 3	3rd Car	3	Leading Axle	Trailing Bogie
	Low Leg Min	MOS 5	2nd Car	4	Trailing Axle	Trailing Bogie
Laterals	High Leg Max	DMOS A 1	1st Car	1	Leading Axle	Leading Bogie
	Low Leg Max	DMOS A 8	1st Car	1	Leading Axle	Leading Bogie
	High Leg Min	DMOS A 2	1st Car	2	Trailing Axle	Leading Bogie
	Low Leg Min	MOS 5	2nd Car	4	Trailing Axle	Trailing Bogie

© University of Pretoria

Table F-3: Summary of Down Direction Analysed Bogies (Figure 4.4)

DOWN	Leading Bogie		Trailing Bogie	
	High Leg	Low Leg	High Leg	Low Leg
DMOS B	A1W8 & A2W7	A1W1 & A2W2	A3W6 & A4W5	A3W3 & A4W4
PTOS	A4W4 & A3W3	A4W5 & A3W6	A2W2 & A1W1	A2W7 & A1W8
MOS	A4W4 & A3W3	A4W5 & A3W6	A2W2 & A1W1	A2W7 & A1W8
DMOS A	A4W4 & A3W3	A4W5 & A3W6	A2W2 & A1W1	A2W7 & A1W8

Table F-4: Summary of Up Direction Analysed Bogies (Figure 4.4)

UP	Leading Bogie		Trailing Bogie	
	High Leg	Low Leg	High Leg	Low Leg
DMOS A	A1W1 & A2W2	A1W8 & A2W7	A3W3 & A4W4	A3W6 & A4W5
MOS	A1W1 & A2W2	A1W8 & A2W7	A3W3 & A4W4	A3W6 & A4W5
PTOS	A1W1 & A2W2	A1W8 & A2W7	A3W3 & A4W4	A3W6 & A4W5
DMOS B	A4W5 & A3W6	A4W4 & A3W3	A2W7 & A1W8	A2W2 & A1W1

© University of Pretoria

APPENDIX G. CURVE RAIL FORCES TRENDS FOR BOGIES

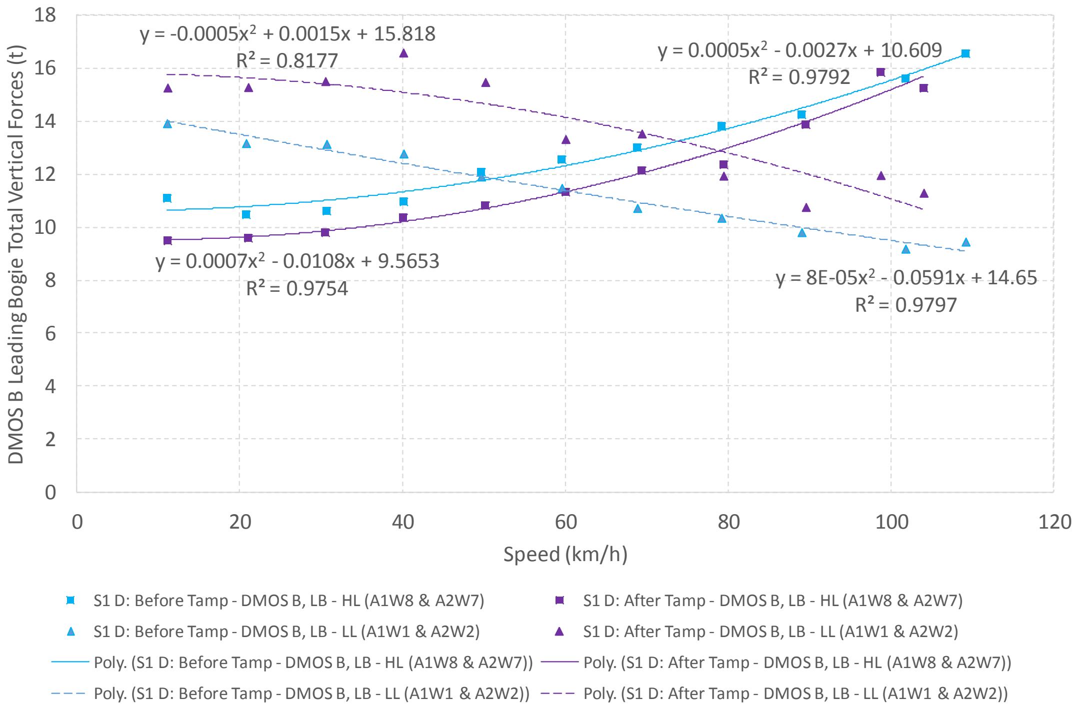

Figure G-1: Vertical Forces (DMOS B Leading Bogie) – S1 Down

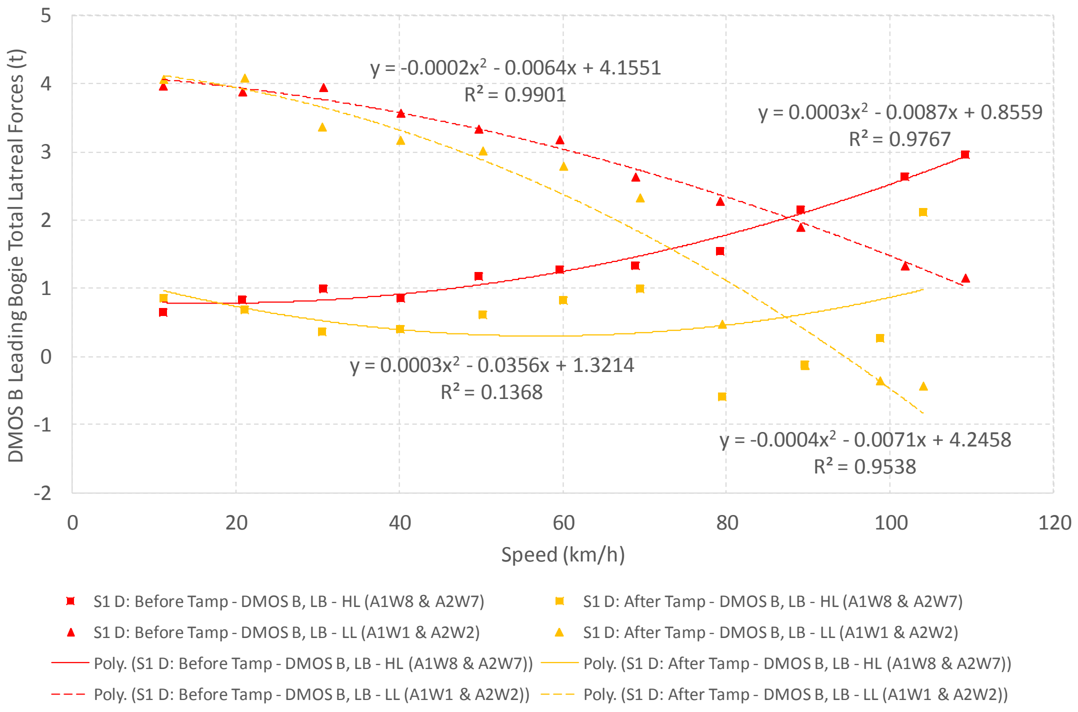

Figure G-2: Lateral Forces (DMOS B Leading Bogie) – S1 Down

© University of Pretoria

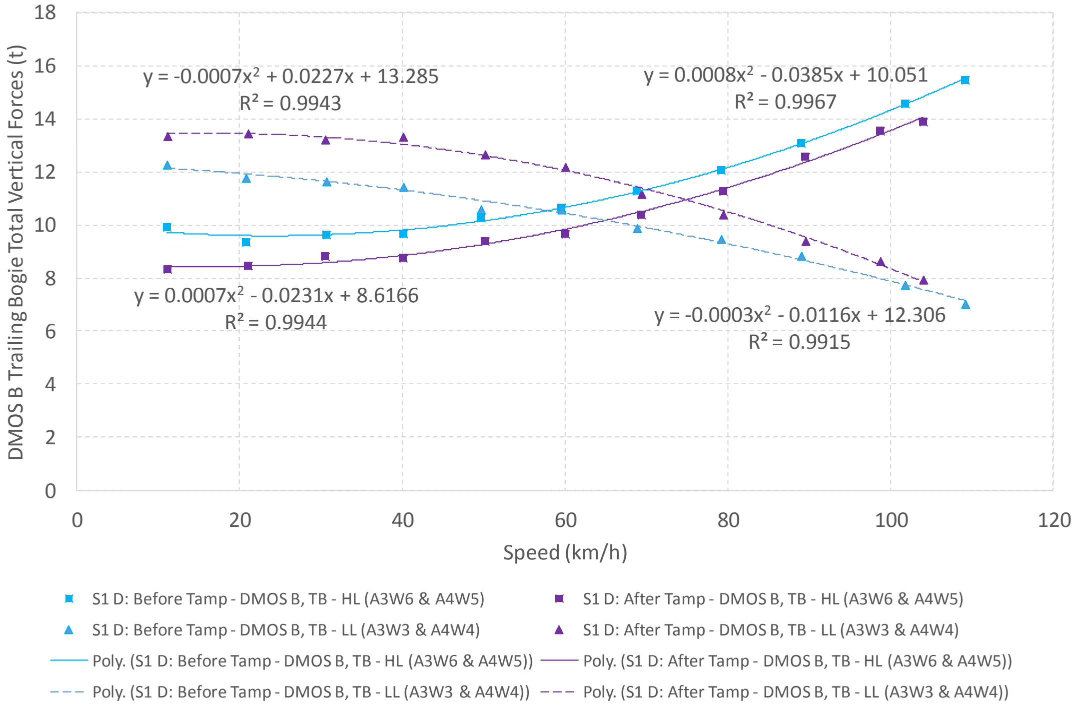

Figure G-3: Vertical Forces (DMOS B Trailing Bogie) – S1 Down

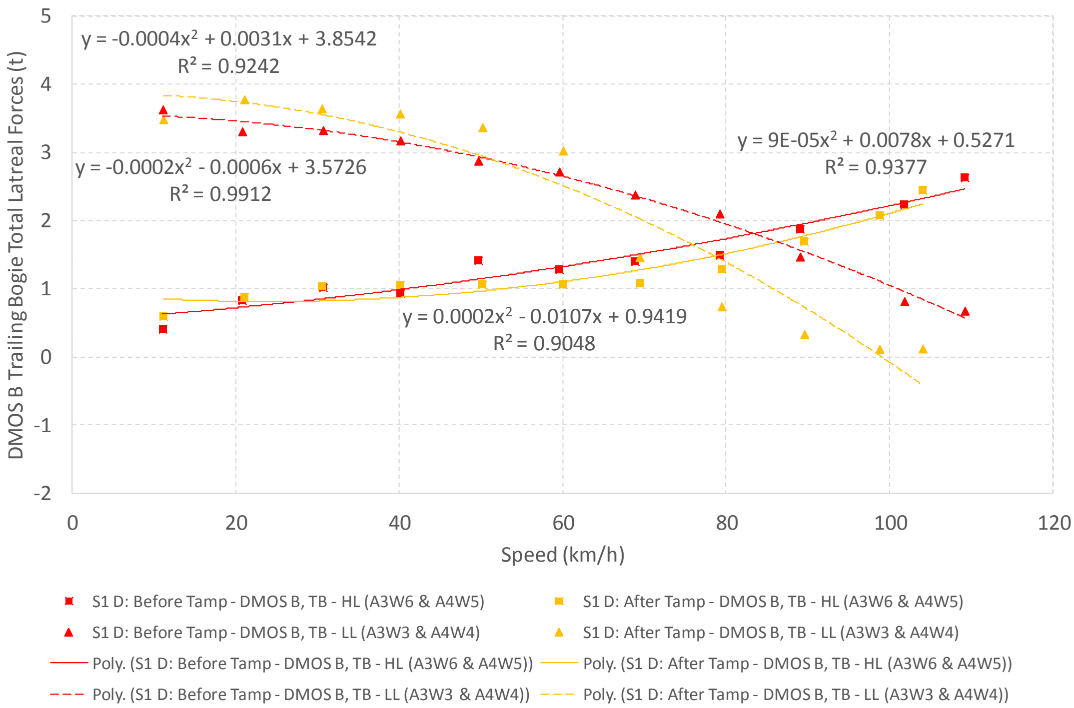

Figure G-4: Lateral Forces (DMOS B Trailing Bogie) – S1 Down

© University of Pretoria

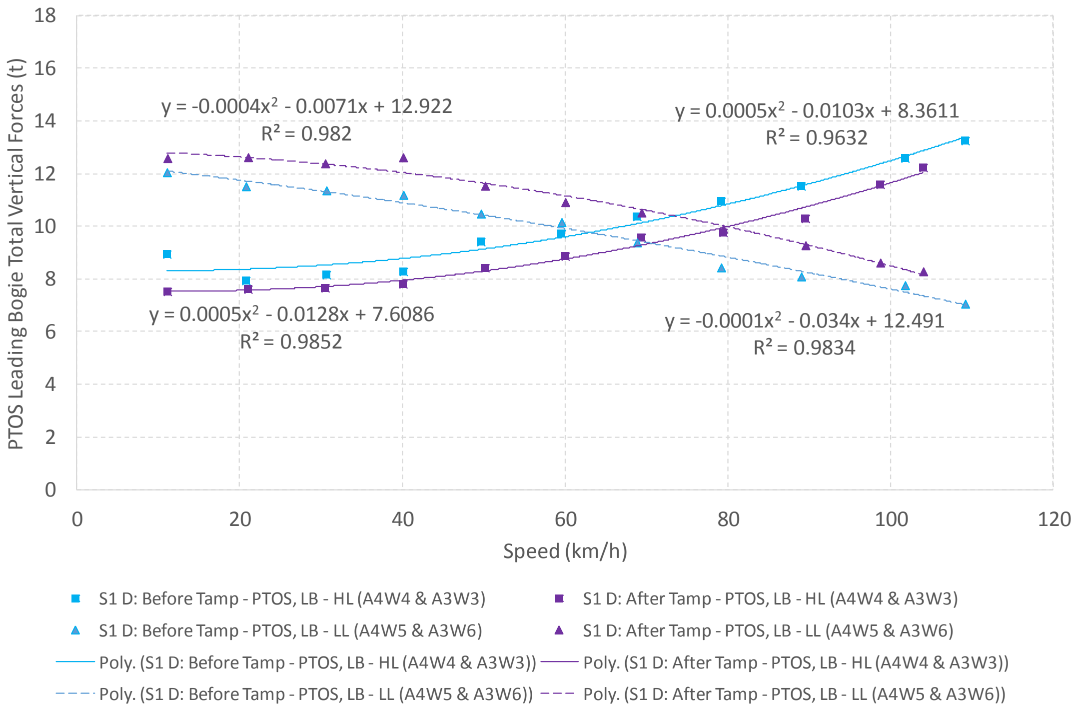

Figure G-5: Vertical Forces (PTOS Leading Bogie) – S1 Down

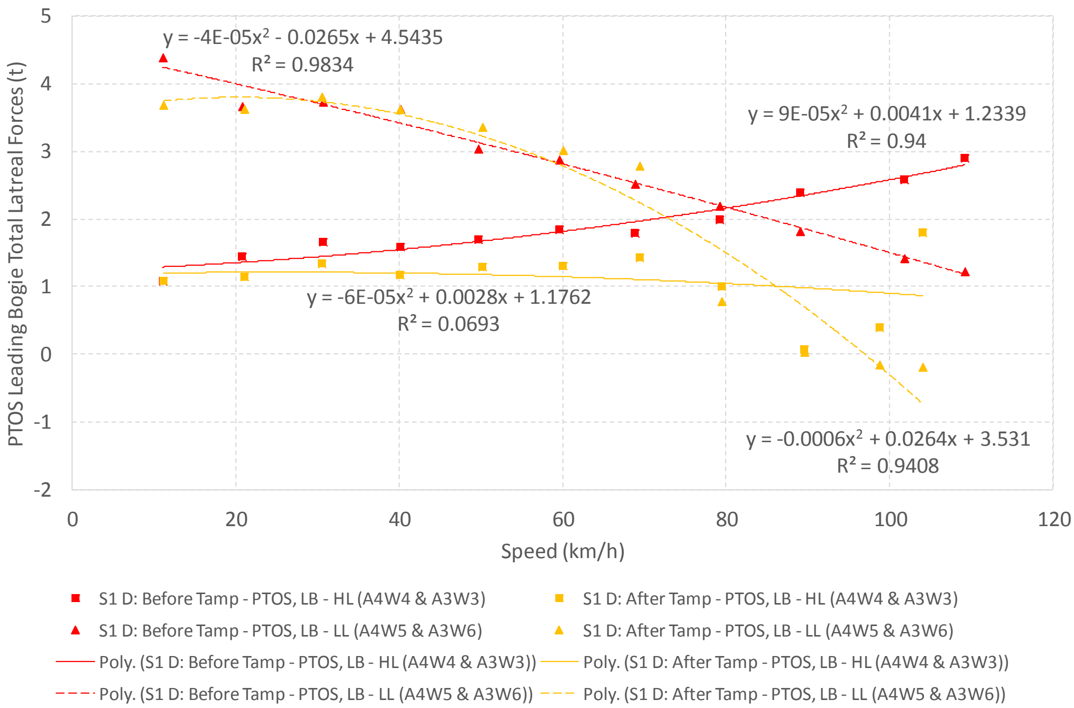

Figure G-6: Lateral Forces (PTOS Leading Bogie) – S1 Down

© University of Pretoria

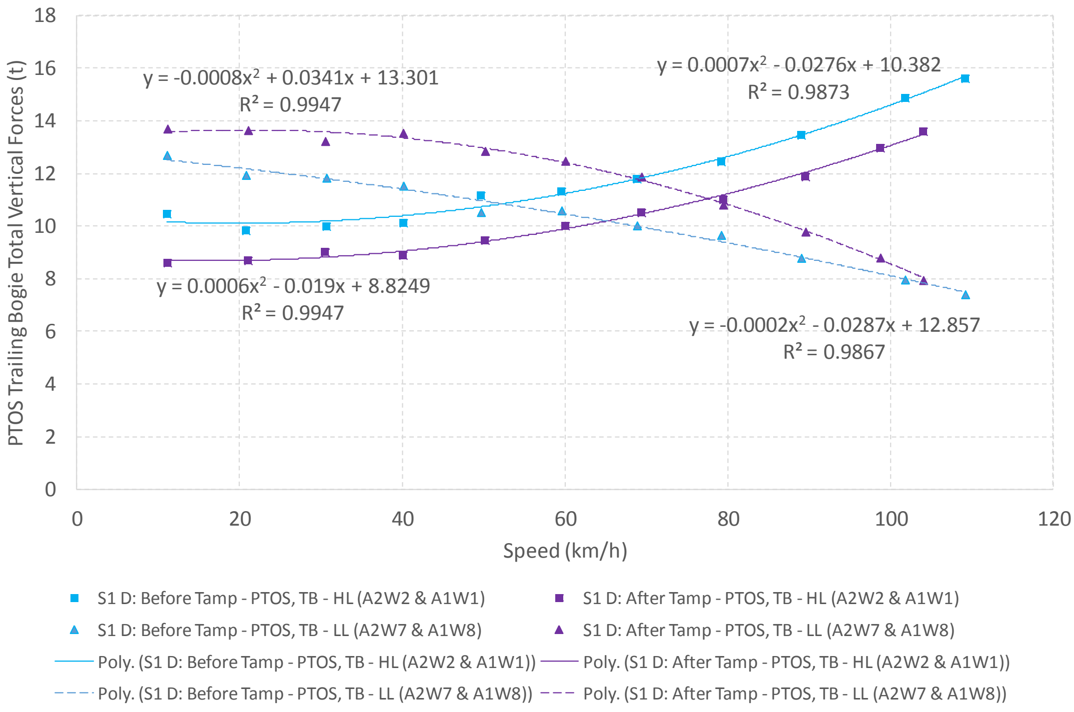

Figure G-7: Vertical Forces (PTOS Trailing Bogie) – S1 Down

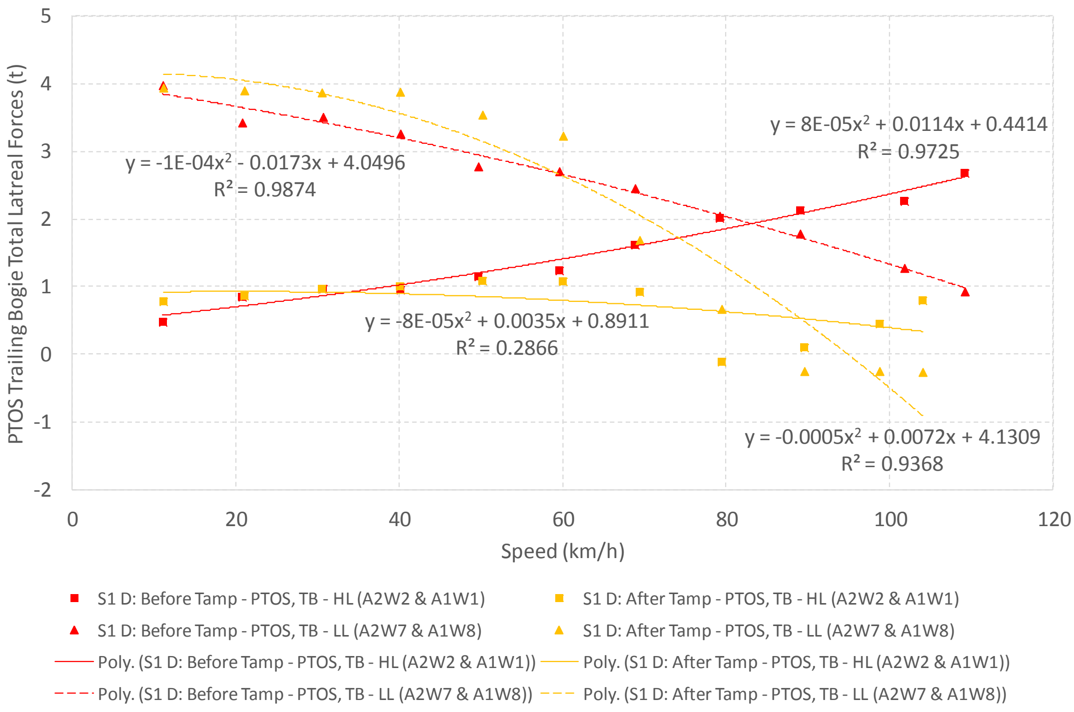

Figure G-8: Lateral Forces (PTOS Trailing Bogie) – S1 Down

© University of Pretoria

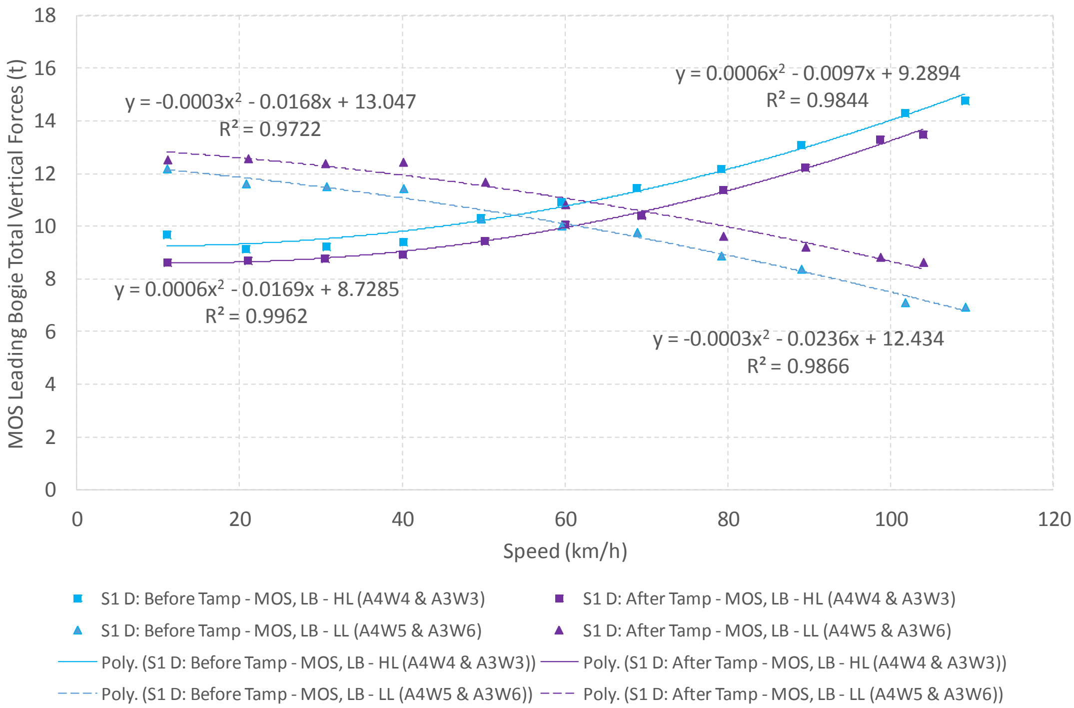

Figure G-9: Vertical Forces (MOS Leading Bogie) – S1 Down

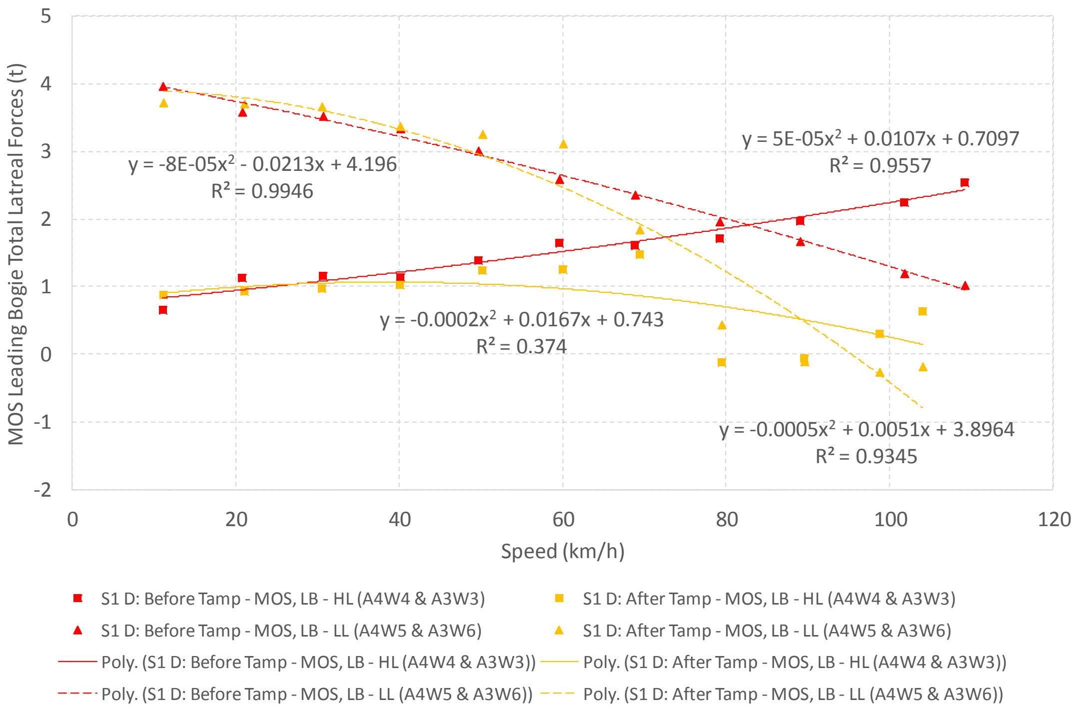

Figure G-10: Lateral Forces (MOS Leading Bogie) – S1 Down

© University of Pretoria

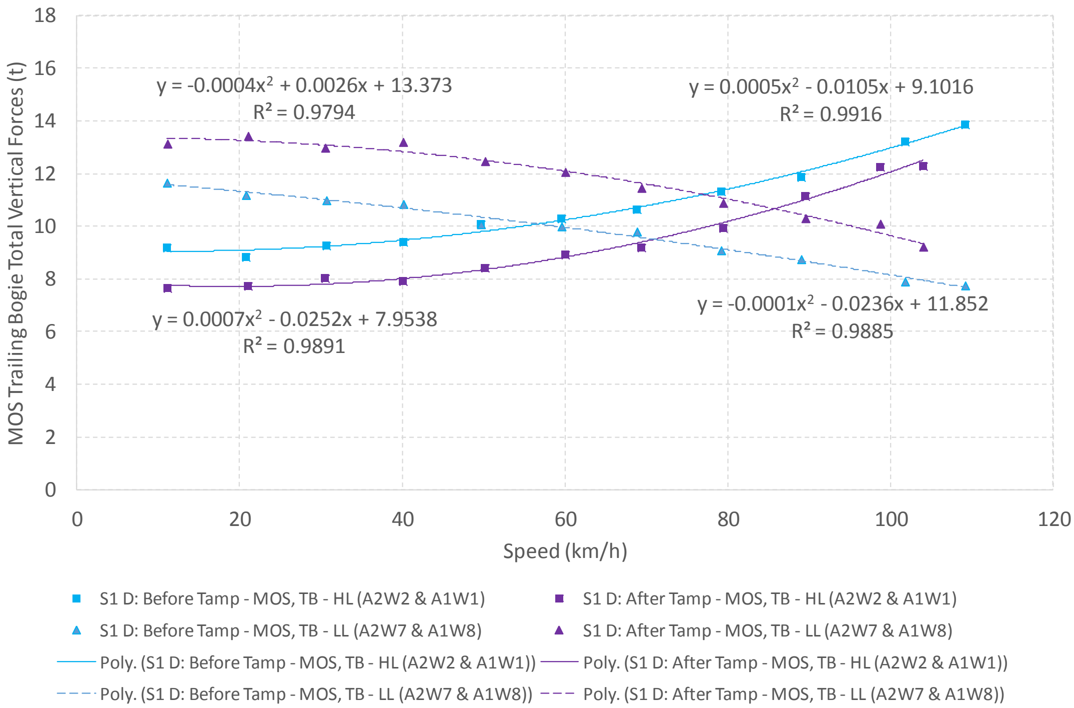

Figure G-11: Vertical Forces (MOS Trailing Bogie) – S1 Down

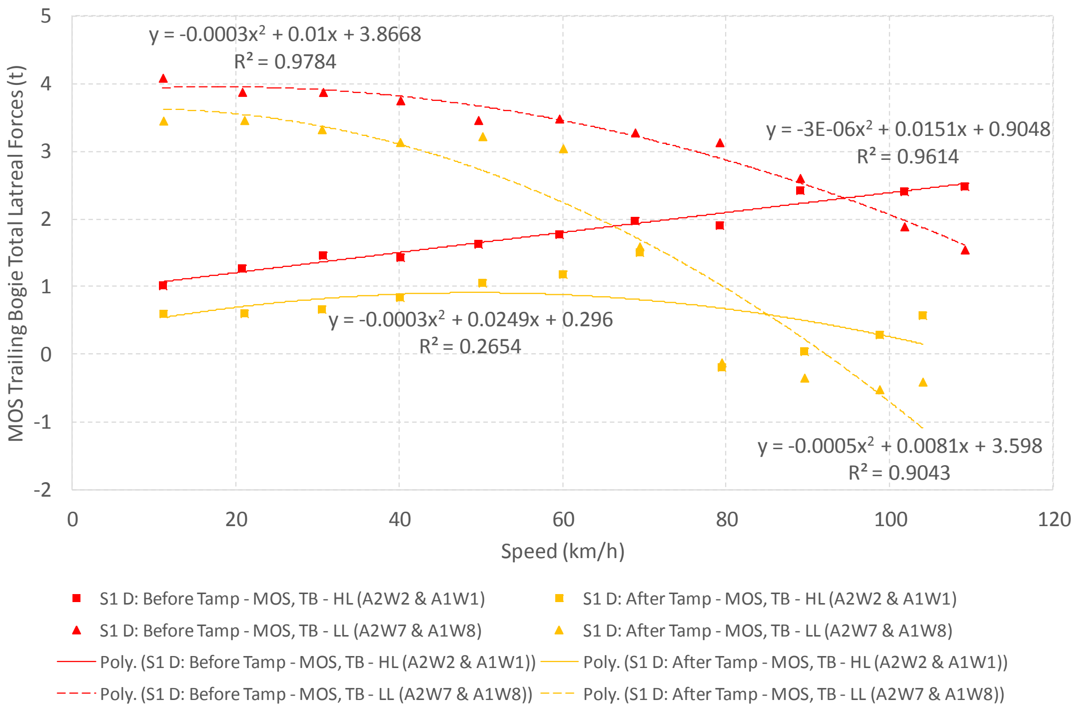

Figure G-12: Lateral Forces (MOS Trailing Bogie) – S1 Down

© University of Pretoria

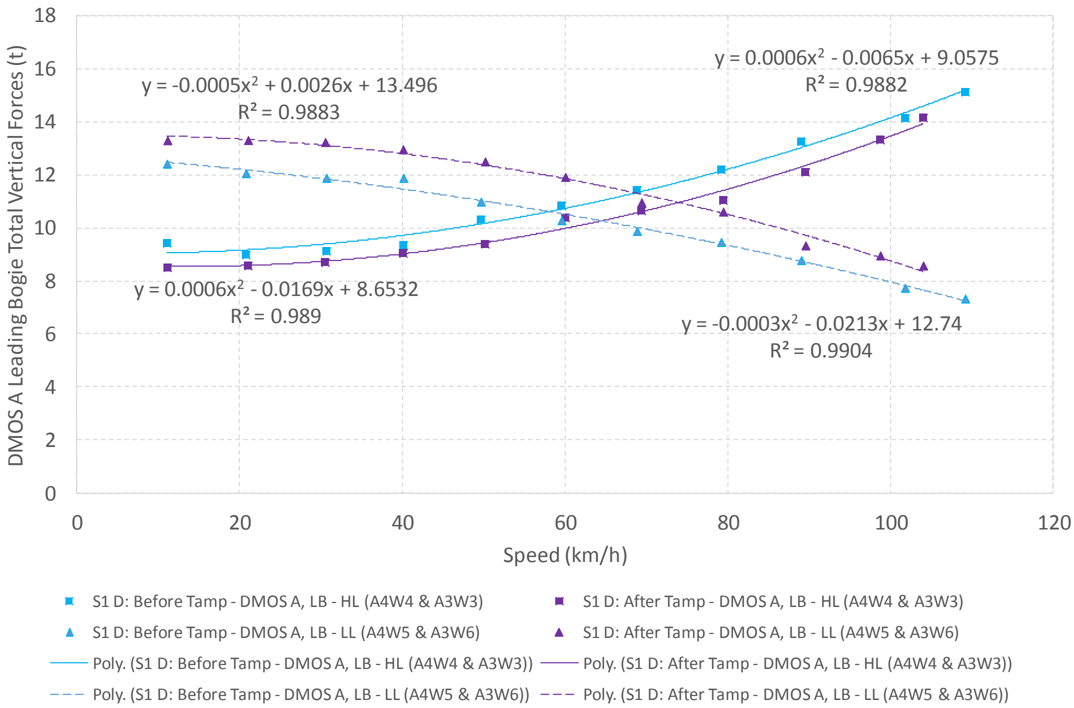

Figure G-13: Vertical Forces (DMOS A Leading Bogie) – S1 Down

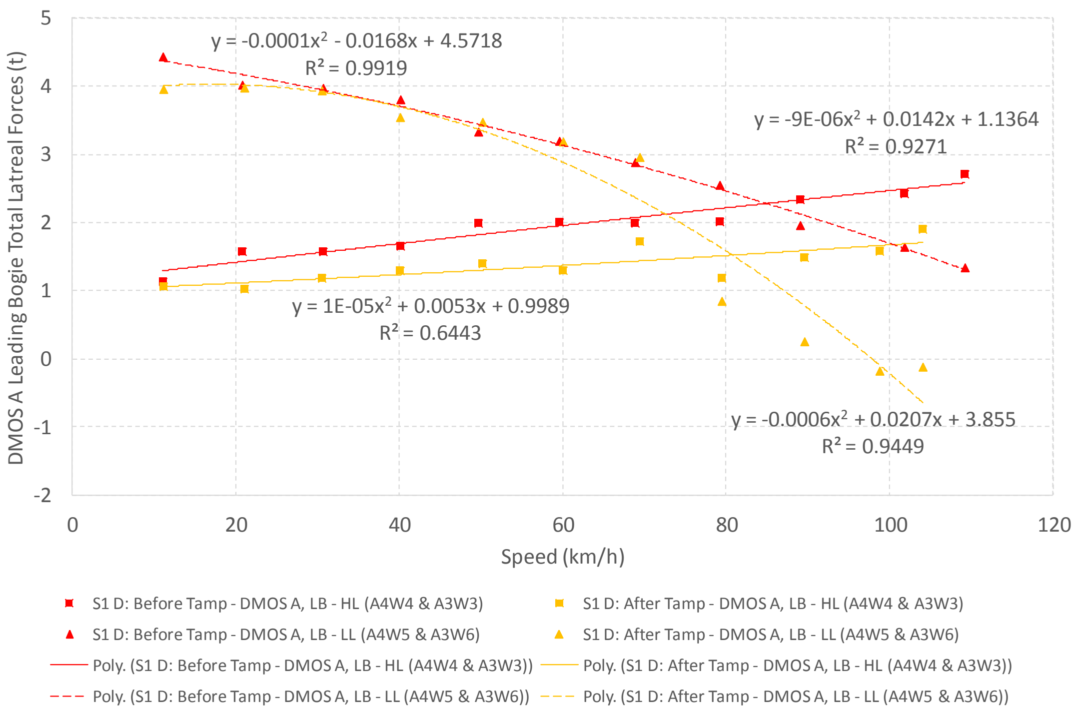

Figure G-14: Lateral Forces (DMOS A Leading Bogie) – S1 Down

© University of Pretoria

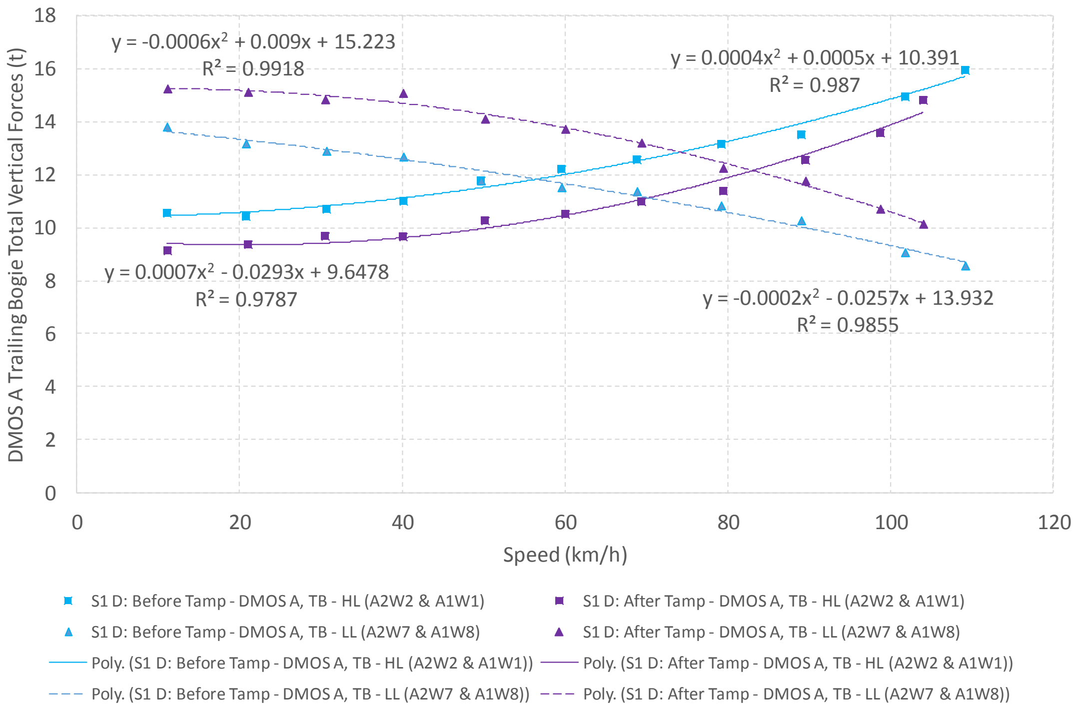

Figure G-15: Vertical Forces (DMOS A Trailing Bogie) – S1 Down

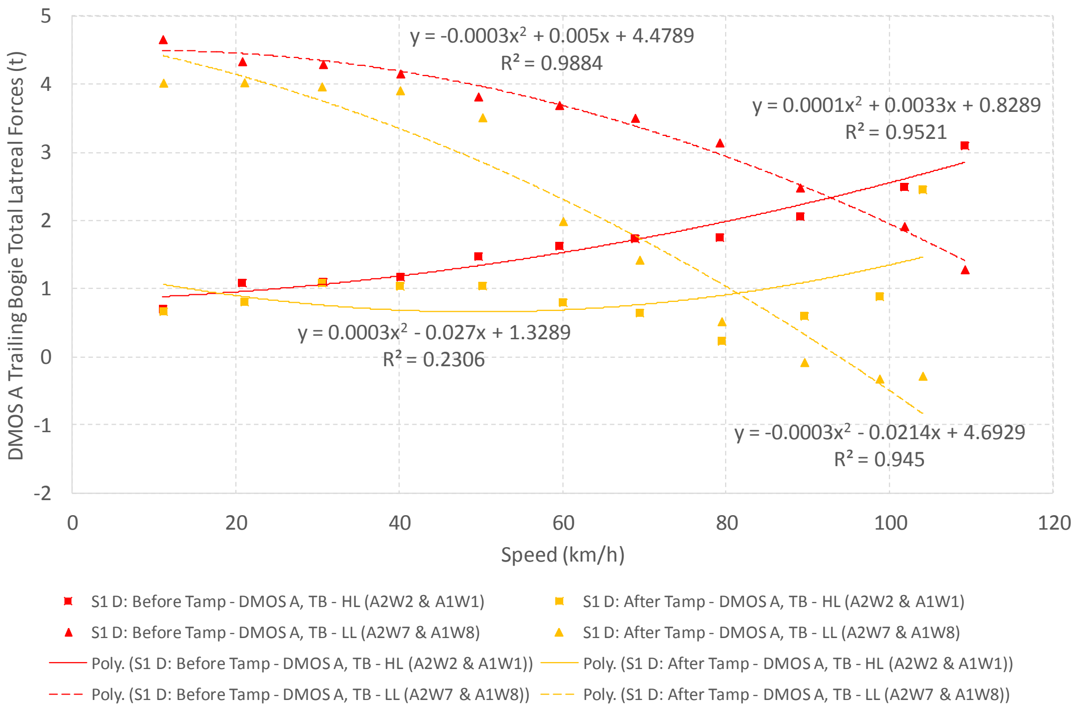

Figure G-16: Lateral Forces (DMOS A Trailing Bogie) – S1 Down

© University of Pretoria

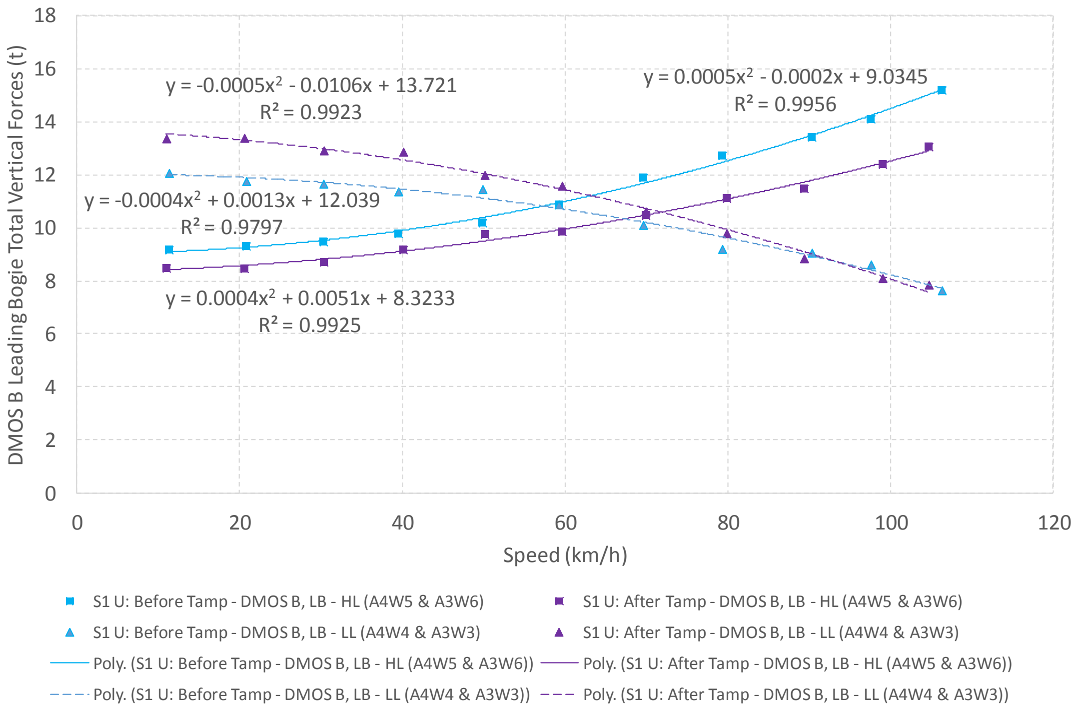

Figure G-17: Vertical Forces (DMOS B Leading Bogie) – S1 Up

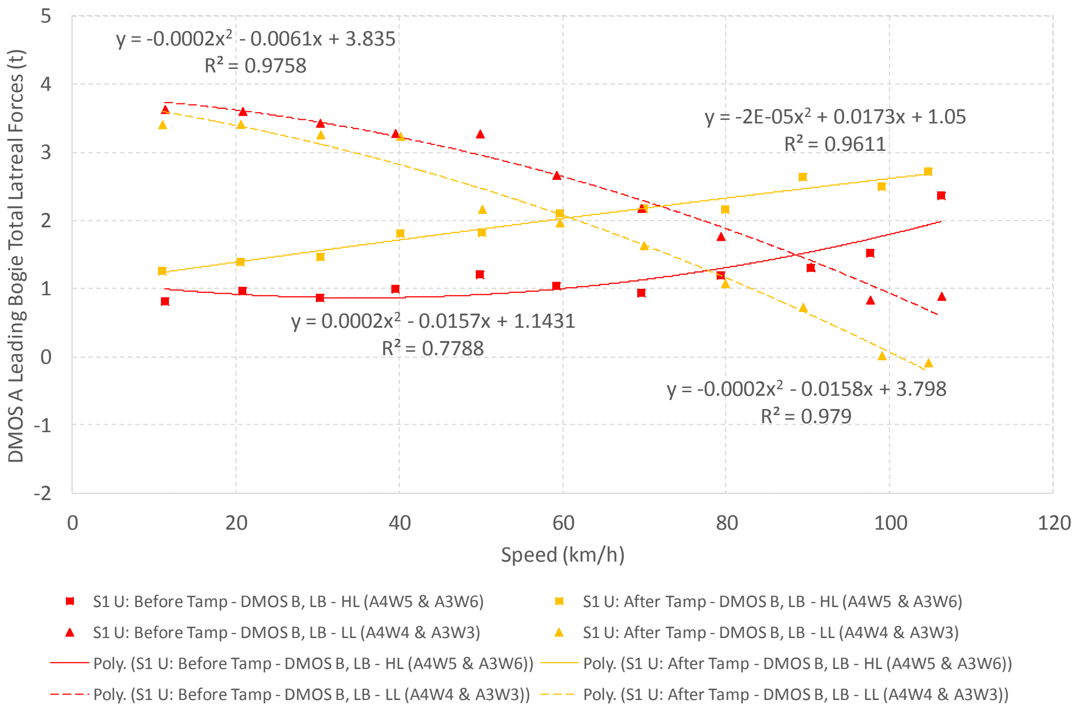

Figure G-18: Lateral Forces (DMOS B Leading Bogie) – S1 Up

© University of Pretoria

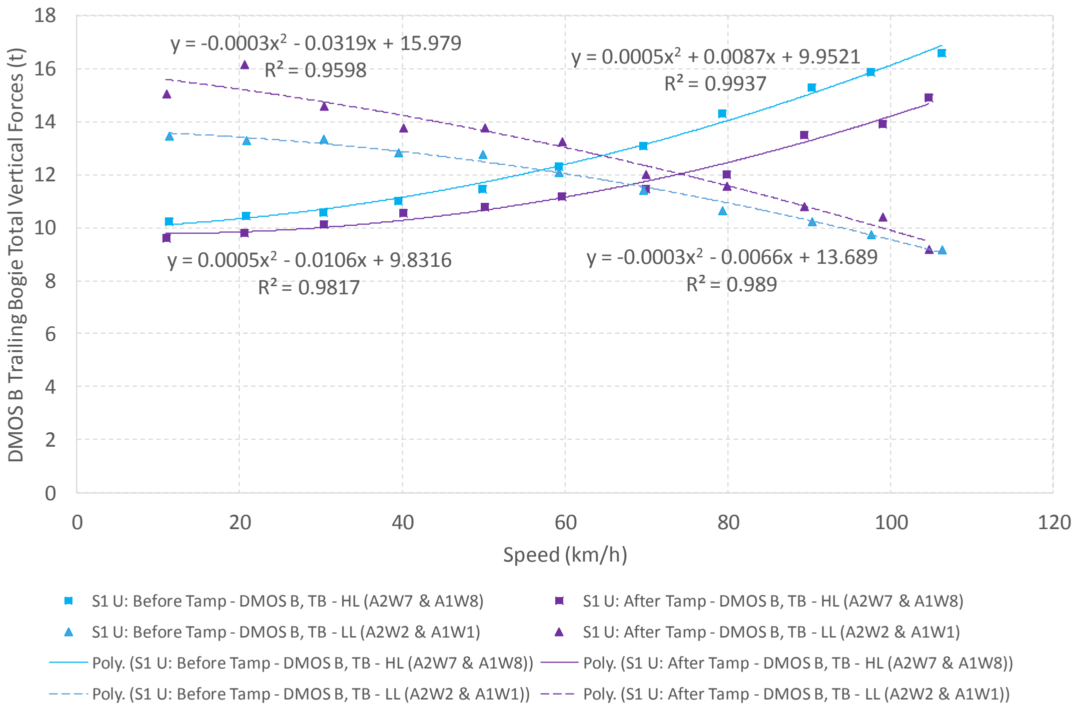

Figure G-19: Vertical Forces (DMOS B Trailing Bogie) – S1 Up

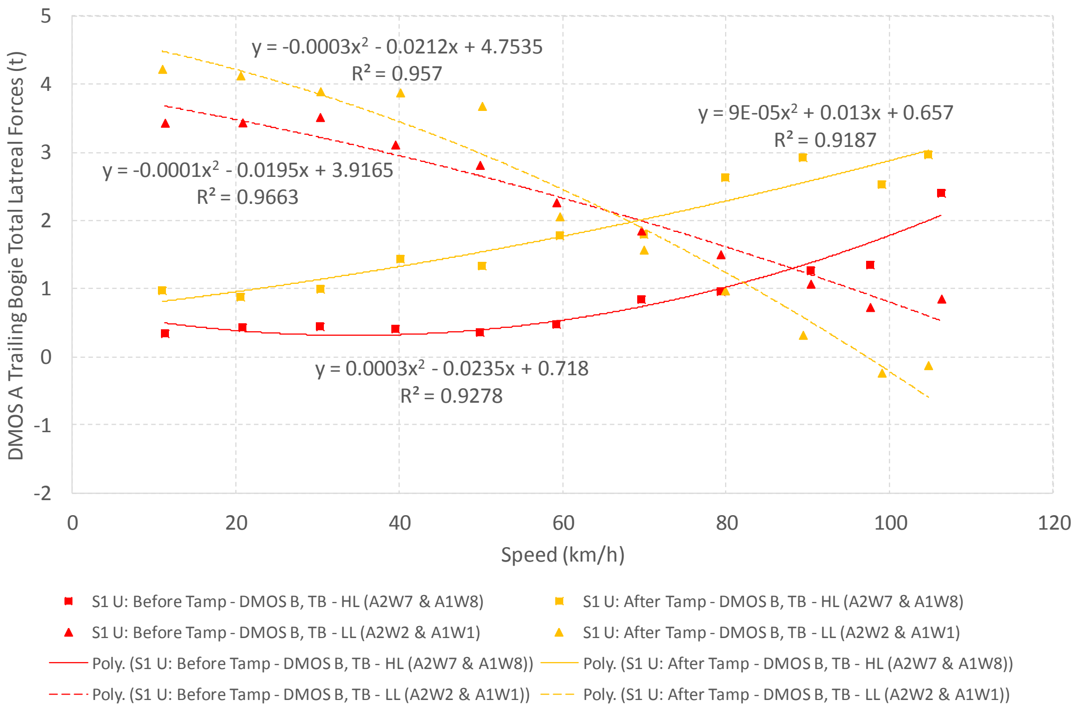

Figure G-20: Lateral Forces (DMOS B Trailing Bogie) – S1 Up

© University of Pretoria

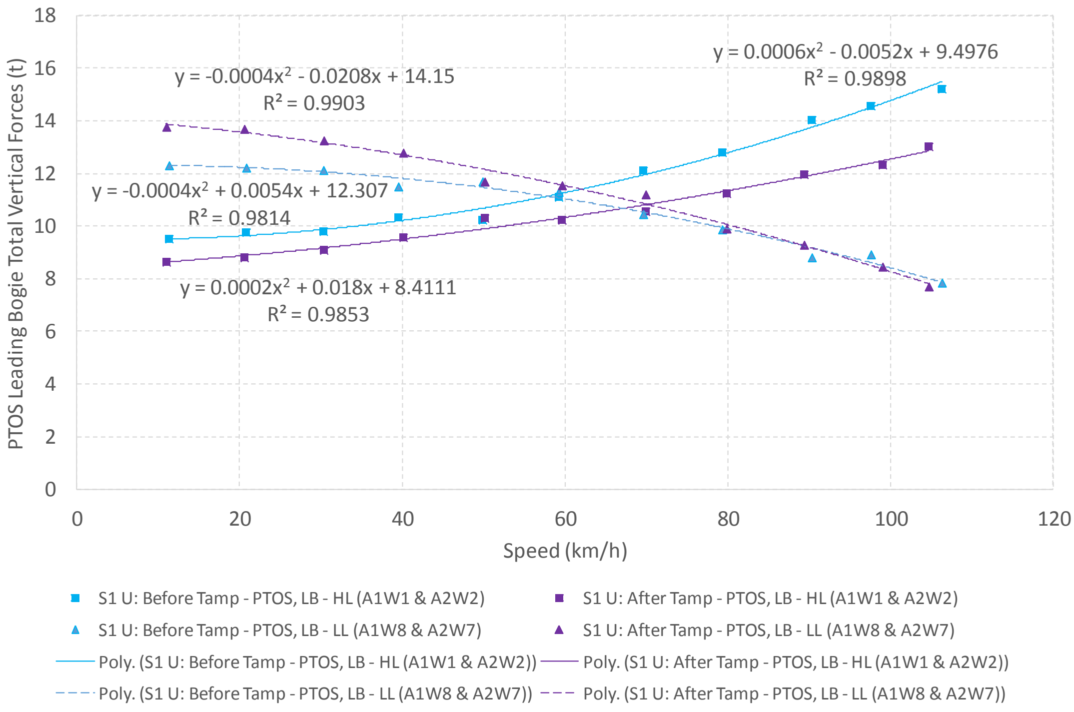

Figure G-21: Vertical Forces (PTOS Leading Bogie) – S1 Up

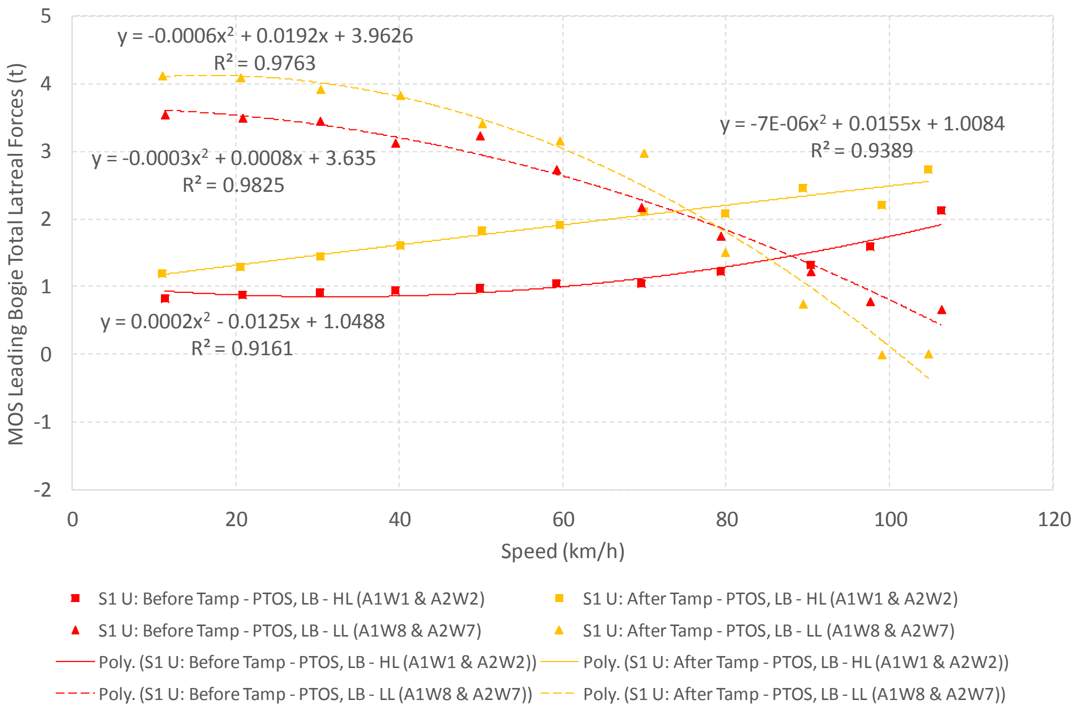

Figure G-22: Lateral Forces (PTOS Leading Bogie) – S1 Up

© University of Pretoria

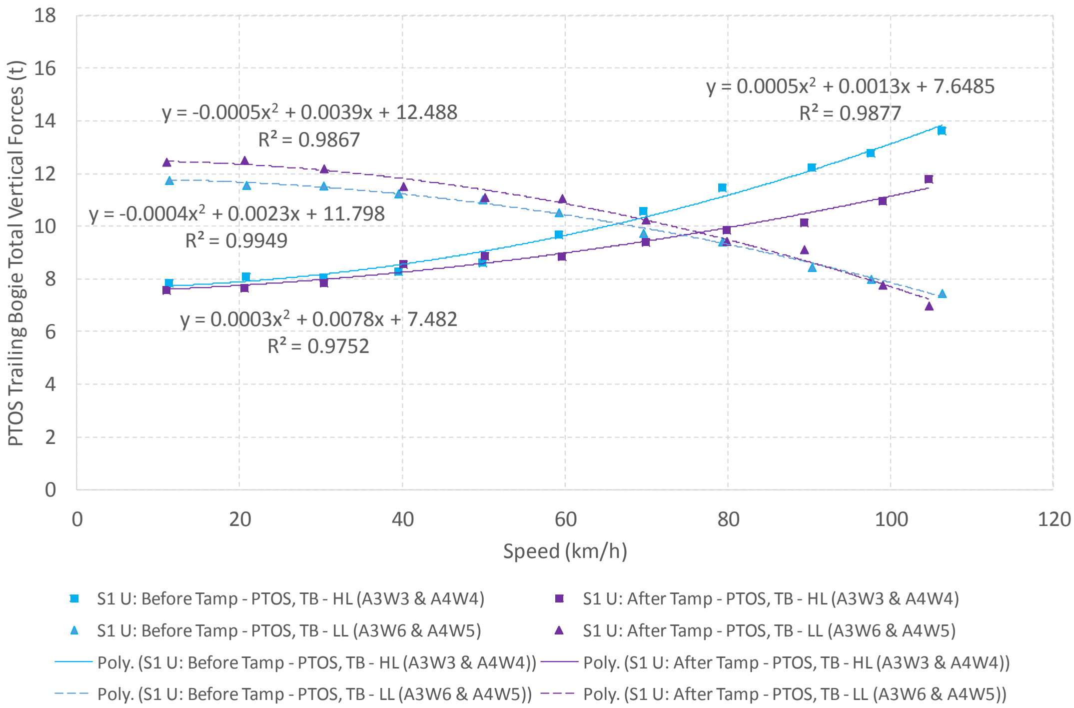

Figure G-23: Vertical Forces (PTOS Trailing Bogie) – S1 Up

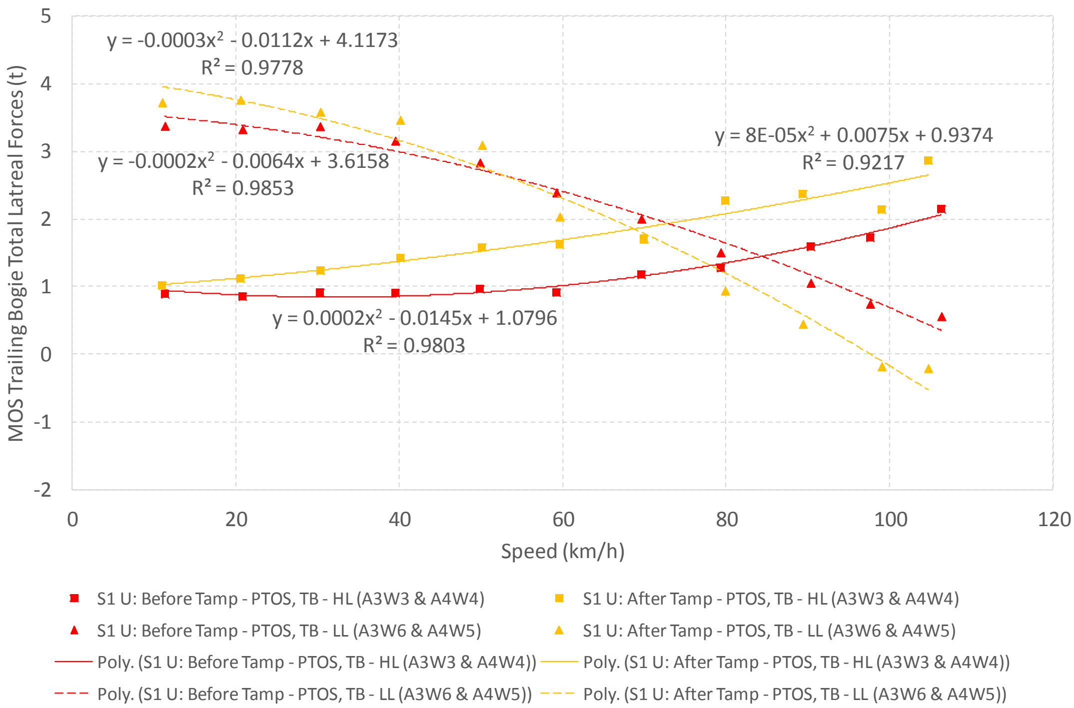

Figure G-24: Lateral Forces (PTOS Trailing Bogie) – S1 Up

© University of Pretoria

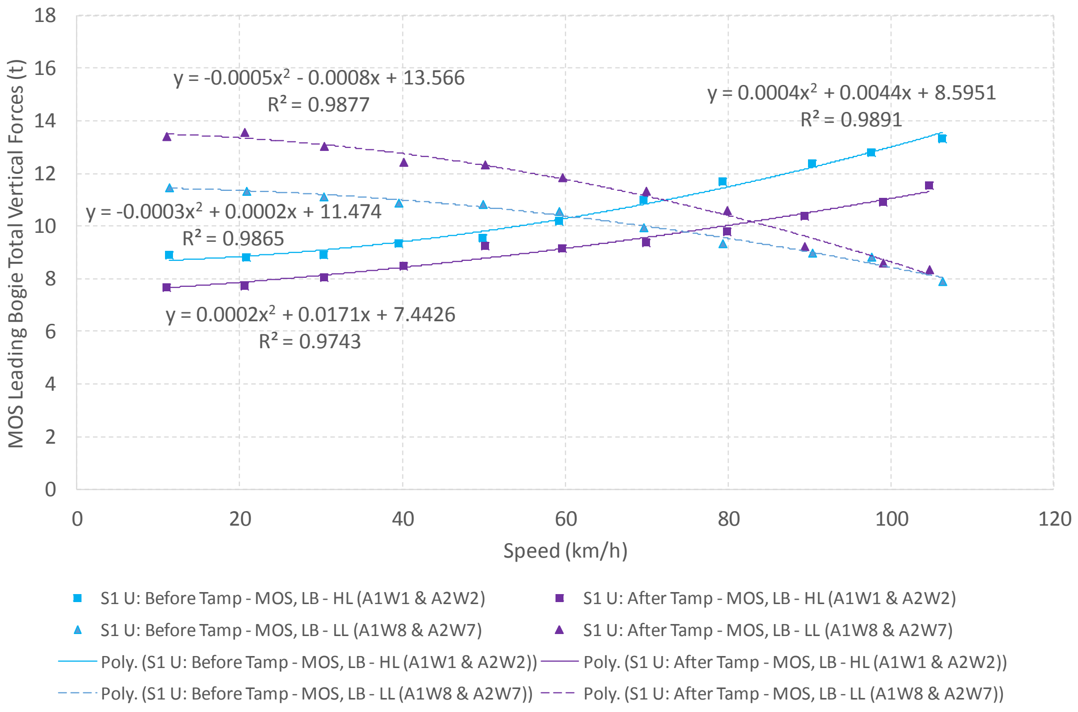

Figure G-25: Vertical Forces (MOS Leading Bogie) – S1 Up

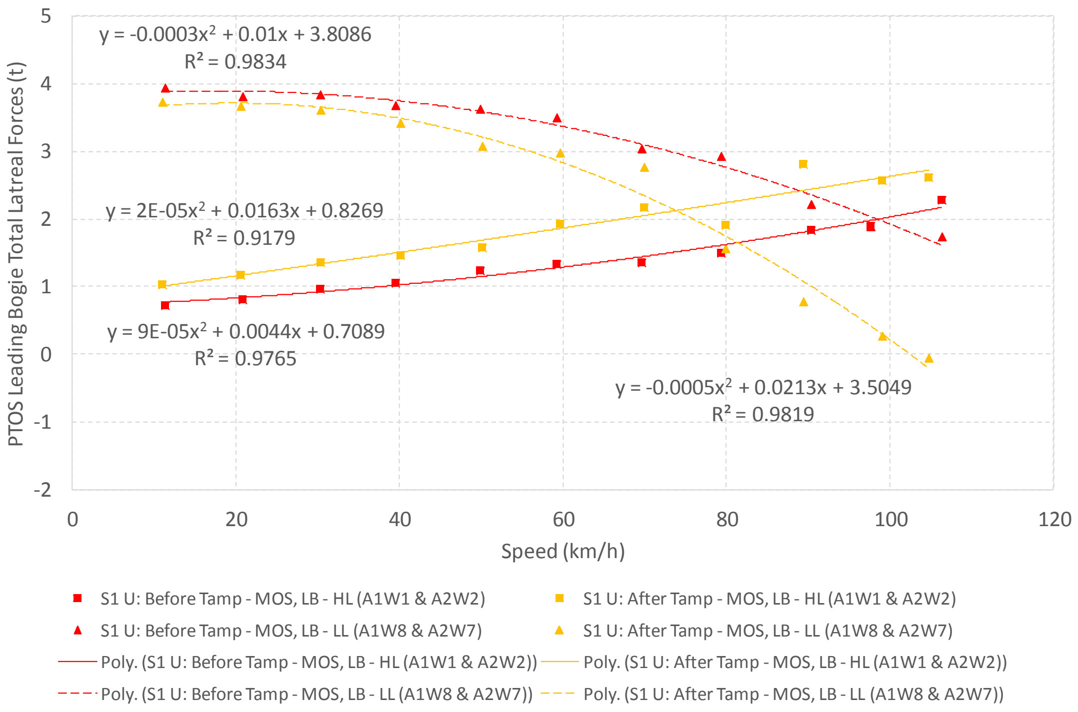

Figure G-26: Lateral Forces (MOS Leading Bogie) – S1 Up

© University of Pretoria

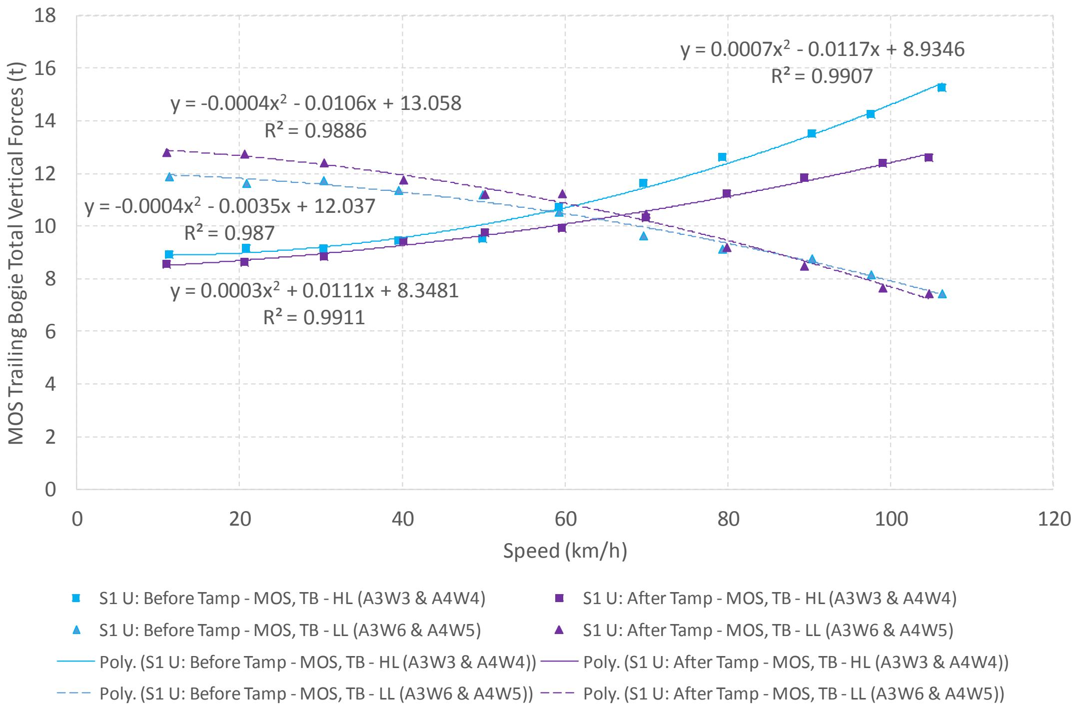

Figure G-27: Vertical Forces (MOS Trailing Bogie) – S1 Up

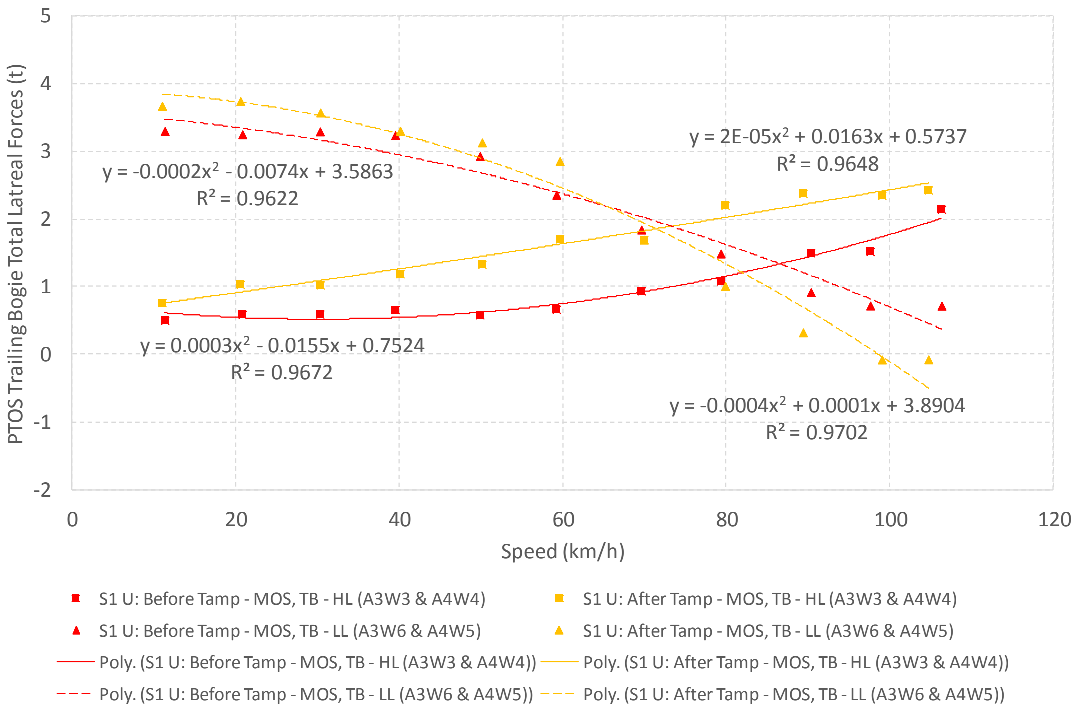

Figure G-28: Lateral Forces (MOS Trailing Bogie) – S1 Up

© University of Pretoria

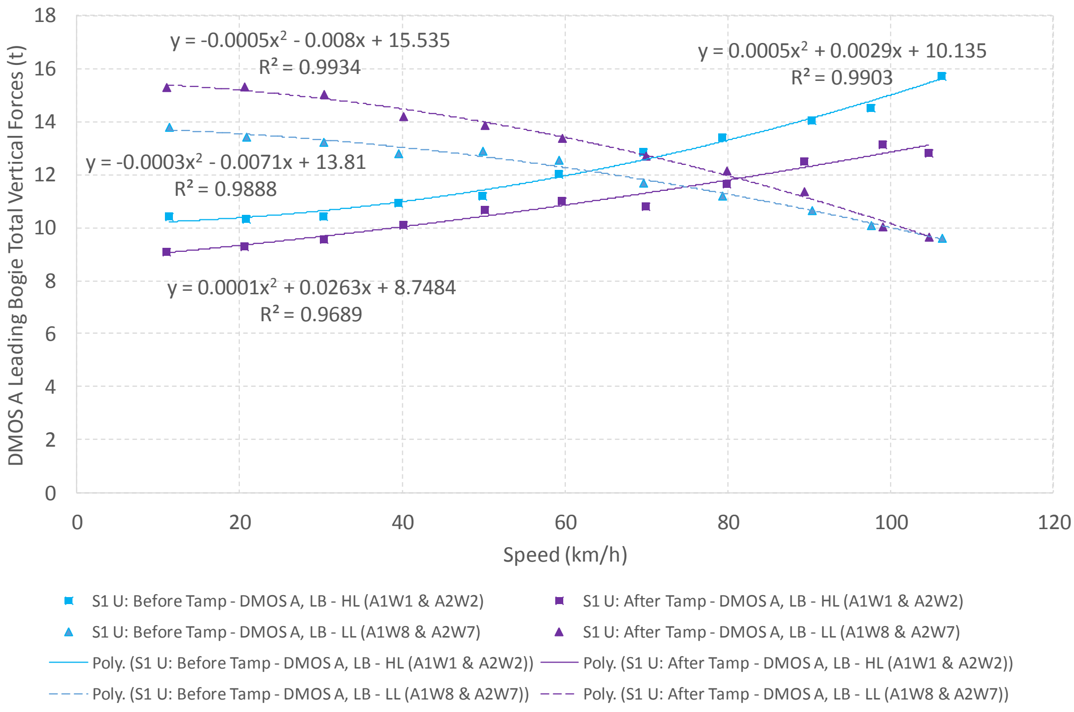

Figure G-29: Vertical Forces (DMOS A Leading Bogie) – S1 Up

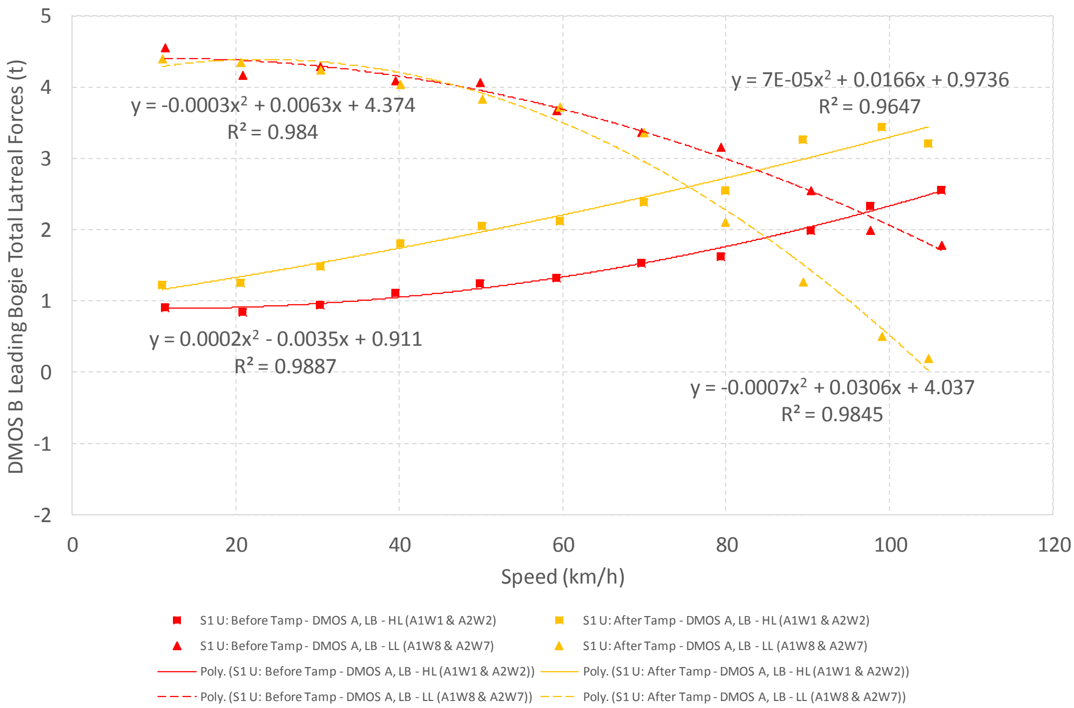

Figure G-30: Lateral Forces (DMOS A Leading Bogie) – S1 Up

© University of Pretoria

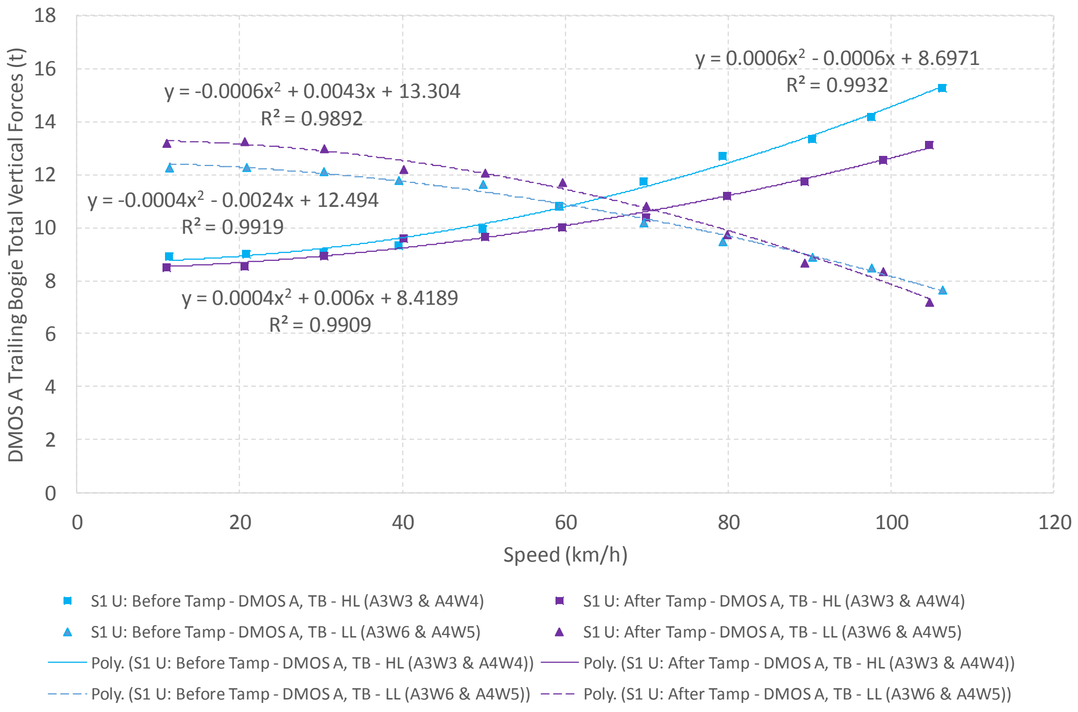

Figure G-31: Vertical Forces (DMOS A Trailing Bogie) – S1 Up

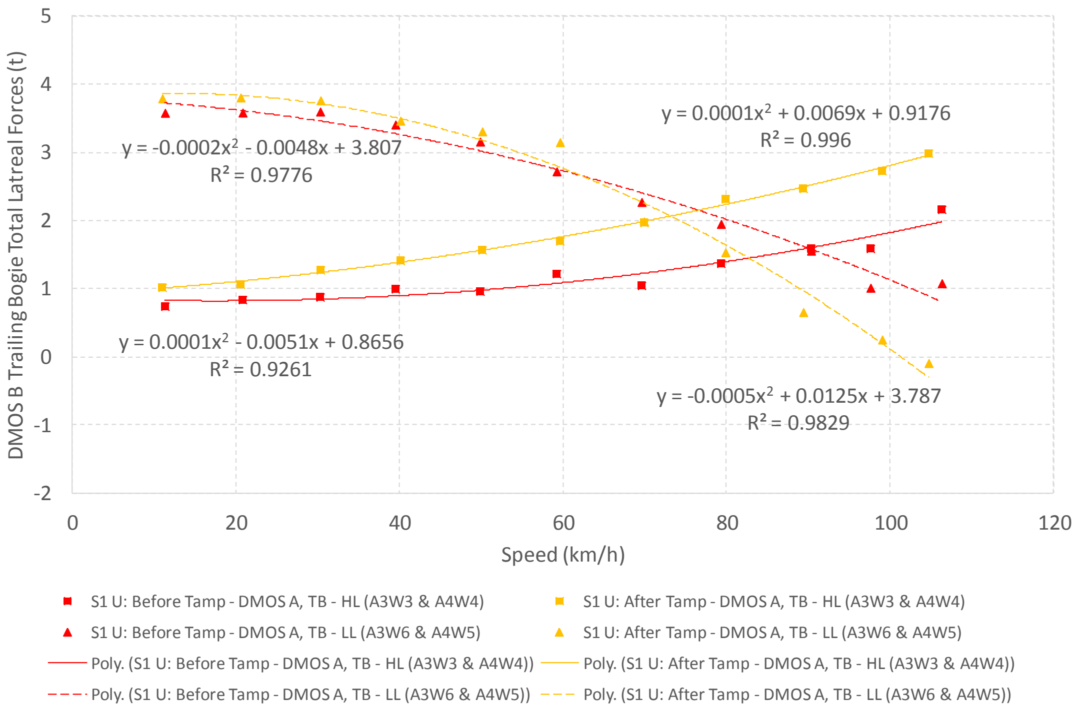

Figure G-32: Lateral Forces (DMOS A Trailing Bogie) – S1 Up

© University of Pretoria

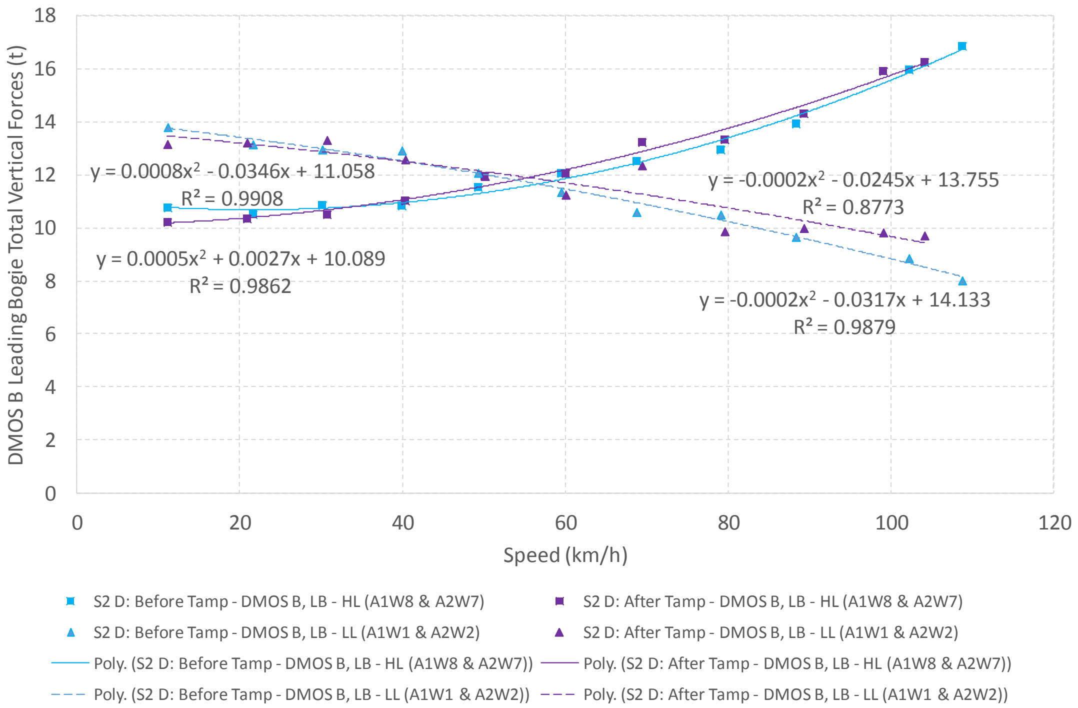

Figure G-33: Vertical Forces (DMOS B Leading Bogie) – S2 Down

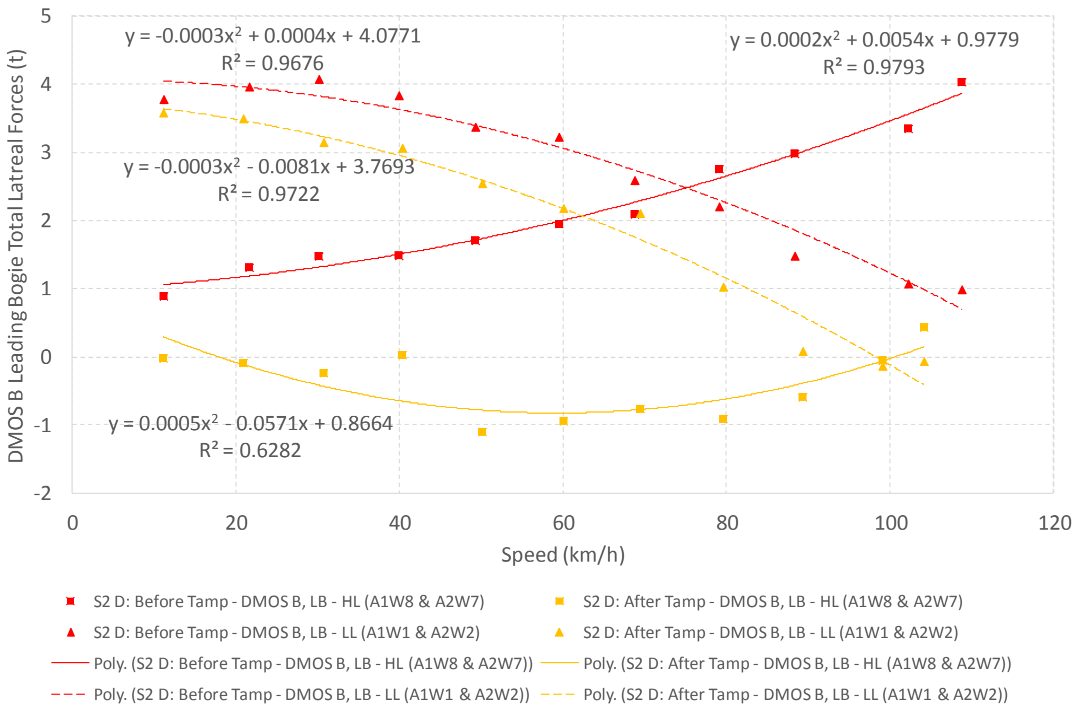

Figure G-34: Lateral Forces (DMOS B Leading Bogie) – S2 Down

© University of Pretoria

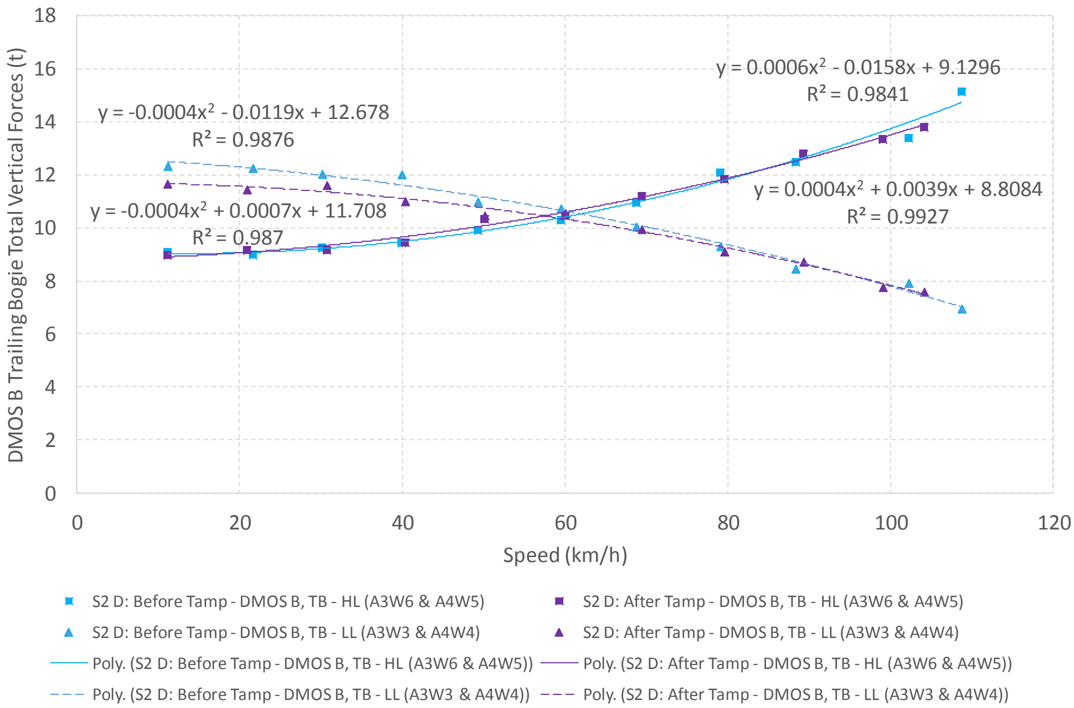

Figure G-35: Vertical Forces (DMOS B Trailing Bogie) – S2 Down

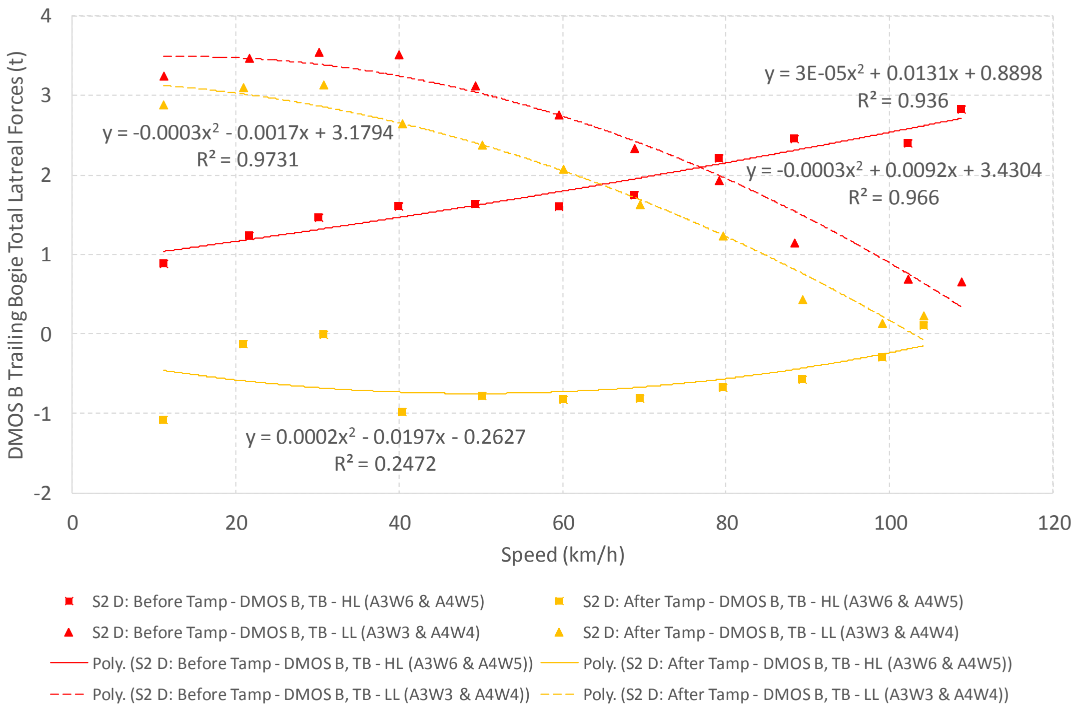

Figure G-36: Lateral Forces (DMOS B Trailing Bogie) – S2 Down

© University of Pretoria

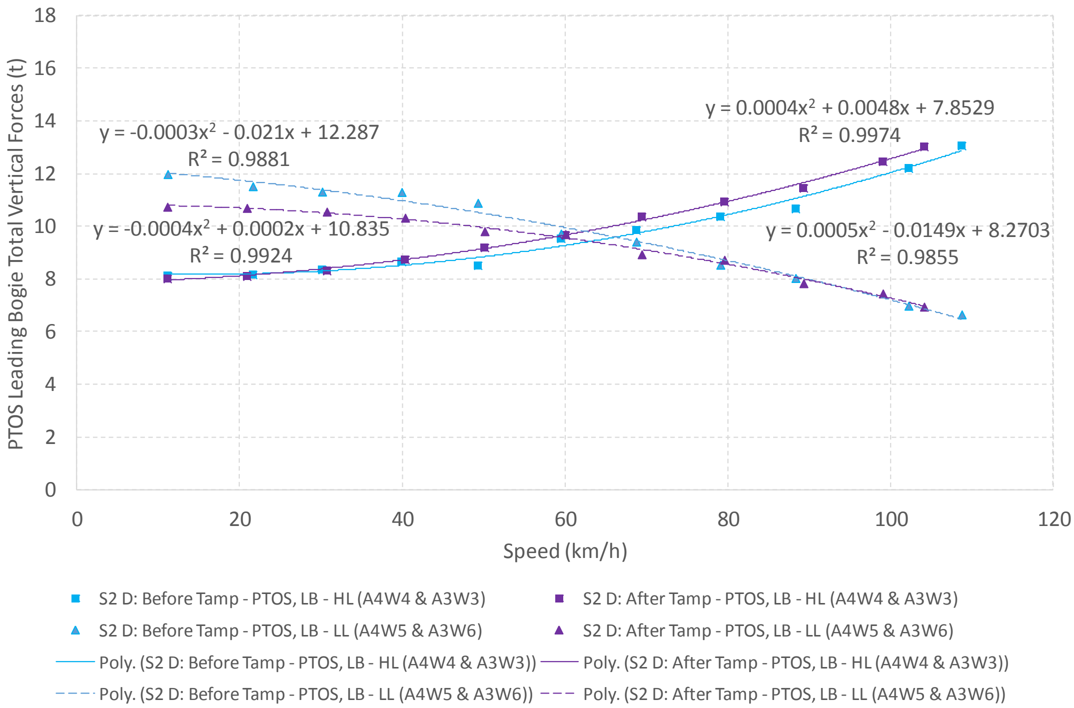

Figure G-37: Vertical Forces (PTOS Leading Bogie) – S2 Down

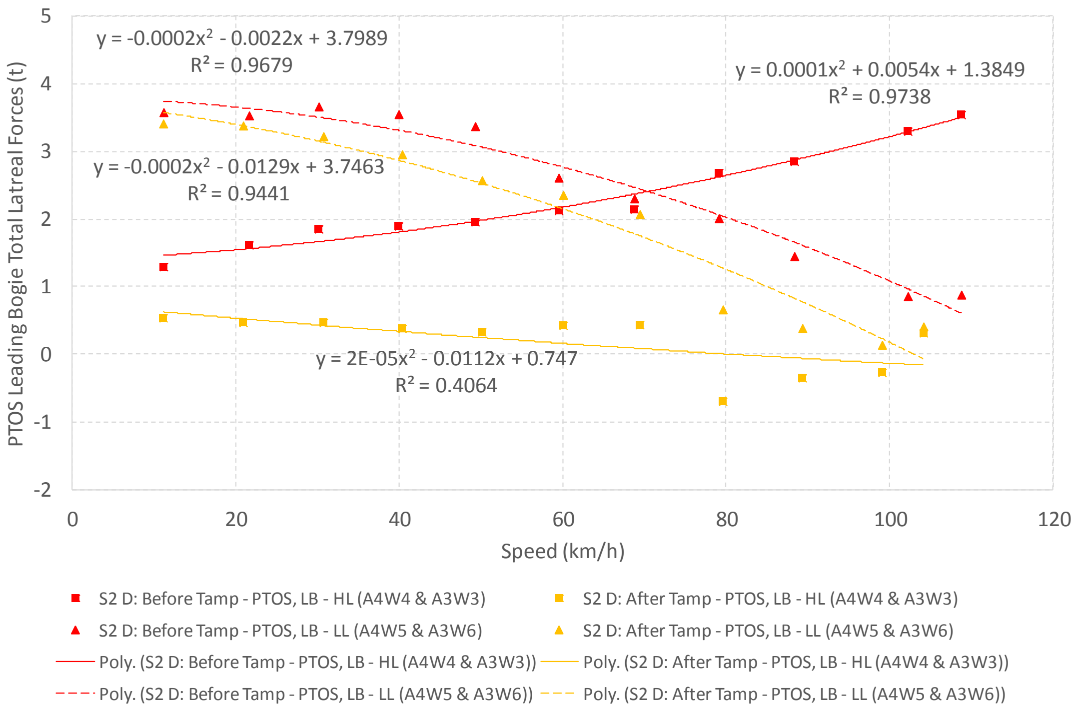

Figure G-38: Lateral Forces (PTOS Leading Bogie) – S2 Down

© University of Pretoria

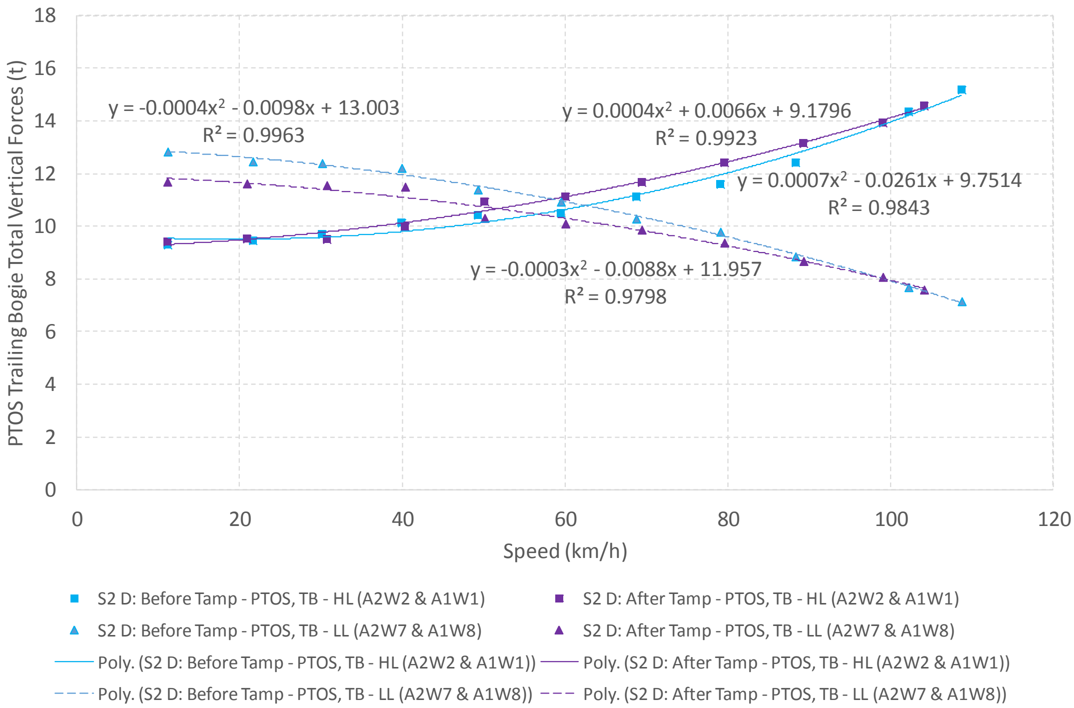

Figure G-39: Vertical Forces (PTOS Trailing Bogie) – S2 Down

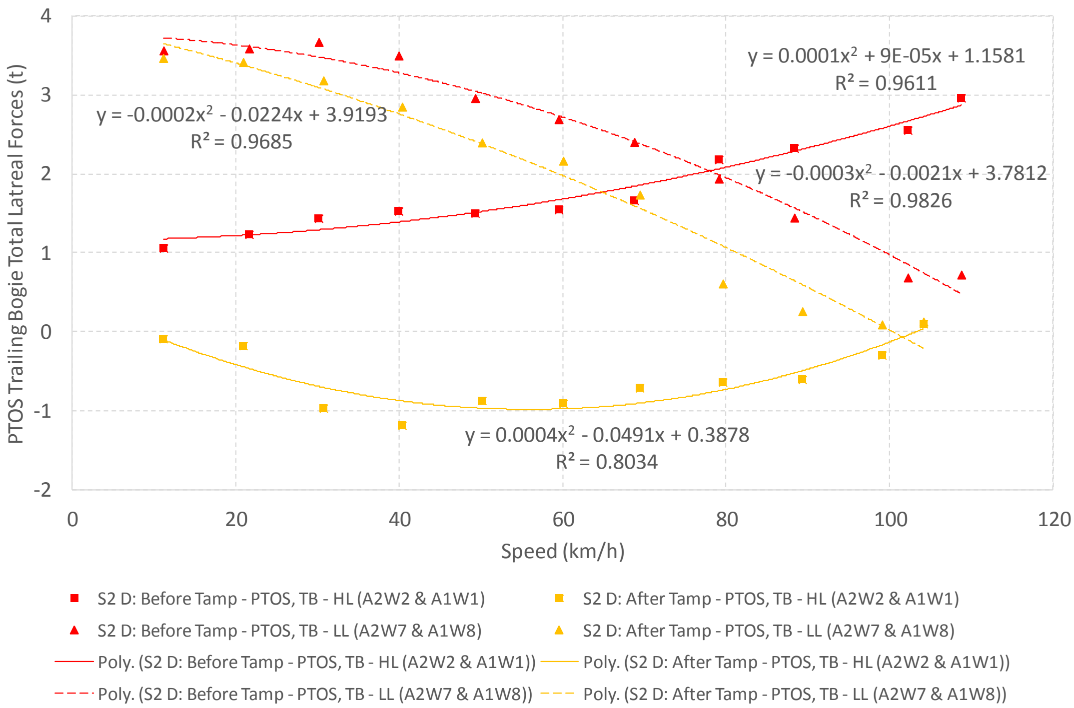

Figure G-40: Lateral Forces (PTOS Trailing Bogie) – S2 Down

© University of Pretoria

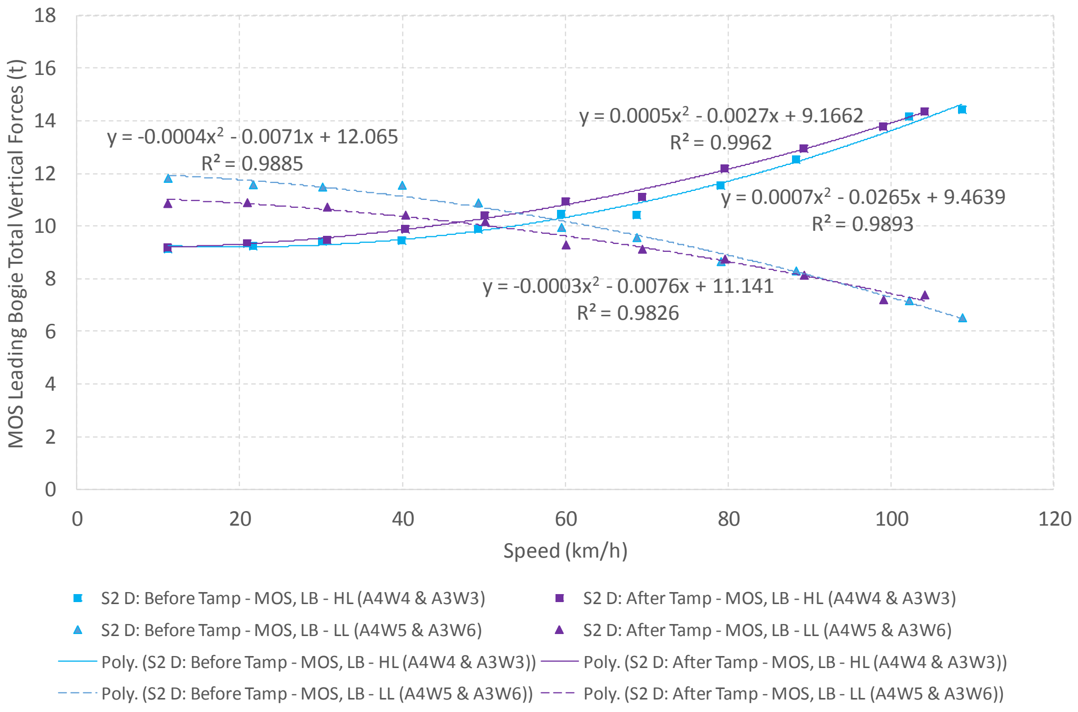

Figure G-41: Vertical Forces (MOS Leading Bogie) – S2 Down

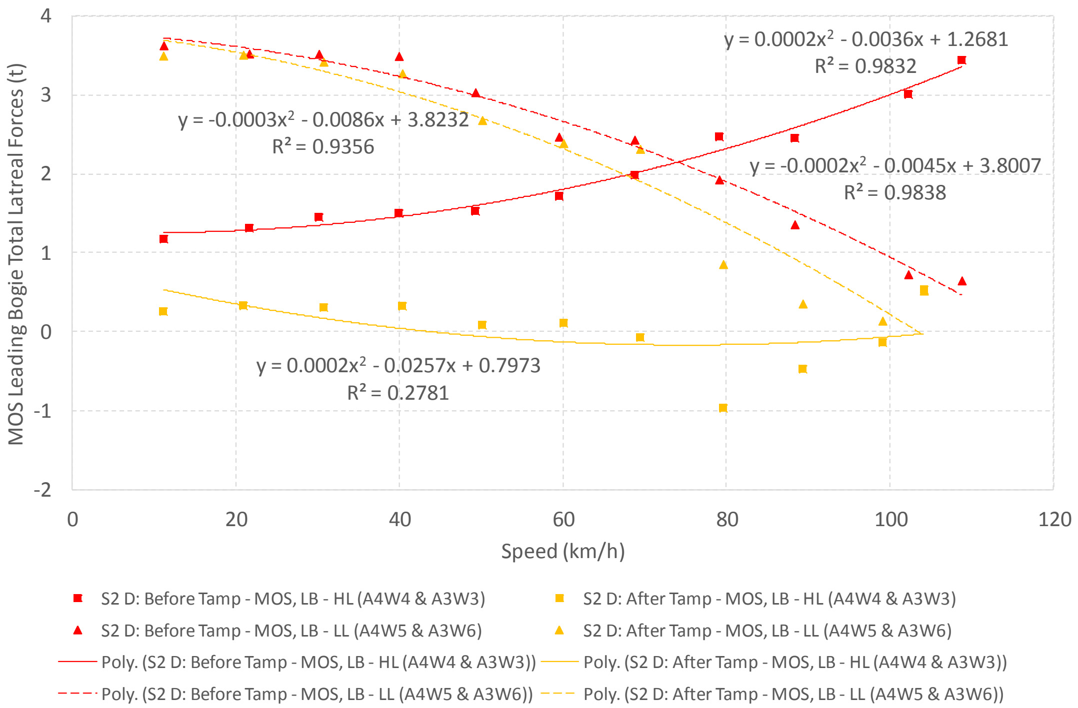

Figure G-42: Lateral Forces (MOS Leading Bogie) – S2 Down

© University of Pretoria

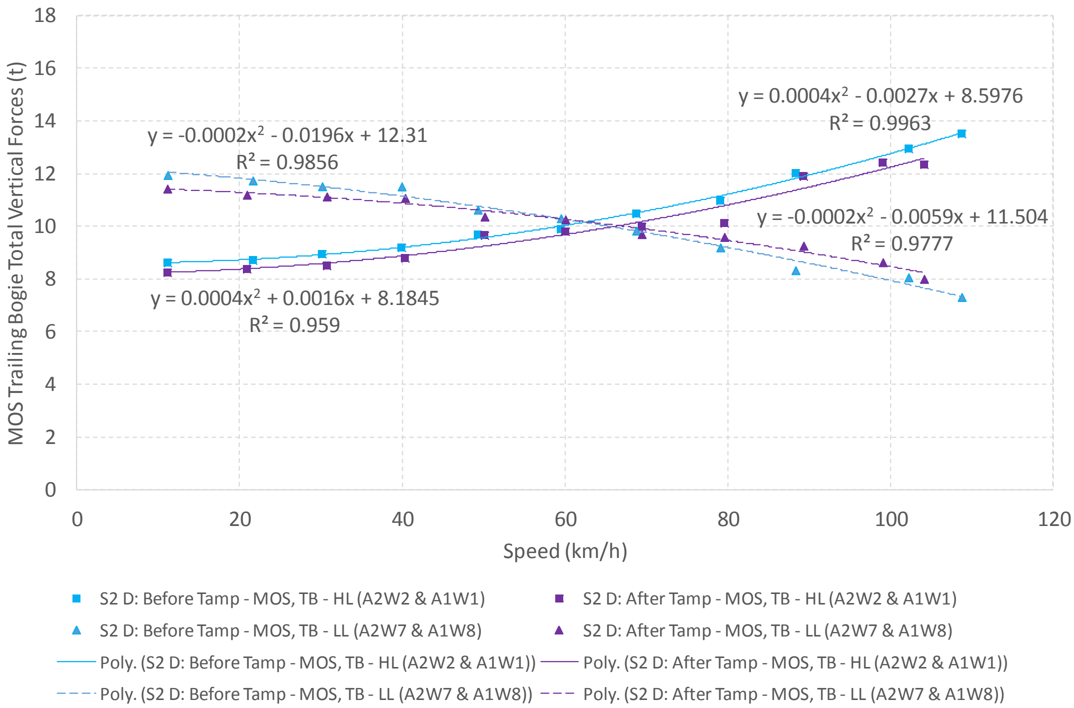

Figure G-43: Vertical Forces (MOS Trailing Bogie) – S2 Down

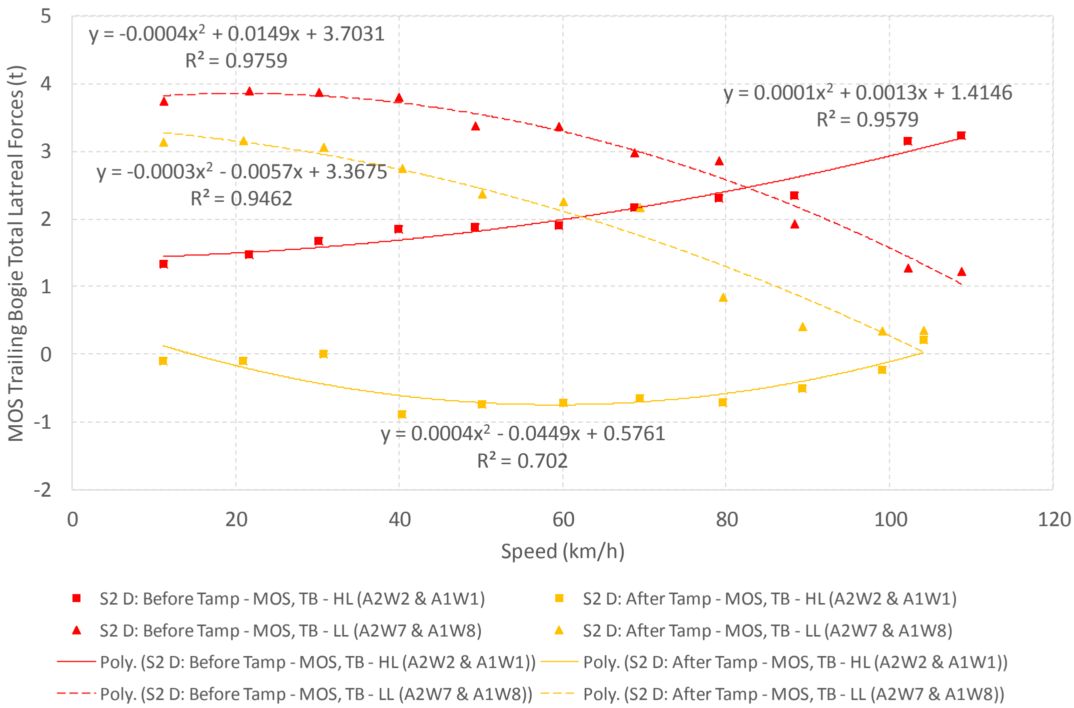

Figure G-44: Lateral Forces (MOS Trailing Bogie) – S2 Down

© University of Pretoria

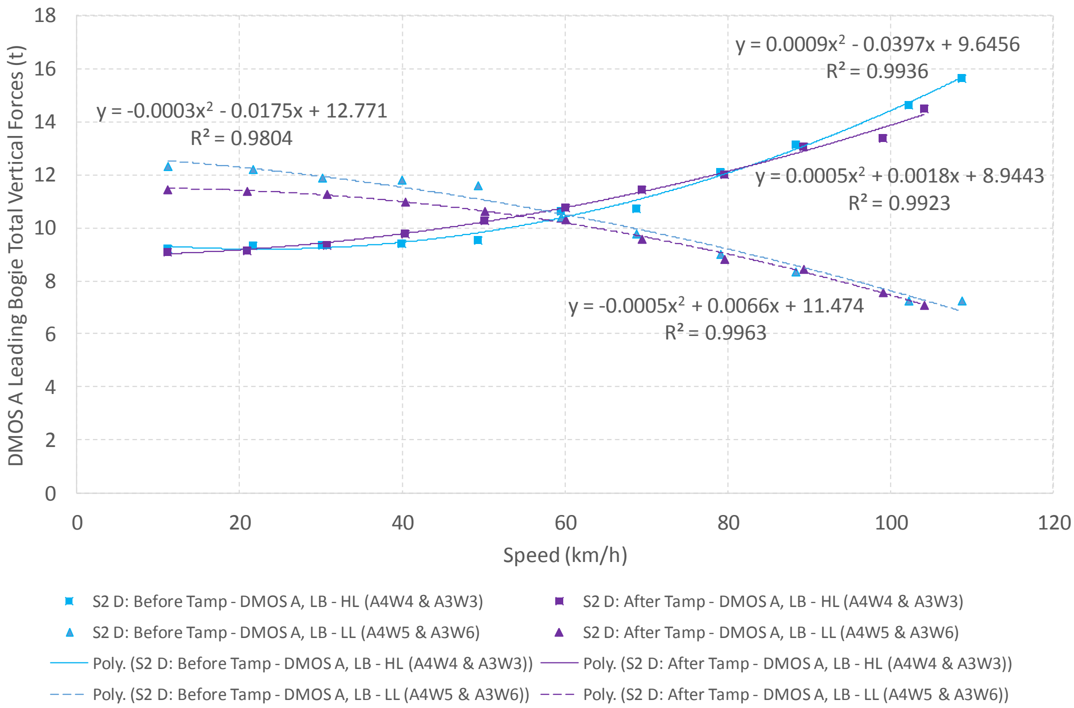

Figure G-45: Vertical Forces (DMOS A Leading Bogie) – S2 Down

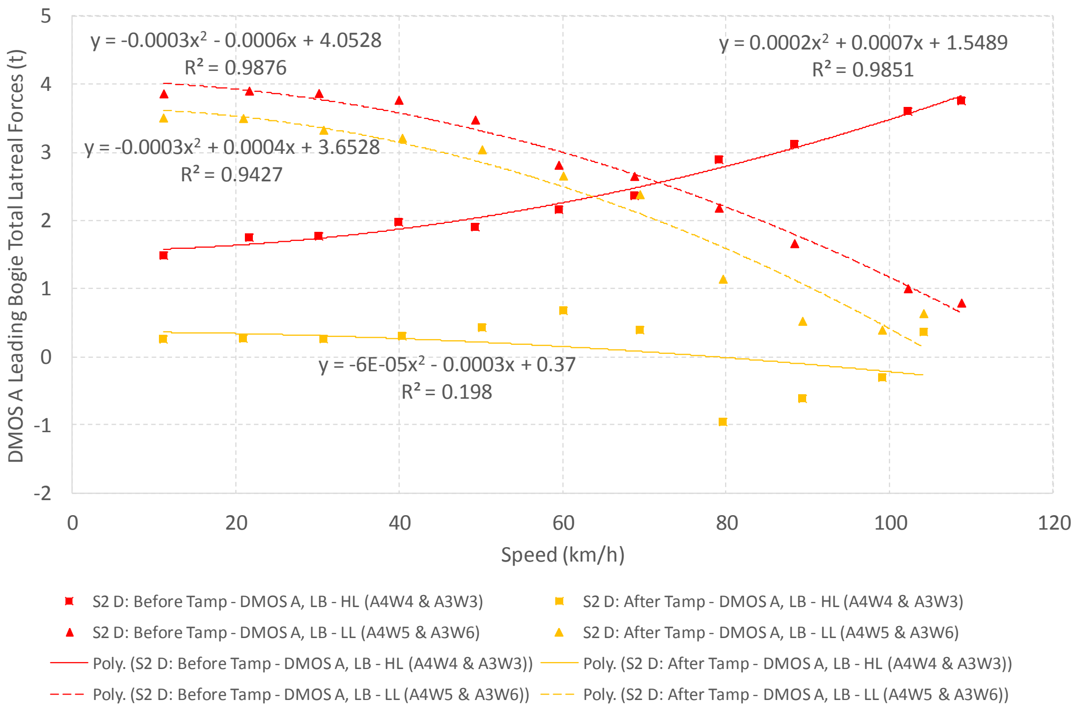

Figure G-46: Lateral Forces (DMOS A Leading Bogie) – S2 Down

© University of Pretoria

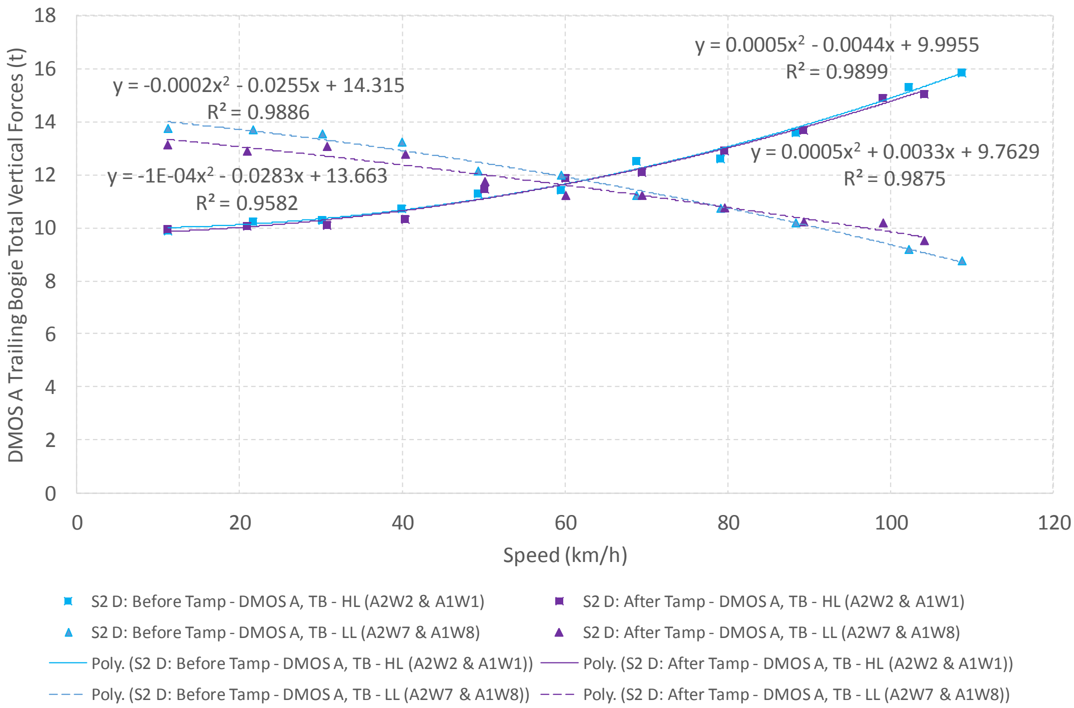

Figure G-47: Vertical Forces (DMOS A Trailing Bogie) – S2 Down

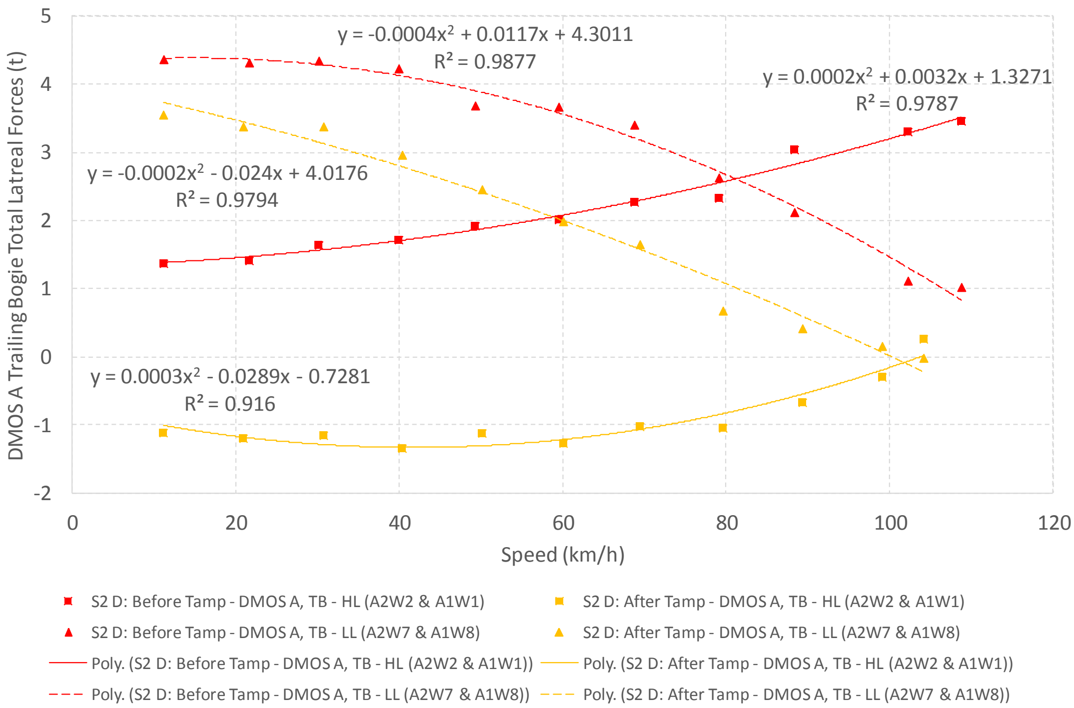

Figure G-48: Lateral Forces (DMOS A Trailing Bogie) – S2 Down

© University of Pretoria

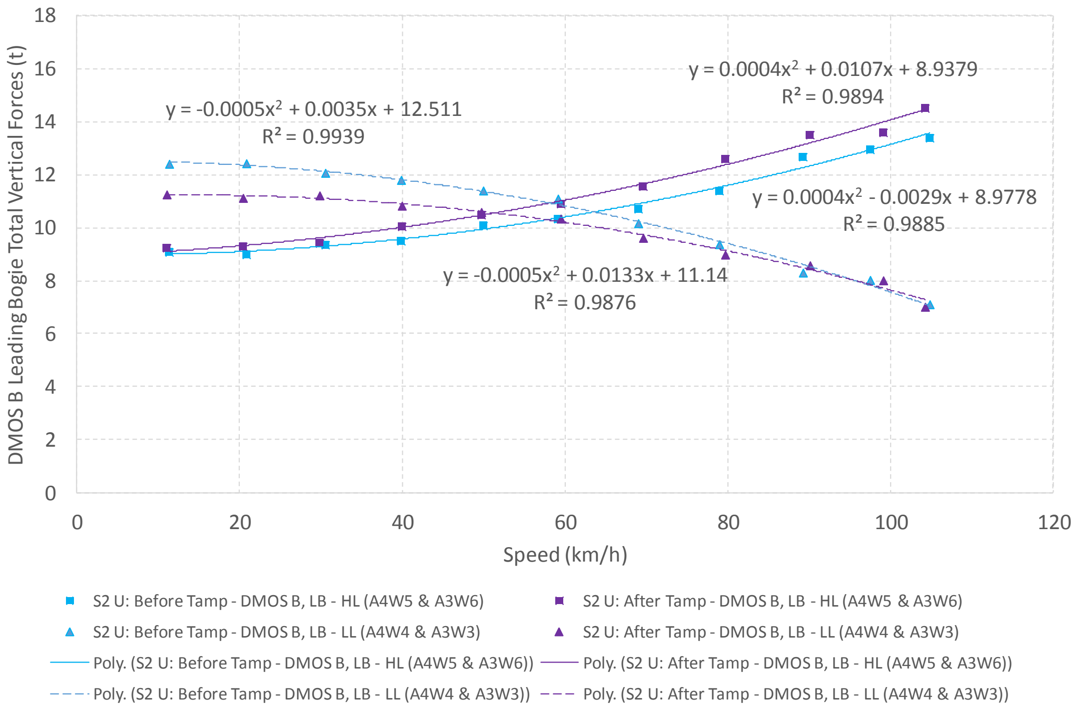

Figure G-49: Vertical Forces (DMOS B Leading Bogie) – S2 Up

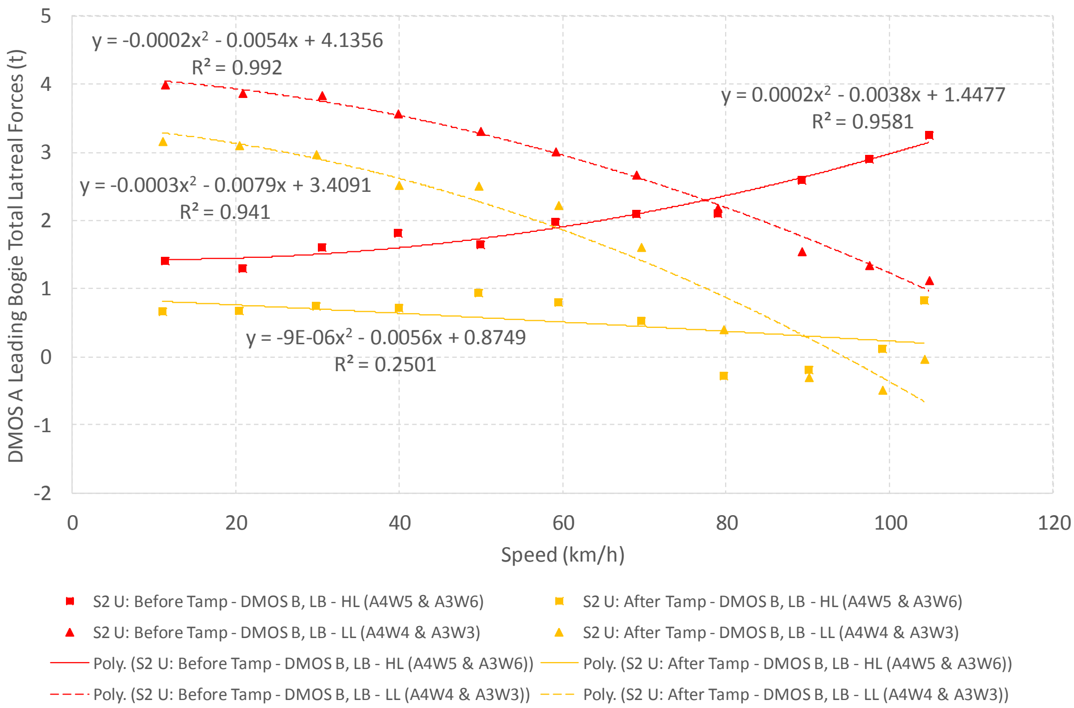

Figure G-50: Lateral Forces (DMOS B Leading Bogie) – S2 Up

© University of Pretoria

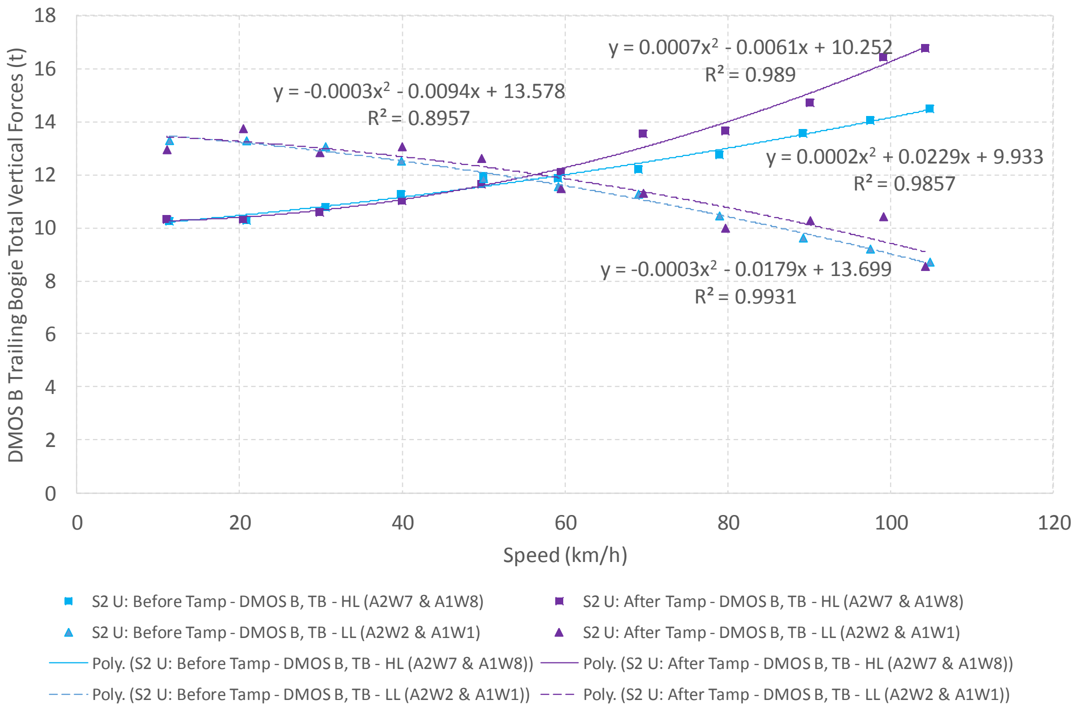

Figure G-51: Vertical Forces (DMOS B Trailing Bogie) – S2 Up

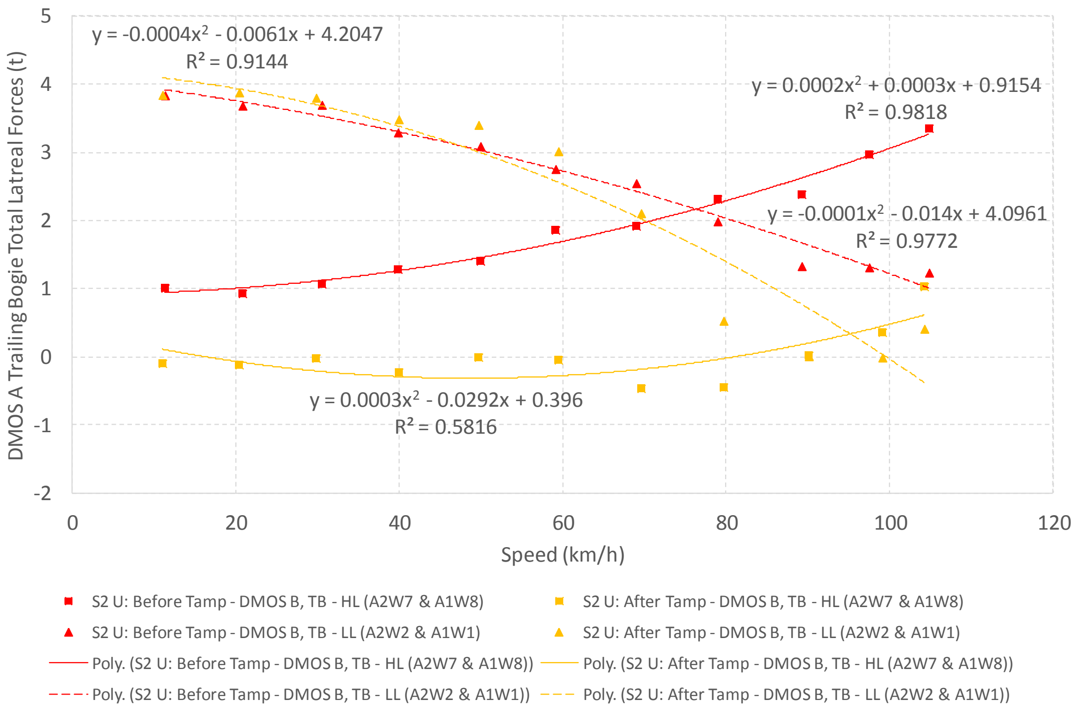

Figure G-52: Lateral Forces (DMOS B Trailing Bogie) – S2 Up

© University of Pretoria

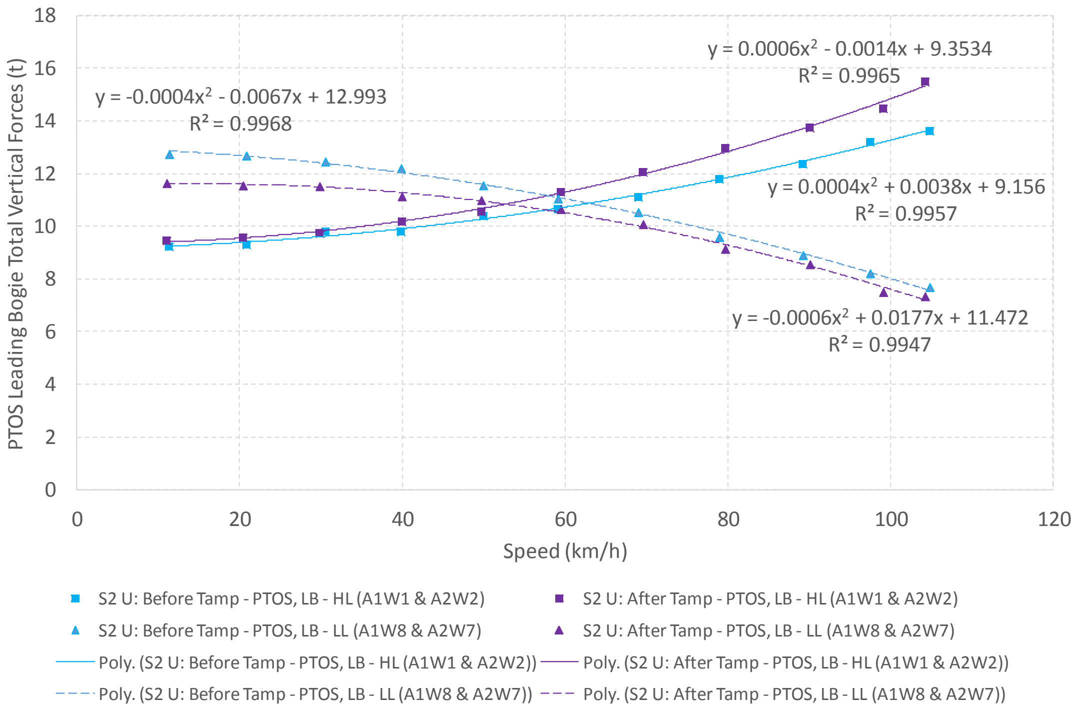

Figure G-53: Vertical Forces (PTOS Leading Bogie) – S2 Up

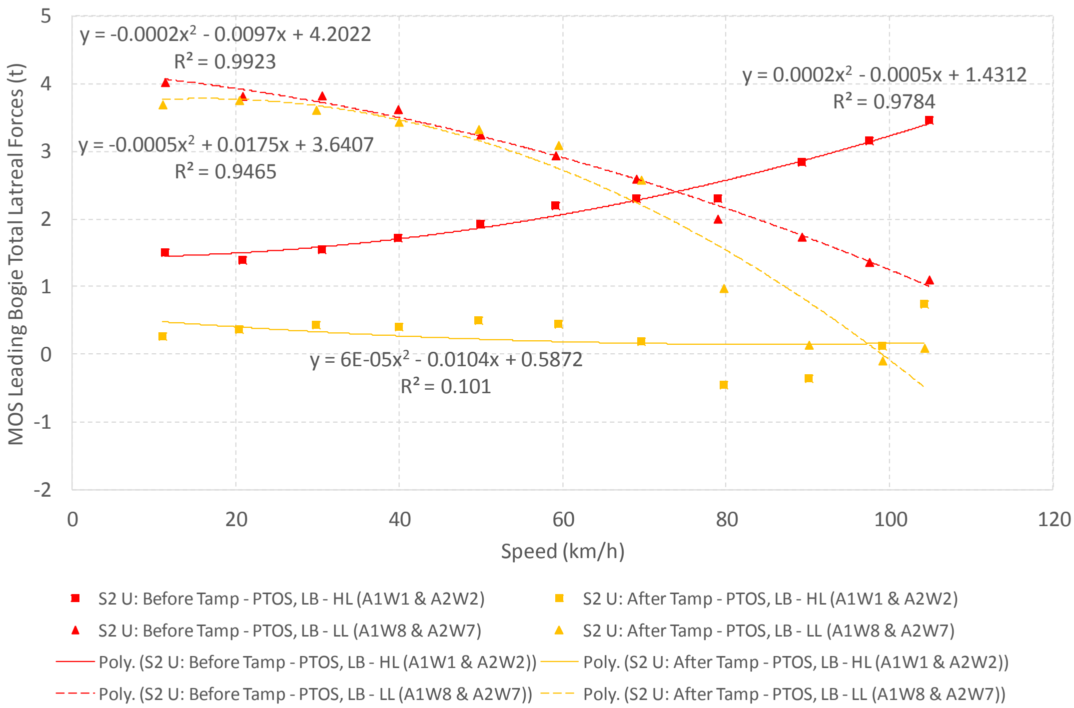

Figure G-54: Lateral Forces (PTOS Leading Bogie) – S2 Up

© University of Pretoria

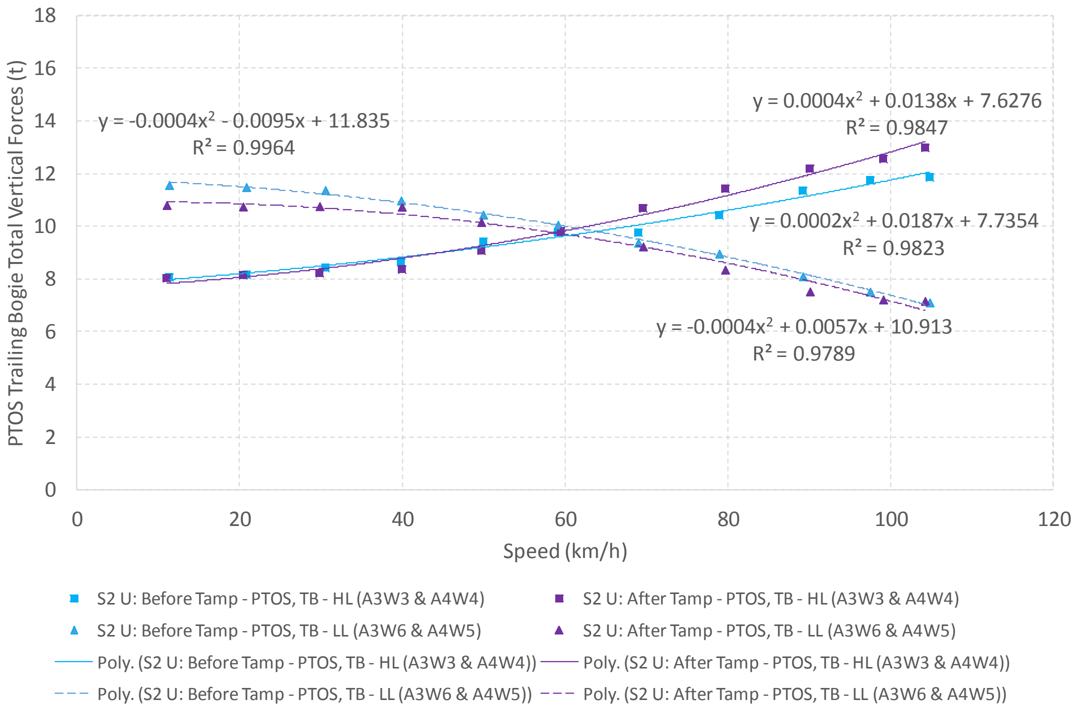

Figure G-55: Vertical Forces (PTOS Trailing Bogie) – S2 Up

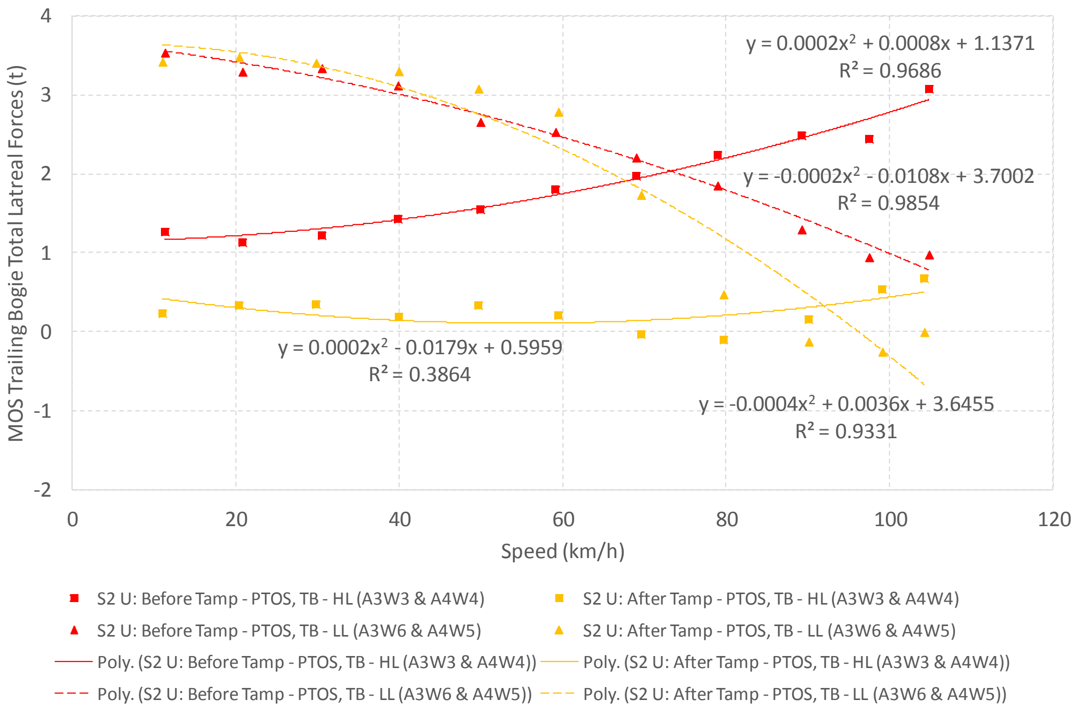

Figure G-56: Lateral Forces (PTOS Trailing Bogie) – S2 Up

© University of Pretoria

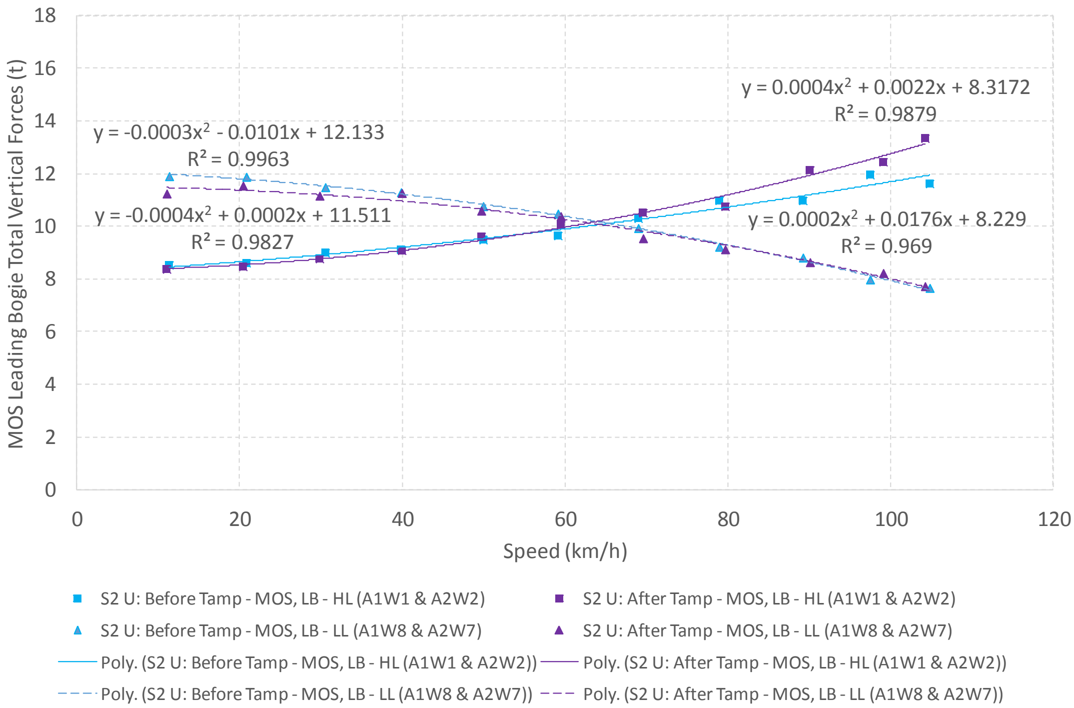

Figure G-57: Vertical Forces (MOS Leading Bogie) – S2 Up

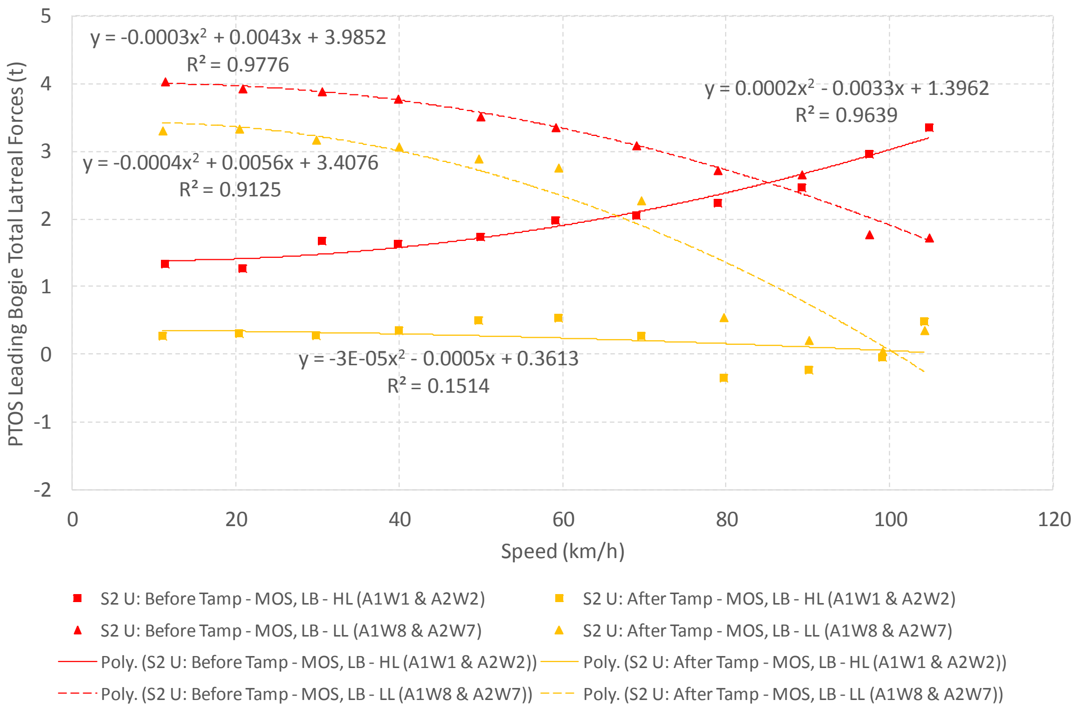

Figure G-58: Lateral Forces (MOS Leading Bogie) – S2 Up

© University of Pretoria

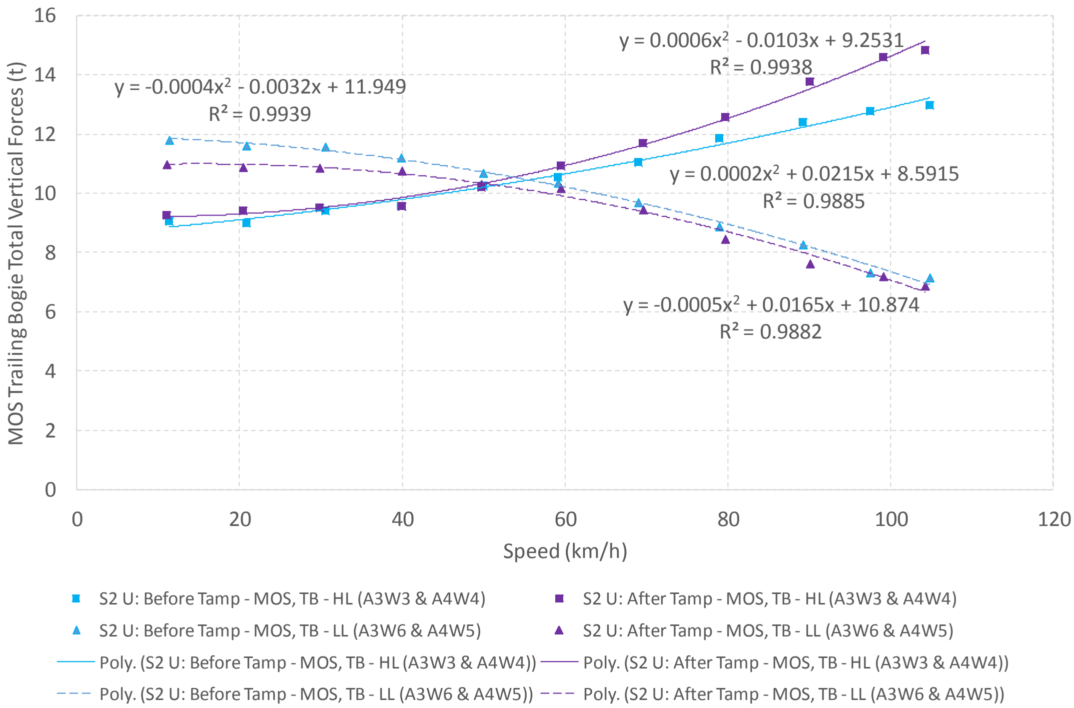

Figure G-59: Vertical Forces (MOS Trailing Bogie) – S2 Up

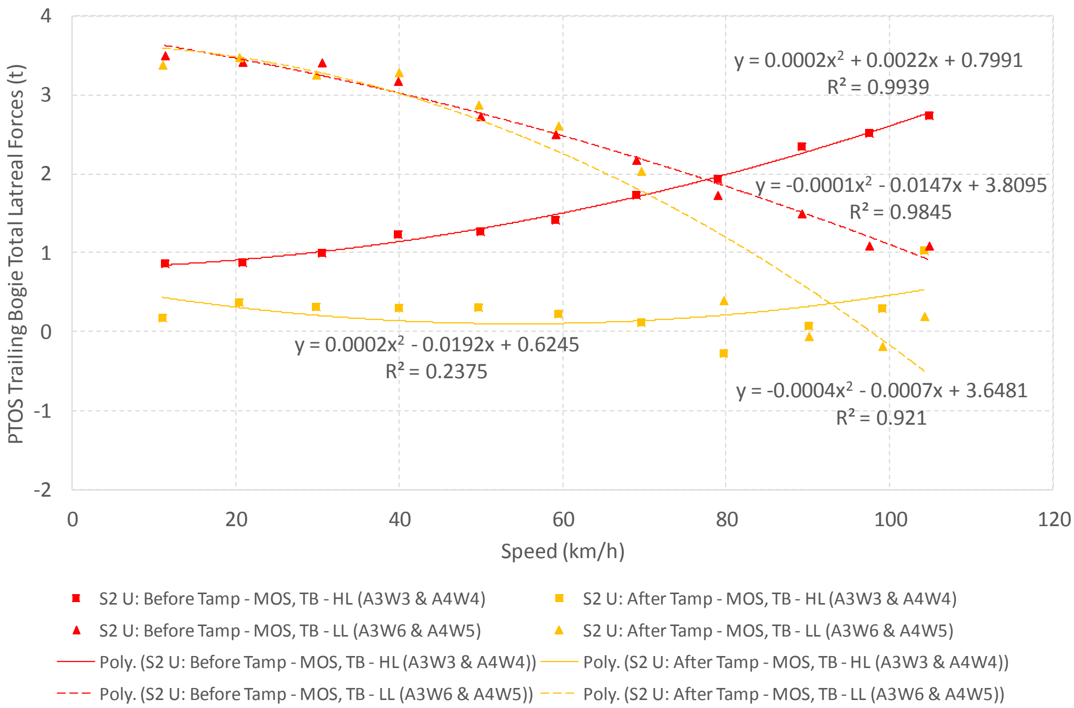

Figure G-60: Lateral Forces (MOS Trailing Bogie) – S2 Up

© University of Pretoria

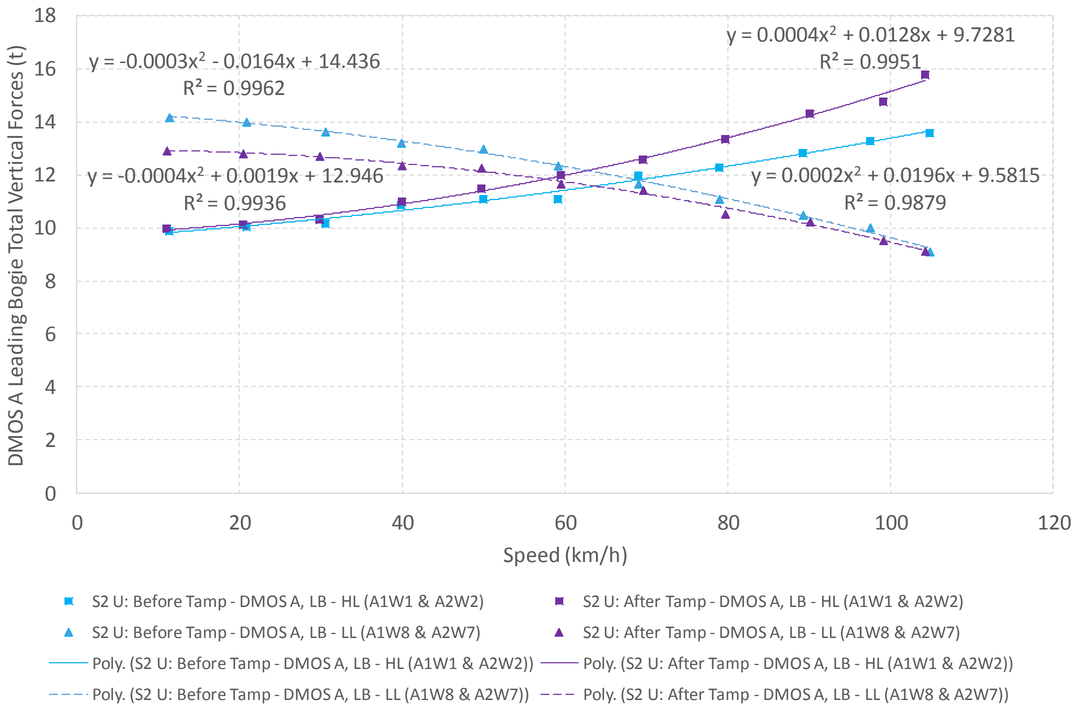

Figure G-61: Vertical Forces (DMOS A Leading Bogie) – S2 Up

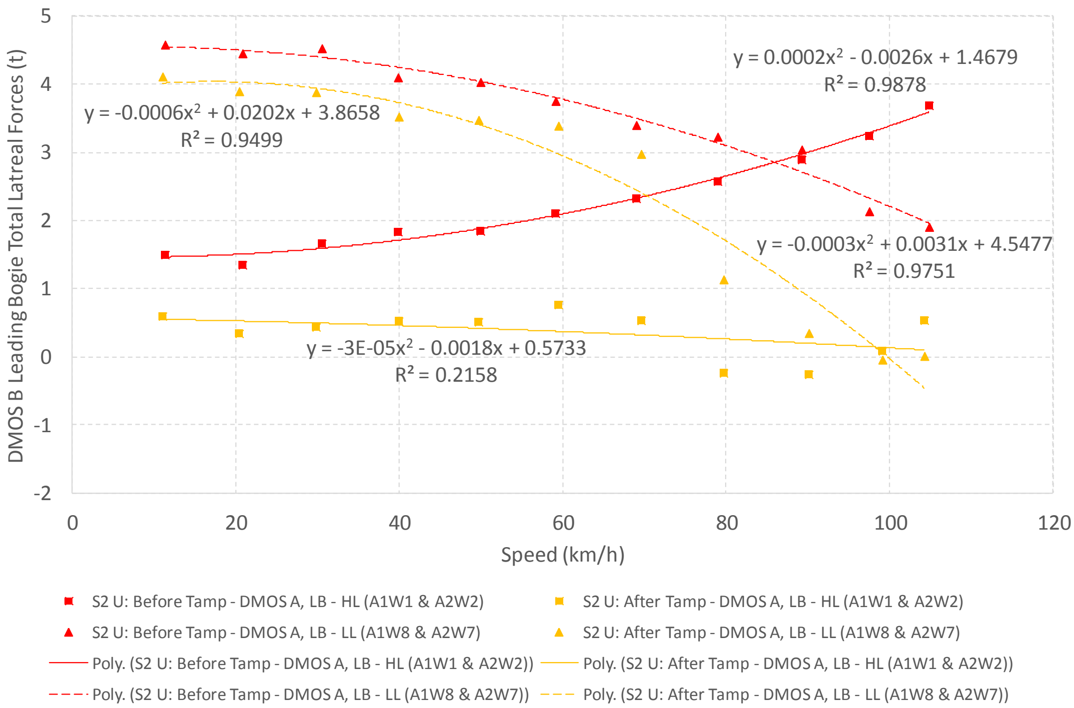

Figure G-62: Lateral Forces (DMOS A Leading Bogie) – S2 Up

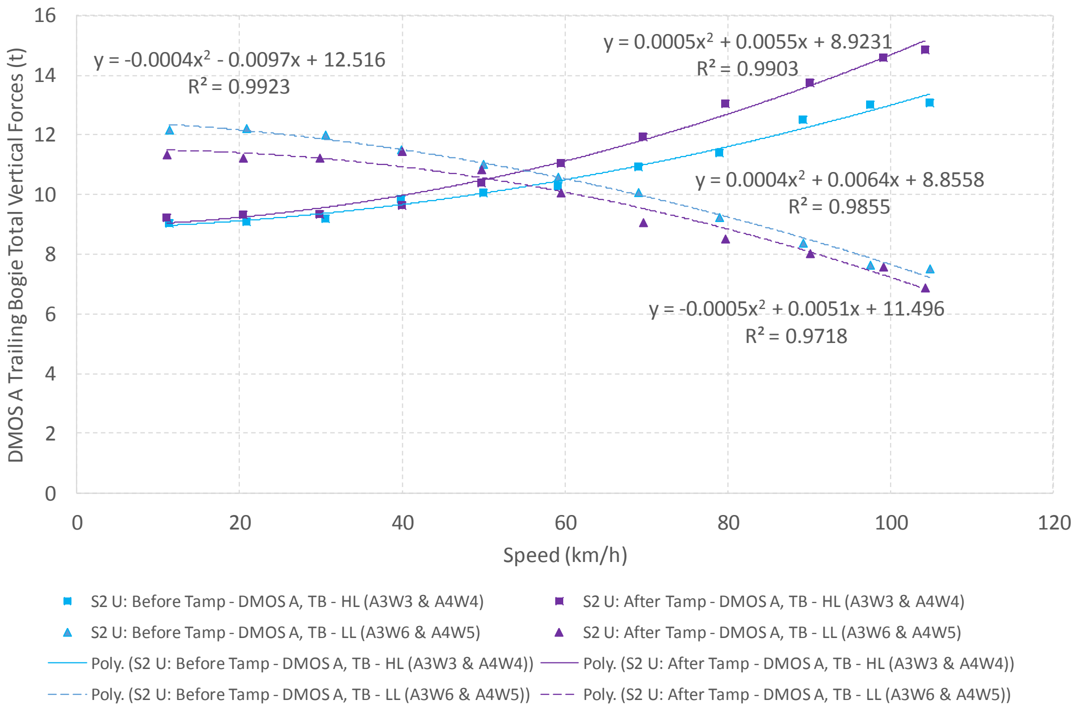

Figure G-63: Vertical Forces (DMOS A Trailing Bogie) – S2 Up

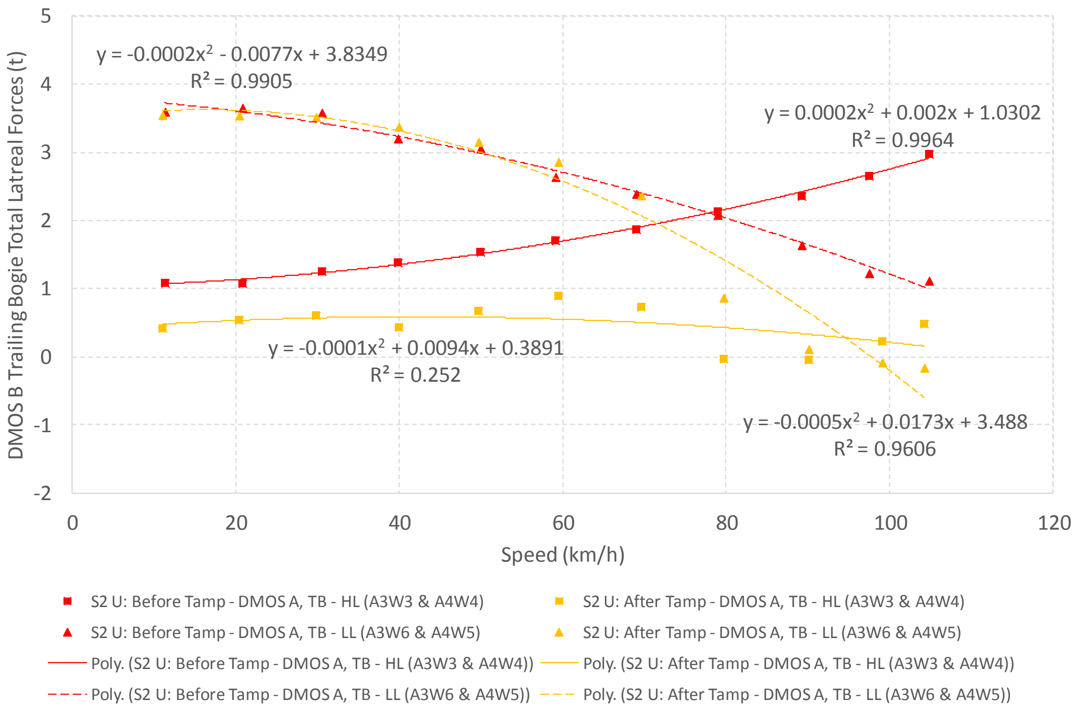

Figure G-64: Lateral Forces (DMOS A Trailing Bogie) – S2 Up

© University of Pretoria

APPENDIX H. CURVE RAIL FORCES TRENDS FOR CARS

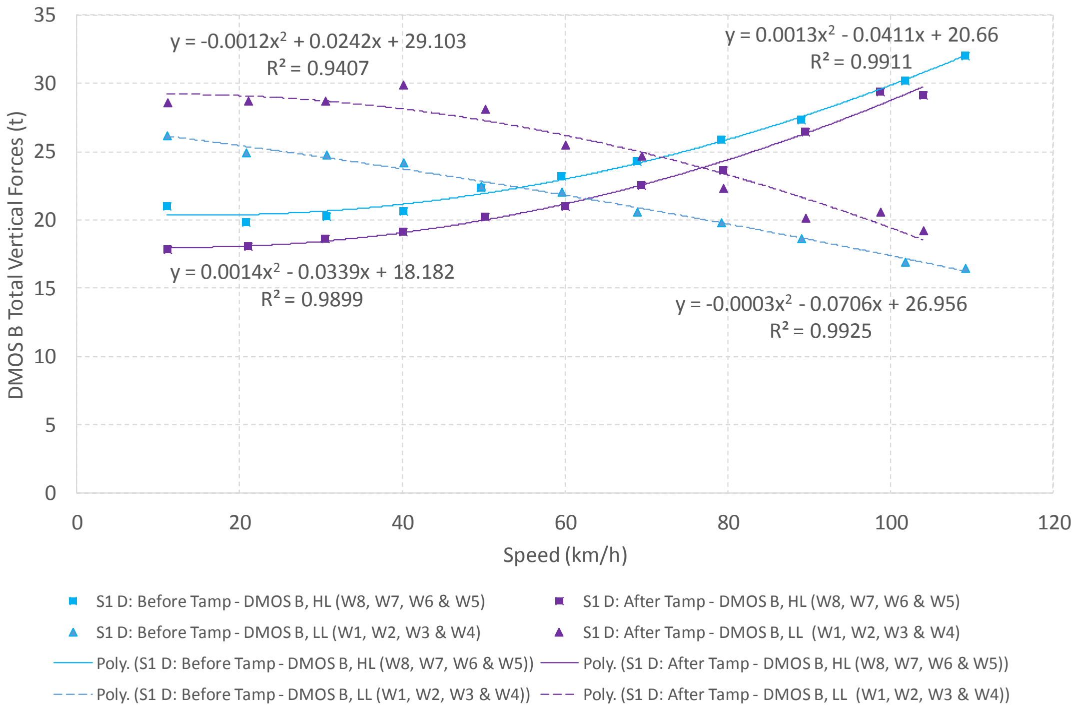

Figure H-1: Vertical Forces (DMOS B) – S1 Down

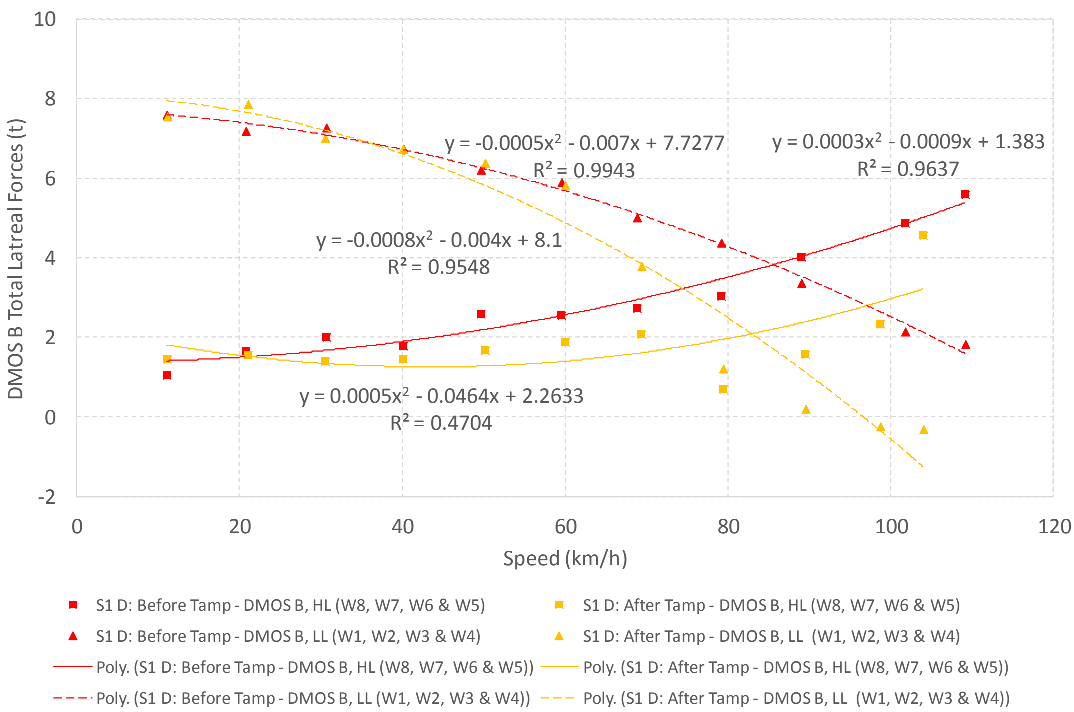

Figure H-2: Lateral Forces (DMOS B) – S1 Down

© University of Pretoria

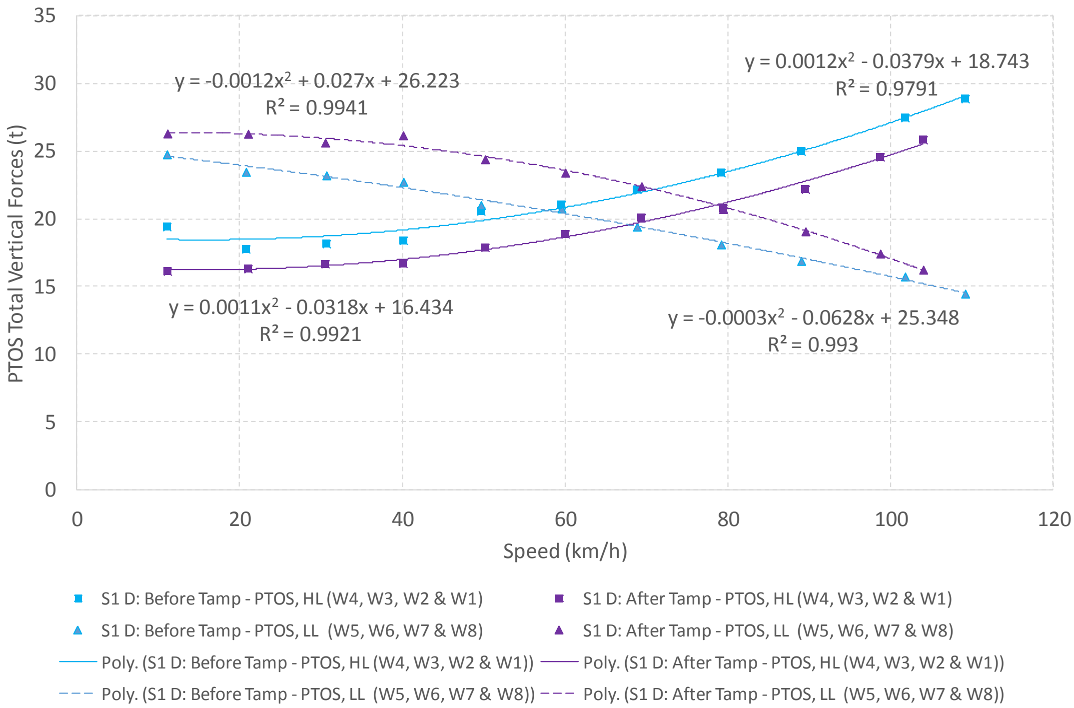

Figure H-3: Vertical Forces (PTOS) – S1 Down

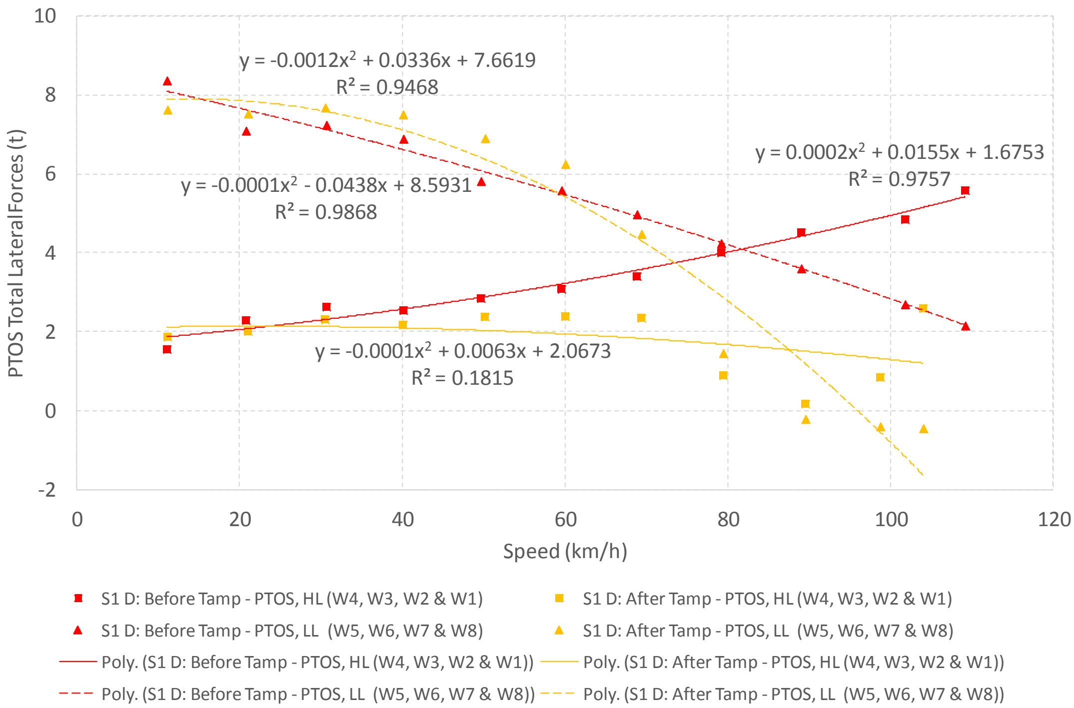

Figure H-4: Lateral Forces (PTOS) – S1 Down

© University of Pretoria

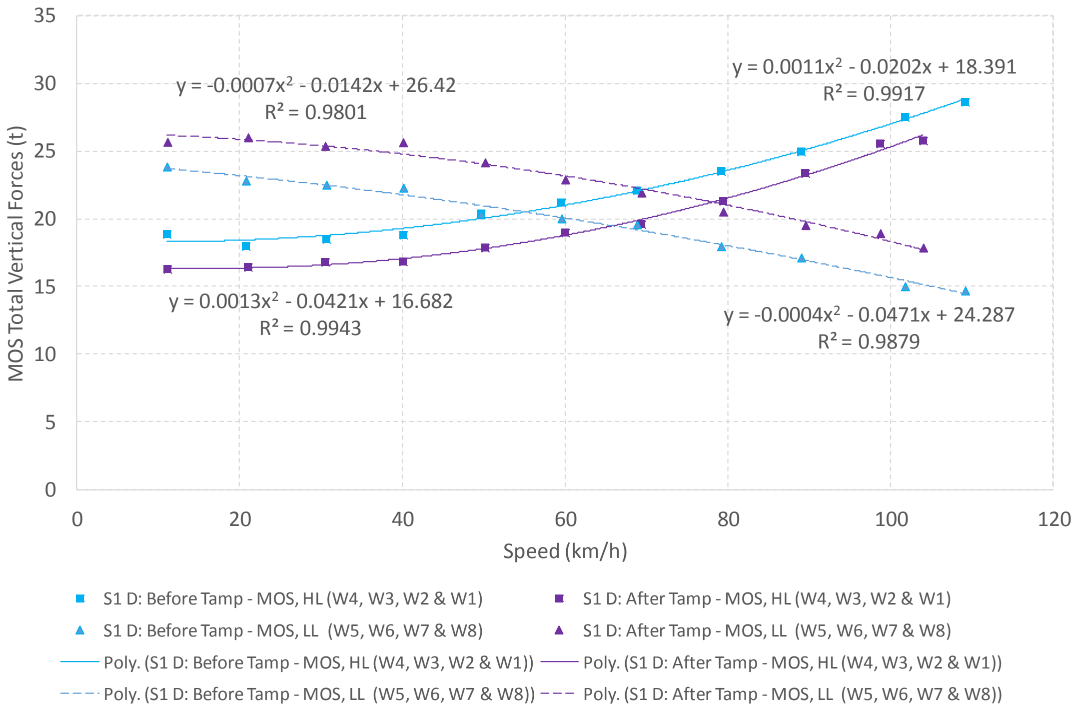

Figure H-5: Vertical Forces (MOS) – S1 Down

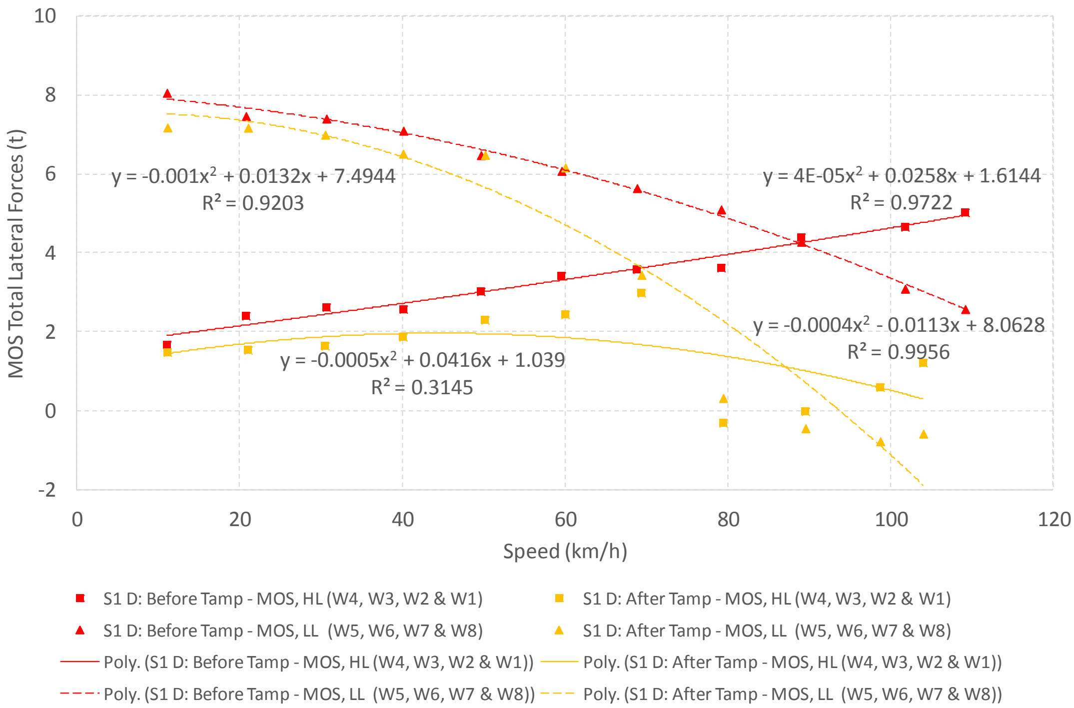

Figure H-6: Lateral Forces (MOS) – S1 Down

© University of Pretoria

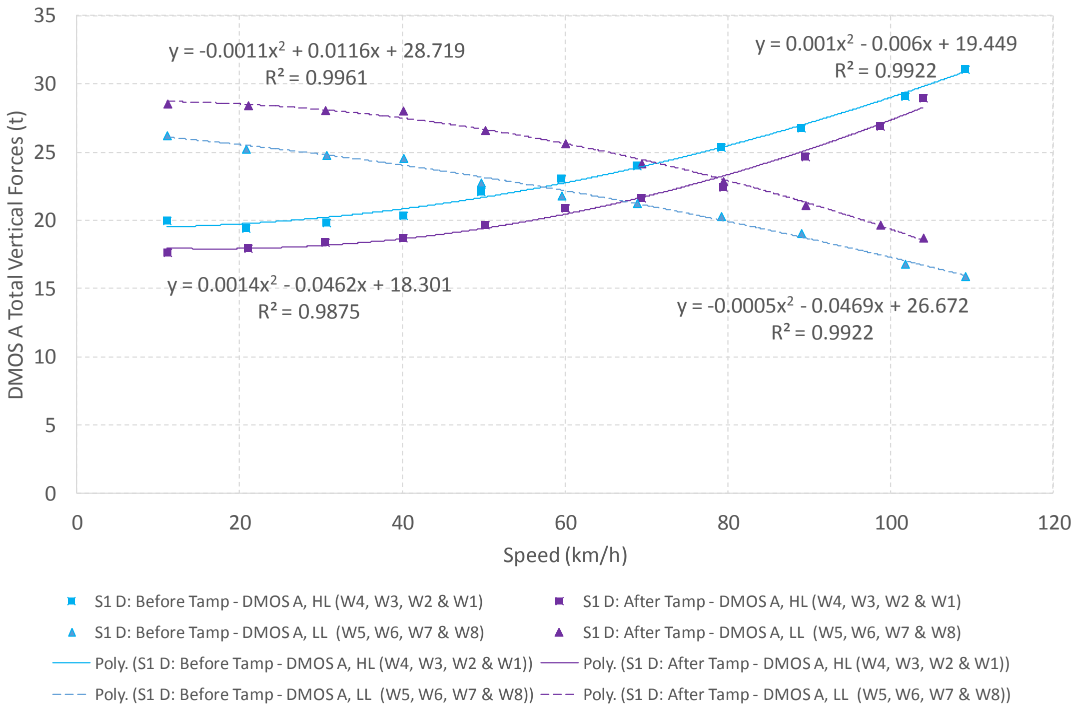

Figure H-7: Vertical Forces (DMOS A) – S1 Down

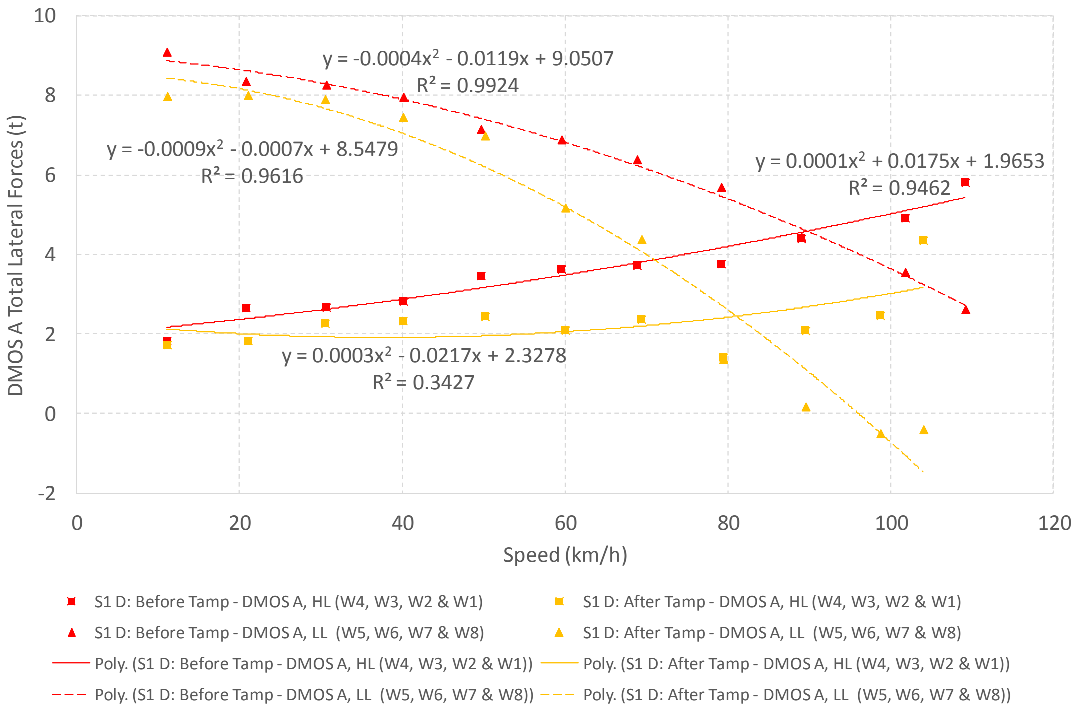

Figure H-8: Lateral Forces (DMOS A) – S1 Down

© University of Pretoria

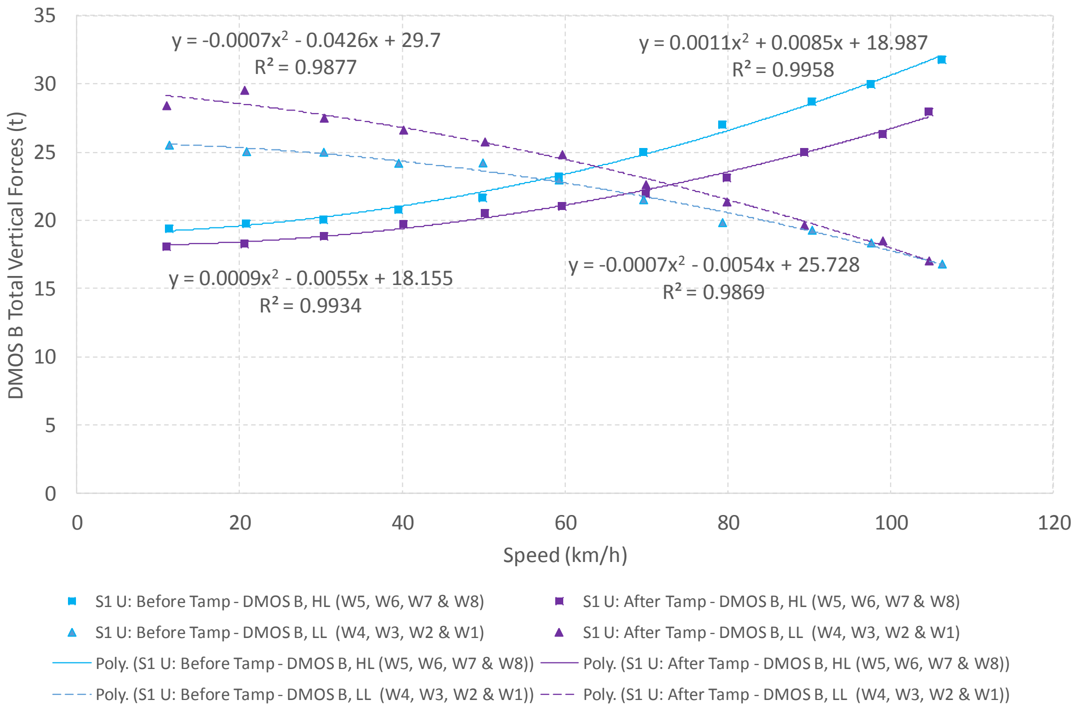

Figure H-9: Vertical Forces (DMOS B) – S1 Up

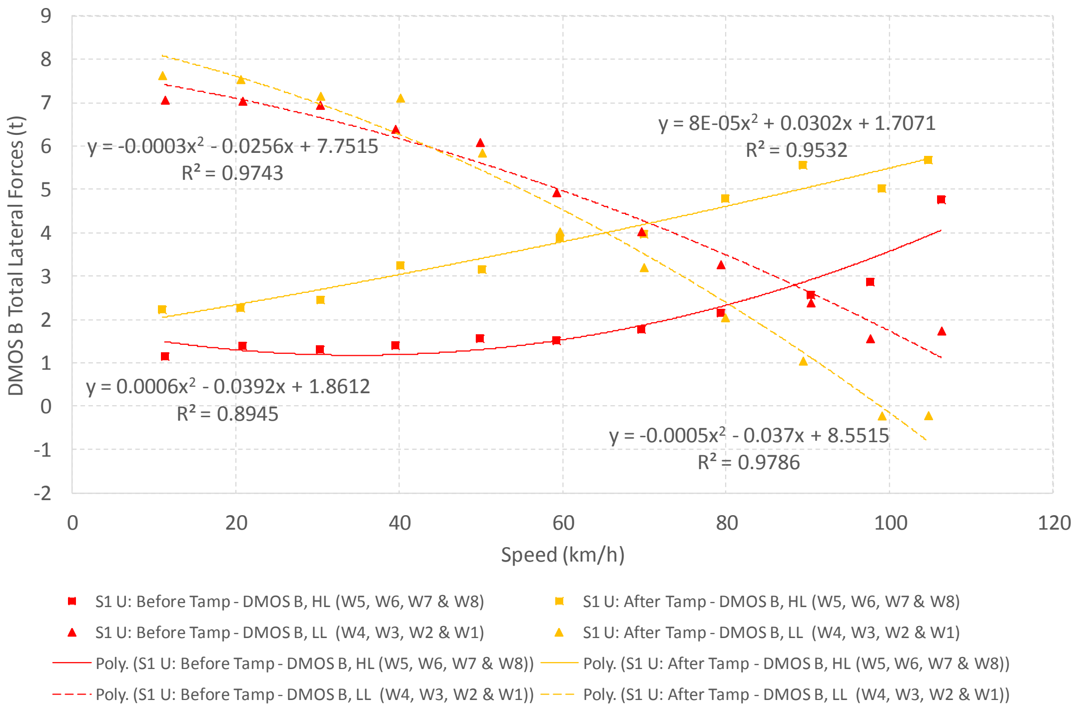

Figure H-10: Lateral Forces (DMOS B) – S1 Up

© University of Pretoria

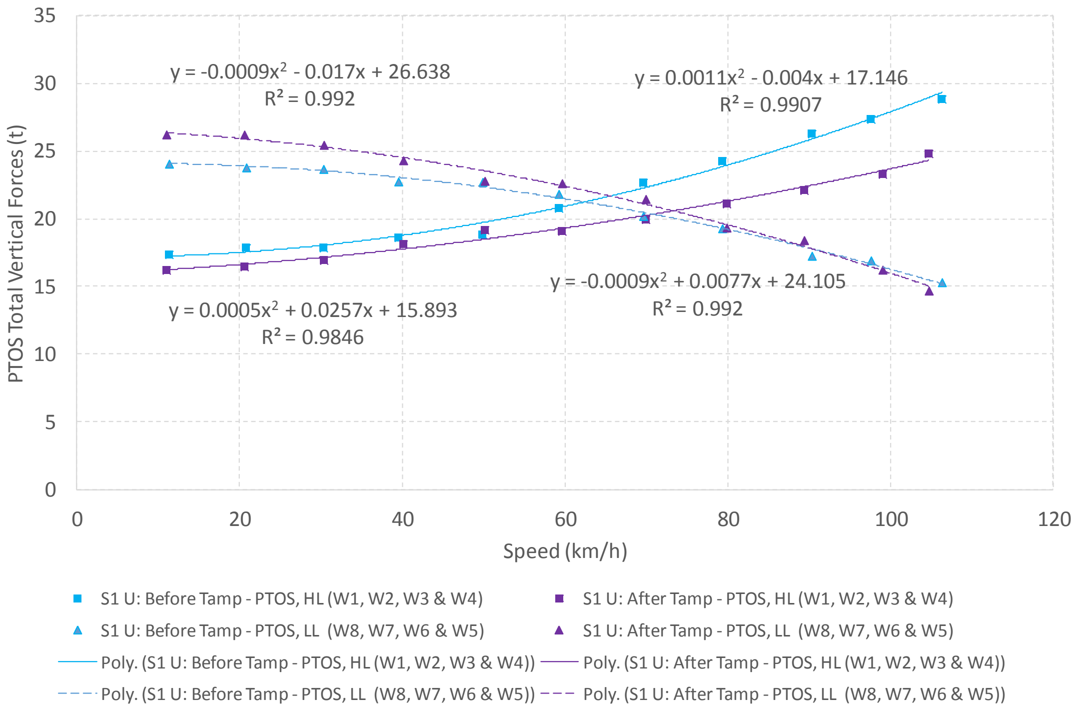

Figure H-11: Vertical Forces (PTOS) – S1 Up

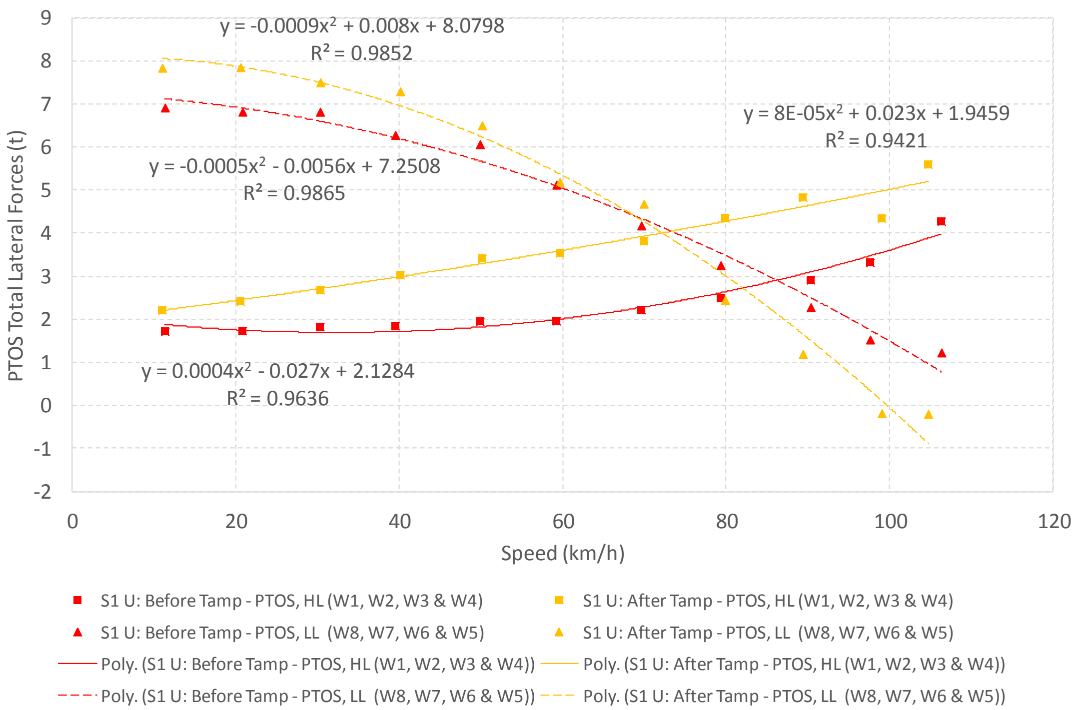

Figure H-12: Lateral Forces (PTOS) – S1 Up

© University of Pretoria

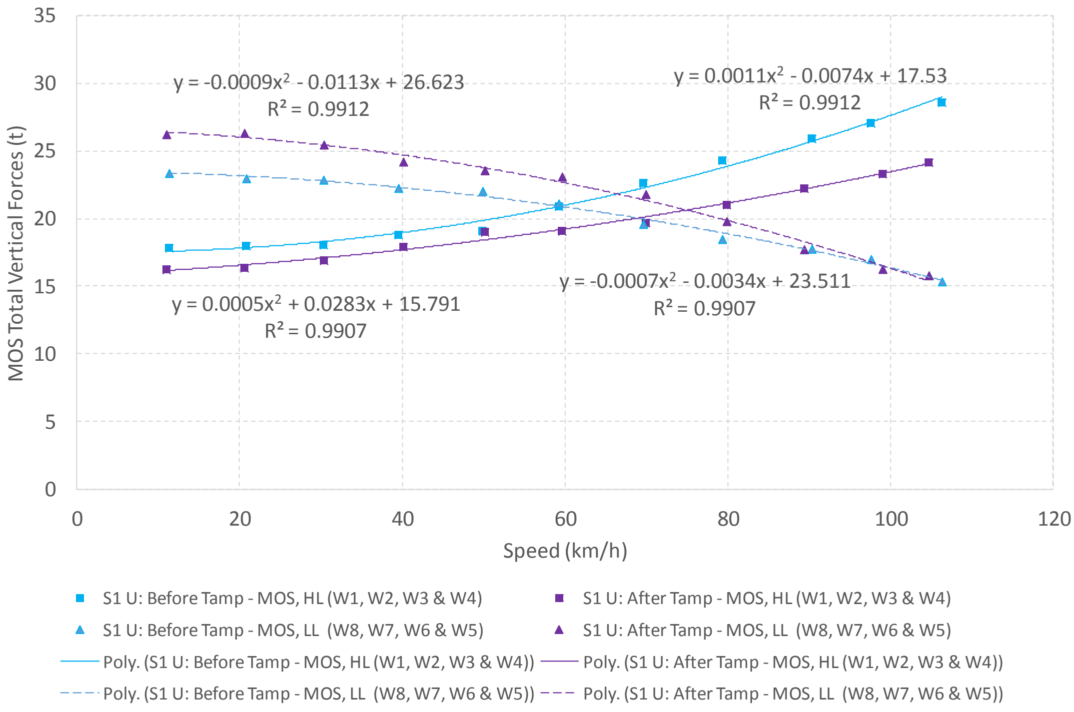

Figure H-13: Vertical Forces (MOS) – S1 Up

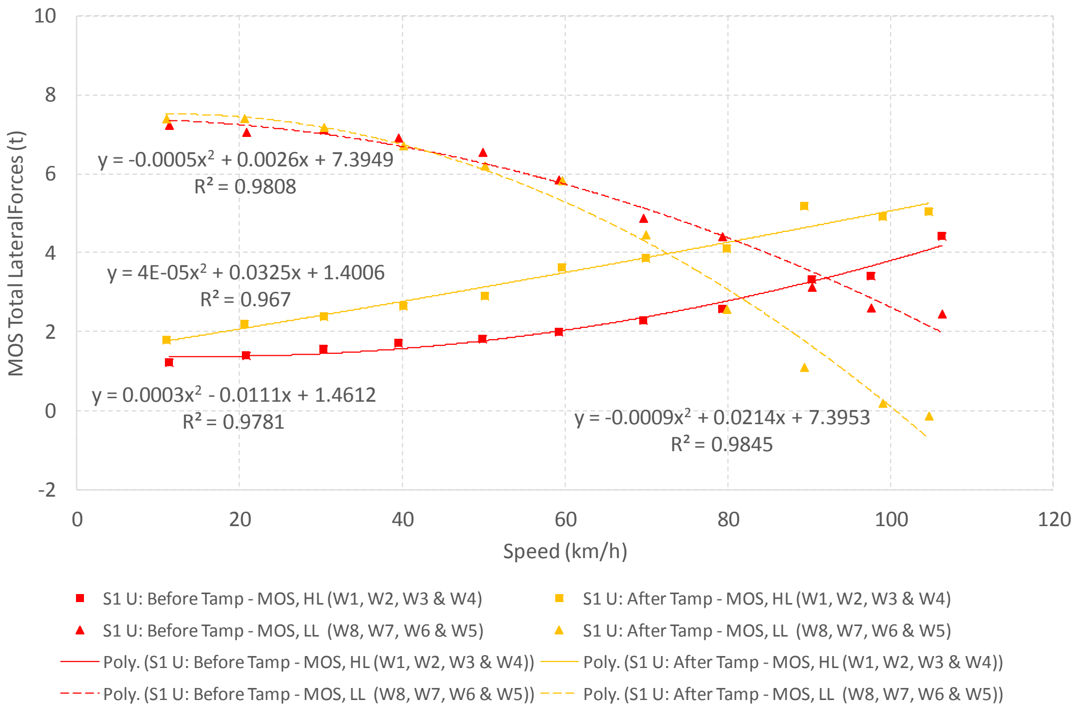

Figure H-14: Lateral Forces (MOS) – S1 Up

© University of Pretoria

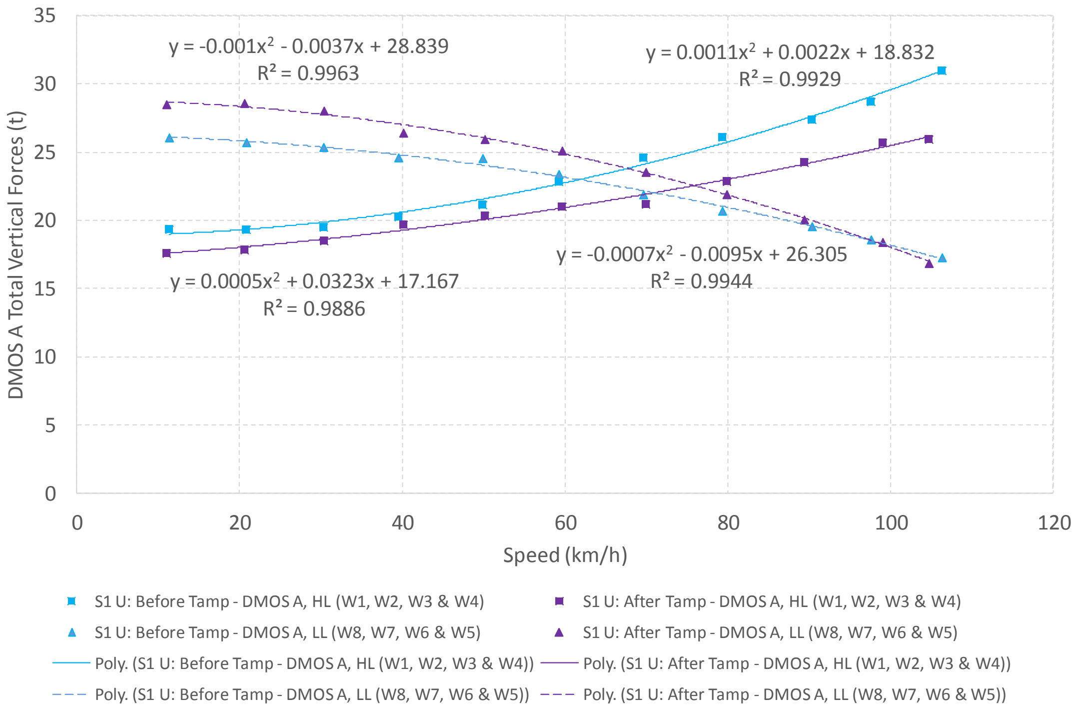

Figure H-15: Vertical Forces (DMOS A) – S1 Up

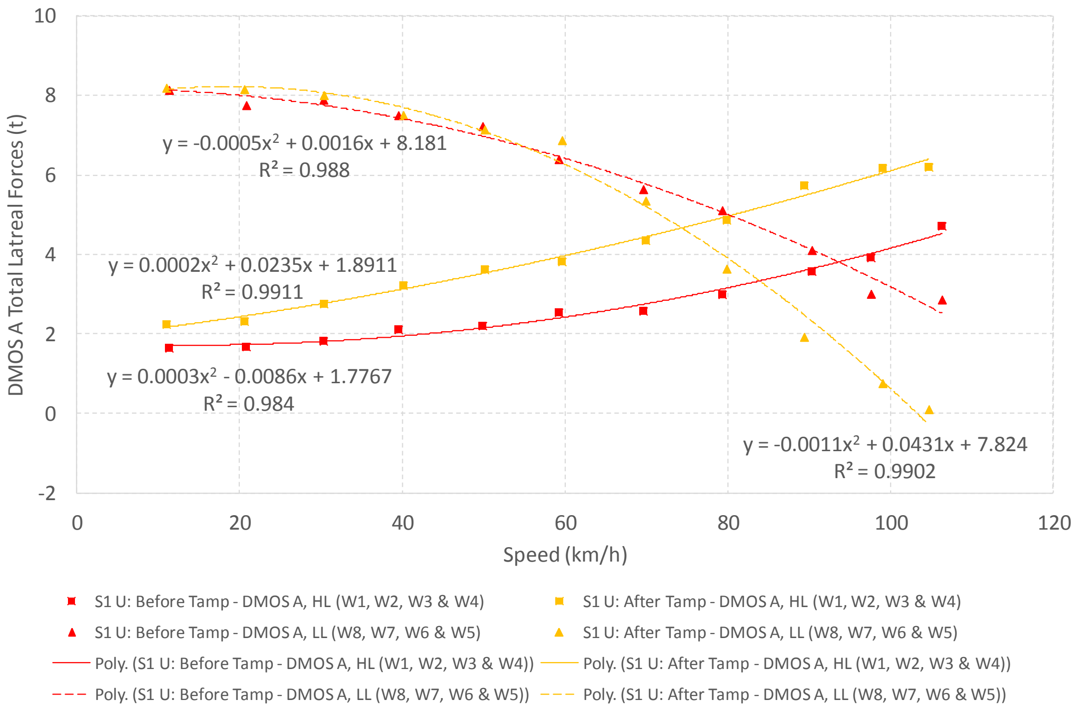

Figure H-16: Lateral Forces (DMOS A) – S1 Up

© University of Pretoria

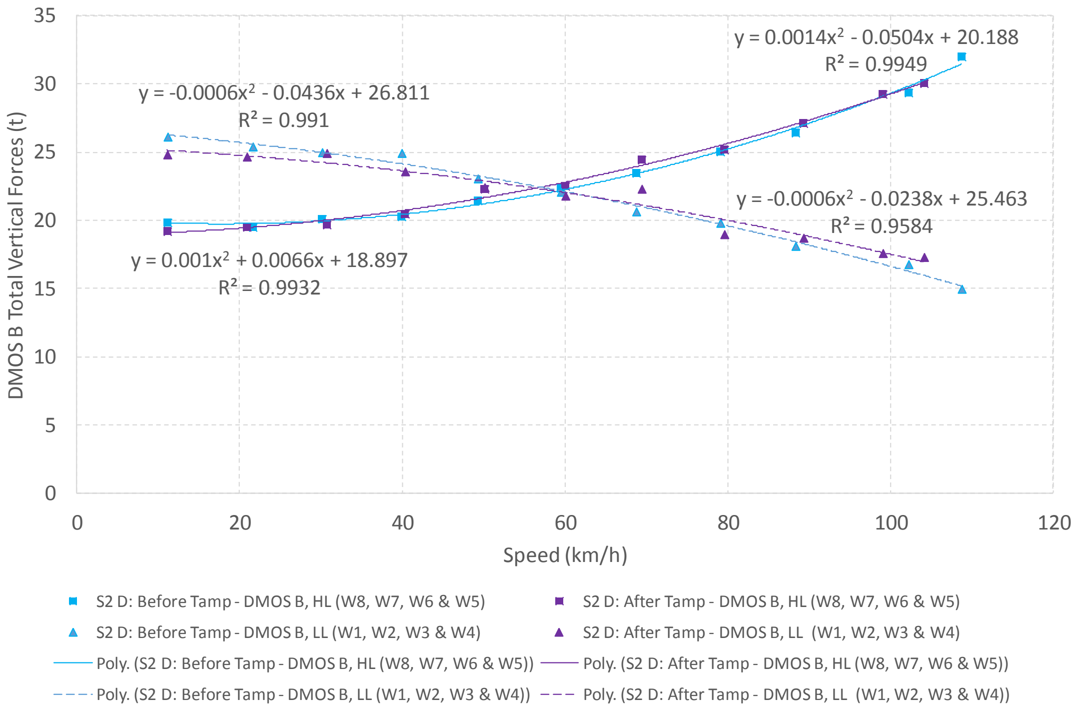

Figure H-17: Vertical Forces (DMOS B) – S2 Down

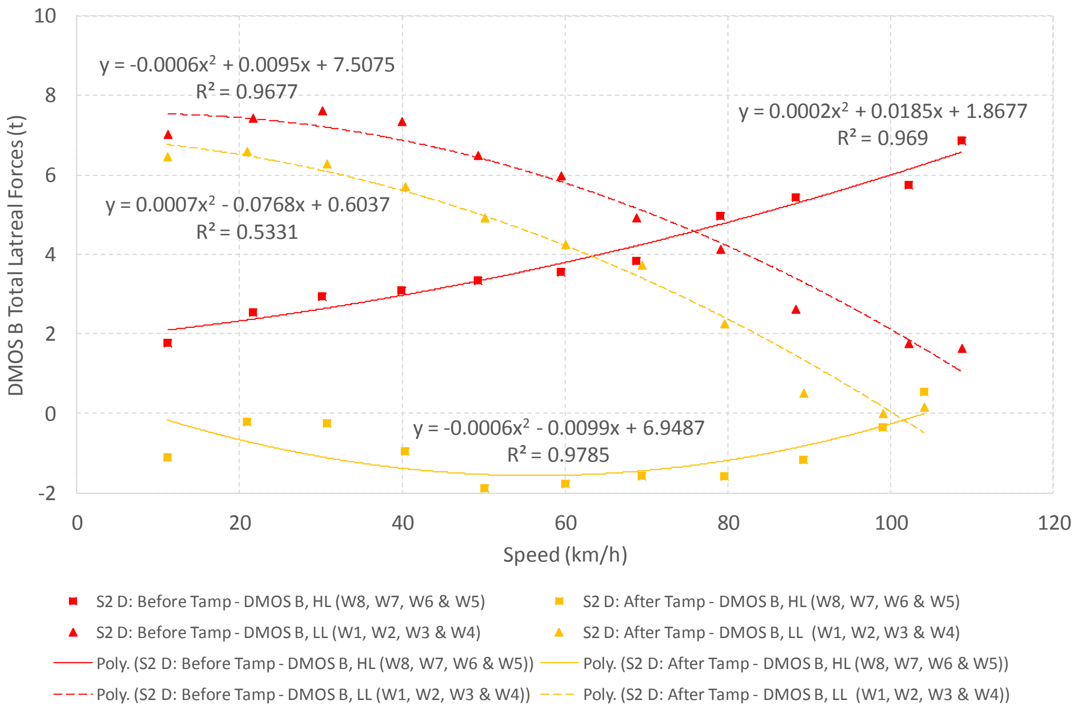

Figure H-18: Lateral Forces (DMOS B) – S2 Down

© University of Pretoria

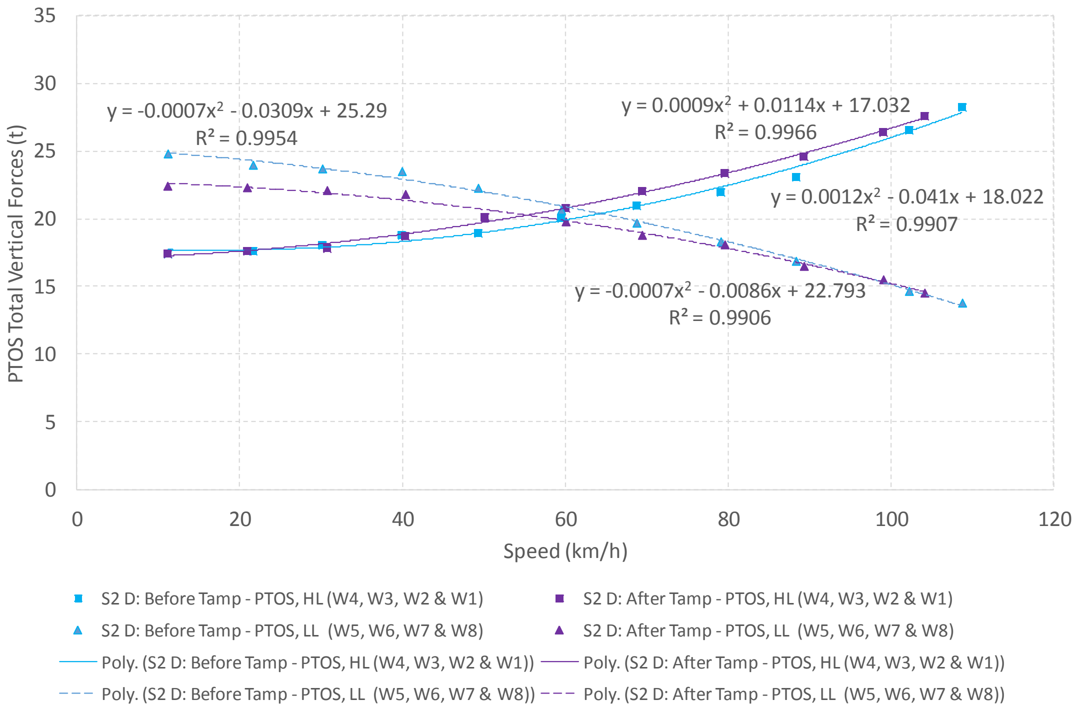

Figure H-19: Vertical Forces (PTOS) – S2 Down

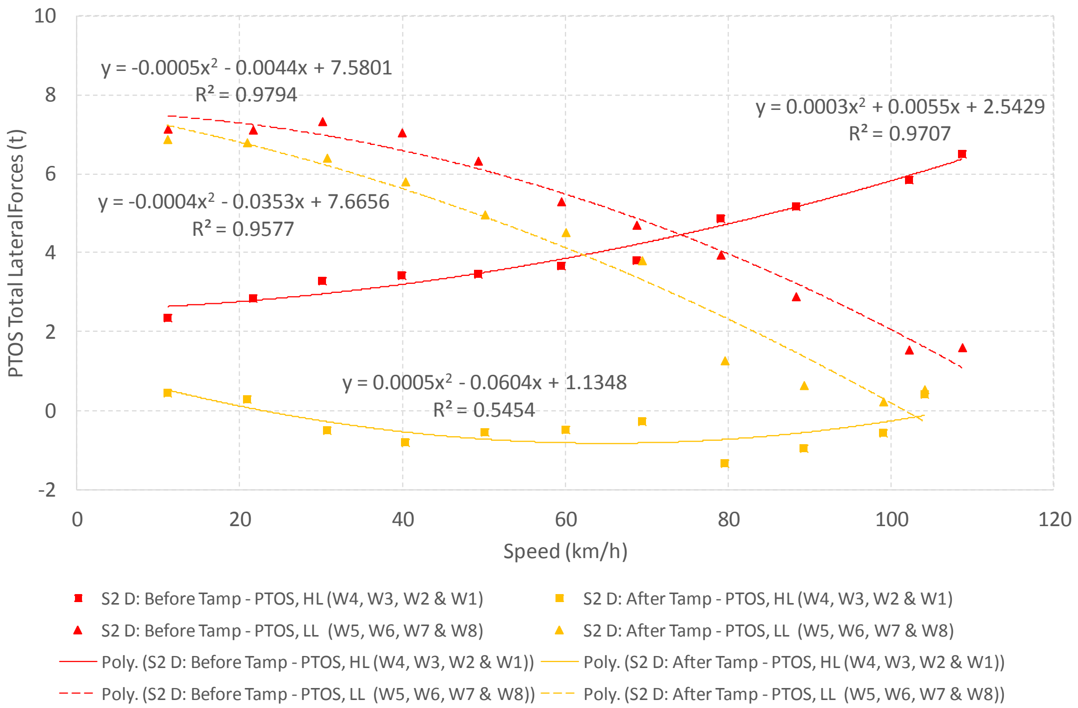

Figure H-20: Lateral Forces (PTOS) – S2 Down

© University of Pretoria

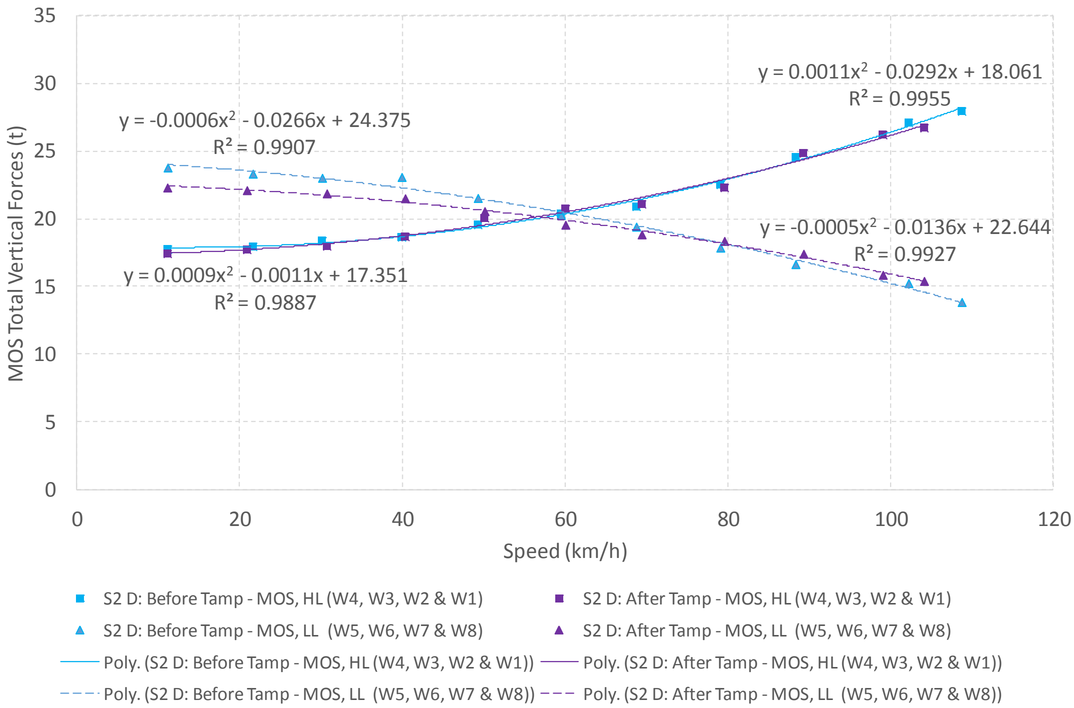

Figure H-21: Vertical Forces (MOS) – S2 Down

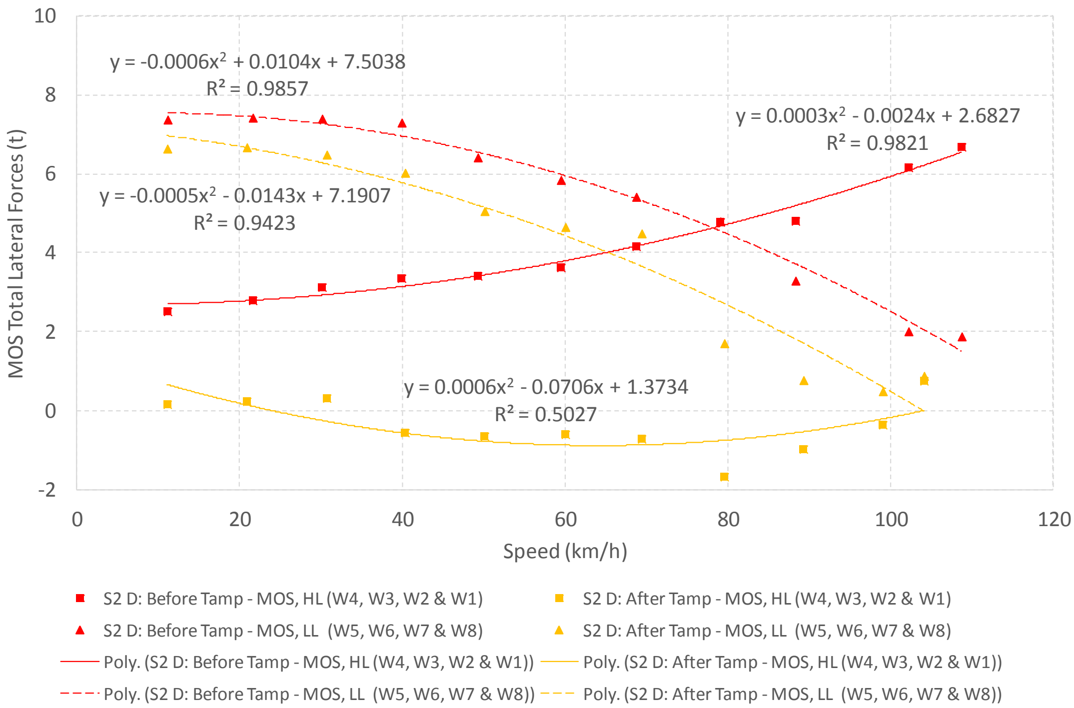

Figure H-22: Lateral Forces (MOS) – S2 Down

© University of Pretoria

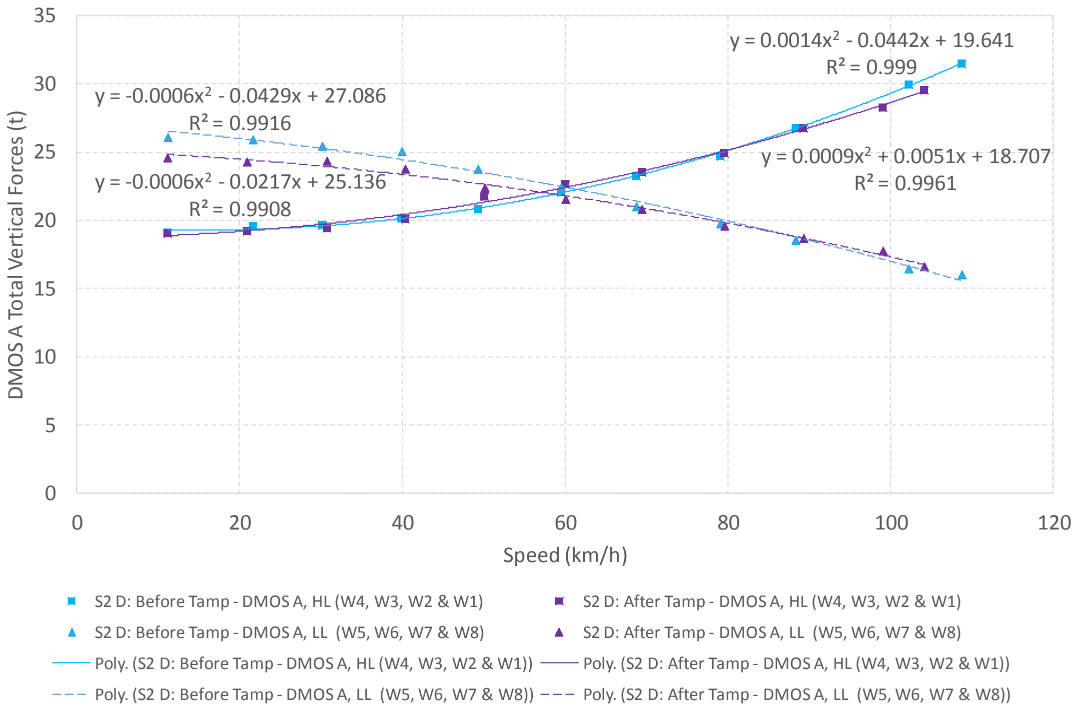

Figure H-23: Vertical Forces (DMOS A) – S2 Down

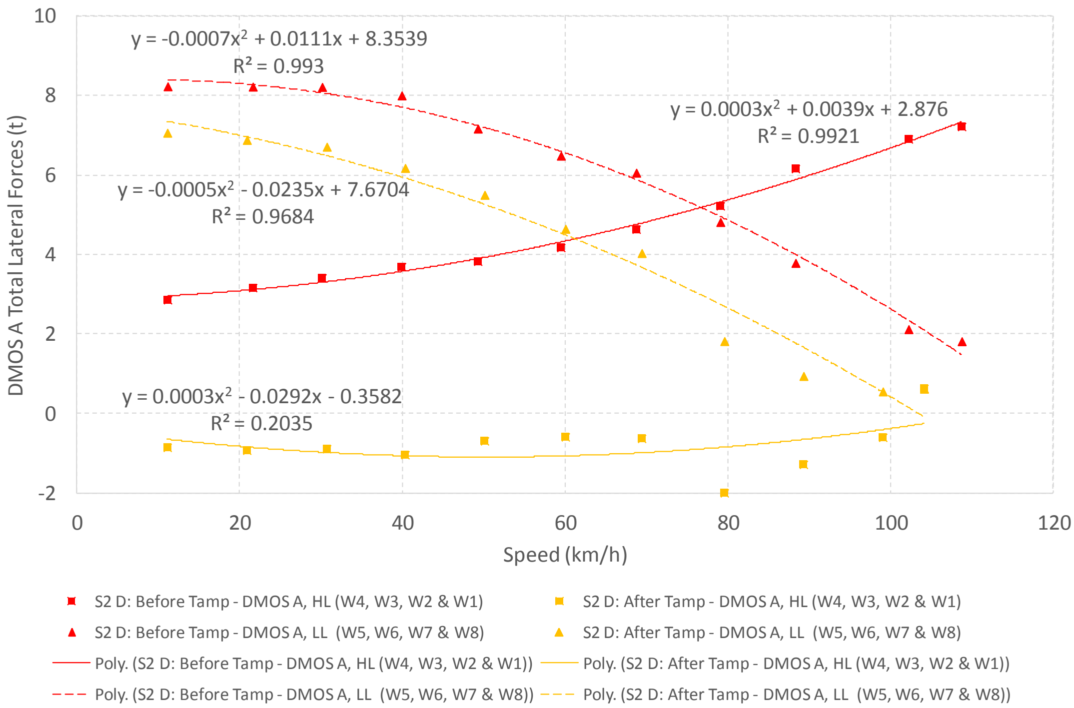

Figure H-24: Lateral Forces (DMOS A) – S2 Down

© University of Pretoria

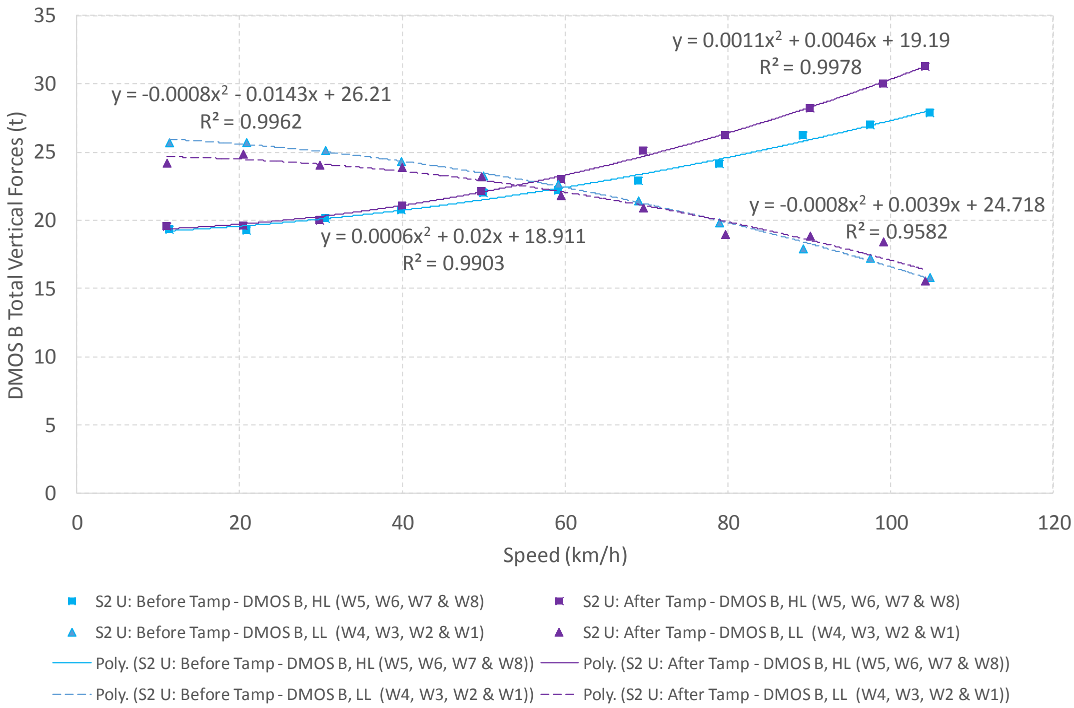

Figure H-25: Vertical Forces (DMOS B) – S2 Up

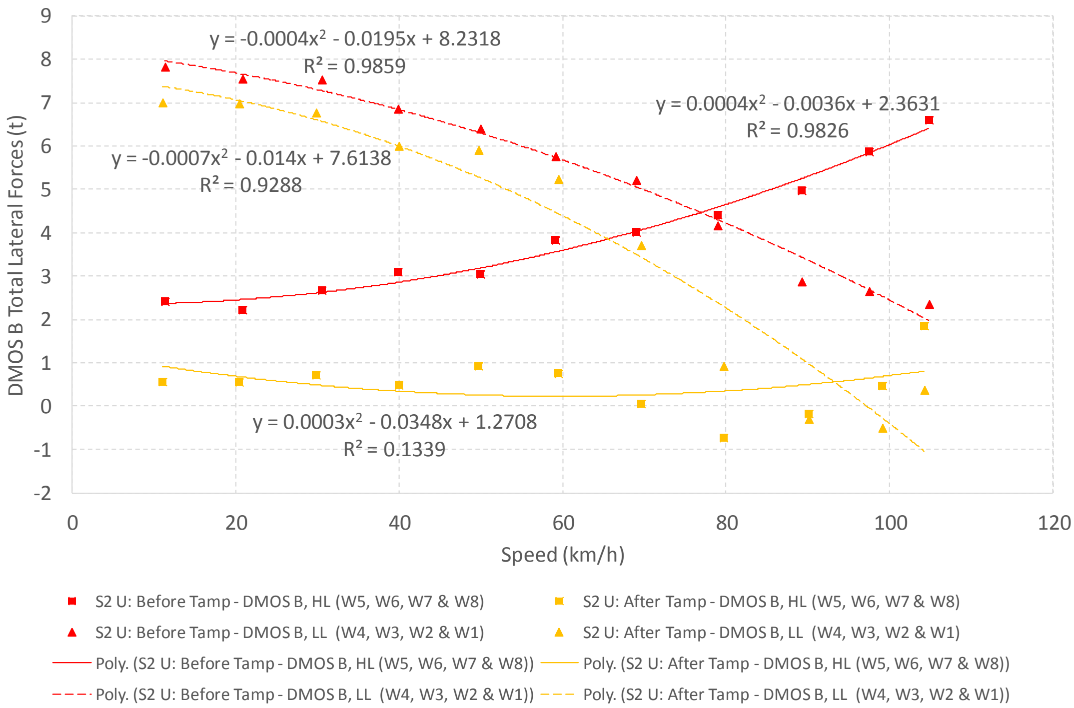

Figure H-26: Lateral Forces (DMOS B) – S2 Up

© University of Pretoria

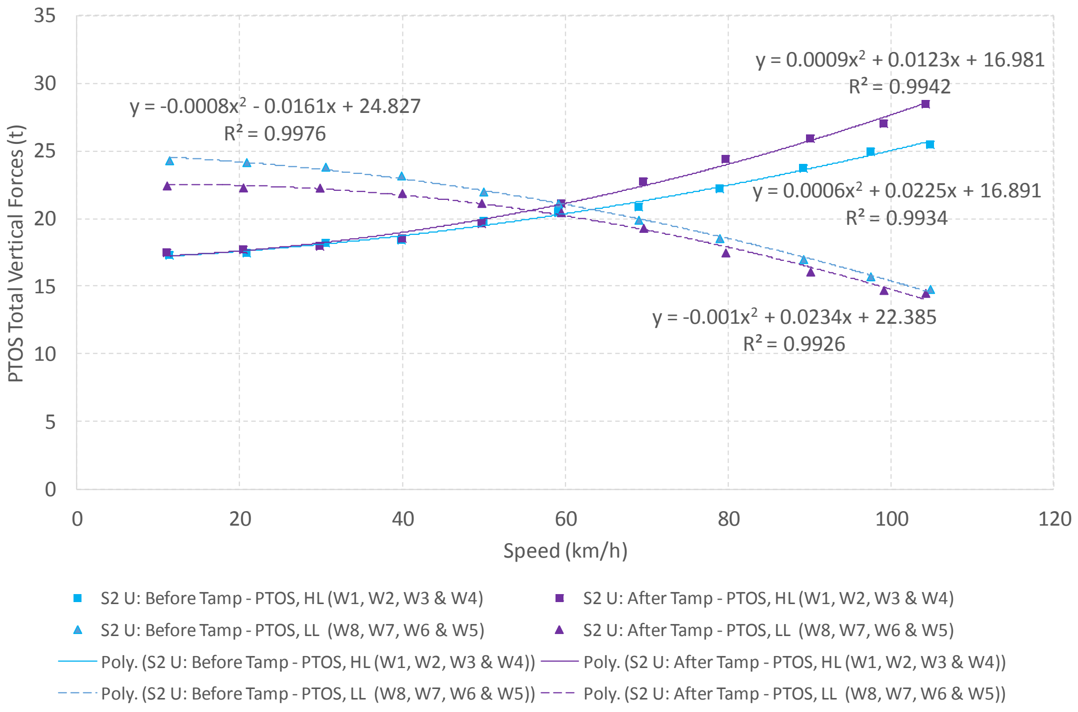

Figure H-27: Vertical Forces (PTOS) – S2 Up

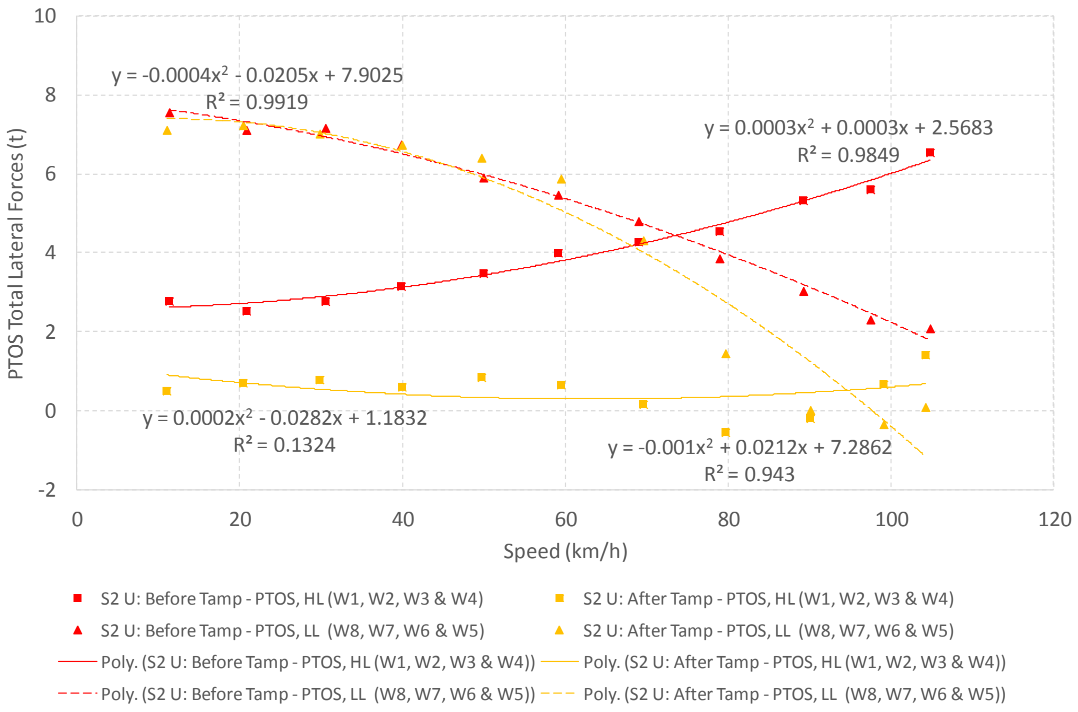

Figure H-28: Lateral Forces (PTOS) – S2 Up

© University of Pretoria

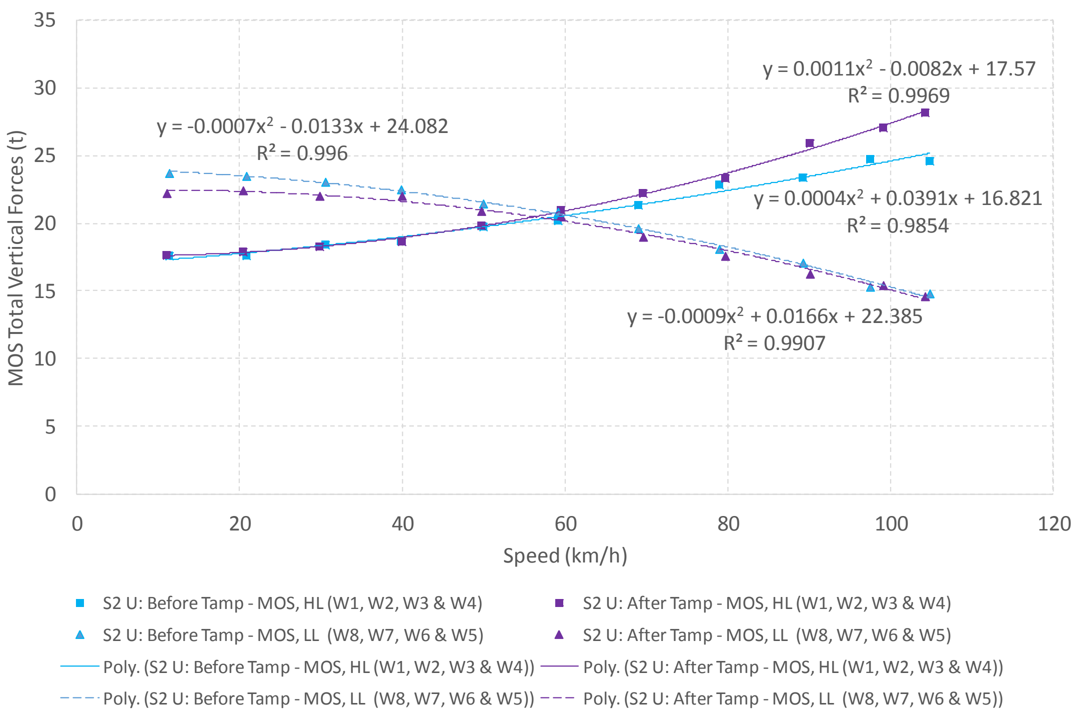

Figure H-29: Vertical Forces (MOS) – S2 Up

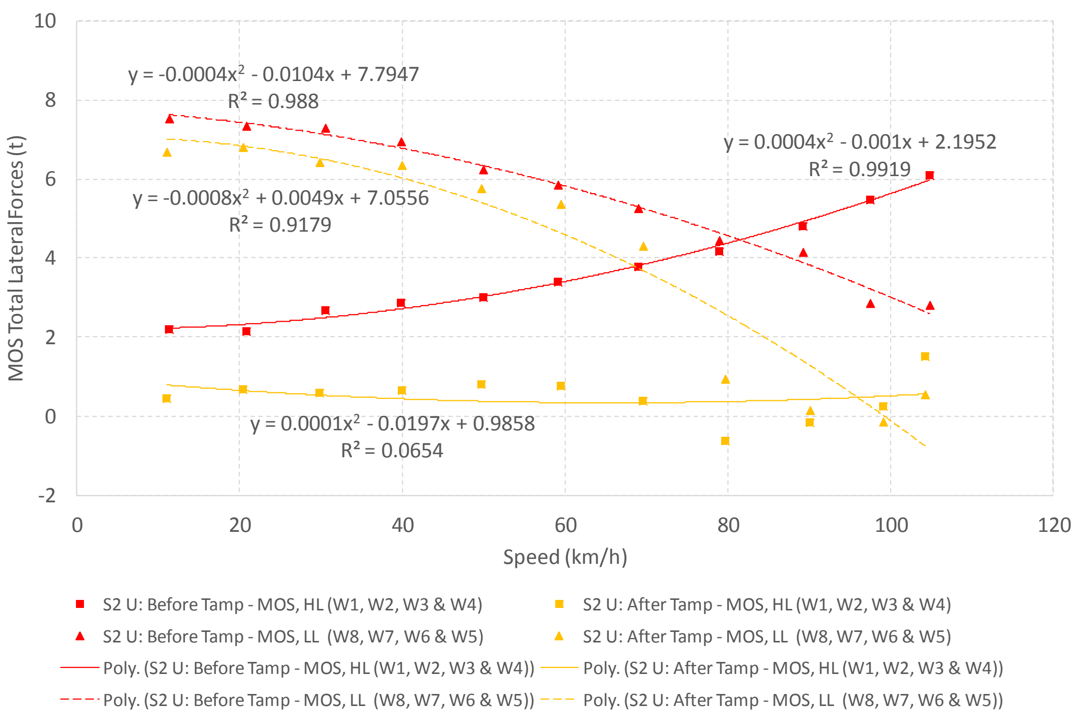

Figure H-30: Lateral Forces (MOS) – S2 Up

© University of Pretoria

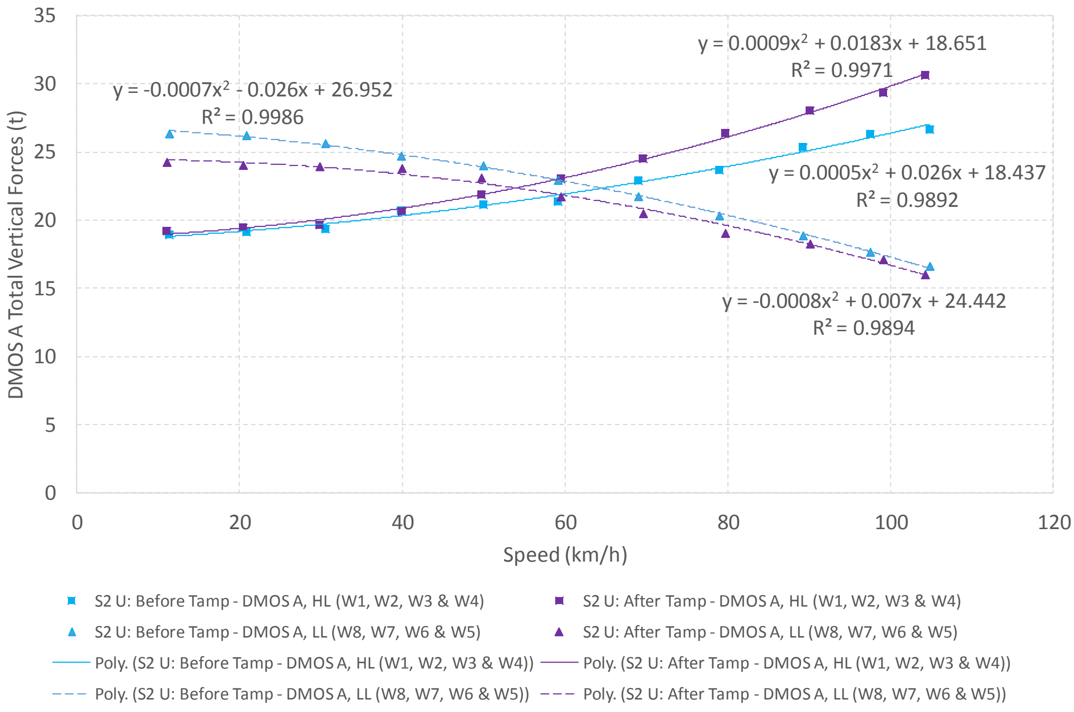

Figure H-31: Vertical Forces (DMOS A) – S2 Up

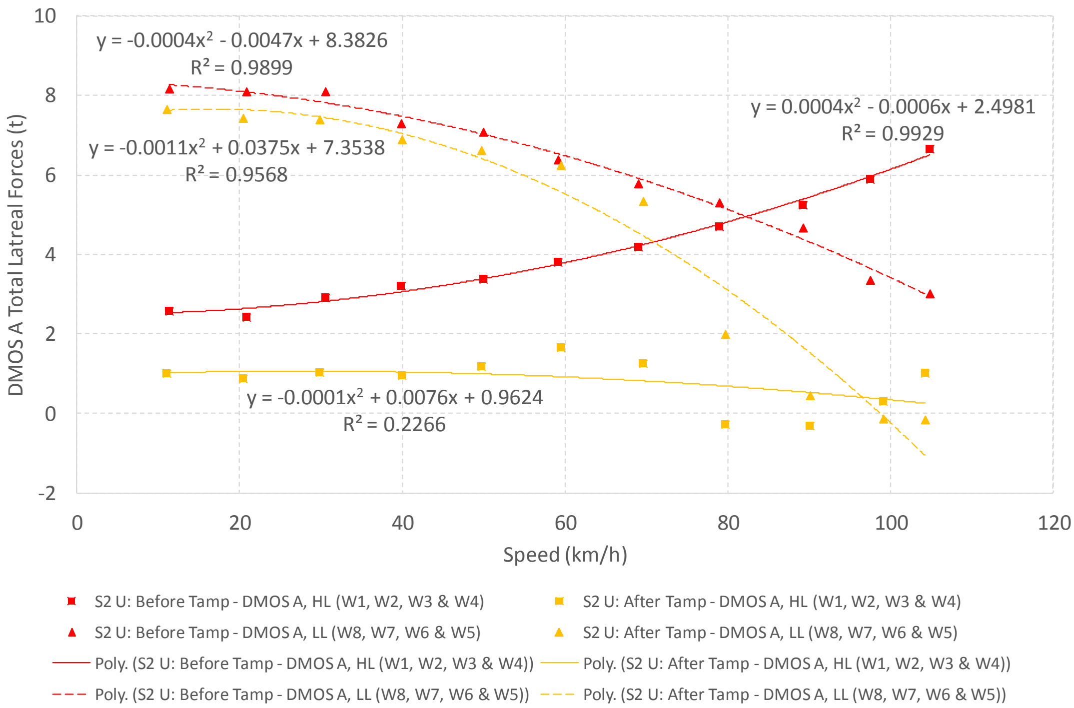

Figure H-32: Lateral Forces (DMOS A) – S2 Up

© University of Pretoria

APPENDIX I. CURVE RAIL FORCES TRENDS FOR 4-CAR TRAINS

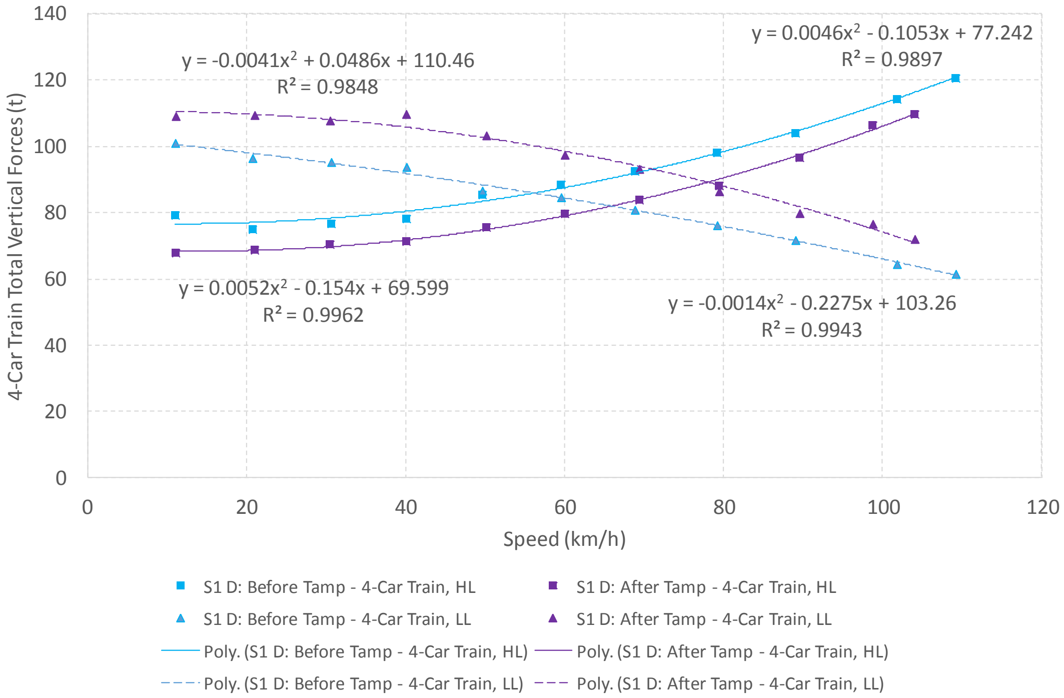

Figure I-1: Vertical Forces (4-Car Train) – S1 Down

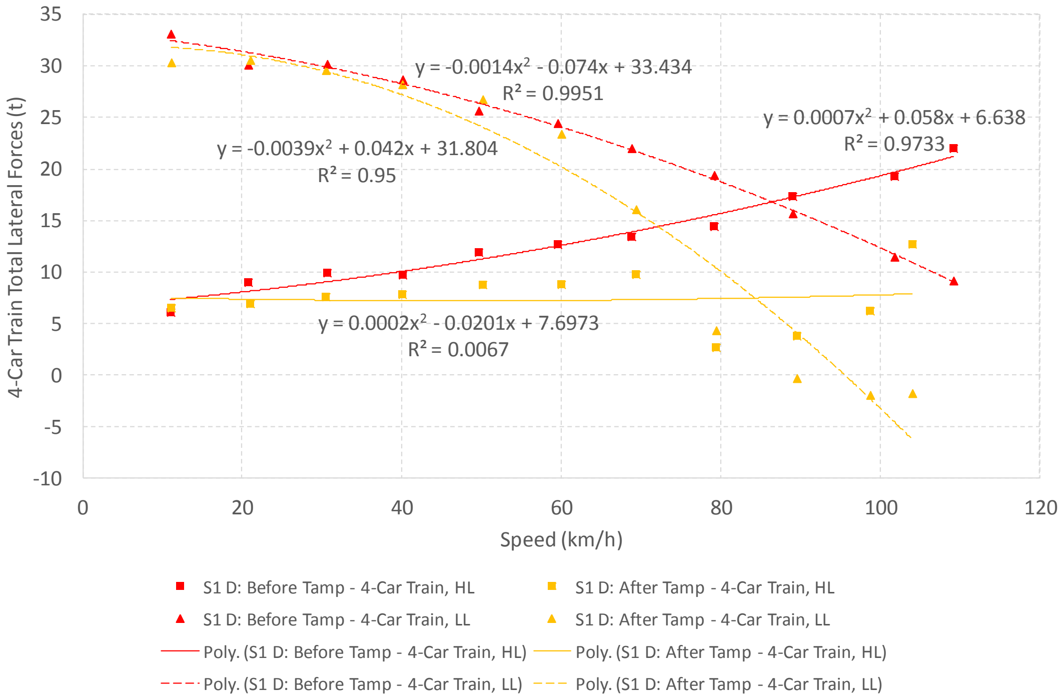

Figure I-2: Lateral Forces (4-Car Train) – S1 Down

© University of Pretoria

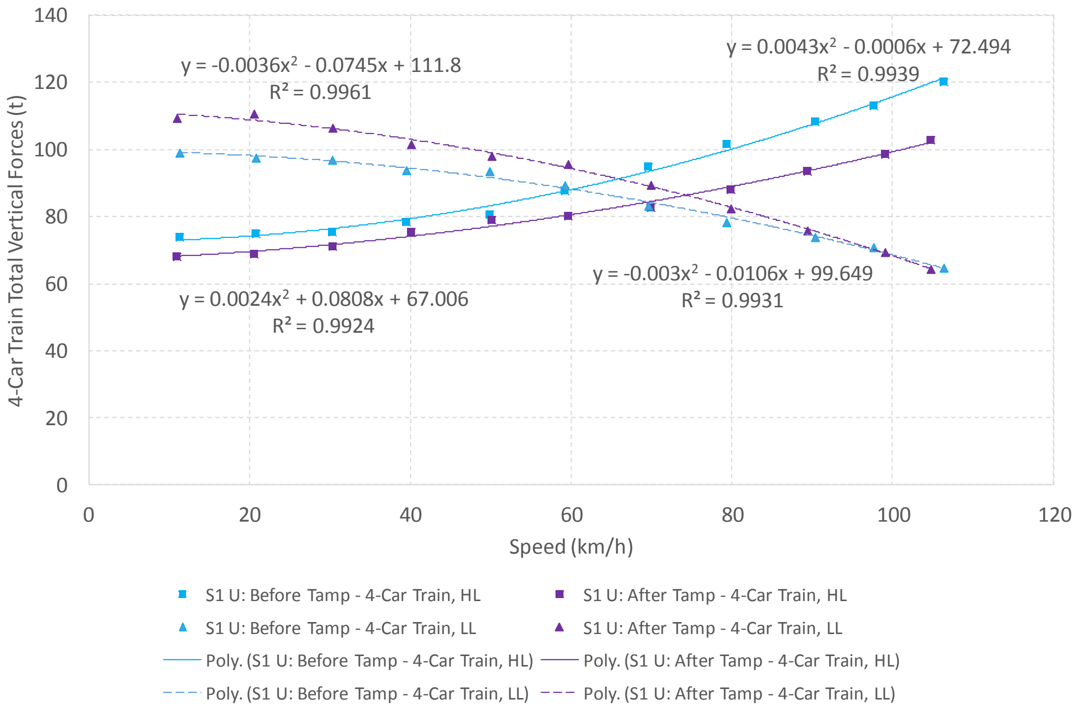

Figure I-3: Vertical Forces (4-Car Train) – S1 Up

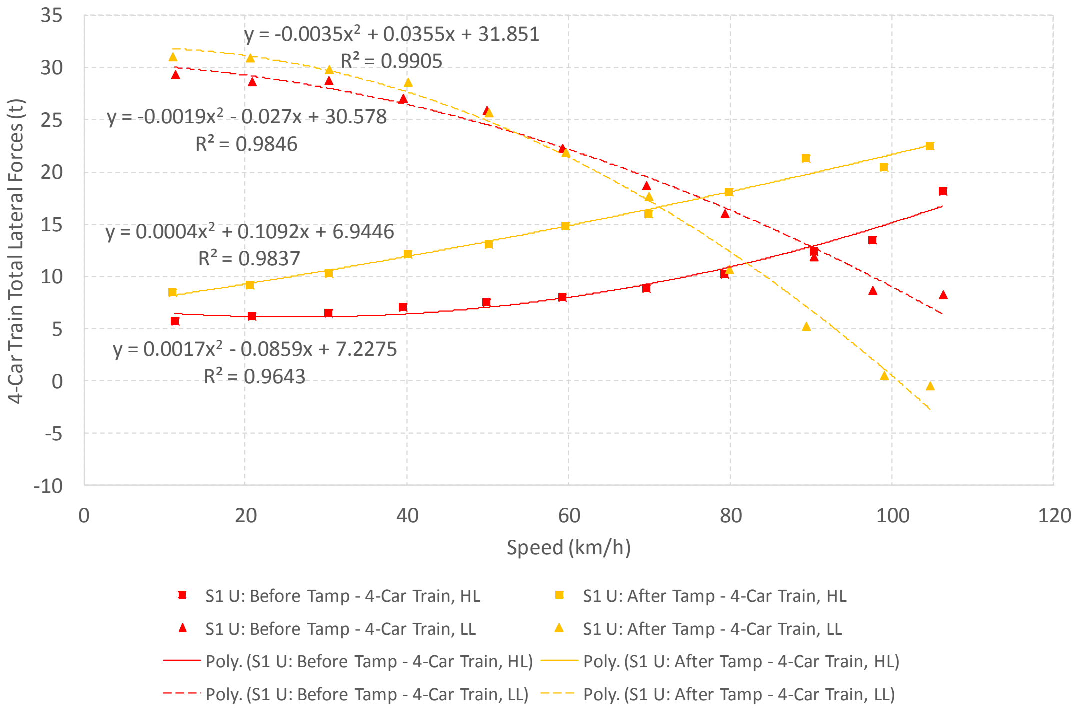

Figure I-4: Lateral Forces (4-Car Train) – S1 Up

© University of Pretoria

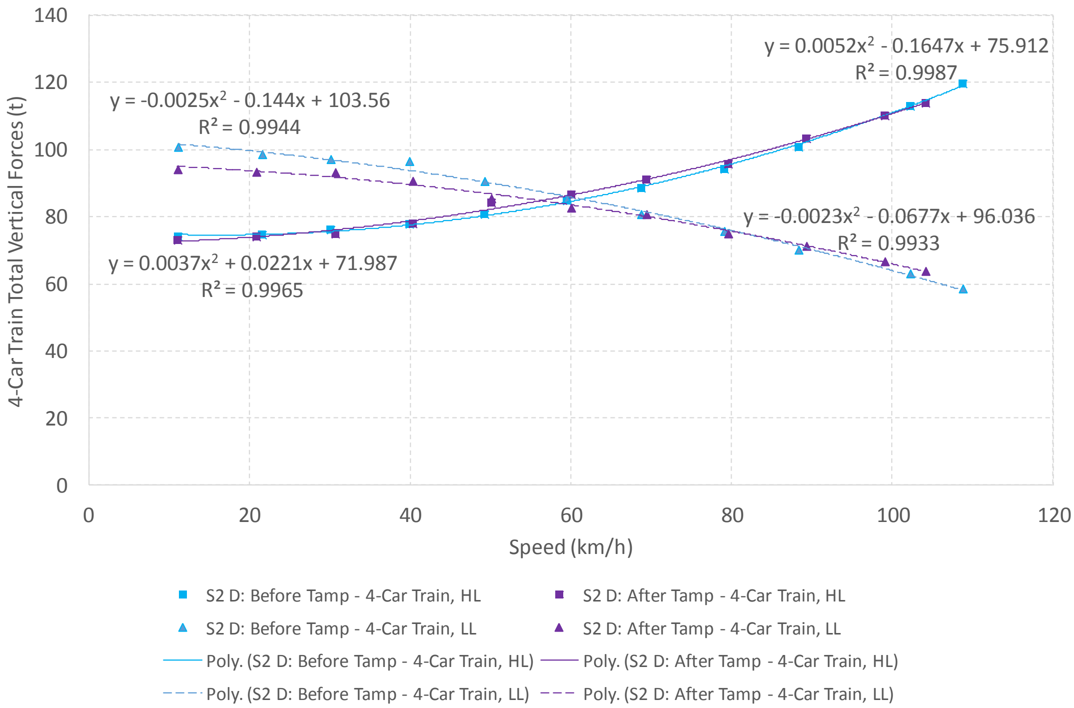

Figure I-5: Vertical Forces (4-Car Train) – S2 Down

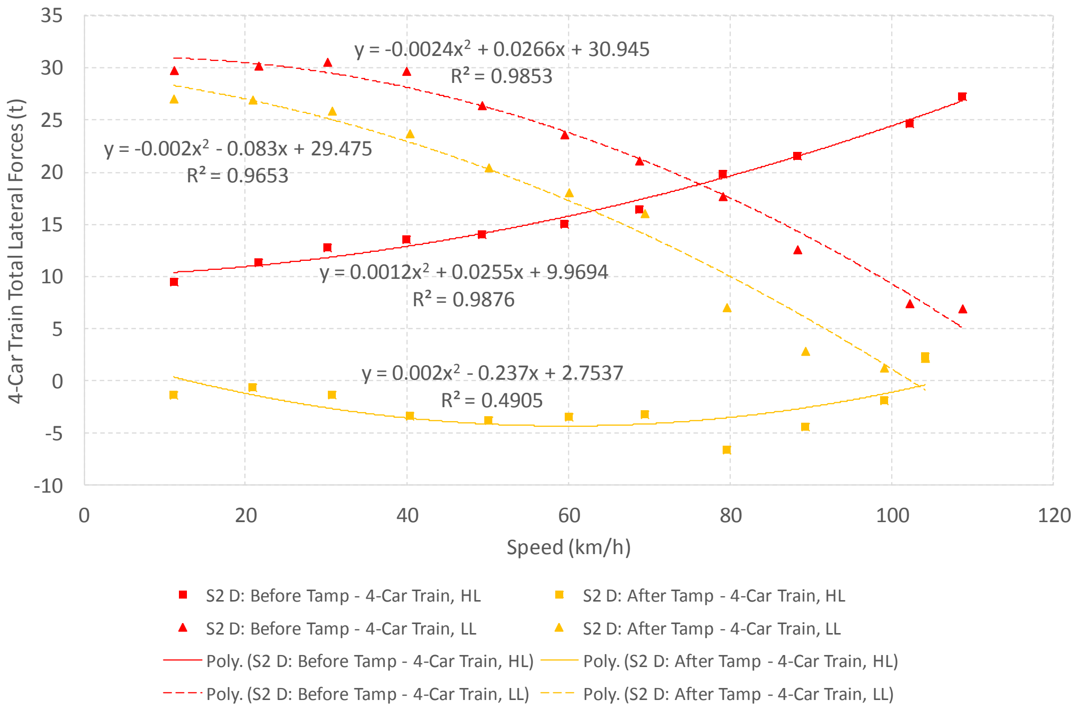

Figure I-6: Lateral Forces (4-Car Train) – S2 Down

© University of Pretoria

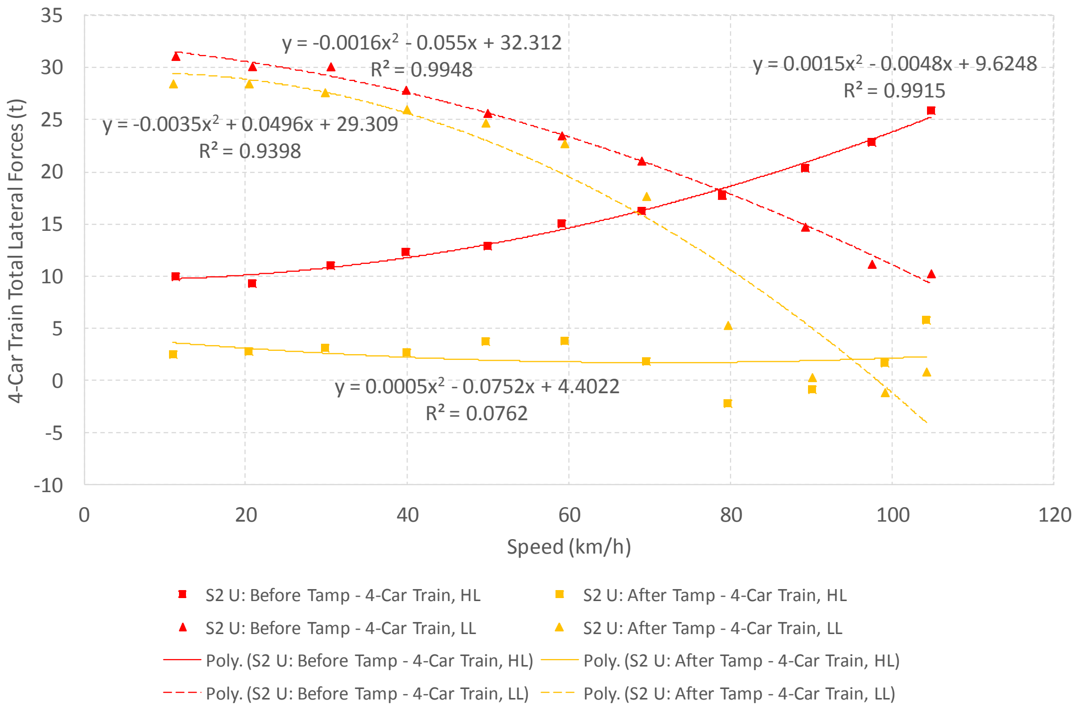

Figure I-7: Lateral Forces (4-Car Train) – S2 Up

© University of Pretoria

APPENDIX J. TREND LINE INFROMATION FOR BOGIES, CARS AND 4-CAR TRAINS

Table J-1: Trend Line Information (Bogies) – S1 Down

	SITE 1: DOWN			Before Tamping		After Tamping	
	Car	Bogie	Rail	Trend Line Equation	R^2	Trend Line Equation	R^2
Verticals	DMOS B	Leading	HL	$y = 0.0005x^2 - 0.0027x + 10.609$	0.9792	$y = 0.0007x^2 - 0.0108x + 9.5653$	0.9754
			LL	$y = 8E-05x^2 - 0.0591x + 14.65$	0.9797	$y = -0.0005x^2 + 0.0015x + 15.818$	0.8177
		Trailing	HL	$y = 0.0008x^2 - 0.0385x + 10.051$	0.9967	$y = 0.0007x^2 - 0.0231x + 8.6166$	0.9944
			LL	$y = -0.0003x^2 - 0.0116x + 12.306$	0.9915	$y = -0.0007x^2 + 0.0227x + 13.285$	0.9943
	PTOS	Leading	HL	$y = 0.0005x^2 - 0.0103x + 8.3611$	0.9632	$y = 0.0005x^2 - 0.0128x + 7.6086$	0.9852
			LL	$y = -0.0001x^2 - 0.034x + 12.491$	0.9834	$y = -0.0004x^2 - 0.0071x + 12.922$	0.9820
		Trailing	HL	$y = 0.0007x^2 - 0.0276x + 10.382$	0.9873	$y = 0.0006x^2 - 0.019x + 8.8249$	0.9947
			LL	$y = -0.0002x^2 - 0.0287x + 12.857$	0.9867	$y = -0.0008x^2 + 0.0341x + 13.301$	0.9947
	MOS	Leading	HL	$y = 0.0006x^2 - 0.0097x + 9.2894$	0.9844	$y = 0.0006x^2 - 0.0169x + 8.7285$	0.9962
			LL	$y = -0.0003x^2 - 0.0236x + 12.434$	0.9866	$y = -0.0003x^2 - 0.0168x + 13.047$	0.9722
		Trailing	HL	$y = 0.0005x^2 - 0.0105x + 9.1016$	0.9916	$y = 0.0007x^2 - 0.0252x + 7.9538$	0.9891
			LL	$y = -0.0001x^2 - 0.0236x + 11.852$	0.9885	$y = -0.0004x^2 + 0.0026x + 13.373$	0.9794
	DMOS A	Leading	HL	$y = 0.0006x^2 - 0.0065x + 9.0575$	0.9882	$y = 0.0006x^2 - 0.0169x + 8.6532$	0.9890
			LL	$y = -0.0003x^2 - 0.0213x + 12.74$	0.9904	$y = -0.0005x^2 + 0.0026x + 13.496$	0.9883
		Trailing	HL	$y = 0.0004x^2 + 0.0005x + 10.391$	0.9870	$y = 0.0007x^2 - 0.0293x + 9.6478$	0.9787
			LL	$y = -0.0002x^2 - 0.0257x + 13.932$	0.9855	$y = -0.0006x^2 + 0.009x + 15.223$	0.9918
Laterals	DMOS B	Leading	HL	$y = 0.0003x^2 - 0.0087x + 0.8559$	0.9767	$y = 0.0003x^2 - 0.0356x + 1.3214$	0.1368
			LL	$y = -0.0002x^2 - 0.0064x + 4.1551$	0.9901	$y = -0.0004x^2 - 0.0071x + 4.2458$	0.9538
		Trailing	HL	$y = 9E-05x^2 + 0.0078x + 0.5271$	0.9377	$y = 0.0002x^2 - 0.0107x + 0.9419$	0.9048
			LL	$y = -0.0002x^2 - 0.0006x + 3.5726$	0.9912	$y = -0.0004x^2 + 0.0031x + 3.8542$	0.9242
	PTOS	Leading	HL	$y = 9E-05x^2 + 0.0041x + 1.2339$	0.9400	$y = -6E-05x^2 + 0.0028x + 1.1762$	0.0693
			LL	$y = -4E-05x^2 - 0.0265x + 4.5435$	0.9834	$y = -0.0006x^2 + 0.0264x + 3.531$	0.9408
		Trailing	HL	$y = 8E-05x^2 + 0.0114x + 0.4414$	0.9725	$y = -8E-05x^2 + 0.0035x + 0.8911$	0.2866
			LL	$y = -1E-04x^2 - 0.0173x + 4.0496$	0.9874	$y = -0.0005x^2 + 0.0072x + 4.1309$	0.9368
	MOS	Leading	HL	$y = 5E-05x^2 + 0.0107x + 0.7097$	0.9557	$y = -0.0002x^2 + 0.0167x + 0.743$	0.3740
			LL	$y = -8E-05x^2 - 0.0213x + 4.196$	0.9946	$y = -0.0005x^2 + 0.0051x + 3.8964$	0.9345
		Trailing	HL	$y = -3E-06x^2 + 0.0151x + 0.9048$	0.9614	$y = -0.0003x^2 + 0.0249x + 0.296$	0.2654
			LL	$y = -0.0003x^2 + 0.01x + 3.8668$	0.9784	$y = -0.0005x^2 + 0.0081x + 3.598$	0.9043
	DMOS A	Leading	HL	$y = -9E-06x^2 + 0.0142x + 1.1364$	0.9271	$y = 1E-05x^2 + 0.0053x + 0.9989$	0.6443
			LL	$y = -0.0001x^2 - 0.0168x + 4.5718$	0.9919	$y = -0.0006x^2 + 0.0207x + 3.855$	0.9449
		Trailing	HL	$y = 0.0001x^2 + 0.0033x + 0.8289$	0.9521	$y = 0.0003x^2 - 0.027x + 1.3289$	0.2306
			LL	$y = -0.0003x^2 + 0.005x + 4.4789$	0.9884	$y = -0.0003x^2 - 0.0214x + 4.6929$	0.9450

© University of Pretoria

Table J-2: Trend Line Information (Bogies) – S1 Up

	SITE 1: UP			Before Tamping		After Tamping	
	Car	Bogie	Rail	Trend Line Equation	R^2	Trend Line Equation	R^2
Verticals	DMOS B	Leading	HL	$y = 0.0005x^2 - 0.0002x + 9.0345$	0.9956	$y = 0.0004x^2 + 0.0051x + 8.3233$	0.9925
			LL	$y = -0.0004x^2 + 0.0013x + 12.039$	0.9797	$y = -0.0005x^2 - 0.0106x + 13.721$	0.9923
		Trailing	HL	$y = 0.0005x^2 + 0.0087x + 9.9521$	0.9937	$y = 0.0005x^2 - 0.0106x + 9.8316$	0.9817
			LL	$y = -0.0003x^2 - 0.0066x + 13.689$	0.9890	$y = -0.0003x^2 - 0.0319x + 15.979$	0.9598
	PTOS	Leading	HL	$y = 0.0006x^2 - 0.0052x + 9.4976$	0.9898	$y = 0.0002x^2 + 0.018x + 8.4111$	0.9853
			LL	$y = -0.0004x^2 + 0.0054x + 12.307$	0.9814	$y = -0.0004x^2 - 0.0208x + 14.15$	0.9903
		Trailing	HL	$y = 0.0005x^2 + 0.0013x + 7.6485$	0.9877	$y = 0.0003x^2 + 0.0078x + 7.482$	0.9752
			LL	$y = -0.0004x^2 + 0.0023x + 11.798$	0.9949	$y = -0.0005x^2 + 0.0039x + 12.488$	0.9867
	MOS	Leading	HL	$y = 0.0004x^2 + 0.0044x + 8.5951$	0.9891	$y = 0.0002x^2 + 0.0171x + 7.4426$	0.9743
			LL	$y = -0.0003x^2 + 0.0002x + 11.474$	0.9865	$y = -0.0005x^2 - 0.0008x + 13.566$	0.9877
		Trailing	HL	$y = 0.0007x^2 - 0.0117x + 8.9346$	0.9907	$y = 0.0003x^2 + 0.0111x + 8.3481$	0.9911
			LL	$y = -0.0004x^2 - 0.0035x + 12.037$	0.9870	$y = -0.0004x^2 - 0.0106x + 13.058$	0.9886
	DMOS A	Leading	HL	$y = 0.0005x^2 + 0.0029x + 10.135$	0.9903	$y = 0.0001x^2 + 0.0263x + 8.7484$	0.9689
			LL	$y = -0.0003x^2 - 0.0071x + 13.81$	0.9888	$y = -0.0005x^2 - 0.008x + 15.535$	0.9934
		Trailing	HL	$y = 0.0006x^2 - 0.0006x + 8.6971$	0.9932	$y = 0.0004x^2 + 0.006x + 8.4189$	0.9909
			LL	$y = -0.0004x^2 - 0.0024x + 12.494$	0.9919	$y = -0.0006x^2 + 0.0043x + 13.304$	0.9892
Laterals	DMOS B	Leading	HL	$y = 0.0002x^2 - 0.0157x + 1.1431$	0.7788	$y = -2E-05x^2 + 0.0173x + 1.05$	0.9611
			LL	$y = -0.0002x^2 - 0.0061x + 3.835$	0.9758	$y = -0.0002x^2 - 0.0158x + 3.798$	0.9790
		Trailing	HL	$y = 0.0003x^2 - 0.0235x + 0.718$	0.9278	$y = 9E-05x^2 + 0.013x + 0.657$	0.9187
			LL	$y = -0.0001x^2 - 0.0195x + 3.9165$	0.9663	$y = -0.0003x^2 - 0.0212x + 4.7535$	0.9570
	PTOS	Leading	HL	$y = 0.0002x^2 - 0.0125x + 1.0488$	0.9161	$y = -7E-06x^2 + 0.0155x + 1.0084$	0.9389
			LL	$y = -0.0003x^2 + 0.0008x + 3.635$	0.9825	$y = -0.0006x^2 + 0.0192x + 3.9626$	0.9763
		Trailing	HL	$y = 0.0002x^2 - 0.0145x + 1.0796$	0.9803	$y = 8E-05x^2 + 0.0075x + 0.9374$	0.9217
			LL	$y = -0.0002x^2 - 0.0064x + 3.6158$	0.9853	$y = -0.0003x^2 - 0.0112x + 4.1173$	0.9778
	MOS	Leading	HL	$y = 9E-05x^2 + 0.0044x + 0.7089$	0.9765	$y = 2E-05x^2 + 0.0163x + 0.8269$	0.9179
			LL	$y = -0.0003x^2 + 0.01x + 3.8086$	0.9834	$y = -0.0005x^2 + 0.0213x + 3.5049$	0.9819
		Trailing	HL	$y = 0.0003x^2 - 0.0155x + 0.7524$	0.9672	$y = 2E-05x^2 + 0.0163x + 0.5737$	0.9648
			LL	$y = -0.0002x^2 - 0.0074x + 3.5863$	0.9622	$y = -0.0004x^2 + 0.0001x + 3.8904$	0.9702
	DMOS A	Leading	HL	$y = 0.0002x^2 - 0.0035x + 0.911$	0.9887	$y = 7E-05x^2 + 0.0166x + 0.9736$	0.9647
			LL	$y = -0.0003x^2 + 0.0063x + 4.374$	0.9840	$y = -0.0007x^2 + 0.0306x + 4.037$	0.9845
		Trailing	HL	$y = 0.0001x^2 - 0.0051x + 0.8656$	0.9261	$y = 0.0001x^2 + 0.0069x + 0.9176$	0.9960
			LL	$y = -0.0002x^2 - 0.0048x + 3.807$	0.9776	$y = -0.0005x^2 + 0.0125x + 3.787$	0.9829

© University of Pretoria

Table J-3: Trend Line Information (Bogies) – S2 Down

	SITE 2: DOWN			Before Tamping		After Tamping	
	Car	Bogie	Rail	Trend Line Equation	R^2	Trend Line Equation	R^2
Verticals	DMOS B	Leading	HL	$y = 0.0008x^2 - 0.0346x + 11.058$	0.9908	$y = 0.0005x^2 + 0.0027x + 10.089$	0.9862
			LL	$y = -0.0002x^2 - 0.0317x + 14.133$	0.9879	$y = -0.0002x^2 - 0.0245x + 13.755$	0.8773
		Trailing	HL	$y = 0.0006x^2 - 0.0158x + 9.1296$	0.9841	$y = 0.0004x^2 + 0.0039x + 8.8084$	0.9927
			LL	$y = -0.0004x^2 - 0.0119x + 12.678$	0.9876	$y = -0.0004x^2 + 0.0007x + 11.708$	0.9870
	PTOS	Leading	HL	$y = 0.0005x^2 - 0.0149x + 8.2703$	0.9855	$y = 0.0004x^2 + 0.0048x + 7.8529$	0.9974
			LL	$y = -0.0003x^2 - 0.021x + 12.287$	0.9881	$y = -0.0004x^2 + 0.0002x + 10.835$	0.9924
		Trailing	HL	$y = 0.0007x^2 - 0.0261x + 9.7514$	0.9843	$y = 0.0004x^2 + 0.0066x + 9.1796$	0.9923
			LL	$y = -0.0004x^2 - 0.0098x + 13.003$	0.9963	$y = -0.0003x^2 - 0.0088x + 11.957$	0.9798
	MOS	Leading	HL	$y = 0.0007x^2 - 0.0265x + 9.4639$	0.9893	$y = 0.0005x^2 - 0.0027x + 9.1662$	0.9962
			LL	$y = -0.0004x^2 - 0.0071x + 12.065$	0.9885	$y = -0.0003x^2 - 0.0076x + 11.141$	0.9826
		Trailing	HL	$y = 0.0004x^2 - 0.0027x + 8.5976$	0.9963	$y = 0.0004x^2 + 0.0016x + 8.1845$	0.9590
			LL	$y = -0.0002x^2 - 0.0196x + 12.31$	0.9856	$y = -0.0002x^2 - 0.0059x + 11.504$	0.9777
	DMOS A	Leading	HL	$y = 0.0009x^2 - 0.0397x + 9.6456$	0.9936	$y = 0.0005x^2 + 0.0018x + 8.9443$	0.9923
			LL	$y = -0.0003x^2 - 0.0175x + 12.771$	0.9804	$y = -0.0005x^2 + 0.0066x + 11.474$	0.9963
		Trailing	HL	$y = 0.0005x^2 - 0.0044x + 9.9955$	0.9899	$y = 0.0005x^2 + 0.0033x + 9.7629$	0.9875
			LL	$y = -0.0002x^2 - 0.0255x + 14.315$	0.9886	$y = -1E-04x^2 - 0.0283x + 13.663$	0.9582
Laterals	DMOS B	Leading	HL	$y = 0.0002x^2 + 0.0054x + 0.9779$	0.9793	$y = 0.0005x^2 - 0.0571x + 0.8664$	0.6282
			LL	$y = -0.0003x^2 + 0.0004x + 4.0771$	0.9676	$y = -0.0003x^2 - 0.0081x + 3.7693$	0.9722
		Trailing	HL	$y = 3E-05x^2 + 0.0131x + 0.8898$	0.9360	$y = 0.0002x^2 - 0.0197x - 0.2627$	0.2472
			LL	$y = -0.0003x^2 + 0.0092x + 3.4304$	0.9660	$y = -0.0003x^2 - 0.0017x + 3.1794$	0.9731
	PTOS	Leading	HL	$y = 0.0001x^2 + 0.0054x + 1.3849$	0.9738	$y = 2E-05x^2 - 0.0112x + 0.747$	0.4064
			LL	$y = -0.0002x^2 - 0.0022x + 3.7989$	0.9679	$y = -0.0002x^2 - 0.0129x + 3.7463$	0.9441
		Trailing	HL	$y = 0.0001x^2 + 9E-05x + 1.1581$	0.9611	$y = 0.0004x^2 - 0.0491x + 0.3878$	0.8034
			LL	$y = -0.0003x^2 - 0.0021x + 3.7812$	0.9826	$y = -0.0002x^2 - 0.0224x + 3.9193$	0.9685
	MOS	Leading	HL	$y = 0.0002x^2 - 0.0036x + 1.2681$	0.9832	$y = 0.0002x^2 - 0.0257x + 0.7973$	0.2781
			LL	$y = -0.0002x^2 - 0.0045x + 3.8007$	0.9838	$y = -0.0003x^2 - 0.0086x + 3.8232$	0.9356
		Trailing	HL	$y = 0.0001x^2 + 0.0013x + 1.4146$	0.9579	$y = 0.0004x^2 - 0.0449x + 0.5761$	0.7020
			LL	$y = -0.0004x^2 + 0.0149x + 3.7031$	0.9759	$y = -0.0003x^2 - 0.0057x + 3.3675$	0.9462
	DMOS A	Leading	HL	$y = 0.0002x^2 + 0.0007x + 1.5489$	0.9851	$y = -6E-05x^2 - 0.0003x + 0.37$	0.1980
			LL	$y = -0.0003x^2 - 0.0006x + 4.0528$	0.9876	$y = -0.0003x^2 + 0.0004x + 3.6528$	0.9427
		Trailing	HL	$y = 0.0002x^2 + 0.0032x + 1.3271$	0.9787	$y = 0.0003x^2 - 0.0289x - 0.7281$	0.9160
			LL	$y = -0.0004x^2 + 0.0117x + 4.3011$	0.9877	$y = -0.0002x^2 - 0.024x + 4.0176$	0.9794

© University of Pretoria

Table J-4: Trend Line Information (Bogies) – S2 Up

	SITE 2: UP			Before Tamping		After Tamping	
	Car	Bogie	Rail	Trend Line Equation	R^2	Trend Line Equation	R^2
Verticals	DMOS B	Leading	HL	$y = 0.0004x^2 - 0.0029x + 8.9778$	0.9885	$y = 0.0004x^2 + 0.0107x + 8.9379$	0.9894
			LL	$y = -0.0005x^2 + 0.0035x + 12.511$	0.9939	$y = -0.0005x^2 + 0.0133x + 11.14$	0.9876
		Trailing	HL	$y = 0.0002x^2 + 0.0229x + 9.933$	0.9857	$y = 0.0007x^2 - 0.0061x + 10.252$	0.9890
			LL	$y = -0.0003x^2 - 0.0179x + 13.699$	0.9931	$y = -0.0003x^2 - 0.0094x + 13.578$	0.8957
	PTOS	Leading	HL	$y = 0.0004x^2 + 0.0038x + 9.156$	0.9957	$y = 0.0006x^2 - 0.0014x + 9.3534$	0.9965
			LL	$y = -0.0004x^2 - 0.0067x + 12.993$	0.9968	$y = -0.0006x^2 + 0.0177x + 11.472$	0.9947
		Trailing	HL	$y = 0.0002x^2 + 0.0187x + 7.7354$	0.9823	$y = 0.0004x^2 + 0.0138x + 7.6276$	0.9847
			LL	$y = -0.0004x^2 - 0.0095x + 11.835$	0.9964	$y = -0.0004x^2 + 0.0057x + 10.913$	0.9789
	MOS	Leading	HL	$y = 0.0002x^2 + 0.0176x + 8.229$	0.9690	$y = 0.0004x^2 + 0.0022x + 8.3172$	0.9879
			LL	$y = -0.0003x^2 - 0.0101x + 12.133$	0.9963	$y = -0.0004x^2 + 0.0002x + 11.511$	0.9827
		Trailing	HL	$y = 0.0002x^2 + 0.0215x + 8.5915$	0.9885	$y = 0.0006x^2 - 0.0103x + 9.2531$	0.9938
			LL	$y = -0.0004x^2 - 0.0032x + 11.949$	0.9939	$y = -0.0005x^2 + 0.0165x + 10.874$	0.9882
	DMOS A	Leading	HL	$y = 0.0002x^2 + 0.0196x + 9.5815$	0.9879	$y = 0.0004x^2 + 0.0128x + 9.7281$	0.9951
			LL	$y = -0.0003x^2 - 0.0164x + 14.436$	0.9962	$y = -0.0004x^2 + 0.0019x + 12.946$	0.9936
		Trailing	HL	$y = 0.0004x^2 + 0.0064x + 8.8558$	0.9855	$y = 0.0005x^2 + 0.0055x + 8.9231$	0.9903
			LL	$y = -0.0004x^2 - 0.0097x + 12.516$	0.9923	$y = -0.0005x^2 + 0.0051x + 11.496$	0.9718
Laterals	DMOS B	Leading	HL	$y = 0.0002x^2 - 0.0038x + 1.4477$	0.9581	$y = -9E-06x^2 - 0.0056x + 0.8749$	0.2501
			LL	$y = -0.0002x^2 - 0.0054x + 4.1356$	0.9920	$y = -0.0003x^2 - 0.0079x + 3.4091$	0.9410
		Trailing	HL	$y = 0.0002x^2 + 0.0003x + 0.9154$	0.9818	$y = 0.0003x^2 - 0.0292x + 0.396$	0.5816
			LL	$y = -0.0001x^2 - 0.014x + 4.0961$	0.9772	$y = -0.0004x^2 - 0.0061x + 4.2047$	0.9144
	PTOS	Leading	HL	$y = 0.0002x^2 - 0.0005x + 1.4312$	0.9784	$y = 6E-05x^2 - 0.0104x + 0.5872$	0.1010
			LL	$y = -0.0002x^2 - 0.0097x + 4.2022$	0.9923	$y = -0.0005x^2 + 0.0175x + 3.6407$	0.9465
		Trailing	HL	$y = 0.0002x^2 + 0.0008x + 1.1371$	0.9686	$y = 0.0002x^2 - 0.0179x + 0.5959$	0.3864
			LL	$y = -0.0002x^2 - 0.0108x + 3.7002$	0.9854	$y = -0.0004x^2 + 0.0036x + 3.6455$	0.9331
	MOS	Leading	HL	$y = 0.0002x^2 - 0.0033x + 1.3962$	0.9639	$y = -3E-05x^2 - 0.0005x + 0.3613$	0.1514
			LL	$y = -0.0003x^2 + 0.0043x + 3.9852$	0.9776	$y = -0.0004x^2 + 0.0056x + 3.4076$	0.9125
		Trailing	HL	$y = 0.0002x^2 + 0.0022x + 0.7991$	0.9939	$y = 0.0002x^2 - 0.0192x + 0.6245$	0.2375
			LL	$y = -0.0001x^2 - 0.0147x + 3.8095$	0.9845	$y = -0.0004x^2 - 0.0007x + 3.6481$	0.9210
	DMOS A	Leading	HL	$y = 0.0002x^2 - 0.0026x + 1.4679$	0.9878	$y = -3E-05x^2 - 0.0018x + 0.5733$	0.2158
			LL	$y = -0.0003x^2 + 0.0031x + 4.5477$	0.9751	$y = -0.0006x^2 + 0.0202x + 3.8658$	0.9499
		Trailing	HL	$y = 0.0002x^2 + 0.002x + 1.0302$	0.9964	$y = -0.0001x^2 + 0.0094x + 0.3891$	0.2520
			LL	$y = -0.0002x^2 - 0.0077x + 3.8349$	0.9905	$y = -0.0005x^2 + 0.0173x + 3.488$	0.9606

© University of Pretoria

Table J-5: Trend Line Information (Cars) – S1 Down

	SITE 1: DOWN		Before Tamping		After Tamping	
	Car	Rail	Trend Line Equation	R^2	Trend Line Equation	R^2
Verticals	DMOS B	HL	$y = 0.0013x^2 - 0.0411x + 20.66$	0.9911	$y = 0.0014x^2 - 0.0339x + 18.182$	0.9899
		LL	$y = -0.0003x^2 - 0.0706x + 26.956$	0.9925	$y = -0.0012x^2 + 0.0242x + 29.103$	0.9407
	PTOS	HL	$y = 0.0012x^2 - 0.0379x + 18.743$	0.9791	$y = 0.0011x^2 - 0.0318x + 16.434$	0.9921
		LL	$y = -0.0003x^2 - 0.0628x + 25.348$	0.9930	$y = -0.0012x^2 + 0.027x + 26.223$	0.9941
	MOS	HL	$y = 0.0011x^2 - 0.0202x + 18.391$	0.9917	$y = 0.0013x^2 - 0.0421x + 16.682$	0.9943
		LL	$y = -0.0004x^2 - 0.0471x + 24.287$	0.9879	$y = -0.0007x^2 - 0.0142x + 26.42$	0.9801
	DMOS A	HL	$y = 0.001x^2 - 0.006x + 19.449$	0.9922	$y = 0.0014x^2 - 0.0462x + 18.301$	0.9875
		LL	$y = -0.0005x^2 - 0.0469x + 26.672$	0.9922	$y = -0.0011x^2 + 0.0116x + 28.719$	0.9961
Laterals	DMOS B	HL	$y = 0.0003x^2 - 0.0009x + 1.383$	0.9637	$y = 0.0005x^2 - 0.0464x + 2.2633$	0.4704
		LL	$y = -0.0005x^2 - 0.007x + 7.7277$	0.9943	$y = -0.0008x^2 - 0.004x + 8.1$	0.9548
	PTOS	HL	$y = 0.0002x^2 + 0.0155x + 1.6753$	0.9757	$y = -0.0001x^2 + 0.0063x + 2.0673$	0.1815
		LL	$y = -0.0001x^2 - 0.0438x + 8.5931$	0.9868	$y = -0.0012x^2 + 0.0336x + 7.6619$	0.9468
	MOS	HL	$y = 4E-05x^2 + 0.0258x + 1.6144$	0.9722	$y = -0.0005x^2 + 0.0416x + 1.039$	0.3145
		LL	$y = -0.0004x^2 - 0.0113x + 8.0628$	0.9956	$y = -0.001x^2 + 0.0132x + 7.4944$	0.9203
	DMOS A	HL	$y = 0.0001x^2 + 0.0175x + 1.9653$	0.9462	$y = 0.0003x^2 - 0.0217x + 2.3278$	0.3427
		LL	$y = -0.0004x^2 - 0.0119x + 9.0507$	0.9924	$y = -0.0009x^2 - 0.0007x + 8.5479$	0.9616

Table J-6: Trend Line Information (Cars) – S1 Up

	SITE 1: UP		Before Tamping		After Tamping	
	Car	Rail	Trend Line Equation	R^2	Trend Line Equation	R^2
Verticals	DMOS B	HL	$y = 0.0011x^2 + 0.0085x + 18.987$	0.9958	$y = 0.0009x^2 - 0.0055x + 18.155$	0.9934
		LL	$y = -0.0007x^2 - 0.0054x + 25.728$	0.9869	$y = -0.0007x^2 - 0.0426x + 29.7$	0.9877
	PTOS	HL	$y = 0.0011x^2 - 0.004x + 17.146$	0.9907	$y = 0.0005x^2 + 0.0257x + 15.893$	0.9846
		LL	$y = -0.0009x^2 + 0.0077x + 24.105$	0.9920	$y = -0.0009x^2 - 0.017x + 26.638$	0.9920
	MOS	HL	$y = 0.0011x^2 - 0.0074x + 17.53$	0.9912	$y = 0.0005x^2 + 0.0283x + 15.791$	0.9907
		LL	$y = -0.0007x^2 - 0.0034x + 23.511$	0.9907	$y = -0.0009x^2 - 0.0113x + 26.623$	0.9912
	DMOS A	HL	$y = 0.0011x^2 + 0.0022x + 18.832$	0.9929	$y = 0.0005x^2 + 0.0323x + 17.167$	0.9886
		LL	$y = -0.0007x^2 - 0.0095x + 26.305$	0.9944	$y = -0.001x^2 - 0.0037x + 28.839$	0.9963
Laterals	DMOS B	HL	$y = 0.0006x^2 - 0.0392x + 1.8612$	0.8945	$y = 8E-05x^2 + 0.0302x + 1.7071$	0.9532
		LL	$y = -0.0003x^2 - 0.0256x + 7.7515$	0.9743	$y = -0.0005x^2 - 0.037x + 8.5515$	0.9786
	PTOS	HL	$y = 0.0004x^2 - 0.027x + 2.1284$	0.9636	$y = 8E-05x^2 + 0.023x + 1.9459$	0.9421
		LL	$y = -0.0005x^2 - 0.0056x + 7.2508$	0.9865	$y = -0.0009x^2 + 0.008x + 8.0798$	0.9852
	MOS	HL	$y = 0.0003x^2 - 0.0111x + 1.4612$	0.9781	$y = 4E-05x^2 + 0.0325x + 1.4006$	0.9670
		LL	$y = -0.0005x^2 + 0.0026x + 7.3949$	0.9808	$y = -0.0009x^2 + 0.0214x + 7.3953$	0.9845
	DMOS A	HL	$y = 0.0003x^2 - 0.0086x + 1.7767$	0.9840	$y = 0.0002x^2 + 0.0235x + 1.8911$	0.9911
		LL	$y = -0.0005x^2 + 0.0016x + 8.181$	0.9880	$y = -0.0011x^2 + 0.0431x + 7.824$	0.9902

© University of Pretoria

Table J-7: Trend Line Information (Cars) – S2 Down

	SITE 2: DOWN		Before Tamping		After Tamping	
	Car	Rail	Trend Line Equation	R^2	Trend Line Equation	R^2
Verticals	DMOS B	HL	$y = 0.0014x^2 - 0.0504x + 20.188$	0.9949	$y = 0.001x^2 + 0.0066x + 18.897$	0.9932
		LL	$y = -0.0006x^2 - 0.0436x + 26.811$	0.9910	$y = -0.0006x^2 - 0.0238x + 25.463$	0.9584
	PTOS	HL	$y = 0.0012x^2 - 0.041x + 18.022$	0.9907	$y = 0.0009x^2 + 0.0114x + 17.032$	0.9966
		LL	$y = -0.0007x^2 - 0.0309x + 25.29$	0.9954	$y = -0.0007x^2 - 0.0086x + 22.793$	0.9906
	MOS	HL	$y = 0.0011x^2 - 0.0292x + 18.061$	0.9955	$y = 0.0009x^2 - 0.0011x + 17.351$	0.9887
		LL	$y = -0.0006x^2 - 0.0266x + 24.375$	0.9907	$y = -0.0005x^2 - 0.0136x + 22.644$	0.9927
	DMOS A	HL	$y = 0.0014x^2 - 0.0442x + 19.641$	0.9990	$y = 0.0009x^2 + 0.0051x + 18.707$	0.9961
		LL	$y = -0.0006x^2 - 0.0429x + 27.086$	0.9916	$y = -0.0006x^2 - 0.0217x + 25.136$	0.9908
Laterals	DMOS B	HL	$y = 0.0002x^2 + 0.0185x + 1.8677$	0.9690	$y = -0.0006x^2 - 0.0099x + 6.9487$	0.9785
		LL	$y = -0.0006x^2 + 0.0095x + 7.5075$	0.9677	$y = 0.0007x^2 - 0.0768x + 0.6037$	0.5331
	PTOS	HL	$y = 0.0003x^2 + 0.0055x + 2.5429$	0.9707	$y = 0.0005x^2 - 0.0604x + 1.1348$	0.5454
		LL	$y = -0.0005x^2 - 0.0044x + 7.5801$	0.9794	$y = -0.0004x^2 - 0.0353x + 7.6656$	0.9577
	MOS	HL	$y = 0.0003x^2 - 0.0024x + 2.6827$	0.9821	$y = 0.0006x^2 - 0.0706x + 1.3734$	0.5027
		LL	$y = -0.0006x^2 + 0.0104x + 7.5038$	0.9857	$y = -0.0005x^2 - 0.0143x + 7.1907$	0.9423
	DMOS A	HL	$y = 0.0003x^2 + 0.0039x + 2.876$	0.9921	$y = 0.0003x^2 - 0.0292x - 0.3582$	0.2035
		LL	$y = -0.0007x^2 + 0.0111x + 8.3539$	0.9930	$y = -0.0005x^2 - 0.0235x + 7.6704$	0.9684

Table J-8: Trend Line Information (Cars) – S2 Up

	SITE 2: UP		Before Tamping		After Tamping	
	Car	Rail	Trend Line Equation	R^2	Trend Line Equation	R^2
Verticals	DMOS B	HL	$y = 0.0006x^2 + 0.02x + 18.911$	0.9903	$y = 0.0011x^2 + 0.0046x + 19.19$	0.9978
		LL	$y = -0.0008x^2 - 0.0143x + 26.21$	0.9962	$y = -0.0008x^2 + 0.0039x + 24.718$	0.9582
	PTOS	HL	$y = 0.0006x^2 + 0.0225x + 16.891$	0.9934	$y = 0.0009x^2 + 0.0123x + 16.981$	0.9942
		LL	$y = -0.0008x^2 - 0.0161x + 24.827$	0.9976	$y = -0.001x^2 + 0.0234x + 22.385$	0.9926
	MOS	HL	$y = 0.0004x^2 + 0.0391x + 16.821$	0.9854	$y = 0.0011x^2 - 0.0082x + 17.57$	0.9969
		LL	$y = -0.0007x^2 - 0.0133x + 24.082$	0.996	$y = -0.0009x^2 + 0.0166x + 22.385$	0.9907
	DMOS A	HL	$y = 0.0005x^2 + 0.026x + 18.437$	0.9892	$y = 0.0009x^2 + 0.0183x + 18.651$	0.9971
		LL	$y = -0.0007x^2 - 0.026x + 26.952$	0.9986	$y = -0.0008x^2 + 0.007x + 24.442$	0.9894
Laterals	DMOS B	HL	$y = 0.0004x^2 - 0.0036x + 2.3631$	0.9826	$y = 0.0003x^2 - 0.0348x + 1.2708$	0.1339
		LL	$y = -0.0004x^2 - 0.0195x + 8.2318$	0.9859	$y = -0.0007x^2 - 0.014x + 7.6138$	0.9288
	PTOS	HL	$y = 0.0003x^2 + 0.0003x + 2.5683$	0.9849	$y = 0.0002x^2 - 0.0282x + 1.1832$	0.1324
		LL	$y = -0.0004x^2 - 0.0205x + 7.9025$	0.9919	$y = -0.001x^2 + 0.0212x + 7.2862$	0.943
	MOS	HL	$y = 0.0004x^2 - 0.001x + 2.1952$	0.9919	$y = 0.0001x^2 - 0.0197x + 0.9858$	0.0654
		LL	$y = -0.0004x^2 - 0.0104x + 7.7947$	0.988	$y = -0.0008x^2 + 0.0049x + 7.0556$	0.9179
	DMOS A	HL	$y = 0.0004x^2 - 0.0006x + 2.4981$	0.9929	$y = -0.0001x^2 + 0.0076x + 0.9624$	0.2266
		LL	$y = -0.0004x^2 - 0.0047x + 8.3826$	0.9899	$y = -0.0011x^2 + 0.0375x + 7.3538$	0.9568

© University of Pretoria

Table J-9: Trend Line Information (4-Car Train) – S1 Down

4 Car Train	SITE 1: DOWN		Before Tamping		After Tamping	
			Trend Line Equation	R^2	Trend Line Equation	R^2
	Verticals	High Leg	$y = 0.0046x^2 - 0.1053x + 77.242$	0.9897	$y = 0.0052x^2 - 0.154x + 69.599$	0.9962
		Low Leg	$y = -0.0014x^2 - 0.2275x + 103.26$	0.9943	$y = -0.0041x^2 + 0.0486x + 110.46$	0.9848
	Laterals	High Leg	$y = 0.0007x^2 + 0.058x + 6.638$	0.9733	$y = 0.0002x^2 - 0.0201x + 7.6973$	0.0067
		Low Leg	$y = -0.0014x^2 - 0.074x + 33.434$	0.9951	$y = -0.0039x^2 + 0.042x + 31.804$	0.9500

Table J-10: Trend Line Information (4-Car Train) – S1 Up

4 Car Train	SITE 1: UP		Before Tamping		After Tamping	
			Trend Line Equation	R^2	Trend Line Equation	R^2
	Verticals	High Leg	$y = 0.0043x^2 - 0.0006x + 72.494$	0.9939	$y = 0.0024x^2 + 0.0808x + 67.006$	0.9924
		Low Leg	$y = -0.003x^2 - 0.0106x + 99.649$	0.9931	$y = -0.0036x^2 - 0.0745x + 111.8$	0.9961
	Laterals	High Leg	$y = 0.0017x^2 - 0.0859x + 7.2275$	0.9643	$y = 0.0004x^2 + 0.1092x + 6.9446$	0.9837
		Low Leg	$y = -0.0019x^2 - 0.027x + 30.578$	0.9846	$y = -0.0035x^2 + 0.0355x + 31.851$	0.9905

Table J-11: Trend Line Information (4-Car Train) – S2 Down

4 Car Train	SITE 2: DOWN		Before Tamping		After Tamping	
			Trend Line Equation	R^2	Trend Line Equation	R^2
	Verticals	High Leg	$y = 0.0052x^2 - 0.1647x + 75.912$	0.9987	$y = 0.0037x^2 + 0.0221x + 71.987$	0.9965
		Low Leg	$y = -0.0025x^2 - 0.144x + 103.56$	0.9944	$y = -0.0023x^2 - 0.0677x + 96.036$	0.9933
	Laterals	High Leg	$y = 0.0012x^2 + 0.0255x + 9.9694$	0.9876	$y = 0.002x^2 - 0.237x + 2.7537$	0.4905
		Low Leg	$y = -0.0024x^2 + 0.0266x + 30.945$	0.9853	$y = -0.002x^2 - 0.083x + 29.475$	0.9653

Table J-12: Trend Line Information (4-Car Train) – S2 Up

4 Car Train	SITE 2: UP		Before Tamping		After Tamping	
			Trend Line Equation	R^2	Trend Line Equation	R^2
	Verticals	High Leg	$y = 0.0021x^2 + 0.1076x + 71.06$	0.9951	$y = 0.004x^2 + 0.0271x + 72.393$	0.9982
		Low Leg	$y = -0.0031x^2 - 0.0698x + 102.07$	0.9984	$y = -0.0035x^2 + 0.0509x + 93.931$	0.9921
	Laterals	High Leg	$y = 0.0015x^2 - 0.0048x + 9.6248$	0.9915	$y = 0.0005x^2 - 0.0752x + 4.4022$	0.0762
		Low Leg	$y = -0.0016x^2 - 0.055x + 32.312$	0.9948	$y = -0.0035x^2 + 0.0496x + 29.309$	0.9398

© University of Pretoria

APPENDIX K. FORCE BALANCING DATA FOR BOGIES AND CARS

Table K-1: Force Balancing (Bogies) – S1 Down

	SITE 1: DOWN			Before Tamping		After Tamping		Δ x (km/h)	Δ x (%)	Δ y (t)	Δ y (%)
	Car	Bogie	Rail	x (km/h)	y (t)	x (km/h)	y (t)				
Verticals	DMOS B	Leading	HL / LL	51.73	11.81	77.49	12.93	25.77	49.81	1.12	9.53
		Trailing	HL / LL	59.13	10.57	76.37	10.94	17.25	29.17	0.36	3.44
	PTOS	Leading	HL / LL	65.53	9.83	80.07	9.79	14.53	22.18	-0.04	-0.45
		Trailing	HL / LL	51.83	10.83	78.60	11.04	26.77	51.65	0.21	1.91
	MOS	Leading	HL / LL	51.89	10.40	69.33	10.44	17.44	33.60	0.04	0.37
		Trailing	HL / LL	57.66	10.16	83.95	10.77	26.29	45.59	0.61	6.04
	DMOS A	Leading	HL / LL	56.27	10.59	75.80	10.82	19.53	34.72	0.23	2.16
		Trailing	HL / LL	58.03	11.77	81.85	11.94	23.82	41.05	0.17	1.47
Laterals	DMOS B	Leading	HL / LL	83.56	2.22	88.12	0.51	4.56	5.46	-1.71	-76.89
		Trailing	HL / LL	89.01	1.93	82.11	1.41	-6.90	-7.75	-0.52	-27.02
	PTOS	Leading	HL / LL	80.58	2.15	91.41	0.93	10.83	13.45	-1.22	-56.68
		Trailing	HL / LL	82.76	1.93	92.34	0.53	9.58	11.58	-1.40	-72.47
	MOS	Leading	HL / LL	81.78	1.92	85.00	0.72	3.22	3.94	-1.20	-62.61
		Trailing	HL / LL	91.65	2.26	93.18	0.01	1.53	1.67	-2.25	-99.50
	DMOS A	Leading	HL / LL	88.06	2.32	82.20	1.50	-5.85	-6.65	-0.81	-35.17
		Trailing	HL / LL	97.67	2.11	79.69	1.08	-17.98	-18.41	-1.02	-48.58

© University of Pretoria

Table K-2: Force Balancing (Bogies) – S1 Up

	SITE 1: UP			Before Tamping		After Tamping		Δ x (km/h)	Δ x (%)	Δ y (t)	Δ y (%)
	Car	Bogie	Rail	x (km/h)	y (t)	x (km/h)	y (t)				
Verticals	DMOS B	Leading	HL / LL	58.62	10.74	69.21	10.59	10.59	18.07	-0.15	-1.38
		Trailing	HL / LL	59.45	12.24	75.35	11.87	15.90	26.75	-0.36	-2.98
	PTOS	Leading	HL / LL	58.57	11.25	70.67	10.68	12.10	20.67	-0.57	-5.06
		Trailing	HL / LL	68.46	10.08	76.70	9.85	8.25	12.04	-0.24	-2.34
	MOS	Leading	HL / LL	61.20	10.36	81.61	10.17	20.41	33.35	-0.19	-1.86
		Trailing	HL / LL	56.97	10.54	67.98	10.49	11.01	19.33	-0.05	-0.48
	DMOS A	Leading	HL / LL	61.81	12.22	81.54	11.56	19.73	31.92	-0.67	-5.45
		Trailing	HL / LL	60.73	10.87	69.05	10.74	8.32	13.71	-0.13	-1.22
Laterals	DMOS B	Leading	HL / LL	94.91	1.45	62.07	2.05	-32.84	-34.60	0.59	40.71
		Trailing	HL / LL	94.56	1.18	67.63	1.95	-26.93	-28.48	0.77	65.29
	PTOS	Leading	HL / LL	86.44	1.46	73.77	2.11	-12.67	-14.66	0.65	44.51
		Trailing	HL / LL	90.39	1.40	70.12	1.86	-20.27	-22.42	0.45	32.33
	MOS	Leading	HL / LL	96.62	1.97	76.73	2.20	-19.89	-20.58	0.22	11.20
		Trailing	HL / LL	83.82	1.56	71.65	1.84	-12.17	-14.52	0.28	18.15
	DMOS A	Leading	HL / LL	93.60	2.34	72.82	2.55	-20.78	-22.20	0.22	9.34
		Trailing	HL / LL	99.52	1.35	73.98	1.98	-25.54	-25.66	0.63	46.49

© University of Pretoria

Table K-3: Force Balancing (Bogies) – S2 Down

	SITE 2: DOWN			Before Tamping		After Tamping		Δ x (km/h)	Δ x (%)	Δ y (t)	Δ y (%)
	Car	Bogie	Rail	x (km/h)	y (t)	x (km/h)	y (t)				
Verticals	DMOS B	Leading	HL / LL	56.92	11.68	55.50	11.78	-1.42	-2.49	0.10	0.84
		Trailing	HL / LL	61.55	10.43	58.24	10.39	-3.31	-5.38	-0.04	-0.36
	PTOS	Leading	HL / LL	67.15	9.52	58.25	9.49	-8.90	-13.26	-0.03	-0.36
		Trailing	HL / LL	62.28	10.84	52.94	10.65	-9.34	-14.99	-0.19	-1.76
	MOS	Leading	HL / LL	58.24	10.29	46.72	10.13	-11.52	-19.79	-0.16	-1.59
		Trailing	HL / LL	65.83	10.15	68.39	10.16	2.57	3.90	0.01	0.12
	DMOS A	Leading	HL / LL	61.11	10.58	52.75	10.43	-8.35	-13.67	-0.15	-1.41
		Trailing	HL / LL	64.92	11.82	58.48	11.67	-6.43	-9.91	-0.15	-1.28
Laterals	DMOS B	Leading	HL / LL	73.89	2.47	98.20	0.08	24.31	32.90	-2.39	-96.73
		Trailing	HL / LL	82.03	2.17	102.90	-0.17	20.87	25.44	-2.34	-107.95
	PTOS	Leading	HL / LL	77.93	2.41	112.96	-0.26	35.04	44.96	-2.68	-110.90
		Trailing	HL / LL	78.29	1.78	102.13	-0.45	23.84	30.45	-2.23	-125.56
	MOS	Leading	HL / LL	78.45	2.22	96.75	0.18	18.30	23.32	-2.03	-91.75
		Trailing	HL / LL	82.61	2.20	97.08	-0.01	14.47	17.52	-2.22	-100.59
	DMOS A	Leading	HL / LL	69.48	2.56	118.42	-0.51	48.94	70.45	-3.07	-119.78
		Trailing	HL / LL	77.84	2.79	85.91	-1.00	8.07	10.37	-3.78	-135.75

© University of Pretoria

Table K-4: Force Balancing (Bogies) – S2 Up

	SITE 2: UP			Before Tamping		After Tamping		Δ x (km/h)	Δ x (%)	Δ y (t)	Δ y (%)
	Car	Bogie	Rail	x (km/h)	y (t)	x (km/h)	y (t)				
Verticals	DMOS B	Leading	HL LL	66.31	10.54	50.93	10.52	-15.38	-23.20	-0.02	-0.23
Verticals	DMOS B	Trailing	HL LL	55.10	11.80	56.05	12.11	0.95	1.72	0.31	2.60
Verticals	PTOS	Leading	HL LL	63.00	10.98	50.72	10.83	-12.28	-19.49	-0.16	-1.43
Verticals	PTOS	Trailing	HL LL	62.44	9.68	59.22	9.85	-3.21	-5.15	0.17	1.71
Verticals	MOS	Leading	HL LL	64.90	10.21	61.95	9.99	-2.96	-4.55	-0.23	-2.21
Verticals	MOS	Trailing	HL LL	57.00	10.47	52.46	10.36	-4.55	-7.98	-0.10	-0.99
Verticals	DMOS A	Leading	HL LL	68.90	11.88	56.97	11.76	-11.93	-17.31	-0.13	-1.06
Verticals	DMOS A	Trailing	HL LL	58.32	10.59	50.52	10.48	-7.80	-13.37	-0.11	-1.06
Laterals	DMOS B	Leading	HL LL	80.00	2.42	89.45	0.30	9.45	11.82	-2.12	-87.54
Laterals	DMOS B	Trailing	HL LL	81.86	2.28	92.09	0.25	10.23	12.50	-2.03	-88.99
Laterals	PTOS	Leading	HL LL	72.52	2.45	102.84	0.15	30.32	41.81	-2.29	-93.78
Laterals	PTOS	Trailing	HL LL	66.85	2.08	91.43	0.63	24.58	36.76	-1.45	-69.72
Laterals	MOS	Leading	HL LL	79.96	2.41	99.35	0.02	19.40	24.26	-2.40	-99.36
Laterals	MOS	Trailing	HL LL	75.89	2.12	88.06	0.48	12.17	16.03	-1.63	-77.12
Laterals	DMOS A	Leading	HL LL	84.39	2.67	97.71	0.11	13.32	15.79	-2.56	-95.85
Laterals	DMOS A	Trailing	HL LL	72.48	2.23	98.45	0.35	25.96	35.82	-1.88	-84.49

© University of Pretoria

Table K-5: Force Balancing (Cars) – S1 Down

	SITE 1: DOWN		Before Tamping		After Tamping		Δ x (km/h)	Δ x (%)	Δ y (t)	Δ y (%)
	Car	Rail	x (km/h)	y (t)	x (km/h)	y (t)				
Verticals	DMOS B	HL / LL	54.18	22.25	76.94	23.86	22.75	42.00	1.61	7.24
	PTOS	HL / LL	58.57	20.64	79.26	20.82	20.69	35.32	0.18	0.89
	MOS	HL / LL	54.37	20.54	77.10	21.16	22.73	41.82	0.62	3.02
	DMOS A	HL / LL	57.09	22.37	77.14	23.07	20.05	35.13	0.70	3.14
Laterals	DMOS B	HL / LL	85.32	3.49	85.27	1.94	-0.06	-0.06	-1.55	-44.35
	PTOS	HL / LL	82.35	4.31	84.80	1.88	2.45	2.97	-2.43	-56.30
	MOS	HL / LL	86.03	4.13	88.72	0.79	2.69	3.13	-3.34	-80.77
	DMOS A	HL / LL	93.22	4.47	81.28	2.55	-11.94	-12.81	-1.92	-42.99

Table K-6: Force Balancing (Cars) – S1 Up

	SITE 1: UP		Before Tamping		After Tamping		Δ x (km/h)	Δ x (%)	Δ y (t)	Δ y (%)
	Car	Rail	x (km/h)	y (t)	x (km/h)	y (t)				
Verticals	DMOS B	HL / LL	57.46	23.11	74.14	22.69	16.68	29.03	-0.41	-1.79
	PTOS	HL / LL	61.98	21.12	73.67	20.50	11.69	18.86	-0.62	-2.95
	MOS	HL / LL	58.77	20.89	74.95	20.72	16.18	27.54	-0.17	-0.83
	DMOS A	HL / LL	61.27	23.10	77.02	22.62	15.76	25.72	-0.47	-2.05
Laterals	DMOS B	HL / LL	88.81	3.11	65.18	4.02	-23.63	-26.60	0.90	29.03
	PTOS	HL / LL	88.26	2.86	71.83	4.01	-16.43	-18.62	1.15	40.17
	MOS	HL / LL	95.11	3.12	74.17	4.03	-20.94	-22.01	0.91	29.24
	DMOS A	HL / LL	96.07	3.72	75.51	4.81	-20.56	-21.40	1.09	29.21

© University of Pretoria

Table K-7: Force Balancing (Cars) – S2 Down

	SITE 2: DOWN		Before Tamping		After Tamping		Δ x (km/h)	Δ x (%)	Δ y (t)	Δ y (%)
	Car	Rail	x (km/h)	y (t)	x (km/h)	y (t)				
Verticals	DMOS B	HL / LL	59.27	22.12	55.26	22.32	-4.01	-6.76	0.20	0.89
	PTOS	HL / LL	64.56	20.38	54.08	20.28	-10.48	-16.24	-0.10	-0.47
	MOS	HL / LL	61.71	20.45	57.19	20.23	-4.53	-7.34	-0.22	-1.06
	DMOS A	HL / LL	61.34	22.20	57.14	21.94	-4.20	-6.84	-0.26	-1.17
Laterals	DMOS B	HL / LL	78.53	4.55	100.18	-0.06	21.66	27.58	-4.62	-101.42
	PTOS	HL / LL	73.40	4.56	100.26	0.11	26.86	36.59	-4.46	-97.69
	MOS	HL / LL	80.65	4.44	102.68	0.45	22.04	27.33	-3.99	-89.86
	DMOS A	HL / LL	77.70	4.99	103.80	-0.16	26.10	33.60	-5.15	-103.14

Table K-8: Force Balancing (Cars) – S2 Up

	SITE 2: UP		Before Tamping		After Tamping		Δ x (km/h)	Δ x (%)	Δ y (t)	Δ y (%)
	Car	Rail	x (km/h)	y (t)	x (km/h)	y (t)				
Verticals	DMOS B	HL / LL	60.99	22.36	53.76	22.62	-7.23	-11.86	0.25	1.13
	PTOS	HL / LL	62.76	20.67	56.33	20.53	-6.42	-10.24	-0.14	-0.66
	MOS	HL / LL	60.85	20.68	55.66	20.52	-5.19	-8.53	-0.16	-0.77
	DMOS A	HL / LL	65.31	22.27	55.14	22.40	-10.18	-15.58	0.13	0.57
Laterals	DMOS B	HL / LL	76.29	4.42	90.72	0.58	14.43	18.92	-3.83	-86.80
	PTOS	HL / LL	73.69	4.22	94.81	0.31	21.12	28.66	-3.91	-92.72
	MOS	HL / LL	77.99	4.55	96.92	0.02	18.93	24.27	-4.53	-99.65
	DMOS A	HL / LL	83.24	5.22	96.28	0.77	13.04	15.67	-4.45	-85.30

© University of Pretoria

APPENDIX L. RAIL FORCES FOR BOGIES AND CARS AT 85 KM/H

Table L-1: Rail Forces Before and After Tamping at 85 km/h (Bogies) – S1 Down

	SITE 1: DOWN			Ops Speed (x) (km/h)	Before Tamping	After Tamping	Δ y (t)
	Car	Bogie	Rail		y (t)	y (t)	
Verticals	DMOS B	Leading	HL	85.0	13.99	13.70	-0.28 (-2%)
			LL	85.0	10.20	12.33	+2.12 (+20.77%)
		Trailing	HL	85.0	12.56	11.71	-0.84 (-6.68%)
			LL	85.0	9.15	10.16	+1 (+10.92%)
	PTOS	Leading	HL	85.0	11.10	10.13	-0.96 (-8.65%)
			LL	85.0	8.88	9.43	+0.55 (+6.19%)
		Trailing	HL	85.0	13.09	11.54	-1.54 (-11.76%)
			LL	85.0	8.97	10.42	+1.44 (+16.04%)
	MOS	Leading	HL	85.0	12.80	11.63	-1.17 (-9.14%)
			LL	85.0	8.26	9.45	+1.19 (+14.4%)
		Trailing	HL	85.0	11.82	10.87	-0.95 (-8.03%)
			LL	85.0	9.12	10.70	+1.58 (+17.31%)
	DMOS A	Leading	HL	85.0	12.84	11.55	-1.28 (-9.96%)
			LL	85.0	8.76	10.10	+1.34 (+15.29%)
		Trailing	HL	85.0	13.32	12.21	-1.1 (-8.25%)
			LL	85.0	10.30	11.65	+1.35 (+13.1%)
Laterals	DMOS B	Leading	HL	85.0	2.28	0.46	-1.82 (-79.68%)
			LL	85.0	2.17	0.75	-1.41 (-65.09%)
		Trailing	HL	85.0	1.84	1.48	-0.36 (-19.56%)
			LL	85.0	2.08	1.23	-0.84 (-40.45%)
	PTOS	Leading	HL	85.0	2.23	0.98	-1.25 (-55.98%)
			LL	85.0	2.00	1.44	-0.56 (-27.97%)
		Trailing	HL	85.0	1.99	0.61	-1.37 (-68.89%)
			LL	85.0	1.86	1.13	-0.72 (-38.78%)
	MOS	Leading	HL	85.0	1.98	0.72	-1.26 (-63.62%)
			LL	85.0	1.81	0.72	-1.09 (-60.3%)
		Trailing	HL	85.0	2.17	0.25	-1.92 (-88.61%)
			LL	85.0	2.55	0.67	-1.87 (-73.35%)
	DMOS A	Leading	HL	85.0	2.28	1.52	-0.75 (-32.91%)
			LL	85.0	2.42	1.28	-1.14 (-47.08%)
		Trailing	HL	85.0	1.83	1.20	-0.63 (-34.39%)
			LL	85.0	2.74	0.71	-2.03 (-74.18%)

© University of Pretoria

Table L-2: Rail Forces Before and After Tamping at 85 km/h (Bogies) – S1 Up

	SITE 1: UP			Ops Speed (x) (km/h)	Before Tamping	After Tamping	Δ y (t)
	Car	Bogie	Rail		y (t)	y (t)	
Verticals	DMOS B	Leading	HL	85.0	12.63	11.65	-0.98 (-7.75%)
			LL	85.0	9.26	9.21	-0.05 (-0.53%)
		Trailing	HL	85.0	14.30	12.54	-1.76 (-12.3%)
			LL	85.0	10.96	11.10	+0.13 (+1.18%)
	PTOS	Leading	HL	85.0	13.39	11.39	-2 (-14.93%)
			LL	85.0	9.88	9.49	-0.38 (-3.84%)
		Trailing	HL	85.0	11.37	10.31	-1.05 (-9.23%)
			LL	85.0	9.10	9.21	+0.1 (+1.09%)
	MOS	Leading	HL	85.0	11.86	10.34	-1.51 (-12.73%)
			LL	85.0	9.32	9.89	+0.56 (+6%)
		Trailing	HL	85.0	13.00	11.46	-1.53 (-11.77%)
			LL	85.0	8.85	9.27	+0.41 (+4.63%)
	DMOS A	Leading	HL	85.0	13.99	11.71	-2.28 (-16.29%)
			LL	85.0	11.04	11.24	+0.2 (+1.81%)
		Trailing	HL	85.0	12.98	11.82	-1.16 (-8.93%)
			LL	85.0	9.40	9.33	-0.06 (-0.63%)
Laterals	DMOS B	Leading	HL	85.0	1.25	2.38	+1.12 (+89.34%)
			LL	85.0	1.87	1.01	-0.86 (-45.95%)
		Trailing	HL	85.0	0.89	2.41	+1.52 (+171.17%)
			LL	85.0	1.54	0.78	-0.75 (-48.81%)
	PTOS	Leading	HL	85.0	1.43	2.28	+0.84 (+58.68%)
			LL	85.0	1.54	1.26	-0.27 (-17.58%)
		Trailing	HL	85.0	1.29	2.15	+0.86 (+66.55%)
			LL	85.0	1.63	1.00	-0.62 (-38.11%)
	MOS	Leading	HL	85.0	1.73	2.36	+0.62 (+35.77%)
			LL	85.0	2.49	1.70	-0.78 (-31.31%)
		Trailing	HL	85.0	1.60	2.10	+0.5 (+31.2%)
			LL	85.0	1.51	1.01	-0.5 (-33.06%)
	DMOS A	Leading	HL	85.0	2.06	2.89	+0.83 (+40.32%)
			LL	85.0	2.74	1.58	-1.16 (-42.3%)
		Trailing	HL	85.0	1.15	2.23	+1.07 (+92.67%)
			LL	85.0	1.95	1.24	-0.71 (-36.33%)

© University of Pretoria

Table L-3: Rail Forces Before and After Tamping at 85 km/h (Bogies) – S2 Down

	SITE 2: DOWN			Ops Speed (x) (km/h)	Before Tamping	After Tamping	Δ y (t)
	Car	Bogie	Rail		y (t)	y (t)	
Verticals	DMOS B	Leading	HL	85.0	13.90	13.93	+0.03 (+0.21%)
			LL	85.0	9.99	10.23	+0.23 (+2.3%)
		Trailing	HL	85.0	12.12	12.03	-0.09 (-0.74%)
			LL	85.0	8.78	8.88	+0.1 (+1.13%)
	PTOS	Leading	HL	85.0	10.62	11.15	+0.53 (+4.99%)
			LL	85.0	8.33	7.96	-0.37 (-4.43%)
		Trailing	HL	85.0	12.59	12.63	+0.04 (+0.31%)
			LL	85.0	9.28	9.04	-0.23 (-2.47%)
	MOS	Leading	HL	85.0	12.27	12.55	+0.28 (+2.28%)
			LL	85.0	8.57	8.33	-0.24 (-2.79%)
		Trailing	HL	85.0	11.26	11.21	-0.04 (-0.35%)
			LL	85.0	9.20	9.56	+0.35 (+3.8%)
	DMOS A	Leading	HL	85.0	12.77	12.71	-0.06 (-0.46%)
			LL	85.0	9.12	8.42	-0.69 (-7.56%)
		Trailing	HL	85.0	13.23	13.66	+0.42 (+3.17%)
			LL	85.0	10.70	10.54	-0.16 (-1.49%)
Laterals	DMOS B	Leading	HL	85.0	2.88	-0.37	-3.25 (-112.77%)
			LL	85.0	1.94	0.91	-1.03 (-52.99%)
		Trailing	HL	85.0	2.22	-0.49	-2.71 (-122.06%)
			LL	85.0	2.04	0.87	-1.17 (-57.21%)
	PTOS	Leading	HL	85.0	2.57	-0.06	-2.62 (-102.08%)
			LL	85.0	2.17	1.20	-0.96 (-44.3%)
		Trailing	HL	85.0	1.89	-0.90	-2.78 (-147.22%)
			LL	85.0	1.44	0.57	-0.86 (-59.92%)
	MOS	Leading	HL	85.0	2.41	0.06	-2.34 (-97.21%)
			LL	85.0	1.97	0.92	-1.04 (-52.7%)
		Trailing	HL	85.0	2.25	-0.35	-2.59 (-115.23%)
			LL	85.0	2.08	0.72	-1.36 (-65.39%)
	DMOS A	Leading	HL	85.0	3.05	-0.09	-3.14 (-102.83%)
			LL	85.0	1.83	1.52	-0.31 (-16.9%)
		Trailing	HL	85.0	3.04	-1.02	-4.06 (-133.37%)
			LL	85.0	2.41	0.53	-1.87 (-77.73%)

© University of Pretoria

Table L-4: Rail Forces Before and After Tamping at 85 km/h (Bogies) – S2 Up

	SITE 2: UP			Ops Speed (x) (km/h)	Before Tamping	After Tamping	Δ y (t)
	Car	Bogie	Rail		y (t)	y (t)	
Verticals	DMOS B	Leading	HL	85.0	11.62	12.74	+1.11 (+9.55%)
			LL	85.0	9.20	8.66	-0.53 (-5.76%)
		Trailing	HL	85.0	13.32	14.79	+1.46 (+10.95%)
			LL	85.0	10.01	10.61	+0.6 (+5.99%)
	PTOS	Leading	HL	85.0	12.37	13.57	+1.2 (+9.7%)
			LL	85.0	9.53	8.64	-0.89 (-9.33%)
		Trailing	HL	85.0	10.77	11.69	+0.92 (+8.54%)
			LL	85.0	8.14	8.51	+0.36 (+4.42%)
	MOS	Leading	HL	85.0	11.17	11.39	+0.22 (+1.96%)
			LL	85.0	9.11	8.64	-0.46 (-5.05%)
		Trailing	HL	85.0	11.86	12.71	+0.84 (+7.08%)
			LL	85.0	8.79	8.66	-0.12 (-1.36%)
	DMOS A	Leading	HL	85.0	12.69	13.71	+1.01 (+7.95%)
			LL	85.0	10.87	10.22	-0.65 (-5.97%)
		Trailing	HL	85.0	12.29	13.00	+0.71 (+5.77%)
			LL	85.0	8.80	8.32	-0.48 (-5.45%)
Laterals	DMOS B	Leading	HL	85.0	2.57	0.33	-2.23 (-86.78%)
			LL	85.0	2.23	0.57	-1.66 (-74.38%)
		Trailing	HL	85.0	2.39	0.08	-2.3 (-96.39%)
			LL	85.0	2.18	0.80	-1.38 (-63.19%)
	PTOS	Leading	HL	85.0	2.83	0.14	-2.69 (-94.92%)
			LL	85.0	1.93	1.52	-0.41 (-21.21%)
		Trailing	HL	85.0	2.65	0.52	-2.13 (-80.37%)
			LL	85.0	1.34	1.06	-0.27 (-20.19%)
	MOS	Leading	HL	85.0	2.56	0.10	-2.45 (-95.67%)
			LL	85.0	2.18	0.99	-1.18 (-54.04%)
		Trailing	HL	85.0	2.43	0.44	-1.99 (-81.85%)
			LL	85.0	1.84	0.70	-1.13 (-61.49%)
	DMOS A	Leading	HL	85.0	2.69	0.20	-2.48 (-92.12%)
			LL	85.0	2.64	1.25	-1.39 (-52.57%)
		Trailing	HL	85.0	2.65	0.47	-2.17 (-82.03%)
			LL	85.0	1.74	1.35	-0.38 (-21.89%)

© University of Pretoria

Table L-5: Rail Forces Before and After Tamping at 85 km/h (Cars) – S1 Down

	SITE 1: DOWN		Ops Speed (x) (km/h)	Before Tamping	After Tamping	Δ y (t)
	Car	Rail		y (t)	y (t)	
Verticals	DMOS B	HL	85.0	26.56	25.42	-1.14 (-4.29%)
		LL	85.0	18.79	22.49	+3.7 (+19.69%)
	PTOS	HL	85.0	24.19	21.68	-2.51 (-10.37%)
		LL	85.0	17.84	19.85	+2 (+11.2%)
	MOS	HL	85.0	24.62	22.50	-2.12 (-8.61%)
		LL	85.0	17.39	20.16	+2.76 (+15.86%)
	DMOS A	HL	85.0	26.16	24.49	-1.67 (-6.38%)
		LL	85.0	19.07	21.76	+2.68 (+14.05%)
Laterals	DMOS B	HL	85.0	3.47	1.93	-1.54 (-44.32%)
		LL	85.0	3.52	1.98	-1.54 (-43.74%)
	PTOS	HL	85.0	4.44	1.88	-2.55 (-57.46%)
		LL	85.0	4.15	1.85	-2.29 (-55.21%)
	MOS	HL	85.0	4.10	0.96	-3.13 (-76.4%)
		LL	85.0	4.21	1.39	-2.82 (-66.94%)
	DMOS A	HL	85.0	4.18	2.65	-1.52 (-36.4%)
		LL	85.0	5.15	1.99	-3.16 (-61.36%)

© University of Pretoria

Table L-6: Rail Forces Before and After Tamping at 85 km/h (Cars) – S1 Up

	SITE 1: UP		Ops Speed (x) (km/h)	Before Tamping	After Tamping	Δ y (t)
	Car	Rail		y (t)	y (t)	
Verticals	DMOS B	HL	85.0	27.66	23.53	-4.13 (-14.93%)
		LL	85.0	20.21	21.30	+1.08 (+5.34%)
	PTOS	HL	85.0	24.75	21.81	-2.94 (-11.87%)
		LL	85.0	18.26	19.16	+0.9 (+4.92%)
	MOS	HL	85.0	24.85	21.69	-3.15 (-12.67%)
		LL	85.0	18.16	18.69	+0.52 (+2.86%)
	DMOS A	HL	85.0	26.97	24.19	-2.77 (-10.27%)
		LL	85.0	20.44	21.02	+0.58 (+2.83%)
Laterals	DMOS B	HL	85.0	2.86	4.85	+1.98 (+69.12%)
		LL	85.0	3.41	1.79	-1.61 (-47.24%)
	PTOS	HL	85.0	2.72	4.48	+1.75 (+64.25%)
		LL	85.0	3.16	2.26	-0.9 (-28.46%)
	MOS	HL	85.0	2.69	4.45	+1.76 (+65.54%)
		LL	85.0	4.00	2.71	-1.29 (-32.22%)
	DMOS A	HL	85.0	3.21	5.33	+2.12 (+65.97%)
		LL	85.0	4.70	3.54	-1.16 (-24.65%)

© University of Pretoria

Table L-7: Rail Forces Before and After Tamping at 85 km/h (Cars) – S2 Down

	SITE 2: DOWN		Ops Speed (x) (km/h)	Before Tamping	After Tamping	Δ y (t)
	Car	Rail		y (t)	y (t)	
Verticals	DMOS B	HL	85.0	26.02	26.68	+0.66 (+2.53%)
		LL	85.0	18.77	19.11	+0.33 (+1.75%)
	PTOS	HL	85.0	23.21	24.50	+1.29 (+5.55%)
		LL	85.0	17.61	17.00	-0.6 (-3.4%)
	MOS	HL	85.0	23.53	23.76	+0.23 (+0.97%)
		LL	85.0	17.78	17.88	+0.09 (+0.5%)
	DMOS A	HL	85.0	26.00	25.64	-0.35 (-1.34%)
		LL	85.0	19.10	18.96	-0.14 (-0.73%)
Laterals	DMOS B	HL	85.0	4.89	1.77	-3.11 (-63.66%)
		LL	85.0	3.98	-0.87	-4.84 (-121.6%)
	PTOS	HL	85.0	5.18	-0.39	-5.56 (-107.37%)
		LL	85.0	3.59	1.78	-1.81 (-50.36%)
	MOS	HL	85.0	4.65	-0.29	-4.93 (-106.1%)
		LL	85.0	4.05	2.36	-1.69 (-41.69%)
	DMOS A	HL	85.0	5.38	-0.67	-6.04 (-112.37%)
		LL	85.0	4.24	2.06	-2.17 (-51.18%)

© University of Pretoria

Table L-8: Rail Forces Before and After Tamping at 85 km/h (Cars) – S2 Up

	SITE 2: UP		Ops Speed (x) (km/h)	Before Tamping	After Tamping	Δ y (t)
	Car	Rail		y (t)	y (t)	
Verticals	DMOS B	HL	85.0	24.95	27.53	+2.58 (+10.34%)
		LL	85.0	19.21	19.27	+0.05 (+0.26%)
	PTOS	HL	85.0	23.14	24.53	+1.39 (+6%)
		LL	85.0	17.68	17.15	-0.52 (-2.94%)
	MOS	HL	85.0	23.03	24.82	+1.78 (+7.72%)
		LL	85.0	17.89	17.29	-0.6 (-3.35%)
	DMOS A	HL	85.0	24.26	26.71	+2.44 (+10.05%)
		LL	85.0	19.68	19.26	-0.42 (-2.13%)
Laterals	DMOS B	HL	85.0	4.95	0.48	-4.46 (-90.15%)
		LL	85.0	3.68	1.37	-2.31 (-62.69%)
	PTOS	HL	85.0	4.76	0.23	-4.53 (-95.14%)
		LL	85.0	3.27	1.86	-1.4 (-42.81%)
	MOS	HL	85.0	5.00	0.03	-4.96 (-99.19%)
		LL	85.0	4.02	1.69	-2.32 (-57.7%)
	DMOS A	HL	85.0	5.34	0.89	-4.45 (-83.37%)
		LL	85.0	5.09	2.59	-2.49 (-48.88%)

© University of Pretoria